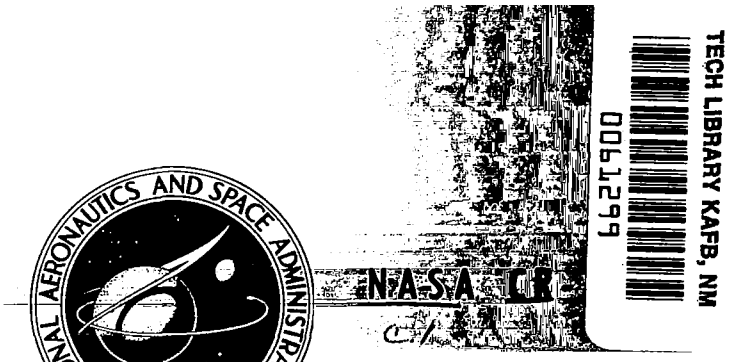

NASA CONTRACTOR REPORT

NASA CR-1975

RIDING AND HANDLING QUALITIES OF LIGHT AIRCRAFT — A REVIEW AND ANALYSIS

by Frederick O. Smetana, Delbert C. Summey, and W. Donald Johnson

Prepared by
NORTH CAROLINA STATE UNIVERSITY
Raleigh, N. C. 27607
for Langley Research Center

NATIONAL AERONAUTICS AND SPACE ADMINISTRATION • WASHINGTON, D. C. • MARCH 1972

1. Report No.	2. Government Accession No.	3. Recipient's Catalog No.
NASA CR - 1975		

4. Title and Subtitle	5. Report Date
RIDING AND HANDLING QUALITIES OF LIGHT AIRCRAFT - A REVIEW AND ANALYSIS	March 1972
	6. Performing Organization Code: 32.100
7. Author(s): Frederick O. Smetana, Delbert C. Summey, and W. Donald Johnson	8. Performing Organization Report No.: None
9. Performing Organization Name and Address: North Carolina State University at Raleigh, Department of Mechanical and Aerospace Engineering, Raleigh, North, Carolina 27607	10. Work Unit No.: 736-05-10-01-00
	11. Contract or Grant No.: NAS1-9603
12. Sponsoring Agency Name and Address: National Aeronautics and Space Administration, Washington, DC 20546	13. Type of Report and Period Covered: Contractor Report
	14. Sponsoring Agency Code

15. Supplementary Notes

16. Abstract

Design procedures and supporting data necessary for configuring light aircraft to obtain desired responses to pilot commands and gusts are presented. The procedures employ specializations of modern military and jet transport practice where these provide an improvement over earlier practice.

General criteria for riding and handling qualities are discussed in terms of the airframe dynamics. Methods available in the literature for calculating the coefficients required for a linearized analysis of the airframe dynamics are reviewed in detail. The review also treats the relation of spin and stall to airframe geometry.

Root locus analysis is used to indicate the sensitivity of airframe dynamics to variations in individual stability derivatives and to variations in geometric parameters. Computer programs are given for finding the frequencies, damping ratios, and time constants of all rigid body modes and for generating time histories of aircraft motions in response to control inputs.

To the end that the work serve as a self-contained riding and handling characteristics design handbook, appendices are included presenting the derivation of the linearized equations of motion; the stability derivatives; the transfer functions; approximate solutions for the frequency, damping ratio, and time constants; an indication of methods to be used when linear analysis is inadequate; sample calculations; and an explanation of the use of root locus diagrams and Bode plots.

17. Key Words (Suggested by Author(s))	18. Distribution Statement
Stability derivatives Bode plots Sample calculations Computer programs	Unclassified - Unlimited

19. Security Classif. (of this report)	20. Security Classif. (of this page)	21. No. of Pages	22. Price*
Unclassified	Unclassified	409	$6.00

*For sale by the National Technical Information Service, Springfield, Virginia 22151

TABLE OF CONTENTS

	Page
GENERAL INTRODUCTION	1
Background	2
Objectives and Organization	4
Factors Contributing to the Pilot's Opinion of Aircraft Handling Qualities	6
Flight Motions of Light Aircraft-General Considerations	11
Control Forces and Deflections-General Considerations	14
LITERATURE REVIEW	15
Scope	16
Symbols	18
Stability Derivatives	27
Power Effects	110
Control Forces and Deflections	122
Inertial Characteristics	152
Stall	156
Spin Entry	165
Human Factors	179
Design for Desirable Riding Qualities	187
THE EFFECT OF VARIATIONS IN STABILITY DERIVATIVES ON THE MOTIONS OF A TYPICAL LIGHT AIRCRAFT	193
Introduction	194

TABLE OF CONTENTS (continued)

	Page
Longitudinal Variations	198
Lateral Variations	203
REFERENCES	301
APPENDICES	311
A - Derivation of Equations of Motion	311
B - Definition of Stability Derivatives	333
C - Transfer Functions	337
D - Simplified Response Characteristics	347
E - Use of the Non-Linear Forms of the Equations of Motion	353
F - Some Notes on the Construction and Interpretation of Bode Plots and Root Locus Diagrams	355
G - Sample Calculations	363
Longitudinal Sample Calculations	
Lateral Sample Calculations	
H - Computer Programs	379
Longitudinal Program	
Lateral Program	
Longitudinal and Lateral Sample Output	
Time Response Program	
I - Bibliography	393

GENERAL INTRODUCTION

BACKGROUND

Recent engine advances, the upsurge in business flying, and general affluence have greatly accelerated the development of new and altered models of general aviation aircraft. These developments follow the traditional industry pattern of evolutionary change rather than revolutionary change. For example, a particular model may not be selling as well as expected, so it is determined that offering the aircraft with additional power would increase its sales appeal. It is then up to the company's engineering department to accomplish this refitting with a minimum of expense. There are the obvious structural modifications to make, the weight and balance to check, and then a check flight to determine whether the ride and handling characteristics remain, according to the subjective opinion of the company pilot, satisfactory. It is, of course, not possible to explore, in this type of flight test program, all possible flight modes and conditions so that one may omit tests at a condition which formerly was not uncomfortable or unsafe but has, because of the changes become so. This seldom happens of course, but place an aircraft with a larger engine in the hands of an inexperienced pilot, and he will probably be surprised that the periods of the longitudinal short period and dutch roll modes increase and their damping decreases; similarly, it is seldom expected by the novice that moving the engine to the wing and adding a second engine may, because of the nacelle design, give a serious pitch-up condition at high angles of attack or that providing adequate static longitudinal stability or weathercock stability at some particular flight condition does not guarantee acceptable dynamic characteristics. Yet these things can, given sufficient and reliable analytical and experimental data, be forecast quite accurately and can be included in the pilot's handbook.

To expect the manufacturer of light aircraft to carry out the comprehensive preliminary design analyses, the extensive wind tunnel tests, and the exhaustive flight tests that were performed for the C-5A, for example, for each of his new aircraft is not being economically realistic. If one could, however, supply the designer of light aircraft with simple-to-use, accurate means of predicting all aspects of the flight performance of his airplane, this would go a long way toward enabling these manufacturers to provide safer, more enjoyable aircraft more economically.

Despite more than 50 years of scientific study, much of the preliminary design is still an art. Desirable handling qualities, for example, are still largely unquantified. The usual procedure is to have an experienced pilot decide whether an airplane handles "satisfactorily." Little effort has been made until recently to determine--by a series of the best available quantitative tests--those control forces and response rates with which a human is confortable and the limiting aircraft accelerations, oscillatory amplitudes, and frequencies for acceptable riding qualities and then incorporating this information into a determination of the geometric, inertial, and power characteristics necessary to achieve them.

Another major problem in light aircraft design is the diversity and fragmentation of reliable experimental and analytical information. In an attempt to contribute to a solution of this problem, the National Aeronautics and Space

Administration supported a review of its published research since 1940 (Refs. 1, 2, 3) with a view toward identifying those items of pertinence to light aircraft design. The present study is an in-depth review, selection, and extension of that portion of this information and certain other information specifically related to the handling and riding qualities of light aircraft. It is intended to serve as a compilation of applicable, available experimental data as well as modern analysis procedures for those interested in these aspects of light aircraft design.

OBJECTIVES AND ORGANIZATION

This work was undertaken with the intention of providing a recent engineering graduate with sufficient understanding, information, and procedures to permit him to predict, with reasonable accuracy, certain riding and handling characteristics of projected light aircraft. To facilitate the presentation, the discussion is limited, for the most part, to those facets of the riding and handling qualities which have a common basis: they trace their origin to the general dynamical behavior of the airframe and its components. This approach takes advantage of the fact that few recent students have not at some time during their collegiate careers seen derived the equations of motion of a rigid body in space and the solution of a system of linear differential equations by the method of Laplace Transforms. Recent graduates are also generally familiar with some of the vocabulary of feedback control systems analysis. The present work, therefore, seeks to build upon this foundation in elaborating modern techniques for predicting essential features of the riding and handling qualities of light aircraft. As a consequence of this choice, however, many perfectly respectable problem areas and effective analysis techniques are not discussed. For these omissions the authors request the reader's forebearance.

The work begins with a discussion of the origin of and basis for riding and handling qualities criteria and how these are distinguished from other familiar criteria, termed here control capability. This section outlines the more familiar handling qualities design and evaluation procedure, that based on control forces and deflections. The relation between such methods and those derived from dynamical considerations is indicated. Next a section reviews briefly, in qualitative terms, the derivation of the linearized equations of motion and the usual methods for analyzing the stability of their solutions. Appendices detail these procedures for those unfamiliar with them.

These sections are intented to provide a basis for appreciating the use which may be made of the data presented in the literature review and that generated during the present investigation. The first portion of the review is basically a compilation of those techniques reported in the literature which the authors regard as most suitable for the calculation of aircraft stability derivatives if given the aircraft's geometry. In preparation is a computer program for performing these calculations. One need then supply only the airframe geometric and inertial parameters and the program will provide numerical values of all the derivatives. This program, along with typical results, will be available as part of a follow-on report which will discuss test and data reduction techniques for extracting the values of stability derivatives from flight data. A short section discusses what is known generally about the effect of applications of power to the values of the individual stability derivatives.

The next portion is concerned with the relation among the stability derivatives, the airframe geometry and mass distribution, the dynamic pressure, and the control forces and control deflections. Included in this discussion of handling qualities are current views of desirable values as represented by the FAR and military specifications.

Information on typical values of light aircraft inertial characteristics and methods of computing them are also included as a section of the literature review. The ratio of aerodynamic control moment to aircraft moment of inertia, of course, is the primary factor in determining the responsiveness of an aircraft to control surface deflections; hence, it seemed desirable to provide suitable information to permit one to make estimates of these characteristics.

Only two conditions involving significant departures from small pertubations are treated: stall and spin. These are included to indicate the state of knowledge regarding some of the limits of the small pertubation analysis.

Finally, a section reviews the information available on the anthopological basis for riding and handling evaluations by human pilots. Included is a new procedure for estimating the riding qualities in terms of the airframe dynamics.

Following the literature review are results of computer studies measuring the sensitivity of aircraft motions to variations in individual stability derivatives. It is, of course, not possible to vary these derivatives in this fashion physically but these studies do indicate those derivatives which influence the motion significantly and must, therefore, be determined with great accuracy. More approximate values are quite acceptable for derivatives which do not strongly affect the motion.

A limited number of more elaborate computer studies are also presented. For these studies all the derivatives which depend upon a given geometric variation are varied appropriately. One can then see the changes in motion which result from a given change in airframe geometry.

For the sake of completeness, Bode plots of the principal longitudinal and lateral transfer functions are then provided, using the original stability derivative values for the example airplane. Some persons find such plots very helpful in visualizing aircraft dynamic responses.

The appendices present derivations of the equations of motion, transformation of these equations to the frequency domain, a computer program for evaluating the constants in the transfer functions given the aircraft geometry and inertia, a computer program for extracting the poles and zeros of a 4th order polynomial transfer function and a computer program to calculate the time histories of the linear velocities and angular displacements given the poles and zeros of the transfer functions; also included are discussions of one and two degree of freedom simplifications of the equations of motion as a means of obtaining approximate predictions of the frequency and damping of the principal modes, example determinations of flight motion of a particular airplane using the methods presented in the text, and the use of unexpanded force terms in generalized non-linear equations of motion to investigate departures from the results of small pertubation theory.

A discussion of the correlation and interpretation of Bode plots and Root Locus diagrams is included. The final appendix presents a bibliography of pertinent documents not specifically cited in the text.

FACTORS CONTRIBUTING TO THE PILOT'S OPINION OF AIRCRAFT RIDING AND HANDLING QUALITIES

Pilots, like other humans, are sensitive to the inertial forces imposed on their bodies by changes in their motion. The relative acceptability of these inertial forces gives rise to the pilot's subjective opinion of the riding qualities of the aircraft. To control the motions of the aircraft, the pilot must exert certain forces on the controls and displace them through certain distances. The magnitudes of these control forces and control displacements and the magnitude and phase relationships between control force and displacement on the one hand and the aircraft's motion on the other hand combine to form the psychological and anthropological basis of the pilot's opinion of the handling qualities of the aircraft.

In addition to the riding and handling qualities defined in this fashion, a pilot's satisfaction with his aircraft also depends upon the aircraft's control capability, which includes such factors as how quickly it will attain a given bank angle, how tight a turn it will make, how great a variation in c.g. location it will tolerate, how often retrimming is required, the minimum airspeed for rudder effectiveness, whether it is possible to fly unyawed with asymmetric power, whether the stall is gentle and the recovery rapid, and whether spin recovery is simple and rapid. The logic for separating what is commonly treated as a single study, aircraft flying qualities, into three divisions as in the present work stems from a number of considerations: handling qualities can, in modern aircraft, be altered to achieve desired values without affecting the riding characteristics or the control capabilities; many of the control capability limits involve very large motions and aerodynamic non-linearities not normally encountered in the motions associated in the pilot's mind with the riding qualities; the control capabilities are primarily a direct result of the aircraft's geometric configuration; riding qualities are strongly affected by inertial characteristics as well as geometric configuration; the pilot makes a direct association between the "ride" and the force applied to his body; for many of the control capabilities, his role is more like that of an observer in that his gratification is dependent not so much upon the forces applied to his body as to the psychologically satisfying condition of being able to will a motion and observe that it is carried out or to being able to refrain from performing a tedious task. It is, of course, true that if one configures the aircraft geometry, mass distribution, and control system to obtain a given set of riding and handling qualities he has at the same time determined, even if unknowingly, much of the aircraft's control capability. Nevertheless, for the present, an aircraft's geometric and inertial parameters will be examined primarily in the light of their influence on riding and handling qualities. The exception to this is the discussion in the literature review of the controllability during stall and spin entry.

As in other matters of opinion, it has proven difficult to identify and to quantify those necessary parameters and their desirable values which are significant in determining the riding and handling qualities of aircraft. Military

flying quality specification, for example, are the result of the combined efforts of many trained engineer-pilots over the years; yet until the release of MIL-F-8785B (ASG) in 1969, most requirements were still stated in qualitative terms. The new specification and the accompanying 688 page background report, AFFDL-TR-69-72, August 1969 (Ref. 4), are the result of more than three years work by a large group of specialists, who consulted more than 660 references, some of them obscure or classified military reports. The new specification sets some quantitative limits on both the riding and handling qualities as well as continuing some qualitative requirements from earlier editions of the specification. The quantitative limits are derived from modern stability analysis, some limited anthropological test data, and pilot comments on the characteristics of variable stability aircraft. The selection of parameters upon which to set requirements appears to have been based upon experience rather than upon a rigorous demonstration that these parameter values do indeed represent the necessary and suffucient conditions for adequate riding and handling qualities.

While the new specification is a great step forward, it is to be hoped that one will soon find standards of acceptable aircraft motions, control forces and displacements, and aircraft response to control displacements which trace their claim from systematic anthropological studies of forces and limb extensions, accelerations, response rates, etc. found to be comfortable by a large number of pilots.

Certainly prior to the issuance of the new specification, and probably even today, the most widely used concept of aircraft flying qualities (handling qualities in the present context) was that developed more than 25 years ago and detailed in the standard textbook of Perkins and Hage and in NACA Report 927, "Appreciation and Prediction of Flying Qualities," by W. H. Phillips. To appreciate the reason that the group of parameters upon which the criteria of these authors are based came into common use, it is well to recall that an aircraft spends most of its flight time in a quasi-equilibrium condition; thus, the forces and, to some extent, the amplitude and phase relations between force application and aircraft response are the traditional basis for the pilot's opinion of the handling qualities.

In developing criteria for the desirability of these forces, deflections, and responses, the attempt was made to express them in terms meaningful to the designer, readily measured and applicable to a wide range of aircraft types. For example, the change in elevator angle with change in trimmed lift coefficient can be shown to be related to the location of the center of gravity in chord lengths from the aerodynamic center, the ratio of horizontal tail area to wing area, the location of the horizontal tail plane aft of the wing aerodynamic center in wing chord lengths, the tail lift curve slope, the relative dynamic pressure and flow direction at the tail compared to that at the wing, and the effectiveness of the elevator in changing the apparent tail angle of attack. Note that these quantities are all non-dimensional and, therefore, applicable to aircraft of varying size and configuration. If one is willing to assume that the tail contribution to aircraft lift coefficient is small, then by measuring the dynamic pressure and aircraft weight during flight the lift coefficient is readily obtained. The elevator angle can be measured easily by installing the movable element of a potentiometer or other position transducer on the elevator shaft. For a given aircraft $d\delta e/dC_L$ can be altered readily only by changing center-of-gravity location. From the pilot's viewpoint, $d\delta e/dC_L$ is significant

because a zero value of this parameter is indicative of the rearmost permissible loading which an aircraft may have before no motion of the stick is required to change speed. Obviously, a pilot will prefer a loading such that at least a small displacement of the stick is required to change speed. Usually, therefore, the aft c.g. limit will be set about .05c ahead of the point for $d\delta e/dC_L=0$

Unfortunately, a pilot is less able to discern variations in $d\delta e/dC_L$ than he is in changes in force with speed. When written as $d(F_S/q)/dC_L$ the parameter depends on the same quantities as $d\delta e/dC_L$ with the addition of the control system gearing and the aerodynamic moments of the elevator about its hinge. Depending upon the elevator design, $d(F_S/q)/dC_L$ can be zero forward or aft of the c.g. location for which $d\delta e/dC_L = 0$. It is desirable to attempt to design the elevator such that $d(F_S/q)dC_L = 0$ occurs at or slightly aft of the c.g. location for which $d\delta e/dC_L = 0$. One would not wish the forces required to change speed to disappear while there is yet some stick motion required nor would one wish the aircraft to continue to change speed if the pilot released the stick. The conditions may both occur if the aircraft has $d(F_S/q)/dC_L = 0$ forward of the c.g. location for which $d\delta e/dC_L = 0$ and is loaded such that the c.g. is between the two points. Hence, it is usually felt necessary to check both parameters during flight test. The aft c.g. limit is then chosen to insure that both parameters have at least perceptable values.

Although an airplane may be loaded with the c.g. so far aft that the control forces and elevator deflections required to change speed are opposite to those normally required, it is not necessarily an uncontrollable airplane. Only if the forces or deflections required for control are too large or require too rapid an application for the pilot to manage can the aircraft really be called uncontrollable. The fact that the controls require actuation in a manner contrary to the usual experience would not of itself be so serious if it were not also for the fact that at these c.g. locations the aircraft will spontaneously rotate to large angles of attack rather rapidly unless countering controls are promptly applied and continuously modulated. If the rotation takes place more rapidly than the speed decreases, large load factors will be developed and the aircraft will quickly destroy itself. Because of the motion damping effects of the horizontal tail, however, the c.g. location at which the elevator angle or stick force per unit of normal acceleration is zero is further aft than when $d\delta e/dC_L=0$ or $d(F_S/q)/dC_L = 0$; thus, even when the aircraft is loaded such that $d(F_S/q)/dC_L=0$, it will retain a finite value for dF_S/dn. Hence vehicle motions--as contrasted to speed changes--will require conventional, although light, forces for control. As the c.g. moves aft from the $dF_S/dn = 0$ location, control becomes progressively more difficult. Determining the c.g. location at which $dF_S/dn = 0$ from flight test provides the designer with a check on the calculated damping effectiveness of the horizontal tail and indicates to the pilot the control margin he has for maneuver if he should inadvertantly load the aircraft such that $d(F_S/q)dC_L = 0$.

In addition to providing a measure of the rearmost permissible c.g. location the parameters $d\delta e/dC_L$, $d(F_S/q)/dC_L$, $d\delta e/dn$, and dF_S/dn are often used to define desirable handling at normal loadings. The presently accepted standards for the values of these or similar parameters are discussed in the literature review. At this point it is sufficient to note that for psychological reasons increasing parameter values seem to be preferred as aircraft size and gross weight increase although human physical capabilities provide the overall upper and lower bounds for all classes of aircraft.

In addition to the stick force arising from aerodynamic hinge moments, a significant contribution is usually supplied by control system friction. This has a material bearing on the pilot's evaluation of the aircraft's handling characteristics. In fact, customer feedback to the manufacture indicates that the average light aircraft pilot seems to prefer a control system which requires a conscious application of force to change speed and which is tolerant of small, inadvertant stick movements. For this reason most lightplane manufacturers evaluate the handling characteristics of their products only in terms of the forces required to change speed and normal acceleration as functions of loading, speed, configuration, and power setting.

In addition to the handling about the y-axis of the aircraft, the pilot will also be concerned with handling about the other two axes. Traditionally such things as the sideslip angle per unit of rudder deflection or rudder force, the amount of rudder needed to compensate for the yawing due to aileron deflection and rolling, and the non-dimensional wing tip helix angle (pb/2U) which is a measure of the rolling capability of the aircraft have been measured to provide quantitative support to the pilot handling impressions. As will be seen from the literature review desirable values are still being specified for most of these parameters.

The reader will note that all of the parameters mentioned thus far are intended to be measured under steady flight conditions. One will generally find little in the way of quantitative requirements on the dynamic behavior of aircraft. This situation arose because older aircraft usually were not very "clean" aerodynamically, had a low ratio of weight to volume, operated at low altitudes, and had relatively large horizontal tailplanes to provide adequate control at low speeds. It can be shown that aerodynamic drag is the principal contributor to the damping of the longitudinal phugoid oscillation; hence a "dirty" airplane--particularly one with relatively low power loading--seldom has unsatisfactory phugoid characteristics. Damping of the dutch roll and longitudinal short period modes is strongly dependent upon the ratio of the restoring force generated by rotation to the moment of inertia about that axis. Thus low density aircraft with large control surfaces operating in dense air usually experience well-damped longitudinal short period and dutch roll oscillations. However, as light aircraft become more dense, operate at higher altitudes, become more "clean", and utilize higher power loadings, it is no longer reasonable to assume that if one assures satisfactory static handling characteristics, as outlined above, then the dynamic flight characteristics, will naturally be satisfactory.

Two additional concerns of recent vintage have also served to focus attention on dynamic characteristics: ride and handling in turbulence. Now that the novelty of flight has disappeared for a significant fraction of the population, standards for what is an acceptable level of ride are continuously being upgraded. Travel in current jet transports has convinced many that (a) flying can be very smooth and (b) an uncomfortable ride can be very fatiguing for passengers and can serve to diminish the effectiveness of a pilot. As a result of these comfort and safety considerations and the growing realization among designers that aircraft riding characteristics can be altered through suitable design just as they can in other vehicles, increasing attention is being directed toward establishing the vehicle behavior identified with good riding qualities. Since the human body associates only changes in motion with vehicle ride, it is apparent that riding qualities can be defined only in terms of the vehicle's dynamic characteristics.

In turbulent weather, the aircraft is struck continually by gusts of more or less random magnitude and orientation. Most of the characteristic motions of the aircraft are excited simultaneously. As a result, pilot work load may be very high depending almost entirely on the vehicle's dynamic characteristics. Well damped aircraft, for example, materially reduce the amount of control input required of the pilot when compared with aircraft having lightly damped longitudinal short period and dutch roll oscillations.

There is even less justification for neglecting consideration of the airframe dynamics when one observes that many of the conventional static stability parameters are merely the zero frequency values of more general transfer functions. They are, therefore, still available, having been generated as a part of the process of evaluating the general dynamical behavior. This point is elaborated somewhat in the next section.

FLIGHT MOTIONS OF LIGHT AIRCRAFT—
GENERAL CONSIDERATIONS

The motion of a rigid body in space is described completely by a system of six equations, three representing the translation of the center of mass (center of gravity) and three representing the angular motion of the body about its center of gravity. General solutions of this system of differential equations are unknown because products and squares of the dependent variables appear in some terms and because the unbalanced aerodynamic forces and moments which produce the motion are not known explicitly. Since these forces and moments are known to depend, among other things, upon the vehicle's inclination relative to the stream, the time rate of change of the inclination, the vehicle velocities, and the vehicle accelerations, it has been usual to represent the forces and moments by Taylor series expansions in these variables about the equilibrium condition. Even if these variables are all related to the six dependent variables and their derivatives, one is faced with the task of evaluating either empirically or analytically the first and higher order partial derivatives of all the forces and moments with respect to each of the dependent variables and their derivatives in order to make possible solutions for particular sets of initial conditions--the only possible solutions because of the presence of the nonlinear product and square terms. The inverse problem, finding the values of all the partial derivatives if the motion is known, clearly has no unique solution.

If it were necessary to follow this procedure in all its detail every time someone wanted to know the motion of an aircraft following a momentary control surface deflection, the motion would probably remain unknown until a series of expensive flight tests established the safety of the particular control surface deflection and the character of the response. Fortunately, most departures from equilibrium are small and, also because there is a plane of symmetry, there is little lateral-longitudinal cross-coupling. As a result, for most flight maneuvers one can neglect products and squares of the dependent variables because they are very small compared with the value of the variables themselves. One can also consider the aircraft's motion to be represented by two independent systems of three differential equations; further, the departures from equilibrium are small enough that the aerodynamic forces and moments can be described with sufficient accuracy by retaining only the linear term of the Taylor expansion. The equations are thus made linear and amenable to a vast literature of solution techniques.

The usual range of values of the partial derivatives in the Taylor expansions of the aerodynamic forces and moments, the so-called stability derivatives,* are such that most aircraft exhibit very characteristic motions in response to momentary control surface deflections. In response to an elevator deflection

---

* For a detailed derivation of the equations of motion, their linearization, and the normalization of the partial derivatives to obtain the conventional stability derivatives, the reader is referred to Appendix A.

the aircraft will exhibit a well-damped oscillation in the neighborhood of 6 radians/sec., the so-called short period mode; at the same time it will also exhibit a very long period (Phugoid) oscillation which may even be slightly divergent. The motions about the other two axes are always coupled. There is an oscillation, called the dutch roll, which usually is not well damped and has a frequency near 6 radians/sec. There is an aperiodic motion, which is usually slightly divergent, called the spiral mode, and a second aperiodic motion, called the rolling mode or roll subsidence, which is heavily damped.

During the past twenty years, it has become common practice to study flight motions by transforming the linear differential equations into algebraic equations through the use of the Laplace transform. One can then solve for the response to a specific control surface deflection readily by matrix techniques. The resulting ratio of aircraft response to control surface deflection is called a transfer function, eg., the function which describes the manner in which the aircraft converts a control surface deflection into a motion. If one then obtains the inverse Laplace transform of these transfer functions, he then has the time history of the aircraft's linear or angular velocity components resulting from a specified control surface deflection. The three dependent variables excited by an elevator motion are usually taken to be u, θ, and α, although w or a_z may sometimes be used instead of α.

Finding the inverse transform is not always straightforward and is really unnecessary if one desires only to determine the frequency and damping of oscillations or the subsidence of aperiodic motions. The transfer function consists of polynomials in the numerator and denominator. By factoring these polynomials and writing them as a product of factors, one can find the values of the Laplace variable, s, for which the numerator or denominator is zero. The value of s for which the numerator vanishes is called a zero, and the value for which the denominator vanishes, a pole. A first order pole represents an aperiodic motion in the time domain. The numerical value describes the rate at which the motion subsides (or diverges). A pair of complex poles represent a periodic motion. The real part expresses the damping and the imaginary part, the natural frequency. Understanding of the significance of this procedure is enhanced, perhaps, if one plots the poles on a plane (the s-plane) with the abscissa the axis of reals and the ordinate the axis of the imaginaries. If a pole lies on the right half plane, the motion is unstable. A pair of complex poles, or roots, on the imaginary axis represent an undamped sinusoid. The distance from the real axis represents the frequency of the sinusoid. The distance from the imaginary axis represents the degree of damping or divergence.

The location of the roots (poles) on the s-plane will, of course, change as the values of the stability derivatives change. By calculating the locus of roots for representative values of stability derivatives from negative infinity to positive infinity it is possible to determine the conditions under which instabilities will exist. This form of analysis, as well as the transfer function approach, also facilitates study of the effect of adding an automatic control system to the aircraft. If one plots the poles and the zeros of the aircraft-control system combination on the s-plane, he can employ

the well-developed methodology of the now classical locus-of-roots analysis to sketch rather accurately the path which the roots must follow as the gain of the feedback element in the combined system is changed from zero to infinity. The concept of the locus of roots of the "open loop" transfer function* is used in later sections of this work to illustrate the allowable range of values for single aircraft stability parameters with all other parameters held constant. Details of the construction of the transfer functions for the airframe and the numerical procedure for evaluating the constants in the transfer functions and extracting the roots may be found in the Appendices.

As noted earlier, the study of the stability of accelerated motions (dynamic stability) has often been treated as separate and apart from a study of the tendencies of the aircraft at equilibrium to return to equilibrium if disturbed (static stability). It will be recognized, however, that the steady state, or infinite time portion of the solutions of the general equations of motion are representative of the "static" stability and handling. One may cite as examples the longitudinal derivatives $d\delta_e/da_z$, dF_s/da_z, dF_s/du, and $d\delta_e/dC_L$ which are often used to describe the handling and stability characteristics. The first is simply the inverse of the zero frequency value of the transfer function $\frac{a_z}{\delta_e}$. Transfer functions written in terms of the Laplace variable s can be transformed into the frequency domain by setting $s = j\omega$. The notation $\frac{a_z}{\delta_e}$ is used to designate the amplitude ratio of the two frequency dependent quantities which form the transfer function. It is also a convenient shorthand way to represent a specific transfer function, particularly its zero frequency value or gain. The last derivative $d\delta_e/dC_L$, which is a measure of the stick-fixed neutral point location** can be obtained from $\frac{\alpha}{\delta_e}$ by multiplying by C_{L_α}. The other two derivatives require that the transfer function $\frac{\delta_e}{F_s}$ be obtained and multiplied by $\frac{a_z}{\delta_e}$ or $\frac{U}{\delta_e}$. An alternate form of dF_s/du, $\frac{dF_s/q}{dC_L}$, which can be found from $\frac{\delta_e}{F_s/q}$, $\frac{\alpha}{\delta_e}$, and C_{L_α}, is frequently used to locate the stick-free neutral point. Thus, while there are occasions when it is sufficient simply to equate the forces or moments acting on the aircraft and set the derivative with respect to an aerodynamic angle equal to zero to determine the static stability tendencies, the fact that the same information is available as a part of the solution for the dynamic stability should encourage one to examine the vehicle motions and tendencies completely.

---

* Closed loop (aircraft plus automatic control system) transfer function with the gain of the feedback element equal to zero.

** The neutral point is that longitudinal location of the center of gravity for which the aircraft has no tendency either to return to its initial condition or to continue to move away from it, if disturbed. The proximity of the c.g. to the neutral point is the conventional measure of the aircraft's static longitudinal stability.

CONTROL FORCES AND DEFLECTIONS— GENERAL CONSIDERATIONS

A pilot's evaluation of the handling qualities of his aircraft has its origin, of course, in his anthropological capacity. He is able to move the control wheel fore and aft through but a limited distance before the reach becomes uncomfortable; he is able to exert only a given maximum force with comfort; a control force below a certain value is disturbing because the pilot can apply it without consciously willing it and he has difficulty modulating it; if the time between control force application and the response of the aircraft is longer than a particular value, the pilot will tend to become confused and may apply erroneous control inputs; if the aircraft responds too rapidly, he cannot control potentially dangerous motions.

In addition to these constraints, the designer must provide a comfortable relationship between wheel fore-and-aft travel and speed changes and between wheel force and aircraft normal acceleration. If these gradients are too small, the aircraft is said to be too sensitive; if they are too large, the aircraft is said to be too unresponsive. The designer must also take care to provide proper control centering for trimmed flight. It is undesirable to permit the stick to move through an appreciable distance without requiring the application of force, nor should the force required to set the stick into motion be larger than the smallest force gradient for speed change or acceleration.

Somewhat similar constraints govern the application of the lateral controls.

To accomplish these objectives, the light aircraft designer will usually manipulate (for control of the longitudinal flight mode) the elevator deflection to wheel deflection ratio, provide aerodynamic balance on the elevator or a flying tab, provide centering springs, control the linkage elasticity and friction, and limit the aircraft's center of gravity travel; he will also select a suitable elevator area, horizontal tail aspect ratio, airfoil section, and horizontal tail area and he will locate the horizontal tail area suitably far aft. The designer will recognize that pitch responsiveness is related to the aircraft's moment of inertia about its y-axis as well as the moment the elevator can produce and that there is a structural limitation as well as a human tolerance to normal acceleration which the pilot should not be able to exceed inadvertently. The designer will also endeavor to provide a reasonably linear relation between control force or deflection and the desired result, such as speed change or normal acceleration.

From the foregoing, it is evident that, to carry out this task in a direct fashion, considerable knowledge of desirable anthropological limits must be available as well as a substantial knowledge of diverse aerodynamic and mechanical characteristics. The state of understanding of this problem is discussed in the literature review which follows.

LITERATURE REVIEW

SCOPE

During a review (Refs. 1, 2, 3) of all NACA/NASA literature published between 1940 and 1968, those reports dealing with aircraft stability and control analyses and tests were set aside as a group. The documents in this group were then screened and the content of those regarded as most applicable to light aircraft design was noted in the report. For the present study, the entire group was reexamined and rereviewed. In addition, the review of NACA documents was extended backward to 1930, and a computer search of Scientific and Technical Aerospace Reports, International Aerospace Abstracts, and Department of Defense archives was made for current (1962 to late 1969) stability and control information from world-wide sources. Included in this were the USAF Flying Quality Specification and Stability and Control Datcom.

As one would suspect, much of the earlier (pre-1944) information has been superceded; more refined analyses and more accurate and reliable test data are now available. Most of the information is also uncorrelated: flight test results are not compared with results from wind tunnel tests; wind tunnel test results are not compared with theoretical analyses. To attempt such a correlation and evaluation here is not possible with the information available to the authors. The reason for this is that the wind tunnel or flight test reports available in the open literature usually do not give sufficient information on the airplane's geometric or inertial parameters to permit satisfactory correlations to be made. The course adopted, therefore, was to list all the stability derivatives likely to be significant in the design of future light aircraft, detail the method of calculation regarded as most reasonable for such aircraft, report the values of these derivatives in such aircraft, and note pertinent references for each derivative. This approach is an expansion (in that it details methods of calculation and typical results) and specialization (to light aircraft) of the approach adopted by Ellison and Hoak (Ref. 5).

Values for these derivatives are required, of course, to calculate the riding qualities of a light aircraft. The handling characteristics* will, for the purposes of the present study, be defined as

(1) The longitudinal control force and control surface position variations with speed and load factor--their maximum and minimum values, phase relationships, and control travel required to achieve them

---

* the reader will recognize that the definition of handling is somewhat broadened here to include items previously identified with aircraft controllability. This has been done because many specification requirements state responsiveness to control application only in terms of angular displacement reached in a given time. In such instances it is helpful to correlate the initial responses to control application--here considered as the handling characteristics--with the final capabilities of the aircraft.

(2) The angular displacement and angular rate variations produced by application of rudder and aileron forces--their maximum and minimum values, phase relationships, degree of linearity, and control travel required

(3) Controllability of the aircraft under special circumstances.

The review which follows cites some of the literature available on the forces, displacements, and application rates found comfortable by most humans. This apparently has been considered in developing the force and rate limits set in Mil F-8785B. For this reason, the discussion below follows the specification fairly closely, yet pointing out those areas not treated and describing methods available in the literature for insuring that the aircraft complies with the specification.

For the present compilation, only that literature containing data applicable to aircraft designed to operate within the following limits was considered:

Maximum gross weight	10,000#
Maximum wing loading	$40\#/ft^2$
Maximum indicated airspeed	300 mph
Maximum Mach number	0.4
Aspect ratio	≥ 5.0
Little or no wing sweep	
Rigid structure	

Those portions of the specifications and other documents referring to aircraft controllability as defined above and to handling in turbulent air or with external stores are not discussed. Also, in examining the literature upon which the following was based, many documents not cited but dealing with the subject were examined. Some were regarded as perhaps less complete than the reports cited, as confirming results found in cited documents, presenting data in a form not so well suited to comparison with theory, or presenting less accurate results than are now available. The reader interested in perusing the more interesting of these documents is referred to Appendix I for a bibliographical listing.

SYMBOLS

Ae	effective aspect ratio
AR	aspect ratio
A_π	a commonly used area for a component which is the reference area for C_{D_π}
a.c.	aerodynamic center of wing
a_o	lift-curve slope at zero lift
a_v	lift-curve slope of vertical tail
BHP	engine brake horsepower
b	wing span
b_a	aileron span
b_v	vertical tail span
C	wing force parallel to the airplane reference line
C_C	coefficient of wing force parallel to the airplane reference line $\frac{C}{\frac{1}{2}\rho U^2 S}$
C_D	drag coefficient $\frac{D}{\frac{1}{2}\rho U^2 S}$
C_{D_f}	zero lift drag, found in C_D section
C_{D_q}	$\frac{\partial C_D}{\partial(\frac{qc}{2U})}$
C_{D_o}	three-dimensional drag coefficient found in lateral stability derivatives section
C_{d_o}	two-dimensional parasite drag coefficient
C_{D_u}	$\frac{U}{2}\frac{\partial C_D}{\partial u}$
C_{D_α}	$\frac{\partial C_D}{\partial \alpha}$

$C_{D_{\dot{\alpha}}}$ $\dfrac{\partial C_D}{\partial(\frac{\dot{\alpha}c}{2U})}$

$C_{D_{\delta_E}}$ $\dfrac{\partial C_D}{\partial \delta_E}$

C_{D_π} component drag coefficient based on the area A_π

C_{h_o} elevator hinge-moment coefficient when $\alpha_t = 0^o$ and $\delta_e = 0^o$

C_{h_δ} variation of control-surface hinge-moment coefficient with deflection $\dfrac{\partial C_h}{\partial \delta}$

C_L lift coefficient $(L/\frac{1}{2}\rho U^2 S)$

C_{L_u} $\dfrac{U}{2}\dfrac{\partial C_L}{\partial u}$

C_{L_α} $\dfrac{\partial C_L}{\partial \alpha}$

$(\dfrac{dC_L}{d\alpha})_\infty$ wing lift curve slope with infinite aspect ratio

$C_{L_{\dot{\alpha}}}$ $\dfrac{\partial C_L}{\partial(\frac{\dot{\alpha}c}{2U})}$

$C_{L_{\delta_E}}$ $\dfrac{\partial C_L}{\partial \delta_E}$

C_ℓ section lift coefficient or rolling moment coefficient $(L/\frac{1}{2}\rho U^2 Sb)$

$C_{\ell_{max}}$ maximum section lift coefficient

C_{ℓ_p} $\dfrac{\partial C_\ell}{\partial(\frac{pb}{2U})}$

C_{ℓ_r} $\dfrac{\partial C_\ell}{\partial(\frac{rb}{2U})}$

$C_{\ell_{\alpha_t}}$ section lift-curve slope of the horizontal tail

C_{ℓ_β} $\frac{\partial C_\ell}{\partial \beta}$

C_{ℓ_δ} change in rolling moment coefficient due to change in aileron deflection (found in control forces section)

$C_{\ell_{\delta_A}}$ $\frac{\partial C_\ell}{\partial \delta_A}$

$C_{\ell_{\delta_E}}$ section lift-curve slope due to elevator deflection (this is not to be confused with rolling moment coefficient)

$C_{\ell_{\delta_R}}$ $\frac{\partial C_\ell}{\partial \delta_R}$

C_m pitching-moment coefficient ($M/\frac{1}{2}\rho U^2 Sc$)

C_{m_T} pitching-moment coefficient due to thrust force

$C_{m_{a.c.}}$ airfoil section pitching moment about the aerodynamic center

C_{m_q} $\frac{\partial C_m}{\partial(\frac{qc}{2U})}$

C_{m_α} $\frac{\partial C_m}{\partial \alpha}$

$C_{m_{\dot{\alpha}}}$ $\frac{\partial C_m}{\partial(\frac{\dot{\alpha}c}{2U})}$

$C_{m_{\delta_E}}$ $\frac{\partial C_m}{\partial \delta_E}$

C_N coefficient of wing force normal to the airplane reference line

C_n yawing-moment coefficient ($N/\frac{1}{2}\rho U^2 Sb$)

C_{n_p} $\frac{\partial C_n}{\partial(\frac{pb}{2U})}$

C_{n_r} $\frac{\partial C_n}{\partial(\frac{rb}{2U})}$

C_{n_β} $\frac{\partial C_n}{\partial \beta}$

$C_{n_{\delta_A}}$ $\frac{\partial C_n}{\partial \delta_A}$

$C_{n_{\delta_R}}$ $\frac{\partial C_n}{\partial \delta_R}$

C_T thrust coefficient $(T/\frac{1}{2}\rho U^2 S)$

C_{T_u} $\frac{U}{2}\frac{\partial C_T}{\partial u}$

C_{y_p} $\frac{\partial C_y}{\partial (\frac{pb}{2U})}$

C_{y_r} $\frac{\partial C_y}{\partial (\frac{rb}{2U})}$

C_{y_β} $\frac{\partial C_y}{\partial \beta}$

$C_{y_{\delta_A}}$ $\frac{\partial C_y}{\partial \delta_A}$

$C_{y_{\delta_R}}$ $\frac{\partial C_y}{\partial \delta_R}$

c mean aerodynamic chord

c_a aileron chord

c_e elevator chord

c_f flap chord

c.g. airplane center of gravity

D drag force

e base of natural system of logarithms or Oswald's span efficiency factor

e_1 induced-angle span efficiency factor

F_A stick-force due to aileron actuation

F_s stick force

f the equivalent parasite area discussed in the C_D section

G ratio of elevator displacement to the product of stick length and stick angular displacement

g acceleration due to gravity (32.2 ft/sec^2)

HP horsepower

h_t height of the horizontal tail a.c. above the c.g. (positive for a.c. above c.g.)

I_{xx} moment of inertia about the x-axis

I_{yy} moment of inertia about the y-axis

I_{zz} moment of inertia about the z-axis

I_{xz} product of inertia

i incidence angle

k_x radius of gyration about the x-axis

k_y radius of gyration about the y-axis

k_z radius of gyration about the z-axis

L lift or rolling moment

ℓ_b length of fuselage or body

ℓ_t length from c.g. to tail quarter chord

ℓ_t' length from wing quarter chord to tail quarter chord

$\frac{\ell_t S_t}{cS_w}$ tail volume factor

ℓ_v length from c.g. to vertical tail aerodynamic center

M pitching-moment about the c.g.

$M_{\substack{fus \\ nac}}$	pitching-moment about the c.g. due to the fuselage and nacelles
$M_{y_{aero}}$	aerodynamic moments about the y-axis (pitching moment)
m	mass in slugs
N	wing force normal to the airplane reference line or yawing moment
n	normal acceleration in g's
p	rolling velocity
$\dot{p}$	rate of change of rolling velocity
$(\frac{pb}{2U})$	helix roll angle
q	dynamic pressure ($\frac{1}{2}\rho U^2$) or pitching velocity
$\dot{q}$	rate of change of pitching velocity
q_t	dynamic pressure at the horizontal tail
q_v	dynamic pressure at the vertical tail
RPM	propeller revolutions per minute
R_N	Reynolds Number
r	yawing velocity
$\dot{r}$	rate of change of yawing velocity
S	wing area
SRP	seat reference point
S_R	rudder area
S_e	elevator area
S_f	flap area
S_s	body side area
S_h	horizontal tail area

s	distance in half chords which is used as a non-dimensionalizing factor $(\frac{2Ut}{c})$
T	thrust
TDPF	tail damping power factor, see figure 72
TDR	tail damping ratio, see figure 72
T_u	$\frac{1}{m}\frac{\partial T}{\partial u}$ (see Appendix A)
t	time or airfoil thickness
t	time
Δt	lag time of the downwash at the tail plane
U	airplane velocity
U_S	stall speed
U_{Trim}	trim speed
W	airplane weight
w_f	maximum width of the fuselage or nacelles
x'	distance from c.g. to wing quarter chord (positive for c.g. ahead of quarter chord)
$\bar{x}$	longitudinal distance rearward from c.g. to wing aerodynamic center
x_a	distance parallel to relative wind from the wing a.c. to the c.g. (positive for a.c. ahead of the c.g.)
y_i	distance from body centerline to inboard edge of aileron
z_T	perpendicular distance from thrust line to c.g. (positive for thrust line below the c.g.)
z_a	vertical distance from wing a.c. to c.g. (positive for a.c. above c.g.)
z_v	distance from the center of pressure of the vertical tail to the aircraft centerline (positive for vertical tail above the x-axis)
z_w	distance from body centerline to quarter-chord point of exposed wing root chord (positive for the quarter-chord point below the body centerline)
Γ	dihedral angle
Λ	wing sweep angle

Ω resultant angular velocity

α angle of attack

$\dot{\alpha}$ rate of change of angle of attack

α_i induced angle of attack

α_o angle of attack for zero lift

α_s stall angle of attack

$\frac{d\alpha_t}{d\delta_E}$ elevator efficiency factor $\left|(dC_L/d\delta_E)/(dC_L/d\alpha_t)\right|$

β sideslip angle

γ flight path angle from the horizontal

δ correction factor for induced drag

δ_A aileron deflection

δ_E elevator deflection

δ_R rudder deflection

δ_a aileron deflection

δ_e elevator deflection

δ_{e_o} elevator angle at zero aircraft lift

δ_f flap deflection

δ_t trim tab deflection

ε downwash angle

$\frac{d\varepsilon}{d\alpha}$ change in downwash angle due to change in angle of attack.

ζ_d Dutch Roll damping ratio

$\zeta_{s.p.}$ short period damping ratio

η efficiency factor for tail, q_t/q, or the propeller efficiency

θ pitch angle

$\dot{\theta}$ rate of change of pitch angle

λ taper ratio (tip chord/root chord)

μ airplane relative density factor ($m/\rho Sb$)

π 3.1416

ρ density

σ sidewash angle

τ correction factor for induced angle or elevator effectiveness factor $(\frac{d\alpha_t}{d\delta_E})$

τ_R time constant for roll mode

ϕ roll angle

$\ddot{\phi}$ second derivative with respect to time of the roll angle

$\frac{\phi_{osc}}{\phi_{av}}$ a measure of the ratio of the oscillatory component of bank angle to the average component of bank angle following a rudder-pedal-free impulse aileron control command

ψ yaw angle

ψ_β phase angle of Dutch Roll component of sideslip

ω_{n_d} Dutch Roll natural frequency

$\omega_{n_{sp}}$ short period natural frequency

Subscript:

a.c. aerodynamic center

c.g. center of gravity

c/4 wing quarter-chord

h horizontal tail

t tail

v vertical tail

w wing

THE STABILITY DERIVATIVES

It is customary, as noted earlier, to represent the aerodynamic and thrust forces on an aircraft by a Taylor expansion about the conditions for steady, level flight. Because of the assumption that perturbations from equilibrium are small, only the linear terms are retained; squares, product terms, and higher order derivatives are neglected. The remaining derivatives, called stability derivatives, being more numerous than the equations of motion, can therefore be evaluated only through special tests or through analyses which limit responses to those resulting from a single variable. The discussion below isolates each of these derivatives, the method from the literature regarded as most suitable for its evaluation, and typical values for light aircraft.

C_L

Usually, by the time an airplane is subjected to a stability analysis, the design has progressed far enough that the lift coefficients for the flight conditions of interest are known for the complete airplane. Since 2-D (section) data are available for many airfoil and airfoil flap configurations, it is desirable to have a means of converting section data to three-dimensional data for a particular airfoil. In Theory of Flight, Richard Von Mises (Ref. 6) gives an estimate of lift coefficient,

$$C_L \simeq \frac{C_\ell}{1 + 2/AR} .$$

An example 2-D plot of C_ℓ versus angle of attack is shown below for the 2412 airfoil section.

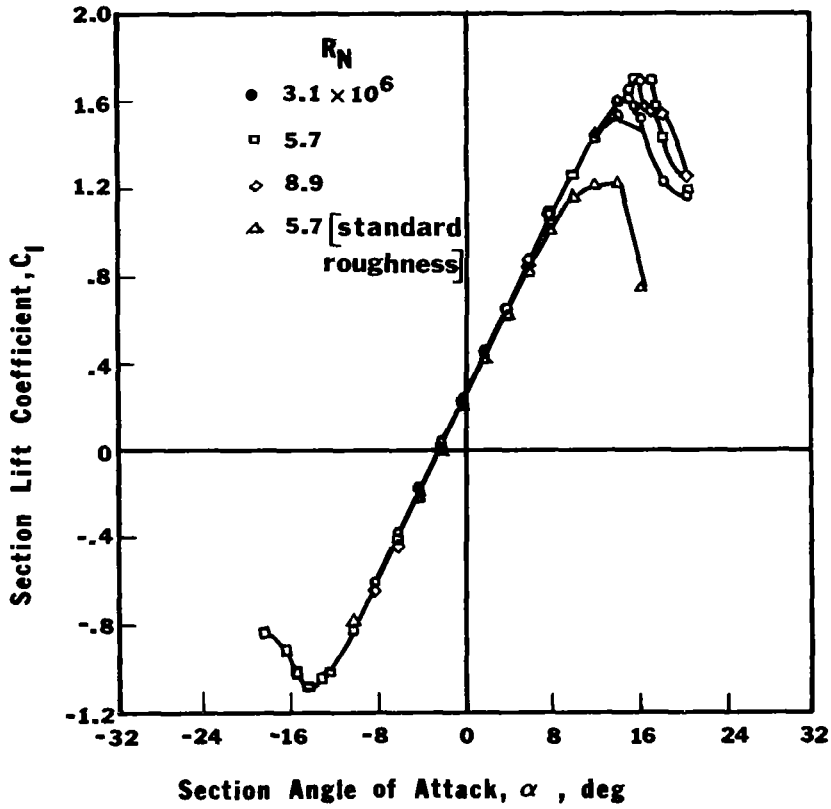

Figure 1. 2-D plot of section lift coefficient versus angle of attack for 2412 airfoil section.

The approximation does not include such factors as taper effects and tip effects.

It should be noted that 2-D section data are available for a large number of airfoils in Theory of Wing Sections (Ref. 7); and the same data are included in TR-824 (Ref. 8).

A refined analysis to determine lift coefficient should include the lift contribution of the tail and, if possible, the lift contribution of the fuselage. The interference effects between the wing and the fuselage may be significant and, for this reason, wind tunnel tests or actual flight tests contribute to determining lift coefficient. The tail coefficient,

$$C_{L_t} = \frac{(\text{Lift})_{\text{tail}}}{(1/2\ \rho U^2)_t\ S_t}$$

can be included in that for the entire aircraft where $\eta_t = q_t/q$:

$$(C_L)_{\text{Airplane}} = C_{L_w} + C_{L_t} \frac{S_t}{S_w} \eta_t + C_{L_{\substack{\text{fuselage} \\ \text{nacelles}}}}.$$

The tail contribution to the total airplane C_L at cruise can be approximated by using the moment equation:

$$C_m = 0.0 = C_{L_w} \frac{x_a}{c} - C_{L_t} \left(\frac{S_t}{S_w} \eta_t\right) \frac{\ell_t}{c}$$

or

$$C_{L_t} = C_{L_w} \frac{x_a}{\ell_t} \frac{S_w}{S_t} \eta_t\ .*$$

The fuselage lift coefficient may be quite difficult to estimate, unless some simplification, such as slender body theory, is applied. NACA TR-540 (Ref. 9) discussed the interference effects between the wing and the fuselage and gives some example lift coefficients for the fuselage at various angles of attack. The table below gives an example of some of these experimental data.

		$\alpha=0^\circ$		$\alpha=4^\circ$		$\alpha=8^\circ$		$\alpha=12^\circ$	
Fuselage	Engine	C_L	C_D	C_L	C_D	C_L	C_D	C_L	C_D
Round	None	.000	.0041	.001	.0042	.005	.0049	.011	.0062
Round	Uncowled	.000	.0189	.001	.0191	.004	.0200	.008	.0216
Round	Cowled	.000	.0069	.008	.0073	.017	.0088	.028	.0115
Rectangular	None	.000	.0049	.005	.0054	.014	.0068	.026	.0097

Table 1. Example lift coefficients for the fuselage at various angles of attack.

* A method for calculating the elevator deflection required for equilibrium cruise is given in the sample calculations in Appendix G.

The fuselage coefficients in the table are based on wing area of the wing fuselage arrangement tested. Thus, by examining the table with a knowledge of the airplane angle of attack, one can estimate the fuselage contribution to the total airplane lift coefficient. For small angles of attack, 0^{o} to 8^{o}, the fuselage lift can probably be neglected without a significant change in the total airplane lift coefficient, unless the fuselage is highly cambered.

Datcom (Ref. 10) gives a method for calculating C_{L_α} of a body based on potential flow theory (see C_{L_α}). Thus, C_L can be approximated by multiplying C_{L_α} by α of the body, which is known.

For light airplanes in the cruising mode of flight, the lift coefficient will probably fall between 0.25 and 0.45. In climbing flight, C_L will probably be larger--0.5 to 0.9. For the landing approach, the usual C_L will probably range from .95 to 1.18. For the Cessna 182, typical values are 0.309 at cruise, 0.719 in climbing flight, and 1.12 in the landing approach.

C_D

The drag coefficient, C_D, is an aerodynamic force coefficient which can be thought of as a damping coefficient. The equilibrium airplane drag effectively damps the thrust by acting in the opposite direction of the relative wind and is always positive in sign. When considering performance of an aircraft, the smallest possible value of C_D is desired; however, in airframe dynamics, C_D is the main contributor to the damping of the phugoid mode. Thus, the larger the value of C_D, the better the damping. Since phugoid damping is not considered of major importance in the flying qualities of the airplane, the performance rather than the flying qualities of the aircraft should dictate the design value of C_D.

A preliminary stage of drag estimation of an airplane in an incompressible flow may be accomplished by adding the individual drags of several components of the airplane. This method is called "drag breakdown." The majority of airplane drag curves can be expressed as

$$C_D = C_{D_f} + \frac{C_L^2}{\pi e AR} \; *$$

where

C_{D_f} = zero lift or parasite drag.

Mathematically, C_{D_f} is the intercept on the C_D axis of a graph of C_D versus C_L^2, and $1/\pi eAR$ is the slope. Only at very low or high values of lift coefficients does the parabolic approximation deviate from the actual drag polar.

The following procedure is commonly used to obtain the value of C_{D_f} for a particular airplane. The drag coefficient of each component is based on an area, A_π, "proper" to that component. For example, one usually bases the drag coefficient for the fuselage on the maximum fuselage area. The equivalent parasite drag area, f, is then expressed as

$$f = C_{D_f} S = \Sigma C_{D_\pi} A_\pi$$

The total f for an airplane is approximately the sum of $C_{D_\pi} A_\pi$ for the individual components, plus five or ten per cent for mutual interference between the components. Another percentage error (3% to 5%) may also be added for small protuberances such as handles, hinges, antennas, and cover plates. Fifteen per cent of the total $C_{D_\pi} A_\pi$ was used to account for protuberances and interferences on the Cessna 182 discussed later in the present study. Once the total f is found, C_{D_f} for the airplane can be determined from

$$C_{D_f} = \frac{f}{S}$$

where

S = wing area.

Total C_D is then

$$C_{D_f} + \frac{C_L^2}{\pi e AR}$$

---

* e can be estimated in the C_{L_α} section.

Values of C_{D_π} and the areas on which they are based are given in the tables below. This information was selected from References 11, 12, 13, and 14.

The wing drag C_{D_π} for airfoils with standard roughness can be obtained from a table given in Reference (15) and shown below. The comparison is based on standard roughness at $R_N = 6 \times 10^6$; the wing C_{D_π} is based on wing area and is tabulated as C_{d_o}. Wing flap deflection may generate an additional C_{D_π} which should be accounted for.

Airfoil Section	$(\frac{t}{c})$	C_{d_o}	C_ℓ	$C_{\ell_{max}}$	α_s	$C_{m_{ac}}$
63_2-415	.15	.0098	.20	1.33	12.	-.070
23016.5	.165	.0102	.15	1.20	12.	-.005
23012.0	.12	.0099	.18	1.22	12.	-.015
2412	.12	.0098	.20	1.22	14.	-.048
23018	.18	.0105	.10	1.05	11.	-.005
2410	.10	.0095	.20	1.22	14.	-.050
63_2-215	.15	.0097	.16	1.26	14.	-.030
64_1-412	.12	.0097	.31	1.34	12.	-.070
64_2-A215	.15	.0102	.20	1.20	14.	-.035
65_2-415	.15	.0100	.22	1.25	14.	-.065
64_1-212	.12	.0088	.18	1.18	11.	-.025

Table 2. Airfoil sections.

The fuselage C_{D_π} can be obtained from the table below by choosing the fuselage most nearly like the one investigated. Twenty per cent of C_{D_π} can be added to account for the canopy and windshield. For the Cessna 182, the fourth fuselage was chosen.

	Ref. Area	C_{D_π}
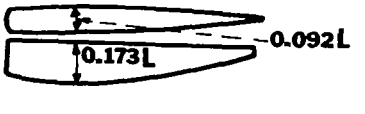	S_c	0.266
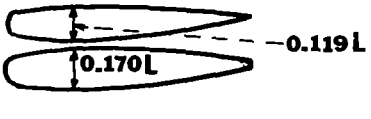	S_c	0.062
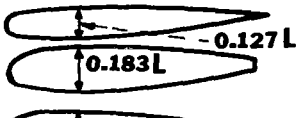	S_c	0.071
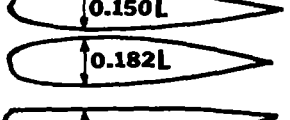	S_c	0.063
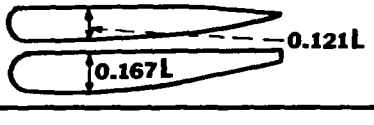	S_c	0.116

Table 3. Fuselage drag where S_c = maximum cross sectional area and L = Fuselage length.

The empennage C_{D_π} values for undeflected control surfaces can be found from Table 4 based on the tail planform area where i_s is the horizontal tail surface incidence.

Tail Arrangement	Description	Area	C_{D_π}
	Tapered fillets, vertical and horizontal tapered surfaces $i_s = 0^o$ $i_s = -4^o$	S_t	 .0043 .0063
	Tapered fillets, tail surfaces with end plates $i_s = 0^o$ $i_s = -4^o$	S_t	 .0058 .0063
	Symmetrical tapered fillets $i_s = 0^o$	S_t	 .0059
	Vertical and horizontal tail surfaces $i_s = 0^o$ $i_s = -4^o$	S_t	 .0070 .0058
	Tail surfaces with end plates $i_s = 0^o$	S_t	 .0058
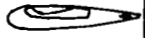	Tapered fillets, horizontal tail surfaces $i_s = 0^o$ $i_s = -4^o$ $i_s = 4^o$	S_t	 .0039 .0083 .0061

Table 4. Empennage drag.

The information required for landing gear drag prediction is given in Table 5. For the nose gear, C_{D_π} is given; however, for the other landing gear, the value of f is given. The tabulated value of f is the value for both wheels of the landing gear assembly.

Configuration	Remarks	$f = C_{D_\pi} A_\pi$
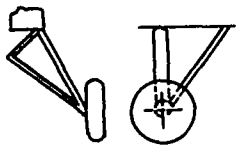	8.50-10 wheels, not faired	1.67
	8.50-10 wheels, faired	1.50
	8.50-10 wheels, no streamline members . .	3.83
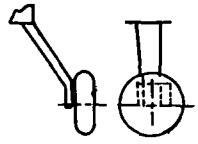	8.50-10 wheels, faired	0.74
	27-in. streamlined wheels, not faired	0.98
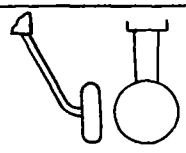	27-in. streamlined wheels, not faired . .	0.84
	8.50-10 wheels, faired	0.68
	21-in. streamlined wheels, not faired . .	0.53
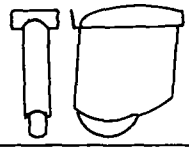	8.50-10 wheels	0.51
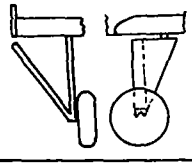	8.50-10 wheels, not faired	1.52
	8.50-10 wheels, faired	1.02
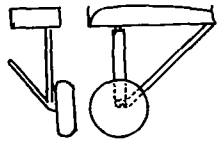	8.50-10 wheels, not faired	1.60
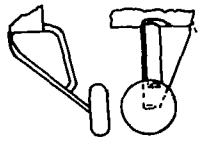	24-in. streamlined wheels, & intersections filleted	0.86
	8.50-10 wheels, no fillets	1.13
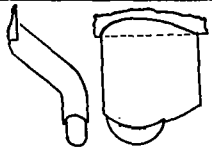	8.50-10 wheels	1.05
	Low pressure wheels, intersections filleted	0.31
	Low pressure wheels, no wheel fairing . .	0.47
	Streamlined wheels, round strut, half fork no fairing	1.25
Nose Gear	For the nose gear C_{D_π} = .5→.8 based on A_π = (wheel diameter)(wheel width)	

Table 5. Landing gear drag.

The C_{D_π} values for other components of interest can be estimated by using the table below:

COMPONENTS	AREA FOR DRAG CALCULATION	C_{D_π}
Nacelles		
1. above wing, small airplane	Cross section area	.250
2. large leading edge nacelle, small airplane	Cross section area	.120
3. small leading edge nacelle, large airplane	Cross section area	.080
4. improved nacelle, no cooling flow	Cross section area	.050
5. improved nacelle, typical cooling air flow	Cross section area	.100
Wing Tanks		
1. centered on tip	Cross section area	.05-.07
2. below wing tip	Cross section area	.07-.10
3. inboard below wing	Cross section area	.15-.30
Wires and Struts		
1. smooth round wires and struts (per foot)	Frontal area	1.2-1.3
2. standard aircraft cable (per foot)	Frontal area	1.4-1.7
3. smooth elliptical wire (per foot)	Frontal area	
fineness ratio 2:1		0.6-0.4
fineness ratio 4:1		.35
fineness ratio 8:1		.3-.2
4. standard streamlined wire (per foot)	Frontal area	.45-.20
5. square wire (per foot)	Frontal area	.16-.20
6. streamlined struts (per foot)	Frontal area	.075-0.10

Table 6. Airplane components.

For smooth round wire of diameter less than $\frac{1}{4}$ inch, assume two end fittings equivalent to three feet of wire.

For smooth round struts of diameter greater than 5/16 inch, assume two end fittings equivalent to one foot of strut.

For smooth elliptical wire, assume two end fittings equivalent to 10 to 15 feet of wire.

For square wire, assume two end fittings equivalent to two feet of wire.

For streamlined struts, assume two end fittings equivalent to five feet of strut if faired, ten feet if unfaired.

The total drag coefficient for the airplane is thus

$$C_D = \frac{\Sigma C_{D_\pi} A_\pi}{S} + \frac{C_L^2}{\pi e AR} .*$$

The drag breakdown method was used to estimate a drag coefficient of 0.0311 for the Cessna 182. Drag coefficients for other light airplanes can be found using the table below taken from Reference (14).

YEAR	AIRPLANE	TYPE	b (ft)	S (ft^2)	W (lbs)	"POWER" (hp)	U (kts)	C_D
1903	Wright-Brothers	biplane	40	510	750	12	26	0.074
1945	Piper "Cub"	personal	35	179	1500	135	110	0.032
1950	Cessna "170"	personal	36	175	2200	140	122	0.032
1942	Messerschmitt-109	fighter	32	172	6700	1200	330	0.036
1943	N. A. P-51 "Mustang"	fighter	37	235	10000	1380	380	0.020

Table 7. Drag coefficients for selected light airplanes

It should be noted that Reference (15) gives another method of estimating drag coefficient which sums friction drag and the profile drag for each of the components.

---

* $e = 1/(1 + \delta)$ and a graph for estimating $(1 + \delta)$ can be found in the discussion of the C_{L_α} section.

C_m

The aerodynamic pitching moment about the c.g. is defined as C_m. In equilibrium flight, the aerodynamic pitching moment must balance the moment coefficient resulting from thrust. Although C_m appears in the list of dimensional stability derivatives in Appendix B of the present study, it is not usually referred to as a stability derivative. The principal effect of C_m is to contribute to the period of the phugoid mode.

Several forces and moments, such as tail, wing, and fuselage lift and drag, and moments about the aerodynamic centers of the wing and tail, contribute to the pitching moment coefficient; however, for equilibrium, power-off flight, the elevator is positioned so that C_m is zero. For powered flight, C_m is the negative of the C_m required to balance the thrust force moment, C_{m_T}. C_{m_T} can be written as

$$C_{m_T} = \frac{T z_T}{qSc}$$

where

z_T = perpendicular distance from thrust line to c.g., positive for thrust line below the c.g.

T = thrust

The particular airplane discussed later was examined with power-off; thus, $C_m = 0$. From the equation above, it is also apparent that C_m is zero when the thrust line passed through the center of gravity ($z_T = 0$).

An equation for C_m is also very helpful in designing or sizing an airplane. The equation can be written simply by summing the aerodynamic moments of the various aircraft components about the c.g. The equation given below is a modification of that contained in TR-927 (Ref. 16). Defining "nose-up" as a positive moment, the moments can be summed using Figure 2. The following equations are based on the assumption that cos α = 1 and sin $\alpha \simeq 0$.

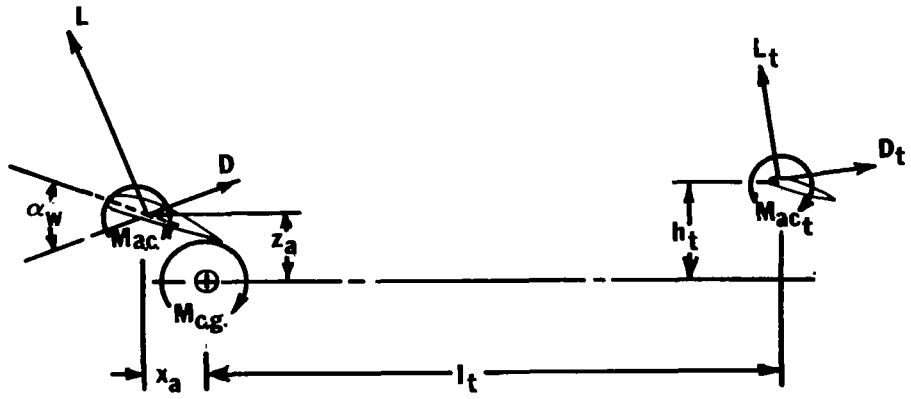

Figure 2. Forces and moments in the plane of symmetry.

$$M_{c.g.} = Lx_a + Dz_a + M_{a.c.} - L_t\ell_t + D_t h_t + M_{a.c._t}$$

where

x_a is positive for a.c. of wing ahead of c.g.
z_a is positive for a.c. of wing above c.g.
h_t is positive for tail a.c. above c.g.
ℓ_t = distance from c.g. to tail quarter chord

Thus, the equation for the moment coefficient can be written as

$$C_{m_{c.g.}} = C_L\frac{x_a}{c} + C_D\frac{z_a}{c} + C_{m_{a.c.}} - C_{L_t}\frac{S_t}{S_w}\frac{\ell_t}{c}\eta_t + C_{D_t}\frac{S_t}{S_w}\frac{h_t}{c}\eta_t + C_{m_{a.c._t}}$$

Since the tail is usually a symmetrical section,

$$C_{L_t} = (C_{L_{\alpha_t}})(\alpha_t)$$

where

$$\alpha_t = (\alpha_w - i_w - \varepsilon + i_t)$$

Thus,

$$C_{m_{c.g.}} = C_L\frac{x_a}{c} + C_D\frac{z_a}{c} + C_{m_{a.c.}} - \alpha_t C_{L_{\alpha_t}}\frac{S_t}{S_w}\frac{\ell_t}{c}\eta_t + C_{D_t}\frac{S_t}{S_w}\frac{h_t}{c}\eta_t + C_{m_{a.c.t}}$$

It should be noted that the above equation does not consider the fuselage or propeller pitching moment. The fuselage pitching moment can be approximated by

$$C_{m_{c.g.\,fuselage}} = (\alpha_{fuselage})(C_{m_\alpha})_{fuselage}\,.$$

$(C_{m_\alpha})_{fuselage}$ is evaluated in the discussion of the C_{m_α} in the present study. The effects of the propeller are discussed in the section dealing with power effects on stability derivatives.

C_T

The thrust coefficient C_T, like C_L is not strictly a stability derivative but is necessary in a dynamic analysis. The coefficient is non-dimensional and is defined as

$$C_T = \frac{\text{Thrust}}{\frac{1}{2} \rho U^2 S} .$$

For the Cessna 182 discussed later, $C_T = 0.0$ since the analysis was made with power-off; however, for power-on cruise $C_T = .04$.

C_{L_u}, C_{D_u} and C_{m_u}

The stability derivatives C_{L_u}, C_{D_u}, and C_{m_u} are the changes in lift, drag, and pitching moment coefficients, respectively, with airspeed. These changes at low speeds are really Reynolds number effects and can usually be considered to be zero. The fact that they are very small for low Mach numbers is pointed out by the figure below taken from Reference (18).

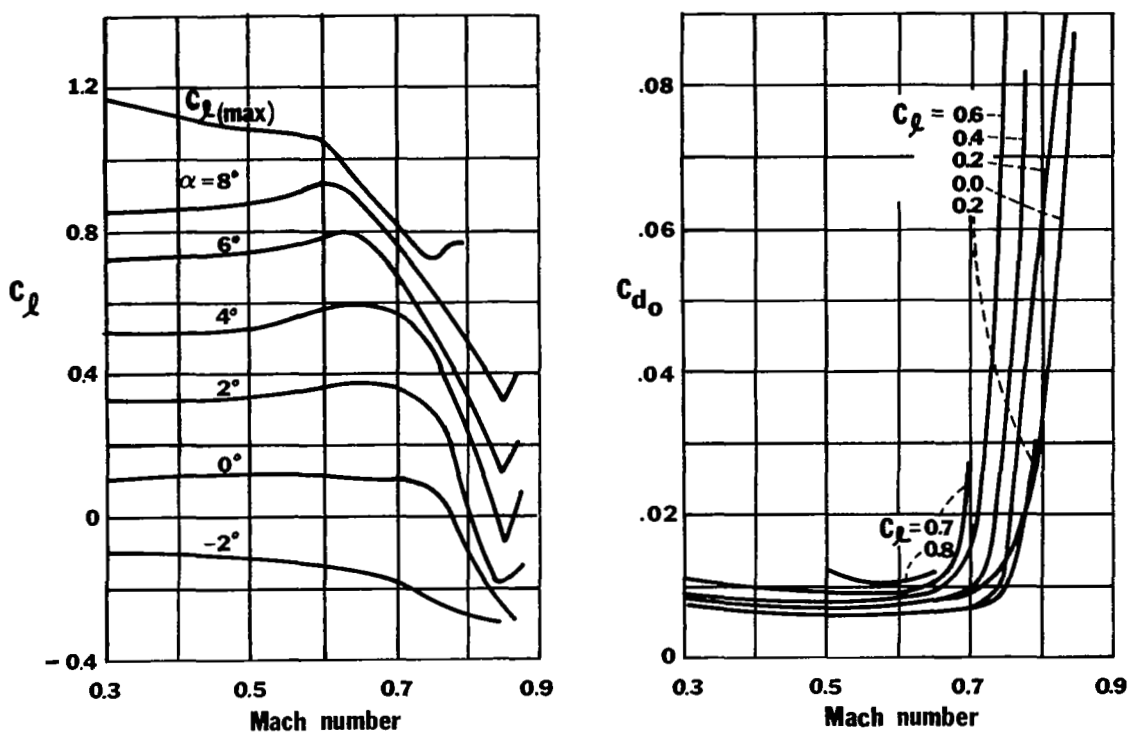

Figure 3. Variation of C_ℓ and C_{d_o} with Mach number.

Since for the cruise condition $C_T \simeq C_D$ and $C_{T_u} \simeq C_{D_u}$ and in the same manner as above C_{T_u} is neglected for cruising flight. It should be noted that for approach and landing maneuvers, C_{T_u} and C_{D_u} may become significant and therefore should not be neglected.

C_{L_u}, C_{D_u}, C_{m_u}, and C_{T_u} were chosen to be zero for the Cessna 182 investigated later in this report.

C_{L_α}

The stability derivative C_{L_α} is the change in lift coefficient with angle of attack and is commonly known as the lift curve slope. This derivative is always positive for angles of attack below the stall. Ordinarily, the wing accounts for 85% to 90% of the total C_{L_α}. This derivative is very important in equilibrium flight and in dynamic conditions. Since an airplane with a higher value of C_{L_α} usually has a lower drag, a high value of C_{L_α} is desirable for optimum performance. Higher values of C_{L_α} are necessarily associated with high aspect ratio, unswept wings. The derivative also makes an important contribution to the damping of the longitudinal short period mode.

That portion of the effective wing angle of attack induced by wing lift can be written from Reference (19):

$$\alpha_i = \frac{C_L}{\pi e_1 AR}$$

where

$e_1 = \frac{1}{1+\tau}$ = induced-angle span efficiency factor
τ = correction factor for induced angle (see Figure 4)
AR = wing aspect ratio

Since the angle of attack for zero lift does not vary with aspect ratio, the geometric angles of attack for the same airfoil wing operating at the same C_L but with two different aspect ratios are related by

$$\alpha_1 = \alpha_2 + \frac{C_L}{\pi}\left(\frac{1}{e_1 AR_1} - \frac{1}{e_1 AR_2}\right)$$

Thus, the expression for the lift curve slope of a wing with one aspect ratio in terms of the lift curve slope at another aspect ratio becomes

$$\left(\frac{dC_L}{d\alpha}\right)_1 = \frac{\left(\frac{dC_L}{d\alpha}\right)_2}{1 + \frac{57.3}{\pi}\left(dC_L/d\alpha\right)_2\left(\frac{1}{e_1 AR_1} - \frac{1}{e_1 AR_2}\right)}$$

where

$dC_L/d\alpha$ = change in lift coefficient per degree

The equation above implies that the lift curve slope is a constant, which is a fairly accurate assumption for angles of attack up to 10 or 12 degrees. However, once the linear range of the 2-D lift curve slope is exceeded, the lift curve slope can only be evaluated for a particular value of α. If condition "2" is that of infinite aspect ratio, the lift curve slope per degree of a finite aspect ratio can be written in terms of the 2-D airfoil lift curve slope, $(dC_L/d\alpha)_\infty$ as

$$\frac{dC_L}{d\alpha} = \frac{\left(\frac{dC_L}{d\alpha}\right)_\infty}{1 + \left(\frac{dC_L}{d\alpha}\right)_\infty \frac{57.3}{\pi e_1 AR}}$$

Typical values for $(C_{L_\alpha})_\infty$ per degree range from about 0.110 for thin airfoils to about 0.115 for thick airfoils at Reynolds Numbers greater than about 10^6. The slope is somewhat less at lower Reynolds Numbers and at the higher (near 1.0) lift coefficients. For exacting use, reference should be made to careful wind tunnel tests of the airfoil being examined.

A rapid approximation to the exact value of e_1 may be achieved by using either or both of the figures below. Figure 4, taken from Reference (19) has both τ and δ plotted for various taper ratios at an aspect ratio of 6.28 (δ is used in the discussion of C_{D_α}). Figure 5 is a plot of $1 + \tau$ and $1 + \delta$ for various aspect ratios at a taper ratio of 1.0 from Reference (20). Thus, if a given design has an aspect ratio $\simeq 6$, Figure 4 may be used; if the design has a taper ratio of 1.0, Figure 5 may be used. For most light airplanes, Figure 4 should give acceptable results.

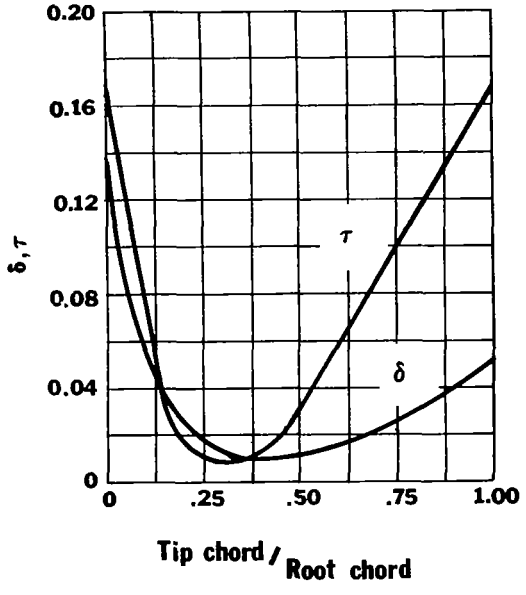

Figure 4. Variation of τ and δ with taper ratios at aspect ratio of 6.28.

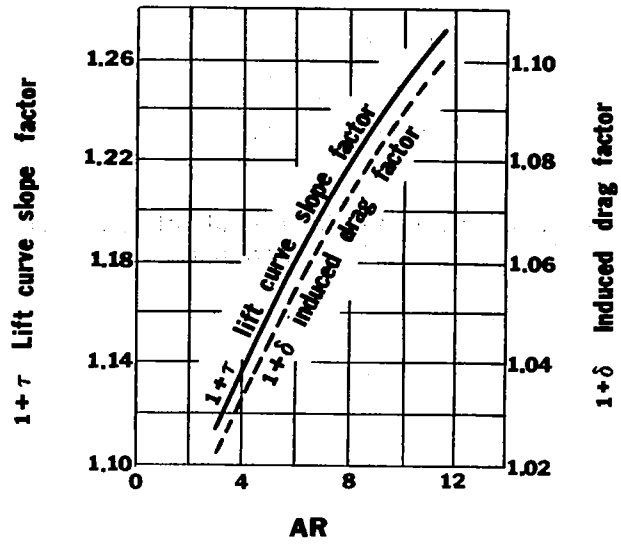

Figure 5. Variation of $1 + \tau$ and $1 + \delta$ with aspect ratios at taper ratio of 1.0.

The lift curve slope of partial or full span flapped wings can often be approximated satisfactorily or directly found by consulting the NACA literature. Many reports have been written concerning various flap configurations on several airfoils or wings. Thus, NASA CR-1485 (Ref. 2) should be very valuable, because it lists NACA reports dealing with specific flap configurations. In the usual case, C_{L_α} is larger for flaps deflected than for flaps retracted. For the cruise condition, an undeflected flap can usually be considered part of the airfoil section, thus requiring no additional calculation. For other flight modes, however, it may be necessary to find C_{L_α} for a given flap deflection. The lift curve slope of the wing is probably known for all flight conditions by the time a dynamic analysis is made, but if not, NASA CR-1485 should be used as a major reference for information on prediction of aerodynamic characteristics of flaps. If the airplane analyzed has partial span flaps instead of full span flaps, the approximate lift curve slope can be obtained from

$$\left(\frac{\overline{dC_L}}{d\alpha}\right) = \frac{S_f}{S}\left(\frac{dC_\ell}{d\alpha}\right)_f + \left(1 - \frac{S_f}{S}\right)\left(\frac{dC_\ell}{d\alpha}\right)$$

where

$\frac{dC_\ell}{d\alpha}$ = local section lift curve slope

S = wing area

f = subscript denoting flap

$\frac{\overline{dC_L}}{d\alpha}$ = mean section value of the lift curve slope between the root and tip section

Although C_{L_α} for the complete airplane, in many cases, is assumed equal to the C_{L_α} of the wing alone, a method of predicting the body and tail C_{L_α} should be available. The method presented here for approximating the body contribution is taken from Reference (10).

$$C_{L_{\alpha_{Body}}} = \frac{2(k_2 - k_1)S_o}{V_b^{2/3}}$$

where

$k_2 - k_1$ = apparent mass factor which is a function of fineness ratio (length/maximum thickness)

V_b = total body volume

S_o = cross sectional area at x_o

x_o = body station where flow ceases to be potential, this is a function of x_1, the body station where the parameter dS_x/dx first reaches its minimum value. (This station where the change in area with respect to x first reaches its lowest value can be estimated from a sketch of the body.)

S_x = body cross sectional area at any body station

ℓ_b = body length.

Figures 6 and 7 represent graphs for estimating both $k_2 - k_1$ and x_o/ℓ_b.

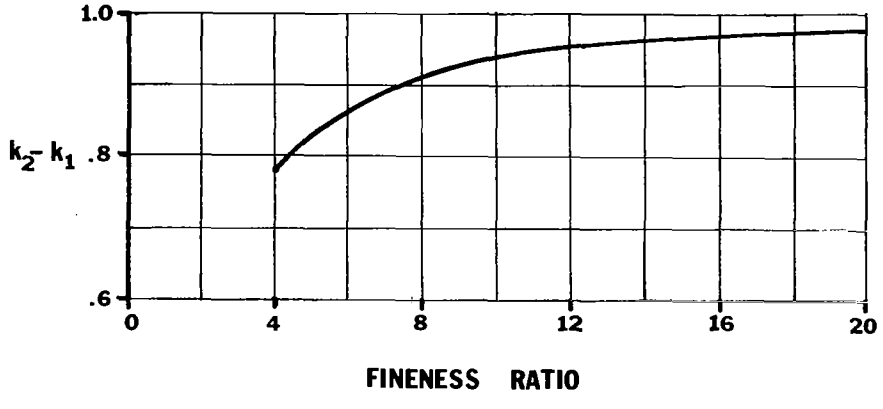

Figure 6. Reduced mass factor.

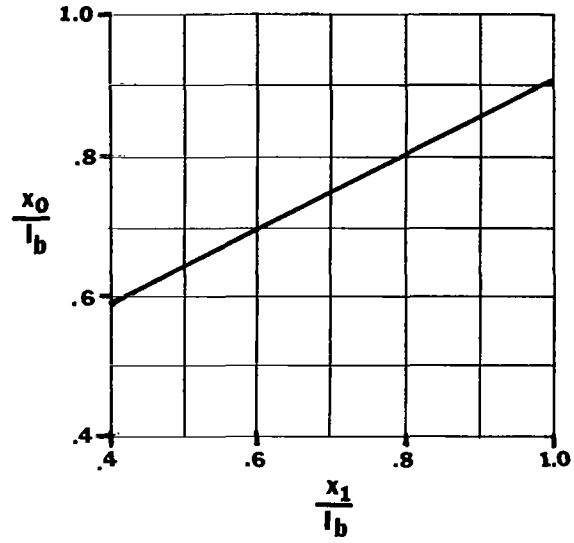

Figure 7. Body station where flow becomes viscous.

For an estimate of some values of $(C_{L_\alpha})_{Body}$, Table 1 from TR-540 (Ref. 9) in the discussion of C_L can be considered. The table is a tabular form of C_L versus α for various fuselage, wing combinations. The value of C_L is based on wing area, and although the fuselages given do not really represent the fuselage of a light airplane, they serve as an indicator for the degree of fuselage contribution to $(C_{L_\alpha})_{Total}$.

The tail as well as the fuselage may make a significant contribution to C_{L_α}. For the usual aerodynamic analysis, the wing C_{L_α} is usually considered to be the total C_{L_α} of the airframe; however, for a dynamic stability analysis, the total C_{L_α} is the change in total C_L resulting from a change in angle of attack only. An airplane in flight must be trimmed after the angle of attack is changed if the new angle of attack is to be maintained. Thus, the trim forces change over the angle of attack range, making it impossible to measure C_{L_α} in flight with everything else (including trim forces) constant.* Wind tunnel tests can be used to obtain the total C_{L_α}, since the model can be restrained. Since the tail contribution is small compared to the wing contribution (usually less than 10%), in many cases, C_{L_α} of the wing alone can be used. For the airplane to be analyzed later in this study, the wing C_{L_α} (4.61) is used.

The tail contribution to C_{L_α} can be estimated as,

$$\text{Total Lift} = \text{Lift}_{wing} + \text{Lift}_{fuselage} + \text{Lift}_{tail}$$

Thus,

$$C_{L_{total}} = C_{L_w} + C_{L_{fuse}} + C_{L_{tail}} \frac{S_t}{S_w} \eta_t$$

The derivative of the above expression is taken to yield

---

* Although impossible to measure exactly, C_{L_α} can be approximated with a good degree of accuracy from flight test records.

$$\left(\frac{dC_L}{d\alpha}\right)_{total} = C_{L_{\alpha_w}} + C_{L_{\alpha_{fuse}}} + \frac{dC_{L_t}}{d\alpha_t}\frac{d\alpha_t}{d\alpha}\frac{S_t}{S_w}\eta_t \ .$$

Since

$$\alpha_t = \alpha_w - i_w + i_t - \varepsilon \ ,$$

$$\frac{d\alpha_t}{d\alpha} = \left(1 - \frac{d\varepsilon}{d\alpha}\right) \ ;$$

thus,

$$\left(\frac{dC_L}{d\alpha}\right)_{total} = C_{L_{\alpha_w}} + C_{L_{\alpha_{fuse}}} + C_{L_{\alpha_{tail}}}\left(1 - \frac{d\varepsilon}{d\alpha}\right)\frac{S_t}{S_w}\eta_t$$

The tail contribution can therefore be written as

$$\left(\frac{dC_L}{d\alpha}\right)_{tail} = C_{L_{\alpha_t}}\left(1 - \frac{d\varepsilon}{d\alpha}\right)\frac{S_t}{S_w}\eta_t$$

Typical values of C_{L_α} for light airplanes fall in the range of 4.0 to 7.0 per radian, depending chiefly on the type of wing used.

C_{D_α}

The stability derivative C_{D_α} is the change in drag coefficient with varying angle of attack. Above the angle of attack for minimum drag the drag coefficient increases as the angle of attack increases; thus, C_{D_α} is positive in sign. C_{D_α} usually has little effect on the short period mode and has only a small effect on the phugoid mode in that a decrease in C_{D_α} usually increases stability.

C_{D_α} is made up of contributions from the wing, fuselage, and tail section, with the wing being by far the largest. The wing drag coefficient can be written as

$$C_D = C_{d_o} + (C_L^2/\pi eAR)$$

where

C_{d_o} = profile drag coefficient

$e = 1/(1 + \delta)$ = Oswald's span efficiency factor *

Thus, $C_{D_{\alpha_{wing}}}$ is

$$C_{D_{\alpha_{wing}}} = \frac{dC_{d_o}}{d\alpha} + \frac{2C_L}{\pi eAR} C_{L_\alpha}$$

For small angles of attack, $(dC_{d_o}/d\alpha)$ is usually small; however, for flight modes other than cruise, $(dC_{d_o}/d\alpha)$ could have a significant value. The wing C_{D_α}, in most cases, serves as a good approximation of the total C_{D_α}.

For fuselage angles of attack less than 10^o, the fuselage C_{D_α} can be ignored, as can the tail C_{D_α}, with good accuracy. Wind tunnel tests should actually be used to measure airplane C_{D_α}, but because the wing C_{D_α} dominates and since the equations are relatively insensitive to changes in C_{D_α}, it is felt that C_{D_α} can be approximated by the wing contribution. Thus,

$$C_{D_\alpha} = \frac{dC_{d_o}}{d\alpha} + \frac{2C_L}{\pi eAR} C_{L_\alpha}$$

The value of C_{D_α} calculated for the Cessna 182 is 0.126 per radian.

---

* A graph for estimating $(1 + \delta)$ can be found in the discussion of C_{L_α}.

C_{m_α}

C_{m_α} is perhaps the most important derivative related to longitudinal stability and control, since it primarily establishes the natural frequency of the short period mode and is a major factor in determining the response of the airframe to elevator motions and gusts. Usually, a large negative value of C_{m_α} is desired (-0.5 to -1.0 for light airplanes), but if C_{m_α} is too large, the required elevator effectiveness may become unreasonably high.

Figure 8, taken from Reference (11), shows that

$$N = L \cos(\alpha - i_w) + D \sin(\alpha - i_w)$$

$$C = D \cos(\alpha - i_w) - L \sin(\alpha - i_w)$$

where

i = incidence angle
t = subscript which refers to the tail
w = subscript which refers to the wing

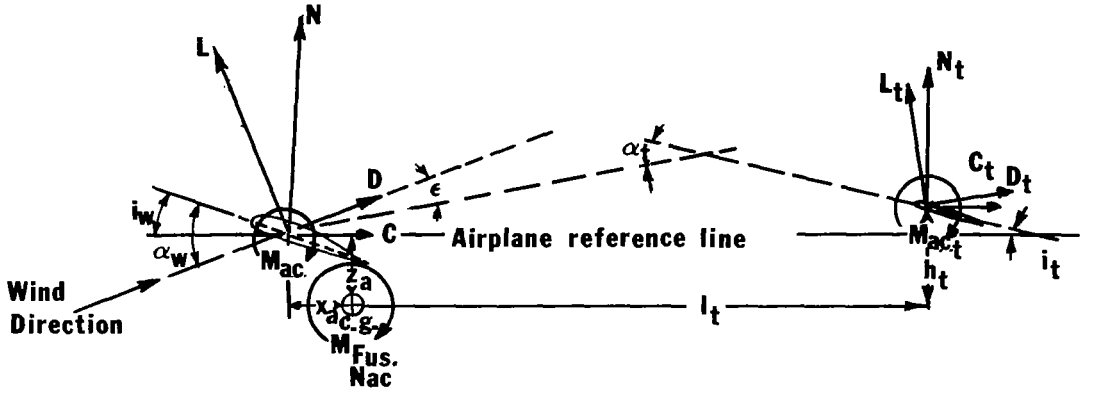

Figure 8. Forces and moments in plane of symmetry.

Neglecting C_{G_t}, the derivative of the pitching moment with respect to C_L can be written as

$$\frac{dC_m}{dC_L} = \underbrace{\frac{dC_N}{dC_L}\frac{x_a}{c} + \frac{dC_C}{dC_L}\frac{z_a}{c} + \frac{dC_{M_{a.c.}}}{dC_L}}_{\text{Contribution of wing}} - \underbrace{\frac{dC_{N_t}}{dC_L}\frac{S_t}{S_w}\frac{\ell_t}{c}\eta_t}_{\substack{\text{Contribution} \\ \text{of} \\ \text{horizontal} \\ \text{tail}}} + \underbrace{\left(\frac{dC_m}{dC_L}\right)_{\substack{\text{Fus.} \\ \text{Nac.}}}}_{\substack{\text{Contribution} \\ \text{of fuselage} \\ \& \text{ nacelles}}}$$

where

$C_{m_{a.c.}}$ = moment coefficient about aerodyanmic center
ℓ_t = length from c.g. to horizontal tail quarter chord
η_t = q_t/q_w

Evaluating some of the derivatives shows that, if $\alpha - i_w$ is small then $\sin(\alpha - i_w) \simeq (\alpha - i_w)$ and $\cos(\alpha - i_w) \simeq 1.0$, $C_D(\alpha - i_w)/C_{L_\alpha}$ is small compared with $(\alpha - i_w)$, and $dC_{d_o}/dC_L \simeq 0$ then

$$\frac{dC_N}{dC_L} = 1 + \frac{2C_L}{\pi eAR}(\alpha - i_w) + C_D \frac{1}{(C_{L_\alpha})_{\text{per radian}}}$$

$$\frac{dC_C}{dC_L} = \frac{2C_L}{\pi eAR} - (\alpha - i_w) - \frac{C_L}{(C_{L_\alpha})_{\text{per radian}}}$$

where

e = span efficiency factor obtained from C_{L_α}
AR = wing aspect ratio

Using the above equations,

$$\left(\frac{dC_m}{dC_L}\right)_{wing} = \left[1.0 + \frac{2C_L}{\pi eAR}(\alpha - i_w)_{\text{radians}} + \frac{C_D}{(C_{L_\alpha})_{\substack{\text{per}\\ \text{radian}}}}\right]\frac{x_a}{c}$$

$$+ \left[\frac{2C_L}{\pi eAR} - (\alpha - i_w)_{\text{radians}} - \frac{C_L}{(C_{L_\alpha})_{\substack{\text{per}\\ \text{radian}}}}\right]\frac{z_a}{c}$$

$$\left(\frac{dC_m}{d\alpha}\right)_{wing} = \left[1.0 + \frac{2C_L}{\pi eAR}(\alpha - i_w)_{\text{radians}} + \frac{C_D}{C_{L_\alpha}}\right]\frac{x_a}{c} C_{L_\alpha}$$

$$+ \left[\frac{2C_L}{\pi eAR} - (\alpha - i_w)_{\text{radians}} - \frac{C_L}{C_{L_\alpha}}\right]\frac{z_a}{c} C_{L_\alpha}$$

where C_{L_α} is per radian. If the c.g. is ahead of the aerodynamic center, x_a is negative (x_a = distance from c.g. to a.c.). If the c.g. position is under the wing a.c., z_a is positive (z_a = vertical distance from c.g. to a.c.).

The angle of attack of the tail is a function of the wing angle of attack, downwash, tail incidence, and wing incidence. Thus,

$$\alpha_t = \alpha_w - \varepsilon + i_t - i_w \ .$$

The first term of a Taylor expansion of C_{N_t} gives

$$C_{N_t} = \left(\frac{dC_N}{d\alpha}\right)_t \alpha_t = \left(\frac{dC_N}{d\alpha}\right)_t (\alpha_w - \varepsilon + i_t - i_w)$$

Therefore,

$$\frac{dC_{N_t}}{dC_L} = \left(\frac{dC_N}{d\alpha}\right)_t \left(\frac{d\alpha_w}{dC_L} - \frac{d\varepsilon}{dC_L}\right)$$

or,

$$\frac{dC_{N_t}}{dC_L} = \frac{(dC_N/d\alpha)_t}{(dC_L/d\alpha)_w}\left(1 - \frac{d\varepsilon}{d\alpha}\right)$$

The above equation can be used to write $(dC_m/dC_L)_t$ as:

$$\left(\frac{dC_m}{dC_L}\right)_t = \frac{-(dC_N/d\alpha)_t}{(dC_L/d\alpha)_w}\left(\frac{S_t}{S_w}\frac{\ell_t}{c}\frac{q_t}{q_w}\right)\left(1 - \frac{d\varepsilon}{d\alpha}\right)$$

or,

$$\left(\frac{dC_m}{d\alpha}\right)_{tail} = -\left(\frac{dC_L}{d\alpha}\right)_t \left(1 - \frac{d\varepsilon}{d\alpha}\right)\frac{S_t}{S_w}\frac{\ell_t}{c}\eta_t$$

Reference (19) gives the change in downwash with respect to α as

$$\frac{d\varepsilon}{d\alpha} = 20\,\frac{dC_L}{d\alpha}\,\frac{(1/\lambda)^{0.3}}{AR^{0.725}}\left(\frac{3c}{\ell_t'}\right)^{0.25}$$

where

λ = tip chord/root chord (use 0.67 for elliptical wing)
AR = wing aspect ratio
ℓ_t' = distance from wing quarter chord to horizontal tail quarter chord.

If the horizontal tail is located ±0.5c or more vertically from the centerline of the wake, a constant of 18 instead of 20 should be used.

Two methods, explained below, may be used to estimate the effects of the fuselage on C_{m_α}. The latter method is considered the more accurate of the two but requires more calculations. The first method requires the evaluation of the equation

$$\left(\frac{dC_m}{d\alpha}\right)_{\substack{\text{Fuselage}\\ \text{or}\\ \text{Nacelles}}} = \frac{k_f w_f^2 \ell_b}{S_w c} \quad \text{(per radian)}$$

where

k_f = empirical factor shown in Figure 9
w_f = maximum width of the fuselage or nacelle
ℓ_b = length of fuselage or nacelle

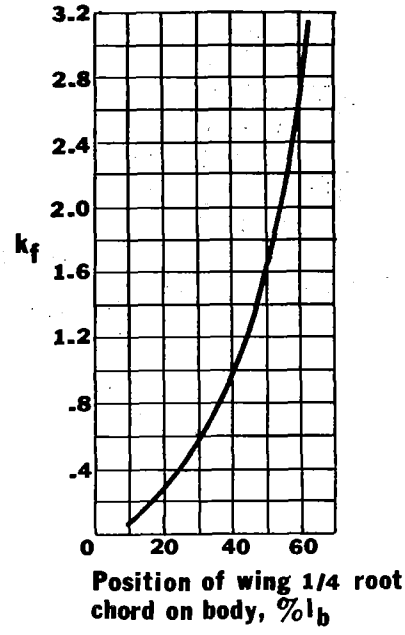

Figure 9. Empirical factor for fuselage or nacelle contributions to C_{m_α}.

The above formula, taken from TR-711 (Ref. 21), is a simple method for estimating the effect of the fuselage or nacelles on C_{m_α}.

The second method, taken from Perkins and Hage (Ref.11), considers the fact that the variation of the fuselage longitudinal pitching moment with angle of attack is greatly affected by the upwash in front of the wing and the downwash behind the wing. The wing's induced flow has a heavy destabilizing influence on the fuselage or nacelle sections ahead of the wing and a stabilizing influence behind the wing. Thus, the location of the wing with respect to the longitudinal axis is of considerable importance. Multhopp (Ref. 22) proposes the following formula to account for this phenomenon:

$$\frac{dM}{d\alpha} = \frac{q}{36.5} \int_o^{\ell_b} w_f^2 \frac{d\beta}{d\alpha} dx$$

or,

$$\frac{dC_m}{d\alpha} = \frac{1}{36.5Sc} \int_o^{\ell_b} w_f^2 \frac{d\beta}{d\alpha} dx$$

where

β = angle of local flow (freestream angle of attack plus the angle of the induced flow ahead of or behind the wing)
w_f = fuselage width
ℓ_b = length of fuselage

The equation can be integrated numerically in the manner illustrated in Figure 10.

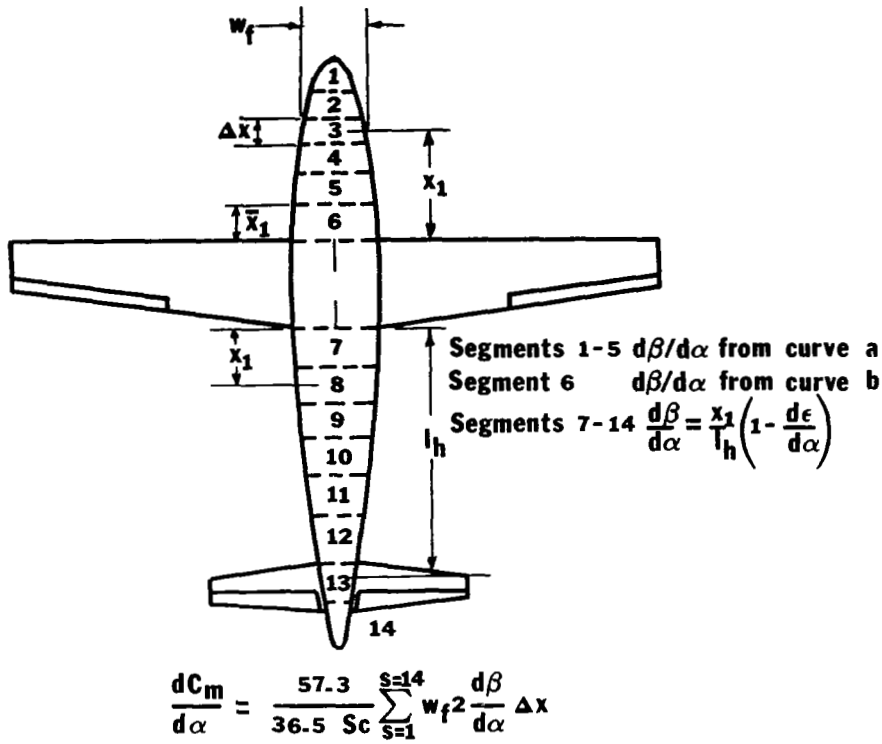

Figure 10. Typical layout for computing fuselage moments.

The integration requires that the average value of $w_f^2(d\beta/d\alpha)\Delta x$ be found for each segment and that the individual segment parts be summed. The curve for $d\beta/d\alpha$ versus positions ahead of the wing leading edge in percent wing chord are given in curve (a) of the following figure. For the section immediately ahead of the wing leading edge, $d\beta/d\alpha$ rises so abruptly that integrated values are given based on the length of this segment aft of the wing chord (curve b). For the segment aft of the wing, it is assumed that $d\beta/d\alpha$ rises linearly from zero at the root trailing edge to $(1 - d\epsilon/d\alpha)$ at the horizontal tail a.c. In the region between the wing leading and trailing edge, $d\beta/d\alpha$ is considered zero. It should be remembered that using the procedure above gives C_{m_α} per radian.

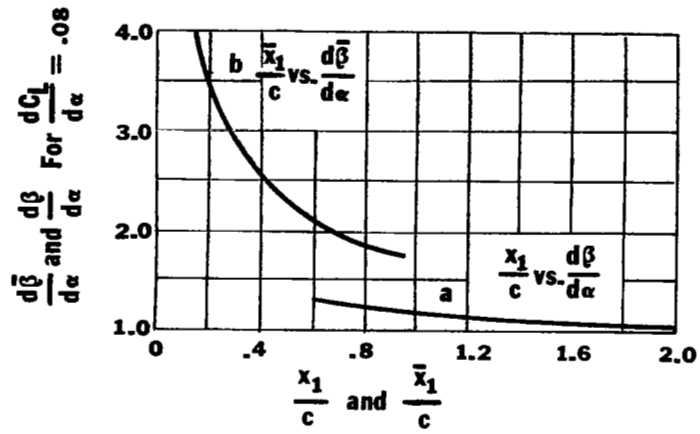

Figure 11. Fuselage pitching moment contribution to C_{m_α}.

It may be desirable to include a factor which takes into account the interference effect of the fuselage or nacelle on the wing C_{m_α}. This additional contribution can be approximated by the formula below and added to the C_{m_α} of the wing.

$$\frac{dC_m}{d\alpha} = \frac{c}{(290)(S)} (w_{L.E.} + 2\, w_{Mid.} - 3\, w_{T.E.})$$

where

$w_{L.E.}$, $w_{Mid.}$, and $w_{T.E.}$ = widths of the fuselage at the wing leading edge, mid-chord, and trailing edge, respectively.

Thus, the total airplane C_{m_α} can be written as the sum of the wing contribution, the fuselage contribution, and the tail contribution:

$$(C_{m_\alpha})_{Airplane} = \left[(1.0 + \frac{2C_L}{\pi eAR}(\alpha - i_w) + \frac{C_D}{C_{L_\alpha}})\frac{x_a}{c} + (\frac{2C_L}{\pi eAR}(\alpha - i_w) - \frac{C_L}{C_{L_\alpha}})\frac{z_a}{c}\right] C_{L_\alpha}$$

$$+ (\frac{dC_m}{d\alpha})_{\substack{Fus. \\ or \\ Nac.}} - (\frac{dC_L}{d\alpha})_t (1 - \frac{d\varepsilon}{d\alpha})\frac{S_t}{S_w}\frac{\ell_t}{c}\eta_t \quad \text{(angles in radians and } C_{L_\alpha} \text{ per radian)}$$

A typical value for C_{m_α} is the one associated with the Cessna 182. For the c.g. at 26% of the mean aerodynamic chord $C_{m_\alpha} = -0.885$. Moving the c.g. forward produces higher negative values for C_{m_α}; moving it aft achieves less negative values. For most light airplanes, C_{m_α} probably falls in the range of -0.5 to -1.0.

$C_{L_{\dot{\alpha}}}$

The stability derivative $C_{L_{\dot{\alpha}}}$ is the change in lift coefficient with the rate of change of angle of attack. This derivative arises from a type of "plunging" motion along the z-axis, during which the angle of pitch, θ, remains zero. For low speed flight, the derivative results primarily from the aerodynamic time lag effect at the horizontal tail, and its sign is positive. For the conventional light airplane, the horizontal tail is immersed in the downwash field of the wing some distance behind the wing. When the wing angle of attack is changed, the downwash field is also altered; however, it takes a finite length of time for the downwash alterations to reach the tail, resulting in a tail lift which lags the motion of the aircraft. $C_{L_{\dot{\alpha}}}$ can also arise from aeroelastic effects at high speed, but these aeroelastic contributions are negligible for light aircraft.

This derivative is unimportant in a dynamic longitudinal stability analysis for light airplanes, since its effect is essentially the same as if the airplane's mass or inertia were changed about the z-axis. Many studies either neglect $C_{L_{\dot{\alpha}}}$ by calling its effects small or fail to mention it at all because of the negligible effects.

An empirical method for calculating $C_{L_{\dot{\alpha}}}$ can be found using the same approach that is used for $C_{m_{\dot{\alpha}}}$. $C_{m_{\dot{\alpha}}}$ is merely the moment resulting from the time lag of the tail lift; thus, $C_{L_{\dot{\alpha}}}$ can be thought of as $C_{m_{\dot{\alpha}}}$ divided by the non-dimensional moment arm *. Thus,

$$C_{L_{\dot{\alpha}}} = \frac{-C_{m_{\dot{\alpha}}}}{\ell_t/c} = \frac{-c\, C_{m_{\dot{\alpha}}}}{\ell_t}$$

The negative sign is included because a positive pitching moment from the tail requires a negative lift (nose-up is a positive pitching moment). Using the equation derived for $C_{m_{\dot{\alpha}}}$, $C_{L_{\dot{\alpha}}}$ can be written as,

$$C_{L_{\dot{\alpha}}} = \frac{\partial C_L}{\partial\left(\frac{c\dot{\alpha}}{2U}\right)} = 2C_{L_{\alpha_t}}\, \varepsilon_\alpha\, \frac{\ell_t'}{c}\, \frac{S_t}{S_w}\, \eta_t$$

where

ℓ_t' = distance between the wing quarter chord and the horizontal tail quarter chord.

A typical range of values of $C_{L_{\dot{\alpha}}}$ for light airplanes is 1.5 to 3.0. For the Cessna 182, $C_{L_{\dot{\alpha}}}$ was found to be 1.74.

---

* the length from the c.g. to the tail quarter chord divided by the mean aerodynamic wing chord, (ℓ_t/c).

$C_{D_{\dot{\alpha}}}$

The stability derivative $C_{D_{\dot{\alpha}}}$ is the change in drag coefficient with rate of change of angle of attack. Like $C_{L_{\dot{\alpha}}}$, $C_{D_{\dot{\alpha}}}$ arises from the aerodynamic lag effect and various "dead-weight" aeroelastic effects. For airplanes in the speed and weight range of light airplanes, however, the drag variation due to both these effects is negligible. Consequently, $C_{D_{\dot{\alpha}}}$ is taken to be zero.

$C_{m_{\dot{\alpha}}}$

The derivative $C_{m\dot{\alpha}}$ is the change in pitching moment coefficient with respect to $\dot{\alpha}$, the time rate of change of the angle of attack. It is quite important in longitudinal dynamics, since it is involved in the damping of the short period mode. A negative value of $C_{m\dot{\alpha}}$ increases short period damping; thus, high negative values are desirable. This derivative is actually caused by a lag effect of the downwash at the horizontal tail of the aircraft.

War Report WR L-430 (Ref. 23) is considered to give the best derivation of an empirical formula for $C_{m\dot{\alpha}}$ based on the lag of the downwash between the trailing edge of the wing and the horizontal tail. The downwash at the tail at the time t depends on the angle of attack of the wing at the time

$$t - \frac{\ell_t'}{U}$$

where

ℓ_t' = length from the quarter chord of the wing to the quarter chord of the horizontal tail

$\frac{\ell_t'}{U}$ = lag time of the downwash

The angle of attack of the tail, α_t, can be written as

$$\alpha_t = \alpha_w - \varepsilon - i_w + i_t$$

For a given maneuver, the angle of attack can be written as a function of time, $\alpha = f(t)$. Thus, expanding the downwash in a Taylor series and ignoring second order terms, the downwash can be written as a function of $(t - \Delta t)$ as

$$\varepsilon = \frac{\partial \varepsilon}{\partial \alpha} f(t - \Delta t)$$

where

$$\Delta t = \frac{\ell_t'}{U}$$

As a simplifying technique, $f(t - \Delta t)$ can be expanded in a Taylor series as

$$f(t - \Delta t) = f(t) - \Delta t\, f'(t) + \frac{(\Delta t)^2}{2} f''(t) - \frac{(\Delta t)^3}{6} f'''(t) + \ldots$$

Thus,

$$\varepsilon = \varepsilon_\alpha \left\{\alpha - \Delta t\, \dot{\alpha} + \frac{(\Delta t)^2}{2} \ddot{\alpha} - \frac{(\Delta t)^3}{6} \dddot{\alpha} + \ldots\right\}$$

A quantity s is now introduced to non-dimensionalize $\dot{\alpha}$, where

$$s = \frac{2Ut}{c}$$

Therefore, $\dot{\alpha}$ can be expressed as

$$\dot{\alpha} = \frac{2U}{c}\frac{d\alpha}{ds} = \frac{2U}{c}\frac{d\alpha}{d(\frac{2U}{c}t)}$$

and $\ddot{\alpha}$ can be expressed as

$$\ddot{\alpha} = \frac{4U^2}{c^2}\frac{d^2\alpha}{d(\frac{4U^2}{c^2}t^2)}$$

The downwash can now be written in terms of s as

$$\varepsilon = \varepsilon_\alpha \{\alpha - 2\frac{l_t'}{c}\frac{d\alpha}{d(\frac{2U}{c}t)} + \frac{(2\frac{l_t'}{c})^2}{2}\frac{d^2\alpha}{d(\frac{2U}{c}t)^2} - \ldots\}$$

The equation for α_t can now be written, with the above equation substituted for the downwash, as

$$\alpha_t = \alpha_w - i_w + i_t - \varepsilon_\alpha \{\alpha - \frac{2l_t'}{c}\frac{d\alpha}{ds} + (\frac{2l_t'}{c})^2\frac{d^2\alpha}{ds^2} - \ldots\}$$

Since α and α_w refer to the same angle of attack,

$$\alpha_t = \alpha(1 - \varepsilon_\alpha) + i_t - i_w + \varepsilon_\alpha\frac{2l_t'}{c}\frac{d\alpha}{ds} - \varepsilon_\alpha\frac{(\frac{2l_t'}{c})^2}{2}\frac{d^2\alpha}{ds^2} - \ldots$$

Since $C_{m_{\dot{\alpha}}}$ results from the lag of the downwash at the tail, only the tail contribution to the pitching moment must be considered when $C_{m_{\dot{\alpha}}}$ is derived. The part of the pitching moment coefficient contributed by the tail can be written as

$$C_m = -C_{L_{\alpha_t}}\eta_t\frac{l_t}{c}\frac{S_t}{S_w}\alpha_t$$

where

l_t = distance from c.g. to $\frac{1}{4}$ chord of tail

Since C_m is a function of tail angle of attack, the expression derived above for α_t can be substituted into the C_m formula to yield

$$C_m = -C_{L_{\alpha_t}}\eta_t\frac{l_t}{c}\frac{S_t}{S_w}\{\alpha(1 - \varepsilon_\alpha) + \varepsilon_\alpha\frac{2l_t'}{c}\frac{d\alpha}{ds} - \varepsilon_\alpha\frac{(\frac{2l_t'}{c})^2}{2}\frac{d^2\alpha}{ds^2} + \ldots\}$$

The partial derivative of C_m with respect to $d\alpha/ds$ can now be expressed as

$$\frac{\partial C_m}{\partial(\frac{d\alpha}{ds})} = -C_{L_{\alpha_t}}\varepsilon_\alpha\frac{l_t}{c}\frac{S_t}{S_w}(\frac{2l_t'}{c})\eta_t$$

or

$$C_{m_{\dot{\alpha}}} = \frac{\partial C_m}{\partial \left(\frac{2U}{c}\dot{\alpha}\right)} = -2C_{L_{\alpha_t}} \varepsilon_\alpha \left(\frac{\ell_t}{c}\right)\left(\frac{\ell_t'}{c}\right) \frac{S_t}{S_w} \eta_t$$

It should be noted that the above formula agrees with the one developed in Perkins and Hage (Ref. 11), except for the manner in which $\dot{\alpha}$ is non-dimensionalized. It should also be pointed out that $C_{m_{\ddot{\alpha}}}$ can be found from the above equation by merely differentiating with respect to $d^2\alpha/ds^2$. In general, however, angular accelerations are considered small when linearized equations of motion are used and there are only small disturbances from equilibrium. Thus, for light airplanes, $C_{m_{\ddot{\alpha}}}$ would not be of great importance.

A typical range of $C_{m_{\dot{\alpha}}}$ for a light airplane is -3.0 to -7.0. For the Cessna 182, $C_{m_{\dot{\alpha}}}$ was calculated at -5.24.

C_{L_q}

The stability derivative C_{L_q} represents the change in airplane lift with varying pitching velocity while the angle of attack of the airplane as a whole remains constant. Contributions are made by both the wing and horizontal tail, but the tail is by far the more important. The general concensus is that C_{L_q} plays only a minor part in estimating the longitudinal response of the aircraft.

Volume V of Aerodynamic Theory by Durand (Ref. 24) explains the physical phenomena associated with C_{L_q}. Figure 12 shows that an airplane flying with velocity U in a circular flight path of radius R and center O has an angular velocity, $d\theta$, such that $U = R(d\theta/dt)$ and α is constant.

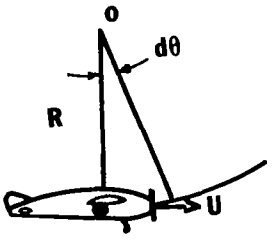

Figure 12. Pitching at constant α.

For small perturbations, $(d\theta/dt) = q$ (Appendix A). If the airplane c.g. is traveling with velocity U while the airplane is rotating with angular velocity q, the direction of motion of any point on the tail, distance ℓ_t behind the c.g., makes an angle $\tan^{-1}(q\ell_t/U)$ with the direction of motion of the c.g. Provided $q\ell_t$ is not too large compared to U, the effective incidence of the tail is increased by approximately $q\ell_t/U$ radians.

The wing contribution to C_{L_q} can be explained in much the same way. The change in angle of attack of the wing (measured at the aerodynamic center) is

$$\Delta\alpha = - q\left(\frac{x_{c.g.} - x_{a.c.}}{U}\right)$$

where

$x_{c.g.}$ = distance to the c.g.
$x_{a.c.}$ = distance to the a.c.

This expression indicates that there is a reduction in lift if the c.g. is behind the a.c. and an increase if the c.g. is in front of the a.c. For a c.g. very near the a.c., the wing contribution is negligible; however, the wing contribution increases as the distance between the c.g. and a.c. increases. It is felt that, for light airplanes, the fuselage contribution to C_{L_q} is smaller than that of the wing; thus, it is neglected here.

A theoretical derivation of C_{L_q} can be obtained from WR L-430 (Ref. 23) by modifying the C_{m_q} derivation to be discussed later. At the horizontal tail, the angle of attack is increased $\ell_t\dot{\theta}/U$ by pitching. The total lift coefficient is, therefore, increased by the amount

$$\Delta C_L = \frac{\ell_t \dot{\theta}}{U} C_{L_{\alpha_t}} \frac{S_t}{S_w} \eta_t$$

where

$C_{L_{\alpha_t}}$ = tail lift curve slope

The following expression is used as a non-dimensionalizing technique.

$$\dot{\theta} = \frac{2U}{c} \left(\frac{c\dot{\theta}}{2U}\right)$$

Thus,

$$\Delta C_L = \frac{\ell_t}{U} \left(\frac{2U}{c} \frac{c\dot{\theta}}{2U}\right) C_{L_{\alpha_t}} \frac{S_t}{S_w} \eta_t$$

Differentiating with respect to $(c\dot{\theta}/2U)$

$$\left.\frac{\partial C_L}{\partial \left(\frac{c\dot{\theta}}{2U}\right)}\right|_{tail} = \frac{2\ell_t}{c} C_{L_{\alpha_t}} \frac{S_t}{S_w} \eta_t$$

or

$$\left.\frac{\partial C_L}{\partial \left(\frac{cq}{2U}\right)}\right|_{tail} = \frac{2\ell_t}{c} C_{L_{\alpha_t}} \frac{S_t}{S_w} \eta_t$$

The wing contribution can be obtained similarly by substituting the distance from the c.g. to the wing quarter chord * for the distance ℓ_t. Thus,

$$\frac{\partial C_L}{\partial \left(\frac{cq}{2U}\right)} = 2 \frac{x'}{c} C_{L_\alpha}$$

where

x' = distance from c.g. to wing quarter chord (positive for c.g. ahead of quarter chord, negative for c.g. behind quarter chord)

C_{L_α} = wing lift curve slope

---

* At this point it is assumed that the a.c. of the wing is very near the wing quarter chord; therefore, the quarter chord is used as the reference.

The airplane C_{L_q} becomes

$$C_{L_q} = \left.\frac{\partial C_L}{\partial\left(\frac{cq}{2U}\right)}\right|_{wing} + \left.\frac{\partial C_L}{\partial\left(\frac{cq}{2U}\right)}\right|_{tail} = 2\frac{x'}{c}C_{L_\alpha} + 2\frac{\ell_t}{c}C_{L_{\alpha_t}}\frac{S_t}{S_w}\eta_t$$

For the Cessna 182 aircraft investigated later in the paper, the c.g. is located very near the quarter chord and the wing contribution is therefore neglected. The value of aircraft C_{L_q} was calculated to be 3.9.

C_{D_q}

The stability derivative C_{D_q} is the change in drag of the airplane with varying pitching velocity while the angle of attack of the airplane as a whole remains constant. This derivative has contributions from both the wing and the fuselage but both contributions are very small. In all of the literature for subsonic flight, C_{D_q} is ignored because it is really unimportant in analyzing flight dynamics and very small in magnitude. C_{D_q} for the Cessna 182 is taken to be 0.

C_{m_q}

The change in pitching moment coefficient due to a change in pitching velocity constitutes the stability derivative C_{m_q}. If an airplane has a positive pitch rate with a constant angle of attack (flying a curved flight path), the angle of attack at the tail is increased, thereby adding more positive lift to the tail and creating a moment to oppose the pitching motion. For this reason, the derivative is sometimes referred to as the "pitch damping" derivative and is usually negative. The wing contribution to C_{m_q} either opposes or increases the pitching motion, depending on the c.g. location (see discussion of C_{L_q}); however, this is relatively insignificant compared to the tail contribution. The fuselage contribution is always neglected for light airplanes.

This particular derivative is very important in longitudinal dynamics because it plays a major role in the damping of the short period mode and a minor role in phugoid damping. High negative values of C_{m_q} (-10.0 to -15.0) usually insure good short period damping for light airplanes.

C_{m_q} can be considered a sum of moments due to the component parts of C_{L_q}. Consequently,

$$C_{m_{q_{tail}}} = \frac{\partial C_m}{\partial\left(\frac{cq}{2U}\right)}\bigg|_{tail} = -\frac{\ell_t}{c}\frac{\partial C_L}{\partial\left(\frac{cq}{2U}\right)}\bigg|_{tail}$$

(The negative sign appears because $C_{m_{q_{tail}}}$ is always negative, while $C_{L_{q_{tail}}}$ is always positive) and

$$C_{m_{q_{wing}}} = \frac{\partial C_m}{\partial\left(\frac{cq}{2U}\right)}\bigg|_{wing} = -\frac{|x'|}{c}\frac{\partial C_L}{\partial\left(\frac{cq}{2U}\right)}\bigg|_{wing}$$

where

$|x'|$ = distance from c.g. to wing quarter chord (always positive).

The sign of $C_{m_{q_{wing}}}$ is opposite that of $C_{L_{q_{wing}}}$; thus, $|x'|$ is used instead of x'. When the a.c. in front of the c.g., $C_{L_{q_{wing}}}$ is negative but $C_{m_{q_{wing}}}$ is positive. The total C_{m_q} is

$$C_{m_q} = -\frac{2x'}{c^2}|x'|\,C_{L_\alpha} - \frac{2\ell_t^{\,2}}{c^2}C_{L_{\alpha_t}}\frac{S_t}{S_w}\eta_t$$

where

x' = distance from c.g. to wing quarter chord (positive for c.g. ahead of quarter chord, negative for c.g. behind quarter chord.

$|x'|$ = magnitude of x'

The value of C_{m_q} calculated for the Cessna 182 is -12.43.

$C_{L_{\delta_E}}$

The change in lift coefficient due to elevator deflection is the stability derivative $C_{L\delta_E}$. Since downward deflection of the elevator is defined as positive, producing a positive lift, $C_{L\delta_E}$ is normally positive in sign. Many erroneously consider this derivative to be the same as the change in equilibrium lift coefficient with respect to elevator deflection, in which the elevator deflection causes a change in the angle of attack, resulting in wing and tail lift changes. For the derivative $C_{L\delta_E}$, the elevator angle is the only quantity which can change; thus, the angle of attack as well as all other angles must remain the same. $C_{L\delta_E}$ does not appear in the characteristic equation of the aircraft, but it does appear in the numerator of the transfer functions; it therefore affects the gain of a particular transfer function.

For a conventional aircraft with the horizontal tail mounted an appreciable distance aft of the center of gravity, $C_{L\delta_E}$ is small, approximately 0.1 to 0.2 per radian. For light airplanes with relatively large tails, $C_{L\delta_E}$ may take on values between 0.3 and 0.5 per radian.

NACA TR-791 (Ref. 25) mentions that $C_{L\delta_E}$ is usually obtained from wind tunnel data; however, an empirical relation from Reference (11) can be used to approximate $C_{L\delta_E}$:

$$C_{L\delta_E} = \frac{dC_{L_t}}{d\alpha_t} \frac{d\alpha_t}{d\delta_E}$$

where

$$(dC_{L_t})/(d\alpha_t) = \text{lift curve slope of the tail}$$

and $d\alpha_t/d\delta_E$ is plotted as a function of elevator area divided by tail area (Figure 13), where $S_E/S_t = 1.0$ for all-movable tail.

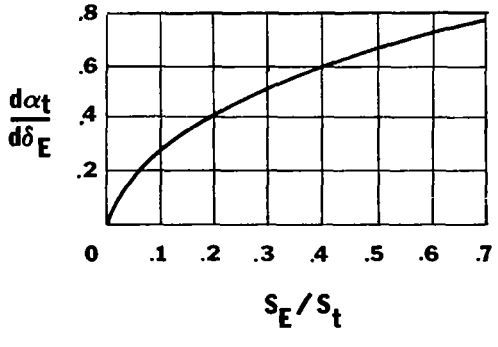

Figure 13. Elevator effectiveness.

The derivative can be estimated more exactly by using the two-dimensional data available in Reference (19) and merely correcting for aspect ratio. The data presented are for the 0009 airfoil and are useful, therefore, for most light airplanes (Figures 14 and 15). Dommash (Ref. 19) mentions that the data

given for the NACA 0009 airfoil with a plain flap illustrate the principles involved and are not intended as exact engineering design data; however, the data should give results well within the satisfactory requirements.

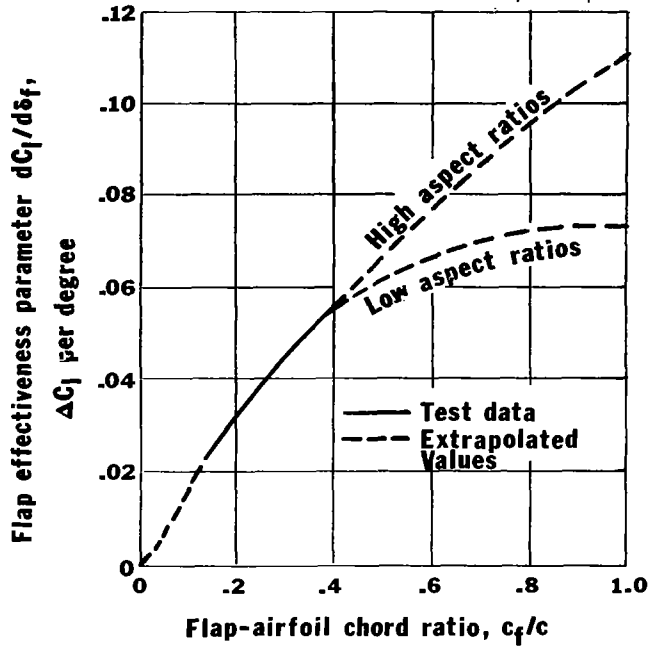

Figure 14. Flap effectiveness parameter versus flap-airfoil chord ratio for NACA 0009 airfoil with plain, unsealed flap and 0.005c gap.

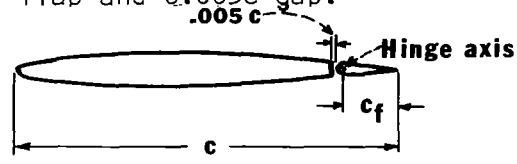

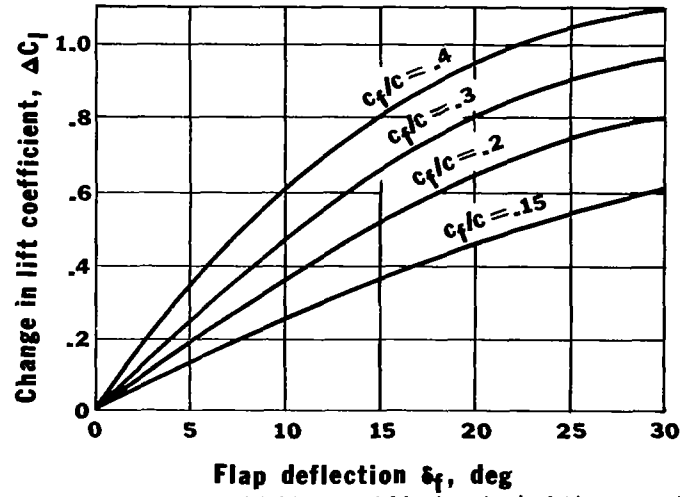

Figure 15. Change in lift coefficient (with constant angle of attack) versus flap deflection for several values of flap-airfoil chord ratios. NACA 0009 airfoil with plain, unsealed flap and 0.005c gap.

The two-dimensional values of $C_{L\delta_E}$ found above can be changed to $C_{\ell\delta_E}$ corrected for aspect ratio using the correction procedure given in Reference (10) for flapped wings:

$$C_{L\delta_E} = C_{\ell\delta_E} \left(\frac{C_{L\alpha_t}}{C_{\ell\alpha_t}}\right) \left(\frac{(\alpha_\delta)_{C_L}}{(\alpha_\delta)_{C_\ell}}\right) K_b$$

where

$C_{\ell\delta_E}$ = section lift curve increment due to flap (elevator) deflection (this derivative should not be confused with the rolling moment coefficient appearing in the lateral dynamics).

$C_{L\alpha_t}$ = lift curve slope of tail without flap deflected (3-D)

$C_{\ell\alpha_t}$ = section lift curve slope of basic airfoil

$\frac{(\alpha_\delta)_{C_L}}{(\alpha_\delta)_{C_\ell}}$ = ratio of 3-D flap effective parameter to the 2-D flap effectiveness parameter obtained from the figure below as a function of wing (tail) aspect ratio and the theoretical value of $(\alpha_\delta)_{C_\ell}$. The theoretical value is also given as a function of flap chord to airfoil chord.

K_b = flap-span factor which is ≈ 1.0 for elevator horizontal tail surface for light airplanes.

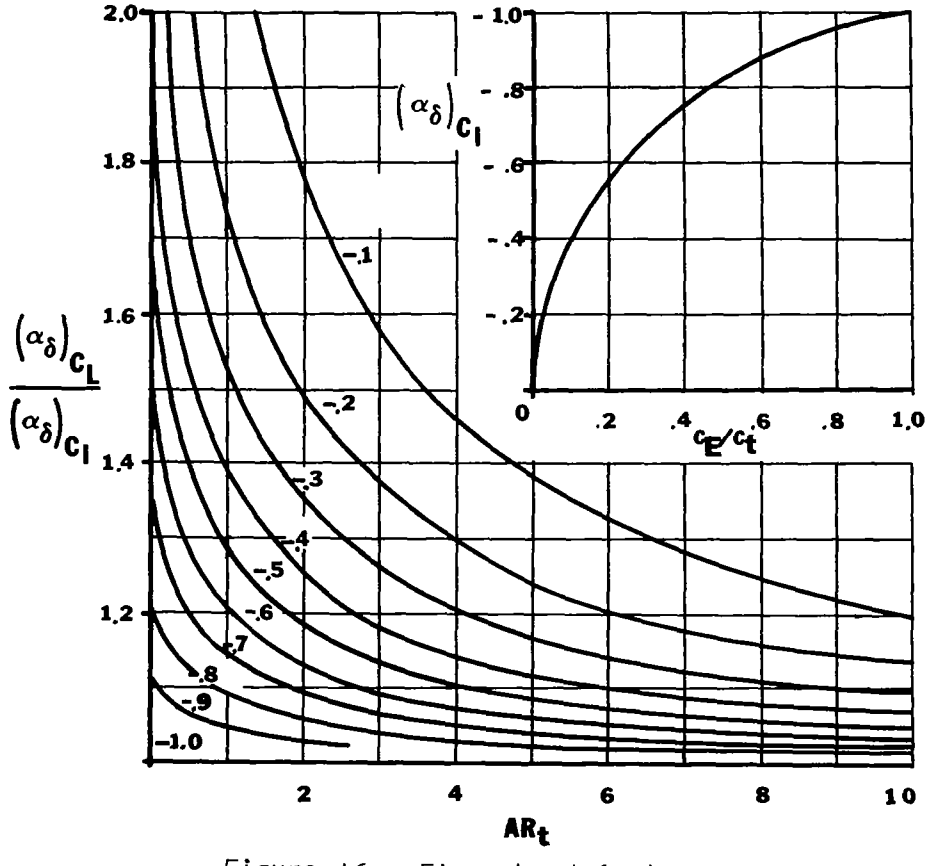

Figure 16. Flap chord factor.

For most light airplanes, $(\alpha_\delta)_{C_L}/(\alpha_\delta)_{C_\ell} \simeq 1.0$ to 1.1; $C_{L\alpha_t}$ and $C_{\ell\alpha_t}$ can be estimated using the procedures enumerated for $C_{L\alpha}$, and $C_{\ell\delta_E}$ can be estimated using the graphs for the 0009 airfoil. The formula for $C_{L\delta_E}$ based on wing area can then be written as

$$C_{L\delta_E} = C_{\ell\delta_E} \left[\frac{C_{L\alpha_t}}{C_{\ell\alpha_t}}\right] \left[\frac{(\alpha_\delta)_{C_L}}{(\alpha_\delta)_{C_\ell}}\right] \frac{S_t}{S_w} \eta_t$$

or, since $(\alpha_\delta)_{C_L}/(\alpha_\delta)_{C_\ell}$ is approximately 1.05 for most light aircraft,

$$C_{L\delta_E} = (1.05)\, C_{\ell\delta_E} \frac{C_{L\alpha_t}}{C_{\ell\alpha_t}} \frac{S_t}{S_w} \eta_t.$$

The value of $C_{L\alpha_E}$ calculated for the Cessna 182 is 0.427.

$C_{D_{\delta_E}}$

The change in drag coefficient due to a change in elevator angle is the control surface stability derivative $C_{D_{\delta_E}}$. For an elevator of reasonable size, the total airplane drag does not change appreciably with elevator deflection. For this reason, $C_{D_{\delta_E}}$ is often neglected. The characteristic equation of the aircraft is not a function of $C_{D_{\delta_E}}$; thus, $C_{D_{\delta_E}}$ affects only the gain of the particular transfer such as u/δ_E.

Probably the best method of estimating $C_{D_{\delta_E}}$ is to perform wind tunnel tests on a particular aircraft model; however, if wind tunnel testing is not feasible, $C_{D_{\delta_E}}$ can be approximated by using data from wind tunnel tests which have already been performed. NACA TR-688 (Ref. 26) discussed the aerodynamic characteristics of several horizontal tails. Using the figures below and the appropriate graphs, $C_{D_{\delta_E}}$ can be estimated. Five tail shapes from NACA TR-688 were chosen for inclusion in this analysis. To estimate $C_{D_{\delta_E}}$, the tail surface which is most like the one in question should be used. The numerical value of $C_{D_{\delta_E}}$ can be taken from plots of C_D versus α for different elevator deflections for each tail surface; however, the values of $C_{D_{\delta_E}}$ must be multiplied by S_t/S so that $C_{D_{\delta_E}}$ will be based on wing area.

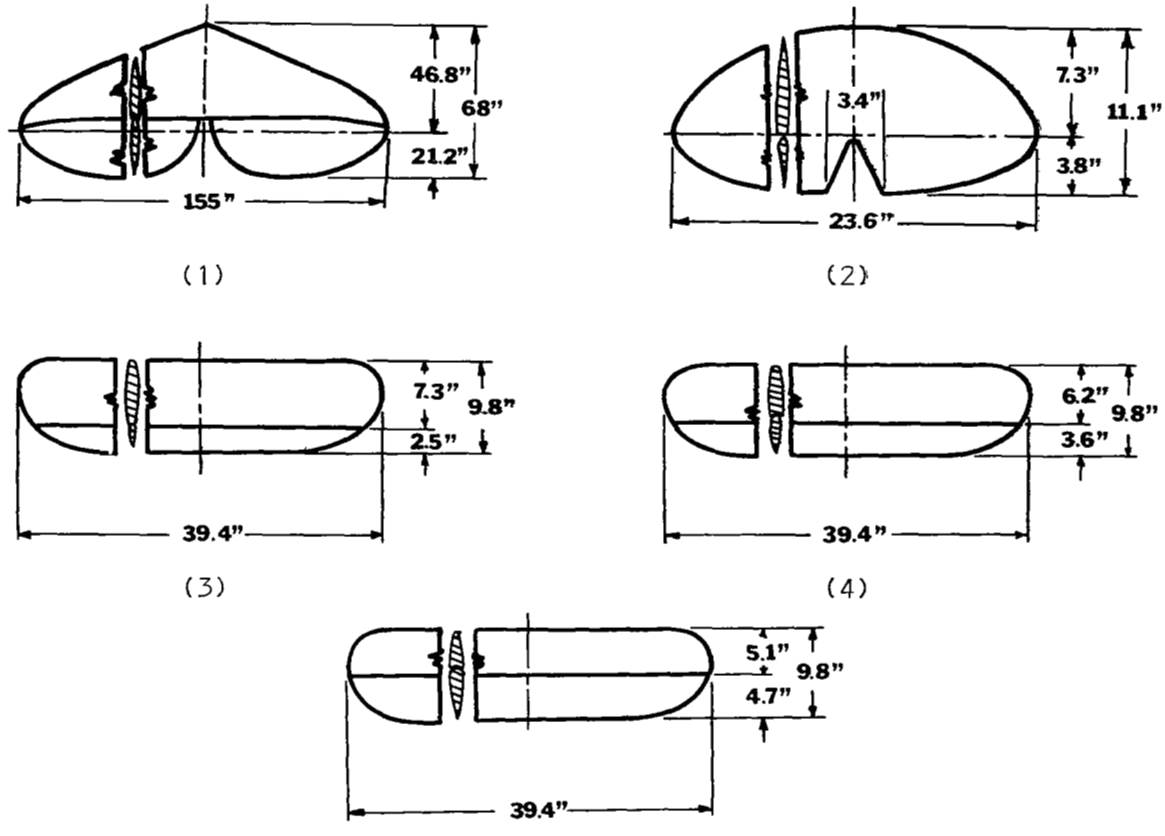

Figure 17. Five tail surfaces selected from NACA TR-688 (Ref. 26).

Tail Surface	AR	Span (in.)	S_t (sq. in.)	S_e (sq. in.)	c_t (in.)	Test U (fps)	Test R_N
1	3.4	155	7015	2450	45.25	88.0	1,960,000
2	3.1	23.6	181	68	7.68	110.0	448,000
3	4.3	39.4	361	81	9.15	-----	---------
4	4.3	39.4	361	117	9.15	-----	---------
5	4.3	39.3	356	162	9.06	-----	---------

Table 8. Dimensional characteristics for horizontal tails.

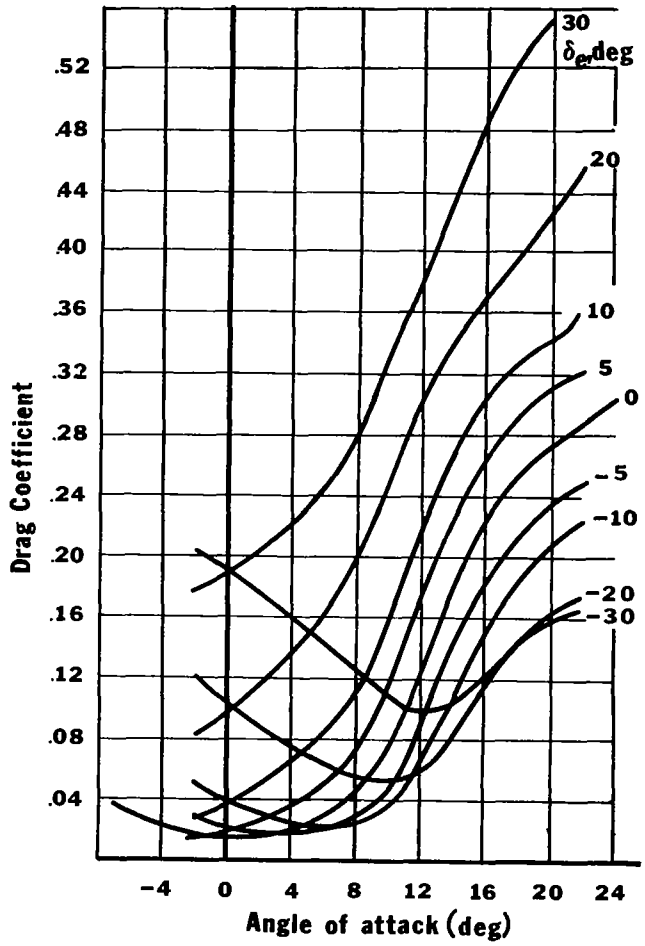

Figure 18. Drag coefficient against angle of attack at various elevator deflections for tail surface 1.

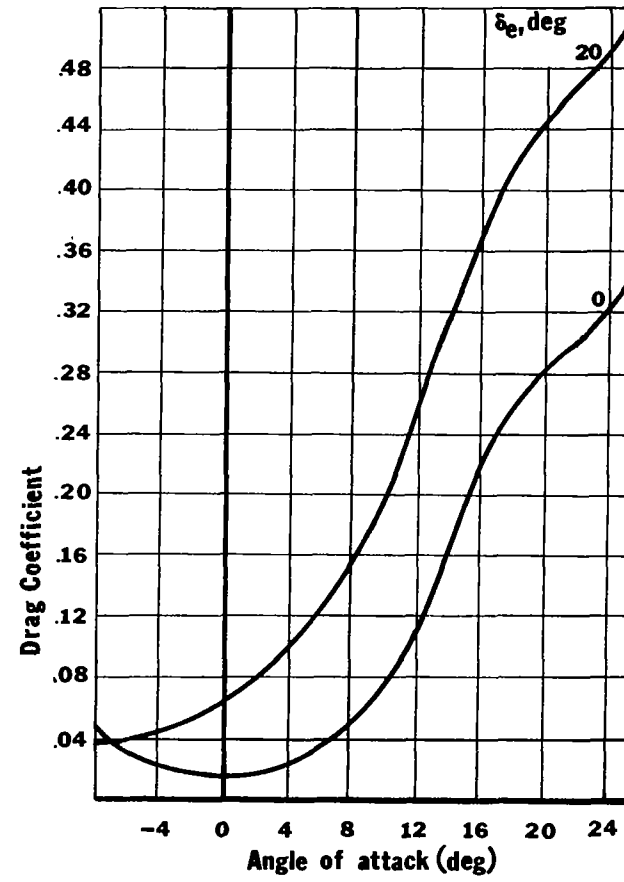

Figure 19. Drag coefficient against angle of attack at various elevator deflections for tail surface 2.

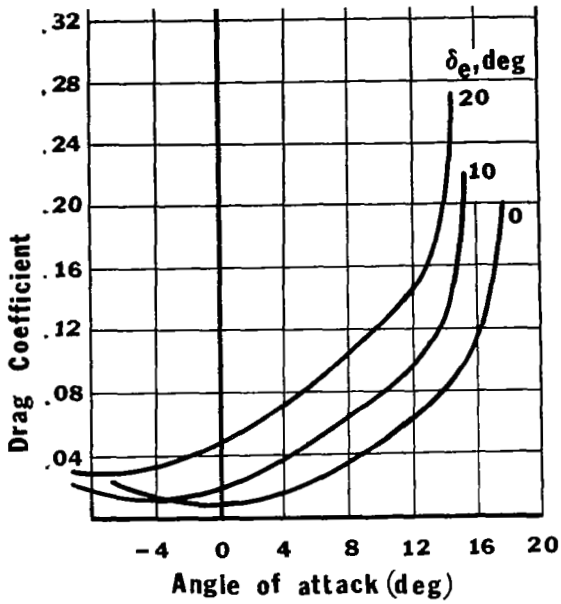

Figure 20. Drag coefficient against angle of attack at various elevator deflections for tail surface 3.

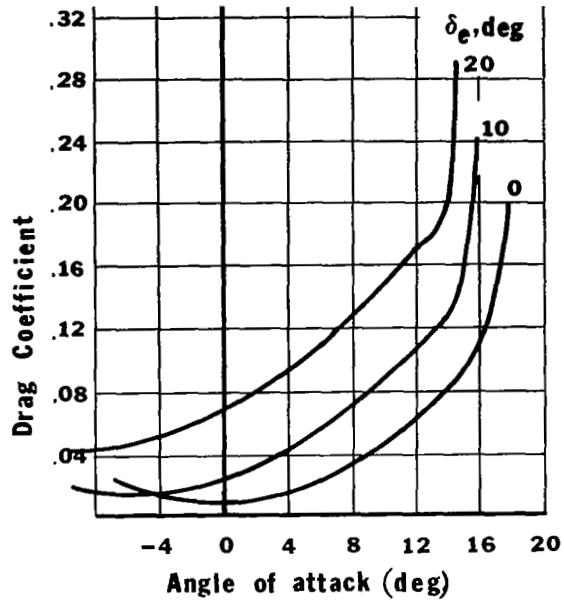

Figure 21. Drag coefficient against angle of attack at various elevator deflections for tail surface 4.

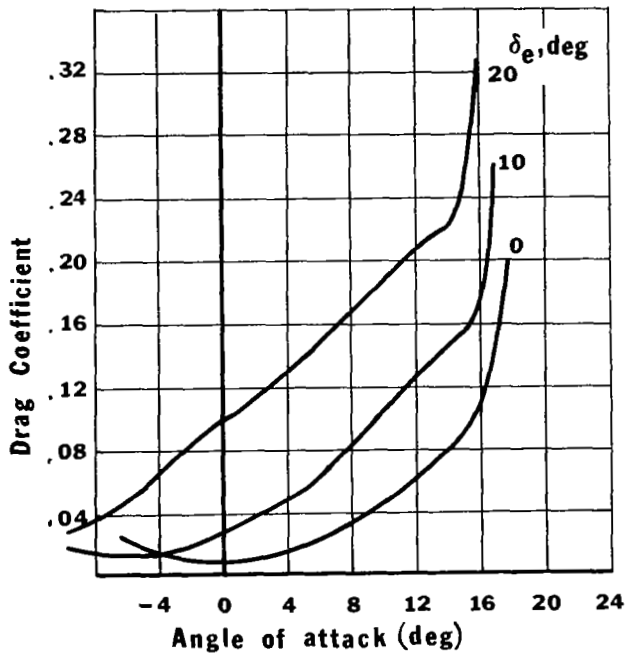

Figure 22. Drag coefficient against angle of attack at various elevator deflections for tail surface 5.

$C_{m_{\delta_E}}$

The stability derivative $C_{m\delta_E}$ is the change in pitching moment coefficient with changes in elevator deflection, usually referred to as "elevator power" or "elevator effectiveness." If $C_{m\delta_E}$ and the maximum deflection of the elevator are known, the maximum rotation moment which the tail can exert can be estimated. It must be remembered that $C_{m\delta_E}$ is evaluated without allowing the airplane to rotate or any other parameters to change; thus, $C_{m\delta_E}$ is really the moment produced by $C_{L\delta_E}$.

The primary function of the elevator is to control the angle of attack of the airplane in equilibrium flight or in maneuvering flight. Depending on the maximum allowable forward center of gravity travel, the horizontal tail is designed to give enough tail power in all flight conditions to control the aircraft. If the needed tail or elevator size is entirely unreasonable, the desired c.g. travel may have to be limited. For all practical purposes the maximum practical $C_{m\delta_E}$ determines the maximum forward center of gravity travel.

Since a positive elevator deflection is defined as down, a positive elevator deflection gives a negative pitching moment contribution, making the sign of $C_{m\delta_E}$ negative. A desirable value of $C_{m\delta_E}$ cannot be stated in general for all aircraft because each case must be analyzed separately. For most light aircraft, however, $C_{m\delta_E}$ should have a value between -0.75 and -2.0.

The numerical value of $C_{m\delta_E}$ can be obtained by multiplying $C_{L\delta_E}$ by the distance from the c.g. to the tail quarter chord divided by the wing mean aerodynamic chord:

$$C_{m\delta_E} = \frac{-\ell_t}{c} C_{L\delta_E}$$

The negative sign appears because $C_{L\delta_E}$ is positive and $C_{m\delta_E}$ must be negative, as discussed above. For the Cessna 182, $C_{m\delta_E}$ was calculated to be -1.28. In the experimental case used for this study, there is a contribution to $C_{m\delta_E}$ due to the moments about the a.c. of the horizontal tail; however, this contribution is so small it is usually neglected.

C_{y_β}

The stability derivative C_{y_β} is the change in side force caused by a variation in sideslip angle. When the airframe has a positive sideslip, β, the relative wind strikes the wing, fuselage, and vertical tail obliquely from the right, resulting in a negative side force. The major contribution to C_{y_β} comes from the vertical tail, with a smaller contribution from the fuselage and a nearly negligible contribution from the wing. This derivative contributes to the damping of the Dutch Roll mode; thus, large negative values of C_{y_β} might seem desirable. Large negative values of C_{y_β}, however, may create a large time lag in the airplane's response and cause it to react sluggishly to the pilot's commands.

In estimating values for C_{y_β}, force-test data for the design in question should be used, if possible. According to TR-1098 (Ref. 27), interference effects are so large that a generalized formula would not be completely satisfactory. Instead, a method of correcting data of a similar design for use in analyzing the design in question is recommended. A more recent publication, Datcom (Ref. 10), probably gives the most accurate method, since interference effects based on experimental results are included.

The wing contribution to C_{y_β} is small, on the order of α^2 (angle of attack in radians), so its accurate estimation is not vital to the total C_{y_β}. For swept wings, TN-1581 (Ref. 28) gives the following formula for C_{y_β} of the wing:

$$(C_{y_\beta})_{wing} = C_L{}^2 \frac{6 \tan \Lambda \sin \Lambda}{\pi\, AR(AR + 4 \cos \Lambda)} \text{ . (per radian)}$$

For zero sweep ($\Lambda = 0^\circ$), $(C_{y_\beta})_{wing}$ is equal to zero. TR-1098(Ref. 27) states that the above formula is not satisfactory in practice and that no correction of $(C_{y_\beta})_{wing}$ is necessary for similar designs since this contribution is so small. The method in Datcom (Ref. 10) gives the effect of wing dihedral on C_{y_β} as follows:

$$(C_{y_\beta})_{wing} = -.0001\ |\Gamma| \text{ per degree,}$$

where Γ is in degrees.

The fuselage contribution is greater than that of the wing and may be estimated by a method adapted from Datcom (Ref. 10). The basic relation is

$$(C_{y_\beta})_{fus} = -\, K_i\ (C_{L_\alpha})_{fus} \left(\frac{\text{Body Reference Area}}{S_w}\right) ,$$

where

$$\text{Body Reference Area} = (\text{fuselage volume})^{2/3},$$

K_i = wing-fuselage interference factor obtained from the graph below,

z_w = distance from body centerline to quarter-chord point of exposed wing root chord (positive for the quarter-chord point below the body centerline),

d = maximum body height at wing-body intersection.

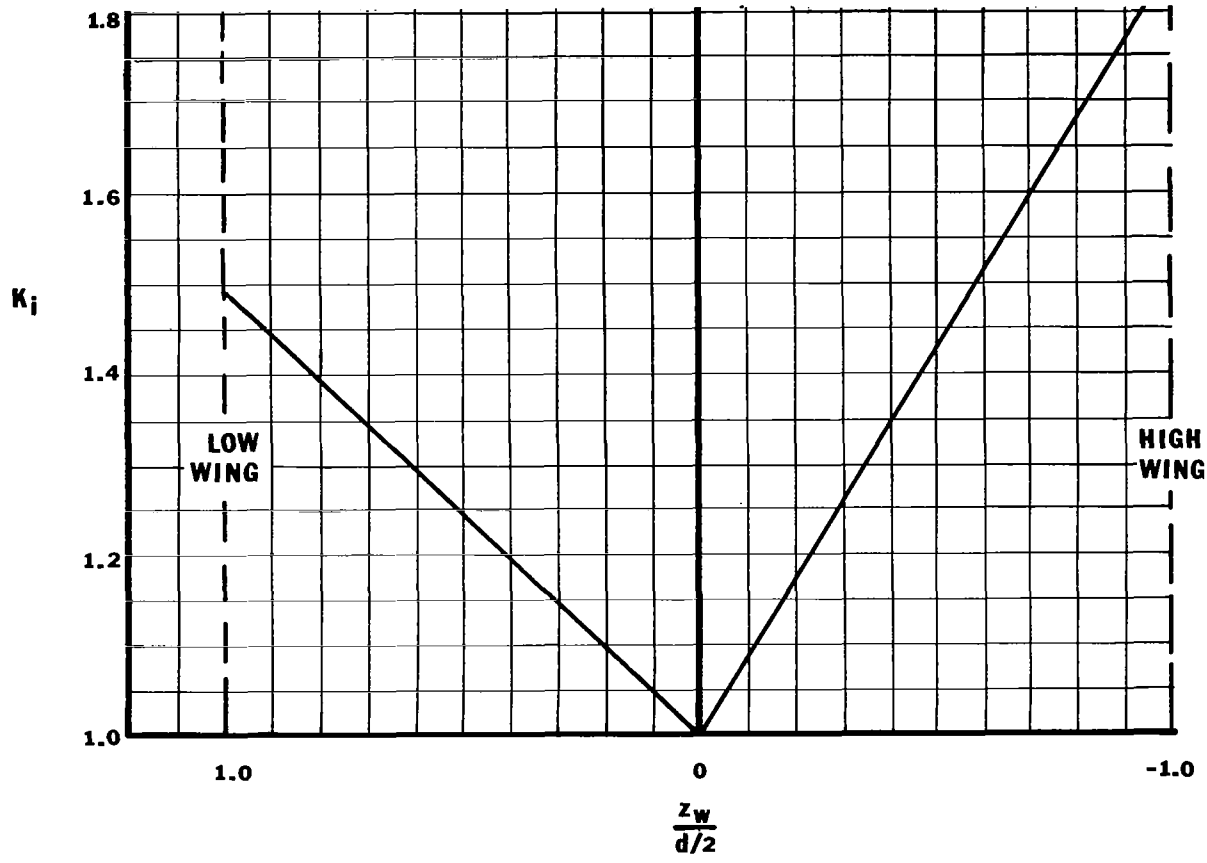

Figure 23. Values for wing-fuselage interference factor.

TR-540 (Ref. 9) gives values of $(C_{L_\alpha})_{fus}$ as .0525 per radian for round fuselages and .1243 per radian for rectangular fuselages. Observation of these

data indicates that, for most conventional light aircraft, the value of $(C_{y\beta})_{fus}$ is small.

The vertical tail is the most important contributor to $C_{y\beta}$, and $(C_{y\beta})_{tail}$ is used in the calculation of tail effects on many of the other lateral stability derivatives. TR-1098 (Ref. 27) gives the following formula for adapting $(C_{y\beta})_{tail}$ of a similar model to the design under consideration:

$$[(C_{y\beta})_{tail}]_{design} = [(C_{y\beta})_{tail}]_{data} \frac{[(C_{L_\alpha})_{tail} S_{tail}]_{design}}{[(C_{L_\alpha})_{tail} S_{tail}]_{data}} \frac{S_{data}}{S_{design}} .$$

The subscript "design" refers to the new configuration, and the subscript "data" refers to the configuration for which $(C_{y\beta})_{tail}$ is already known. Datcom (Ref.10) presents probably the most comprehensive method of obtaining $(C_{y\beta})_{tail}$ yet developed. In this method, the following formula is shown:

$$(C_{y\beta})_{tail} = - k (C_{L_\alpha})_V (1 + \frac{\partial\sigma}{\partial\beta}) \frac{q_V}{q} \frac{S_V}{S_W} .$$

The value of $(C_{L_\alpha})_V$ must be determined, using the effective aspect ratio of the vertical tail, to convert the two-dimensional lift-curve slope to the three-dimensional value. The importance of this approach is stressed in WR L-487 (Ref. 29), in which data of free-flight tests show that, for vertical tails of the same area, with the aspect ratio increased from 1.0 to 2.28, effectiveness increases 67%. The value of k, an empirical factor, may be obtained from the following graph as a function of the ratio of vertical tail span to fuselage diameter in the tail region, $(b_V/2r_1)$.

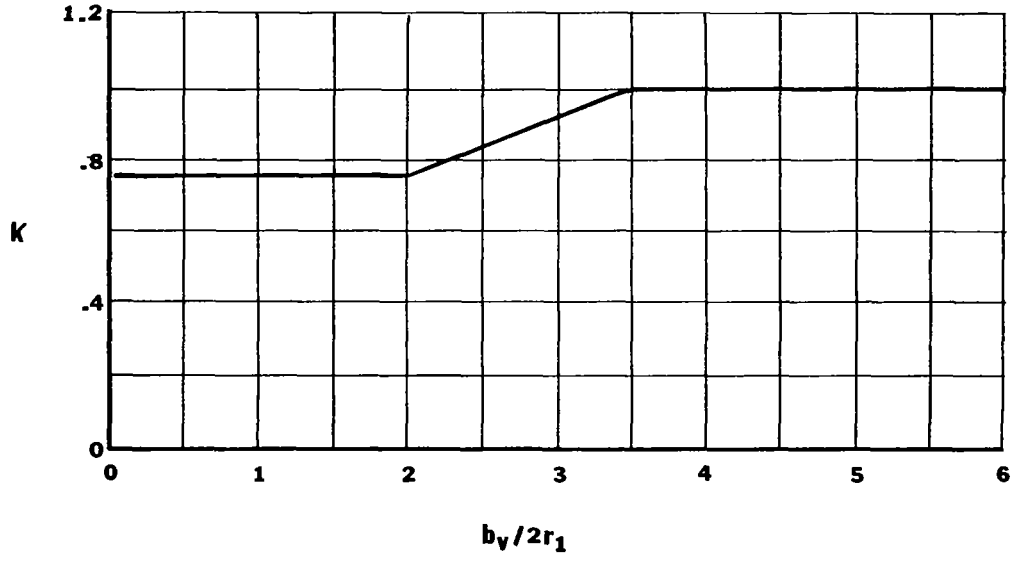

Figure 24. Values for k as a function of the ratio of vertical tail span to fuselage diameter in the tail region.

The value of the combination sidewash and dynamic pressure ratio parameter for zero sweep is the empirically-derived expression,

$$\left(1 + \frac{\partial\sigma}{\partial\beta}\right) \frac{q_v}{q} = .724 + 1.53 \left(\frac{S_v}{S_w}\right) + .4 \frac{z_w}{d} + .009 \, (AR),$$

where

z_w = distance, parallel to z-axis, from wing root quarter-chord point to fuselage centerline,

d = maximum diameter of fuselage.

A comparison of calculated values of this parameter (using the above formula) with tested values indicates that the average error is less than five percent. Putting together each of the components, the following formula from Datcom (Ref. 10) for total $C_{y\beta}$ results:

$$(C_{y\beta})_{total} = - K_i \, (C_{L\alpha})_{fus} \left(\frac{\text{Body Reference Area}}{S_w}\right) - .0001|\Gamma|$$

$$- k \, (C_{L\alpha})_v \left(1 + \frac{\partial\sigma}{\partial\beta}\right) \frac{q_v}{q} \frac{S_v}{S_w} .$$

Incorporating the above formula and the characteristics of a typical light airplane yields $C_{y\beta}$ = -.31 per radian, which seems to be a typical value.

C_{l_β}

The stability derivative C_{ℓ_β}, normally referred to as the "effective dihedral derivative," is the change in rolling moment coefficient caused by variation in sideslip angle. In popular usage, a "positive dihedral effect" means a negative value of C_{ℓ_β}. During aircraft sideslipping, the rolling moment produced is the result of wing dihedral effect and the moment resulting from the vertical tail center of pressure located above the equilibrium x-axis. For most conventional configurations, the value of C_{ℓ_β} is negative; however, this value can easily be adjusted by changing the amount of built-in wing dihedral.

C_{ℓ_β} is quite important to lateral stability, since it aids in damping both the Dutch Roll mode and the spiral mode. For favorable Dutch Roll damping characteristics, small negative values of C_{ℓ_β} are desired, but for improved spiral stability, large negative values are necessary. A compromise is thus in order, as indicated in TN-1094 (Ref. 30), which shows that best general flight behavior is obtained when the effective dihedral angle is approximately 2^o.

In actual practice, C_{ℓ_β} is usually not determined analytically because of the large errors involved as compared with force-test data on the design in question. If possible, force-test data should be used to determine the amount of wing dihedral, thus determining the value of C_{ℓ_β}. An analytical approach for straight and level flight ($\beta = -\psi$) is given in Perkins and Hage (Ref. 11) for calculating C_{ℓ_β} of the total aircraft. This formula is given below, followed by a discussion of methods for obtaining each component:

$$(C_{\ell_\beta})_{total} = (C_{\ell_\beta})_W + (C_{\ell_\beta})_V + (\Delta C_{\ell_\beta})_1 + (\Delta C_{\ell_\beta})_2 + (C_{\ell_\beta})_{W,\Gamma=0}$$

From Perkins and Hage, the wing dihedral contribution to C_{ℓ_β} is

$$(C_{\ell_\beta})_W = \left(\frac{C_{\ell_\beta}}{\Gamma}\right)\Gamma + (\Delta C_{\ell_\beta})_{tip\ shape}$$

The effect of wing tip shape on the value of ΔC_{ℓ_β} is shown below.

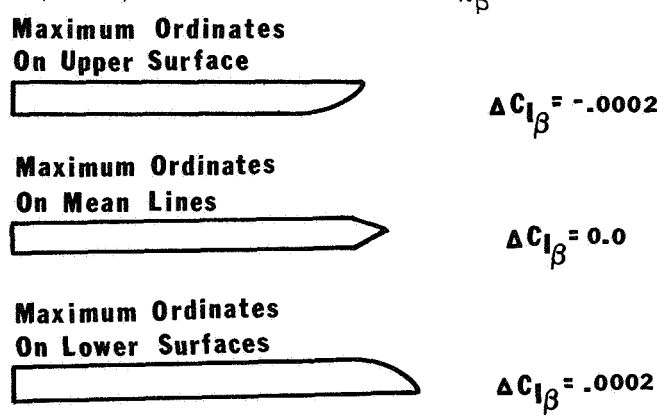

Figure 25. Effect of wing tip shape on C_{ℓ_β} per radian.

The value of (C_{ℓ_β}/Γ) for a particular aspect ratio and taper ratio may be obtained from the following graph.

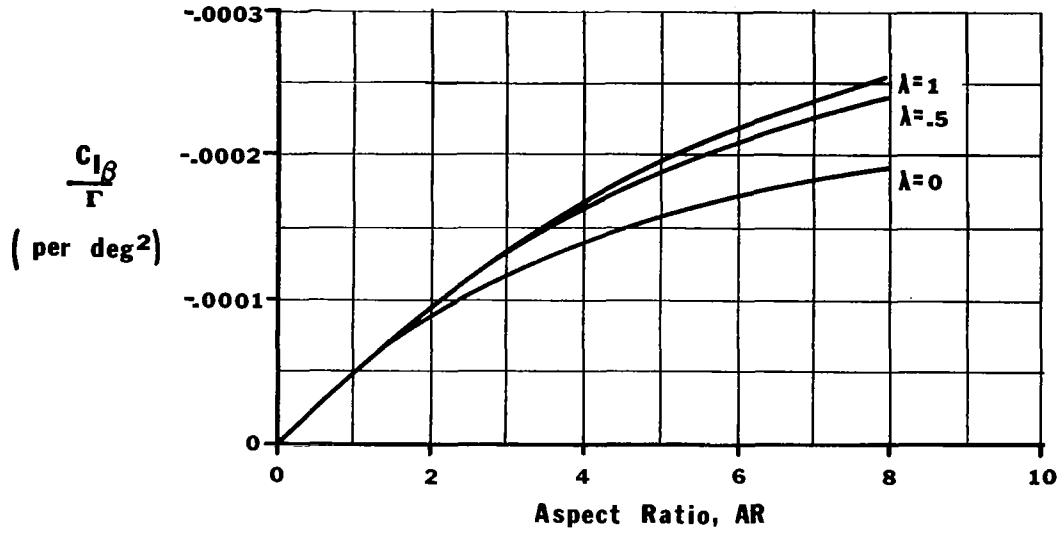

Figure 26. Values for (C_{ℓ_β}/Γ) for various aspect and taper ratios.

A theoretical study for unswept, elliptical wings with zero dihedral is presented in TR-1269 (Ref. 31), producing the following equation for wing contribution to C_{ℓ_β}:

$$(C_{\ell_\beta})_{\substack{w, \\ \Gamma=0}} = C_L\left[-\frac{16}{3\pi^2 AR} + .05\right] \text{ per radian}$$

Also presented is a revised formula, which considers changes in taper ratio:

$$(C_{\ell_\beta})_{\substack{w, \\ \Gamma=0}} = C_L\left[-\frac{k(.71\,\lambda + .29)}{AR\,\lambda} + .05\right] \text{ per radian}$$

where

k = 1.0 for straight wing tips
k = 1.5 for round wing tips

If the vertical tail is located above the longitudinal axis, the vertical tail contribution is easily calculated from computation of the normal force caused by sideslip. Thus,

$$(C_{\ell_\beta})_V = -\,a_V \frac{S_V}{S_W}\frac{z_V}{b_W}\eta_V = -\,(C_{n_\beta})_V \frac{z_V}{\ell_V}$$

where

z_V = distance from the center of pressure of the vertical tail to the airplane's x-axis (positive for vertical tail above the x-axis).

Most studies on this subject consider two interference effects on the vertical tail--wing-fuselage and wing-vertical tail interference--both influenced by the wing's location. These effects are tabulated in Perkins and Hage, as shown in Table 9.

	Wing-fuselage $(\Delta C_{\ell_\beta})_1$	Wing-vertical Tail $(\Delta C_{\ell_\beta})_2$
High Wing	-.0006	.00016
Mid Wing	0	0
Low Wing	.0008	-.00016

Table 9. Values for interference effects on the vertical tail per radian.

Typical values of C_{ℓ_β} range from -.03 to -.12 per radian.

C_{n_β}

The stability derivative C_{n_β}, often called the "weathercock" or static directional derivative, is the change in yawing moment coefficient resulting from a change in sideslip angle. Physically, C_{n_β} is the result of the airframe sideslipping, with the relative wind striking it obliquely, causing a yawing moment about the center of gravity. The vertical tail, fuselage, and wing contribute to C_{n_β}, with the vertical tail the dominant factor. For positive sideslip, the vertical tail causes a positive yawing moment; thus, C_{n_β} is usually positive, even though the fuselage contribution is normally negative. The wing contribution is usually positive, but quite small compared to that of the vertical tail and fuselage.

The value of C_{n_β} determines primarily the Dutch Roll natural frequency and affects the spiral stability of the aircraft. It is generally agreed that values of C_{n_β} as high as practically possible are desirable for good flying qualities. Values for C_{n_β} should be obtained from force-test data for the model in question where possible.

At present, two analytical methods of calculating total C_{n_β} appear most complete. The first is that presented in Perkins and Hage (Ref. 11) for straight, level flight ($\beta = -\psi$). The value of C_{n_β} for the total plane can be obtained from the composite formula,

$$(C_{n_\beta})_{total} = (C_{n_\beta})_W + (C_{n_\beta})_{fus} + (C_{n_\beta})_V + \Delta_1 C_{n_\beta} + \Delta_2 C_{n_\beta}$$

Perkins and Hage also give a value for $(C_{n_\beta})_W$ as

$$(C_{n_\beta})_W = .00006\ (\Lambda^o)^{1/2} \text{ per degree}$$

For unswept wings, TM-906 (Ref. 32) gives

$$(C_{n_\beta})_W = \frac{C_L^2}{4\pi AR} \text{ per radian}$$

This formula is modified in TN-1581 (Ref. 28) for sweep, by the following relation:

$$(C_{n_\beta})_W = C_L^2 \left[\frac{1}{4\pi AR} - \frac{\tan \Lambda}{\pi\ AR(AR + 4\cos \Lambda)} \left(\cos \Lambda - \frac{AR}{2} - \frac{AR^2}{8 \cos \Lambda}\right)\right.$$

$$\left. + 6 \frac{\bar{x}}{c} \frac{\sin \Lambda}{AR}\right] \quad \text{per radian}$$

where

$\bar{x}$ = longitudinal distance rearward from c.g. to wing aerodynamic center

A value of $(C_{n_\beta})_{fus}$ can be obtained from Perkins and Hage by use of

$$(C_{n_\beta})_{fus} = \frac{-.96\ K_\beta}{57.3} \left(\frac{S_s}{S_w}\right) \left(\frac{\ell_b}{b_w}\right) \left(\frac{h_1}{h_2}\right)^{1/2} \left(\frac{w_2}{w_1}\right)^{1/3}$$

The value of K_β, an empirical constant, can be obtained from the following graph as a function of fineness ratio and c.g. location. The distance from the nose to the c.g. is d; S_s is the body side area. The other variables are shown below.

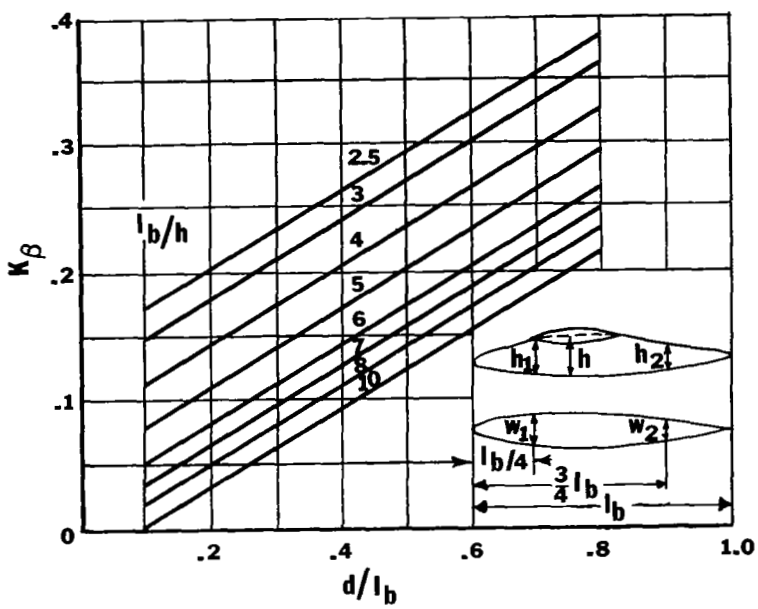

Figure 27. Empirical constant K_β as a function of fineness ratio and c.g. location.

Perkins and Hage also present the following formula for vertical tail contribution to C_{n_β}:

$$(C_{n_\beta})_V = a_V \frac{S_V}{S_W} \frac{\ell_V}{b_W} \eta_V$$

The value of a_V, lift-curve slope of vertical tail, is determined by using the effective aspect ratio, which is calculated

$$Ae = 1.55 \frac{b_V^2}{S_V}$$

The value of a_V can now be obtained from the following graph for a particular value of Ae. This value is based on a conventional, low horizontal tail configuration; therefore, for designs significantly different, one is referred to Datcom (Ref. 10) for an alternate method of finding Ae.

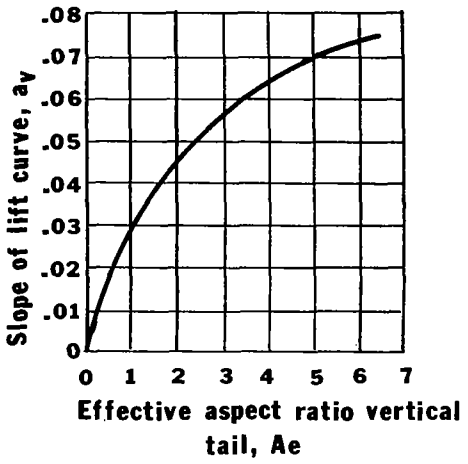

Figure 28. Values of a_v as a function of vertical tail aspect ratio.

The vertical tail efficiency factor, η_v, is also needed for the design in question. Two interference factors must be determined to complete the calculation of total $C_{n\beta}$. The first of these, $\Delta_1 C_{n\beta}$, is the wing-fuselage interference factor, a function of wing location. The following chart is used to determine its value.

WING POSITION	$\Delta_1 C_{n\beta}$ PER DEGREE
High Wing	.0002
Mid Wing	.0001
Low Wing	0

Table 10. Values for $\Delta_1 C_{n\beta}$ as a function of wing location.

The second interference factor, $\Delta_2 C_{n\beta}$, is the result of sidewash at the vertical tail caused by wing-fuselage interference. Its value may be determined from the following graph as a function of wing position and maximum fuselage height.

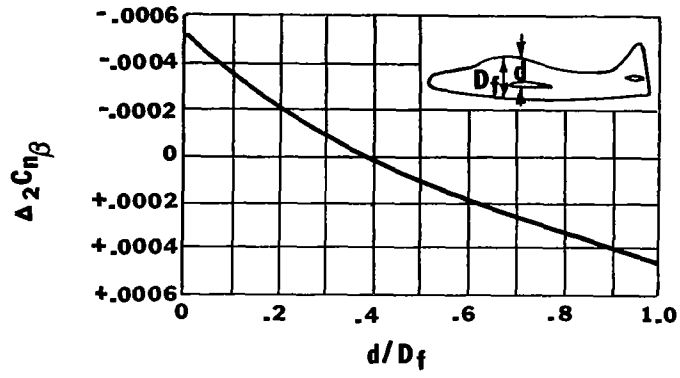

Figure 29. Values for $\Delta_2 C_{n_\beta}$ as a function of wing position and maximum fuselage height.

Now that each of the components has been determined, the value for total C_{n_β}, using the method of Perkins and Hage, can be evaluated. They indicate that a $C_{n_\beta} \geq .0005 (\sqrt{W}/b)$ is necessary for adequate directional stability.

The second method of obtaining total C_{n_β} is presented in Datcom (Ref. 10) where a wing-fuselage correction is added to the vertical tail contribution, resulting in

$$(C_{n_\beta})_{total} = - K_n \frac{\text{Body Side Area}}{S_w} \frac{\ell_b}{b_w} - (C_{y_\beta})_{tail} \frac{\ell_v}{b_w}$$

The interference factor, K_n (per degree), may be determined from the following graph as a function of aircraft geometry and Reynolds Number.

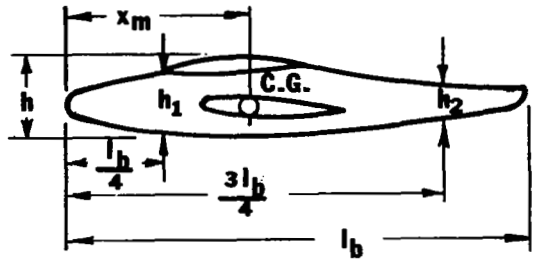

S_{B_S} = Body Side Area
w = Maximum Body Width

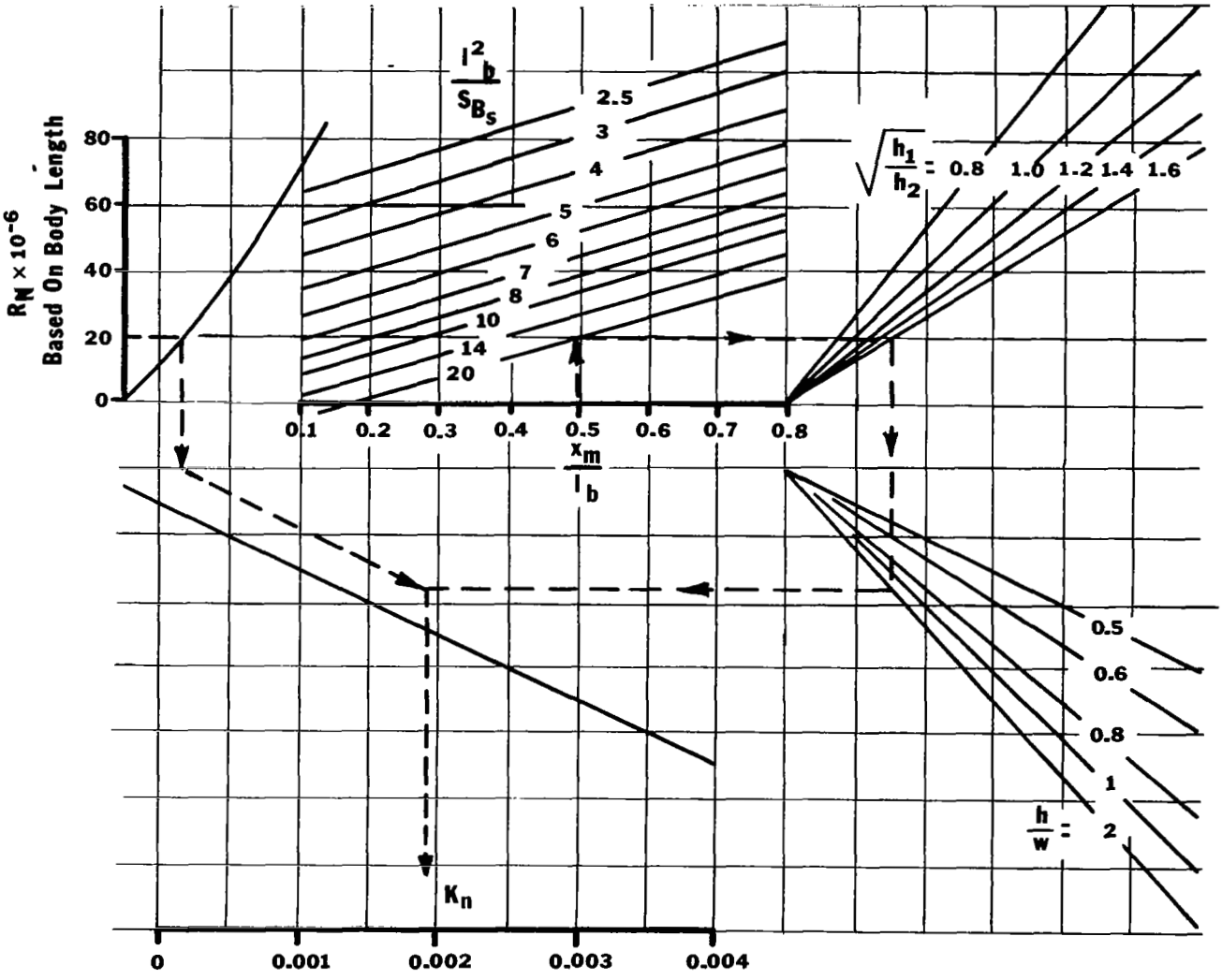

Figure 30. Empirical interference factor, K_n, as a function of aircraft geometry and Reynolds Number.

The value of $(C_{y_\beta})_{tail}$ may be obtained from the discussion of the stability derivative C_{y_β} in the present study.

For light aircraft, typical values of C_{n_β} seem to range from 0.03 to 0.12 per radian.

C_{y_p}

The stability derivative C_{y_p} is the change in side force resulting from rolling velocity, with the vertical tail the main contributor, even though, for some configurations, the wing may make a significant contribution. The rolling velocity, p, creates an effective angle of attack on the tail, which, in turn, produces a side force. The sign of C_{y_p} may be either positive or negative. It is relatively insignificant and commonly neglected.

In TN-1581 (Ref. 28), a completely theoretical approach, the following formula for C_{y_p} of the wing is presented:

$$C_{y_p} = C_L \frac{AR + \cos \Lambda}{AR + 4 \cos \Lambda} \tan \Lambda$$

For zero sweepback, this formula gives $C_{y_p} = 0.0$, which agrees with other theoretical treatments. From wind tunnel tests on wings alone, TR-968 (Ref. 33) adds C_L/AR to the above formula to account for wing tip suction, resulting in

$$C_{y_p} = C_L \left[\frac{AR + \cos \Lambda}{AR + 4 \cos \Lambda} \tan \Lambda + \frac{1}{AR}\right]$$

This reduces to $C_{y_p} = C_L/AR$ for zero sweepback, which does not appear small enough to be considered negligible.

The wing contribution is usually minor compared to the vertical tail contribution. From NASA MEMO 4-1-59L (Ref. 34), using a theoretical method of discrete-horseshoe-vortices, with the horizontal tail in the mid-position, a value of $(C_{y_p})_{tail}$ is $(-.8)[b_v/(b_w/2)]$ for the vertical tail contribution. Also, in TR-1086 (Ref. 35), a formula for tail contribution is

$$(C_{y_p})_{tail} = (C_{L\alpha})_{\substack{vert \\ tail}} \cdot \frac{S_v}{S_w} \left[-\frac{2}{b_w}(z_v \cos \alpha - \ell_v \sin \alpha) + \left(\frac{\partial \sigma}{\partial \left(\frac{pb}{2U}\right)}\right)_{av}\right]$$

where

z_v = height of vertical tail center of pressure above the longitudinal axis

σ = sidewash angle at the vertical tail

The ratio $(\partial\sigma/[\partial(pb/2U)])_{av}$ is the average effect of sidewash on the vertical tail and can be obtained from the following graph as a function of angle of attack and vertical tail to semispan ratio for a wing with aspect ratio in the vicinity of 6.

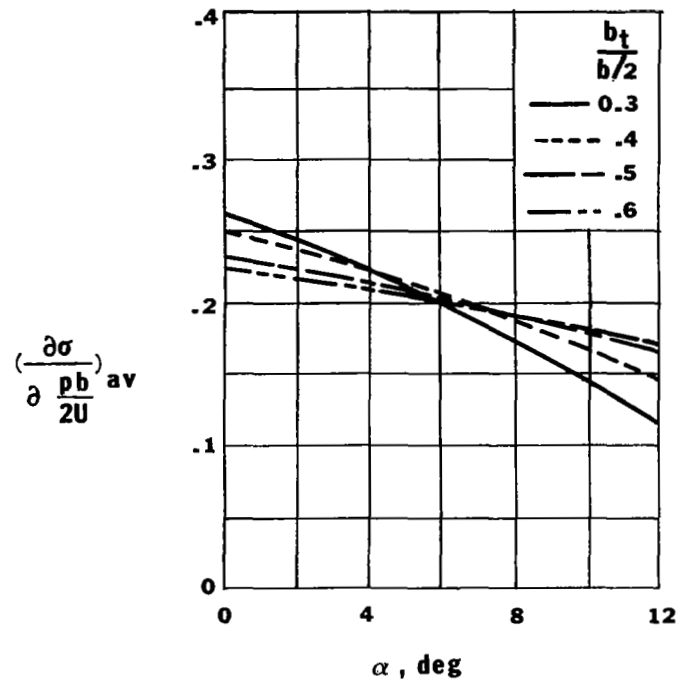

Figure 31. Estimation of average sidewash angle at the vertical tail with wing aspect ratio equal to 6.

In TR-1098 (Ref. 27), the relation for tail contribution is

$$(C_{y_p})_{tail} = 2\left[\frac{z_v}{b_w} - \left(\frac{z_v}{b_w}\right)_{\alpha = 0}\right](C_{y\beta})_{tail}$$

which seems quite small for cruise at an angle of attack near zero.

Datcom (Ref. 10) also presents a method for calculating C_{y_p}, but, for conventional light aircraft with zero wing sweep, it appears that C_{y_p} is very near zero. The following formula is taken from this work:

$$C_{y_p} = \left(\frac{C_{y_p}}{C_L}\right) C_L + \left(\frac{(\Delta C_{y_p})_\Gamma}{(C_{\ell_p})_{\Gamma = 0}}\right) C_{\ell_p}$$

The following graphs, which have been adapted from Datcom for light aircraft, show (C_{y_p}/C_L) as a function of wing sweep and taper ratio, and $[(\Delta C_{y_p})_\Gamma/(C_{\ell_p})_{\Gamma=0}]$ as a function of dihedral angle.

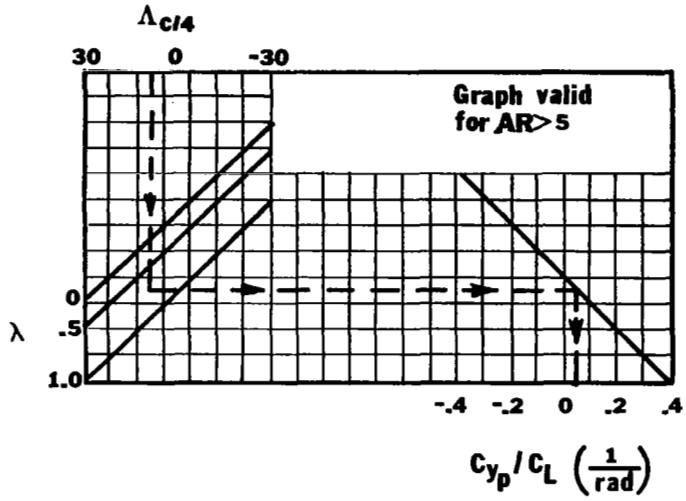

Figure 32. Values for (C_{y_p}/C_L) as a function of wing sweep and taper ratio.

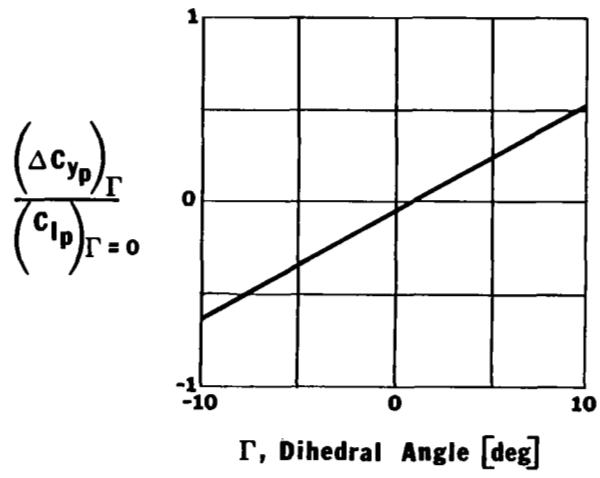

Figure 33. Values for $[(\Delta C_{y_p})_\Gamma/(C_{\ell_p})_{\Gamma=0}]$ as a function of dihedral angle.

TN-4066 (Ref. 36), which uses flight measurements to determine stability derivatives, states that, in practice, C_{y_p} may lie between 0.3 and -0.3. Using this range of C_{y_p}, the other stability derivatives were calculated, with C_{y_p} showing a small effect only on C_{y_β} and C_{n_p}. Thus, it appears that $C_{y_p} = 0.0$ is probably as accurate an estimate as is necessary.

C_{l_p}

The stability derivative $C\ell_p$, the roll damping derivative, is the change in rolling moment coefficient due to variation in rolling velocity. For a positive roll, $C\ell_p$ is the result, primarily, of an increase in lift on the down moving wing and a decrease in lift on the up moving wing, thus creating a moment which opposes the motion of the roll. This moment is negative, making $C\ell_p$ negative in sign. The wing, horizontal tail, and vertical tail contribute to $C\ell_p$, with the wing the dominant factor for airframes with conventional-size tails. $C\ell_p$ is the principal determinant of the damping-in-roll characteristics of the aircraft.

The basic wing contribution to $C\ell_p$ may be found from the graph below as a function of aspect and taper ratio for a wing with zero or small sweep, a lift coefficient of zero, and lift curve slope of 2π. For swept wings, the reader is referred to TR-1098 (Ref. 27), from which this figure was adapted.

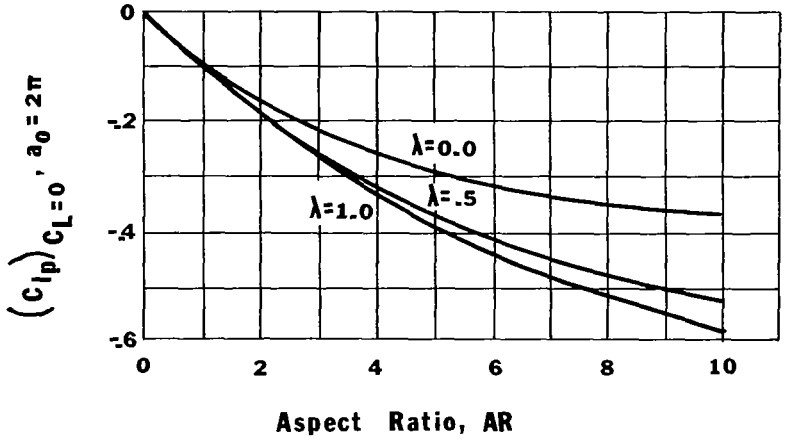

Figure 34. Wing contribution to $C\ell_p$ for wing with zero or small sweep.

The present study assumes a linear lift curve slope with no correction for non-linearities in lift coefficient. In order to use Figure 34 to calculate wing $C\ell_p$ for lift curve slopes other than 2π, several means of correcting the data must be considered. TN-1839 (Ref. 37) presents the following method:

$$(C\ell_p)_{(a_o)_w} = (C\ell_p)_{a_o} = 2\pi/\text{rad} \left[\frac{AR + 4\cos\Lambda}{\left(\frac{2\pi}{(a_o)_w}\right) AR + 4\cos\Lambda}\right],$$

which, for zero sweep, reduces to

$$(C\ell_p)_{(a_o)_w} = (C\ell_p)_{a_o} = 2\pi/\text{rad} \left[\frac{AR + 4}{\left(\frac{2\pi}{(a_o)_w}\right) AR + 4}\right].$$

The effect of wing dihedral on C_{ℓ_p} is considered by TN-1732 (Ref. 38) in a correction for wing C_{ℓ_p}; however, since most light aircraft have dihedral of seven degrees or less, this correction appears quite small. The drag contribution to wing C_{ℓ_p} is given in TN-1924 (Ref. 39), for swept wings with elliptic-chord distribution, by the following formula:

$$(C_{\ell_p})_{wing} = (C_{\ell_p})_{(a_o)_w} - \frac{1}{8} \frac{C_L^2}{\pi\, AR \cos^2 \Lambda} \left[1 + 2 \sin^2 \Lambda \frac{AR + 2 \cos \Lambda}{AR + 4 \cos \Lambda}\right] - \frac{1}{8} C_{D_o} ,$$

which reduces, for zero sweep, to the following relation:

$$(C_{\ell_p})_{wing} = (C_{\ell_p})_{(a_o)_w} - \frac{1}{8} \left(\frac{C_L^2}{\pi\, AR} + C_{D_o}\right) = (C_{\ell_p})_{(a_o)_w} - \frac{1}{8} C_{D_o},$$

where

C_D = experimentally determined drag coefficient.

Thus, for an aircraft with a linear lift curve slope, small dihedral, and zero sweep, the following formula for wing C_{ℓ_p} results:

$$(C_{\ell_p})_{wing} = \left[(C_{\ell_p})_{a_o = 2\pi}\right] \left[\frac{AR + 4}{\frac{2\pi}{(a_o)_w} AR + 4}\right] - \frac{1}{8} C_{D_o}.$$

By considering the horizontal tail as an isolated airfoil, the basic value for $(C_{\ell_p})_h$ may also be determined from Figure 34 as a function of horizontal tail aspect ratio, taper ratio, and amount of sweep. This procedure is the same as that for calculating the wing contribution; thus, $(C_{\ell_p})_h$ must be corrected for lift curve slope other than 2π. The value obtained is scaled down by the method of TR-1098 (Ref. 27):

$$(C_{\ell_p})_h = 0.5 \frac{S_h}{S_w} \left(\frac{b_h}{b_w}\right)^2 (C_{\ell_p})_{a_o = 2\pi/rad} \left[\frac{AR + 4 \cos \Lambda}{\frac{2\pi}{(a_o)_h} AR + 4 \cos \Lambda}\right] .$$

The factor 0.5 is included to account for the flow rotation at the tail caused by the wing; Λ is the amount of sweep of the horizontal tail. The horizontal tail is assumed to have negligible dihedral.

The vertical tail contribution to C_{ℓ_p} is also given in TR-1098 (Ref. 27):

$$(C_{\ell_p})_v = 2 \left(\frac{z_v}{b_w}\right)^2 (C_{y\beta})_{tail} ,$$

or

$$(C_{\ell_p})_v = 2 \left(\frac{z_v}{b_w}\right) \left[\frac{z_v}{b_w} - \left(\frac{z_v}{b_w}\right)_{\alpha = 0^o}\right] (C_{y\beta})_{tail} ,$$

where

z_v = height of center of pressure of vertical tail above the x-axis (different for each angle of attack).

From these formulas, it is obvious that the vertical tail contribution is negligible at low angles of attack. A much more elaborate formula for estimating vertical tail contribution is given in TN-2587 (Ref. 40), but because of the relative unimportance of this contribution to total $C\ell_p$, that method is not included.

In summary, for an aircraft with zero sweep a value for total $C\ell_p$ may be obtained by simply adding the various contributions as follows:

$$(C\ell_p)_{total} = \left[(C\ell_p)_{a_o = 2\pi}\right] \left[\frac{AR + 4}{(\frac{2\pi}{(a_o)_w})AR + 4}\right] - \frac{1}{8} C_D$$

$$+ 0.5 \frac{S_h}{S_w}(\frac{b_h}{b_w})^2 \left|(C\ell_p)_{a_o=2\pi}\right| \left[\frac{AR + 4}{(\frac{2\pi}{(a_o)_h})AR + 4}\right]$$

$$+ 2.0 (\frac{z_v}{b_w}) \left[\frac{z_v}{b_w} - (\frac{z_v}{b_w})_{\alpha = 0^o}\right] (C_{y\beta})_{tail} .$$

An adaptation from TN-1309 (Ref. 41) for various sideslip angles is

$$(C\ell_p)_{total} = \left[(C\ell_p)_{total}\right]_{\beta = 0^o} \cos^2 \beta \quad .$$

Typical values of $C\ell_p$ range from -.25 per radian to -.60 per radian.

C_{n_p}

The stability derivative C_{n_p} is the change in yawing moment caused by rolling, with the wing and vertical tail the main contributors. For a positive roll, the produced yawing moment is a result of the unsymmetrical lift distribution causing increased drag on the left wing and decreased drag on the right wing and is, therefore, negative. The vertical tail contribution may be either positive or negative, depending on tail geometry, angle of attack, and sidewash from the wing. Dutch Roll damping is influenced by C_{n_p} in that the larger its negative value, the less Dutch Roll damping. therefore, a positive C_{n_p} is desired.

Using an elliptical lift distribution, Perkins and Hage (Ref. 11) give the following formula for C_{n_p}:

$$(C_{n_p})_W = -\frac{C_L}{8} .$$

The results of wind tunnel testing on a wing with AR = 5.16, λ = 1.0, and 0^o wing sweep is reported in TR-968 (Ref. 33). The resulting formula for $(C_{n_p})_W$, by a curve fit, is

$$(C_{n_p})_W = -.043\ C_L - .0044$$

for $0 < C_L < 1.05$. This report shows that, for large C_L (in the stall region), C_{n_p} reverses signs, and large positive values are obtained. This same trend occurs at smaller C_L when sweepback is encountered. Below is a formula for use with sweepback, from TN-1581 (Ref. 28).

$$(C_{n_p})_W = C_L \frac{AR + 4}{AR + 4\cos\Lambda}\left[1 + 6\left(1 + \frac{\cos\Lambda}{AR}\right)\frac{\tan^2\Lambda}{12}\right]\left(\frac{C_{n_p}}{C_L}\right)_{\Lambda = 0^o}$$

The ratio $(C_{n_p}/C_L)_{\Lambda = 0^o}$ as a function of aspect ratio and taper ratio may be obtained from the following figure.

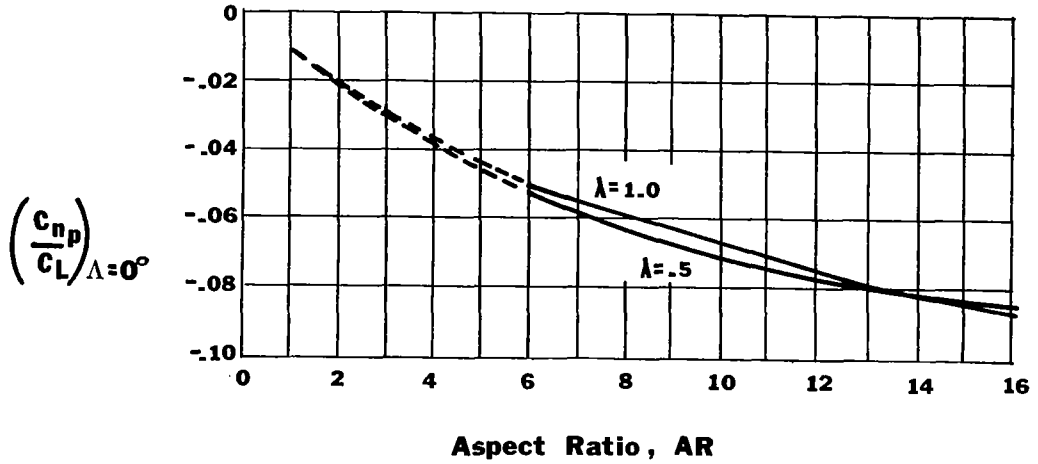

Figure 35. Values of (C_{n_p}/C_L) for zero sweep.

TN-2587 (Ref. 40) explains, through the following formula, how the vertical tail contribution to C_{n_p} is influenced by sidewash variations:

$$(C_{n_p})_V = 57.3\, a_V \frac{S_V}{S_W}\frac{1}{b_W}(z_V \sin\alpha + \ell_V \cos\alpha)\left[\frac{2}{b_W}(z_V \cos\alpha - \ell_V \sin\alpha) - \left(\frac{\partial\sigma_1}{\partial\frac{pb}{2U}} + \frac{\partial\sigma_2}{\partial\frac{pb}{2U}}\right)\right].$$

Values for $\partial\sigma_1/[\partial(pb/2U)]$, effect of wing sidewash, as a function of $(h_t/b_{W/2})$, may be obtained from the following graph, reproduced from TN-2332 (Ref. 42), for wings with aspect ratios in the vicinity of six, where h_t is the distance from the wing centerline to the center of pressure of the vertical tail (positive above the wing centerline).

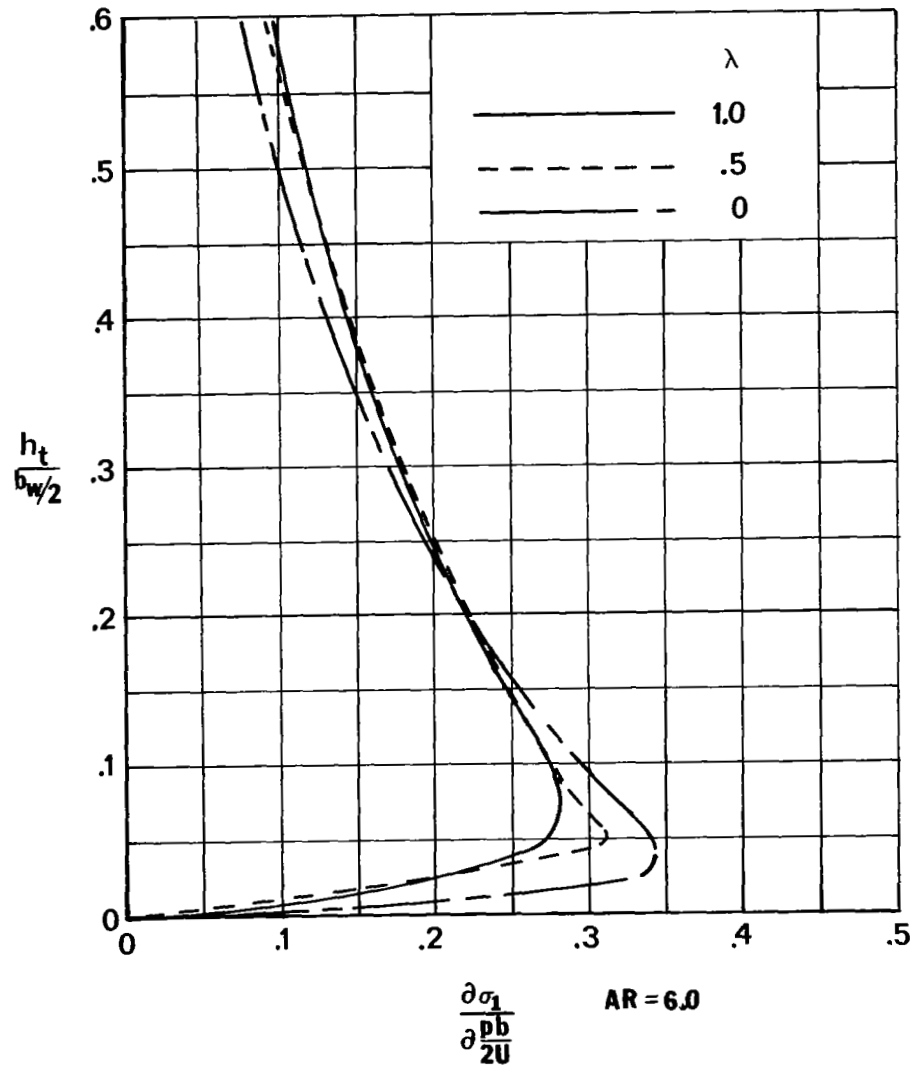

Figure 36. Effect of wing sidewash on vertical tail.

The effect of fuselage sidewash, $\partial\sigma_2/[\partial(pb/2U)]$, may be determined from the following formula adapted from TN-2587 (Ref. 40):

$$\frac{\partial\sigma_2}{\partial\frac{pb}{2U}} = 9.30\left(\frac{\Delta h}{b_w}\right)^2 \frac{3}{b_w},$$

where

$$\frac{\Delta h}{b_w} = \frac{z_v - (z_v \cos\alpha - \ell_v \sin\alpha)}{b_w}.$$

For zero angle of attack, this sidewash factor reduces to zero and is quite small for low angles of attack. With these factors, a value of $(C_{n_p})_v$ can be determined and added to the wing contribution to yield total C_{n_p}.

$$(C_{n_p})_{total} = (C_{n_p})_w + (C_{n_p})_v$$

Typical values for C_{n_p} range from -.01 per radian to -.10 per radian.

C_{y_r}

The stability derivative C_{y_r} is the change in side force resulting from a change in yawing velocity. As the airframe undergoes a positive yaw, an effective positive side force develops on the vertical tail, which is the dominant contributor to C_{y_r}. Since this force is normally small, C_{y_r} usually has a small positive value.

The wing contribution is normally negligible, as indicated by TN-1669 (Ref. 43), which is the result of wind tunnel tests on rectangular wings with zero sweep and aspect ratio of 5.16. The following formula is produced by curve-fitting the data of this report, which gives $(C_{y_r})_{wing}$ as a function of lift coefficient for an angle of attack below the stall region:

$$(C_{y_r})_w = .143\ C_L - .05.$$

The tail contribution may be estimated by the formula below from TR-1098 (Ref. 27) which gives $(C_{y_r})_{tail}$ as a function of the values for $(C_{y\beta})_{tail}$ or $(C_{n\beta})_{tail}$ discussed in connection with the stability derivative $C_{y\beta}$ in the present study:

$$(C_{y_r})_{tail} = -\ 2\ \frac{\ell_v}{b}(C_{y\beta})_{tail},$$

or

$$(C_{y_r})_{tail} = 2\ (C_{n\beta})_{tail}.$$

For wind tunnel tests of a model oscillating in yaw, TR-1130 (Ref. 44) indicates that much larger values for C_{y_r} are obtained than from other testing methods. These results are presented graphically in Figure 37, including fuselage, wing, and tail effects. The fuselage effects are relatively large and negative in sign.

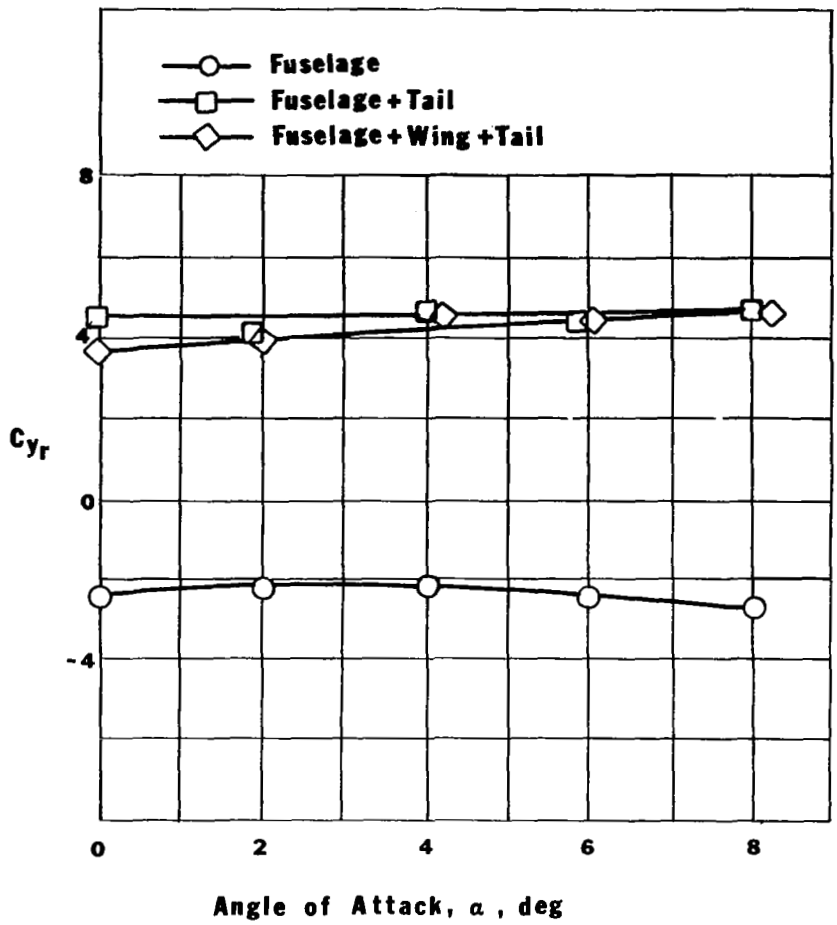

Figure 37. Values for fuselage, wing, and tail contributions to C_{y_r}.

TN-4066 (Ref. 36), which utilizes flight test data to calculate stability derivatives, indicates that C_{y_r} could range from -0.3 to 0.3 without showing any significant effects on the other stability derivatives. This helps demonstrate the insignificance of C_{y_r} to the lateral stability of light aircraft.

C_{l_r}

The change in rolling moment due to variation in yawing velocity constitutes the stability derivative C_{ℓ_r}. The wing provides the major contribution, with the vertical tail having a minor effect. When there is a positive yaw rate, the left wing moves faster than the right wing, producing more lift on the left wing and, consequently, a positive rolling moment. The tail contribution may be either positive or negative, depending on tail geometry and angle of attack of the airplane. Although C_{ℓ_r} has little effect on Dutch Roll damping, it is quite important to the spiral mode. For spiral stability, it is desirable that C_{ℓ_r} be as small a positive number as possible.

The wing contribution to C_{ℓ_r} is presented in TR-589 (Ref. 45) as a function of lift coefficient by the following formulas:

$$(C_{\ell_r})_{wing} = C_L/3 \text{ for rectangular lift distribution,}$$

or

$$(C_{\ell_r})_{wing} = C_L/4 \text{ for an elliptical lift distribution.}$$

In TN-1669 (Ref. 43), the results of wind tunnel tests of a NACA 0012 airfoil of aspect ratio 5.16 and zero sweep indicate that $(C_{\ell_r})_{wing} = C_L/4$ agrees with experimental data for lift coefficients below the stall regime. The wing contribution to C_{ℓ_r} as a function of aspect ratio, taper ratio, and sweep angle is presented in Figure 38, adapted from Datcom (Ref. 10).

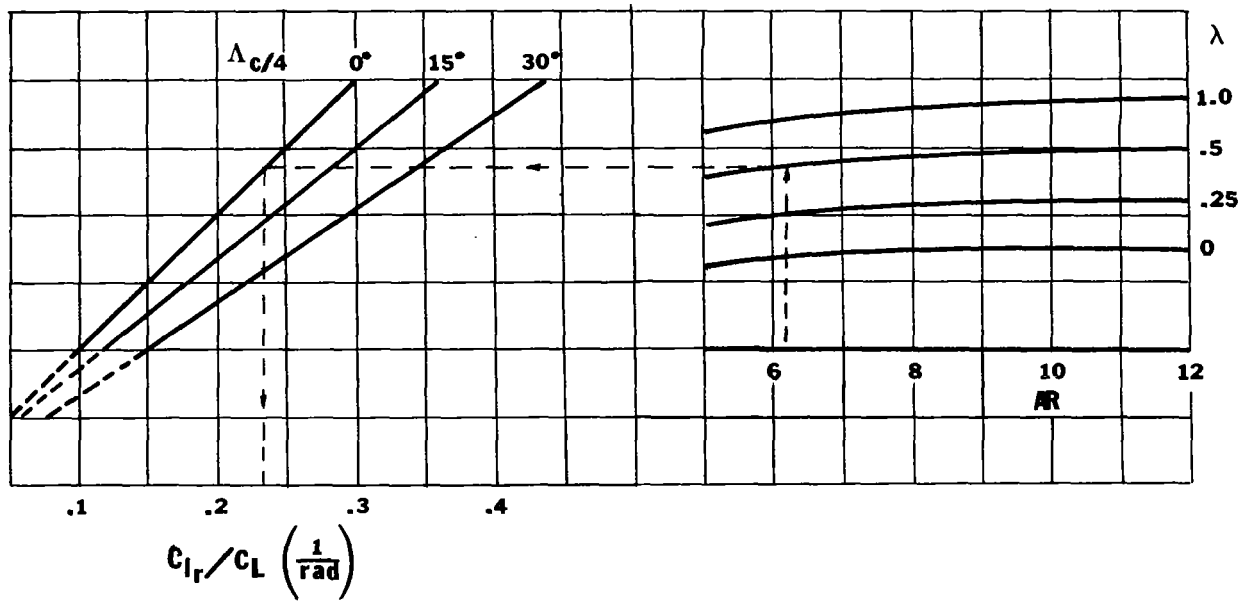

Figure 38. Wing contribution to C_{ℓ_r} as a function of aspect ratio, taper ratio, and sweep angle.

The minor contribution of the vertical tail to C_{ℓ_r} may be calculated from the formula below from TN-1984 (Ref. 46):

$$(C_{\ell_r})_{tail} = -2 \frac{\ell_v}{b_w} \frac{z_v}{b_w} (C_{y\beta})_{tail},$$

or

$$(C_{\ell_r})_{tail} = -2 \frac{\ell_v}{b_w} (C_{\ell_\beta})_{tail} .$$

By adding the wing and vertical tail contributions, total C_{ℓ_r} may be determined.

Typical values of C_{ℓ_r} range from .04 per radian to .12 per radian.

C_{n_r}

C_{n_r}, commonly known as the yaw damping derivative, is the change in yawing moment due to variation in yawing velocity. As the airframe undergoes a positive r, a yawing moment which opposes the motion is produced. This moment consists of contributions from the wing, fuselage, and vertical tail, all of which are negative in sign. TN-1080 (Ref. 47) states that the vertical tail contributes about 70% to 90% of C_{n_r} for conventional designs. The derivative C_{n_r} is the main contributor to the damping of the Dutch Roll mode and also plays a significant role in determining spiral stability, making it vital to lateral stability. For best effects in each of these modes, large negative values of C_{n_r} are desired.

The wing contribution to C_{n_r} as a function of lift and drag coefficients is given in TR-1098 (Ref. 27) by the following relation:

$$(C_{n_r})_{wing} = C_L^2 \left[(\Delta C_{n_r})_1 / C_L^2\right] + C_{D_o} \left[(\Delta C_{n_r})_2 / C_{D_o}\right] .$$

Originally presented in TN-1581 (Ref. 28), this formula is the result of simple sweep theory with strip integration; consequently, $\left[(\Delta C_{n_r})_1 / C_L^2\right]$ and $\left[(\Delta C_{n_r})_2 / C_{D_o}\right]$ are functions of sweep, taper ratio, and aspect ratio. For wings with zero sweep and aspect ratio greater than five, however, these terms are constant at the following approximate values:

$$\frac{(\Delta C_{n_r})_1}{C_L^2} = -0.020 ,$$

and

$$\frac{(\Delta C_{n_r})_2}{C_{D_o}} = -0.30 .$$

With these restrictions, the above formula reduces to

$$(C_{n_r})_{wing} = -0.02\ C_L^2 - 0.3\ C_{D_o} .$$

The graph that follows from TN-1669 (Ref. 43) shows, for a rectangular wing, the close agreement between the above theory and experimental data for wing contribution to C_{n_r}.

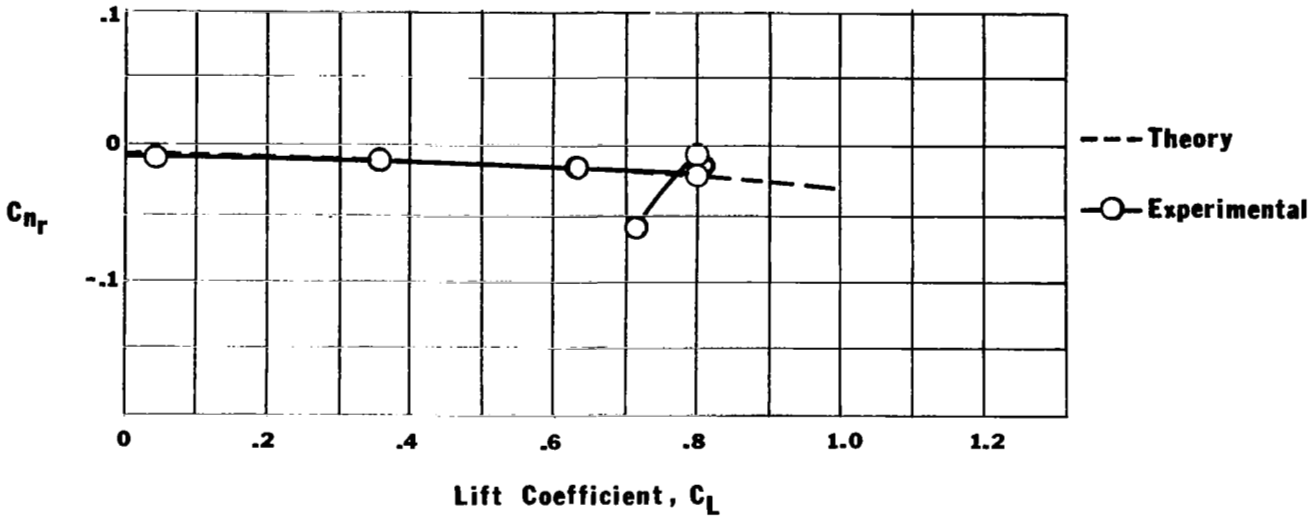

Figure 39. Results of experimental data on wing contribution to C_{n_r}.

This graph points out the relative insignificance of wing contribution to C_{n_r}.

The tail contribution to C_{n_r} is presented in TR-1098 (Ref. 27), as follows:

$$(C_{n_r})_{tail} = 2 \left(\frac{\ell_v}{b_w}\right)^2 (C_{y\beta})_{tail} ;$$

Blakelock (Ref. 18) treats this contribution as,

$$(C_{n_r})_{tail} = -2 \frac{S_v}{S_w} \left(\frac{\ell_v}{b_w}\right)^2 (C_{L\alpha})_v \eta_v .$$

The vertical tail efficiency factor, η_v, compensates for the interference between the fuselage and the vertical tail. When there is no interference, η_v is equal to one. Total C_{n_r} is then determined by adding the wing and vertical tail contributions, since the fuselage contribution is negligible.

Another approach to calculating total C_{n_r} is free-oscillation tests, as presented in WR L-387 (Ref. 48). These tests on a mid-wing airplane include effects of wing, fuselage, and vertical tail on C_{n_r}. The wing contribution is calculated as

$$(C_{n_r})_{wing} = -.33 \left(\frac{1 + 3\lambda}{2 + 2\lambda}\right) C_{D_o} - .02 \left(1 - \frac{AR - 6}{13} - \frac{1 - \lambda}{2.5}\right) C_L^2 ,$$

which, for an aspect ratio of six and taper ratio of one, seems to agree closely with the previous formula for wing contribution. WR L-387 (Ref. 48) also

states that the fuselage contribution often ranges from -.003 to -.006, small enough to be neglected. The vertical tail contribution from Reference (48) is

$$(C_{n_r})_{tail} = -2\left(\frac{\ell_v}{b_w}\right)(C_{n_\beta})_{tail} .$$

Combining these two formulas, the result is the empirical expression below, showing C_{n_r} for a conventional, mid-wing airplane:

$$C_{n_r} = -2\left(\frac{\ell_v}{b_w}\right)(C_{n_\beta})_{tail} - \left[.33\left(\frac{1+3\lambda}{2+2\lambda}\right)C_{D_o} + .02\left(1 - \frac{AR-6}{13} - \frac{1-\lambda}{2.5}\right)C_L{}^2\right] .$$

Typical values of C_{n_r} for general aviation aircraft range from -.05 per radian to -.14 per radian.

$C_{y_{\delta_A}}$

The stability derivative $C_{y\delta_A}$ is the change in side force coefficient with variation in aileron deflection. For most conventional light aircraft, this derivative is zero; however, for an airframe with low aspect ratio and highly swept wings, it may have a value other than zero.

$C_{l_{\delta_A}}$

The stability derivative $C_{\ell_{\delta_A}}$, known as the aileron effectiveness or "aileron power", is the variation in rolling moment coefficient with change in aileron deflection. Since left aileron down is defined as positive, a positive deflection produces a rolling moment to the right, which is also positive, making $C_{\ell_{\delta_A}}$ positive. Desirable values of $C_{\ell_{\delta_A}}$ are given in terms of the wing tip helix angle (pb/2U) for a full aileron deflection. For light aircraft, this range is normally from 0.07 to 0.08 radians. In Perkins and Hage (Ref. 11), strip integration can be used to evaluate $C_{\ell_{\delta_A}}$ as,

$$C_{\ell_{\delta_A}} = \frac{2(C_{L_\alpha})_w \tau}{S_w b_w} \int_a^b c\, y\, dy.$$

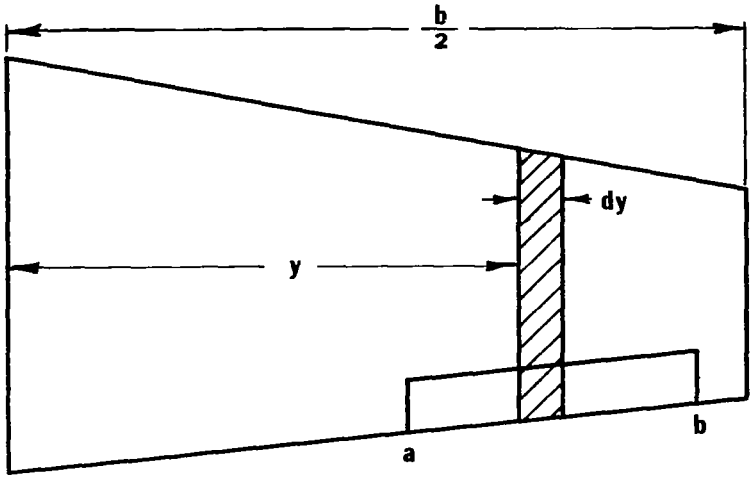

Figure 40. Illustration of strip integration.

In order to integrate, the chord, c, as a function of the spanwise distance, y, must be known. For straight, tapered wings, this relationship is

$$c = c_R \left[1 - \frac{y}{b_w/2} (1 - \lambda)\right],$$

where

c_R = root chord.

The value of τ may be obtained from the following graph as a function of aileron chord to wing chord ratio.

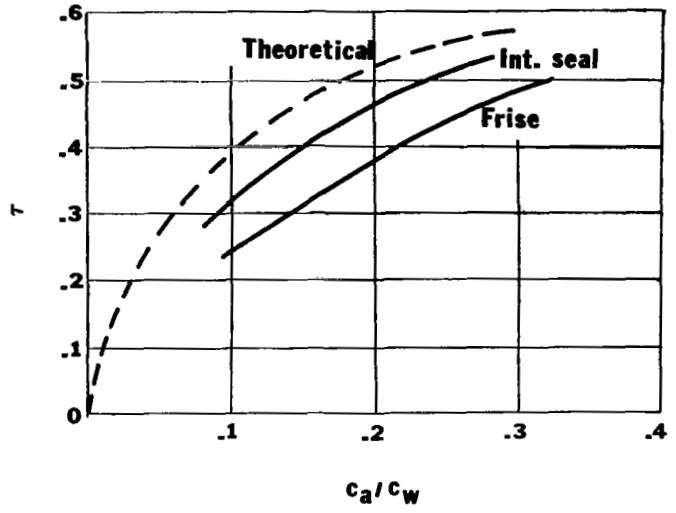

Figure 41. Values for τ as a function of aileron chord to wing chord ratio.

The method of strip integration presented above is seldom used in practice because of large errors incurred in assuming a discontinuous lift distribution. In reality, the lift distribution adjusts to the aileron deflection quickly but smoothly. This being the case, the value of $C_{l_{\delta_A}}$ is normally found from the spanwise load distribution data as presented in TR-635 (Ref. 49). These data are reproduced below for $(C_{l_{\delta_A}}/\tau)$ as a function of the extent of the unit antisymmetrical angle of attack.

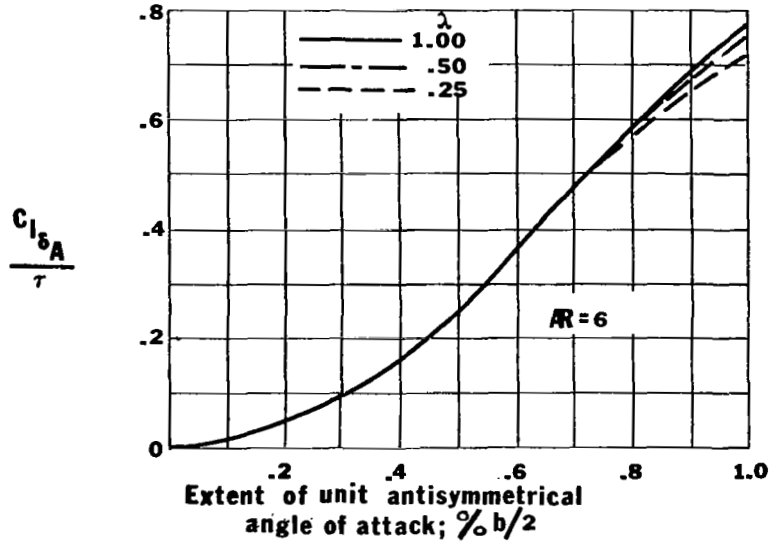

Figure 42. Values for $(C_{l_{\delta_A}}/\tau)$ as a function of the extent of unit antisymmetrical angle of attack.

A value of $(C\ell_{\delta_A}/\tau)$ is obtained from Figure 42 by first using the distance from the body centerline to the outboard edge of the aileron divided by the wing semispan to get a value, from which is subtracted a value obtained by using the distance from the body centerline to the inboard edge of the aileron divided by the wing semispan. The value of $(C\ell_{\delta_A}/\tau)$ from the graph is multiplied by a value of τ from the preceding graph to give $C\ell_{\delta_A}$ per radian.

Typical values of $C\ell_{\delta_A}$ range from 0.1 to 0.25 per radian.

$C_{n_{\delta_A}}$

The stability derivative $C_{n\delta_A}$, the change in yawing moment coefficient with variation in aileron deflection, results from the difference between drag on the up and down ailerons. Since a positive deflection is with the aileron on the left wing down, $C_{n\delta_A}$ is usually negative, even though it is heavily dependent on the position and size of the ailerons and the angle of attack of the airframe. A negative value for $C_{n\delta_A}$ is known as "adverse yaw coefficient due to ailerons" because it is the result of initial yawing of the airframe in a direction opposite that desired for a turn. Thus, the desired value of $C_{n\delta_A}$ is either zero or a very small positive value.

To compute a value for $C_{n\delta_A}$, a formula, adapted partially from Datcom (Ref. 10), is

$$C_{n\delta_A} = 2K\, C_L\, C_{\ell_{\delta_A}}.$$

Here, δ_A is again positive for left aileron down and right aileron up, with K being an empirical factor obtained from the following graph.

$$\eta = \frac{Y_i}{b_w/2} = \frac{\text{spanwise distance from centerline to the inboard edge of the control surface}}{\text{semispan}}$$

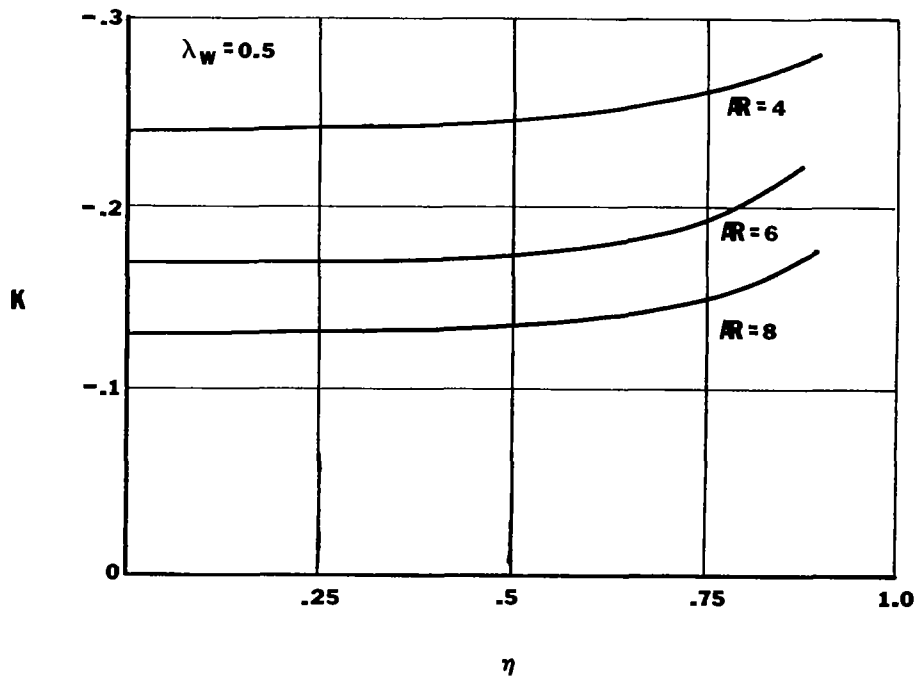

Figure 43. Empirical factor K as a function of η for taper ratio = 0.5.

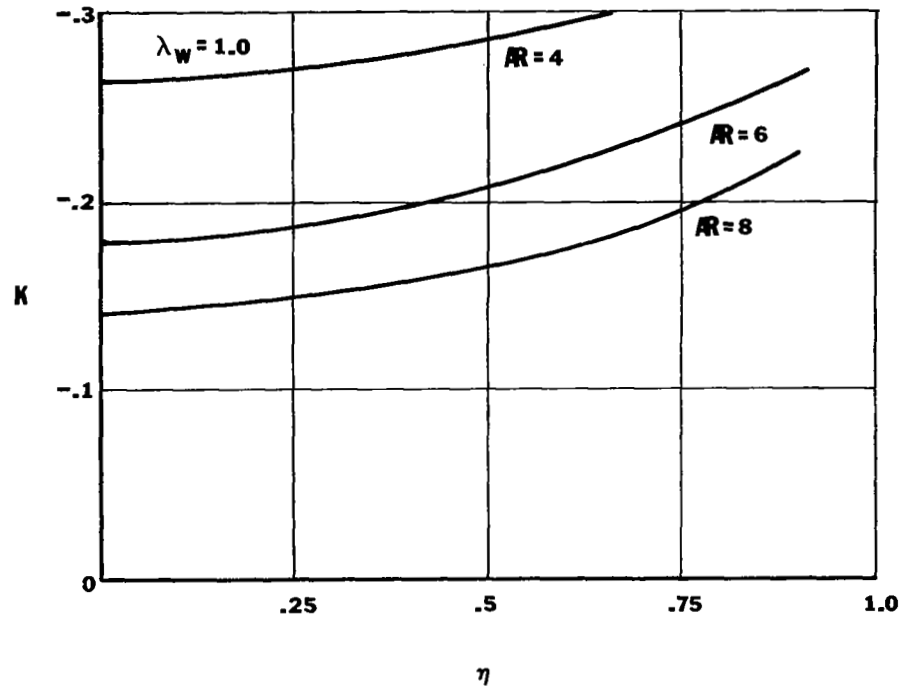

Figure 44. Empirical factor K as a function of η for taper ratio = 1.0.

Typical values of $C_{n\delta_A}$ range from -0.004 to -0.09 per radian.

$C_{y_{\delta_R}}$

The stability derivative $C_{y_{\delta_R}}$ is the change in side force resulting from rudder deflection. For a positive rudder deflection, or rudder toward the left wing, a positive side force results; hence, the value of $C_{y_{\delta_R}}$ is positive.

For an airplane without autopilot, the effect of $C_{y_{\delta_R}}$ is relatively unimportant to lateral stability and often is assumed equal to zero.

In Etkin (Ref. 50), the following formula for estimating $C_{y_{\delta_R}}$ is set forth:

$$C_{y_{\delta_R}} = a_v \tau \frac{S_v}{S_w} ,$$

where

a_v = lift curve slope of the vertical tail (calculated as shown in discussion of C_{n_β}),

τ = a function of rudder area to vertical tail area ratio as found from the graph below.

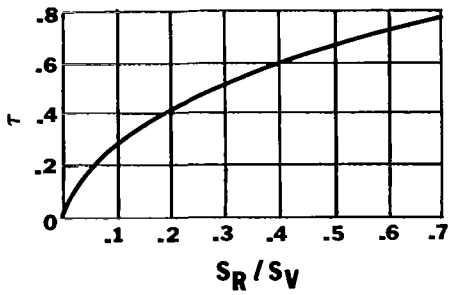

Figure 45. Values for τ as a function of rudder area to vertical tail area ratio.

Typical values of $C_{y_{\delta_R}}$ range from .12 per radian to .24 per radian.

$C_{l_{\delta_R}}$

The stability derivative $C_{\ell_{\delta R}}$ is the variation in rolling moment coefficient with change in rudder deflection. Because the rudder is normally located above the x-axis, a positive rudder deflection (rudder to the left) causes a positive rolling moment, making $C_{\ell_{\delta R}}$ positive. This value may possibly be negative for an unusual airframe configuration or an abnormal angle of attack. For conventional light aircraft, this derivative is of only minor importance and is usually neglected.

The following formula adapted from Etkin (Ref. 50) may be used to determine $C_{\ell_{\delta R}}$:

$$C_{\ell_{\delta R}} = a_V \tau \frac{S_V}{S} \frac{z_V}{b_W}$$

where

z_V = distance from the x-axis to aerodyanmic center of the vertical tail

The value of τ may be obtained from the graph below as a function of rudder area to vertical tail area ratio.

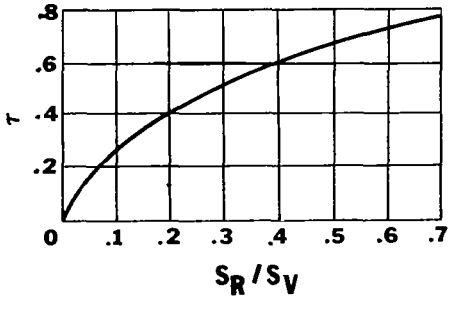

Figure 46 Values for τ as a function of rudder area to vertical tail area ratio.

$C_{n_{\delta_R}}$

The stability derivative $C_{n\delta_R}$ is the variation in yawing moment coefficient with a change in rudder deflection. Also known as the "rudder power," this derivative is negative, since a positive rudder deflection toward the left wing creates a negative yawing moment.

Perkins and Hage (Ref. 11) give

$$C_{n\delta_R} = - a_V \tau \frac{S_V}{S_W} \frac{\ell_V}{b_W} \eta_V .$$

The value of τ may be obtained from the following graph for a particular rudder area to vertical tail area ratio.

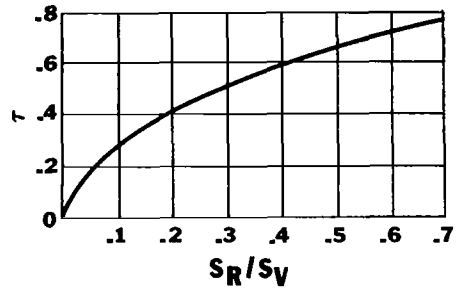

Figure 47. Values for τ as a function of rudder area to vertical tail area ratio.

The value of $C_{n\delta_R}$ is normally on the order of -.06 per radian but may vary greatly, depending on the airframe configuration. Power has a great effect on $C_{n\delta_R}$, as seen in the following graph from TR-781 (Ref. 51) for a single engine plane with propeller rotating to the right, flying at a speed of 111 miles per hour.

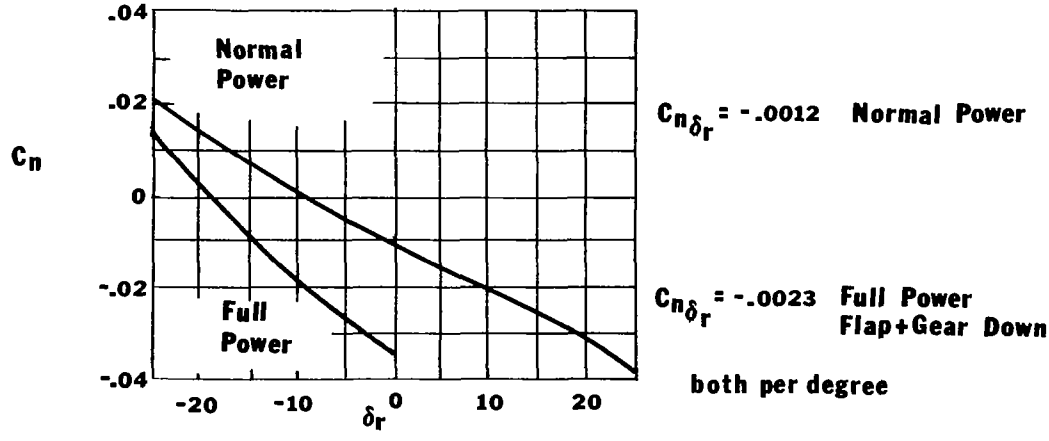

Figure 48. Effect of aircraft power on $C_{n\delta_R}$.

POWER EFFECTS

Although the primary function of a propulsion system is to overcome airplane drag, the location of the system with respect to aerodynamic surfaces may influence some aerodynamic parameters and, ultimately, aircraft stability. Thus, as wing loadings increase, more pronounced power effects are to be expected. The literature indicates that analytical determination of power effects for light aircraft is, at best, an approximation. Many references suggest only the origin of a particular effect and estimate only its order of magnitude. The following will discuss the significant reports dealing with power, the characteristic changes to be expected in longitudinal and lateral stability due to power application, and the analytical procedure given in Datcom (Ref. 10) for estimating the effects of power on longitudinal stability.

Power effects for light aircraft can usually be classified as 1) direct propeller effects and 2) slipstream effects, with more accurate estimation possible for propeller than for slipstream effects. Since the engine is directly in front of the horizontal and vertical tails, the slipstream effects on single engine aircraft may be more difficult to predict than those on twin or multiengine aircraft, especially in the lateral mode. The lack of documentation on ways to predict analytically the effects of power on lateral stability bears out this conclusion.

The need for higher-powered aircraft during World War II led to considerable interest in effects of power on aircraft stability. WR L-710 (Ref. 102) indicates that power has a significant influence on both the longitudinal and lateral stability and control characteristics. Using this report, one concludes that power applied to single-engine, low-wing models decreases longitudinal stability and effective dihedral. Directional stability and rudder and elevator effectiveness were usually increased by applications of power. At the same time, the report warns that power-on wind tunnel tests should be used to predict actual flight stability and control, lest the researcher be misled by theoretical data.

NACA TR-690 (Ref. 103) is a report of the effects of propeller operation on the flow about eight wind tunnel models. A tabulation of downwash angles, the dynamic pressures at the tail, and the pitching-moment contribution of the propeller and the wing is presented. TR-941 (Ref. 104) correlates some pertinent experimental data on power effects obtained during the War Years. It gives semiempirical procedures to predict power-on longitudinal stability characteristics with flaps undeflected, and agrees well with experimental data.

In two Technical Notes, 1339 (Ref. 105) and 1379 (Ref. 106), Hagerman discusses the effects of power on the longitudinal and lateral stability of a single-engine, high-wing airplane model. He found that, for longitudinal stability, power greatly increased the lift increments and the tail-off lift curve slope while, in general, it decreased the stability of the model for all three flap configurations tested. For lateral stability, application of power had no effect on the effective dihedral, with the flap neutral; however, with both single and double slotted flaps deflected, power increased the effective dihedral. The directional stability of the entire model was increased except with flaps neutral at low lift coefficients. Rudder effectiveness was decreased

with flaps neutral and double slotted flaps deflected and increased with single slotted flaps deflected. Trim changes caused by power were small, indicating good control. TN 1327 (Ref. 107) on lateral stability, written about the same time as Hagerman's work, reveals that power decreased the dihedral effect regardless of the flap condition, increased the directional stability, and increased overall lateral stability as lift coefficient was increased.

The problem of power effects also justified the investigation undertaken in TN 1474 (Ref. 108), which sought to off-set power effects by using an unsymmetrical tail on the single-engine airplane. Although the tests and analyses showed that extreme asymmetry in the horizontal tail indicated a reduction in power effects on the longitudinal stability, the "practical" arrangement tested did not show marked improvement. Three years after the asymmetric investigation, a dynamic free-flight study of dynamic longitudinal stability as influenced by static stability measured in wind-tunnel force tests under conditions of constant thrust and constant power was undertaken. (Ref. 109) The results agreed with previous studies that the longitudinal "steadiness" of airplanes is affected to a much greater extent by changes in constant-thrust static margin than by changes in constant-power static margin.

TN D-3726 (Ref. 110), a recent report directly related to light aircraft, discusses the effects of power on the landing configuration stick-fixed and stick-free static longitudinal stability for the aircraft (including both twin and single engine aircraft) with the most pronounced power effects. When the power was cycled from approach to maximum at an airspeed of 80 knots the pilot had to push with a force of approximately eight pounds to counter the resulting nose-up pitch. This characteristic also presented a problem when the power was being reduced in the landing phase. For light aircraft, power effects caused by propeller slipstream can become quite large. At a speed of 110 knots, approximately 10 degrees of rudder and 90 pounds of force was required to maintain heading when changing power from maximum to idle. This was considered excessive by the pilot.

Another recent paper (Ref. 111) on light aircraft gives methods for analyzing power-on static longitudinal stability. The methods are similar to those given in Datcom (Ref. 10); however, the paper also describes how power effects can be analyzed using airplane stick force, elevator deflection, and neutral points. The method utilizes a point-to-point calculation technique for each speed or load factor variation from trim.

In 1969 and 1970, NASA investigated longitudinal and lateral stability characteristics of both a light single engine and a light twin engine aircraft in a full scale tunnel (Refs. 112 and 113). These investigations were carried out for several conditions of power, as indicated by the extensive data in each report. These two reports may be used either to obtain a rough estimate or to help verify the exactness of analytical procedures for estimating power effects on aircraft similar to those investigated.

Although the literature mentioned above may give the general trends for power effects, analytical techniques are often hard to find, cumbersome to use, and inaccurate. For the present, Datcom (Ref. 10) probably gives the best analytical procedures for predicting power effects. They are extensions from those of Perkins and Hage (Ref. 11), among others (Refs. 114 and 115), with improvements added where possible. Datcom's methods of estimating power effects on lift and

pitching moment variation with angle of attack are summarized below. Curves of both ΔC_L and ΔC_m versus α can be plotted for several flight conditions using these procedures; thus, C_{L_α} and C_{m_α} due to power can be evaluated. Scrutiny of the present discussion points out that the estimation of power effects deals only with static longitudinal stability. It would seem that an approximation of power effects for the dynamic derivatives could be achieved by estimating the change in η_t with power, computed analytically in a similar manner to that given below, and using this corrected value. Some of the methods given can also be used to estimate lateral stability derivative changes with power. For example, $(C_{N_\alpha})_p$ is analagous to $(C_{y_\psi})_p$ or $(-C_{y_\beta})_p$ for cruising flight and could be used to estimate $(C_{y_\psi})_p$ or $(C_{y_\beta})_p$. When approached from the engineering viewpoint, similar methods could also be used in determining slipstream effects on the vertical tail.

Again the reader should remember that, at best, analytical prediction of power effects is crude.

Lift Increment Due to Propeller Thrust

$$(\Delta C_L)_T = nC_T \sin \alpha_T$$

where
n = number of engines
α_T = thrust axis angle of attack to free stream in degrees

Lift Increment Due to Propeller Normal Force

$$(\Delta C_L)_{N_p} = \frac{nN_p}{qS_w} \cos \alpha_T = nf(C_{N_\alpha})_p (\alpha_p)\left(\frac{S_p}{S_w}\right) \cos \alpha_T \text{ (per radian)}$$

where α_p = angle between local airstream and thrust in degrees
S_p = propeller disc area
f = propeller inflow factor
$(C_{N_\alpha})_p$ = propeller normal-force derivative at $T_c' = 0$ per radian

$$\alpha_p = \alpha_T - \frac{\partial \varepsilon_u}{\partial \alpha}(\alpha_w - \alpha_o)$$

where α_o = wing angle of attack for zero lift in degrees
$\frac{\partial \varepsilon_u}{\partial \alpha}$ = wing upwash derivative given in Figure 49.

The factor f accounts for the increase in velocity at the propeller plane due to the induced flow of the propeller and is given in Figure 50 as a function of

$$\frac{S_w C_T}{8R_p^2}$$

where R_p = propeller radius in feet.

$$(C_{N_\alpha})_p = \left[(C_{N_\alpha})_p\right]_{K_N=80.7} \left[1 + 0.8\left(\frac{K_N}{80.7} - 1\right)\right] \quad \text{(per radian)}$$

where $K_N = 262\left(\frac{b_p}{R_p}\right)_{.3R_p} + 262\left(\frac{b_p}{R_p}\right)_{.6R_p} + 135\left(\frac{b_p}{R_p}\right)_{.9R_p}$ (per blade)

with b_p = blade width in feet

$\left[(C_{N_\alpha})_p\right]_{K_N=80.7}$ = propeller normal-force derivative at C_T and given in Figure 51 as a function of β, the nominal blade angle at 0.75 radians; this blade angle should be obtained from a performance engineer or from a power plant engineer.

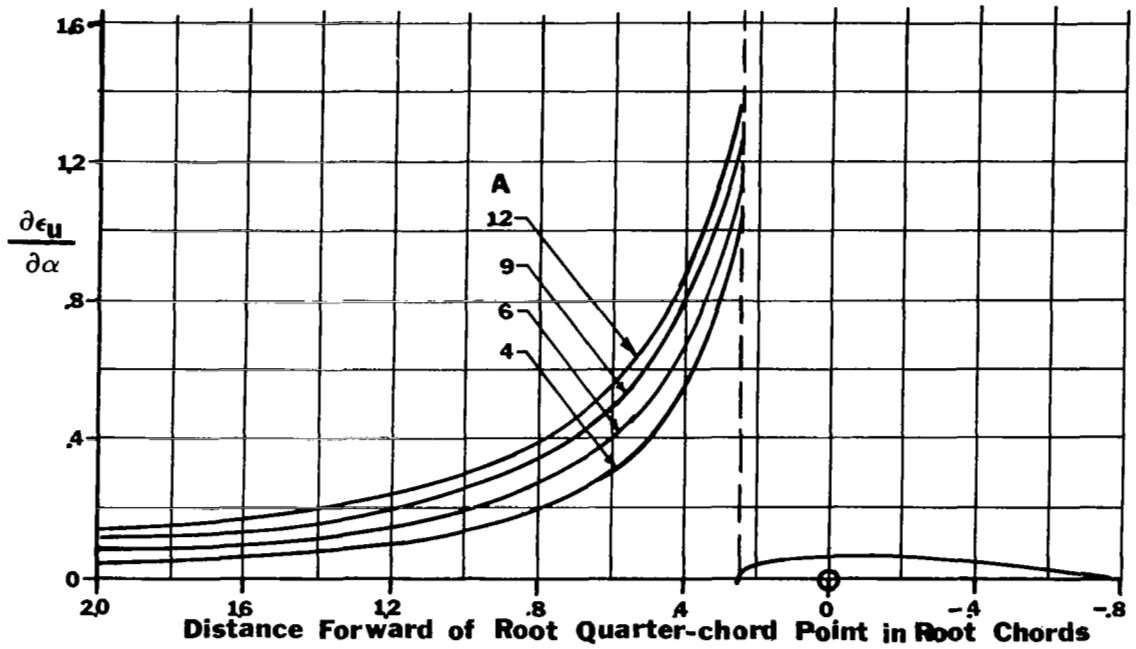

Figure 49. Upwash gradient at plane of symmetry for unswept wings.

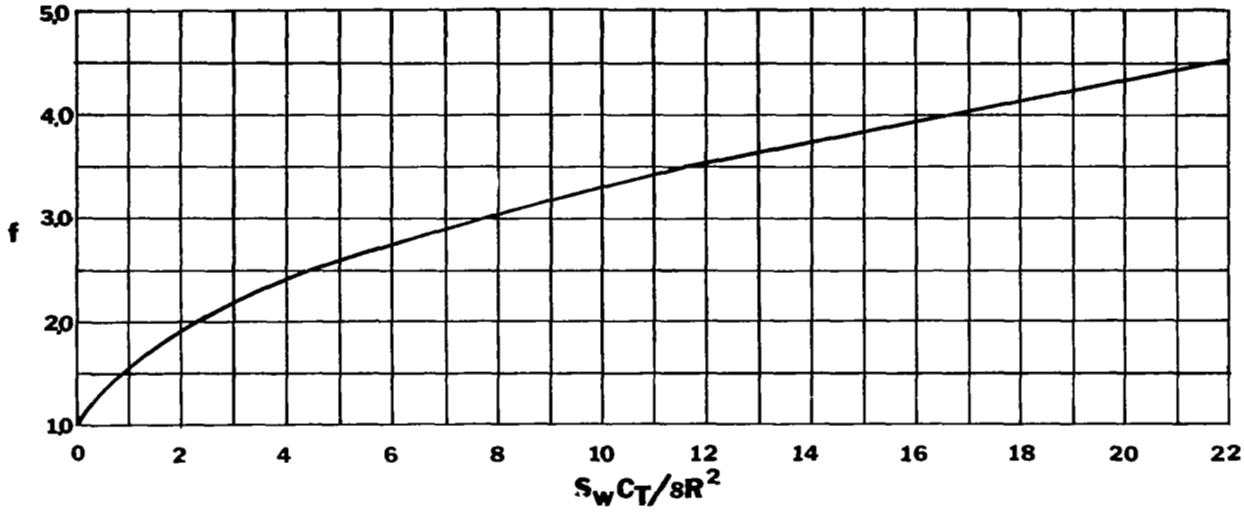

Figure 50. Propeller inflow factor.

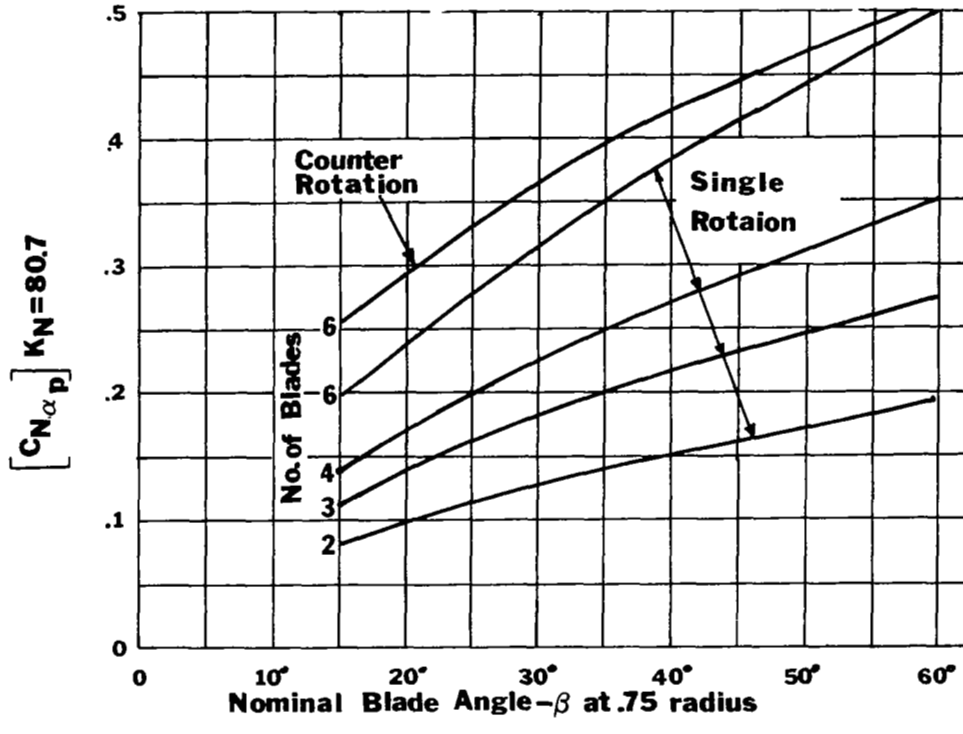

Figure 51. Propeller normal force parameter.

Lift Increment Due to a Change in Slipstream Dynamic Pressure on the Wing

$$(\Delta C_L)_{\Delta\eta_s} = K_1 \Delta\eta_s \, (C_L)_{\substack{\text{prop} \\ \text{off}}} \frac{S_i}{S_w}$$

where K_1 = correction parameter for additional wing lift due to power and given in Figure 52, where AR_i = effective aspect ratio of wing immersed in the slipstream,

$A_i = 2R_p/c_i$,

c_i = average chord of wing immersed in slipstream.

$\Delta\eta_s = \frac{\Delta q_s}{q}$ = ratio of change in dynamic pressure in propeller slipstream to freestream dynamic pressure and given by

$$\Delta\eta_s = \frac{S_w C_T}{\pi R_p^2} \text{ (per engine).}$$

S_i = wing area immersed in the slipstream in square feet.

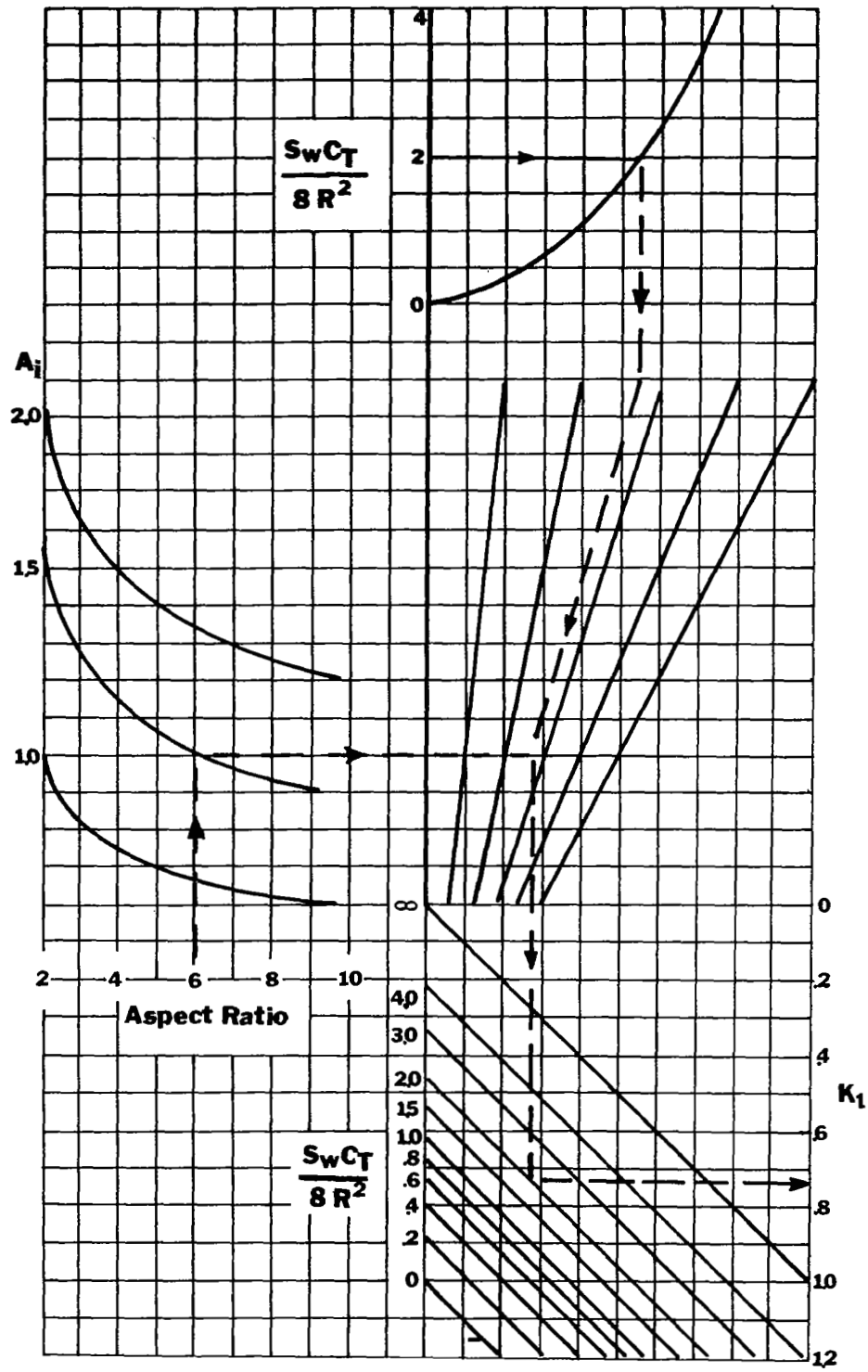

Figure 52. Correlation parameter for additional wing lift due to propeller power.

Lift Due to the Change in Angle of Attack Induced by the Propeller Flow Field

$$(\Delta C_L)_{\alpha_w} = (1 + \Delta n_s)\, C_{L_\alpha}\, \Delta\alpha\, \frac{S_i}{S_w}$$

$$\text{where } \Delta\alpha = \frac{-\varepsilon_p}{1 - \frac{\partial \varepsilon_u}{\partial \alpha}}$$

$$\varepsilon_p = \frac{\partial \varepsilon_p}{\partial \alpha_p}\, \alpha_p$$

$$\alpha_p = \alpha_T - \frac{\partial \varepsilon_u}{\partial \alpha}(\alpha_w - \alpha_o)$$

The propeller downwash derivative is given by

$$\frac{\partial \varepsilon_p}{\partial \alpha_p} = C_1 + C_2\, (C_{N_\alpha})_p$$

where C_1 and C_2 are presented in the figure below and $(C_{N_\alpha})_p$ is given in one of the previous sections.

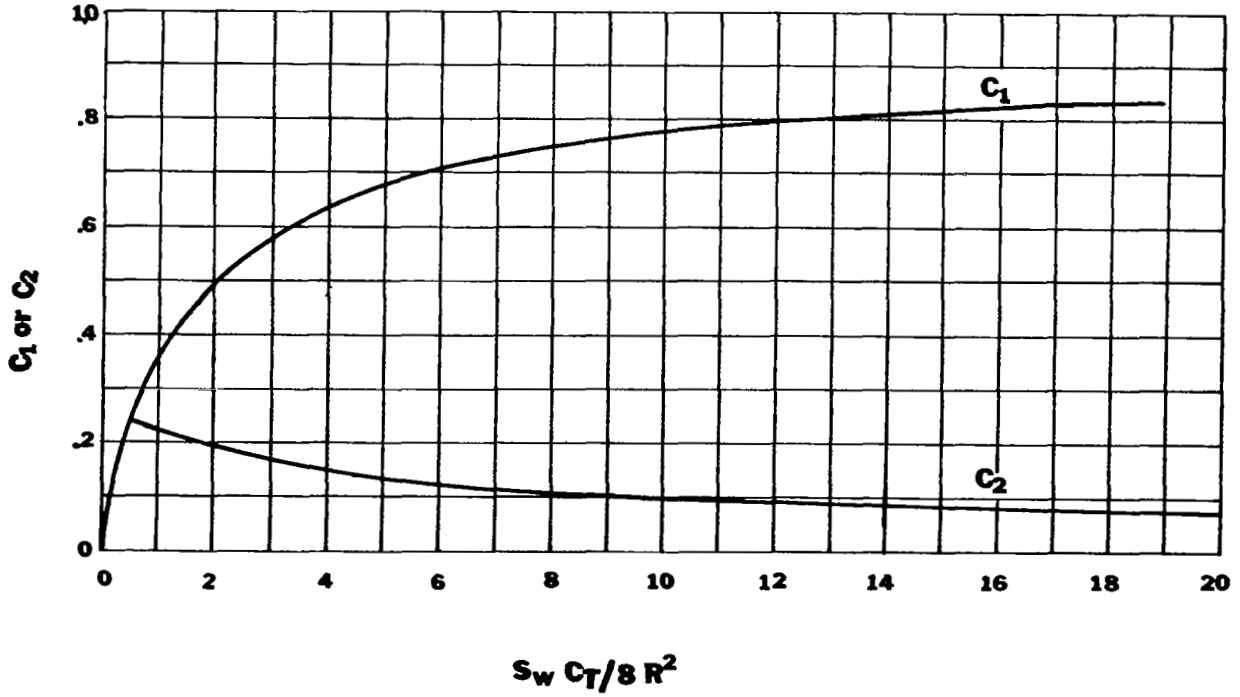

Figure 53. Factors for determining downwash due to propellers.

Lift Increment Due to the Horizontal Tail

$$(\Delta C_L)_t = -(\Delta C_m)_t \frac{c}{\ell_t}$$

where $(\Delta C_m)_t$ = total change in pitching moment of the horizontal tail due to power and can be calculated using

$$(\Delta C_m)_t = (\Delta C_{m_t})_q + (\Delta C_{m_t})_\epsilon$$

given in the next section--pitching moment variations with power.

Total Lift Increment Due to Power

$$(\Delta C_L)_{power} = (\Delta C_L)_T + (\Delta C_L)_{N_p} + (\Delta C_L)_{\Delta\eta_s} + (\Delta C_L)_{\alpha_w} + (\Delta C_L)_t$$

Pitching Moment Increment Due to the Offset of the Thrust Axis from Origin of Axis

$$(\Delta C_m)_T = C_T \frac{z_T}{c}$$

Pitching Moment Due to the Propeller Normal Force

$$(\Delta C_m)_{N_p} = (\Delta C_L)_{N_p} \frac{x_p}{c} \frac{1}{\cos \alpha_T}$$

where x_p = distance from the intersection of the propeller plane with the thrust axis to the wing quarter chord.

$(\Delta C_L)_{N_p}$ is evaluated in a previous section.

Pitching Moment Due to the Change in the Lift of the Wing Caused by Power Effect

$$(\Delta C_m)_L = -\left[(\Delta C_L)_{\Delta\eta_s} + (\Delta C_L)_{\alpha_w}\right] \frac{x_w}{c}$$

where x_w = distance parallel to x-axis from wing quarter-chord to aerodynamic center of wing area immersed in the slipstream, in feet

$(\Delta C_L)_{\Delta\eta_s}$ and $(\Delta C_L)_{\alpha_w}$ are evaluated in a previous section.

Pitching Moment Due to Change in Dynamic Pressure Acting on the Horizontal Tail

$$(\Delta C_{m_t})_q = -C_{L_t} \frac{\Delta q_t}{q} \frac{S_t}{S_w} \frac{\ell_t}{c}$$

where $\frac{\Delta q_t}{q}$ is presented in the figure below.

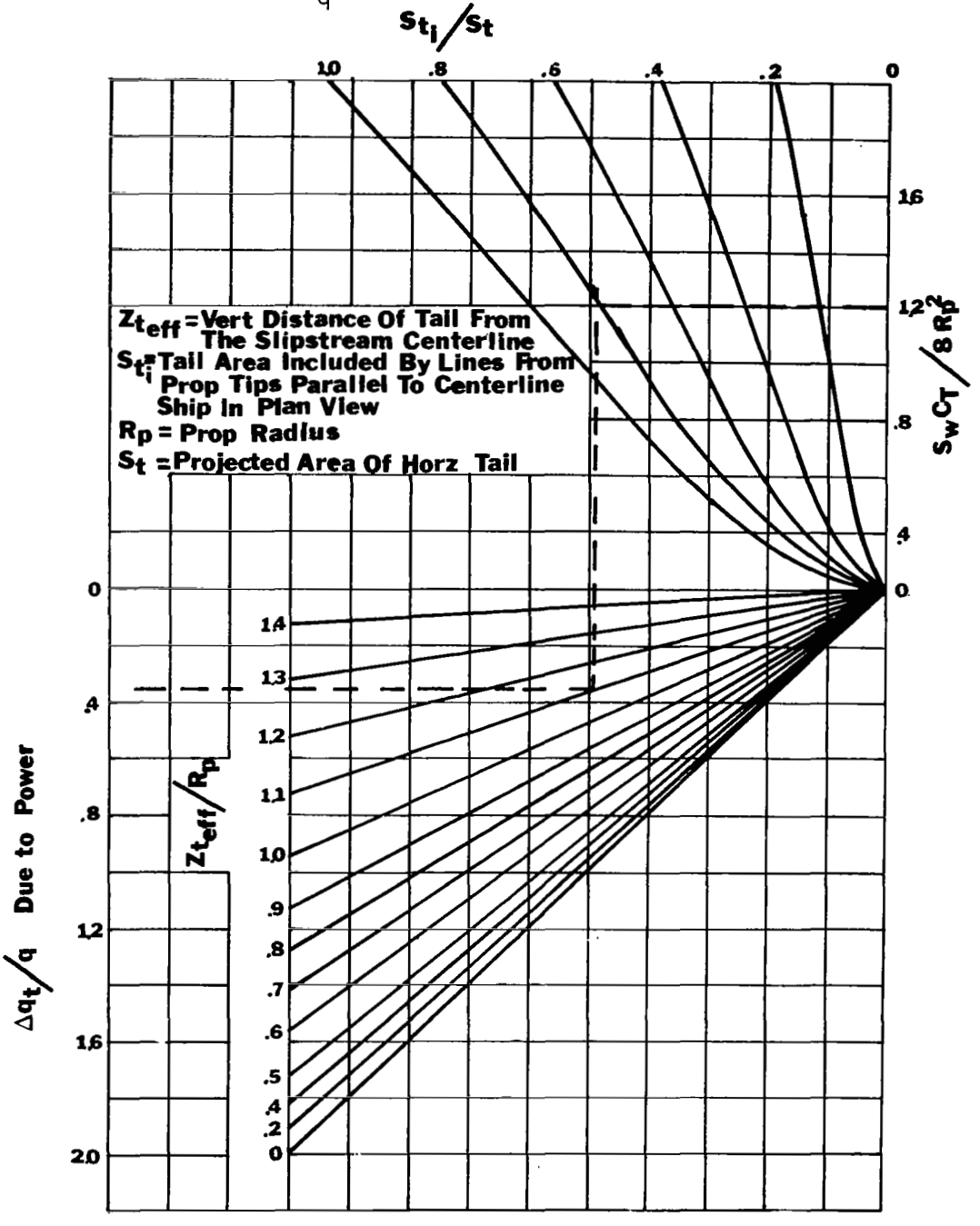

Figure 54. Effect of propeller power on dynamic pressure ratio at the horizontal tail.

Pitching Moment Due to the Change in Angle of Attack of the Horizontal Tail

$$(\Delta C_{m_t})_\varepsilon = C_{L_{\alpha_t}} \Delta\varepsilon \frac{S_t}{S_w} \frac{\ell_t}{c} \left(\frac{q_t}{q}\right)_{power}$$

where $\Delta\varepsilon$ is given in Figure 55 for single engine airplanes and Figure 56 for multi-engine airplanes. $\varepsilon_{prop\ off}$ can be obtained from a formula in the C_L section.

$$\left(\frac{q_t}{q}\right)_{power} = \left(\frac{q_t}{q}\right)_{prop\ off} + \frac{\Delta q_t}{q}$$

where $\frac{\Delta q_t}{q}$ is evaluated in Figure 54 above.

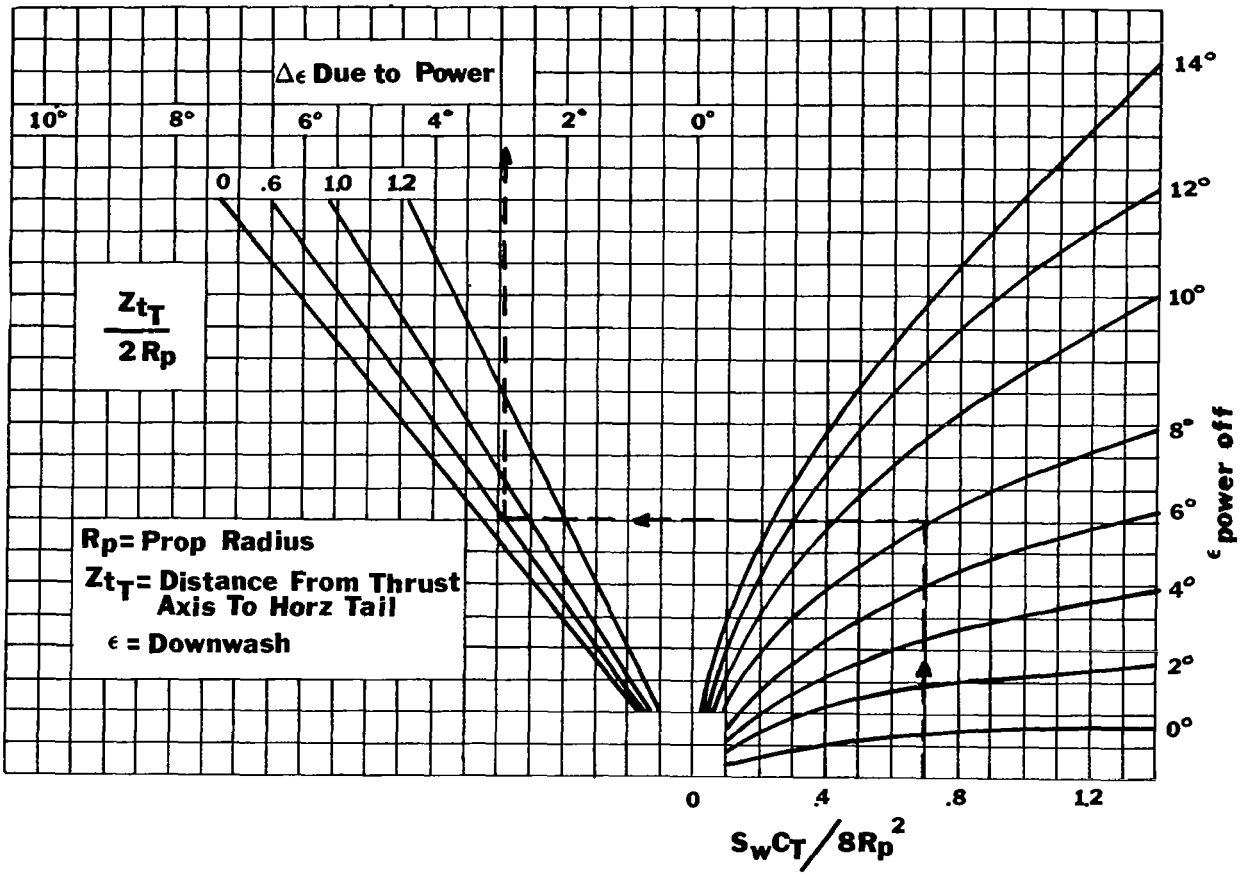

Figure 55. Increment in downwash due to propeller power for single-engine airplanes.

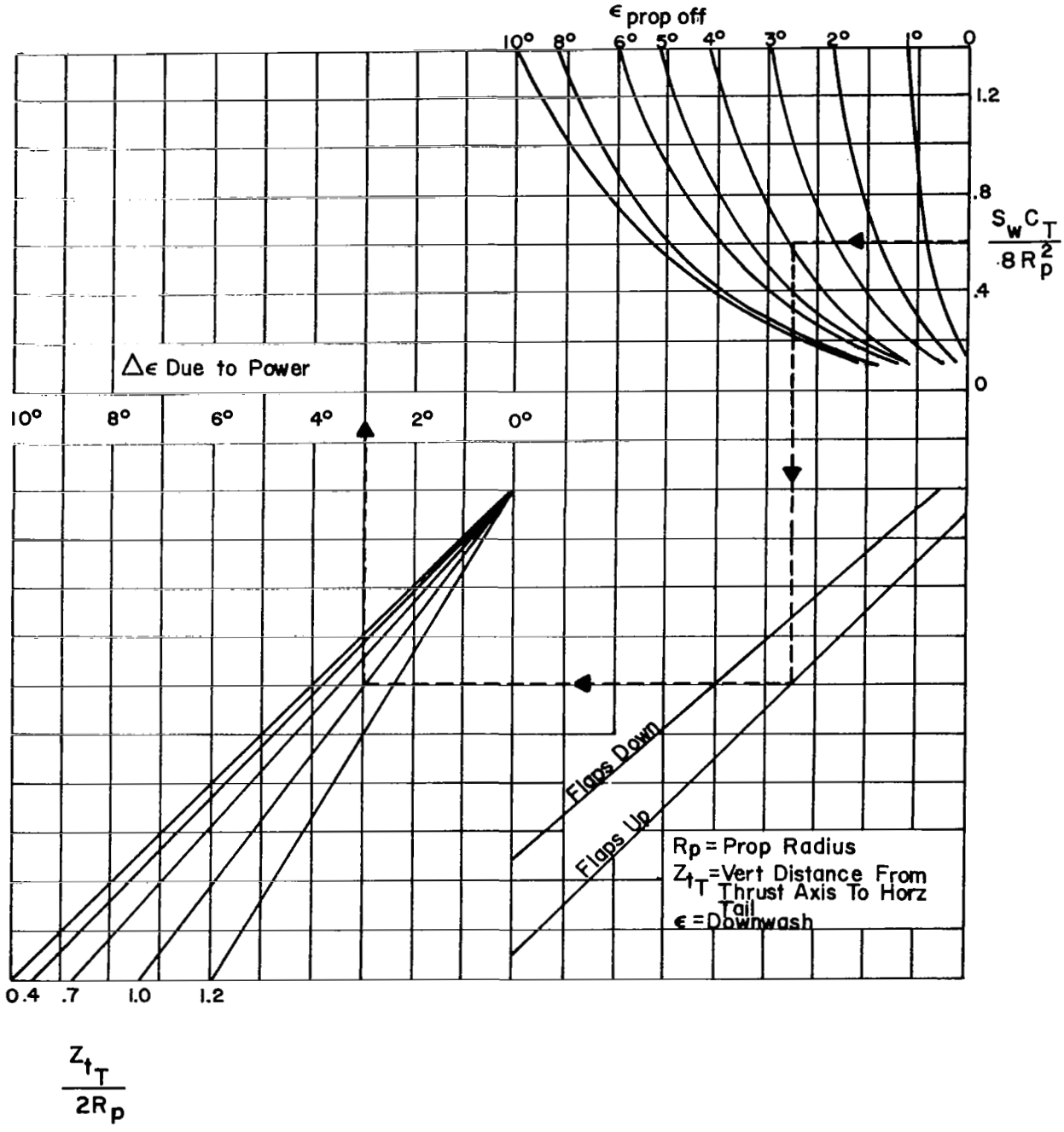

Figure 56. Increment in downwash due to propeller power for multi-engine airplanes.

Total Change in Pitching Moment Due to the Propeller Power Effects

$$(\Delta C_m)_{power} = (\Delta C_m)_T + (\Delta C_m)_{N_p} + (\Delta C_m)_L + (\Delta C_{m_t})_q + (\Delta C_{m_t})_\varepsilon$$

CONTROL FORCES AND DEFLECTIONS

Pitch Control

As indicated previously, the state of knowledge regarding desirable aircraft handling qualities up to 1948 is codified in NACA TR-927 (Ref. 16) and in the text by Perkins and Hage (Ref. 11). These works have served those of the present generation of aeronautical engineers without access to large research and development budgets virtually as holy writ, and the handling qualities of most aircraft of less than 10,000 pounds gross weight now flying reflect this technology. It is therefore desirable to examine the parameters cited in these works, their values, and the factors which produce them in some detail as a foundation for recent advances in understanding and new results.

For an aircraft which employs a trim tab to set longitudinal flight velocity, it can be shown that at any given trimmed speed the incremental stick force variation with speed is given by Perkins and Hage (Ref. 11) as

$$\frac{dF_s}{dU} = -2\, GS_e c_e \eta_t \frac{W}{S} \frac{C_{h_\delta}}{C_{m_\delta}} \left(\frac{dC_m}{dC_L}\right)_{Free} \left(\frac{1}{U_{Trim}}\right),$$

where

G = ratio elevator displacement to the product of stick length and stick angular displacement,

and

$$\left(\frac{dC_m}{dC_L}\right)_{Free} = \left(\frac{dC_m}{dC_L}\right)_{Fix} + \frac{C_{h_\alpha}}{C_{h_\delta}} \frac{C_{L_{\alpha_t}}}{C_{L_{\alpha_w}}} \frac{\ell_t}{c} \frac{S_t}{S_w} \eta_t \frac{d\alpha_t}{d\delta_e} \left(1 - \frac{d\varepsilon}{d\alpha}\right).$$

Since

$$C_{m_\delta} = - C_{L_{\alpha_t}} \frac{\ell_t}{c} \frac{S_t}{S_w} \eta \frac{d\alpha_t}{d\delta_e},$$

and

$$\left(\frac{dC_m}{dC_L}\right)_{Fix} = \frac{C_{m_\alpha}}{C_{L_\alpha}},$$

then

$$\frac{dF_s}{dU} = -2\frac{GS_e c_e}{U_{Trim}} \eta_t \frac{W}{S_w} \frac{C_{h_\delta}}{C_{m_\delta}} \left[\frac{C_{m_\alpha}}{C_{L_\alpha}} - \frac{C_{h_\alpha}}{C_{h_\delta}} \frac{C_{m_\delta}}{C_{L_{\alpha_w}}} \left(1 - \frac{d\varepsilon}{d\alpha}\right)\right].$$

A pull force is negative. It is seen that for a given aircraft, the stick force gradient at trim depends upon the trim speed, the weight, and the c.g. location. Short of major geometric modifications, the force gradients for a given speed, weight, and c.g. location can be changed by modifying G and the hinge moment parameters, C_{h_α} and C_{h_δ}. The effect of elevator balance point, elevator nose

shape, elevator trailing-edge shape, mass balancing and sealing on C_{h_α} and C_{h_δ} are treated extensively in TR-868 (Ref. 52). Figures 57, 58, 59, 60, and 61 illustrating these effects are taken from this work. A guide for using these charts follows Figure 61.

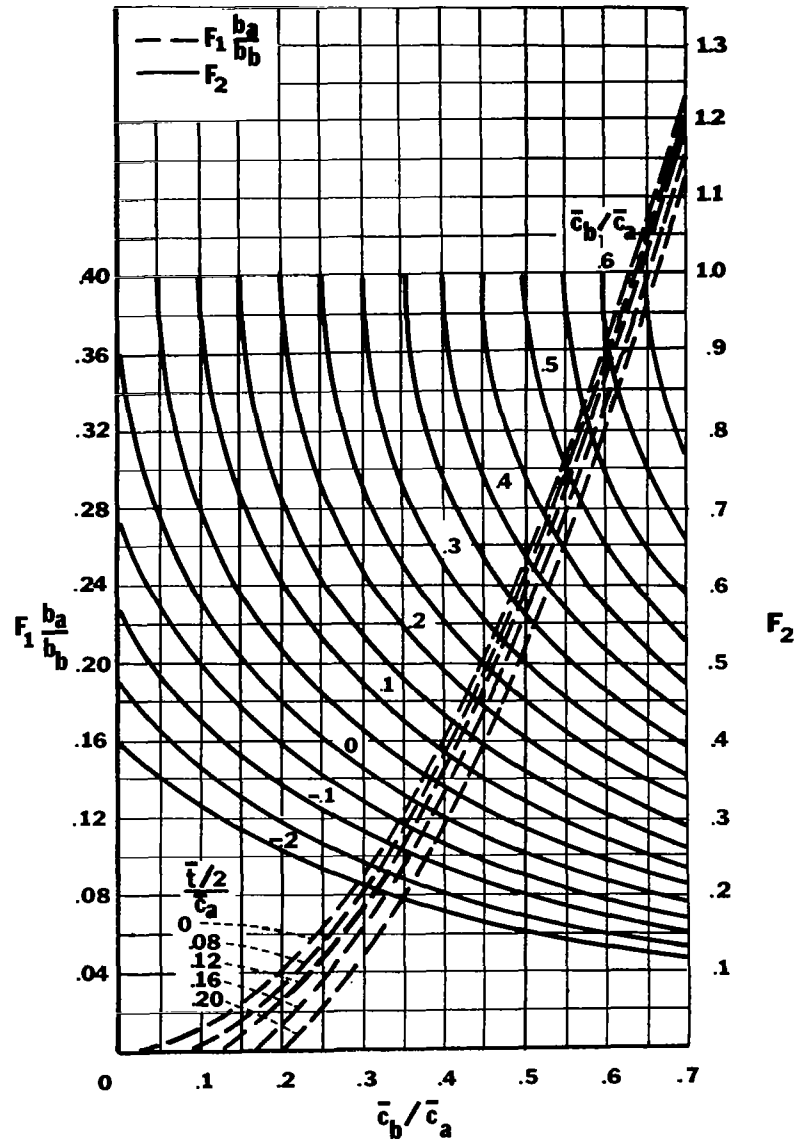

Figure 57. Charts for determining numerical values of overhang factor F_1 and of nose-shape factor F_2 from geometric constants of balanced ailerons.

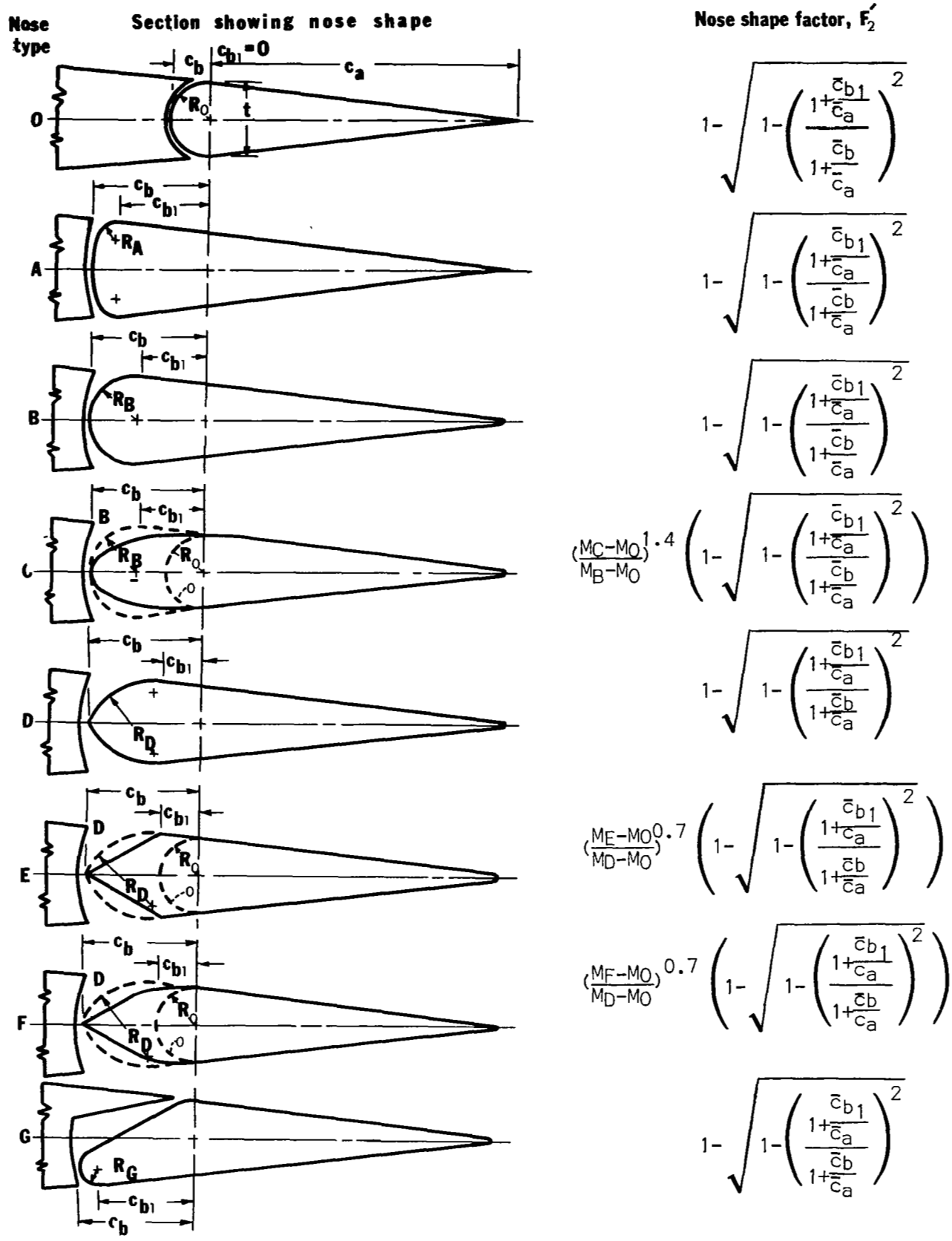

Figure 58a. Various nose shapes considered in correlation of plain, overhang, and Frise balances and corresponding expressions for nose-shape factor.

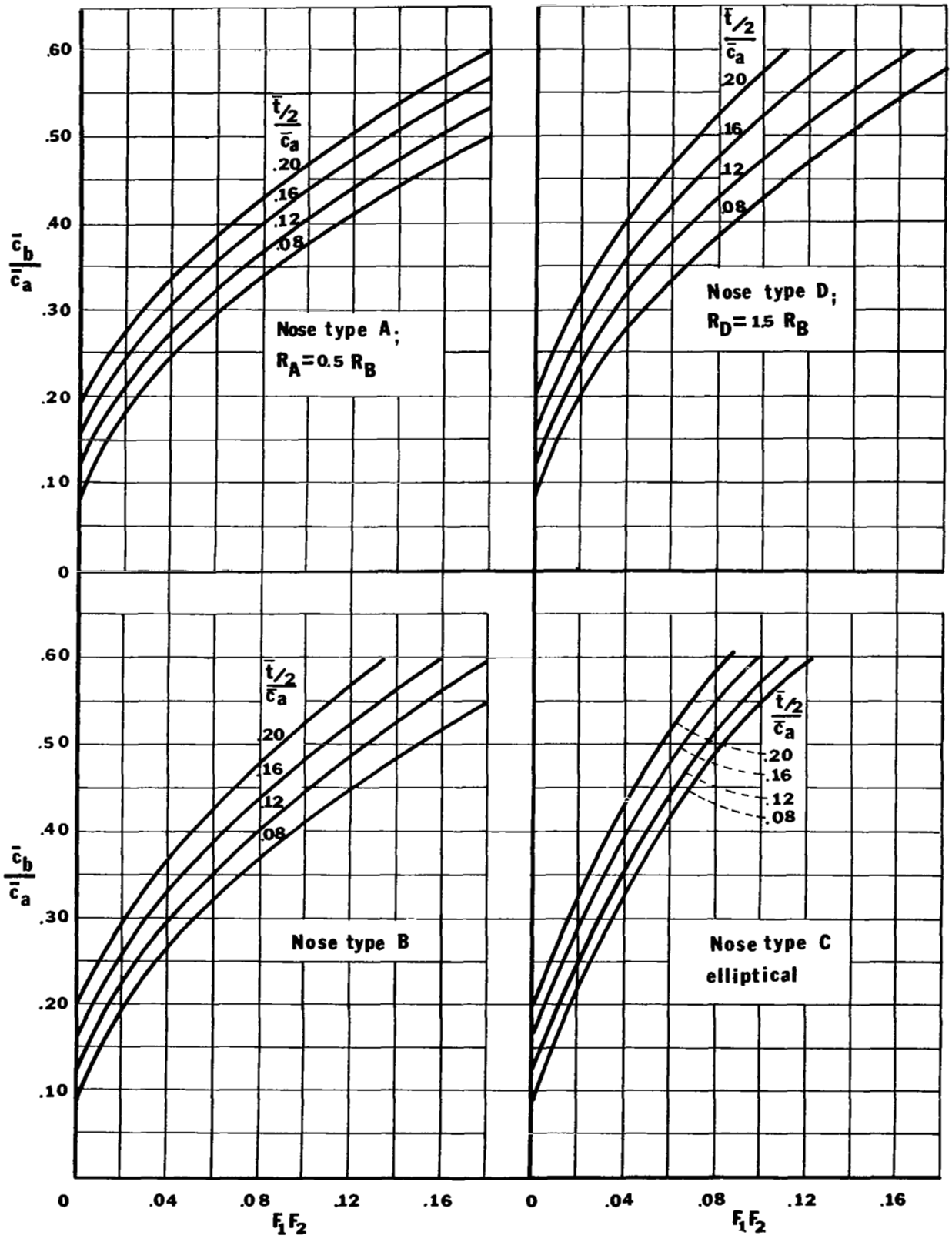

Figure 58b. Charts for estimating the required lengths of overhangs having various nose shapes. Letters A,B,C, and D refer to the corresponding nose shapes of Figure 58a.

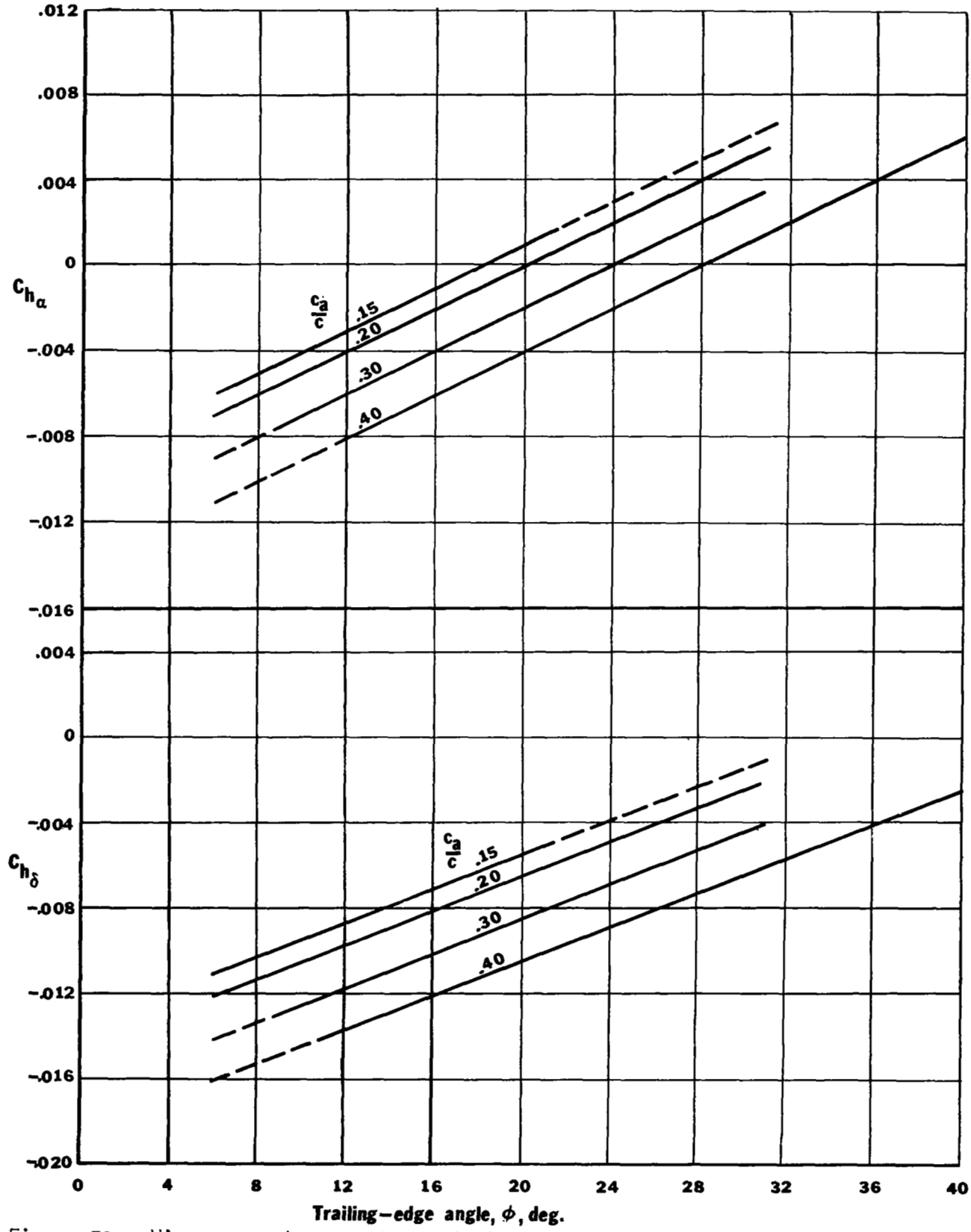

Figure 59. Hinge moment parameters of plain 2-D ailerons with various chords and values of ϕ. Gaps sealed; c_a/c=aileron to wing chord ratio.

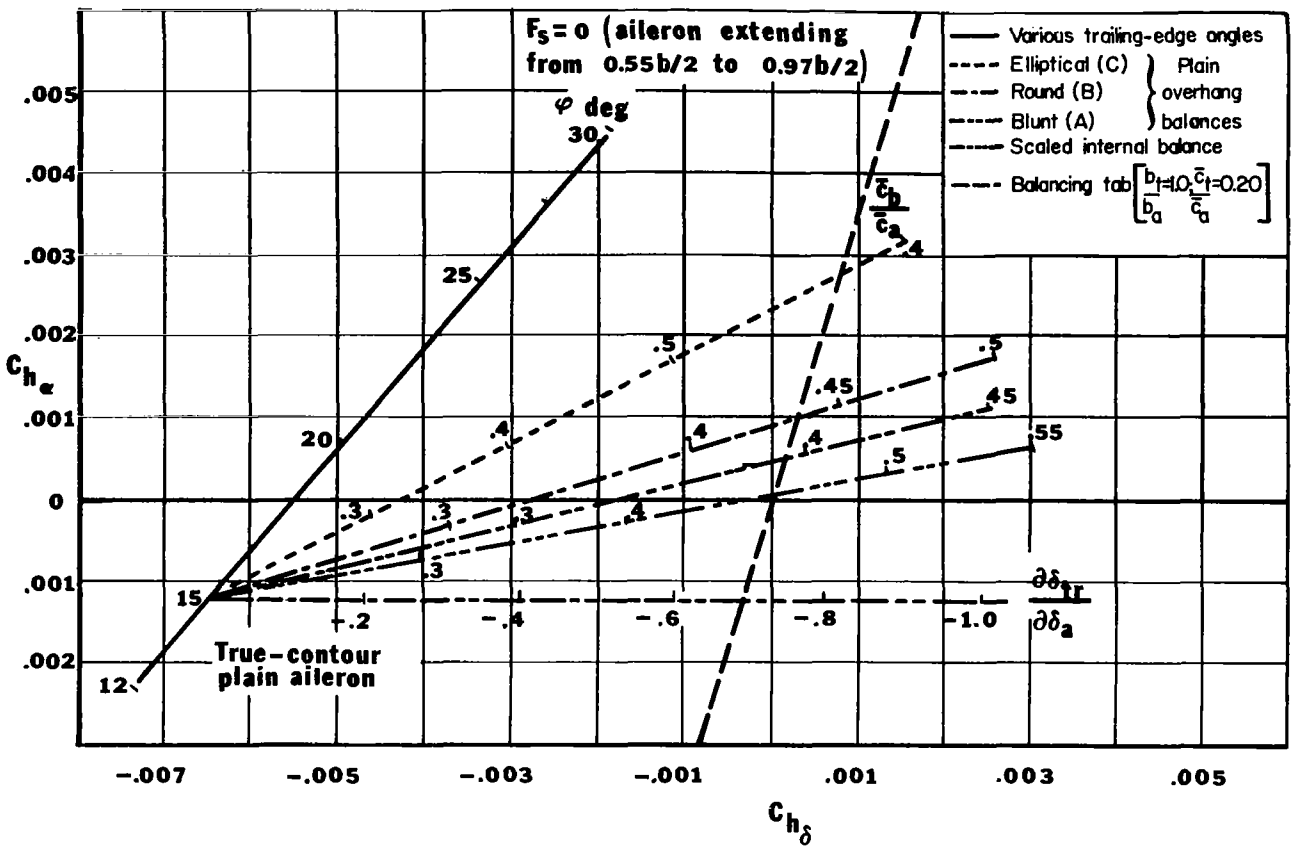

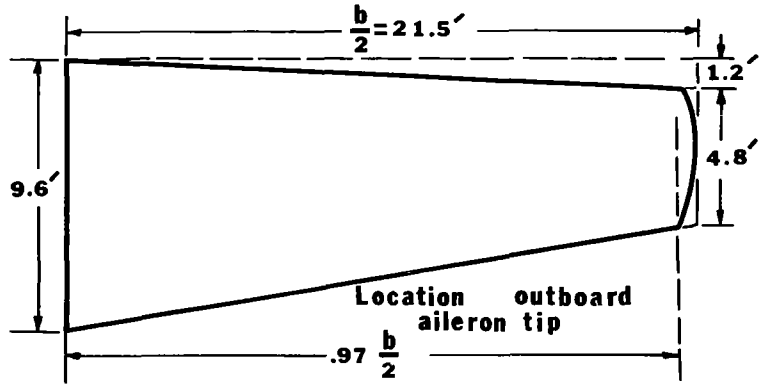

AIRPLANE CONSTANTS

Wing span, b, ft.	43
Wing area, S, sq ft	308
Aspect ratio, AR.	6.0
Taper ratio, λ	.5
Root airfoil section.	NACA 23015
Tip airfoil section	NACA 23009
Airplane weight, lbs.	12,000
Stick length, ft.	2.33

Figure 60. Effects of aerodynamic balances on aileron hinge-moment parameters estimated from correlations. $\frac{ca}{c} = 0.25$.

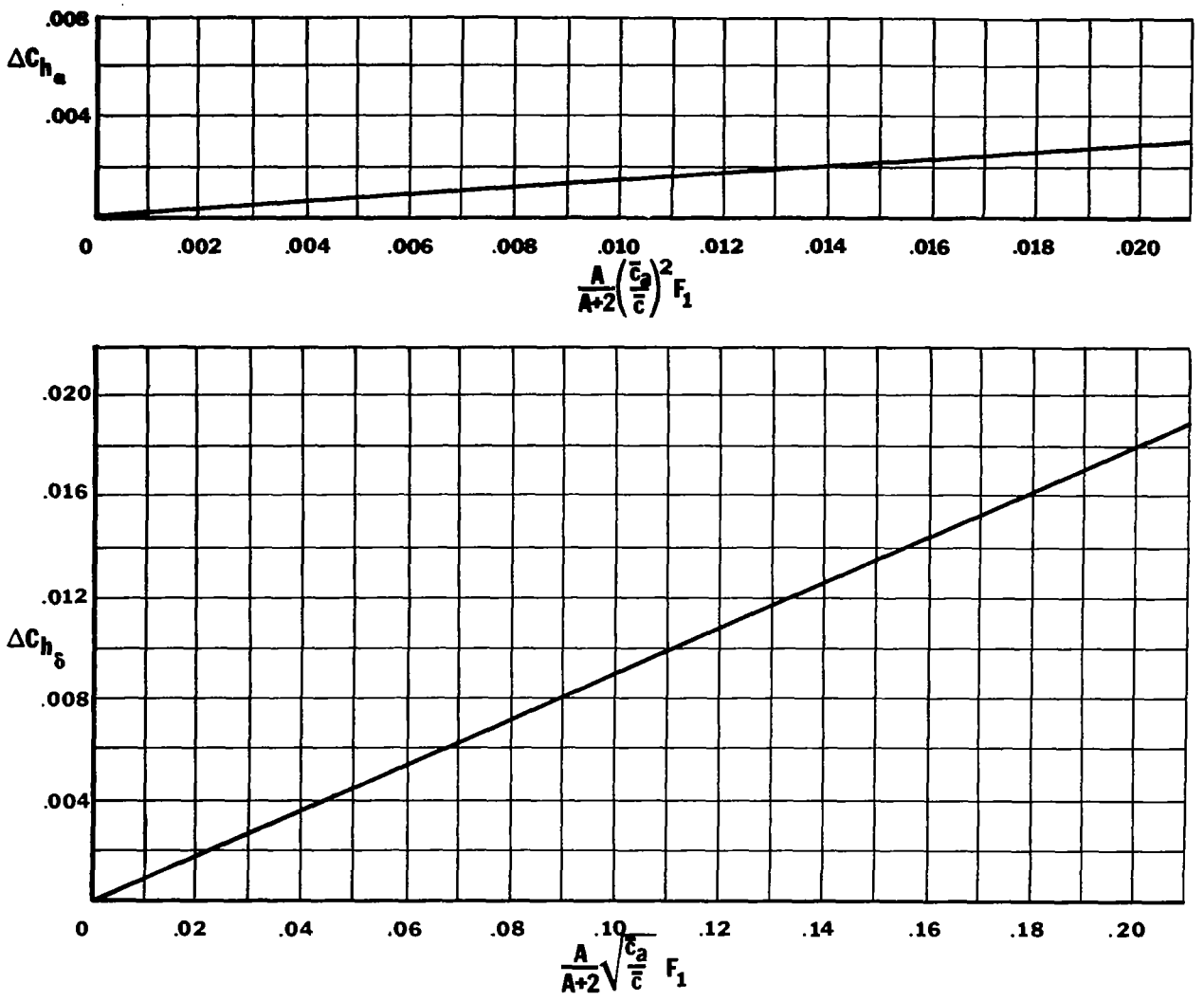

Figure 61a. Effect of sealed internal balances on the hinge-moment parameters of control surfaces. M=0.2 or less.

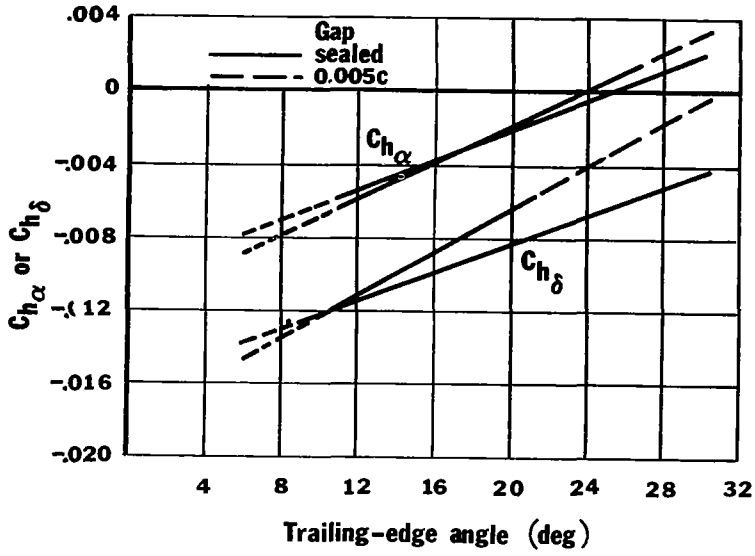

Figure 61b. Effect of gap on hinge-moment variation with trailing edge angle. NACA 0009 airfoil; 2-D model, $\frac{c_a}{c}$ =0.30.

The general expressions for changes in the hinge moment characteristics which result from geometric changes are

$$\Delta C_{h_\alpha} = \frac{AR}{AR+2}\left[0.017F_1 + 5.05 \times 10^{-4}\,\Delta\phi\right] ,$$

and

$$\Delta C_{h_\delta} = \frac{AR}{AR+2}\left[0.10F_1F_2' + 5.7 \times 10^{-4}\,\Delta\phi\right] .$$

The trailing edge angle data are for balances with a gap of .005$\bar{c}$.

One first selects a nose shape from Figure 58 and secures therefrom a value of F_2'. This involves, in addition, a selection of $\bar{c}_b/\bar{c}_a$. The symbols M_O, M_B, M_C, M_D, M_E, and M_F refer to moments about the hinge axis of the profile areas of exposed overhang balances of types corresponding to the subscripts O, B, C, and so forth. The balance profile area is defined as the total profile area of the airfoil ahead of the hinge axis. F_2=F_2' for nose shapes O, A, B, D, and G. F_2 can also be found from Figure 57. The same figure is used to determine F_1. One then calculates F_1F_2' and uses Figure 61b or the equations above to check whether the initial selection of nose shape and nose overhang will give the desired modification in hinge moment characteristics. Additional modifications in C_{h_α} and C_{h_δ} can then be obtained from trailing edge angle variations as indicated in Figures 59 and 61a or the equations above.

For sealed balances, the equations are

$$\Delta C_{h_\alpha} = \frac{AR}{AR+2}\left[0.14\left(\frac{\bar{c}_a}{\bar{c}}\right)^2 F_1 + 5 \times 10^{-4}\,\Delta\phi\right],$$

and

$$\Delta C_{h_\delta} = \frac{AR}{AR+2}\left[0.09\sqrt{\frac{\bar{c}_a}{\bar{c}}}\;F_1 + 4 \times 10^{-4}\,\Delta\phi\right].$$

The increments represented by these equations are to be added to the hinge moment coefficients produced by control surfaces with no area forward of the hinge line. The results of calculations for the basic hinge moment coefficients of thin, simple shapes shown in TR-868 (Ref. 52) can be represented by

$$C_{h_\alpha} \simeq -.0003\,\frac{c_a}{c} \qquad \frac{c_a}{c} < 0.4\ ,$$

and

$$C_{h_\delta} \simeq -.023\left(\frac{c_a}{c}\right)^{1/2} \qquad \frac{c_a}{c} < 0.4\ .$$

It should be noted, however, that these values will be altered to some extent by the condition of the flow over the basic wing (condition of boundary layer, presence of tip vortices, etc.) and by the particular shape of the control surface. For this reason, precise values are usually obtained experimentally. Further details may be found in Reference 52.

One final consideration should be mentioned here: To reduce drag, inertially-induced control surface deflection, the possibility of flutter, and effects of control surface droop, and the control surface actuation force, the control surface is also mass balanced about the hinge line. This will often require that lead weights be placed in the nose of the aerodynamic balance or attached by long arms to the hinge axis.

Report 927 (Ref. 16) illustrates suitable values for C_{h_α} and C_{h_δ} for a typical example. This is reproduced as Figure 62. In general, one desires to keep the values of C_{h_α} and C_{h_δ} small. This will also keep the stick forces to reasonable values for high speeds or heavy weights.

Some of the means for altering the effective G mechanically (springs and bob weights) are discussed by Perkins and Hage (Ref. 11). Fully powered control systems, of course, can use other means if necessary to produce the desired feel. (See, for example, TN D-632 (Ref. 53).)

Formerly, considerable effort was expended toward specifying acceptable values for dF_S/dU, but recently specification writers (both in FAR part 23 (Ref. 54) and in MIL-F-8785B (Ref. 4)) have asked only that dF_S/dU be stable

at all flight conditions, e.g., that increasing pull forces and aft motion of the elevator control be required to maintain lower than trim airspeed. There is no requirement that dF_s/dU be linear.*

In addition to calling for stable force-speed gradients, both FAR part 23 and MIL-F-8785B specify the maximum out-of-trim forces an aircraft should require in a variety of flight conditions. The table below summarizes these maximum forces and conditions.

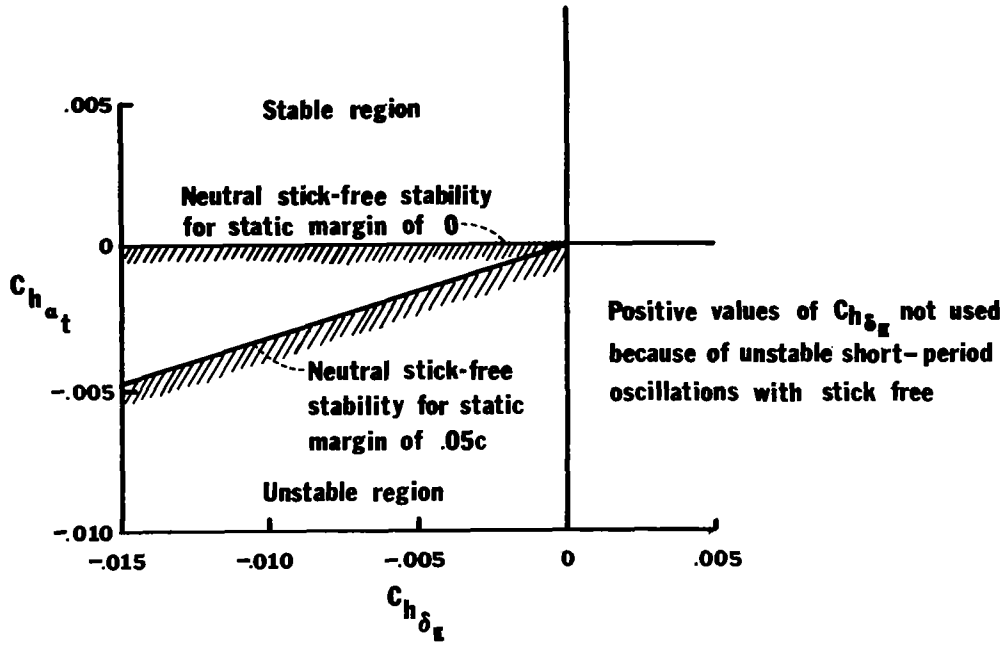

Figure 62. Boundary between stable and unstable values of C_{h_α} and $C_{h_{\delta_E}}$ for the example given in TR-927. Unstable side of boundaries indicated by cross-hatching.

---

* Indeed, dF_s/dU is directly proportional to U away from trim. Other causes of non-linear force variations include the fact that all the derivatives in the equation are evaluated at specific points only. At high values of C_L, for example, C_{L_α} is less than for C_L near 0. Thus, one should take care that the derivative values used for calculations are those valid for the range of angles being considered.

CONDITION	MAXIMUM FORCE	REFERENCE
1.5 U_{Stall} with power off and gear and flaps down at most forward c.g.	10 lbs	FAR 23.145
Any cruise speed between $1.3U_S$ and U_{max}; Approach speeds between $1.1U_S$ and $1.8U_S$	40 lbs	FAR 23.175
Maximum force for prolonged application; Temporary application Stick Wheel	10 lbs 60 lbs 75 lbs	FAR 23.143
Take-off	20 lbs pull to 10 lbs push	MIL-F-8785B § 3.2.3.3.2
Landing	Must be a pull force of not more than 35 lbs	MIL-F-8785B § 3.2.3.4.1
Dives with aircraft trimmed for level flight with trim at dive entry	< 50 lbs push, < 10 lbs pull } stick < 75 lbs push, < 15 lbs pull } wheel < 10 lbs stick < 20 lbs wheel	MIL-F-8785B § 3.2.3.5

Table 11. Specification requirements for maximum out-of-trim forces.

The general expression for stick force is given in Perkins and Hage (Ref. 11) as

$$F_s = -GS_e c_e \frac{\rho U^2}{2} \eta_t \left[C_{h_o} + C_{h_\alpha} (\alpha_w - \varepsilon - i_w + i_t) + C_{h_\delta} \delta_{e_o} + C_{h_{\delta_t}} \delta_t \right]$$
$$+ \left[\frac{C_{h_\alpha}}{C_{L_{\alpha_w}}} \frac{2\frac{W}{S}}{\rho U^2} \left(1 - \frac{d\varepsilon}{d\alpha} \right) - \frac{C_{h_\delta}}{C_{m_\delta}} \frac{2\frac{W}{S}}{\rho U^2} \frac{C_{m_\alpha}}{C_{L_\alpha}} \right],$$

where

α_o = aircraft angle of attack for zero lift,
i_w = wing incidence angle,
i_t = tail plane incidence angle,
C_{h_o} = residual hinge moment coefficient (hinge moment not caused by deflection or angle of attack),
δ_{e_o} = elevator angle at zero aircraft lift,
δ_t = trim tab deflection.

Note that for trimmed flight, δ_t is such that $F_s = 0$. For aircraft with irreversible longitudinal control systems, F_s is the force which the control system must apply to the elevator or stabilator, but the force which the pilot feels is determined by control system design.

The only mention found in the literature for desirable control deflection gradients is the requirement in MIL-F-8785B §3.2.2.2.2 (Ref. 4) that the pilot apply not less than 5 lbs force for each inch of stick travel.

Anything which changes the flow field in the neighborhood of the horizontal control surface can have an effect on its actuating forces. Such changes can be the result of applications of power (which result in increases in η_t and contributions to the downwash field from the propeller slipstream) or alterations in the lift configuration, as with deflection of flaps (which also result in altered downwash fields). The change in wing pitching moment accompanying the deflection of flaps varies the trimming moment which the tail is required to generate and thus changes the stick force or the trim tab setting required. Additional moments associated with the application of power develop when the thrust does not act through the c.g. and because propellers generate in-plane forces in upwash fields. Some of these effects tend to reduce stick forces and gradients; others tend to increase them; none of them are easy to estimate accurately from theoretical considerations alone. Wind tunnel or flight testing is necessary for accurate evaluation. For most aircraft, the application of power results in a more positive value of C_{m_α} and a reduction in control forces. The discussion in Perkins and Hage (Ref. 11) enables one to arrive at some very approximate quantitative values for these effects. The problem of undesirable trim changes with application of power or extension of gear and/or flaps is apparently a fairly common one since several of the light aircraft tested for TN D-3726 (Ref. 55) evidenced substantial shifts in stick force with the application of power or the extension of flaps or gear.

In addition to the forces required to change speed, the forces needed to change flight direction contribute significantly to the pilot's impression of the vehicle's handling qualities. In the longitudinal mode, these are usually

stated as the stick force per "g". The forces required to change direction are higher than those required to initiate a change in speed alone at the same dynamic pressure because an additional trim moment is required to pitch the aircraft to an angle of attack sufficient to generate the additional lift needed to curve the flight path and because rotation (up-pitching) induces a positive angle of attack component in the flow about the tail plane, which one must counter with a compensatory elevator deflection.

To find the elevator stick force for an arbitrary maneuver, it is necessary to solve the general equations for the normal acceleration produced by that elevator motion which results from the specified application of stick force. For simplicity and standardization in analysis and in flight tests, however, maneuvers designed to evaluate stick force per g are limited to steady pull-ups in the xz plane of inertial space and to steady turns in the xy plane of inertial space. The general expressions for stick per g in these circumstances are

$$\left(\frac{dF_s}{dn}\right)_{\text{Pull-ups}} = \frac{G\eta_t S_e c_e (W/S) C_{h_\delta}}{C_{m_\delta}} \left[\frac{C_{m_\alpha}}{C_{L_\alpha}} + \frac{C_{h_\alpha}}{C_{h_\delta}} \frac{\ell_t}{c} \frac{S_t}{S_w} \eta_t \frac{d\alpha_t}{d\delta_e} \left(1 - \frac{d\varepsilon}{d\alpha}\right)\right]$$

$$- 57.3\, G\eta_t S_e c_e g \ell_t \frac{\rho}{2} \left[C_{h_\alpha} - \frac{C_{h_\delta}{}^*}{\frac{d\alpha_t}{d\delta_e}}\right],$$

and

$$\left(\frac{dF_s}{dn}\right)_{\text{turns}} = \frac{G\eta_t S_e c_e (W/S) C_{h_\delta}}{C_{m_\delta}} \left[\frac{C_{m_\alpha}}{C_{L_\alpha}} + \frac{C_{h_\alpha}}{C_{h_\delta}} \frac{\ell_t}{c} \frac{S_t}{S_w} \eta_t \frac{d\alpha_t}{d\delta_e} \left(1 - \frac{d\varepsilon}{d\alpha}\right)\right]$$

$$- 57.3\, G\eta_t S_e c_e g \ell_t \frac{\rho}{2} \left(1 + \frac{1}{n^2}\right) \left(C_{h_\alpha} - \frac{C_{h_\delta}{}^*}{\frac{d\alpha_t}{d\delta_e}}\right).$$

Note that the stick force gradients will be linear in pull-ups so long as G, C_{m_α}, C_{L_α}, C_{h_α}, C_{h_δ}, $(d\alpha_t/d\delta_e)$, $(d\varepsilon/d\alpha)$, $C_{L_{\alpha t}}$, and η_t retain the same values as for n=1. Note also that as turns tighten, the stick force per g approaches the same value as for pull-ups.

On the question of linearity, MIL-F-8785B (Ref. 4) specifies that the local value of dF_s/dn shall not differ by more than 50% from its average value. The force limits in maneuvers are stated differently for stick and wheel controls, the rationale being that stick controllers are easier to manipulate precisely at low forces and wheel controllers permit larger forces to be applied. Not unexpectedly, the force limits are stated in terms of the limit load factor which the structure can sustain. One would not wish to be able to exceed this load factor with a very light force; nor, on the other hand, would one wish the stick forces to be so great that the maneuver capabilities of the craft could

---

* C_{h_δ} is often increased by 10% to account roughly for the fuselage damping.

not be achieved. For the limit load factor of 3.8 typical of most light aircraft, the specification stipulates that for stick controllers the maximum stick force per g shall be no more than 28 lbs per g nor less than 20 lbs per g. The minimum gradient is 7.5 lbs per g.

With wheel controllers, the maximum values are at least 42.8 lbs per g but not more than 120 lbs per g. The minimum value is 16 lbs per g.

"The term gradient does not include that portion of the force versus n curve within the preloaded breakout force or friction band." These, according to paragraph 3.5.2.1 (Ref. 4) should be between 1/2 and 3 lbs for a stick and 4 lbs for a wheel.

FAR part 23 (Ref. 54) places no numerical limits on the elevator stick force in maneuvering flight other than to say (23.143) that the force on the pitch control should never exceed 60 lbs (stick) or 75 lbs (wheel) during temporary applications or 10 lbs during prolonged applications. The popular flying journals generally do not report such data perhaps because its acquisition requires the installation of considerable instrumentation or because the omission of quantitative standards in the FAR's suggests to some either a lack of significance or a lack of popular appreciation for the meaning of quantitative values in describing handling. Since there are few reports dealing with light aircraft available elsewhere, it is difficult to determine the force gradients now common in light aircraft.

Two sources, however, are helpful. TND-3726 (Ref. 55) reports that, for some of the light aircraft investigated, stick force gradients varied between 8 and 17 lbs per g for speeds of less than 100 knots. When compared with the requirements of MIL-F-8785B (Ref. 4), these aircraft have gradients lower than desired. On the other hand, tests on a light aircraft adapted for military use (Ref. 56) showed compliance with the specification at all flight conditions and aircraft loadings. Based on these limited samplings, one would expect to find a wide variation in the handling during maneuvers exhibited by contemporary light aircraft.

One additional area given prominance by MIL-F-8785B but not referred to elsewhere in quantitative terms is the phase relation between the application of control force and the motion of the cockpit control on the aerodynamic control surface. Paragraph 3.5.3.1 requires that control deflection should not lead the application of control force. Paragraph 3.5.3 specifies that the control surface deflection shall not lag the cockpit control forces by more than 30° in phase angle for application frequencies equal or less than $\omega_{n_{sp}}$. In control systems where the aerodynamic surfaces are actuated by rigid linkages from the wheel or stick these requirements of course are always met. If, however, the system contains elastic elements, linkage force boosters, or remotely controlled actuators this may not be the case. The characteristics of such systems will require investigation and possible alteration to insure compliance with the specification. Reference 56 presents results taken with typical force and angular position transducers which could be used along with oscillographic or tape recorders to obtain data suitable for analysis of the control system phase responses.

Roll Control

If one reviews the literature dealing with the handling qualities of light aircraft in the roll mode chronologically, he becomes aware of a subtle shift of emphasis from concern primarily with achievement of a given rolling rate at low speeds and limitation of aileron forces at high speeds to concern with total pilot work load (including rudder and elevator coordination required) during rolls and to the angle attained in a specified period of time. This is not surprising when one recalls that during the era of World War II good rolling performance in fighter aircraft (weighing generally less than 10,000 lbs, at least at the beginning of the war) was essential to survival in dog fights. As knowledge of how to achieve this performance aerodynamically grew and the control forces at high speed were reduced by power boost systems, attention could be devoted to factors affecting safety and precision rather than simple survival. Hence, the 1969 revision of MIL-F-8785B (Ref.4) devotes considerable attention to limiting the forces the pilot must apply to rudder and elevator during aileron application. It also changed the requirement for the attainment of a given pb/2U to the attainment of a given bank angle in a fixed time on the premise that such a requirement was more meaningful in establishing collision avoidance capabilities and was equally suited to establishing the desirability of other areas of rolling performance.

The shift in areas of concern with time also had its analog in the analytical techniques employed and the parameter values identified. Whereas one would begin a discussion of roll handling with consideration of those control forces, control deflections, and their gradients which affect the pilot's opinion of an aircraft's roll handling qualities, it will be recognized that such things as the phase relationships between control application and aircraft response, the presence of spurious responses which require control input to counter, and the precision with which desired maneuvers can be executed also contribute significantly to his overall impression of handling characteristics. These factors plus the inevitable coupling of lateral and directional modes and the fact that aerodynamically the aircraft has no inherent bank orientation and thus no static roll stability in the conventional sense, make it necessary to employ a more general approach to roll handling analysis than the simpler view suitable for the treatment of pitch handling. The discussion which follows begins, therefore, with the simple, one-dimensional view and moves on to detail methods which the specification writers have used in an effort to quantify other phases of acceptable roll handling.

The general, linear treatment of steady, one-dimensional roll has been available since the mid-1940's. (See References 11 and 16, for example.) With the assumption that all derivatives remain constant irrespective of aileron deflection, speed, altitude, and rolling rate, and that the time required to attain the maximum rolling rate for a given aileron deflection can be considered

zero*, one can write

$$\phi = -\frac{U}{b}\left(\frac{C_{\ell_\delta}}{C_{\ell_p}}\right)\delta_a \; t \; ,$$

for the bank angle as a function of aileron deflection and

---

* One-dimensional rolling motion is described by the equation

$$I_{xx}\ddot{\phi} = \frac{\partial L}{\partial p}\, p + \frac{\partial L}{\partial \delta_a}\frac{\delta_a}{2} \; ,$$

whose solution for a step aileron input is

$$\phi = -\left(\frac{C_{\ell_\delta}}{C_{\ell_p}}\right)\frac{U}{b}\,\delta_a \; t \; + \left[\frac{1 - e^{\left(\frac{C_{\ell_p} b^2 q S_w t}{2U \; I_{xx}}\right)}}{\frac{C_{\ell_p} b^2 q S_w}{2U \; I_{xx}}}\right]$$

In this equation, $q = 1/2\ \rho U^2$. Since the denominator of the second term ** (equal to $(1/\tau_R)$) generally has a value of -10 or more (negative), it is obvious that for times in excess of about 1.0 sec the second term contributes very little to the bank angle attained. MIL-F-8785B, §3.3.1.2 requires that the maximum value of τ_R for light aircraft is 1.0. §3.3.1.4 further states that the rolling mode and the spiral mode shall not couple, ie, the time constants have the same value, to produce an oscillatory mode. For a simulator study of this case, the reader is referred to TND-5466 (Ref. 57).

For the complete three-dimensional treatment of rolling response to aileron deflection, the appendices to the present study should be examined.

** See Appendix D for a discussion of the stability derivatives most important in determing the value of the rolling mode time constant, τ_R.

$$\phi = - \frac{2F_a \frac{C_{\ell_\delta}}{C_{\ell_p}} t}{\rho U b \, S_a c_a G \, C_{h_\delta} \left[1 - 2 \frac{C_{h_\alpha}}{C_h} \frac{C_{\ell_\delta}}{C_{\ell_p}} \left(\frac{y'}{b} \right) \right]}$$

for the bank angle as a function of control force. δ_a is the total (up plus down, assumed to be equal and equally effective) aileron deflection. y' is the spanwise location of the aileron centroid. It is seen that at low speed the rolling performance increases with increasing speed until the force limits are reached; at this point the bank angle possible per unit time decreases with increasing speed. The ratio $(C_{\ell_\delta}/C_{\ell_p})$ is a function of taper ratio, aileron-to-wing chord ratio, and per cent of span denoted to ailerons. In addition to making this ratio as large as practicable (maximum possible value is about 1.5), one desires to adjust

$$\frac{C_{h_\alpha}}{C_{h_\delta}} \frac{C_{\ell_\delta}}{C_{\ell_p}} \frac{y'}{b}$$

to be approximately 0.5 so as to increase the roll capability at high speeds. Careful attention to aileron geometry is therefore necessary to obtain the proper ratio of $C_{h\alpha}$ to $C_{h\delta}$. TR-868 (Ref. 52) is an excellent source of experimental data on geometric effects and design methods.

It is apparent from the foregoing that if one minimizes friction and elasticity in the aileron linkage, the factors contributing to wheel or stick force and to rolling performance are well known. Even non-linearities in the derivatives $C_{h\delta}$, $C_{h\alpha}$, etc., while requiring that tedious computations be made to obtain $\phi(t)$, are well documented for a large number of configurations. Thus it is a fairly straightforward matter to translate control force, control deflection, and rolling performance limitations into hardware specifications. It remains then to state the appropriate values for these qualities.

The maximum force given in FAR part 23 (Ref. 54) and MIL-F-8785B (Ref. 4) seem, for the most, to have been selected by experience from many years of pilot comments; nevertheless, comparison of these results with available anthropological data (See discussion of Human Factors in this work) for the comfortable application of lateral forces shows good agreement. The table below gives a summary of the specification requirements.

REQUIREMENT	REFERENCE
Temporary: Stick 60# Wheel 75# (Max) Prolonged 10#	FAR 23.143
Stick 20# (Max) Wheel 40# (Max) The minimum force for maximum rolling performance shall not be less than the breakout force plus 1/4 of the above values.	MIL-F-8785B § 3.3.4.2
Control centering and breakout forces shall not be more than 2# (stick) or 3# (wheel) nor less than 1/2 #.	§3.5.2.1
Rolling performance: aircraft must reach a 60° bank angle in 1.7 sec in cruise and a 30° bank in 1.3 sec for approach	§3.3.4.14
Not more than 5# (stick) or 10# (wheel) should be required to achieve a 45° bank with rudder free and the ailerons trimmed for wings in level flight.	§3.3.2.6
Not more than 60° of wheel rotation, in either direction } ±80° for a completely mechanical system	§3.3.4.4
There shall be no objectionable non-linearities in variation of rolling response to wheel motion.	§3.3.4.3
Control surface response shall not lag cockpit control force input by more than 30° phase angle for frequencies less than $1/\tau_R$ or ω_{nd}, whichever is larger.	§3.5.3
Cockpit control deflection shall not lead cockpit control force.	§3.5.3.1

Table 12. Specification requirements for comfortable application of lateral forces.

The requirements quoted in the preceding table are those restricted to Class I (small light airplanes such as light utility, primary trainer, and light observation up to about 12,000 lbs gross weight); category B which includes climb, cruise, and descent and category C which includes take-off, approach, and landing; and Level I, ie, having flying qualities clearly adequate for the Mission Flight Phase. This approach was selected for the present work because it was desired to show the present state of understanding of what is required to obtain satisfactory handling qualities.

The requirement on the time constant of the rolling mode was given previously as not less than 1.0 sec. Examination of the equation of motion cited previously will also show that the aircraft will respond well to sinusoidal aileron inputs up to frequencies of

$$\frac{C_{\ell_p} b^2 q S_w}{2U I_{xx}} \text{ rad/sec},$$

where

$$q = 1/2\ \rho U^2.$$

This is generally above the range at which the pilot can track. Thus, if the phase lag in the control system is less than 30° up to this frequency, the pilot will find the aircraft able to generate roll rates corresponding to wheel position virtually as rapidly as he can turn the wheel or move the stick.

It is noteworthy that in preparing this specification, its writers have provided quantitative limits on

(1) The rolling performance of which the aircraft must be capable,

(2) The maximum and minimum forces needed to produce maximum rolling velocity,

(3) Permissible breakout and centering forces,

(4) The maximum control deflection.

These, coupled with the frequency response requirements mentioned earlier and the ban on objectionable non-linearities, present a complete and quantitative description of the factors contributing to the pilot's satisfaction with roll mode handling.

The usual methods of producing a rolling motion is the differential deflection of outboard portions of trailing edge of the wing, or ailerons. If one wishes to roll to the right, he deflects the right aileron up to reduce lift on that wing and deflects the left aileron down to increase lift on that wing. Usually, such operation is a portion of a coordinated turn to the right. The drag on the right wing is decreased and the drag on the left wing increased by this aileron deflection. The resulting yawing moment (called adverse yaw),

if unbalanced by a rudder deflection, reduces the effective rolling velocity by moving the right wing at a higher forward velocity than the left wing. The lift on the right wing is therefore greater (and less on the left) than would be the case if the adverse yaw were not present.

Adverse yaw is also undesirable because if unopposed it excites the lightly damped Dutch Roll oscillation. The pilot thus finds himself producing often disconcerting yawing motions unintentionally. The specification requirements limiting its extent include §3.3.2.5 (Ref. 4) which provides that no more than 50 lbs of rudder force be required to make a coordinated (β=0) turn at cruise speeds or 100 lbs in the approach configuration for high performance fighter aircraft. There is also §3.3.2.4, which provides that adverse sideslip shall not exceed 10° and that proverse sideslip shall not exceed 3° during flight phase categories B and C (cruise, climb, descent, and take-off and landing). TND-3726 (Ref. 55) suggests that pilots find a sideslip angle of 10° in response to a rudder-locked aileron deflection the maximum acceptable. Some of the aircraft tested for this report exhibited sideslip angles in excess of 13°. Reference 56 reports that a converted light aircraft carrying military stores under the wing reached sideslip angles in excess of 10° and required 125 lbs of rudder force to perform a coordinated turn at low speed. The military stores were responsible for a 5° increase in sideslip angle.

In the absence of a rudder force to counter the adverse yawing moment, the aircraft will develop sufficient sideslip to permit a balancing yawing moment due to sideslip to be produced. Since all light aircraft employ some dihedral to aid in maintaining the wings' level during normal flight* and since this stabilizing rolling moment due to sideslip acts to reduce the roll rate achieved by a given aileron deflection, it is important for good rolling response that adverse yaw be held to a minimum. §3.3.6.3.2 of MIL-F-8785B (Ref. 4) states that the positive dihedral effect shall not be so great that more than 75% of the roll control power available to the pilot, and no more than 10 lbs of aileron stick force or 20 lbs of wheel force are required for sideslip angles which might be experienced in service deployment.

The comments of AFFDL-TR-69-72 (Ref. 4) relative to sideslip requirements developed for the specification seem particularly pertinent: " the primary source of data from which the sideslip requirement evolved (See AFFDL-TR-67-98)" are those tests for which the ratio of bank angle to sideslip angle during Dutch Roll equaled about 1.5. "The pilot comments associated with these configurations indicated that pilot's difficulties were almost exclusively associated with sideslip, rather than with bank angle tracking as was the case for $|\phi/\beta|_d \simeq 6$ configurations. Analysis of the data revealed that the amount of sideslip a pilot will accept or tolerate is a strong function of the phase

---

* FAR part 23 (Ref. 54) states that "the static lateral stability, as shown by the tendency to raise the low wing in a slip, must be positive for any landing gear and flap position."

angle of the Dutch Roll component of sideslip. When the phase angle is such that β is primarily adverse, the pilot can tolerate quite a bit of sideslip. On the other hand, when the phasing is primarily proverse, the pilot can only tolerate a small amount of sideslip because of difficulty of coordination.

"There is more to coordination, however, than whether the sideslip is adverse or proverse; the source and phasing of the disturbing yawing moment also significantly affect the coordination problem. If the yawing moment is caused by aileron and is in the adverse sense, then in order to coordinate the pilot must phase either right rudder with right aileron or left rudder with left aileron. Since pilots find this technique natural, they can generally coordinate well even if the yawing moment is large. If on the other hand, the yawing moment is in the proverse sense or is caused by roll rate, coordination is far more difficult. For proverse yaw-due-to-aileron the pilot must cross control; and for either adverse or proverse yaw-due-to-roll-rate, required rudder inputs must be proportional to roll rate. Pilots find these techniques unnatural and difficult to perform. Since yawing moments may also be introduced by yaw rate, it can be seen that, depending on the magnitude and sense of the various yawing moments, coordination may either be easy or extremely difficult. If coordination is sufficiently difficult that pilots cannot be expected to coordinate routinely, the flying quality requirements must restrict rudder-pedals free unwanted motions to a size acceptable to pilots."

"Analysis further revealed that it was not so much the absolute magnitude of the sideslip that bothered the pilot, but rather the maximum change occuring in sideslip. The latter was a better measure of the amount of coordination required. Thus the data...were plotted...as the maximum change in sideslip occuring during a rudder-pedals-fixed rolling maneuver, $\Delta\beta_{max}$, versus the phase angle of the Dutch Roll component of sideslip ψ_β. The phase angle, ψ_β, is a measure of the sense of the initial sideslip response, whether adverse or proverse, while $\Delta\beta_{max}$ is a measure of the amplitude of the sideslip generated. Both the sense and amplitude affect the coordination problem."

For small aileron control commands (§3.3.2.4.1), the amount of allowable sideslip is given in the figure below.

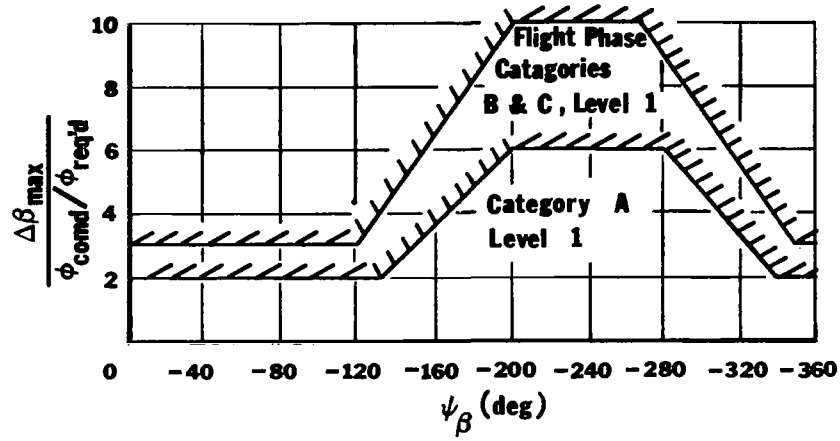

Figure 63. Allowable sideslip for small aileron control commands,

This requirement applied for step aileron control commands up to the magnitude which causes a 60° bank angle change in two seconds or

$$\frac{2\pi}{\omega_{n_d}\sqrt{1-\zeta_d^2}} \text{ seconds,}$$

whichever is greater.

The difference in allowable $\Delta\beta_{max}$ with ψ_β "is almost totally due to the difference in ability to coordinate during turn entries and exits. ψ_β is a direct indicator of the difficulty a pilot will experience in coordinating a turn entry. For $-180° \geq \psi_\beta \geq -270°$, normal coordination may be effected.... As ψ_β varies from -270° to -360° coordination becomes increasingly difficult, and in the range $-360° \leq \psi_\beta \leq -90°$ cross controlling is required to effect coordination. Since pilots do not normally cross control and, if they must, have great difficulty in doing so for $-360° \leq \psi_\beta \leq -90°$, oscillations in sideslip either go unchecked or are amplified by the pilot's efforts to coordinate with rudder pedals."

To extend roll-sideslip coupling requirements to larger control deflections, §3.3.2.3 states that the value of the parameter

$$\phi_{osc}/\phi_{average} = \frac{\phi_1 + \phi_3 - 2\phi_2}{\phi_1 + \phi_3 + 2\phi_3} ,$$

where ϕ_1, ϕ_2, ϕ_3 represent successive peaks in the bank angle time history (ϕ_2 is a minimum peak), shall be within the limits shown on the figure below.

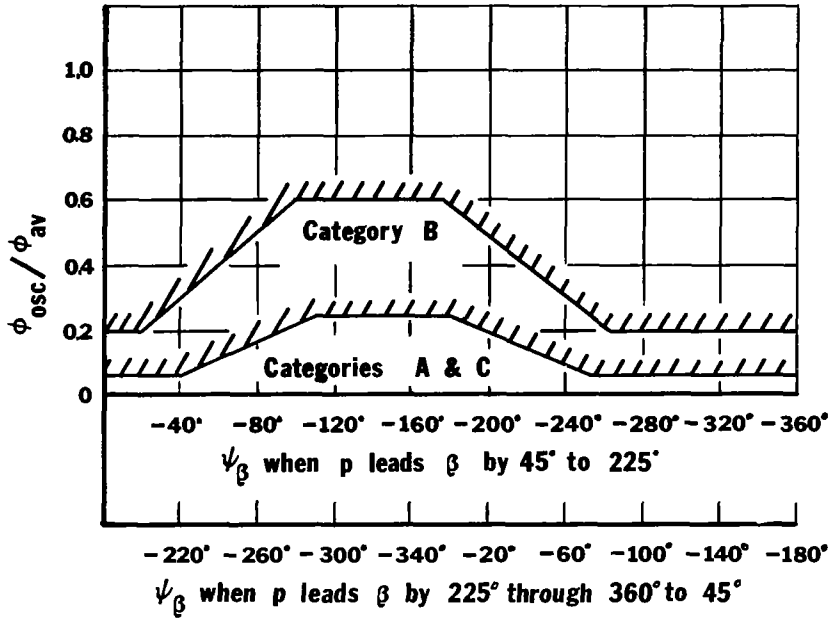

Figure 64. Limits for extending roll-sideslip coupling requirements to larger control deflections.

Similar requirements designed to insure control precision in the roll mode are given in §3.3.2.2.1, which requires that P_{osc}/P_{AV} be as shown in the figure below.

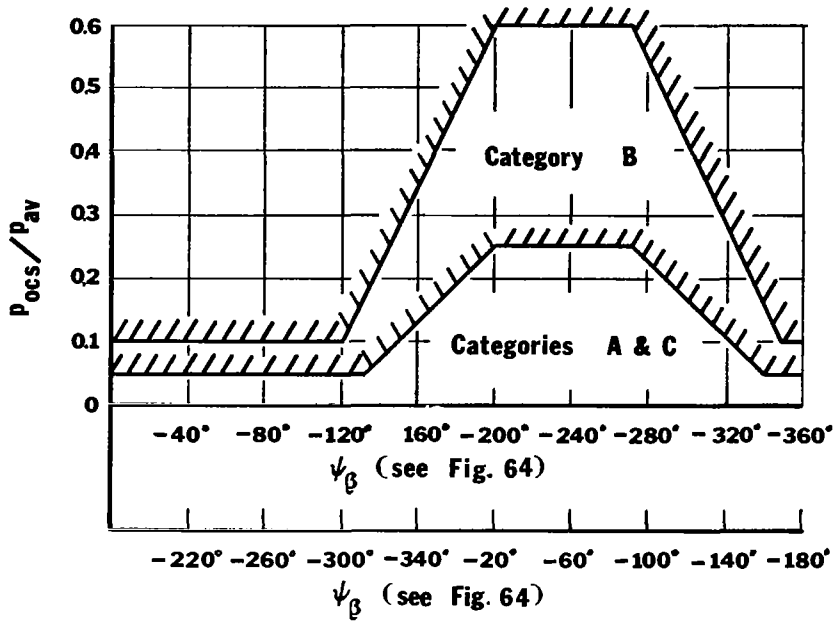

Figure 65. Requirements for insuring control precision in the roll mode.

This requirement applied for step aileron control commands up to the magnitude which causes a 60° bank angle change in

$$\frac{3.4\pi}{\omega_{n_d}\sqrt{1-\zeta_d^2}} \text{ seconds.}$$

For larger roll rates, §3.3.2.2 states that following a rudder-pedals-free step aileron control command, the roll rate at the first minimum following the first peak shall be of the same sign and no less than 60% (categories A and C) or 25% (category B) of the roll rate of the first peak.

Additional evidence of the bearing which rolling moment due to sideslip has on pilot's opinion of an aircraft's handling qualities is provided by §3.3.2.1 which states that roll acceleration, rate, and displacement responses to side gusts shall be investigated for airplanes with large rolling moments due to sideslip.

As mentioned at the beginning of this section, modern concern with aircraft handling characteristics has centered on precision of response and total pilot work load. The paragraphs of MIL-F-8785B (Ref. 4) cited above demonstrate this concern clearly. TND-3726 (Ref. 55), citing the fact "that the stability and control characteristics of the airplanes (tested) are

generally satisfactory but deteriorate with reduced speed, increased power, aft center-of-gravity location and changes to the landing configuration,.. and are critically degraded in turbulent air" and that "in general, each stability and control degradation is relatively small" suggest that "reduced pilot rating results from the combined effects of all deteriorations" and that it is "therefore necessary to consider the combined effect of all the stability and control characteristics in order to properly assess the pilot ratings." The authors of TND-3726 (Ref. 55) suggest that this be done by evaluating a work load factor defined as

$$\text{work load factor} = \int_0^{30\ \text{sec}} |F_e|\,dt + \int_0^{30\ \text{sec}} |F_a|\,dt + \int_0^{30\ \text{sec}} |F_r|\,dt.$$

The integrals are the areas under the curves of the three pilot-applied force time histories taken over a 30 sec period with the aircraft originally in a trimmed state. "The satisfactory airplane presents a work load factor of approximately 300; whereas the unsatisfactory airplane approaches a factor of 500." Clearly, a requirement of this type will ultimately be made part of the flying quality specifications.

Many of the quantitative tests from which the specification writers gained guidance were performed in simulators or in variable stability airplanes. Results reported in TND-746 (Ref. 58) and TND-779 (Ref. 59) for example, showed the importance of the Dutch Roll frequency and damping in establishing the limiting behavior which the pilot could control. TND-221 (Ref. 60) reports pilots require 0.23 sec to begin to move the stick laterally and 0.33 sec longitudinally. TND-173 (Ref. 61) reports results of a study to provide artificial longitudinal stability. TND-1782 (Ref. 62) provides data on the transfer function of human pilots. It should be noted, however, that such data cannot be accepted without some qualification: human pilots display a very high degree of adaptability to devices designed to measure their response capabilities and thus exhibit different transfer functions with increasing time or as the control task is varied.

Several very recent full-scale wind tunnel studies on the stability and control characteristics of representative light aircraft are reported in References 63, 64, and 65. Results of a program of artificial stability augmentation and work load reduction on a popular light twin is presented in considerable engineering detail in Reference 66. This program is notable in beginning with a competent analytical attack on the problem (and in detailing the numerical calculations), in devising an ingenious roll-yaw coupler especially suited to this type aircraft, and in presenting details, including transfer functions, of the flight hardware.

Finally, for a very interesting review of the chronology of man's understanding of aircraft stability and control, the reader is referred to the 1970 von Kármán Lecture given by Dean Perkins (Ref. 67).

Yaw Control

The uses of the yaw control in aircraft include, according to AFFDL-TR-69-72 (Ref. 4),

(a) To perform a cross-wind landing--either employ a steady rudder-pedal-induced sideslip or else a decrab maneuver.

(b) To augment roll rate anywhere within the flight envelope.

(c) To raise a wing when the pilot is busy with his hands, such as when taking a clearance.

(d) For tracking.

(e) For wing-overs...to obtain a rapid change in heading or bank angle.

(f) For close-formation flying.

(g) To lose altitude as in a forward sideslip or to improve visibility.

(h) To counter yawing moments from propeller torques, speed change, asymmetric thrust, stores, etc.

(i) To taxi.

The reader will note that from a handling standpoint these uses are of two types: primary control of motion about the yaw axis and precision of control in coupled lateral-directional motions. Primary control about the yaw axis is much like primary control about the pitch axis: the aircraft can be provided with inherent static stability, the forces experienced by the pilot are a good measure of the out-of-trim condition, and most of the longitudinal stability parameters have directional analogs. Thus, one can write

$$F_r = G\left(\frac{\rho U^2}{2}\right)\eta_v S_r c_r \left[C_{h_\alpha}\beta + C_{h_\delta}\left(\frac{C_{n_\beta}}{C_{n_{\delta_r}}}\right)\beta - C_{h_{\delta_t}}\delta_t\right],$$

$$\frac{dF_r}{d\beta} = -G\left(\frac{\rho U^2}{2}\right)\eta_v S_r c_r \left[C_{h_\alpha} + C_{h_\delta}\left(\frac{C_{n_\beta}}{C_{n_{\delta_r}}}\right)\right],$$

and

$$\frac{d\beta}{d\delta_r} = -\frac{C_{n_{\delta_r}}}{C_{n_\beta}} \quad .$$

With the usual assumption of constancy in the values of the stability derivatives, these relations provide a means to compare the primary directional handling parameters of proposed aircraft with the specification requirements quoted below. Note that to keep the variation in force required with changes in speed reasonable and thus minimize the need for retrimming it is necessary to make C_{h_α} and C_{h_δ} as small as possible. Such a step will also aid in keeping the force required to produce given sideslips (and thus aid in rolling maneuvers) within reason.

Primary yaw control in the present connotation consists of those functions which can be provided only by rudder deflection. Included in this list would be items such as (a), (e), (g), (h), and (i). The precision-of-control items in the list indicate that for these circumstances the rudder is used principally to complement aileron control, to improve its precision by countering adverse yawing moments ($C_{n_{\delta r}}$ or C_{n_p}) or to provide small additional favorable rolling moments (C_{ℓ_r}). The table below shows how the desire to permit these uses was translated into quantitative requirements.

REQUIREMENT	REFERENCE
Maximum rudder force temporary 150# steady 20#	FAR 23.143
Rudder force <50# to counter sideslip in rolls.	MIL-F-8785B §3.3.2.5
Coordinated turn which reaches 45° of bank should require less than 40# of rudder.	§3.3.2.5
50# of rudder force must induce a roll rate of 3°/sec.	§3.3.4.5
If the aircraft is trimmed with symmetric power it must be able to change speed ±30% without requiring more than 100# of rudder force.	§3.3,5.1
No more than 100# of rudder force must be necessary for asymmetric loading.	§3.3.5.1.1

(continued on next page)

REQUIREMENT	REFERENCE
The ratio β/δ_r must be essentially linear to ±15° with the slope permitted to be smaller for β>15° but still positive. The ratio β/F_r must be essentially linear to ±10°. F_r may be less for larger values but never zero.	§3.3.6.1
For the aircraft trimmed for ϕ=0 flight these requirements apply at sideslip angles produced or limited by (a) full rudder pedal deflection (b) 250# rudder pedal force (c) maximum aileron control or surface deflection.	§3.3.6
Control centering and breakout forces shall be between 1# and 7#.	§3.5.2.1
Control surface response shall not lag cockpit control force input by more than 30° (phase angle) for frequencies equal to or less than $1/\tau_R$.	§3.5.3
Cockpit control deflection shall not lead control force.	§3.5.3.1
It shall be possible to take off and land with normal pilot skill in 90° cross winds from either side with velocities up to 20 knots. Rudder forces shall not exceed 100#.	§3.3.7
Rudder control power shall be adequate to maintain wings level and sideslip zero without retrimming throughout dives and pullups. In the service flight envelope, shall not exceed 180#.	§3.3.8
It shall be possible to taxi at any angle to a 35-knot wind.	§3.3.7.3
Rudder forces shall not exceed #180 to maintain a straight path in the event of sudden loss of thrust during take-off.	§3.3.9.1

Table 13. Yaw control requirements.

Current light aircraft often require fairly large (~185 lbs) rudder forces in 15° steady sideslips (Ref. 56) or as a result of the application of power--up to 90 lbs change between idle power and maximum power at a given airspeed (Ref. 55). Pilots considered the latter unsatisfactory although it would satisfy the specification. Note that brake forces in automobiles in excess of 100 lbs are generally regarded as undesirable while forces in excess of 200 lbs are regarded as unacceptable. In this regard, the FAR maximum rudder force requirement appears to be far more reasonable than that of MIL-F-8785B (Ref. 4), particularly considering that diminuative women should be able to operate a light airplane comfortably. The specifications are also notable in omitting any quantitative limitation on rudder pedal travel. While this is another aspect of the present unsatisfactory state of directional control requirements, the condition likely stems from the fact that most directional control during flight is now accomplished through aileron manipulation which the pilot can perform very precisely and for which the force-deflection-response relations are prescribed in great detail.

It is felt by several pilots consulted by the authors that the force limits quoted in the military specifications should be applied only to the faster and heavier aircraft of the general aviation class. It was their contention that one should reduce these limits progressively as maximum speed and weight are reduced so that for the lightest and slowest aircraft in the class the maximum forces will be no greater than 1/3 or 1/2 the specification values. The reasoning apparently follows the usual human expectation that larger vehicles require larger forces to control them. That this is not necessary, however, is evident from the popular acceptance of power steering and power brakes on automobiles. With these devices the forces are made more or less independent of car size. It is to be expected, therefore, that as "fly-by-wire" control systems are installed more widely in aircraft a trend toward standardization of control feel, riding qualities, and handling qualities for aircraft of all sizes, speeds, and weights will develop.

Handling in Turbulent Air

The discussion above has assumed that the air mass through which an aircraft is flying is uniformly stationary with respect to inertial space. Nature, however, is seldom so accomodating, and many aircraft experience severe deterioration in handling qualities during flight in turbulent air (Ref. 55). Analysis reported in Reference 4 indicates that a first order treatment of the problem can be performed. Gusts are considered to be isotropic away from the ground. Gust velocity variation with spatial frequency for two models is used to obtain gust components of $u(x)$, $v(x)$, and $w(x,y)$. From these, one can calculate gust components for α, β, p, q, and r and, subsequently, the altered values of the stability derivatives. It is seen therefore that all airframe dynamic modes can be excited in gusts. If these are insufficiently damped, if the lateral-directional coupling is excessive, or if the static stability is marginal, the pilot's work load will increase markedly if he attempts to maintain a reasonably precise course or comfortable ride. Outstanding handling qualities in still air are consequently a necessary prerequisite to acceptable handling in turbulent air.

INERTIAL CHARACTERISTICS

The airplane designer is directed to the section of this study dealing with spin entry for a discussion of dynamic response resulting from changes in moments of inertia; techniques for estimating moments of inertia are detailed here.

When an airplane is rotated about its center of gravity, the resulting torque, Γ, is equal to the product of the moment of inertia about the c.g. and the angular acceleration ($\Gamma = I\, d\omega/dt$). Since the torque is applied by a control surface, the angular acceleration can be found for a particular control deflection by dividing the torque by the moment of inertia. The three angular degrees of freedom for the airplane are pitch, roll, and yaw; thus, it is necessary to know the moments of inertia about the x, y, and z airplane body axes. One product-of-inertia term, I_{xz}, also appears in the equations of motion (see Appendix A), but this term is usually small, and, for many analyses, is considered zero, indicating that all the axes are principal axes.

Moments of inertia can be obtained by experimental measurements or can be estimated from airplane mass and geometric characteristics. The usual method for determining experimentally the moments of inertia is a pendulum method.

The application of the pendulum method to the experimental determination of moments of inertia of airplanes is discussed in TR-467 (Ref. 68). The moments of inertia about the x and y axes are found by swinging the airplane as a compound pendulum, whereas the moment of inertia about the z axis is determined by oscillating the airplane as a bifilar-torsional pendulum. The differential equation which describes the pendulum motion is of the form,

$$I \frac{d^2\theta}{dt^2} + b\theta = 0$$

where I = measured moment of inertia
b = constant depending on the weight and dimensions of the pendulum
θ = angular displacement.

The period can be written as $T = 2\pi/\sqrt{b/I}$, and the moment of inertia can be solved by solving for I. For each of the cases mentioned above, the true moments of inertia are determined by correcting the measured moments of inertia for (1) the buoyancy of the structure, (2) the air entrapped within the structure, and (3) the additional mass effect. These three factors cause an apparent additional moment of inertia, which is evaluated on the basis of (1) the airplane size and shape normal to the direction of motion and (2) the results of tests of the additional mass effect of flat plates. Reference 68 should be used to evaluate the required corrections. The additional mass effect (moment of inertia influenced by the surrounding medium) results from the fact that the period of the pendulum's vibrating in air is to some extent dependent on the momentum imparted by its motion through the air. The momentum imparted to the body is proportional to the momentum of the body; thus, the equivalent additional mass may be used.

The precision of the pendulum method to estimate true moments of inertia is approximately ±2.5 percent, ±1.3 percent, and ±0.8 percent for the x, y, and z axes respectively. Several types of airplanes of gross weight less than

10,000 pounds have been tested at the NACA laboratories, the results of which were compiled and published as NACA TN-780 (Ref. 69) which supersedes TN-375. Only a few of the airplanes tested are characteristic of the light airplane designs of today. This report, however, is valuable in obtaining an approximate number for the moments of inertia and the radii of gyration. Agard Report 224 (Ref. 101) also discusses methods of obtaining the moments of inertia by the spring oscillation method. Schematic representation of typical methods for determining (within 5% or better) the rolling and pitching moments of inertia are given as well as other references which may be helpful in using these methods.

Because of the equipment required to measure the moment of inertia by the pendulum method, probably the most popular method utilizes the weight and location of component parts outlined in TN-575 (Ref. 70). This is a step-by-step, tabulated method which yields the moments of inertia about the three axes, the products of inertia, and the center of gravity locations. It is believed that the moments of inertia can be estimated within 10% by this method and can be applied by completing Table 14, which is explained below.

The first step in the procedure is to define a set of three mutually perpendicular reference planes, x´z´, y´z´, and x´y´, as shown in the figure below.

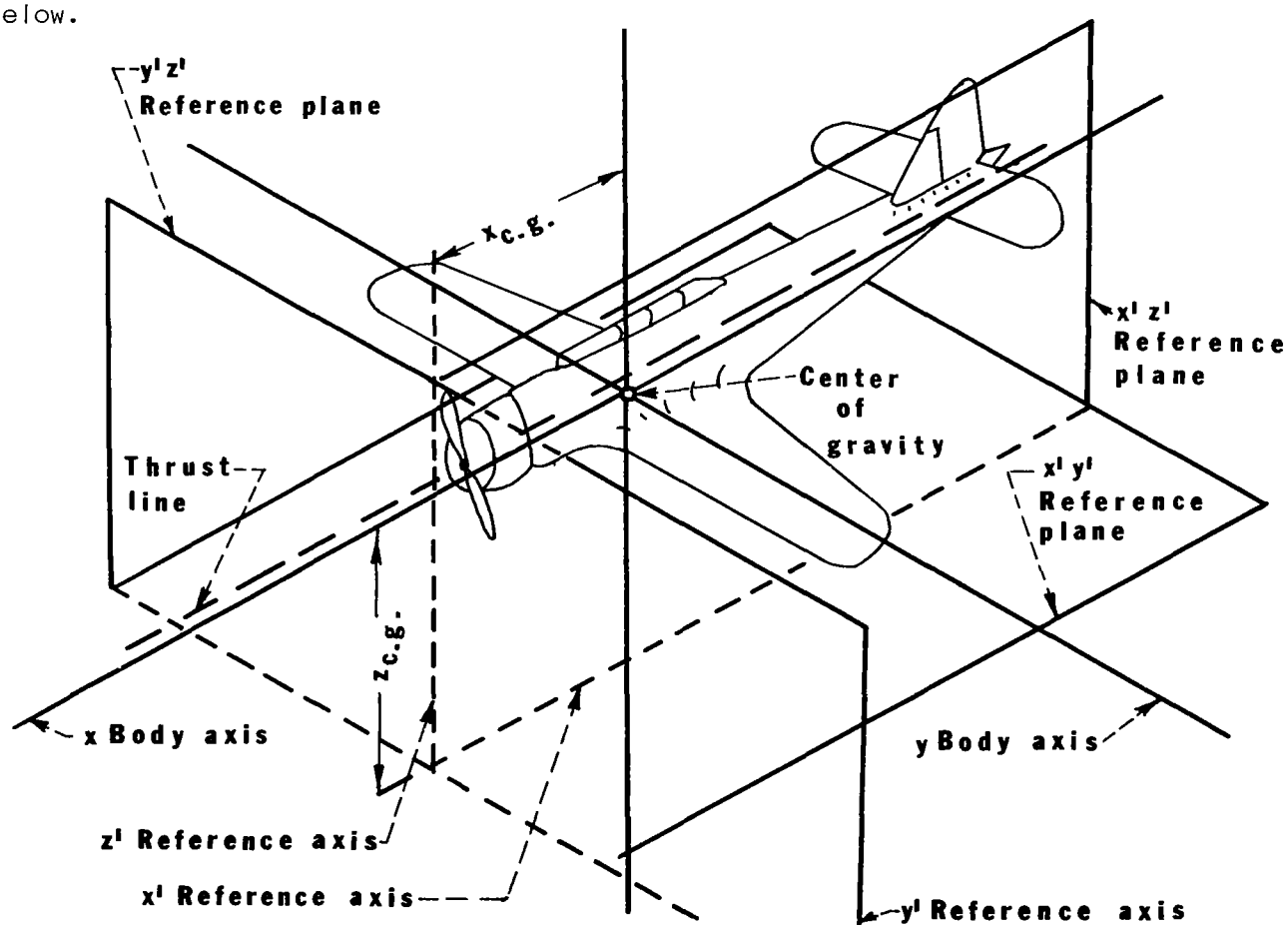

Figure 66. Set of three mutually perpendicular reference planes.

The plane of symmetry is chosen as the x´z´ reference plane, since it contains the c.g. The y´z´ reference plane is usually set at the nose of the airplane, while the x´y´ reference plane can be established at the top or the bottom. These reference planes define the origin of the coordinate axes.

The table which must be completed is shown below and explained column by column.

(1) Item	(2) Wt. (w)	(3) x	(4) y	(5) z	(6) wx	(7) wz	(8) wx^2	(9) wy^2	(10) wz^2	(11) ΔI_{xx}	(12) ΔI_{yy}	(13) ΔI_{zz}	(14) wxz
Totals													

Table 14. Sample table for obtaining inertial characteristics.

Column (1) Elements of the airplane which are considered (flaps, wheels, baggage doors, engine, seats, pilot, fuel, etc.).

Column (2) Weight of each individual element.

Columns (3), (4), & (5) Distance from the x´, y´ and z´ axes to the element. It is important to note that some of these distances may be either positive or negative.

Columns (6) & (7) Moments contributed by each element. Since the airplane is symmetric about the x´z´ plane, wy = 0; therefore, it does not appear.

Columns (8), (9), & (10) The product of the squares of the individual distances and the item weight.

Columns (11), (12), & (13) The estimation of the moments of inertia of the larger items about their own center of gravity.

Column (14) The total product of inertia, I_{xz}.

The information in the above columns can be used to find

(1) c.g. Location--The x and z c.g. locations ($x_{c.g.}$ and $z_{c.g.}$) can be found by dividing the totals of columns (6) and (7) respectively by the total weight.

(2) Moments of Inertia--The total moments of inertia of the airplane about the three reference axes are

$$I_{x'x'} = \Sigma wy^2 + \Sigma wz^2 + \Sigma\Delta I_{xx}$$

$$I_{y'y'} = \Sigma wx^2 + \Sigma wy^2 + \Sigma\Delta I_{yy}$$

$$I_{z'z'} = \Sigma wx^2 + \Sigma wy^2 + \Sigma\Delta I_{zz}$$

The moments of inertia about the c.g. can be written as

$$I_{yy} = I_{y'y'} - W(x_{c.g.}^2 + z_{c.g.}^2)$$

$$I_{xx} = I_{x'x'} - W(z_{c.g.}^2)$$

$$I_{zz} = I_{z'z'} - W(x_{c.g.}^2)$$

where W = total airplane weight

(3) Product of Inertia--The product of inertia, I_{xz}, about the c.g. can be found by the formula,

$$I_{xz} = \Sigma wxz - W(x_{c.g.} + z_{c.g.})$$

Even for the large items, the products of inertia about their own c.g. can usually be neglected. Also, for light aircraft, the products of inertia for the complete aircraft are usually small or negligible. Thus, for a first approximation, assuming the products of inertia to be zero is fairly accurate. If greater accuracy is required, the formula above can be used.

Some typical values of moments of inertia can be seen for light aircraft by examining the table below:

Airplane Weight (lbs.)	Number of Engines	I_{xx} (slug-ft^2)	I_{yy} (slug-ft^2)	I_{zz} (slug-ft^2)
2200	1	902	1335	1922
2650	1	941	1479	2110
3350	1	1495	2207	2878
4650	2	8884	1939	11,001
15,000	2	64,811	17,300	64,543
2100	2	766	1275	1805

Table 15. Typical light aircraft moments of inertia.

STALL

The flow over a body is said to stall when the pressure gradient becomes so unfavorable that the velocity at the surface is zero and the mainstream is no longer attached to the body. When stall occurs on airfoils, there is both a loss of lift and an increase in drag. In general, stall can be defined as that flow condition which follows the first lift-curve peak. TN-2502 (Ref. 71) indicates three classifications for stall at low speeds: 1) trailing-edge stall, 2) leading-edge stall, and 3) thin airfoil stall.

Trailing-edge stall is preceded by the movement of the point of turbulent boundary-layer separation forward from the trailing edge with increasing angle of attack (usually characteristic of airfoils of 15% thickness or more). This type of stall is distinguished by a gradual, continuous force and moment variation with a well-rounded lift-curve peak.

The leading-edge stall is an abrupt flow separation of the laminar boundary layer near the leading edge, generally without subsequent flow reattachment (usually typical of airfoils 9% to 15% thick). Little or no change in lift-curve slope should be expected prior to maximum lift and an abrupt, often substantial, decrease in lift should occur after maximum lift is attained. A combined leading-and trailing-edge stall is possible.

The thin airfoil stall is preceded by flow separation from the leading edge, with the reattachment point moving progressively downstream with increasing angle of attack. This thin airfoil stall has a rounded lift-curve peak, generally preceded by a discontinuous force and moment variation for airfoils with a rounded leading edge.

The stalls mentioned above are shown in the figure below.

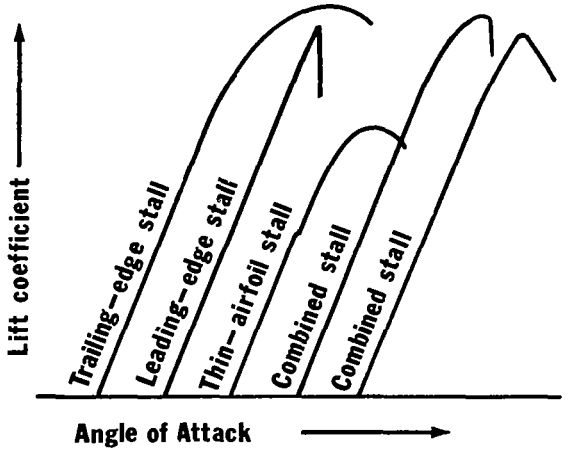

Figure 67. Characteristic stall types.

Not every airfoil can be classified uniquely into a given stall category, nor is each type of stall limited to a certain range of thickness ratios.

Since stall characteristics play a major role in the design of any airplane, it is important to know at the outset at what angle of attack the stall occurs, depending on the weight, speed, and maximum lift coefficient of the airplane. The abrupt stall has proven to be quite dangerous because the pilot receives little or no warning before attaining a critical attitude. Also, if stall occurs during landing or take-off, the pilot has little or no altitude in which to recover. Many parameters affect the stall of a body or wing: taper, aspect, and thickness ratios; Reynolds number; camber; washout; and leading-edge shape. Before considering the parameters which affect stall, some mention should be made of the requirements for good stall warning and recovery. Technical Report AFFDL-TR-69-72 (Ref. 4) defines stall warning requirements, stall characteristics, and stall recovery requirements for light military aircraft.

Stall Warning

> The stall aproach shall be accompanied by an easily perceptible warning.

Acceptable warning for all types of stalls consists of shaking of the cockpit controls, buffeting or shaking of the airplane, or a combination of these. The onset of this warning should occur within the ranges specified by the two tables below.

Warning speed for stalls at 1g normal to the flight path. Warning onset for stalls at 1g normal to the flight path shall occur between the following limits:

Flight Phase	Minimum Stall Warning Speed	Maximum Stall Warning Speed
Approach	Higher of $1.05U_S$ or $U_S + 5$ knots	Higher of $1.10U_S$ or $U_S + 10$ knots
All Other	Higher of $1.05U_S$ or $U_S + 5$ knots	Higher of $1.15U_S$ or $U_S + 15$ knots

Table 16. Warning speed for stalls at 1g normal to the flight path.

Warning range for accelerated stalls. Onset of stall warning shall occur outside the Operational Flight Envelope associated with the Airplane Normal State and within the following angle-of-attack ranges:

Flight Phase	Minimum Stall Warning Angle of Attack	Maximum Stall Warning Angle of Attack
Approach	$\alpha_o + 0.82\ (\alpha_s - \alpha_o)$	$\alpha_o + 0.90\ (\alpha_s - \alpha_o)$
All Other	$\alpha_o + 0.75\ (\alpha_s - \alpha_o)$	$\alpha_o + 0.90\ (\alpha_s - \alpha_o)$

where α_s is the stall angle of attack and α_o is the angle of attack for zero lift.

Table 17. Warning range for accelerated stalls.

Stall angle of attack is the angle of attack at constant speed for the configuration, weight, and c.g. position which is the lowest of the following:

(a) The angle of attack for the highest steady load factor, normal to the flight path, that can be obtained at a given Mach number;

(b) The angle of attack for a given speed or Mach number at which uncontrollable pitching, rolling, or yawing occurs (i.e., loss of control about a single axis);

(c) Angle of attack for a given speed or Mach number, at which intolerable buffeting is encountered.

The increase in buffeting intensity with further increase in angle of attack should be sufficiently marked to be noted by the pilot. This warning may be provided artificially only if it can be shown that natural stall warning is not feasible.

Stall Characteristics

In unaccelerated stalls, the airplane shall not exhibit uncontrollable rolling, yawing, or downward pitching at the stall in excess of 20°.

It is desired that no pitch-up tendencies occur in unaccelerated or accelerated stalls. In unaccelerated stalls, mild nose-up pitch may be acceptable

if no elevator control force reversal occurs and if no dangerous, unrecoverable, or objectionable flight conditions result. A mild nose-up tendency may be acceptable in accelerated stalls if the operational effectiveness of the airplane is not compromised and

(a) The airplane has adequate stall warning;

(b) Elevator effectiveness is such that it is possible to stop the pitch-up promptly and reduce the angle of attack;

(c) At no point during the stall, stall approach, or recovery does any portion of the airplane exceed structural limit loads.

These requirements apply to all stalls resulting from rates of speed reduction up to four knots per second (4.6 miles per hour, per second). Stall characteristics are unacceptable if a spin is likely to result.

Stall Prevention and Recovery

> It shall be possible to prevent the complete stall by moderate use of the controls at the onset of the stall warning. It shall be possible to recover from a complete stall by use of the elevator, ailerons, and rudder controls with reasonable forces, and to regain level flight without excessive loss of altitude or build-up of airspeed. Throttles shall remain fixed until speed has begun to increase when an angle of attack below the stall has been regained. In the straight-flight stalls with the airplane trimmed at a speed not greater than 1.4 U_S and with a speed reduction rate of at least 4.0 knots per second, elevator control power shall be sufficient to recover from any attainable angle of attack. On multiengine aircraft, it shall be possible to recover safely from stalls with the critical engine inoperative.

This requirement applies with the remaining engines up to thrust for level flight at 1.4 U_S, but these engines may be throttled back during recovery.

Although some light aircraft may have special stalling problems, such as nacelles stalling at high speeds where they can produce a significant lift, causing the airplane to attain dangerous attitudes, the stall problem is usually solved if the wing has good stall characteristics. NACA TR-703 (Ref. 72) is a set of design charts prepared to show the effects of wing geometry on the stalling characteristics of tapered wings; a summary of these effects is presented in Table 18.

GEOMETRIC PROPERTY/WING	EFFECTS ON STALL
Taper	Increasing taper tends to move the stalling point progressively outboard and to decrease the stalling margin of most of the remaining wing.
Aspect Ratio	An increase in aspect ratio tends to flatten the section lift distribution; up to an aspect ratio of 18, the effect on the stalling point is relatively small.
Thickness	An increase in root thickness ratio beyond 0.15 causes the stalling point to move inboard, except for the lowest values of Reynolds numbers tested, and tends to reduce the rate at which the section lift and maximum section lift diverge inboard of the initial stalling point.
Camber	Increasing camber linearly from root to tip (4%) appears to be useful to good stall characteristics only for low taper ratios.
Washout	Although washout is expensive in regard to drag considerations, it offers an effective means of improving stalling characteristics. Washout becomes more effective as Reynolds number is increased.
Reynolds Number	An increase in Reynolds number tends to move the initial stalling point inboard.
Sharp Leading Edge	A sharp leading edge reduces the maximum section lift coefficient so that stalling takes place inboard where the sharp edge is located.

Table 18. Effects of wing geometry on stall characteristics of tapered wings.

Thus, for good stall characteristics, wings with low taper ratios, moderate thickness (10% to 15%), low to moderate Reynolds numbers, 1^{o} to 3^{o} washout, and a sharp leading edge at the root seem the most desirable.

WR L-145 (Ref. 73) points out that surface roughness and propeller effects should also be considered as parameters affecting airplane stall. The airplanes tested for the report were military aircraft of the mid 1940's. Because of the armament required, the airplanes were equipped with numerous access doors, inspection plates, and numerous other features that tend to make the wing extremely rough and allow air leakage through it. It was found that a wing which was faired and sealed gave a higher $C_{L_{max}}$ then an unfaired wing, even though both wings stalled at approximately the same angle of attack. The study also indicated that propeller operation generally increases the severity of the stall, especially on single-engine airplanes. The rotation within the slipstream increases the effective angle of attack of the wing section behind the up-going propeller blades and decreases the effective angle of attack of the wing section behind the down-going propeller blades. An asymmetrical stall pattern is thus produced, leading to a sometime severe roll.

WR L-296 (Ref. 74) indicates that airplanes of the 1930's solved the problem of stall by providing a definite warning of the approaching stall through backward movement, position, and forces on the control column. Monoplanes usually had little or no taper with "inefficient" wing-fuselage junctures, causing a gradually developing stall, beginning at midspan. Thus, the stalled condition developed progressively after a reasonably definite warning; also, lateral control was often maintained up to or beyond the stall. Many of the airplanes designed in the 1940's depicted trends toward higher wing loadings and landing speeds; less emphasis was placed on stalling tendencies, thus leading to airplanes with poor stalling characteristics. WR L-296 also indicates that sharp leading edges at the wing root may improve poor stall tendencies. Another proposed solution is limitation of longitudinal control to prevent the wing from reaching maximum lift. To be effective, a warning must occur at an angle of attack considerably below that of maximum lift because gusts or inertia effects may momentarily carry the airplane beyond the warning attitude. An investigation was made in WR L-296 (Ref. 74) of a "stall-control flap." The basic wing tested was a 23012 section with a 60% chord flap. The idea was to deflect the stall-control flap so that the modified airfoil would have a shape similar to the 4412 airfoil, which has good stall characteristics because of its relatively flat lift-curve peak. The flap was considered aerodynamically satisfactory with or without high lift devices, even though it may be very expensive to install. The graph below indicates the effect of the flap deflection on lift-curve shape.

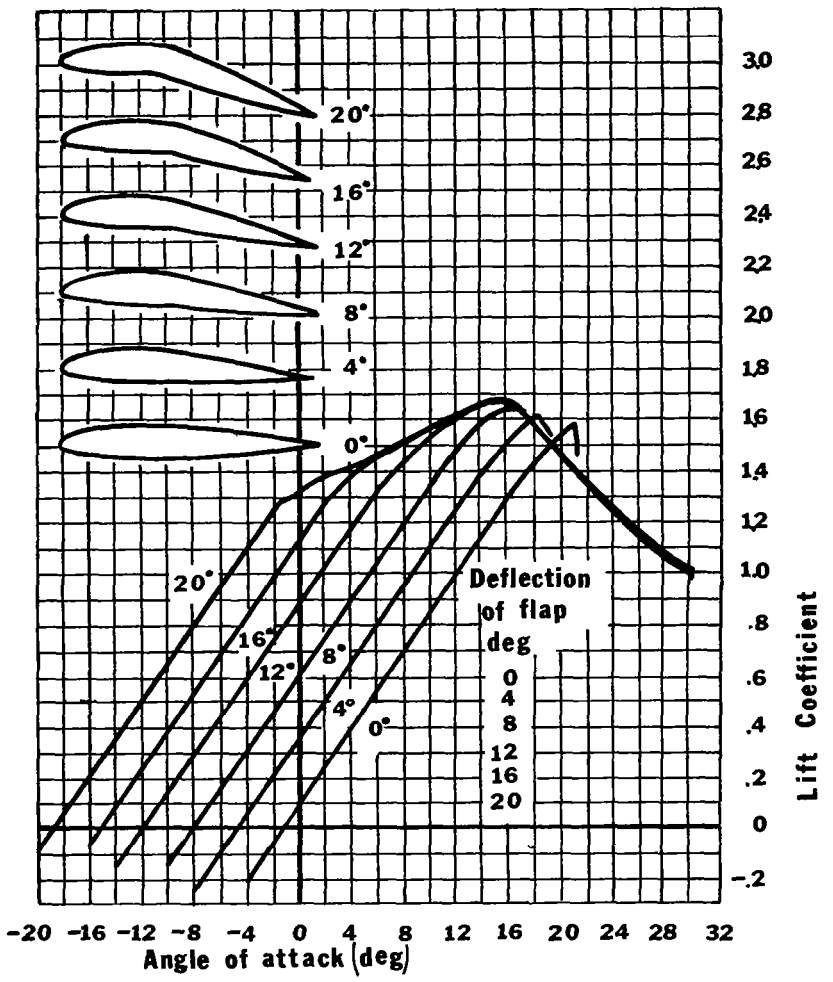

Figure 68. Investigation of a stall control flap in WR L-296 (Ref. 74).

NACA TN-1868 (Ref. 75) is a study made to correlate pilots' opinions of the stall warning properties of 16 airplanes, ranging from single-engine fighters to four-engine bombers, with a number of quantitative factors obtained from time, history flight records for speeds near stall. The altitude test range was 4,000 to 12,000 feet, with stalls attained in straight flight by gradually approaching the stall with the normal acceleration factor as close to unity as possible. The tests indicate that, in general, the stall warning is considered satisfactory by the pilots when characterized by any of the following qualities:

(a) Airplane buffeting at speeds 3 to 15 mph above stalling speed and of a magnitude to produce incremental indicated values of normal acceleration factor from 0.04 to 0.22;

(b) Preliminary controllable rolling motion from 0.04 to 0.06 radians per second occuring anywhere within a range of 2 to 12 mph above the stalling speed;

(c) At least 2.75 inches rearward travel of the control stick during the 15 mph speed range immediately preceding the stall.

The two graphs below indicate the satisfactory and unsatisfactory ranges of both normal acceleration increments, Figure 69, and rearward movement of the control stick, Figure 70, versus speed above the stall. Each line represents a separate test of one of the 16 airplanes. A_Z is the normal acceleration increment.

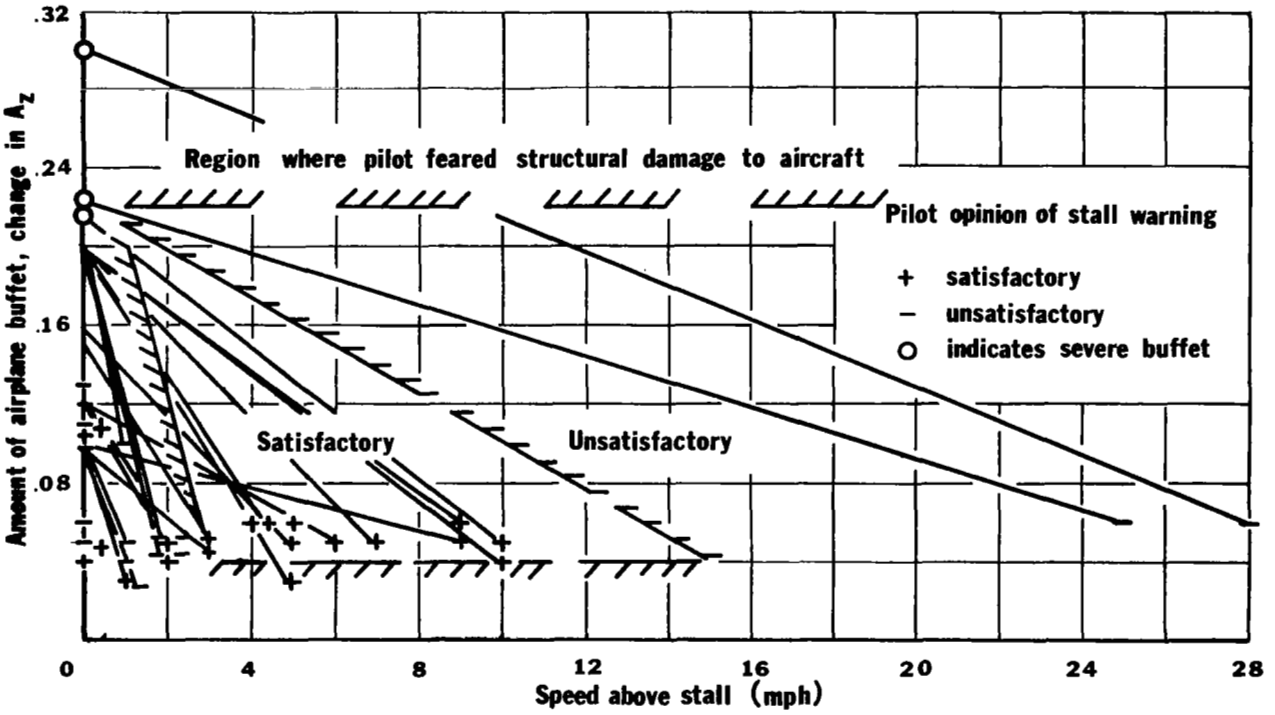

Figure 69. Correlation of pilot opinion of stall warning with airplane buffet at various speeds above stall.

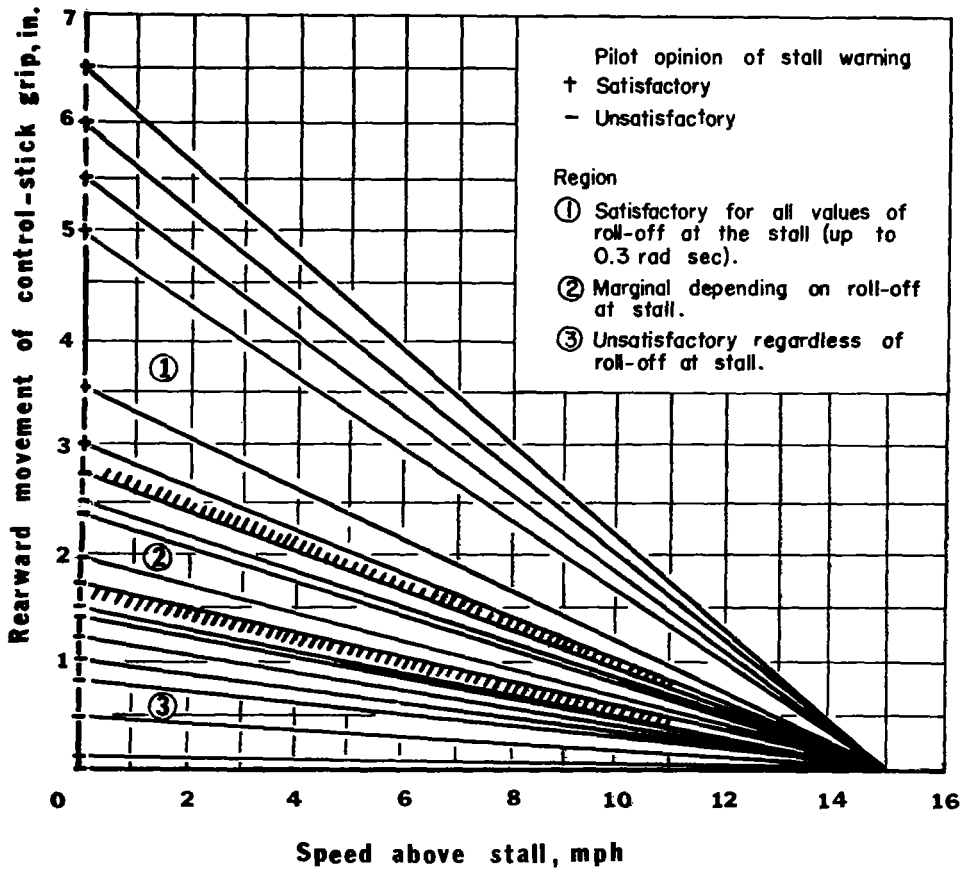

Figure 70. Correlation of pilot opinion of stall warning with rearward movement of control stick in the speed range immediately above stall.

In a summary of various stall-warning devices, TN-2676 (Ref. 76) points to the fact that a warning light, stall-warning dial, rudder shaker, or stick shaker may be necessary for any aircraft with very poor stall-warning characteristics. Such indicators can possibly be actuated by such devices as a leading-edge orifice, leading-edge tab, spoiler and pitot-static tube, trailing-edge pitot static tube, or trailing-edge vane. Light airplanes without hydraulic control systems will probably never need to use these devices.

TN-2923 (Ref. 77) describes the testing of a low-wing, light airplane model during the stall and into the incipient spin. A more detailed review of this report is presented below in the discussion of spin entry.

It should be noted that in seeking to analyze the motions of aircraft near stall, the usual assumption that the longitudinal stability derivatives are constants is no longer true. The derivatives are very strong functions of α. Also, downwash and sidewash fields are very strong and unstable under these conditions. Dynamic pressure may vary considerably along the span. Finally, a deep stall is usually accompanied by sufficiently large motions that one can no longer assume with accuracy that products and squares of pertubation velocities can be neglected. For these reasons, extreme care must be used in attacking this problem analytically.

SPIN ENTRY

The capacity for attaining a spinning attitude while performing ordinary flight maneuvers and the fact that many light aircraft accidents have been attributed in the last few years to stall/spin problems has led to extensive research by NACA/NASA concerning spin entry and recovery. More than 25 NACA/NASA reports deal with spin applicable to light aircraft design. Much of this literature was written in the late 1940's and early 1950's because the higher wing and fuselage loadings of more modern aircraft are not characteristic of the majority of the general aviation aircraft.

A developed spin is usually considered to be a motion in which an airplane in flight, at some angle of attack between the stall and 90°, descends rapidly toward the earth while rotating, with the wings nearly perpendicular to a vertical or near-vertical axis. Special consideration must be given to spins in the design stage, since controls effective in normal flight might be inadequate for recovery from the spin. The same factors which may cause difficulty in attaining a spin also may impede recovery from it, once attained. Besides the problem of providing adequate controls for recovery, there is also the problem of pilot disorientation resulting from the developed spin; thus, preventing the spin or recovering during the incipient phase (the motion between the initial stall and the developed spin) is essential. Civil Air Regulations require that the pilot of a personal-owner airplane recover from a one-turn spin upon release of controls by the pilot; this may mean that controls be designed to float against the spin.

Of the numerous significant reports reviewed for this study, two are considered of primary interest--Airplane Spinning by James S. Bowman (Ref. 78) and Status of Spin Research for Recent Airplane Designs by A. I. Neihouse, et al (Ref. 79). The latter discussed spin-tunnel testing and its correlation with actual flight tests, the influence of airplane geometry on spinning, and a summary of the spinning characteristics of 21 model airplanes, including model and full scale correlation. Airplane Spinning is a state-of-the-art summary of spin prediction and alleviation.

Experience has indicated that spins and spin recoveries of airplanes can be investigated safely and at a comparatively moderate cost using small dynamic models in a spin tunnel.* It is important that the model be designed so that geometrically similar paths of motion between the model and the airplane are attained in the spin; this is accomplished by holding the force, mass, and time ratio constant as well as the ratio of linear dimensions in the model design. It is hand-launched with a spinning motion into the spin tunnel, and the vertical speed of the column of air is adjusted to maintain a spinning attitude of the model at a particular height in the tunnel. It is assumed that, for most spins, the pilot would probably have the airplane

---

* a vertical wind tunnel controlled by a propeller with very fast response time

controls set approximately at "normal spinning control configuration"--that is, stick full back, and laterally neutral, rudder full with the spin. After the spin is established, the model control surfaces (rudder, elevator, and ailerons) are deflected to attempt recovery. Experience has shown that the criterion for satisfactory recovery for model tests is recovery within $2\frac{1}{4}$ turns of the model after the control surface deflections. Based on this analysis, when the recovery in the spin tunnel requires more than this number of turns, the controls are not sufficiently effective and the corresponding airplane probably would have unsatisfactory recovery characteristics. One poor recovery out of several recovery attempts is usually considered as undesirable as consistently poor recoveries. The philosophy is to assume that a proposed design is inadequate for spin recovery unless it can be proven satisfactory.

A developed spin involves a balance of aerodynamic and inertial moments and forces; thus, the effectiveness of any control in promoting or in terminating the spin depends not only on the aerodynamic moments and forces produced by the control but also on the inertial characteristics of the airplane. A spin about any axis in space can be considered as a rotational motion about any axis through the center of gravity. The equations for the moments acting in a spin* are

$$\dot{p} = \frac{U^2}{2\mu k_x^2} C_l + \frac{I_{yy} - I_{zz}}{I_{xx}} qr$$

$$\dot{q} = \frac{U^2}{2\mu k_y^2} C_{m,b} + \frac{I_{zz} - I_{xx}}{I_{yy}} rp$$

$$\dot{r} = \frac{U^2}{2\mu k_z^2} C_n + \frac{I_{xx} - I_{yy}}{I_{zz}} pq$$

The airplane spinning attitude (steep or flat) and its rate of rotation depend primarily on the yawing and pitching moment characteristics of the airplane. Low damping in yaw at spinning attitudes or high autorotative yawing moments lead to flat (high α), fast rotating (high Ω) spins. Some interesting facts can be pointed out by approximating the pitching-moment equation obtained in equating the aerodynamic and inertial pitching moments:

$$\Omega^2 = - \frac{M_{Y_{aero}}}{\frac{1}{2}(I_{zz} - I_{xx}) \sin 2\alpha}$$

Remembering that a positive pitching moment is nose up, it can be seen that a nose-down (negative) pitching moment may nose the airplane down but lead to a higher rate of rotation and may, in fact, flatten the spin. For given directional and lateral characteristics, the pitching moment can influence the motion so that it may vary from a high rotative spin to a low rotative spin.

The effect of any control in bringing about spin recovery depends upon the moments that the control provides and upon the effectiveness of those

---

* assuming the x, y, and z axes are principal axes and that engine effect can be ignored.

moments in producing a change in angular velocity and thus in upsetting the spin equilibrium. Experience has shown that the best way to alleviate the spinning motion is to provide a yawing moment about the z body axis to oppose the spin rotation; thus, the rudder is usually considered the most important control, especially for light airplanes. It also appears that elevator effectiveness and aileron effectiveness, in the final analysis, depend upon their ability to alter the yawing moment of the spin.* Thus, it would seem that the most effective way to influence the spin and to bring about recovery is to obtain a yawing moment by applying a moment about an axis which experiences the least resistance to a change in angular velocity.** For example, the most proficient way to obtain an antispin yawing moment for recovery may be to roll the airplane in such a direction that a gyroscopic yawing moment to oppose the spin is obtained. Similarly, if mass is heavily concentrated in the wings, movement of elevators downward may provide the most effective means of applying an antispin yawing moment. Thus, because of inertial coupling of a rotating body, if the moment about one axis is changed, the moments about the other axes are also changed.

By inspecting the equation given earlier for $\dot{r}$, it can be seen that the rudder is the most important control when $I_{xx} - I_{yy} \simeq 0$ because μ(defined as $m/\rho Sb$) and k_z are relatively small, and C_n is a function of rudder deflection. For modern, high speed fighters and research airplanes, large negative values of $I_{xx} - I_{yy}$ predominate, since the mass is heavily concentrated in the fuselage. For these airplanes, it would be extremely important to make the inertia terms antispin (negative for right spin) for recovery. This can be accomplished by controlling the algebraic sign of the pitching velocity, e.g., by tilting the inner wing (right wing in a right spin) down relative to the spin axis. This tilting of the wing downward makes pitching velocity positive ($q \simeq \Omega \sin \phi$ for low values of I_{xx}) and gives rise to a cross-coupled effect, which acts in a direction that terminates the spinning. Light airplanes, however, fall, for the most part, into the category of airplanes designed in the late 1930's and early 1940's. These light airplanes have relatively small changes in the inertia terms which contribute to $\dot{r}$, indicating that the rudder should be the most important control.

The principal factors in spinning are mass distribution, by far the most important single parameter, and tail design, particularly important for conditions of zero or near-zero loading (small $I_{xx} - I_{yy}$). By knowing the mass distribution and tail design, it is possible, in many cases, to predict whether an airplane has satisfactory spin-recovery characteristics. The mass distribution of airplanes can be grouped into three general loading categories, as shown on the following page.

---

* It should be pointed out that if spoilers are used instead of ailerons, the spoilers are generally ineffective in the developed spin because of the area shielded in the spinning attitude.

** a moment about the axis with the least amount of inertia.

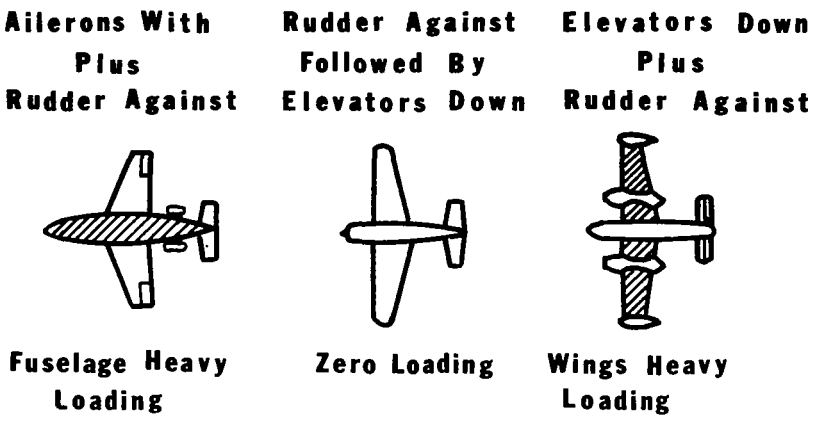

Figure 71. Primary recovery controls as determined by mass distribution.

The type of loading shown on the right is classified as wing-heavy loading, in which the roll moment of inertia is greater than the pitch moment of inertia. The airplane on the left is an example of fuselage-heavy loading, in which the roll moment of inertia is less than the pitch moment of inertia. The airplane in the center has roll and pitch moments of inertia which are about equal; this condition is referred to as zero loading.

The loading of the airplane can dictate what controls are required for recovery, as explained in WR L-168, A Mass-Distribution Criterion for Predicting the Effect of Control Manipulation on the Recovery from a Spin (Ref. 80). Deflecting the rudder against the spin is always recommended, but, for satisfactory recovery, deflection of other controls is sometimes required. For the case of wing-heavy loading, down elevator is the primary recovery control, while ailerons against should also be beneficial; for fuselage-heavy loading, the aileron is the primary recovery control. In the latter case, the aileron needs to be deflected with the spin--for example, stick right for a spin to the right. Predicting what the effects will be for the zero loading is difficult; but, almost invariably, the proper recovery procedure is to move the rudder against the spin and, a short time later, move the elevator down. The above recovery techniques seem to indicate that spin recovery is simple, but it is sometimes hard to class a given airplane in one of the three categories above and, once classed, the controls still may or may not produce enough antispin moment to achieve recovery.

Tail design is also an important factor in designing an airplane to recover from spins. Since most light planes fall into the zero loading category, the rudder is of primary importance to a good design. In a spin, there is a dead air region over much of the vertical tail caused by the wake of the stalled horizontal tail. For optimum rudder effectiveness, part of the rudder must be outside this stalled wake. Another factor which affects tail design from the spin standpoint is that there should be a substantial amount of fixed area beneath the horizontal tail to provide damping of the spinning motion. A criterion for good tail design was determined in the middle 1940's

(TN 1045, Ref. 81 and TN 1329, Ref. 82) on the basis of spin-tunnel tests with about 100 different designs. This criterion is called the tail damping power factor (TDPF), a measure of the damping provided by the fixed area beneath the horizontal tail and the control power provided by the unshielded part of the rudder. The tail-damping power factor can be calculated as shown below in parts a, b, and c of Figure 72.

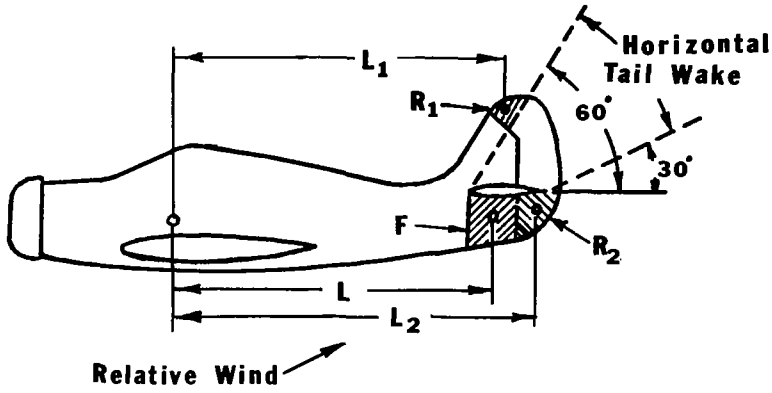

Full-length rudder; α assumed to be 45°

Part a

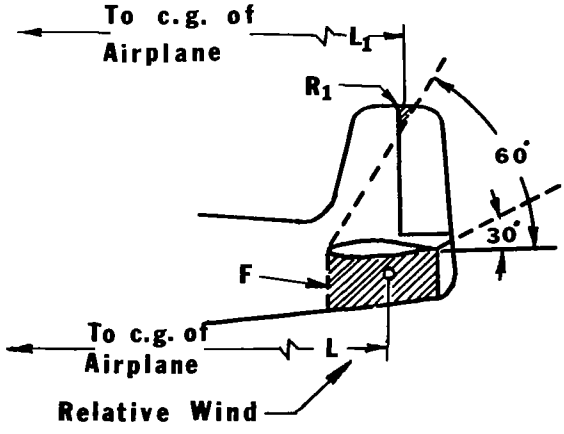

Partial-length rudder; α assumed to be 45°
TDR < 0.019

Part b

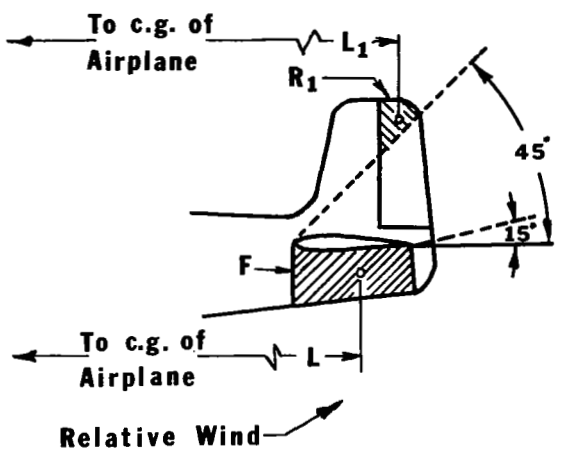

Partial-length rudder; α assumed to be 30°
TDR > 0019

$$TDPF = \left(\frac{FL^2}{S(b/2)^2}\right)\left(\frac{R_1L_1 + R_2L_2}{S\ b/2}\right) \text{ and } TDR = \frac{FL^2}{S(b/2)^2}$$

Part c

Figure 72. Calculation of tail-damping power factor.

The tail damping power factor required to insure satisfactory recovery is given in the figure below.

$$\mu = \frac{\text{Airplane Density}}{\text{Air Density}} = \frac{m/Sb}{\rho}$$

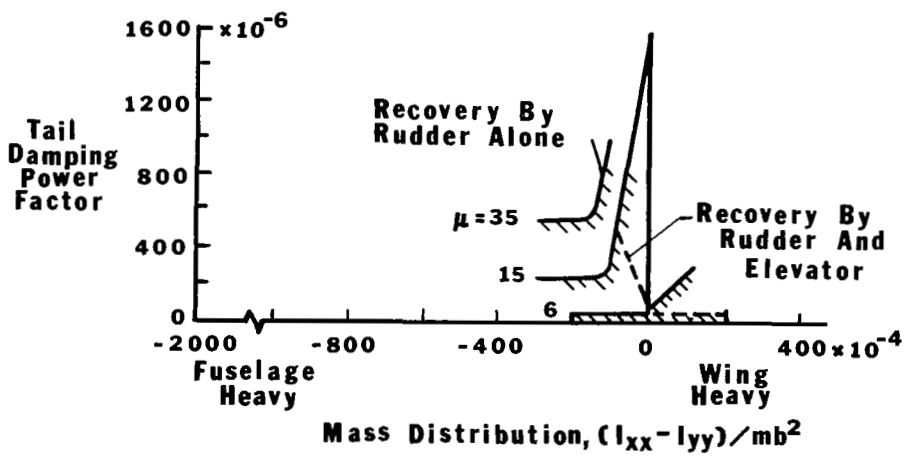

Figure 73. Tail design requirements.

All the data are in the area of zero or near-zero loading, where the rudder is a primary recovery control and the tail design is of particular importance. As can be seen from the graph in Figure 68, only a limited part of the total existing range of mass distributions applies. The plot shows boundaries indicating the minimum values of the tail-damping power factor required to insure satisfactory recovery. The hatched side of the boundaries is the unsatisfactory side. The solid lines are for recovery by rudder alone, and the broken line shows the boundary for recovery by rudder and elevator. The boundaries are presented in terms of the relative density factor μ. The value of $\mu = 6$ is representative of light, single-engine, personal-owner airplanes, while $\mu = 35$ is representative of that for executive jets.

TN-1329, Tail-Design Requirements for Satisfactory Spin Recovery for Personal-Owner-Type Light Airplanes, (Ref. 82) is a report dealing specifically with light airplane design. Its conclusions are based on tests of 60 models in the Langley spin tunnels. Results of this investigation are shown in the plot below.

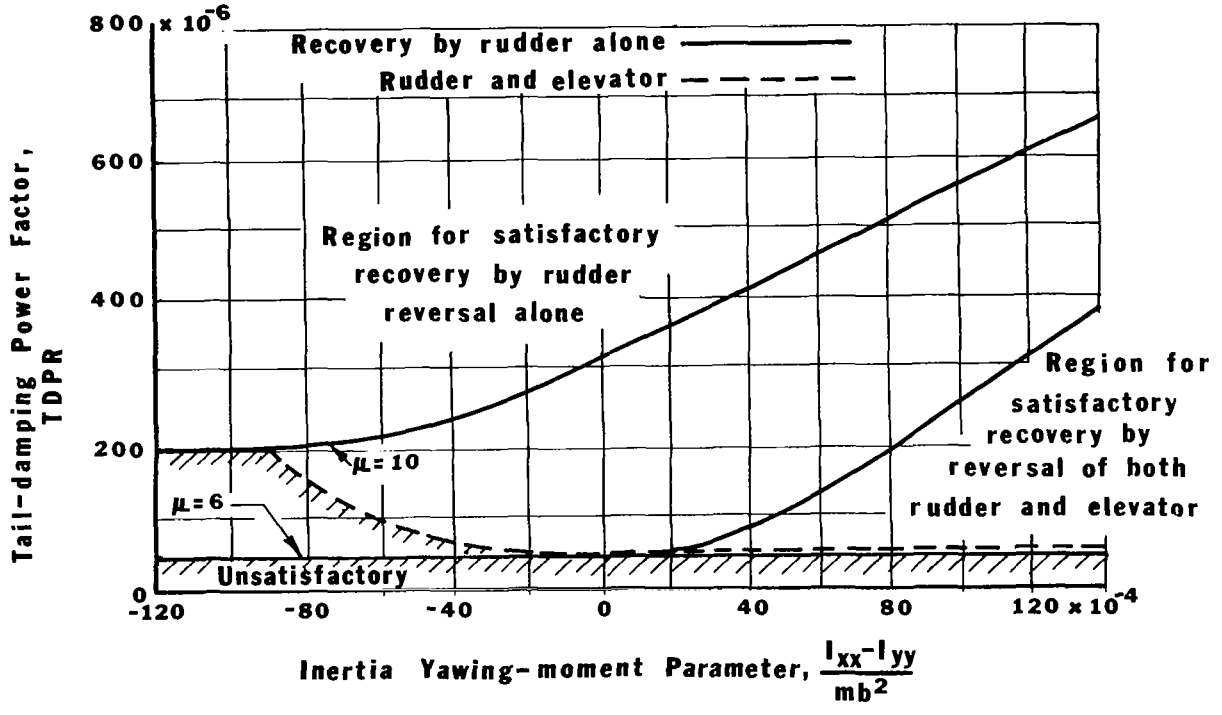

Figure 74. Vertical-tail design requirements for personal-owner-type airplanes.

An important plot which indicates other influences of mass distribution on optimum control movement for recovery from spin is presented below.

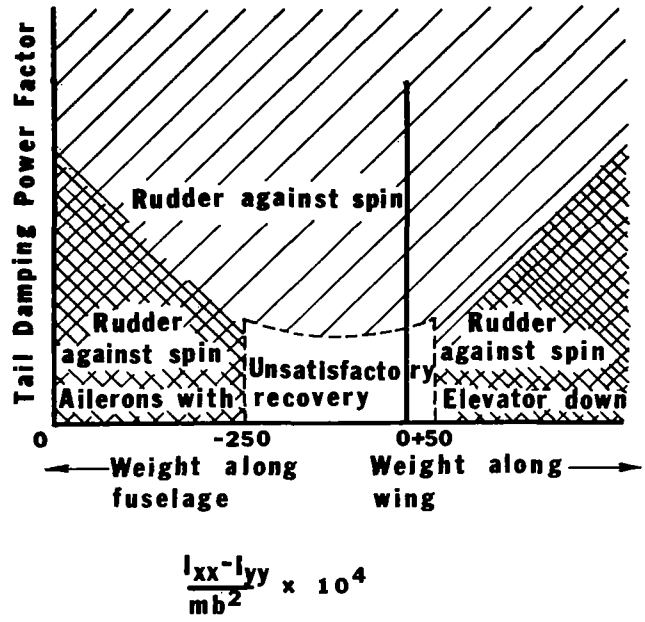

Figure 75. Influence of mass distribution on optimum control movement for recovery from spin.

The unsatisfactory region exists because the difference in inertia is low. As the difference increases either way the control surface (elevator in the case of positive increase, aileron in the case of negative increase) gains effectiveness. Based on the inertias, the reversal of aileron effect should occur at $I_{xx} - I_{yy} = 0$; however, due to the aerodynamic effects, the reversal of aileron effect is shifted from 0 to $[(I_{xx}-I_{yy})/mb^2] \times 10^4 = -50$. Thus, in this vicinity, ailerons with the spin (stick right in a right spin) generally loose their favorable effect and become adverse; for ailerons against the spin, the converse is true. This result, it is believed, is primarily a result of a secondary effect associated with positive C_{n_β} of the airplane and a resulting relative prospin increment in yawing moment because of the increment in inward sideslip that invariably occurs when ailerons are set with the spin. Another important graph, shown below, is a summary of the most important factors in spinning and indicates the present state-of-the-art.

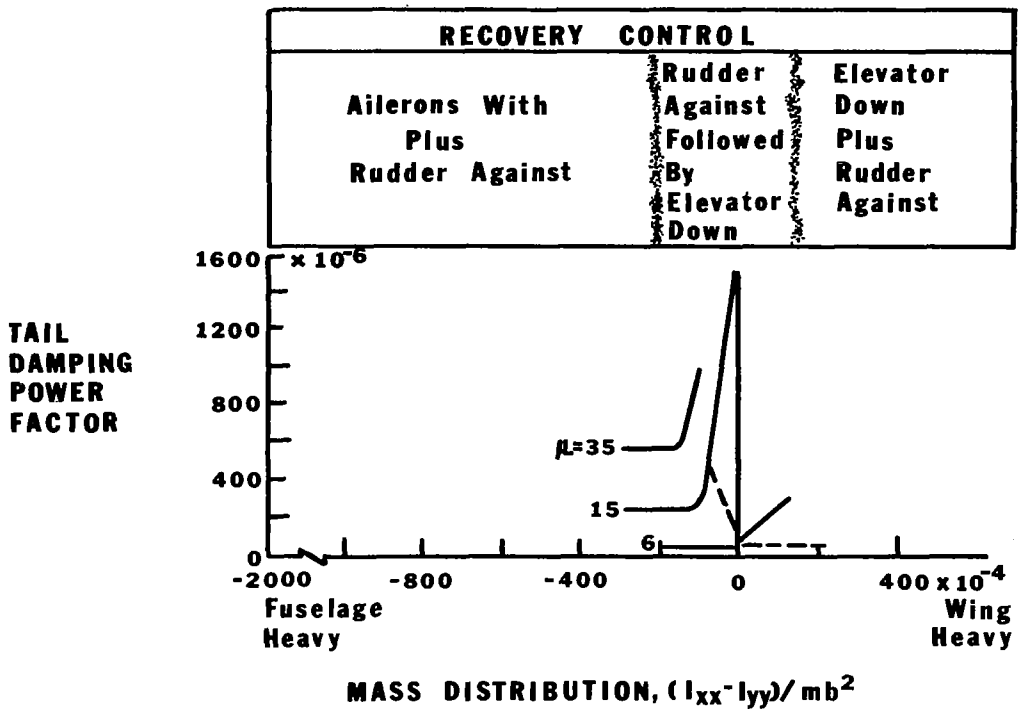

Figure 76. Summary of the most important factors in spinning.

The figure above agrees with current literature; however, it was previously considered in rudder-elevator recovery procedures that rudder application should lead elevator application. For an erect spin down elevator increases the shielding of the rudder more than up elevator; thus, maintaining elevator up provides maximum rudder effectiveness during rudder reversal. It should be noted that, for the extreme loadings on both ends of the scale, no criteria have been developed for predicting the effectiveness of the controls for satisfactory recovery. The safest way to insure good spin recovery is by spin tunnel or flight testing.

The prescribed methods for spin recovery have been given above for the particular mass configuration desired, but a recovery may still be hard to achieve. In flight, an airplane enters a spin following roll-off just above the stalling angle of attack after being brought up from lower angles of attack. It usually takes an airplane two to five turns to attain a fully developed spin after starting the incipient-spin motion, with the number of turns depending upon configuration and control technique. One important fact should be remembered; recoveries are generally achieved much more readily when attempted during the incipient phase of the spin than when attempted after the spin becomes fully developed. Thus, some consideration should be given to the techniques of noticing a spin entry attitude and to ways of avoiding the fully developed spin.

TN-2352 (Ref. 83) is a spin-tunnel investigation of a low-wing personal-owner aircraft which was conducted to provide design information for proportioning personal-owner or liaison airplanes for satisfactory recovery from spins

and for spin proofing. The investigation was intended to be extensive enough to determine the configurations most likely to meet the spin-recovery requirements given in Part 3 of The Civil Air Regulation (Ref. 54) and summarized below.

For an airplane licensed in the normal category:

(1) A 1½-turn recovery after a 1-turn spin by releasing controls (controls assisted to the extent necessary to overcome friction)
(2) "Uncontrollable spin" check--airplane capable of recovering from a 1-turn spin with ailerons at neutral by first completely reversing elevator and then, if necessary, fully reversing the rudder.

For airplanes licensed in the acrobatic category:

(1) A 4-turn recovery after 6 turns of the spin by releasing controls
(2) Recovery from a 6-turn spin in 1½ additional turns after neutralization of rudder and elevator, ailerons at neutral
(3) "Uncontrollable spin" check--airplane capable of recovering from a 6-turn spin with ailerons at neutral by first completely reversing elevator and then, if necessary, fully reversing the rudder
(4) Recovery from "abnormal spins"--a 2-turn recovery after 6 turns of the spin with ailerons initially either full with or full against the spin by neutralizing ailerons and fully reversing rudder and elevator
(5) A 1½-turn recovery from a 1-turn spin by neutralization of rudder and elevator with flaps and landing gear extended.

An extensive amount of testing of this light airplane indicated that satisfactory recovery can be readily obtained even if the tail-damping power factor is not very great, provided the recovery technique used is full rapid rudder reversal followed approximately ½ turn later by forward movement of the stick. The results also indicated that for recovery by merely neutralizing both controls, especially for rearward c.g. positions, high values of tail-damping power factor may have an adverse effect upon recoveries. It was found that different wing planforms had little effect on the model spin and recovery characteristics. It was concluded that unless the rudder can be designed to float against the spin, recovery from a spin by releasing controls might be difficult unless the elevator can be made to float at deflections farther down than neutral. It was also concluded that other requirements for recovery by various movements of the controls as specified in the aforementioned regulations could probably be met for the various model configurations and mass distributions investigated by maintaining the center of gravity at a forward position and utilizing a high tail-damping power factor. For fuselage heavy loading and low TDPF a premature forward stick movement may retard recovery. Mass changes were significant at low TDPF but not at high TDPF. It may be of interest to mention that the model spun with a total angular velocity of approximately 0.35 to 0.5 revolutions per second.

An investigation of the effect of center of gravity location on the spinning characteristics of a low-wing monoplane model is given in TR-672 (Ref. 84).

Moving the c.g. forward steepens the spin, increases $\Omega b/2U$, and improves recovery; similarly, moving the c.g. back tends to flatten the spin, decrease $\Omega b/2U$, and retard recovery. A report in the same series of investigations, TR-691 (Ref. 85), gives the effects of airplane relative density. The findings in this report are that, in most cases, an increase in relative density produces flatter spins, higher velocities, lower values of $\Omega b/2U$, and slower recoveries.

NACA TN-570 (Ref. 86) is directly applicable to light airplane design. This particular report investigates the effect of different tail arrangements on the spinning characteristics of a low-wing monoplane model. Results of this investigation indicate that a reduction in tail length results in spins with higher angles of attack, higher values of $\Omega b/2U$, and slower rates of descent. Recoveries from the spin seem to depend critically upon the exact location of the vertical surfaces. It is also concluded that, by making certain reasonably small changes in the tail arrangement, all the spinning characteristics, except the amount of sideslip, can be changed through wide ranges. This again points out the importance of tail design in light airplane spin recovery.

TN-608 (Ref. 87) is another investigation in which a series of models were tested in the spin tunnel. It was found that rectangular and faired tips give the steepest spins and flaps tend to retard recovery; for controls with the spin, tail B (below) gives steeper spins than tail A, with generally satisfactory recovery for either tail, while tail C generally gives slower recoveries.

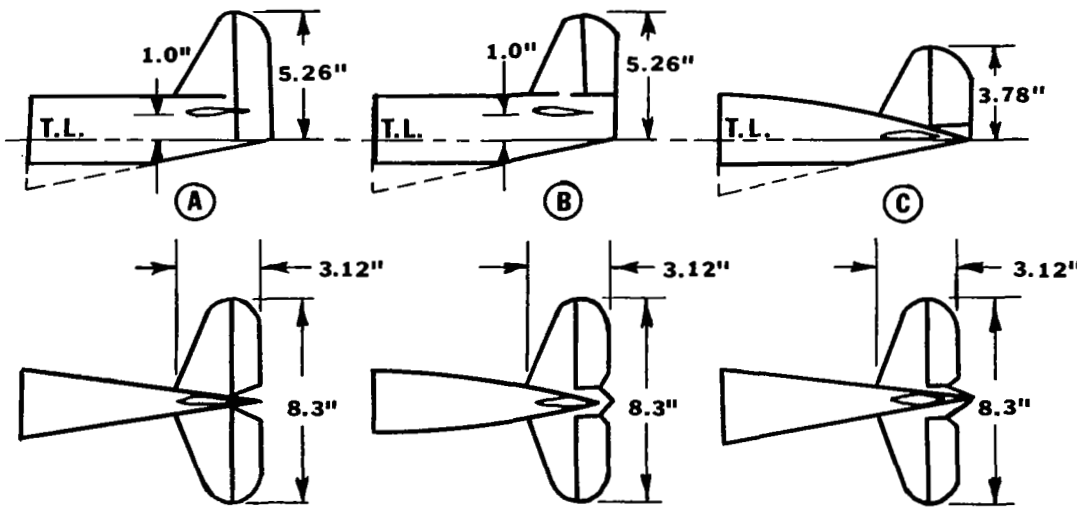

Empennage Arrangements Investigated

Figure 77. Effects of various aircraft tails on spin recovery.

The effect of such devices as antispin fillets and dorsal fins on spin recovery characteristics can be found in TN-1779 (Ref. 88). Data from 21 different models were used to determine the action of fillets in damping of spin rotation, and 30 models were investigated for the effect of dorsal fins. The effectiveness of antispin fillets for spin recovery appear to depend primarily upon the fact that the fuselage area below the fillets becomes effective in damping the spin rotation. Whether or not the fillets improve the recovery characteristics of a given design is still a function of the tail-damping power factor of the design and the mass distribution. Dorsal fins generally have little effect on spin and recovery characteristics.

TN-1801 (Ref. 89) should be mentioned because it is a spin investigation of a twin-tail light airplane model with linked and unlinked aileron controls. It was found that when the rudders and ailerons are linked for two-control operation, the model generally does not spin. The spins obtained in this study were steep, and the tests resulted in satisfactory recovery.

TN-2923 (Ref. 77) is another report in which a light airplane was tested. The motion of a personal-owner or liaison airplane through the incipient spin was analyzed. It was found that, after the initial stall and immediately after the model becomes unstalled, the rates of yaw and pitch are relatively small, and the rates of roll begin to decrease. There also is little loss of altitude up to this time and the results indicate that, even though the airplane may be inverted, a time soon after the roll-off has started appears to be a desirable time to attempt to terminate the motion. It is felt that the motions attained in this investigation are indicative of the motions of a low-wing, light airplane in the incipient spin. Although evaluation of the parameters in incipient-spin motion is not treated specifically in the equations of motion presented in Appendix A of the present study, these parameters could be obtained by proper application of the techniques used in that derivation. Below are some example plots of angular displacements and angular velocities versus time for the incipient spin caused by a right roll-off shown in Figures 78 and 79.

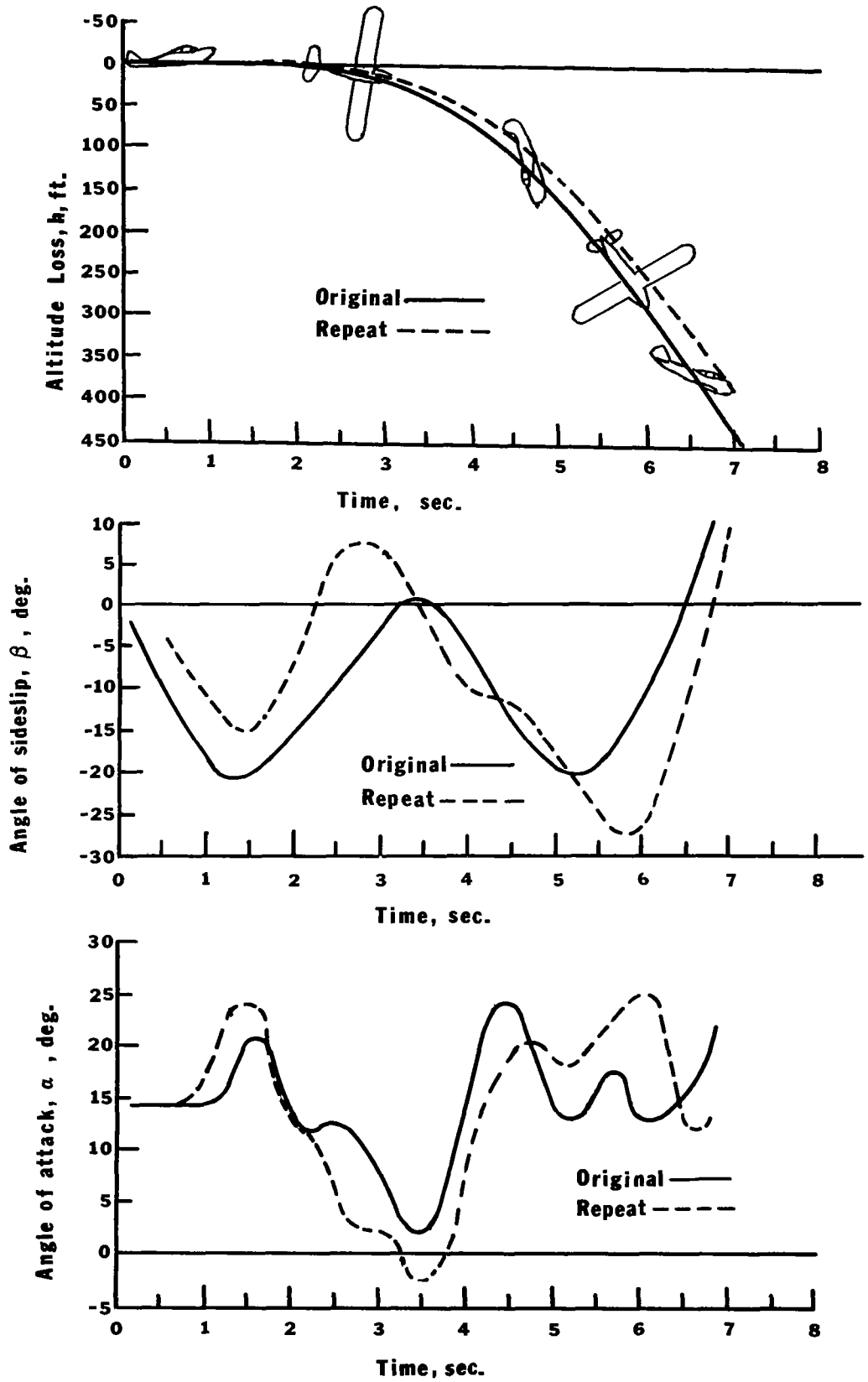

Figure 78. Angular displacements versus time for the incipient spin caused by a right roll-off.

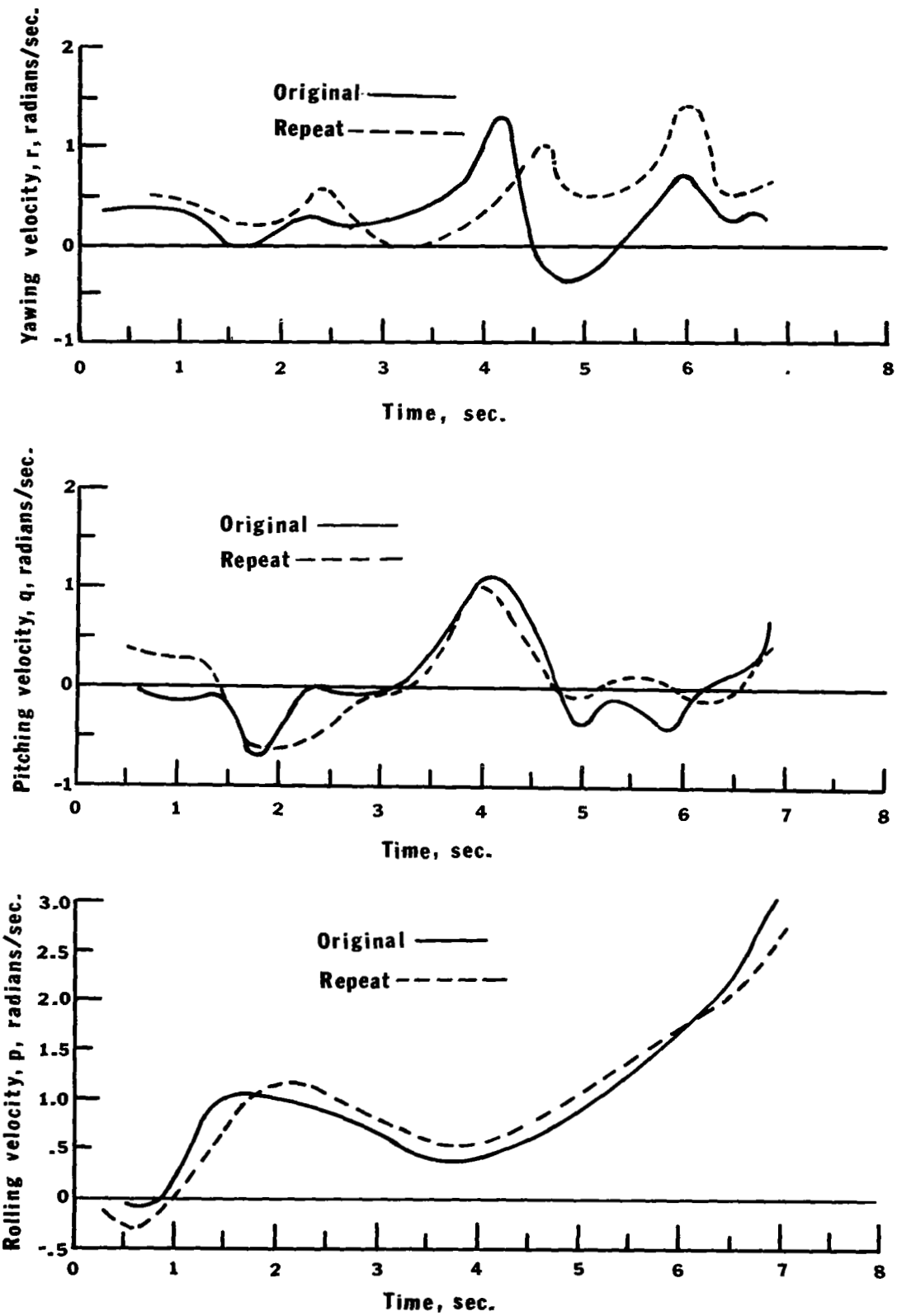

Figure 79. Angular velocities versus time for the incipient spin caused by a right roll-off.

HUMAN FACTORS

For maximum safety to an aircraft and its occupants, the pilot must be able to control aircraft motion during all flight conditions. One possible means of attaining this objective is to design the aircraft controls for the "average" man; however, AFSC DH 1-3 (Ref. 90) indicates that less than one per cent of the population is "average" in the five dimensions considered. Thus, designing for the "average" man appears unsound. The concept of "design limits" offers a more realistic approach. With this idea in mind, the following discussion centers on the pilot's comfort from a "design limit" viewpoint. Using anthropological data, comfort limits for pilots of general aviation aircraft are examined.

Setting the proper minimum force reduces the likelihood of accidental activation of a control, especially those controls on which the pilot must continuously keep his hands or feet. An upper limit is needed to insure that required control forces do not exceed the pilot's capabilities. Several generalizations concerning force applications to control devices are given in AFSC DH 1-3 (Ref. 90):

a) Force application is equally accurate for hands and feet;

b) Controls centered in front of the operator permit maximum force application;

c) Control force greater than 30 to 40 lbs applied by hand or greater than 60 lbs by foot is fatiguing;

d) The preferred hand and arm are generally 10% stronger than the non-preferred.

The capability which 95%, or the fifth percentile, of a population can be expected to exert is considered the standard.

From AFSC DH 1-3, the table below shows arm strength for different angles of elbow flexion.

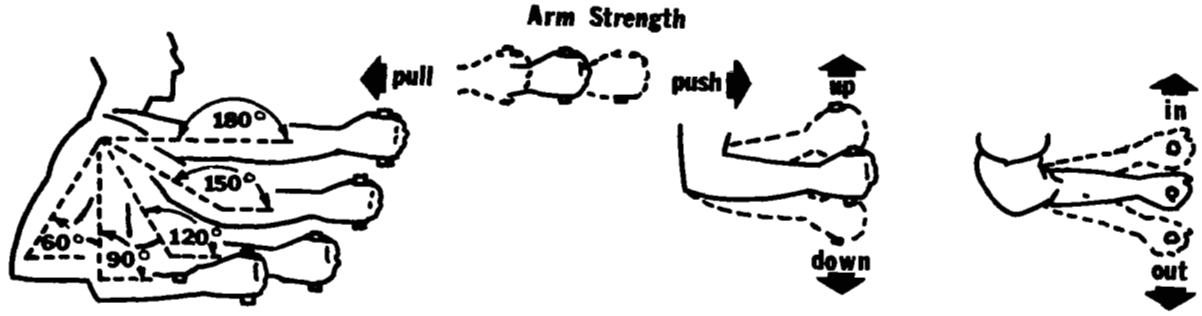

SEATED												
ELBOW FLEXION	PUSH		PULL		UP		DOWN		IN		OUT	
	R	L	R	L	R	L	R	L	R	L	R	L
180°	50	42	52	50	14	9	17	13	20	13	14	8
150°	42	30	56	42	18	15	20	18	20	15	15	8
120°	36	26	42	34	24	17	26	21	22	20	15	10
90°	36	22	37	32	20	17	26	21	18	16	16	10
60°	34	22	24	26	20	15	20	18	20	17	17	12

Table 19. Arm strength for different angles of elbow flexion.

The maximum force exerted on an aircraft control stick by the right arm of male Air Force personnel in the sitting position, according to Morgan (Ref. 91), is reproduced in Table 20.

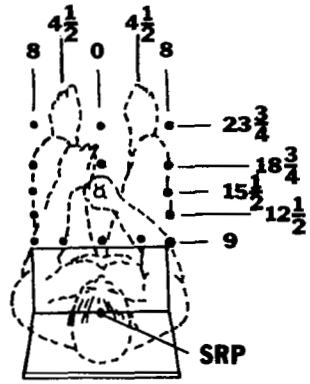

RIGHT ARM ON AIRCRAFT CONTROL STICK (POUNDS)					
DISTANCE IN INCHES FROM					
SRP*	MIDPLANE	PUSH	PULL	LEFT	RIGHT
9	8 (left)	12	26	24	34
	4½ (left)	18	28	31	31
	0	26	34	30	23
	4½ (right)	34	39	26	15
	8 (right)	37	39	26	12
12 1/2	8 (left)	18	33	23	31
	8 (right)	43	49	22	16
15 1/2	8 (left)	23	39	20	25
	0	43	54	24	20
	8 (right)	53	55	24	13
18 3/4	8 (left)	36	45	16	22
	0	64	56	8	15
	8 (right)	70	58	22	14
23 3/4	8 (left)	29	51	11	19
	0	54	62	14	13
	8 (right)	56	58	20	12

*Forward; control is 13 1/2 inches above seat reference point.

Table 20. Maximum force exerted on an aircraft control stick by the right arm.

From this same reference, similar information for amount of force on an aircraft control wheel is given in the table below.

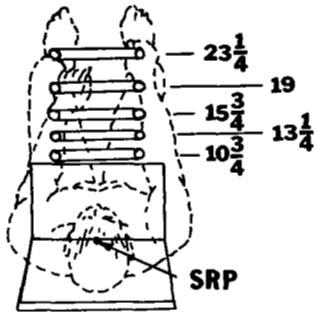

RIGHT ARM ON AIRCRAFT CONTROL WHEEL (POUNDS)					
DISTANCE IN INCHES FORWARD FROM SRP*	CONTROL POSITION	PUSH	PULL	LEFT	RIGHT
	90° (left)	32	23	23	27
	45° (left)	48	40	21	24
10 3/4	0	52	44	26	20
	45° (right)	40	39	31	24
	80° (right)	19	18	21	15
13 1/4	90° (left)	32	33	26	21
	90° (right)	25	31	25	19
	90° (left)	32	42	27	19
15 3/4	0	61	66	27	27
	90° (right)	32	49	29	20
	90° (left)	37	60	22	27
19	0	64	73	25	30
	90° (right)	33	61	33	22
	90° (left)	82	73	21	26
23 1/4	0	105	77	20	35
	90° (right)	49	74	26	22
*Wheel grips 18 inches above SRP and 15 inches apart.					

Table 21. Amount of force exerted on an aircraft control wheel.

Since each of these tests gives the maximum force for the right arm of a male, it must be remembered that the standard left arm, which is usually weaker, and the possibility of female pilots for general aviation aircraft would dictate lower maximum forces. These limits on wheel forces need not be so stringent if a worst case analysis shows them to be impractical, since the pilot could use both hands if necessary. When possible, use of two hands on the wheel should be avoided on landing, as the pilot may need his right hand to perform other tasks. Damon (Ref. 92) gives the left rotation of the wheel as approximately 25 lbs and right rotation as about 30 lbs.

The maximum force that can be exerted in extension of the leg at the hip and knee for 17 test conditions on male British civilians in the sitting position is given in Morgan (Ref. 91).

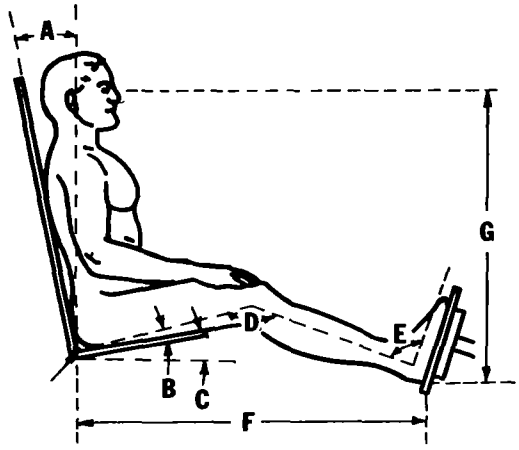

Test Conditions				Avg. force (lb)
A	B	C	D	
0	0	0	90	63
0	0	0	113	89
0	0	0	135	156
0	5	0	164	559
0	6	0	94	73
0	8	0	93	87
0	10	0	80	77
0	10	0	90	59
0	10	0	135	270
0	10	0	165	346
0	15	0	149	227
0	15	0	160	845
0	15	0	169	530
0	16	0	129	319
0	17	0	117	212
0	17	0	151	684
0	33	0	106	184

Table 22. Maximum force exerted in extension of the leg at the hip and knee.

Morgan (Ref. 91) also considers the maximum force that can be exerted in extension of the ankle, corresponding to foot pedal operation (Table 23), by male Air Force personnel for 18 test conditions.

Test Conditions				Percentiles (lb)
A	E	F	G	5th
13	10	35¼	37	14
13	10	38½	37	54
13	30	35¼	37	25
13	30	38½	37	64
13	50	35¼	37	24
13	50	38½	37	48
13	10	35¼	39	15
13	10	38½	39	37
13	30	35¼	39	26
13	30	38½	39	60
13	50	35¼	39	22
13	50	38½	39	50
13	10	35¼	41	18
13	10	38½	41	35
13	30	35¼	41	32
13	30	38½	41	50
13	50	35¼	41	23
13	50	38½	41	50

Table 23. Maximum force exerted in extension of the ankle.

The following table, adapted from MIL-F-8785B (Ref. 4), gives force limits for the elevator, ailerons, and rudder.

CONTROL	MAXIMUM (lbs)	MINIMUM (lbs)
Elevator		
Stick controllers	28.0	3.0
Wheel controllers	120.0	6.0
Ailerons		
Stick controllers	20.0	5.5
Wheel controllers	40.0	10.5
Rudder		
Pedals		
for short duration	100.0	--
for steady coordinated turns	40.0	--

Table 24. Force limits for the elevator, ailerons, and rudder.

Bureau of Aeronautics Report AE-61-4-II (Ref. 93) discusses friction forces in the control system as they affect the pilot's tracking accuracy and recommends that friction forces for hand controls in excess of three pounds be avoided, since they do not improve performance but do increase pilot fatigue. At the same time, this report also recommends that no hand control require less than two pounds of force and no pedal movement require less than seven pounds of force for increased pilot tracking accuracy.

It is not considered necessary to set standards for switches and dials, since they will most likely not require limit forces; however, Woodson and Conover (Ref. 94) suggest that, for increased efficiency, rotary knob diameters range from one-half to two inches and have a maximum resistance of one pound or less.

Often, the force to be overcome is used as a feedback cue; thus, it is necessary to reproduce a previously experienced force and associate with it a certain reaction of the aircraft. The ability to reproduce a given force, as stated by McCormick (Ref. 95), varies with type of control and amount of force to be exerted, as shown in the graph below. The controls tested were of the pressure type, so various amounts of pressure could be applied with little or no displacement, making amount of displacement constant. The devices tested were a stick, an aircraft-type wheel, and a rudder-like pedal. The difference between the actual force reproduction and the desired reproduction was expressed in limens (the standard deviation divided by the standard pressure). This figure indicates that, for pressures of five pounds or less, the errors in reproducing the desired forces are proportionally greater. For five to ten pounds, the errors are somewhat less, but still greater than those of forces ten to forty pounds; pressures greater than forty pounds, over long periods of time, are apt to cause pilot fatigue.

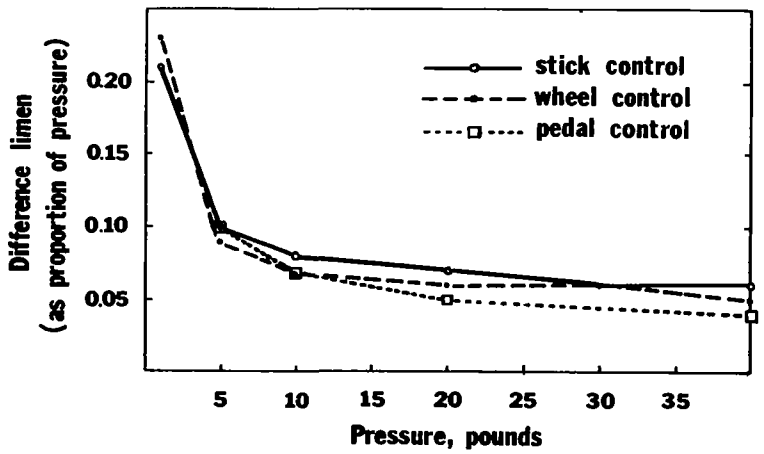

Figure 80. Results of data on reproducing control forces.

Of considerable importance in the design of any control system are the limitations on the pilot's response time, or the speed, considering the effect of load, at which the pilot can actuate the controls. Orlansky (Ref. 96) reports an experiment to determine the maximum rate at which pilots can push or pull a control stick as the load per unit displacement changes. From this and other studies, he concludes that, for a 35-lb load, the maximum rate of stick movement is about 50 in./sec, pushing a stick is nearly 25% faster than pulling, and the rate of control stick motion decreases as the load on the stick increases. The Handbook of Human Engineering Data (Ref. 97) indicates that, as the distance for a positioning movement increases, the operator increases his speed of movement; the time required for the response does not increase as much as would be expected. For example, data from this handbook indicate that the time for total movement increases 15% when the distance is doubled and 25% if the distance is tripled. Also noted is the loss of time in making a position movement when the pilot must change directions with the control, when about 15% to 24% of the movement time is involved in stopping the movement in one direction and beginning it in another direction. Continuous curved motions, therefore, are desired over motions with sharp directional changes.

The pilot's response time is the sum of his reaction time and his movement time. Reaction time, as defined in AFSC DH 1-3 (Ref. 90), is the period between the onset of the signal to respond and the beginning of the actual response. Among the factors affecting reaction time are type of signal, motion unit responding, precision of the response, age and sex of the responder, preparation for the response, practice for complex responses, and ambient conditions. AFSC DH 1-3 reports that hand response is 20% faster than foot response, and the preferred limb is about three percent faster than the non-preferred. The Handbook of Human Engineering Data (Ref. 97) gives mean reaction times for simple movements ranging from about 0.22 sec to 0.3 sec. The conclusion from these data is that the auditory system reacts faster than the visual system.

The foregoing information has been included to indicate the anthropological basis for satisfactory handling: the actuation force levels, limb displacements, and phase relationships with which a pilot is comfortable. It is then the designer's task to provide satisfactory aircraft response using these anthropological data to describe the input to the aircraft control system. The reader will note that the primary emphasis of this report is on insuring satisfactory aircraft response. While many future light aircraft will retain entirely manual control systems which require the designer to make certain compromises between what forces, displacements, etc. he would like to present the pilot with the responses that these inputs can produce, some future light aircraft will employ artificial feel systems which can present the pilot with what he would like while at the same time providing satisfactory responses. When the system is capable of optimizing both these facets it then becomes important to insure that anthropological requirements are considered in detail.

DESIGN FOR DESIRABLE RIDING QUALITIES

In the past the primary design and specification efforts for aircraft have rightly been concerned with insuring safe operation and successful completion of the mission. Progress in these areas now appears to have reached the point that some attention may be directed toward providing the pilot with a comfortable ride as well. A significant portion of what the pilot describes as riding qualities depends upon the design of his seat and other restraints. Noise-induced vibrations also contribute to the pilot's gross impression of the ride. For the present discussion, however, consideration will be restricted to those aspects of ride which can be altered by the aerodynamic design of the aircraft. Thus the concern will be desirable values of linear and angular accelerations associated with the airframe dynamics.

As stated earlier it is these changes in velocity which the pilot feels as imposed forces on his body and which he interprets as major contributors to the riding qualities of his aircraft. Unfortunately, no substantive discussion of the relation between the magnitude and frequency of these accelerations and the acceptability of the ride was found in the literature. The following arguments, however, lead to criteria which may find utility.

There are five characteristic motions associated with rigid aircraft. The spiral mode has a very long time constant and is aperiodic. It is therefore unlikely to induce significant accelerations in normal operation or to occur at a rate which will be uncomfortable. The roll mode, also aperiodic, is very heavily damped and is generally not sensed by the pilot. This leaves the three oscillatory modes as the source of ride discomforts.

Consider first the longitudinal case. From the second equation of A-34 it is evident that to a first order

$$a_z = \dot{w} - U_o q = Z_u u + Z_w w + Z_{\delta_G}\delta_G$$

The notation δ_G is used here to indicate an effective aerodynamic input, similar to a flap on elevator deflection, due to a vertical gust, $\overline{w}$. Thus,

$$\frac{\overline{w}}{U} = \delta_G$$

Since this form is similar to that resulting from a simple control input it may be used to describe pilot induced oscillations as well as gust induced oscillations. Only the value of Z_{δ_G} and δ_G must be changed. Following this tack, then

$$\frac{a_z}{\delta_E} = \frac{Z_u u}{\delta_E} + Z_w \frac{w}{\delta_E} + Z_{\delta_G} .$$

This may be evaluated through the use of Equations C-4 and C-7.

The resulting Bode plot has two well-defined peaks corresponding to the Phugoid mode and the short period mode. Since the peak accelerations are really the values of interest, it is helpful to develop approximate forms for the amplitude of a_z/δ_E corresponding to these two peaks. The numerator of the transfer function contains four zeros: one at the origin, one just to the right of it, one far to the right of the origin and one far to the left of the origin. The latter two have no influence on the phugoid mode and very little on the short period mode.

The denominator has the two second order factors corresponding to the phugoid and short period modes. It will be recalled that the phugoid factor

$$\frac{s^2}{\omega_{n_p}^2} + \frac{2\zeta_p s}{\omega_{n_p}} + 1$$

reduces to $2\zeta_p$ when $\omega = \omega_{n_p}$ and can be approximated by $\omega_{n_{sp}}^2/\omega_{n_p}^2$ when $\omega = \omega_{n_{sp}}$. The short period factor is about 1.0 when $\omega = \omega_p$ and $2\zeta_{sp}$ when $\omega = \omega_{sp}$. For these two conditions the transfer function becomes

$$\frac{a_z}{\delta_E} \simeq \frac{K\, Ta_1 \omega_{n_p}^2}{2\zeta_p}$$

$$\frac{a_z}{\delta_E} \simeq \frac{K\, Ta_1 \omega_{n_{sp}}^2}{\frac{\omega_{n_{sp}}^2}{\omega_{n_p}^2}(2\zeta_{sp})} = \frac{K\, Ta_1 \omega_{n_p}^2}{2\zeta_p} \quad .$$

When the gain and time constant, Ta1, are evaluated as given by Ref. 17 one has

$$\frac{a_z}{\delta_E} = -\frac{\rho U_o^4}{4g\ W/S}\left(\frac{C_{L_\alpha} C_{m_{\delta_E}}}{C_{m_\alpha}}\right)\frac{\omega_{n_p}^2}{\zeta}$$

where the damping ratio refers to the mode being considered. In terms of the gust velocity, $\bar{w}$, this can be written

$$a_z = \frac{\bar{w}\rho U_o^3}{4g\ W/S}\left(\frac{C_{L_\alpha} C_{m_{\delta_G}}}{C_{m_\alpha}}\right)\frac{\omega_{n_p}^2}{\zeta}$$

The quantities in parentheses are relatively constant with speed in the range over which light aircraft operate. Since

$$\omega_{n_p}\omega_{n_{sp}} \simeq \text{constant}$$

and

$$\omega_{n_{sp}} \sim U_o$$

then

$$a_z \sim \bar{w}\, U_o/\zeta$$

ζ_{sp} is approximately independent of speed while ζ_p increases with U_o^2.

Note that increasing the wing loading is favorable for improved ride while reducing oscillatory damping results in a poorer ride. Two additional comments are in order regarding this relation: (1) $\bar{w}$ here is the amplitude of an oscillatory gust having a frequency of either ω_{n_p} or $\omega_{n_{sp}}$. a_z will be less for oscillatory gusts of any other frequency. (2) The equations from which the relation was derived assume no steady pitching velocity. Hence one cannot find the value of a_z/δ_E in a steady pull-up from this relation.

Typically, the damping of the phugoid mode is about 1/10 that of the short period mode while its frequency is about 1/20 that of the short period mode. This means that the accelerations associated with the phugoid mode can be ten times as large as those associated with the short period mode. On the other hand, since desirable values of short period mode frequency range between about 1 and 6 radians/sec for effective handling, the period of time required for the phugoid acceleration to build up to its peak is on the order of 5 to 30 seconds. During this period of time the pilot has the opportunity to take corrective action. Autopilots also damp this motion effectively. In any case, a pilot is not likely to associate phugoid induced accelerations with ride but rather with handling. It is evident, however, that both ride and handling and therefore safety can be improved significantly by increasing the damping.

The phugoid mode is also accompanied by a longitudinal acceleration which has a magnitude about 1/10 to 1/6 as large as a_z. Since either the pilot or an autopilot will attempt to suppress a_z at ω_{n_p}, it seems reasonable to ignore a_x. Note that variations in a_x are essentially zero at $\omega_{n_{sp}}$. Other than possible nausea resulting from the long period swaying motion and the pilot fatigue incurred in controlling it, the phugoid oscillation can probably be ignored. It appears therefore that one may take the following as the ride criteria in the x-z plane:

$$a_z = \frac{\bar{w}\rho U_o^3}{4g\ W/S}\left(\frac{C_{L_\alpha} C_{m_{\delta_G}}}{C_{m_\alpha}}\right)\frac{\omega_{n_p}^2}{\zeta_{sp}} \qquad *$$

$\omega_{n_{sp}}$ between 1 and 6 rad/sec.

A similar argument can be made for the lateral acceleration with the result that

$$\frac{a_y}{\delta_R} = K_{a_y}\,\frac{\rho S U_o^3}{2W}\,\frac{\omega_d}{2\zeta_d}$$

---

* The anthropological basis for suitable values is treated later.

where

$$K_{a_y} = \frac{(C_{\ell_p} C_{y_\beta} C_{n_r} - C_{y_{\delta_R}} C_{n_\beta} C_{\ell_p})^2}{(C_{\ell_\beta} C_{n_r} - C_{\ell_r} C_{n_\beta})\left[C_{\ell_r}(C_{y_\beta} C_{n_{\delta_R}} - C_{y_{\delta_R}} C_{n_\beta}) + C_{n_r}(C_{y_{\delta_R}} C_{\ell_\beta} - C_{y_\beta} C_{\ell_{\delta_R}})\right]}$$

In terms of a lateral gust with oscillation amplitude $\bar{v}$, this becomes

$$a_y = \bar{v} K_{a_y}' \frac{\rho S U_o^2}{4W} \frac{\omega_d}{\zeta_d}$$

where K_{a_y}' indicates that $C_{n_{\delta R}}$ and $C_{y_{\delta R}}$ have been replaced by $C_{n_{\delta G}}$ and $C_{y_{\delta G}}$. ω_d is directly proportional to U_o while ζ_d is approximately constant. The criteria for side acceleration are, therefore,

$$a_y = \bar{v} K_{a_y}' \frac{\rho S U_o^2}{4W} \frac{\omega_d}{\zeta_d}$$

$$\omega_d \text{ between 1 and 6 rad/sec.}$$

with the maximum value for a_y to be specified. a_y of course refers only to perturbations from straight line flight.

Additional components must be added to the accelerations to account for steady rotation. For example, in a steady turn with $\theta = 0$ the accelerometer indications are

$$A_y = U_o R_o - g \sin \phi_o$$

$$A_z = Q_o U_o - g \cos \phi_o \quad .$$

If the turn is coordinated,

$$R_o = \frac{g}{U_o} \sin \phi_o \ ,$$

$$A_y = 0 \quad ,$$

$$Q_o = \frac{g}{U_o} \frac{1-\cos^2\phi_o}{\cos\phi_o} \ ,$$

and

$$A_z = \frac{-g}{\cos \phi_o} \quad .$$

The accelerations felt by the pilot are those values which differ from $A_z = g$ and $A_y = 0$. Thus in a coordinated turn the comfort limit is determined by

$$A_z = g \left(\frac{1}{\cos \phi_o} - 1\right) .$$

McFarland (Ref. 98) suggests a comfort limit of 10 ft/sec^2 for linear accelerations. According to this criterion coordinated turns in clear air should not exceed bank angles of 40°. If the air is turbulent the allowable bank angle apparently would be reduced.

While a pilot may tolerate these acceleration levels during turning flight because they are unavoidable and are imposed for relatively short periods of time, it does not appear reasonable that a 180 lb. pilot would find nearly 60 lbs. of force applied sinusoidally along any of his principal axes for an extended period of time comfortable. It is also reasonable to expect that because of his construction, a pilot will be more sensitive to lateral forces than to vertical forces. While no substantive information is available to support the author's qualitative experience, it is suggested that because of these considerations

$$a_z \simeq 4 \text{ ft/sec}^2$$

and

$$a_y \simeq 2 \text{ ft/sec}^2$$

may be more suitable acceleration limits for the dutch roll and short period motions than that offered by McFarland. Since such accelerations are substantially below those imposed by steady turns, the pilot probably will not be as sensitive to them during turns as at other times. The 40° bank angle limit may therefore be acceptable during turns, provided the a_y and a_z limits quoted above are met during straight-line flight.

Interestingly enough, McFarland suggests a limit of 5° bank angle at low altitudes and 25° bank angle at high altitudes for tilt angles with which passengers would be comfortable. If the 25° tilt occurred in a steady turn, it would correspond to a 3.2 ft/sec^2 acceleration increment along the z-direction.

McFarland was also concerned with tolerable levels of angular acceleration. However, it can be shown that the gain of

$$\frac{\ddot{\theta}}{\delta_E} \simeq K_{\ddot{\theta}} \frac{\omega_{sp}^2}{\zeta_{sp}}$$

is about 10^{-3} times the gain of

$$\frac{a_z}{\delta_E} \simeq K_{a_z} \frac{\omega_{sp}^2}{\zeta_{sp}} .$$

It appears, therefore, that angular accelerations are of no significance if a_z and a_y are maintained at the levels indicated.

Other data of interest to the riding quality discussion are presented in Figure 81. This shows a summary of pilot comments on the short period mode handling qualities of a jet fighter. Note that good handling characteristics will virtually insure good riding qualities according to the criteria developed here.

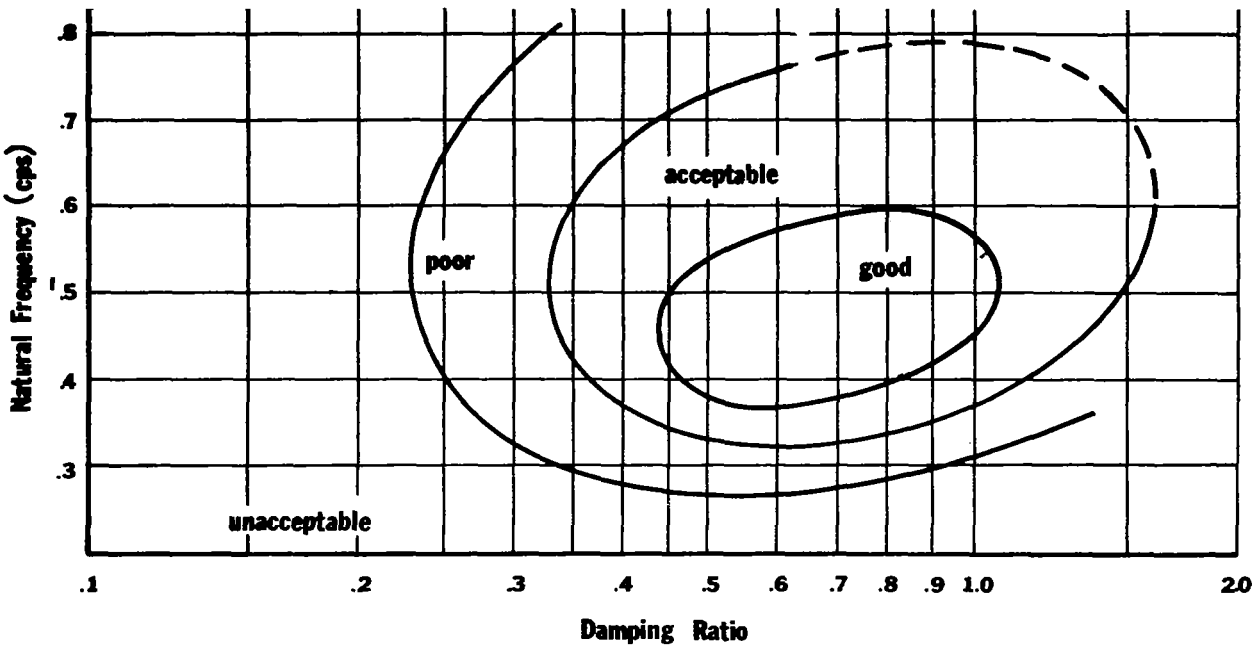

Figure 81. Results of pilot opinion ratings on the handling qualities of a jet fighter (Ref. 99).

One final comment regarding the riding qualities of an aircraft in gusty air may be made. Rigid aircraft exhibit fairly rapid attenuation of normal acceleration response for $\omega > \omega_{sp}$. For example, at frequencies in the range where human internal organ resonances are excited (~42 rad/sec), a_z is less than 10% as much as at ω_{sp} for a given amplitude oscillatory gust. Only if the aircraft has a poorly damped fuselage bending mode or wing bending mode at these frequencies would one expect there to be significant structural shake resulting in pilot discomfort.

THE
EFFECT OF VARIATIONS IN STABILITY DERIVATIVES
ON THE
MOTIONS OF A TYPICAL LIGHT AIRCRAFT

INTRODUCTION

Specification of aircraft geometry, mass distribution, and control system characteristics to yield given riding and handling qualities is unfortunately an interative procedure and therefore a laborious process. One can construct the necessary transfer functions, but there is no unique method to assign numerical values to particular stability derivatives which assumes that these values will bear the often necessary interrelation with one another nor correspond to physically realizable geometry or mass distributions. The approach employed here proceeded through several phases. The first was to take an existing light aircraft, in this case a Cessna 182*, compute its stability derivatives, substitute in the transfer function, and extract the roots. The derivatives were then varied individually to determine the sensitivity of the locus of roots to changes in that particular parameter. This procedure also permits one to determine approximately the range of values which the particular derivative may have for satisfactory performance. It is only an approximate range because some derivatives cannot physically be varied independently of others. This aspect of the procedure and its significance will become clear in the subsequent discussion. Once reasonable values are obtained for the desirable values of the stability derivatives, particularly those which have a strong effect on movement of the roots, one then proceeds to determine the geometric and mass distributions which will produce these values and are at the same time self-consistent. This phase will be elaborated later.

In preparing the figures for the stability derivative variation, the derivatives chosen for examination were generally within plus or minus one order of magnitude of those calculated for the Cessna 182**, at cruise. Included with the figures for the locus of roots due to a variation of a single stability derivative are tables which indicate how the gain of each particular transfer function varies as a function of the stability derivative. Table 16 through Table 31 and Table 35 through Table 46 are tabulations of the numerator roots for the longitudinal and lateral stability derivative variations, respectively. Included at the end of this section are a series of six Bode plots (Figures 90 through 95) illustrating the motions of the aircraft in response to control surface step inputs. The numerical values used to prepare these graphs are those for a Cessna 182 at cruise.

---

* The principal geometric dimensions for the Cessna 182 are shown in Figures 61a and 61b. The longitudinal and lateral derivatives used for the analysis are tabulated in Tables 14a and 14b.

** The values were calculated by the methods presented in earlier sections of this report. They compare favorably with those calculated by Cessna according to a personal communication.

ENGINE

CONTINENTAL MODEL O-470-R
230 HP AT 2600 RPM

AREAS

WING (INCLUDING FUSELAGE)	174.06 SQ FT
AILERON	18.30 SQ FT
FLAP	20.67 SQ FT
STABILIZER (INCLUDING FUSELAGE)	22.10 SQ FT
FIN AND DORSAL	11.62 SQ FT
RUDDER	6.95 SQ FT
ELEVATOR TAB	1.75 SQ FT
ELEVATOR (TOTAL)	16.61 SQ FT

GENERAL DATA

EMPTY WEIGHT (APPROX)		1580 LBS
GROSS WEIGHT	TAKEOFF 2950 LBS	LANDING 2800 LBS
PROP DIAMETER (MAX)		82 IN
WING AIRFOIL ROOT		NACA 2412
VERT. TAIL AIRFOIL ROOT		NACA 0009.5 TIP NACA 0008
HORZ. TAIL AIRFOIL ROOT		NACA 0009 TIP NACA 0006

ANGLES OF INCIDENCE

WING-ROOT CHORD	+1° 30' MIN
WING-TIP CHORD	-1° 30' MIN
STABILIZER	-3°±15' MIN

DIHEDRAL

WING	+1° 44' MIN

MOMENTS OF INERTIA

I_{xx}	948 SLUG-FT^2
I_{yy}	1346 SLUG-FT^2
I_{zz}	1967 SLUG-FT^2

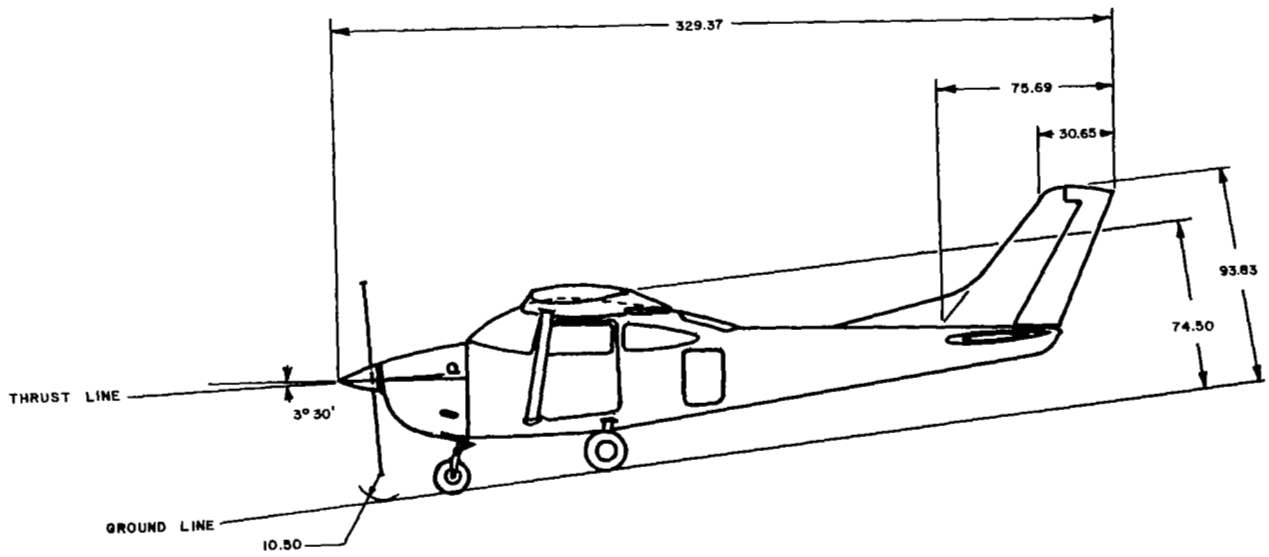

Figure 82a. Three View Drawing of Cessna 182 With Principal Dimensions

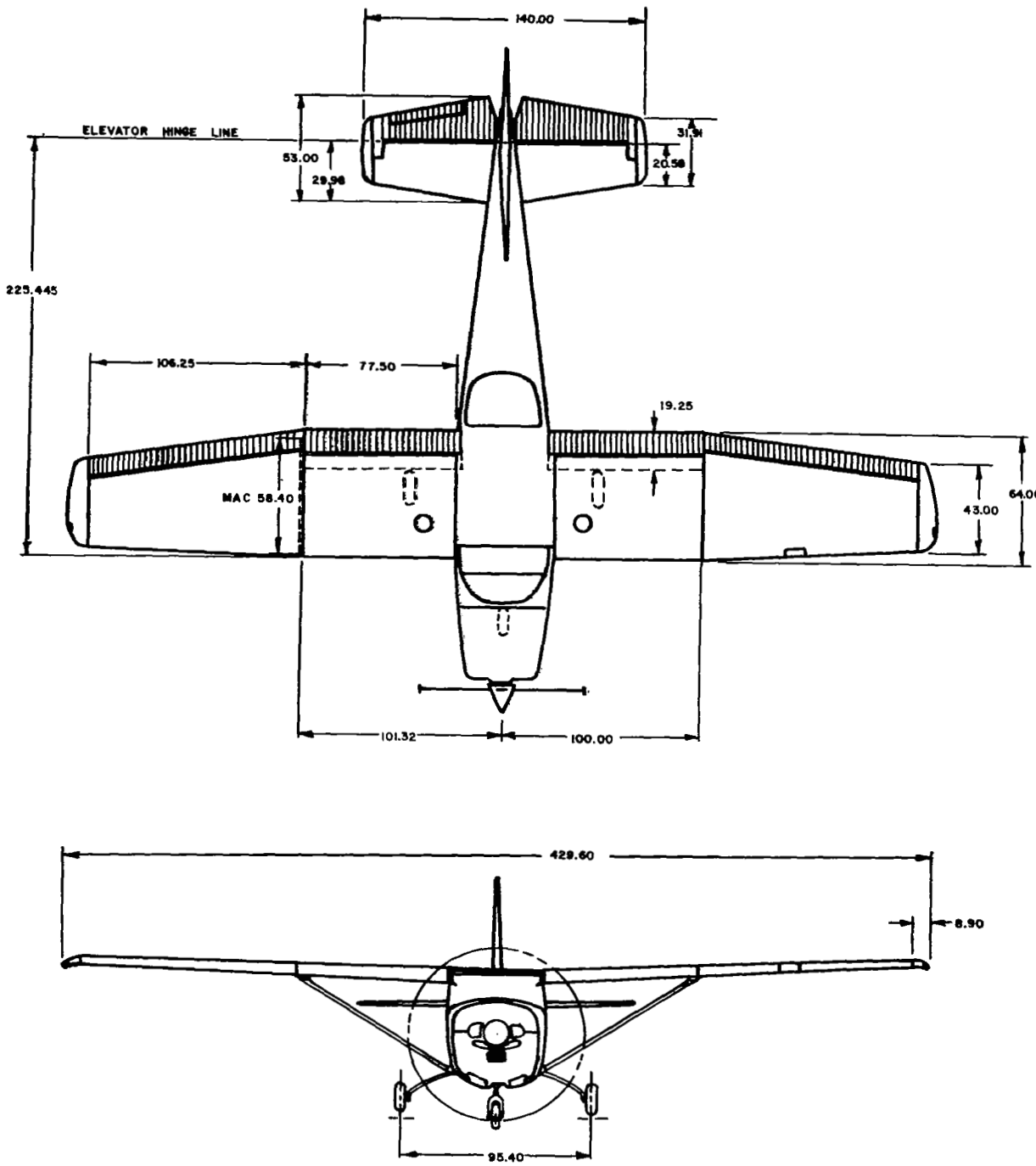

Figure 82b. Three View Drawing Continued

C_L	0.309
C_D	0.0311
C_m	0.0
C_T	0.0
C_{L_u}	0.0
C_{D_u}	0.0
C_{m_u}	0.0
C_{T_u}	0.0
C_{L_α}	4.61/rad.
C_{D_α}	0.126/rad.
C_{m_α}	-0.885/rad.
$C_{L_{\dot{\alpha}}}$	1.74/rad.
$C_{D_{\dot{\alpha}}}$	0.0
$C_{m_{\dot{\alpha}}}$	-5.24/rad.
C_{L_q}	3.9/rad.
C_{D_q}	0.0
C_{m_q}	-12.43/rad.
$C_{L_{\delta_E}}$	0.427/rad.
$C_{D_{\delta_E}}$	0.0596/rad.
$C_{m_{\delta_E}}$	-1.28/rad.
ρ	0.00205 slugs/ft.^{3}
U	219.0 ft./sec.
γ	0^o

Table 25a. Longitudinal stability derivatives.

C_{y_β}	-0.3086
C_{ℓ_β}	-0.089
C_{n_β}	0.06455
C_{y_p}	-0.0373
C_{ℓ_p}	-0.4708
C_{n_p}	-0.0292
C_{y_r}	0.2103
C_{ℓ_r}	0.0958
C_{n_r}	-0.09924
$C_{y_{\delta_R}}$	0.187
$C_{\ell_{\delta_R}}$	0.0147
$C_{n_{\delta_R}}$	-0.0658
ρ	0.00205 slugs/ft.^{3}
U	219.0 ft./sec.
γ	0^o

Table 25b. Lateral stability derivatives (per radian).

LONGITUDINAL VARIATIONS

Figures 83a and 83b show the effect of C_L variations on the longitudinal dynamics. It will be seen that there is little change in the location of the short period roots for all usual values of C_L. The phugoid mode, however, is significantly altered by changes in C_L. At high C_L's, both the frequency and damping ratio are increased. At C_L's near zero, the roots become real with one going unstable. Thus one would expect difficulty in maintaining speed stability in a shallow, high-speed dive.

The effort to provide low drag for good performance leads to a neutrally damped phugoid, as pointed out in Figures 84a and 84b. Stability augmentation is therefore required if one is to obtain both low ($\sim$0) drag and good riding and handling (low work load) qualities.

C_m and C_T must be considered simultaneously because C_m provides the aerodynamic moment to counter the moment produced by the thrust. In gliding flight, $C_m = 0$. Figures 85a and 86a show that the short period mode is not affected by changes in either C_m or C_T. Figures 85b and 86b show the effect on the phugoid mode of altering C_m and C_T respectively. Adding power will make C_T positive and C_m negative. Reference to the figures will show that making C_m negative will cause the phugoid roots to split along the real axis with one going unstable. On the other hand making C_T positive results in an unstable phugoid oscillation. Thus while it is not possible to conclude from these figures alone the detailed airplane behavior when power is added (because C_m and C_T cannot be varied independently in flight but only through design changes such as the location of the engine thrust line), it is obvious that the application of power is destabilizing.

Figures 87a and 87b indicate the variations in longitudinal dynamics produced by changing C_{L_α}. Increasing C_{L_α} is seen to reduce the frequency and to increase the damping of the short period mode. A sufficiently large value of C_{L_α} suggest aperiodic short period roots. The time for the phugoid to damp to half amplitude is little affected by changing C_{L_α} (Figure 87b), but the oscillation frequency is a direct function of C_{L_α}. All usual values of C_{L_α} are therefore acceptable for satisfactory aircraft riding qualities.

From Figure 88a, it is seen that the short period mode is virtually insensitive to moderate changes in C_{D_α}. Increasing values of C_{D_α} destabilizes the phugoid mode (Figure 88b). Instability is most likely to occur in the approach configuration where C_{D_α} is greatest. The maximum acceptable value is about twice the value calculated for the Cessna 182.

Figures 89a and 89b show the movement of the short period and phugoid roots respectively due to a variation in C_{m_α}. For most light airplanes as usually loaded, C_{m_α} will probably lie between -.3 and -1.5. In this range, the time to damp the short period oscillation to half-amplitude is independent of the value of C_{m_α}, while the frequency increases as C_{m_α} assumes greater negative values. C_{m_α} with greater negative values than -1.5 gives short

period mode frequencies higher than the 5-6 rad/sec limit desired. Values of C_{m_α} greater thar about -0.23 cause the short period oscillation to disappear and become two aperiodic modes.

Reasonable variations in C_{m_α} (Figure 89b) also have little effect on the time to damp the phugoid oscillation. The phugoid frequency increases as C_{m_α} becomes more negative, while values more than about -0.05 cause the phugoid to degenerate into aperiodic motions. It is seen therefore that the proper value of C_{m_α} is usually determined by requirements for acceptable short period mode characteristics. A notable exception may be mentioned, however. A recent paper (Ref. 116) discussed results obtained with a light aircraft modified to evaluate the pilot acceptance of various short period mode damping ratios. The damping ratio was made unity (i.e. both roots lie on the negative real axis) by increasing C_{m_α} (making it less negative). One would expect that the pilot would be pleased with this condition since it means that the aircraft would track rapid elevator commands without oscillating. Instead, the pilot found it quite objectionable, saying that it was difficult to maintain airspeed stability. The paper therefore recommends that damping ratios approaching unity not be used. The falacy in the argument is immediately obvious when one examines the effects of near zero C_{m_α} values on the phugoid mode. The roots become aperiodic with one going unstable as C_{m_α} increases. Of course the pilot would find this undesirable. It is therefore important that unity damping ratio for the short period mode <u>not</u> be achieved by increasing C_{m_α} alone. As discussed below the most satisfactory single means of obtaining this behavior (unity damping ratio) is to make C_{m_q} more negative. Increasing the tail length is the most effective geometric change one can make to accomplish this increase is damping. Because of the very significant lengthening required, however, it is desirable to combine this with <u>small</u> rearward shift in operating c.g. (effectively a small increase in C_{m_α}).

Figures 90a, 90b, 91a, and 91b show that the roots are relatively insensitive to changes in $C_{L_{\dot\alpha}}$ and $C_{D_{\dot\alpha}}$. Changing $C_{L_{\dot\alpha}}$ by an order of magnitude from its original value moves the roots only slightly for both the short period and phugoid modes. $C_{D_{\dot\alpha}}$ is usually considered to be zero for most light aircraft. If a value were calculated, it would be at least an order of magnitude smaller than $C_{L_{\dot\alpha}}$, at least as small as .177. Thus, for all normal values of $C_{D_{\dot\alpha}}$, both phugoid and short period roots remain in virtually the same location.

Figures 92a and 92b indicate that $C_{m_{\dot\alpha}}$ is quite important in the short period mode but unimportant in the phugoid mode. More negative values of $C_{m_{\dot\alpha}}$ decrease the frequencies and increase the damping. High negative values can even lead to two highly damped aperiodic modes. Values greater than zero should be avoided. In the normal range of values, an error in $C_{m_{\dot\alpha}}$ of 20% could cause a 5% error in the calculated frequency of oscillation. The phugoid mode roots are relatively unaffected, even when $C_{m_{\dot\alpha}}$ is changed by an order of magnitude.

Figures 93a, 93b, 94a, and 94b indicate that both the short period mode and the phugoid mode are relatively insensitive to variations in C_{L_q} and C_{D_q}. It is noteworthy that a value of $C_{L_q} = 0$ would give almost the same characteristics as the value calculated.

C_{m_q} is quite important to the frequency and damping of the short period mode but relatively unimportant to those of the phugoid mode. The short period roots for various values of C_{m_q} are similar in behaviour to the roots for various values of $C_{m_{\dot{\alpha}}}$ (see above). As C_{m_q} becomes more negative, the frequency decreases and the damping increases for the short period mode (Figure 95a). For the normal range of C_{m_q} values, the damping is more sensitive to changes in C_{m_q} than the frequency of oscillation. For very negative values of C_{m_q}, aperiodic motions are achieved. Variations of C_{m_q} have almost no effect on the phugoid damping. The frequency of the phugoid mode decreases as C_{m_q} becomes more negative, as can be observed from Figure 95b. C_{m_q}, of course, is always negative.

The above results are discussed below from the viewpoint of acceptable riding qualities, since the proper range of the more important stability derivatives is significant in achieving these qualities. The important derivatives which affect the short period mode appear to be C_{L_α}, C_{m_α}, $C_{m_{\dot{\alpha}}}$, and C_{m_q}. It would be desirable to have the short period damp to one-half amplitude in one second or less, with a damping ratio greater than 0.6 and to have the frequency less than five radians per second for acceptable riding qualities and less than four radians per second for good riding qualities. Any reasonable value of C_{L_α} will provide a damping ratio greater than 0.6, a frequency less than 4.25 rad/sec and a time for damping to one-half amplitude of less than 0.25 seconds. C_{m_α} values between -.23 and -1.0 give acceptable short period riding qualities with a frequency of less than 5.0 rad/sec and a damping ratio greater than 0.6. It is desirable to have $C_{m_{\dot{\alpha}}}$ lie between -4.0 and -17.0; the more negative the value, the lower the frequency and higher the damping. C_{m_q} should have values between -6.0 and -29.0 for good riding qualities.

The frequency and damping criteria mentioned above probably should be regarded as applying only to aircraft without artificial stability augmentation. The geometric changes necessary to improve the riding and handling qualities further (i.e. to obtain unity damping ratio for an undamped natural frequency of 6 radians per second) sufficiently degrade aircraft performance and payload capacity as to make these changes unattractive. Improvements in riding and handling qualities, however, can be obtained with stability augmentation without sacrificing either performance or payload.

The phugoid mode must also be considered when discussing riding qualities. This mode should have a damping ratio of at least 0.04, with a maximum frequency of about 0.3 rad/sec. If the period is over three to four seconds, it can be tracked by the pilot although the pilot work load will be high. The phugoid frequency is really not very critical as long as it does not approach the short period range. The derivatives C_m and C_T contribute only to the phugoid mode and should be considered together. More positive values of C_T yield unstable phugoid roots; for the particular airplane analyzed, C_m becomes more negative as C_T became more positive which leads to an increase in phugoid frequency and a decrease in damping. C_L has the most effect on the frequency of the phugoid mode, while C_D mainly affects damping. For the normal range of C_L values (.1-1.5), the frequencies may take on values as high as 0.3 to 0.4 rad/sec; however, as the frequency increases, the damping also increases. The larger the value of C_D, the better the riding qualities; however, performance requirements must dictate the value of C_D.

Values of C_{m_α} between -0.01 and -2.5 appear to give satisfactory phugoid response by affecting the frequency while keeping the damping essentially constant. C_{m_q} has a small effect on the phugoid frequency, but values between 0.0 and -30 give desirable phugoid riding qualities.

In the above discussion, a range of desirable or acceptable values of the important stability derivatives has been given for the phugoid and short period riding qualities. It should be emphasized that the derivatives have been discussed as if they were independent of the other derivatives, while in reality they are not. In the table below, the most important longitudinal stability derivatives are given with the range of values which should result in the desirable handling qualities indicated above. It should be remembered that even though values of C_{m_q} between 0.0 and -30.0 appear acceptable, if the values are very near zero then it will probably be impossible to obtain acceptable values for other stability derivatives.

Stability Derivative	Acceptable Range
C_D	0.03* to 1.0
C_{m_α}	-0.23 to -1.0
$C_{m_{\dot{\alpha}}}$	-4.0 to -17.0
C_{m_q}	0.0 to -30.0

Table 26. Acceptable range for longitudinal stability derivatives.

Since the longitudinal stability derivatives cannot really be varied independently, it was felt that the movement of the roots due to the changes in the airplane's geometry would be more informative than just a variation of the longitudinal stability derivatives. In the case of longitudinal dynamics, the movement of the roots was calculated for various c.g. locations, horizontal tail areas, tail lengths, and tail efficiencies. It should be noted that these variations were made without changing the original inertia characteristics of the airplane. As an example of how inertia changes would effect the geometric variations, the short period plot of ℓ_t indicates the roots with and without the inertia changes. It should also be pointed out that the tail area was varied in such a way that the tail aspect ratio was held constant. The figures and tables below can be used to track the roots.

The phugoid and short period frequencies decreased as the c.g. was moved aft, until aperiodic modes were obtained for both (Figure 96 and Table 44). The short period damping decreased and the phugoid damping remained almost constant as the c.g. moved aft up to 42.5% m.a.c. The short period roots were aperiodic with the c.g. at 42.5% m.a.c., while with the c.g. at 45%

*Lower values of C_D will require artificial damping to meet the phugoid damping criterion.

m.a.c., the phugoid roots were aperiodic with one unstable root. For a c.g. location at 47.5%, there was a phugoid-short period coupling as well as one very stable short period root and an unstable phugoid root.

The variations in horizontal tail area with tail aspect ratio held constant showed that the short period damping increased and the frequency decreased for tail areas greater than that of the Cessna 182. Tail areas less than the original area gave lower frequencies and lower short period damping (Figure 97a). The phugoid damping was virtually unaffected by the variations in tail area while the natural frequency showed only small changes.

For the variation in tail length without inertia effects, the short period damping increased and the frequency decreased for tail lengths greater than that of the Cessna 182 (Figure 98a). Tail lengths less than the original length gave lower frequencies with lower short period damping. Two aperiodic roots are obtained for tail lengths slightly below 45% of the original length. The trajectory of the short period roots considering inertia changes was similar to that calculated without considering inertia changes but exhibited higher damping ratios for longer tail lengths and lower damping ratios for shorter tail lengths. The phugoid damping was almost unaffected by variation in tail length from 200% to 45% of the original value, as seen in Figure 98b. The frequency did decrease as tail length decreased, but no unreasonable frequencies were obtained for the range of tail length variations. As may be expected, the variation of tail efficiency, η_t, gave results similar to those for tail length variation (Figures 99a and 99b).

LATERAL VARIATIONS

Figure 100 shows the effect of C_{y_β} variations on lateral dynamics. In Figure 100a, the Dutch Roll natural frequency appears nearly unaffected by changes in C_{y_β}; however, Dutch Roll damping increases slowly for more negative values of C_{y_β}. For practical airframe configurations, C_{y_β} is never positive. Figures 100b and 100c show the nearly negligible effect of C_{y_β} on the spiral and roll modes, respectively. In general, the three modes seem relatively insensitive to changes in C_{y_β}.

The effect of C_{ℓ_β} variation on the Dutch Roll mode is seen in Figure 101a, where large negative values of C_{ℓ_β} decrease the damping and increase the natural frequency, and positive values improve damping and decrease the natural frequency; however, for typical values of C_{ℓ_β}, the Dutch Roll mode is only slightly affected. The spiral mode, as pointed out in Figure 101b, is more stable for large negative values of C_{ℓ_β} but less stable for both small negative values and any positive values. Thus an aircraft may be made more spirally stable by increasing the wing dihedral; however, there is a limit to the amount of dihedral because of the adverse effect of large negative values of C_{ℓ_β} on the Dutch Roll mode. The roll mode (Figure 101c) is also more stable for larger negative values of C_{ℓ_β}, but substantial changes are necessary for the effect to be very noticeable.

The Dutch Roll frequency is highly sensitive to changes in C_{n_β}, Figure 102a, with large positive values causing very high frequencies; small negative values, which are possible for airframes with small vertical tails, produce an unstable system. Dutch Roll damping is relatively unaffected by changes in C_{n_β}. The spiral mode (Figure 102b) is moderately sensitive to changes in C_{n_β}; it becomes more stable as C_{n_β} grows smaller and becomes negative. The roll mode (Figure 102c) is unaffected by changes in C_{n_β}.

Variation in C_{y_p} has no effect on any of the lateral modes, as indicated in Figures 103a, 103b, and 103c.

Figure 104a shows that the Dutch Roll mode is only slightly affected by variation in C_{ℓ_p}. The spiral mode in Figure 104b is somewhat more sensitive; less negative values of C_{ℓ_p} increase the stability; positive values of C_{ℓ_p} are not physically possible. Obviously, the roll mode in Figure 104c is highly sensitive to changes in C_{ℓ_p}, the damping-in-roll derivative, as it becomes more stable for increasingly negative values of C_{ℓ_p}. For very small negative values and for positive values, the roll and spiral modes couple to produce the roll-spiral oscillatory mode. MIL-F-8785B, (Ref. 4), specifically prohibits this.

Figure 105a shows the effect on the Dutch Roll mode of variations in C_{n_p}. Large negative values cause an increase in natural frequency, whereas positive values decrease the frequency and damping until the system becomes unstable. The spiral mode (Figure 105b) is virtually unaffected by changes in C_{n_p}, and the roll mode (Figure 105c) becomes less stable for large negative values of C_{n_p}.

Variation in C_{y_r} has almost no effect on any of the lateral modes, as Figures 106a, 106b, and 106c indicate.

Larger positive values of C_{ℓ_r} (Figure 107a) increase the Dutch Roll damping, but have little effect on the natural frequency. More positive values, though, seem to give an unstable spiral mode (Figure 107b) and a less stable roll mode (Figure 107c).

Figure 108 shows the effect of variations in C_{n_r} on all three modes. For larger negative values of C_{n_r}, the Dutch Roll becomes two aperiodic modes, with one root moving toward the roll mode root and another root approaching the spiral root. These roots meet and, at one point, two oscillatory modes exist. This situation, however, may not be physically obtainable. For less negative values of C_{n_r}, the Dutch Roll damping decreases, but the roll and spiral modes are little affected.

The previous results are examined below from the viewpoint of acceptable riding qualities. Consideration is given specifically to the allowable range of several important stability derivatives governing these qualities. Two stability derivatives, C_{n_β} and C_{n_r}, seem to have the most effect on the Dutch Roll mode. Using a minimum ζ_d (Dutch Roll damping ratio) of the larger of .19 and $.35/\omega_{n_d}$ and limiting the natural frequency to a range from one radian per second to about five radians per second, a range of values for these two derivatives was determined. C_{n_β}, which determines the natural frequency, should lie between about .01 and about .15 per radian. Also C_{n_r}, the yaw-damping derivative, was found to have a minimum value of -.45 per radian to satisfy the requirement for minimum ω_{n_d} and a maximum value of -.09 per radian to give a damping ratio of at least .19.

The stability derivative C_{ℓ_β} seems to have the most effect on the spiral mode. For best riding qualities, at least a neutrally stable spiral mode is desired. To attain this, a value of C_{ℓ_β} more negative than -.05 is needed. This may be accomplished, physically, by increasing the amount of aircraft wing dihedral, but large negative values of C_{ℓ_β} adversely affect the Dutch Roll mode by increasing the frequency and decreasing the damping, thus, a C_{ℓ_β} of about -0.4 per radian is considered the most negative value permissible.

The stability of the roll mode is determined primarily by C_{ℓ_p}, the damping-in-roll derivative. For a $1/\tau_R$ less than about 0.7, which seems desirable for easy handling, the value of C_{ℓ_p} must be less than -.04 per radian; however, too large a negative value of C_{ℓ_p} may cause the aircraft to react sluggishly to the pilot's commands, and one of the requirements for easy maneuverability is that the aircraft be able to roll a certain number of degrees in a finite amount of time.

The following table lists the important lateral stability derivatives with their suggested range of values for desirable handling qualities.

Stability Derivatives	Acceptable Range (per radian)
C_{n_β}	.01 to .15
C_{n_r}	-0.45 to -0.09
C_{ℓ_β}	-0.40 to -0.05
C_{ℓ_p}	less than -0.04

Table 27. Acceptable range for lateral stability derivatives.

Since the lateral stability derivatives cannot physically be varied independently, it seems necessary to discuss the movement of the roots of the characteristic equation due to a variation of the airplane's geometry. For the lateral dynamics case, the length to the vertical tail, ℓ_v, the area of the vertical tail, S_v, the wing dihedral angle, and a combination of vertical tail area and wing dihedral were varied.

The effect on the Dutch Roll (Figure 109a) of increasing ℓ_v is to increase both frequency and damping of this mode. The reason for this can be gathered by examining the effect on Dutch Roll characteristics of C_{n_β} and C_{n_r} variations. Increasing ℓ_v makes C_{n_β} more positive. This has a direct influence on the frequency of the Dutch Roll. Increasing ℓ_v also makes C_{n_r} more negative. For small increases in the magnitude of C_{n_r}, the damping of the Dutch Roll is increased but the period is unaffected. Finally, for large negative values of C_{n_r}, the period of the Dutch Roll increases and the damping also increases. For ℓ_v up to 150% of the original, C_{n_β} seems to dominate as the frequency rises quite rapidly, but for ℓ_v greater than 150% the frequency levels off and the system becomes more highly damped as C_{n_r} becomes dominant. For decreasing ℓ_v, both the frequency and damping decrease until, at about 35% of the original tail length, the system becomes unstable. The spiral mode (Figure 109b) becomes more stable for both increasing and decreasing ℓ_v. This is possible since in the expression, $C_{\ell_p}\ C_{n_\beta}/(C_{\ell_\beta}\ C_{n_r} - C_{n_\beta}\ C_{\ell_r})C_{y_p}$, which governs the spiral root, C_{n_r}, C_{n_β}, and C_{ℓ_r} all change with ℓ_v variation. The roll mode (Figure 109c) is unaffected by changes in vertical tail length since C_{ℓ_p} is not dependent on ℓ_v. The moment of inertia I_{zz} was held constant for one set of ℓ_v variations and allowed to change for the second set of ℓ_v variations. The results of both are shown in Figure 109 and inertia changes produce only small deflections in the curves with the general trends remaining the same.

Figure 110a shows the effect of vertical tail area variation on the Dutch Roll mode. Increasing S_v gives both a higher frequency and a slightly more damped system since C_{n_β} and C_{n_r} are again substantially affected by changes in vertical tail area. (C_{n_r} becomes less negative as S_v decreases; for the same conditions C_{n_β} may go through zero and become negative) with a value of about 48% of the original tail area, the system becomes unstable. The spiral mode (Figure 110b) becomes more stable for decreasing vertical tail area, since this produces small positive or even negative values of C_{n_β} (Figure 102b). The roll mode (Figure 110c) remains unaffected since C_{ℓ_p} is

only slightly affected by changes in vertical tail area.

The effect of variations in wing dihedral on the Dutch Roll mode is modest as shown in Figure 111a. However, the spiral mode (Figure 111b) is heavily dependent on wing dihedral, since this determines the value of C_{ℓ_β}, the "effective dihedral" derivative. Positive dihedral angle gives a more stable spiral mode and negative dihedral causes the mode to become unstable. The roll mode (Figure 111c) is essentially constant for wing dihedral variation.

The combination of changing both vertical tail area and wing dihedral is shown in Figure 112. The Dutch Roll mode (Figure 112a) is the same as that for S_V variation alone since dihedral angle has little effect on this mode. However, the spiral mode (Figure 112b), which previously became less stable for increasing S_V, now can be made more stable by an increase in the dihedral angle. Thus the Dutch Roll and spiral modes may both be improved by simultaneously increasing vertical tail area and dihedral angle. The roll mode (Figure 112c) remains unaffected.

Short Period Mode Roots for the C_L Variation

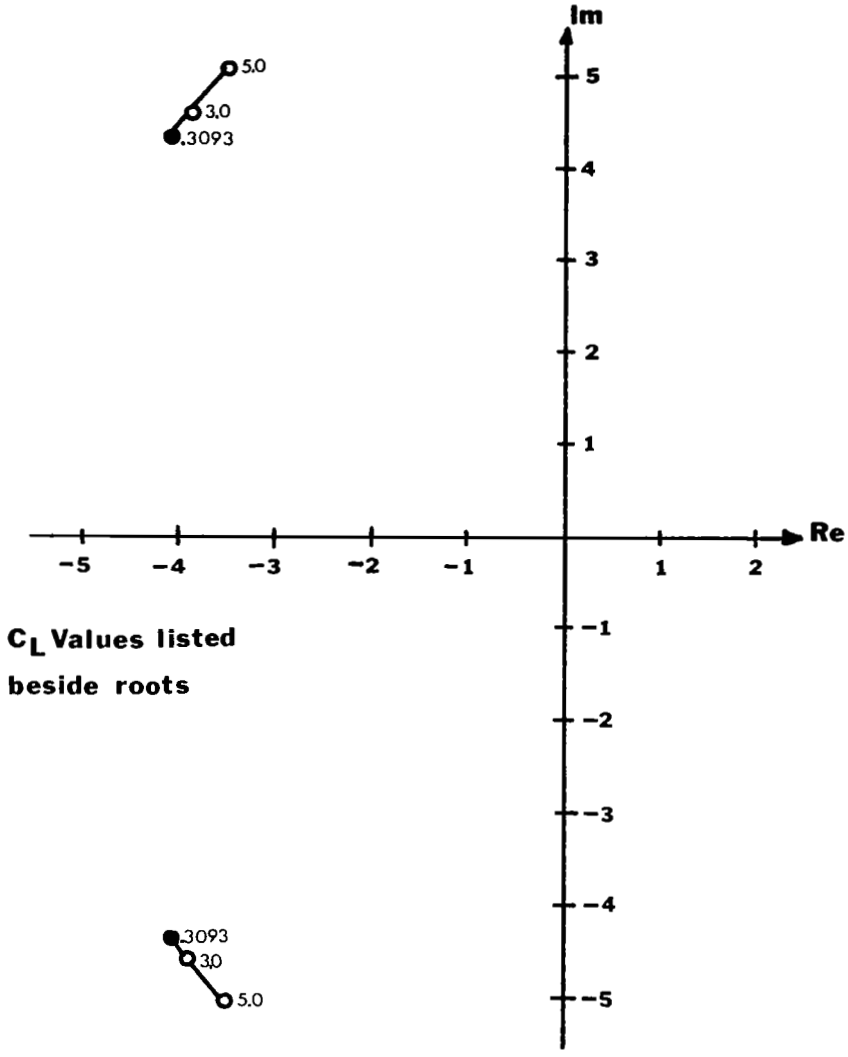

Figure 83a

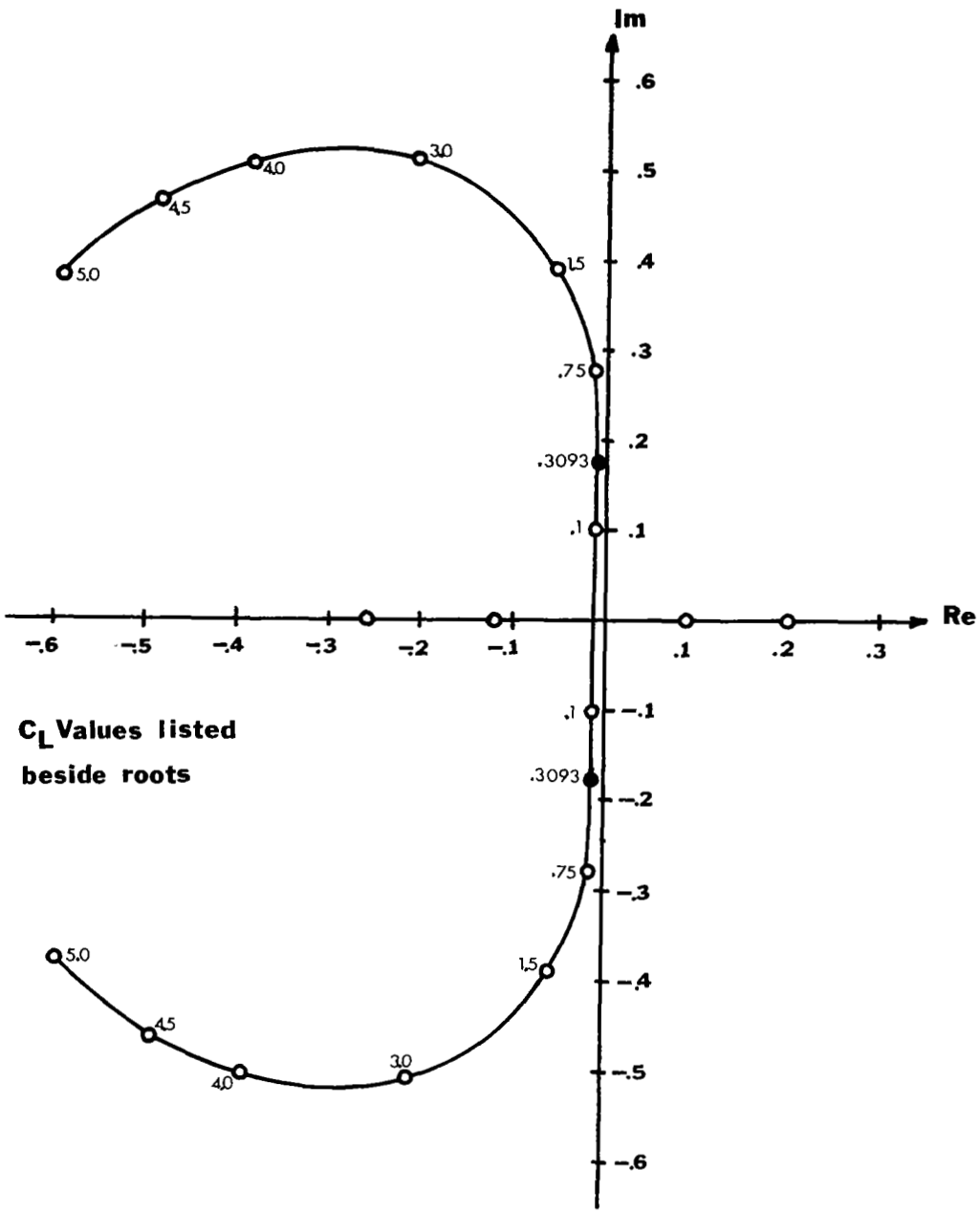
Phugoid Mode Roots for the C_L Variation
Im
Re
.6
.5
.4
.3
.2
.1
-.1
-.2
-.3
-.4
-.5
-.6
-.6
-.5
-.4
-.3
-.2
-.1
.1
.2
.3
5.0
4.5
4.0
3.0
1.5
.75
.3093
.1
C_L Values listed
beside roots

Figure 83b

NUMERATOR ROOTS

STABILITY DERIVATIVE	REAL	IMAGINARY	REAL	REAL
		u		
-0.5	- 0.71701	0.0	-26.93581	21.6049
-0.1	- 1.29165	0.0	-21.27941	15.1774
0.1	- 2.12606	0.0	-17.28866	11.34820
0.3093	- 7.68330	0.0	- 7.93156	6.84425
0.75	- 5.92058	±15.08719		1.58786
1.5	- 6.66843	±26.45906		0.56020
3.0	- 9.03239	±40.57417		0.24139
4.0	-10.68138	±47.65224		0.17489
4.5	-11.51191	±50.80265		0.15371
5.0	-12.34472	±53.75583		0.13711
		$\Delta\alpha$		
-0.5	-0.28084	0.0	0.24735	-195.51762
-0.1	-0.13526	0.0	0.10320	-195.46607
0.1	-0.01509	±0.11668		-195.44030
0.3093	-0.01472	±0.20640		-195.41333
0.75	-0.01393	±0.32196		-195.35655
1.5	-0.01259	±0.045569		-195.25991
3.0	-0.00991	±0.64493		-195.06664
4.0	-0.00812	±0.74498		-194.93780
4.5	-0.00723	±0.79032		-194.87339
5.0	-0.00633	±0.83322		-194.80897
		θ		
-0.5	-0.09750	0.0	-9.99285	
-0.1	-0.03463	0.0	-2.05621	
0.1	-0.03088	0.0	-2.06020	
0.3093	-0.04605	0.0	-2.04529	
0.75	-0.14779	0.0	-1.94407	
1.5	-0.76817	0.0	-1.32461	
3.0	-1.04730	±1.70249		
4.0	-1.04790	±2.45078		
4.5	-1.04820	±2.81025		
5.0	-1.04851	±3.16440		

Table 28. Numerator roots for C_L variations.

Short Period Mode Roots for C_D Variation

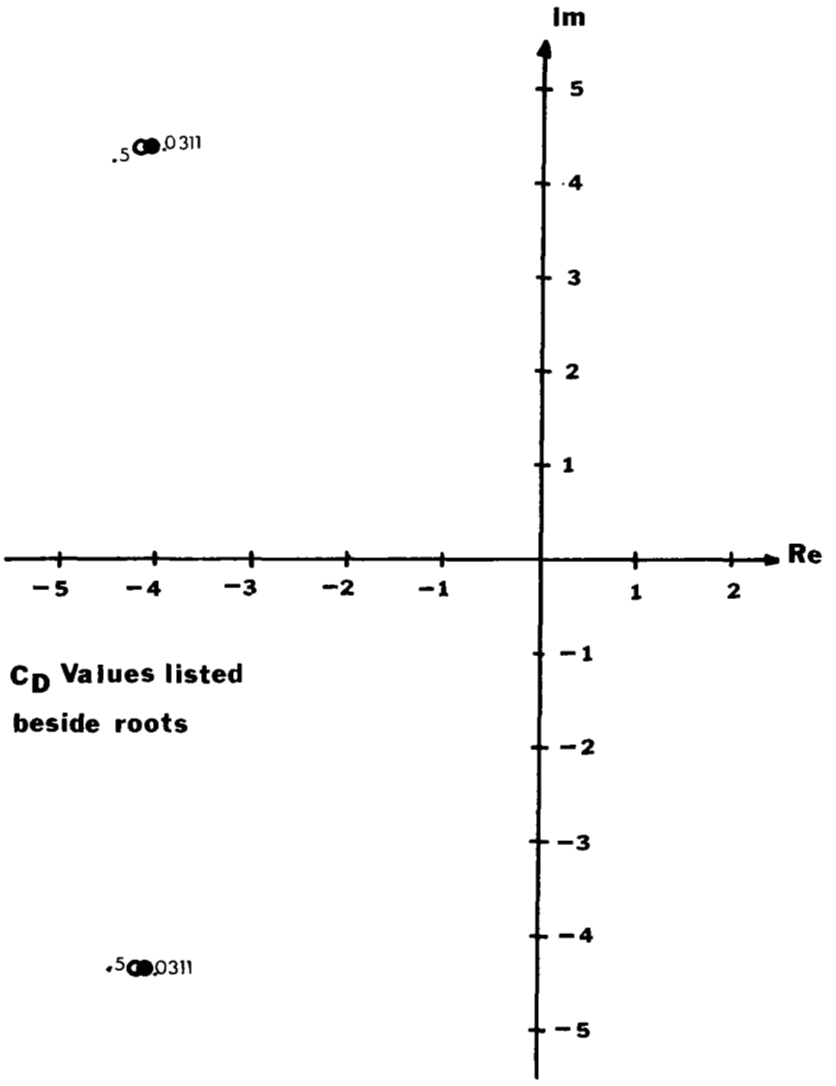

Figure 84a

Phugoid Mode Roots for the C_D Variation

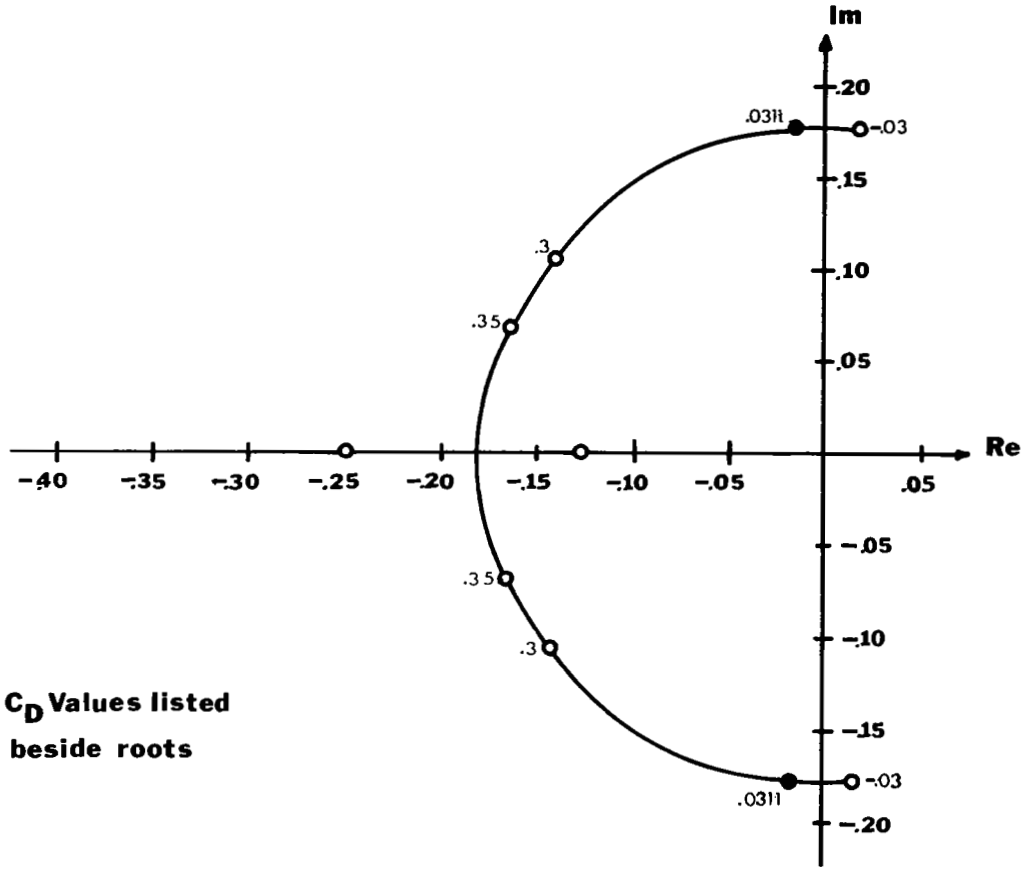

Figure 84b

NUMERATOR ROOTS

u

STABILITY DERIVATIVE	REAL	IMAGINARY	REAL	REAL
-0.03	-7.17723	0.0	-8.39084	6.82668
0.0311	-7.68330	0.0	-7.93156	6.84425
0.3	-7.90719	±1.21744		6.91800
0.35	-7.92566	±1.32588		6.93144
0.4	-7.94408	±1.42569		6.94479
0.5	-7.98077	±1.60575		6.97118

Δα

-0.03	0.01478	±0.20640		-195.41334
0.0311	-0.01472	±0.20640		-195.41333
0.3	-0.14171	±0.15078		-195.41328
0.35	-0.16542	±0.12430		-195.41327
0.4	-0.18914	±0.08393		-195.41326
0.5	-0.35238	0.0	-0.12191	-195.41324

θ

-0.03	0.01315	0.0	-2.01601
0.0311	-0.04605	0.0	-2.04529
0.3	-0.30099	0.0	-2.17126
0.35	-0.34860	0.0	-2.19476
0.4	-0.39622	0.0	-2.21826
0.5	-0.49148	0.0	-2.26524

Table 29. Numerator roots for C_D variations.

Short Period Mode Roots for the C_m Variation

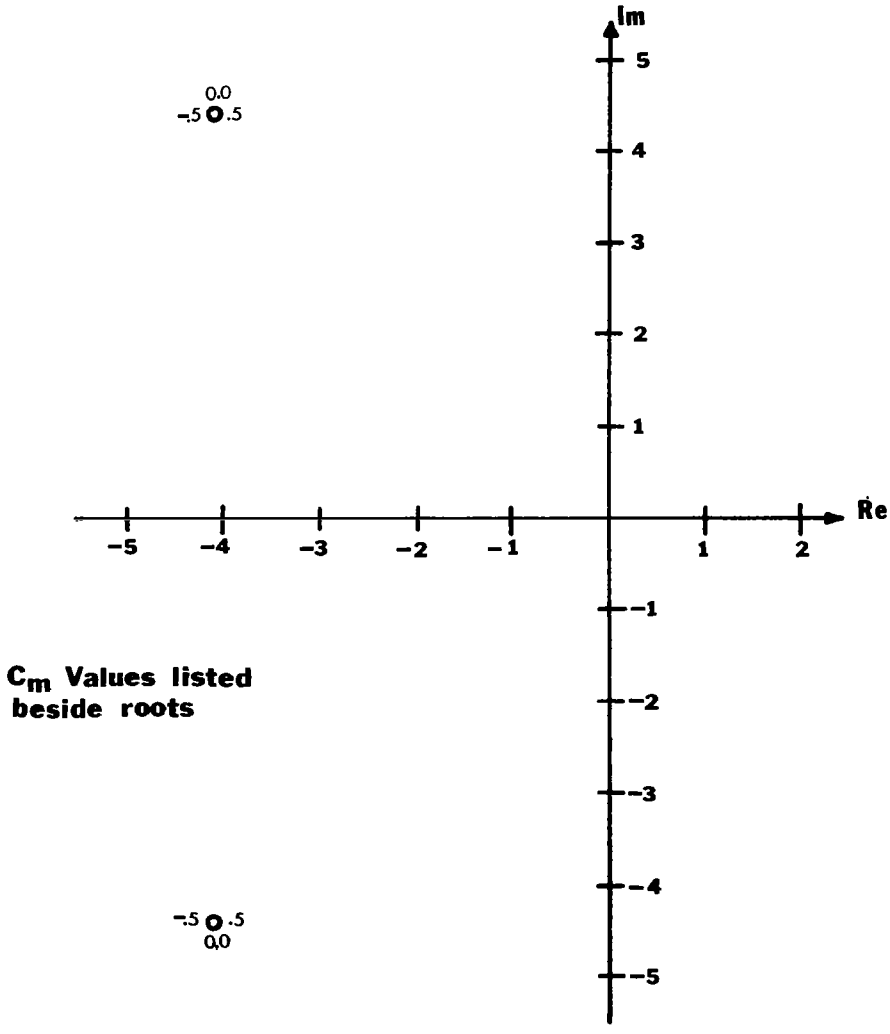

Figure 85a

Phugoid Mode Roots for the C_m Variation

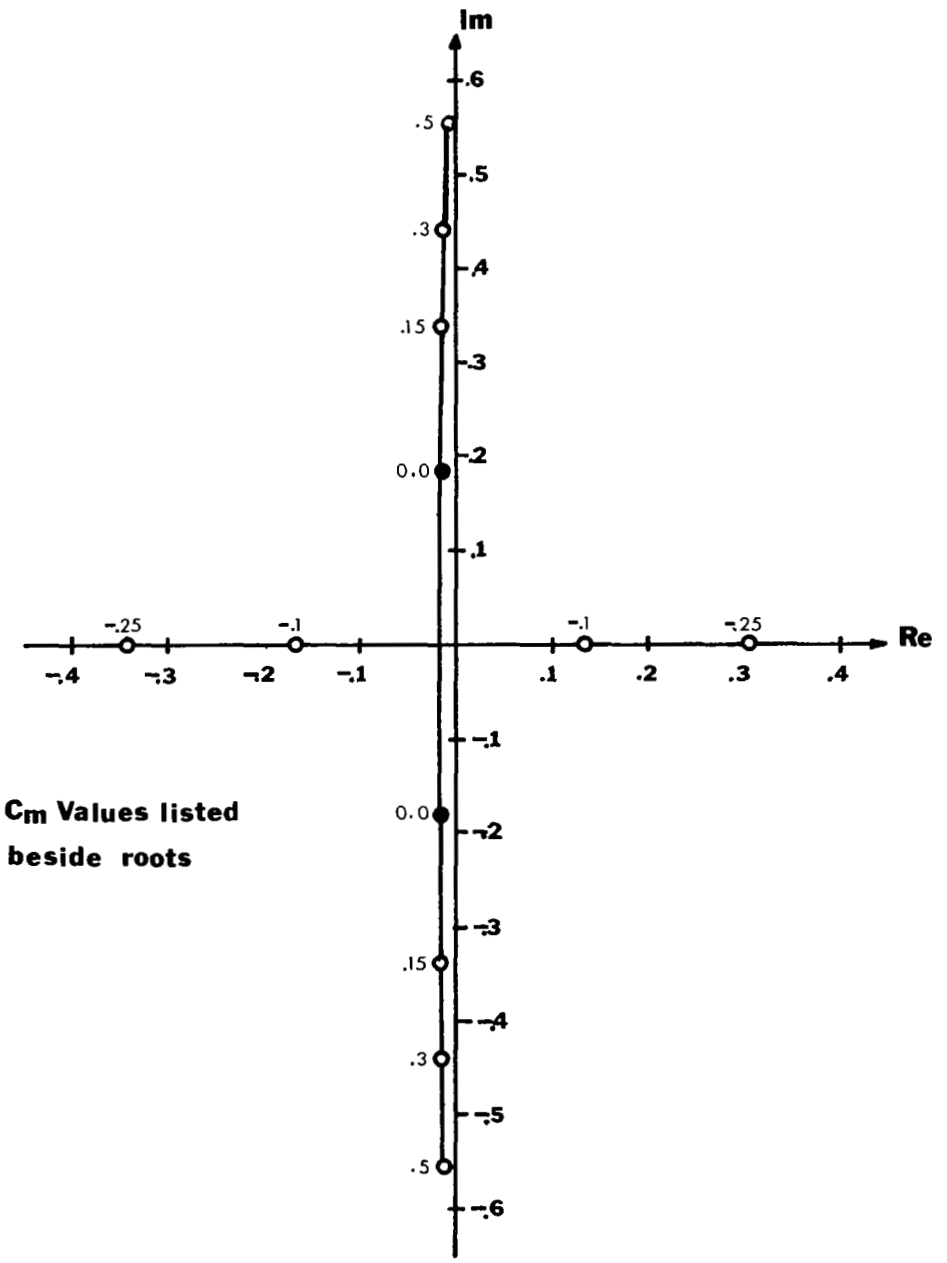

Figure 85b

NUMERATOR ROOTS

STABILITY DERIVATIVE	REAL	IMAGINARY	REAL	REAL
		u		
-0.5	-7.68330	0.0	-7.93156	6.84425
-0.25	-7.68330	0.0	-7.93156	6.84425
-0.1	-7.68330	0.0	-7.93156	6.84425
0.0	-7.68330	0.0	-7.93156	6.84425
0.15	-7.68330	0.0	-7.93156	6.84425
0.30	-7.68330	0.0	-7.93156	6.84425
0.50	-7.68330	0.0	-7.93156	6.84425
		$\Delta\alpha$		
-0.5	-0.00400	±0.14062		-195.43477
-0.25	-0.00936	±0.17668		-195.42405
-0.1	-0.01257	±0.19507		-195.41762
0.0	-0.01472	±0.20640		-195.41333
0.15	-0.01793	±0.22227		-195.40690
0.30	-0.02115	±0.23704		-195.40047
0.50	-0.02544	±0.25535		-195.39189
		θ		
-0.5	-0.01557	0.0	-2.05353	
-0.25	-0.03078	0.0	-2.04944	
-0.1	-0.03993	0.0	-2.04696	
0.0	-0.04605	0.0	-2.04529	
0.15	-0.05524	0.0	-2.04277	
0.30	-0.06445	0.0	-2.04022	
0.50	-0.07677	0.0	-2.03679	

Table 30. Numerator roots for C_m variations.

Short Period Mode Roots for the C_T Variation

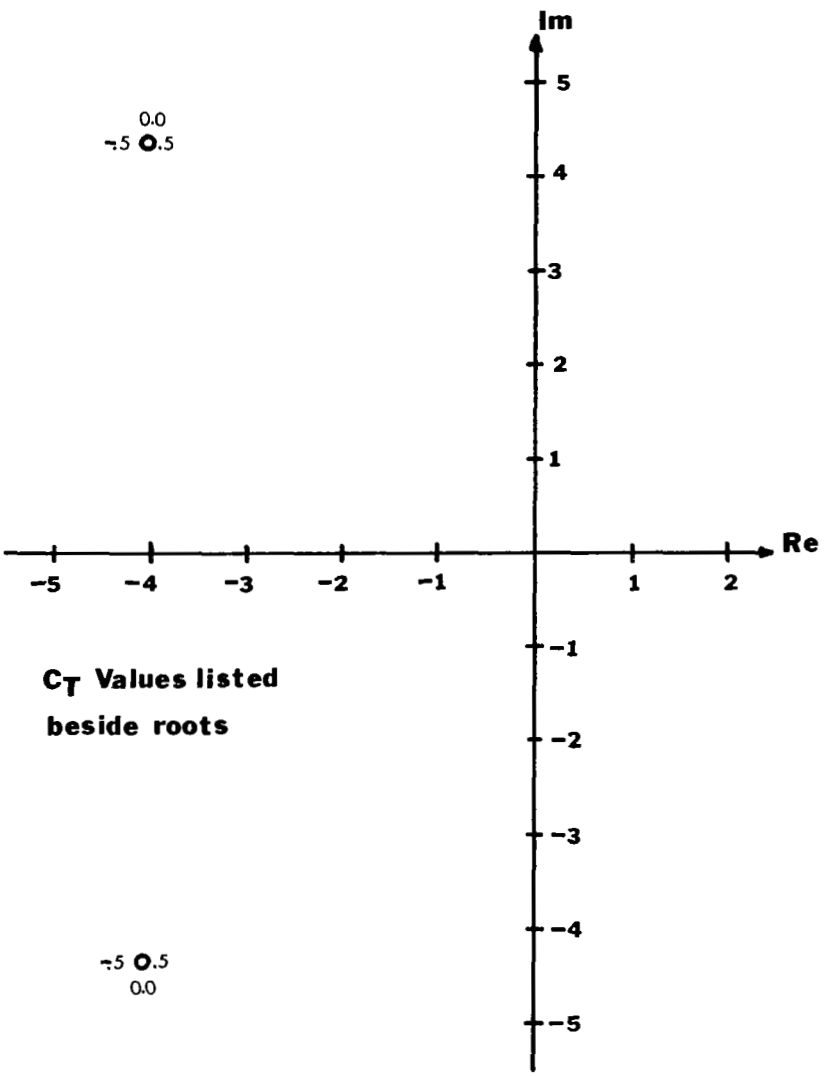

Figure 86a

Phugoid Mode Roots for the C_T Variation

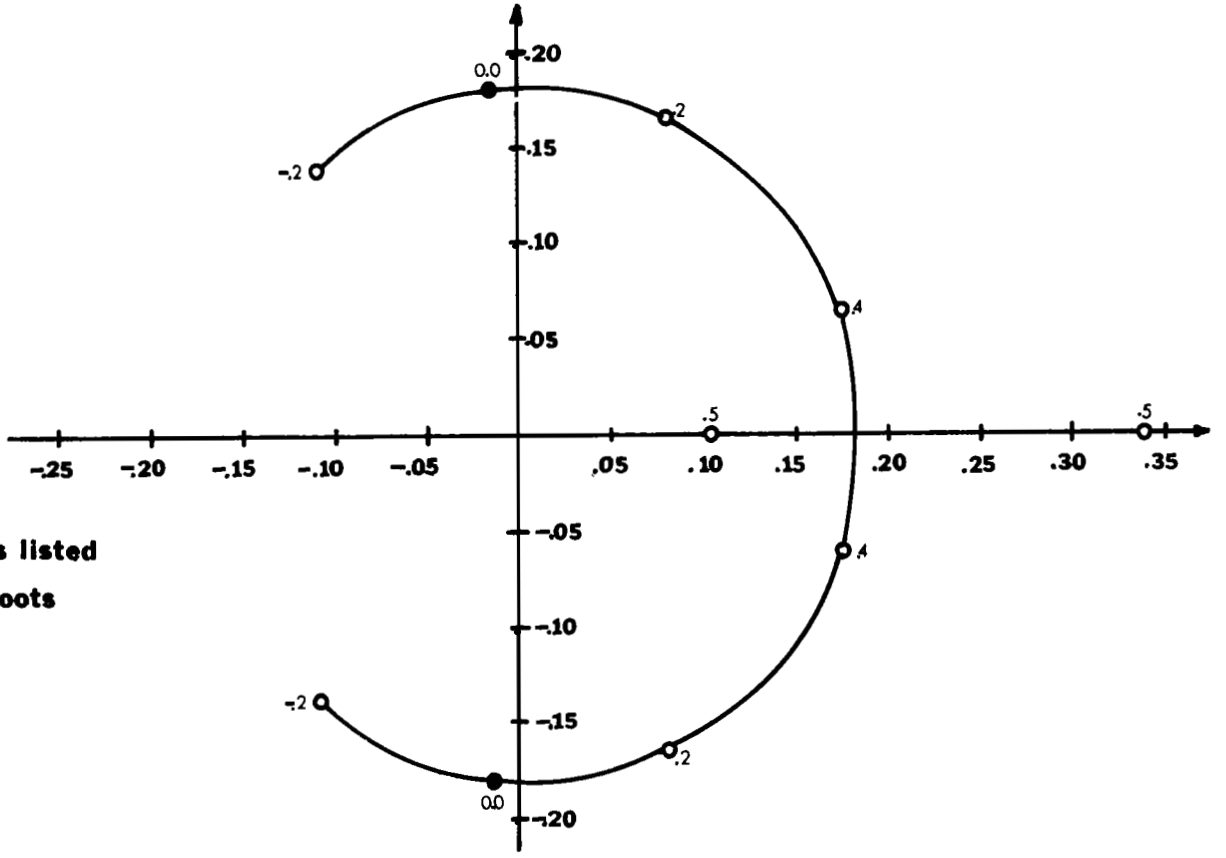

C_T Values listed beside roots

Figure 86b

NUMERATOR ROOTS

u

STABILITY DERIVATIVE	REAL	IMAGINARY	REAL	REAL
-0.5	-7.68330	0.0	-7.93156	6.84425
-0.2	-7.68330	0.0	-7.93156	6.84425
0.0	-7.68330	0.0	-7.93156	6.84425
0.2	-7.68330	0.0	-7.93156	6.84425
0.4	-7.68330	0.0	-7.93156	6.84425
0.5	-7.68330	0.0	-7.93156	6.84425

$\Delta\alpha$

-0.5	-0.40952	0.0	-0.09450	-195.41718
-0.2	-0.10940	±0.17076		-195.41487
0.0	-0.01472	±0.20640		-195.41333
0.2	0.07997	±0.19522		-195.41180
0.4	0.17466	±0.12527		-195.41027
0.5	0.17346	0.0	0.26937	-195.40950

θ

-0.5	-0.52196	0.0	-2.04256
-0.2	-0.23624	0.0	-2.04437
0.0	-0.04605	0.0	-2.04529
0.2	0.14399	0.0	-2.04605
0.4	0.33390	0.0	-2.04669
0.5	0.42882	0.0	-2.04697

Table 31. Numerator roots for C_T variations.

Short Period Mode Roots for the C_{L_α} Variation

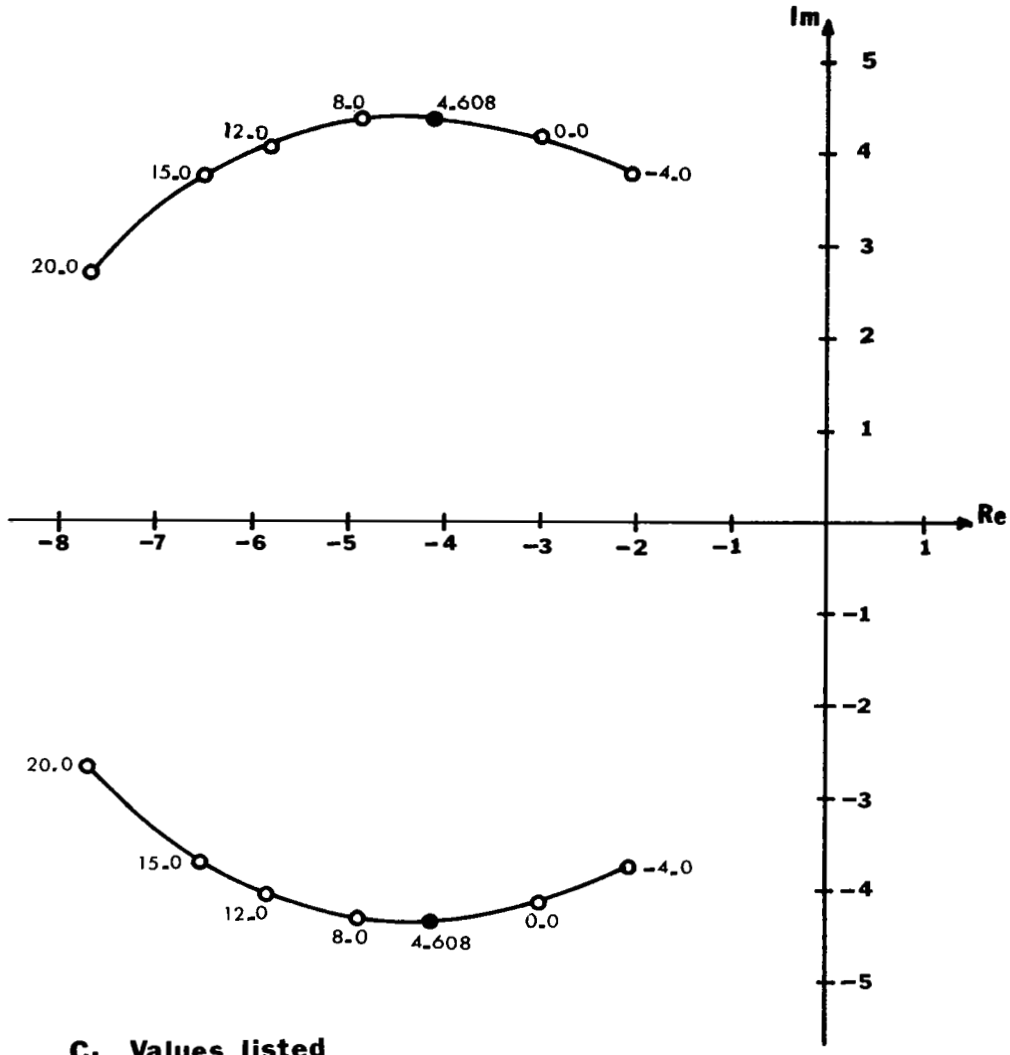

C_{L_α} Values listed beside roots

Figure 87a

Phugoid Mode Roots for the C_{L_α} Variation

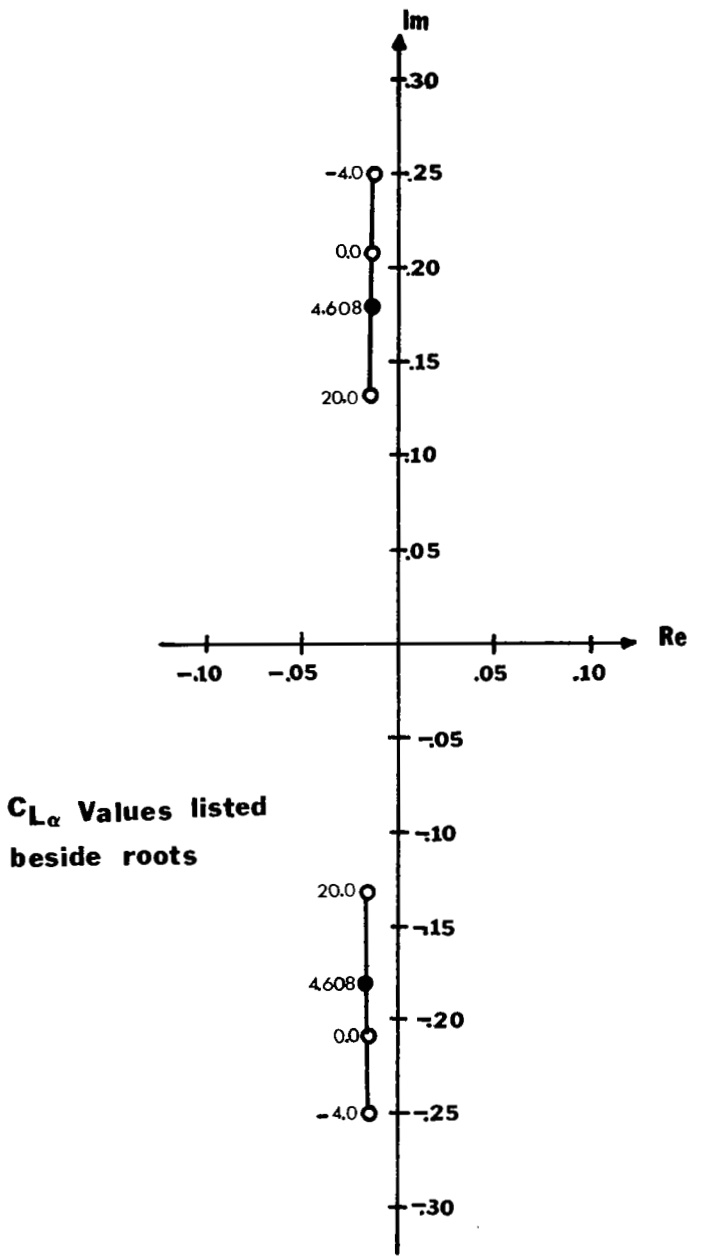

Figure 87b

NUMERATOR ROOTS

u

STABILITY DERIVATIVE	REAL	IMAGINARY	REAL	REAL
- 4.0	3.85691	±4.24363		-12.44010
0.0	0.48723	0.0	4.46793	-11.56084
4.608	6.84425	0.0	-7.68330	- 7.93156
8.0	- 8.98685	±4.10263		7.60946
12.0	-10.23230	±5.68619		8.22106
15.0	-11.10984	±6.45655		8.56664
20.0	-12.50753	±7.33119		9.01289

Δα

- 4.0	-0.01472	±0.20640		-195.41333
0.0	-0.01472	±0.20640		-195.41333
4.608	-0.01472	±0.20640		-195.41333
8.0	-0.01472	±0.20640		-195.41333
12.0	-0.01472	±0.20640		-195.41333
15.0	-0.01472	±0.20640		-195.41333
20.0	-0.01472	±0.20640		-195.41333

θ

- 4.0	-0.01518	0.0	2.00513
0.0	0.04672	±0.15901	
4.608	-0.04605	0.0	-2.04529
8.0	-0.03914	0.0	-3.66043
12.0	-0.03619	0.0	-5.55989
15.0	-0.03503	0.0	-6.98343
20.0	-0.03389	0.0	-9.35520

Table 32. Numerator roots for C_{L_α} variations.

Short Period Mode Roots for the C_{D_α} Variation

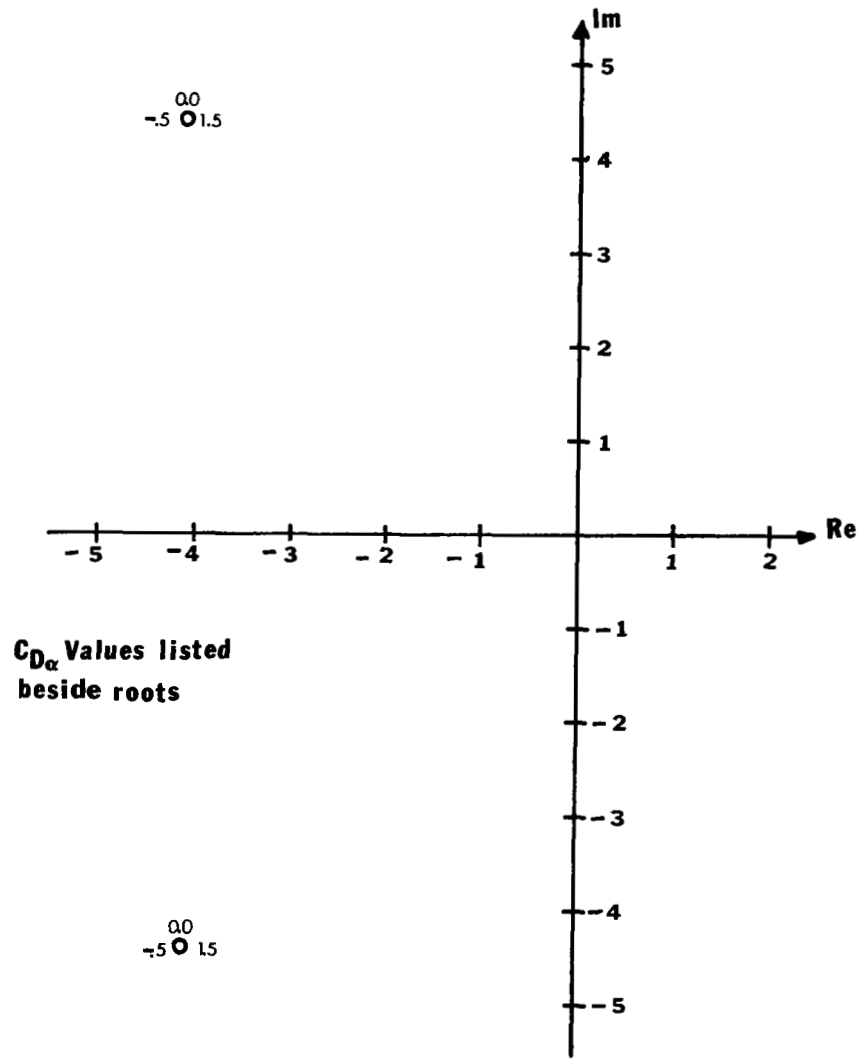

Figure 88a

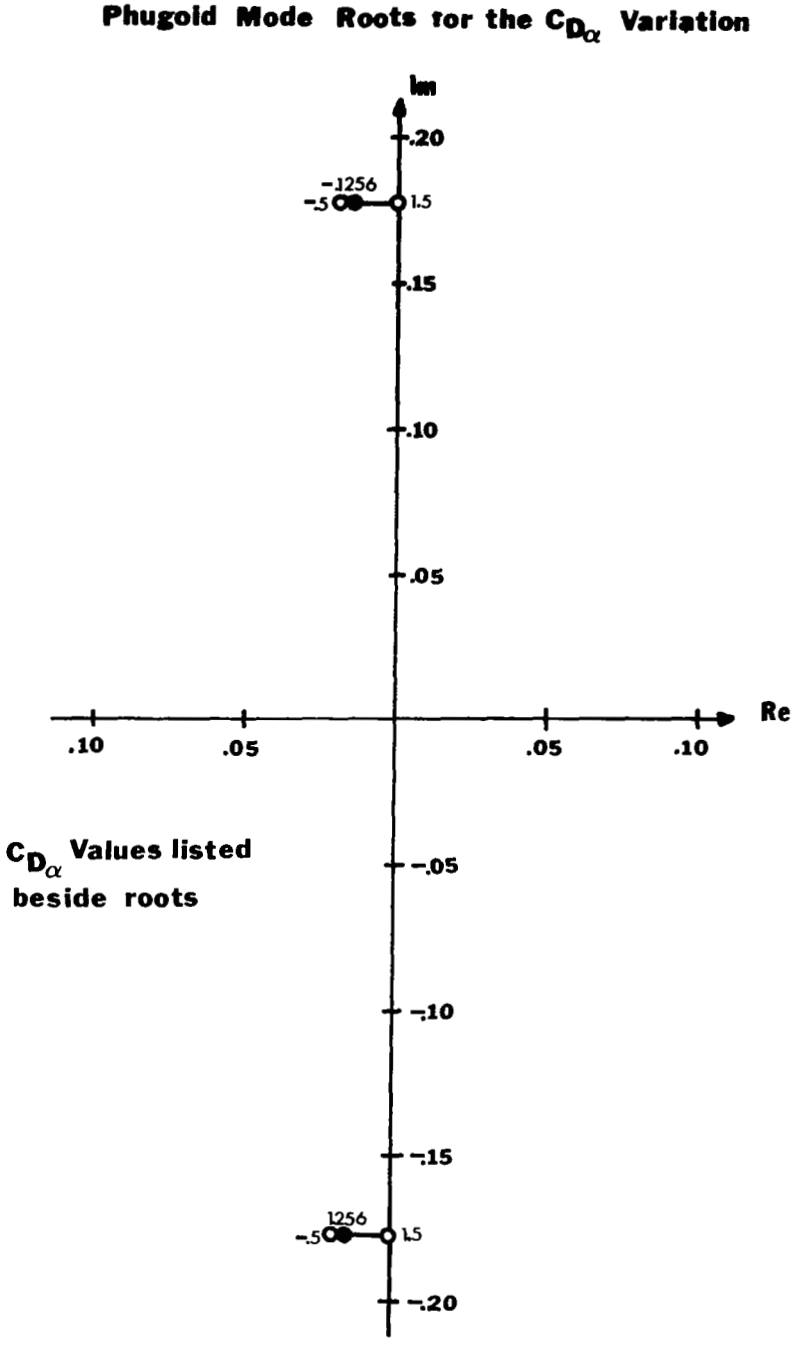
Phugoid Mode Roots for the C_{D_α} Variation
Im
.20
-1256
-.5
1.5
.15
.10
.05
Re
.10
.05
.05
.10
C_{D_α} Values listed beside roots
-.05
-.10
-.15
1256
-.5
1.5
-.20

Figure 88b

NUMERATOR ROOTS

u

STABILITY DERIVATIVE	REAL	IMAGINARY	REAL	REAL
-0.5	-5.98845	±18.51477		1.10150
0.1256	-7.68330	0.0	- 7.93156	6.84425
1.5	-0.43878	0.0	-32.75372	29.04580

$\Delta\alpha$

-0.5	-0.01472	±0.20640		-195.41333
0.1256	-0.01472	±0.20640		-195.41333
1.5	-0.01472	±0.20640		-195.41333

θ

-0.5	-0.09055	0.0	-2.00078
0.1256	-0.04605	0.0	-2.04529
1.5	0.04537	0.0	-2.13671

Table 33. Numerator roots for C_{D_α} variations.

Short Period Mode Roots for the C_{m_α} Variation

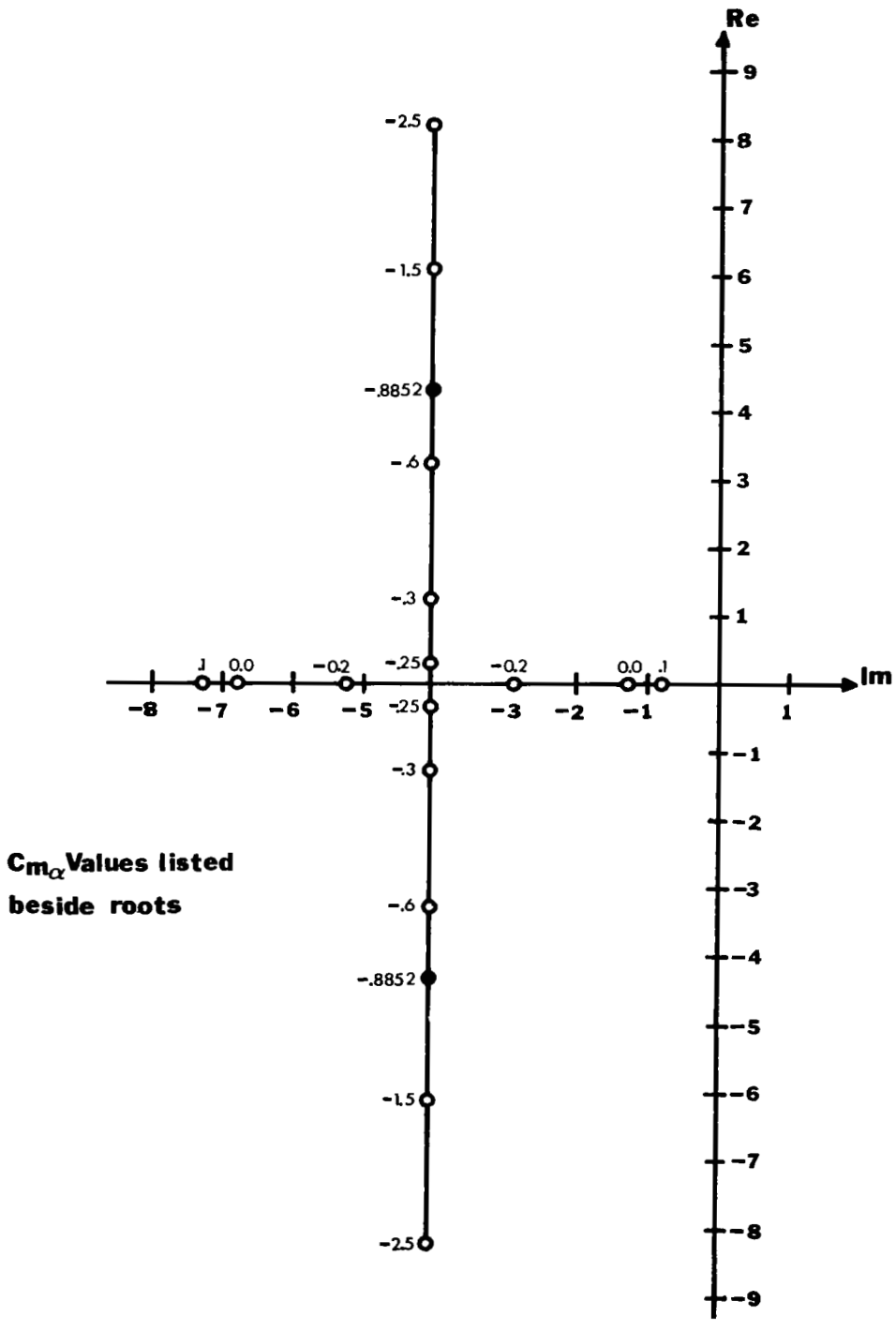

Figure 89a

Phugoid Mode Roots for the Cm_α Variation

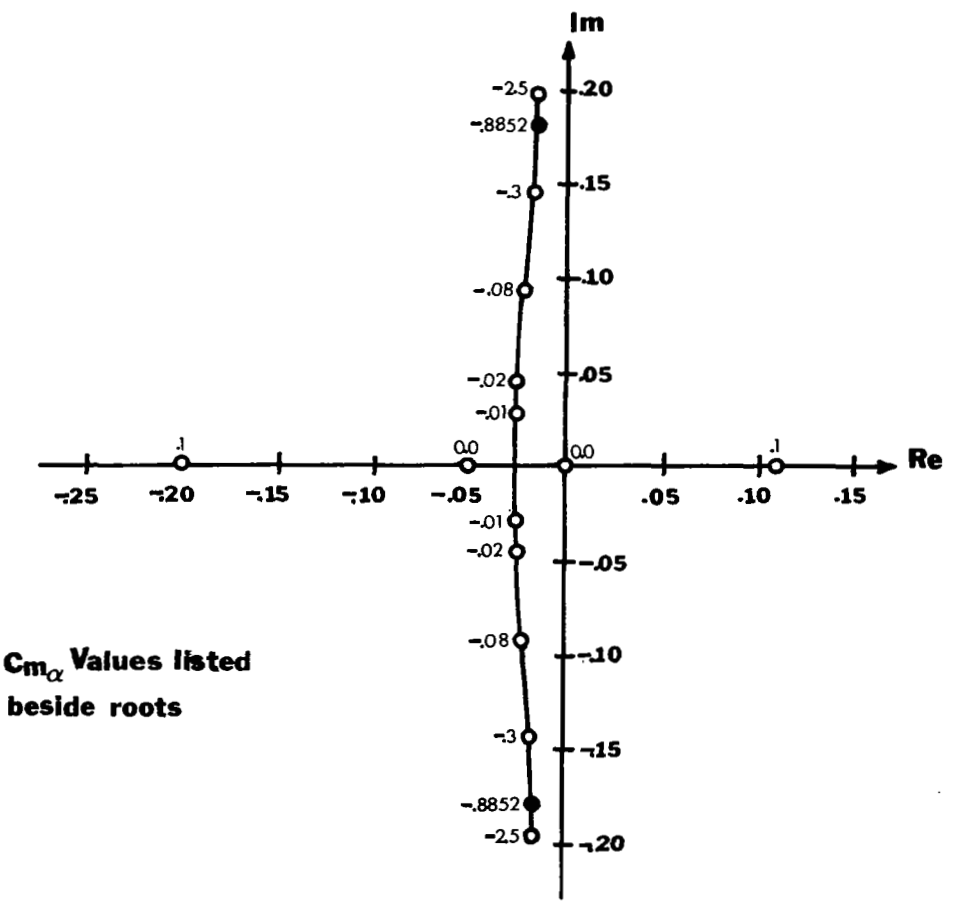

Figure 89b

NUMERATOR ROOTS

u

STABILITY DERIVATIVE	REAL	IMAGINARY	REAL	REAL
-2.5	-6.91423	±4.94608		5.05789
-1.5	-7.46700	±2.95479		6.16344
-0.8852	-7.68330	0.0	- 7.93156	6.84425
-0.6	-5.99482	0.0	- 9.93315	7.15734
-0.3	-5.33012	0.0	-10.92447	7.48395
-0.25	-5.24383	0.0	-11.06490	7.53808
-0.2	-5.16223	0.0	-11.20053	7.59212
-0.08	-4.98270	0.0	-11.50937	7.72143
-0.02	-4.90034	0.0	-11.65618	7.78587
-0.01	-4.88704	0.0	-11.68021	7.79660
0.0	-4.87385	0.0	-11.70412	7.80732
0.1	-4.74795	0.0	-11.93702	7.91432
		$\Delta\alpha$		
-2.5	-0.01472	±0.20640		-195.41333
-1.5	-0.01472	±0.20640		-195.41333
-0.8852	-0.01472	±0.20640		-195.41333
-0.6	-0.01472	±0.20640		-195.41333
-0.3	-0.01472	±0.20640		-195.41333
-0.25	-0.01472	±0.20640		-195.41333
-0.2	-0.01472	±0.20640		-195.41333
-0.08	-0.01472	±0.20640		-195.41333
-0.02	-0.01472	±0.20640		-195.41333
-0.01	-0.01472	±0.20640		-195.41333
0.0	-0.01472	±0.20640		-195.41333
0.1	-0.01472	±0.20640		-195.41333
		θ		
-2.5	-0.05433	0.0	-1.78232	
-1.5	-0.04893	0.0	-1.94544	
-0.8852	-0.04605	0.0	-2.04529	
-0.6	-0.04480	0.0	-2.09151	
-0.3	-0.04356	0.0	-2.14008	
-0.25	-0.04335	0.0	-2.14816	
-0.2	-0.04315	0.0	-2.15625	
-0.08	-0.04268	0.0	-2.17565	
-0.02	-0.04244	0.0	-2.18535	
-0.01	-0.04240	0.0	-2.18697	
0.0	-0.04237	0.0	-2.18858	
0.1	-0.04198	0.0	-2.20474	

Table 34. Numerator roots for C_{m_α} variations.

Short Period Mode Roots for the $C_{L_{\dot{\alpha}}}$ Variation

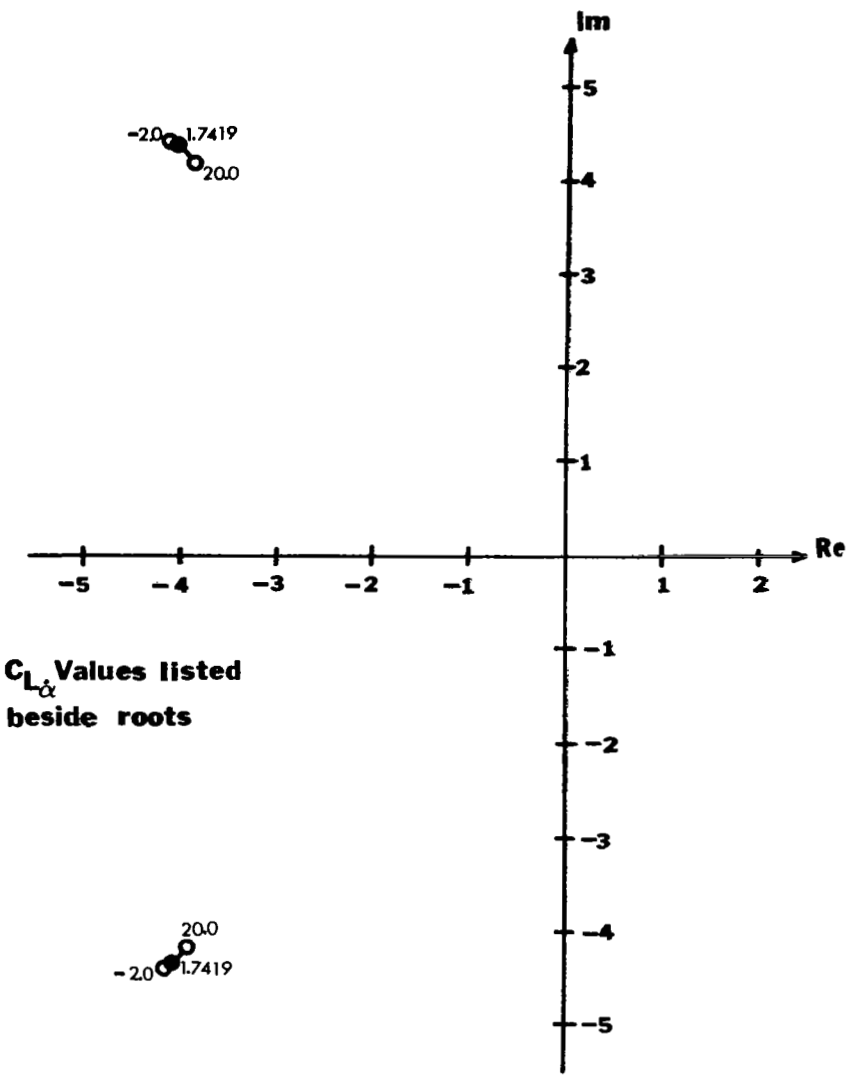

Figure 90a

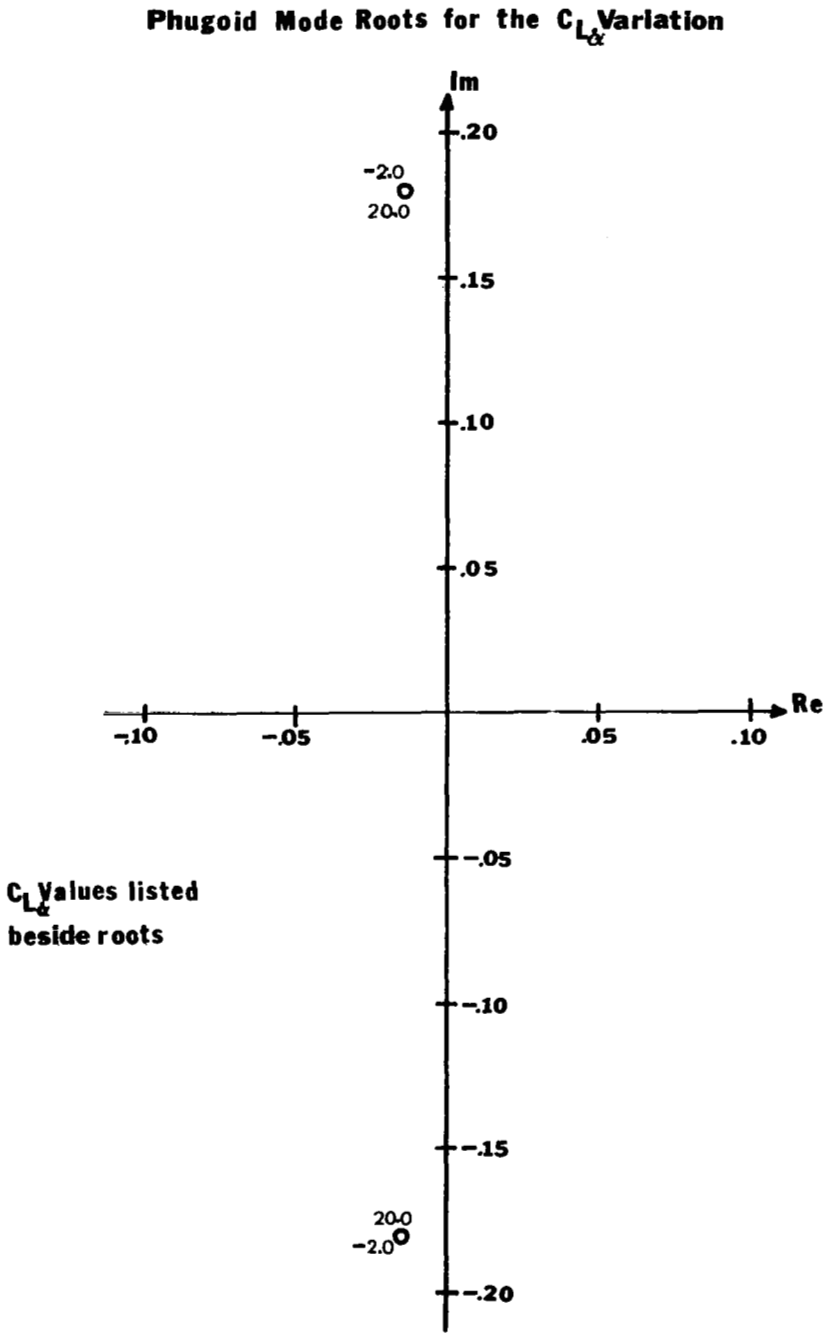
Phugoid Mode Roots for the C_{L_α} Variation
Im
.20
.15
.10
.05
-2.0
20.0
-.10
-.05
.05
.10
Re
-.05
-.10
-.15
20.0
-2.0
-.20
C_{L_α} values listed
beside roots

Figure 90b

NUMERATOR ROOTS

u

STABILITY DERIVATIVE	REAL	IMAGINARY	REAL	REAL
- 2.0	-7.81212	±1.36416		6.76371
1.7419	-7.68330	0.0	- 7.93156	6.84425
20.0	-4.97289	0.0	-10.61842	7.21373

$\Delta\alpha$

- 2.0	-0.01472	±0.20640		-195.41333
1.7419	-0.01472	±0.20640		-195.41333
20.0	-0.01472	±0.20640		-195.41333

θ

- 2.0	-0.04604	0.0	-2.08659
1.7419	-0.04605	0.0	-2.04529
20.0	-0.04608	0.0	-1.86499

Table 35. Numerator roots for $C_{L_{\dot{\alpha}}}$ variations.

Short Period Mode Roots for the $C_{D_{\dot{\alpha}}}$ Variation

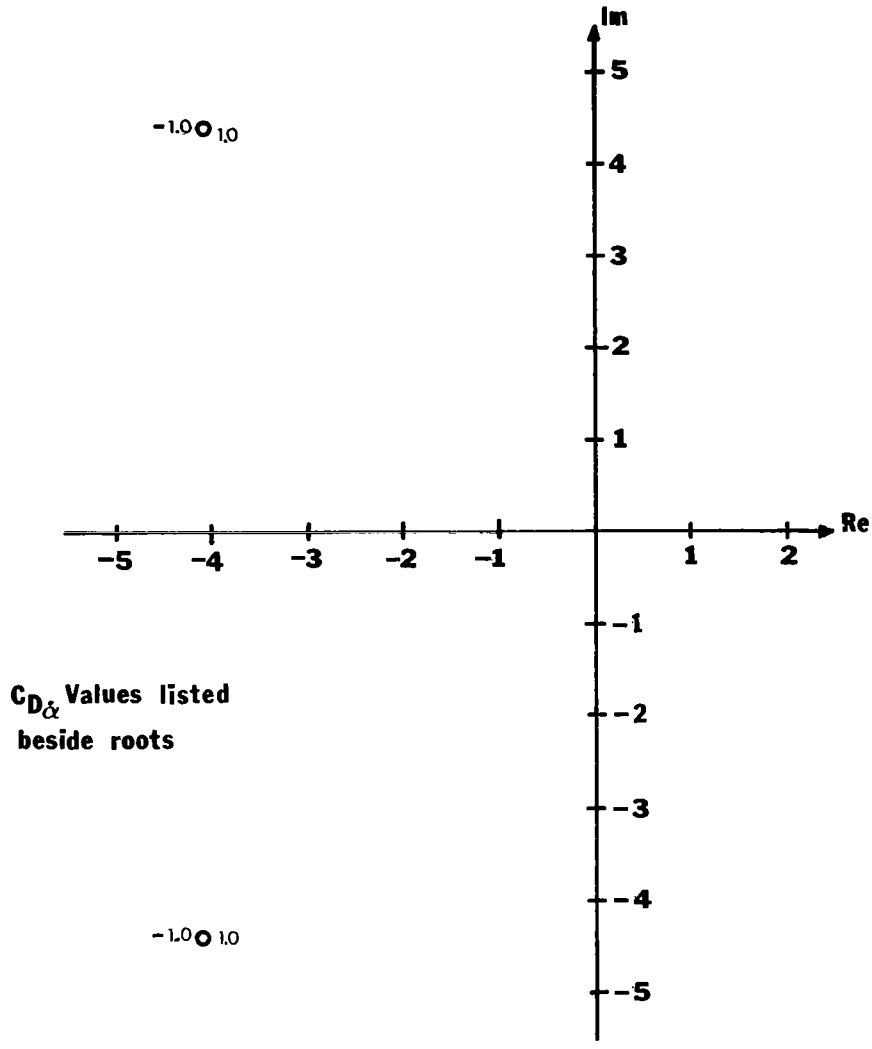

Figure 91a

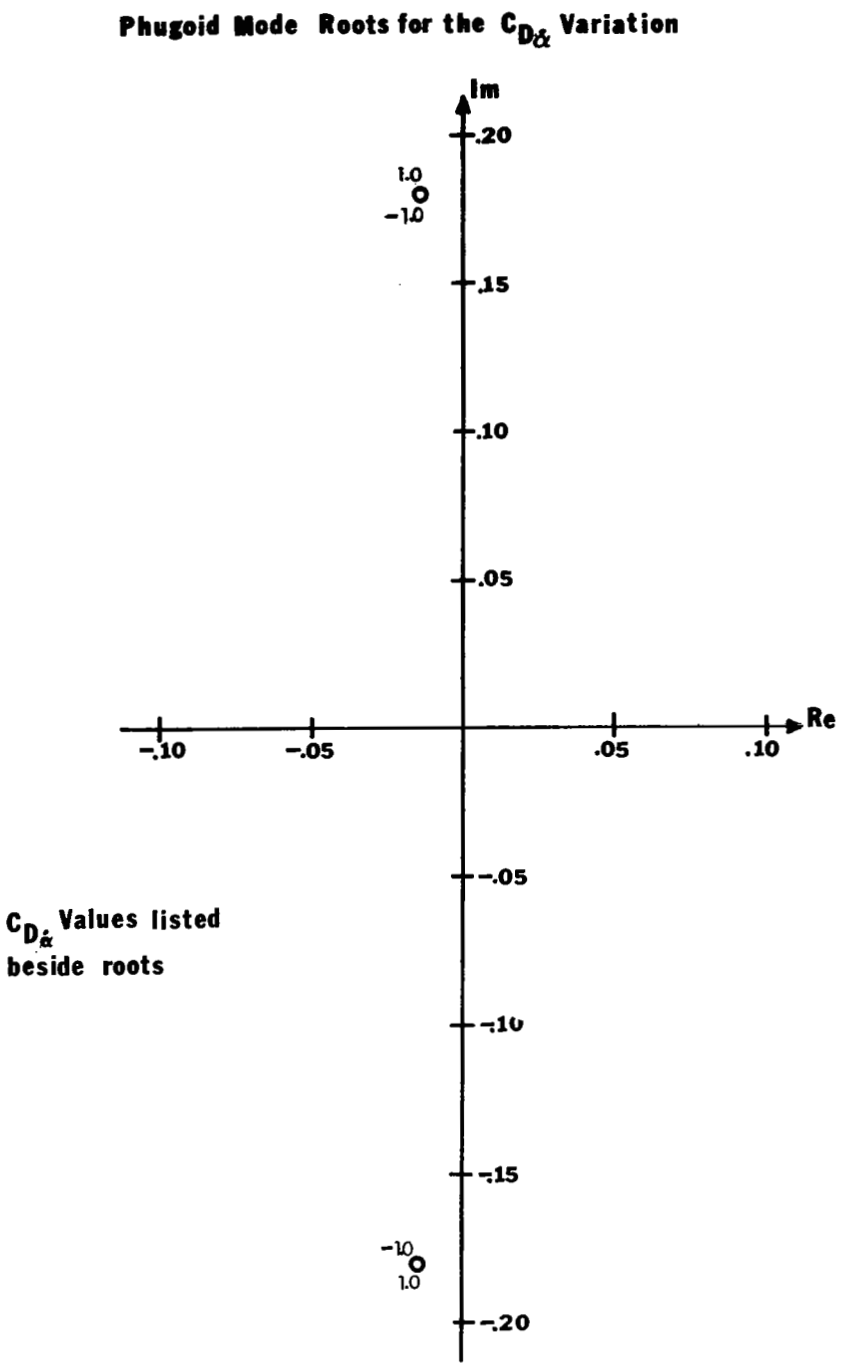
Phugoid Mode Roots for the $C_{D_{\dot{\alpha}}}$ Variation
Im
.20
1.0
-1.0
.15
.10
.05
-.10
-.05
.05
.10
Re
-.05
-.10
-.15
-1.0
1.0
-.20
$C_{D_{\dot{\alpha}}}$ Values listed beside roots

Figure 91b

NUMERATOR ROOTS

STABILITY DERIVATIVE	REAL	IMAGINARY	REAL	REAL
		u		
-1.0	-4.34161	0.0	-16.68519	5.55105
0.0	-7.68330	0.0	- 7.93156	6.84425
1.0	-5.29188	±4.46484		9.03719
		$\Delta\alpha$		
-1.0	-0.01472	±0.20640		-195.41333
0.0	-0.01472	±0.20640		-195.41333
1.0	-0.01472	±0.20640		-195.41333
		θ		
-1.0	-0.04601	0.0	-2.04686	
0.0	-0.04605	0.0	-2.04529	
1.0	-0.04608	0.0	-2.04371	

Table 36. Numerator roots for $C_{D_{\dot{\alpha}}}$ variations.

Short Period Mode Roots for the $C_{m_{\dot{\alpha}}}$ Variation

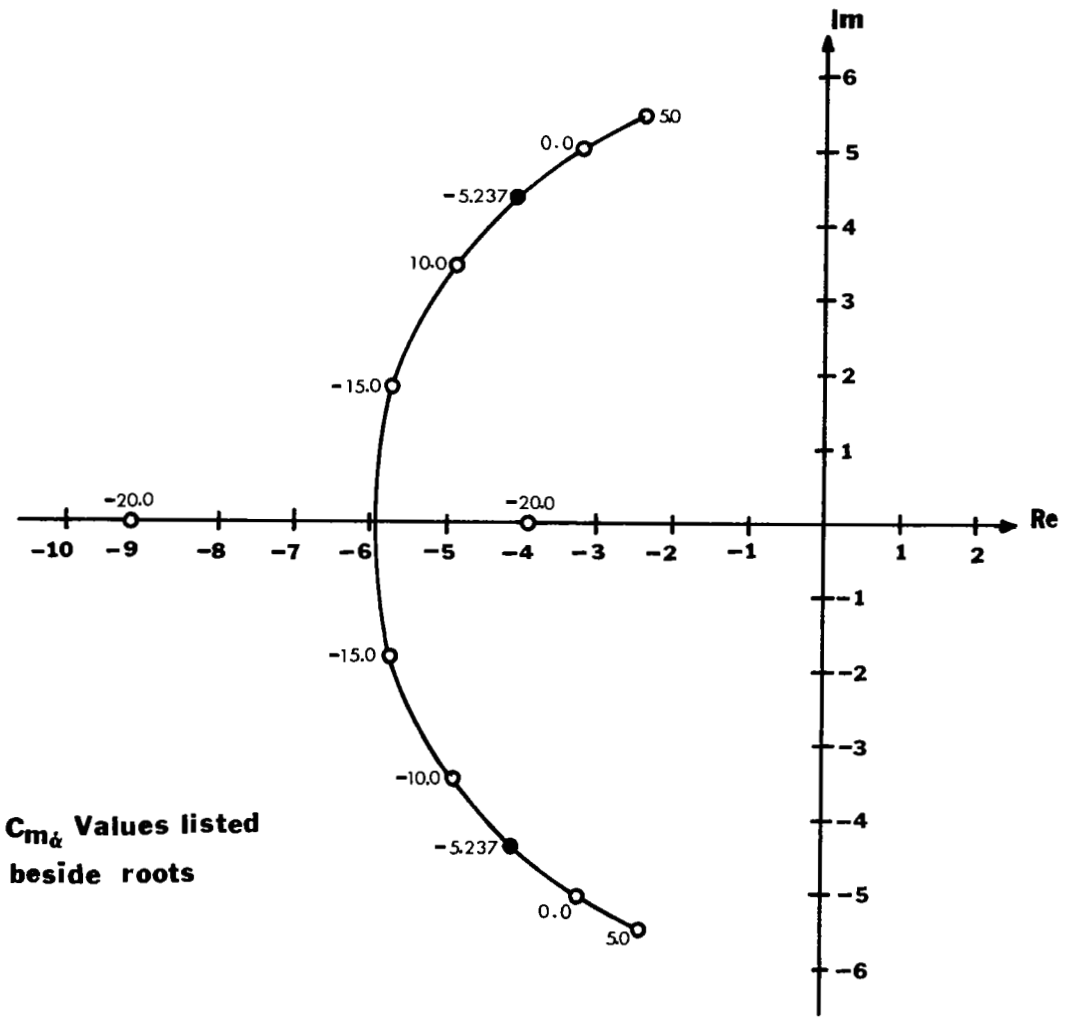

Figure 92a

Phugoid Mode Roots for the $C_{m_{\dot{\alpha}}}$ Variation

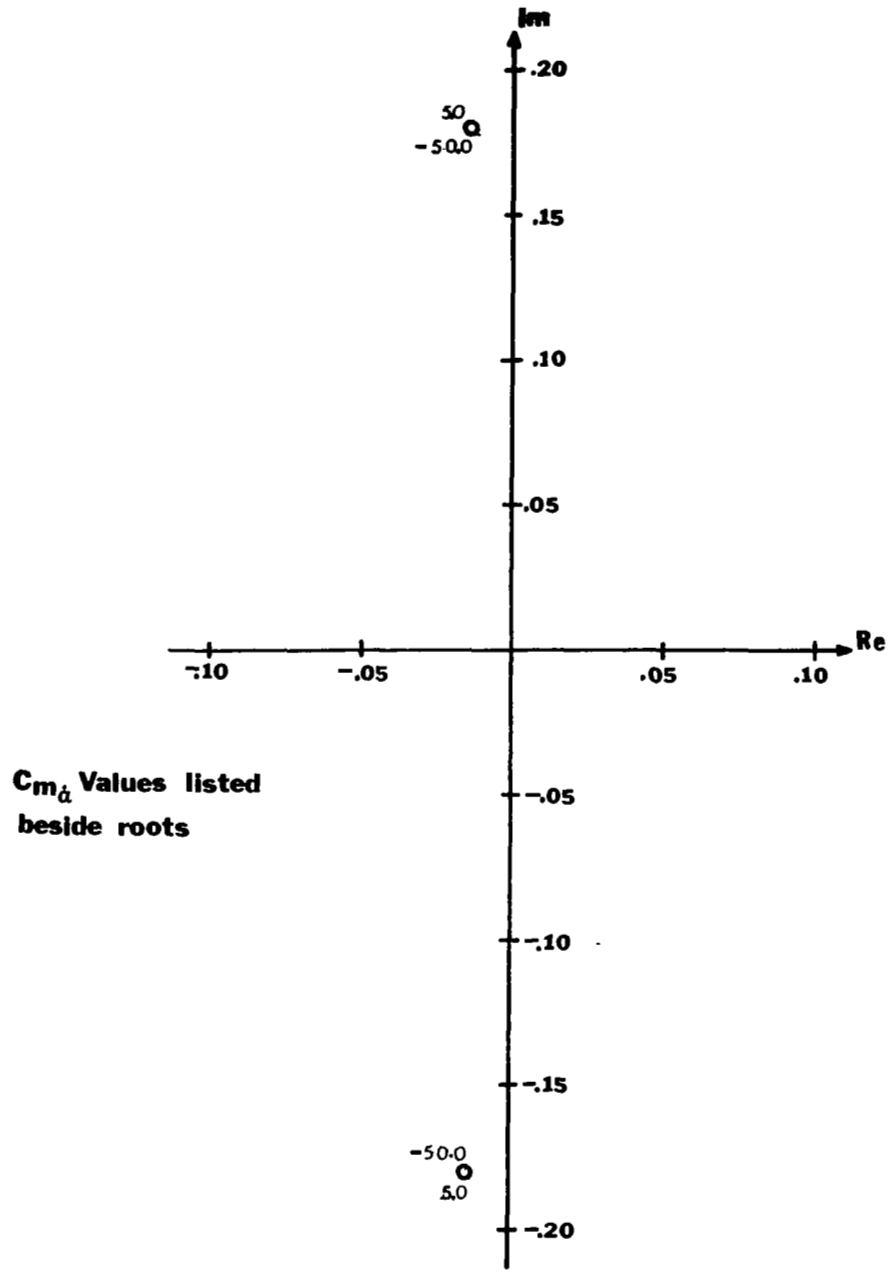

Figure 92b

NUMERATOR ROOTS

u

STABILITY DERIVATIVE	REAL	IMAGINARY	REAL	REAL
-50.0	-3.90188	0.0	-24.11478	4.43293
-20.0	-4.97207	0.0	-14.47813	5.79415
-15.0	-5.34358	0.0	-12.77020	6.11235
-10.0	-5.92015	0.0	-10.89391	6.46725
- 5.237	-7.68330	0.0	- 7.93156	6.84425
0.0	-7.17309	±2.36959		7.30864
5.0	-6.59500	±3.15130		7.80707

$\Delta\alpha$

-50.0	-0.01472	±0.20640		-195.41333
-20.0	-0.01472	±0.20640		-195.41333
-15.0	-0.01472	±0.20640		-195.41333
-10.0	-0.01472	±0.20640		-195.41333
- 5.237	-0.01472	±0.20640		-195.41333
0.0	-0.01472	±0.20640		-195.41333
5.0	-0.01472	±0.20640		-195.41333

θ

-50.0	-0.04594	0.0	-2.22363
-20.0	-0.04601	0.0	-2.10095
-15.0	-0.04602	0.0	-2.08177
-10.0	-0.04603	0.0	-2.06293
- 5.237	-0.04605	0.0	-2.04529
0.0	-0.04606	0.0	-2.02623
5.0	-0.04607	0.0	-2.00835

Table 37. Numerator roots for $C_{m_{\dot{\alpha}}}$ variations.

Short Period Mode Roots for the C_{L_q} Variation

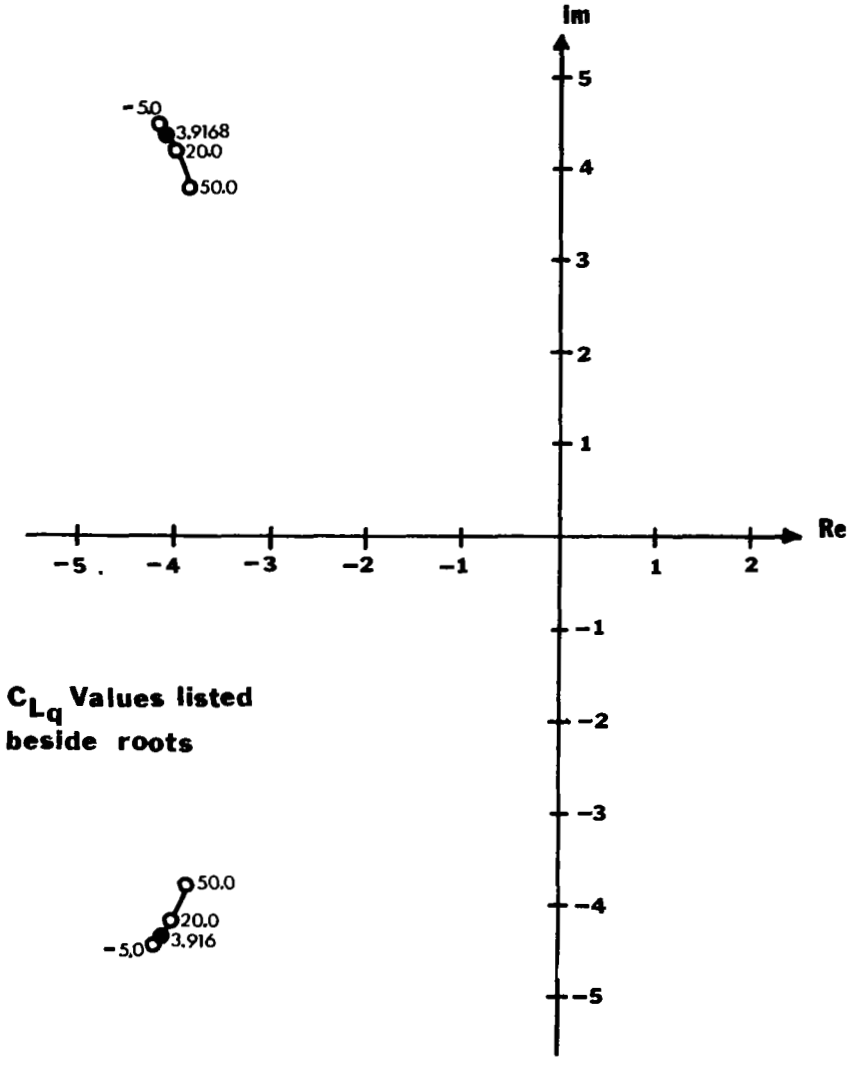

Figure 93a

Phugoid Mode Roots for the C_{L_q} Variation

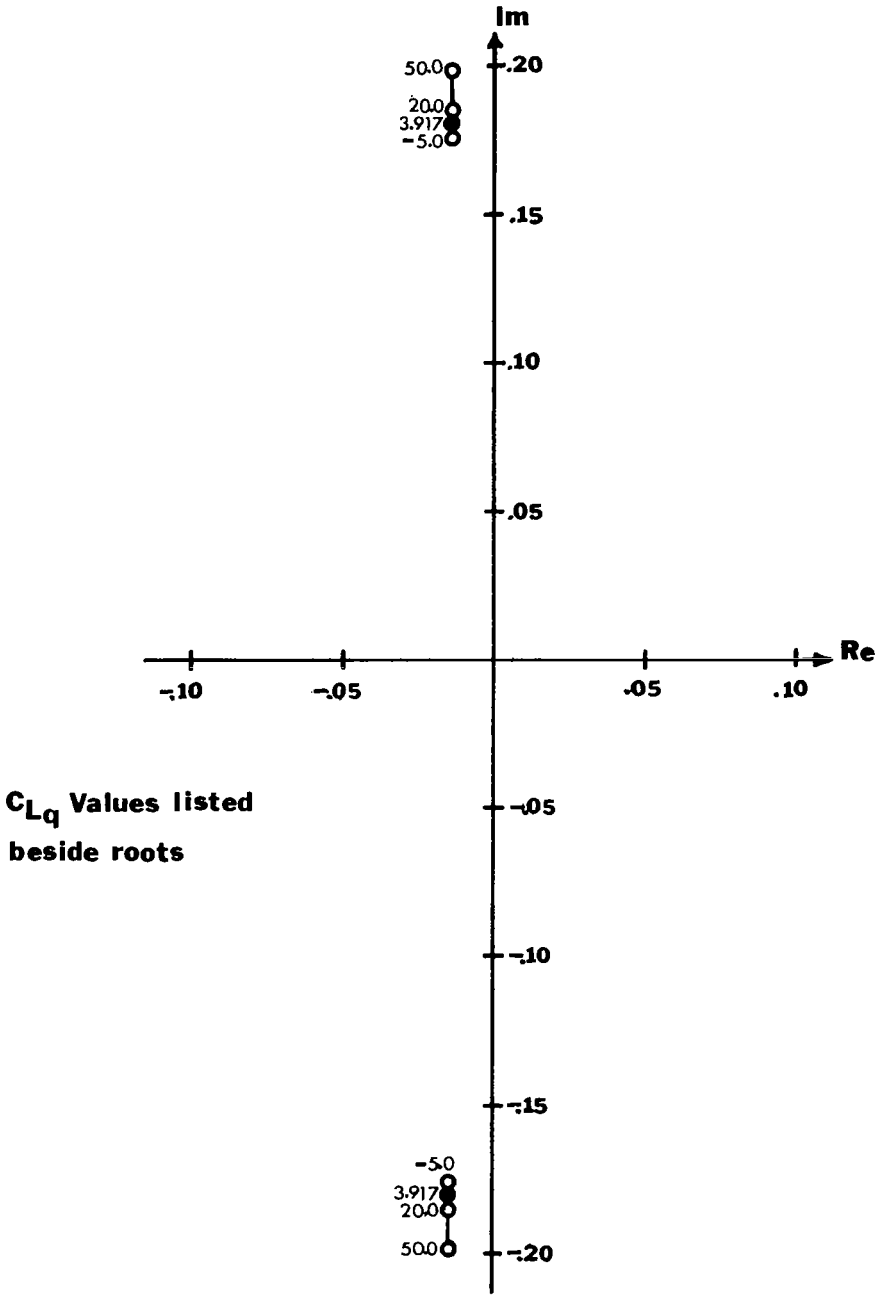

Figure 93b

NUMERATOR ROOTS

STABILITY DERIVATIVE	REAL	IMAGINARY	REAL	REAL
u				
- 5.0	-7.73020	±1.83643		6.60700
3.9168	-7.68330	0.0	- 7.93156	6.84425
20.0	-5.52374	0.0	-10.37532	7.27783
50.0	-4.21075	0.0	-12.23076	8.09894
Δα				
- 5.0	-0.01475	±0.20171		-204.55258
3.9168	-0.01472	±0.20640		-195.41333
20.0	-0.01465	±0.21575		-178.92893
50.0	-0.01449	±0.23718		-148.18066
θ				
- 5.0	-0.04605	0.0	-2.04529	
3.9168	-0.04605	0.0	-2.04529	
20.0	-0.04605	0.0	-2.04529	
50.0	-0.04605	0.0	-2.04529	

Table 38. Numerator roots for C_{L_q} variations.

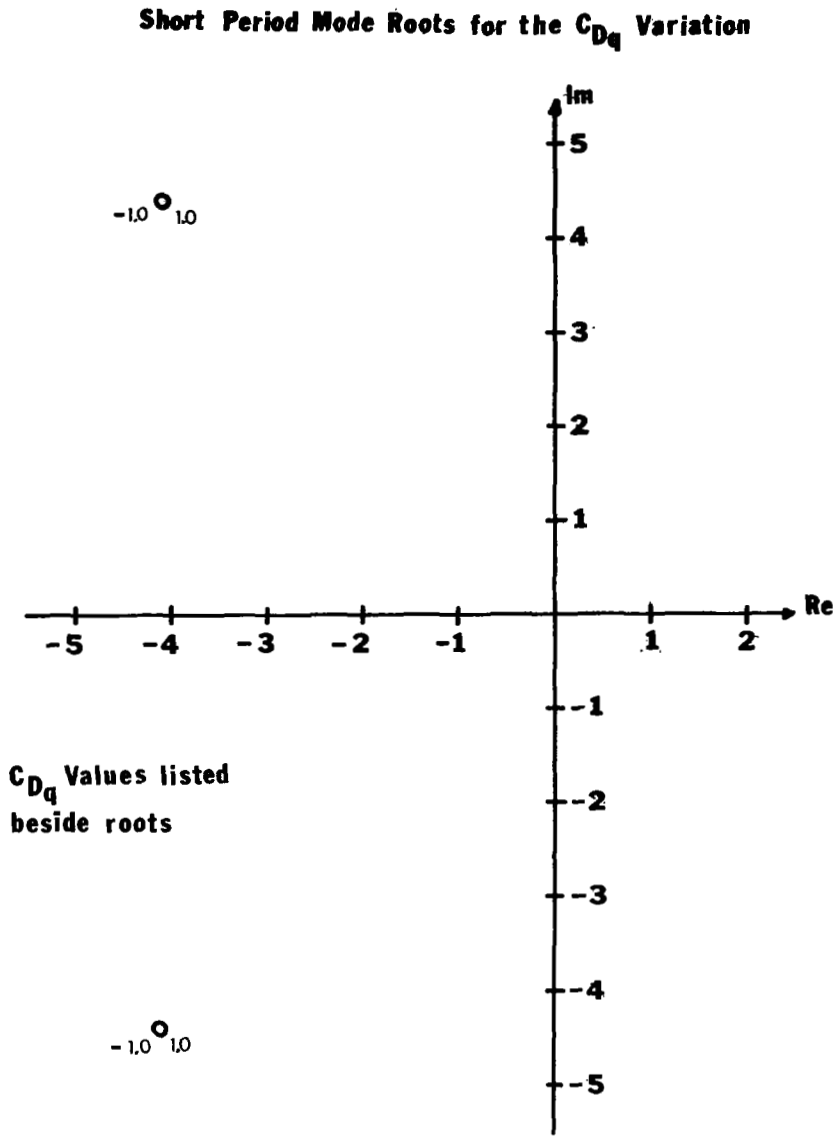
Short Period Mode Roots for the C_{D_q} Variation
Im
5
4
3
2
1
-1
-2
-3
-4
-5
Re
-5
-4
-3
-2
-1
1
2
-1.0
1.0
-1.0
1.0
C_{D_q} Values listed beside roots

Figure 94a

Phugoid Mode Roots for the C_{D_q} Variation

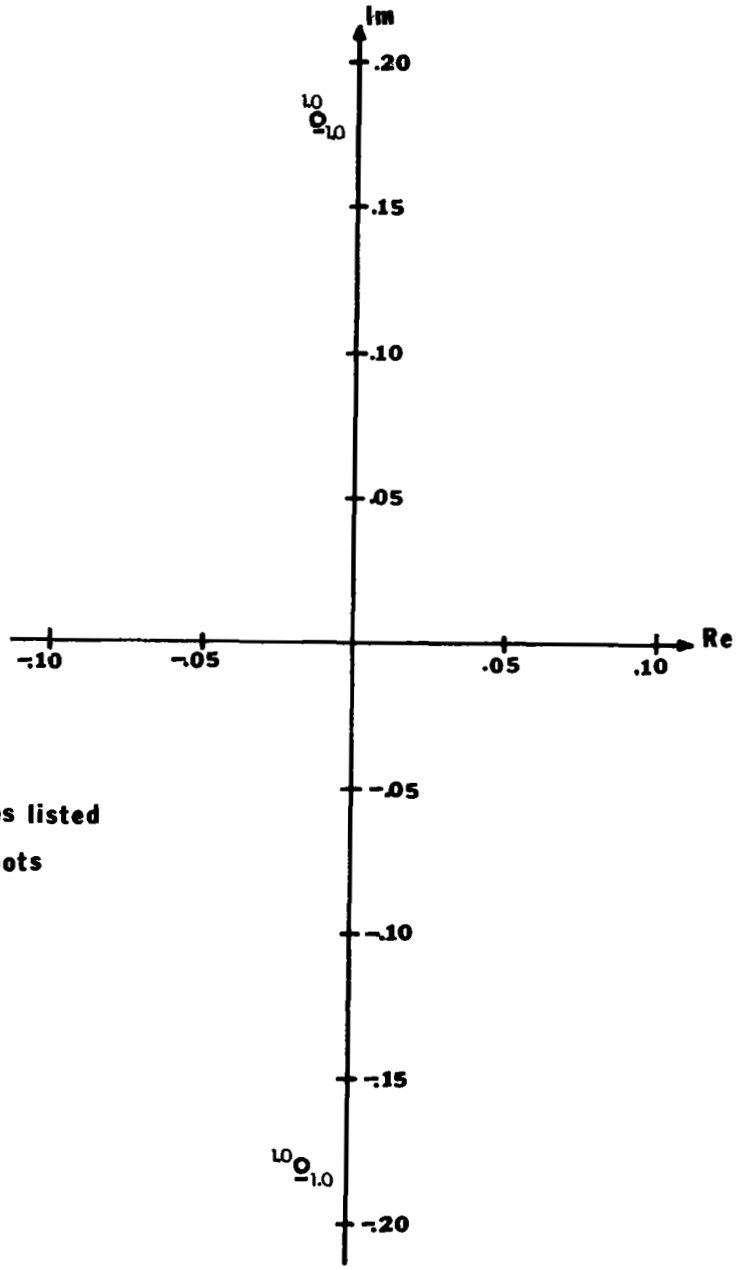

C_{D_q} Values listed beside roots

Figure 94b

NUMERATOR ROOTS

STABILITY DERIVATIVE	REAL	IMAGINARY	REAL	REAL
		u		
-1.0	-4.88199	0.0	-16.37834	5.21643
0.0	-7.68330	0.0	- 7.93156	6.84425
1.0	-5.50557	±3.67822		9.51381
		Δα		
-1.0	-0.01395	±0.20645		-195.41487
0.0	-0.01472	±0.20640		-195.41333
1.0	-0.01549	±0.20634		-195.41179
		θ		
-1.0	-0.04605	0.0	-2.04529	
0.0	-0.04605	0.0	-2.04529	
1.0	-0.04605	0.0	-2.04529	

Table 39. Numerator roots for C_{D_q} variations.

Short Period Mode Roots for the C_{m_q} Variation

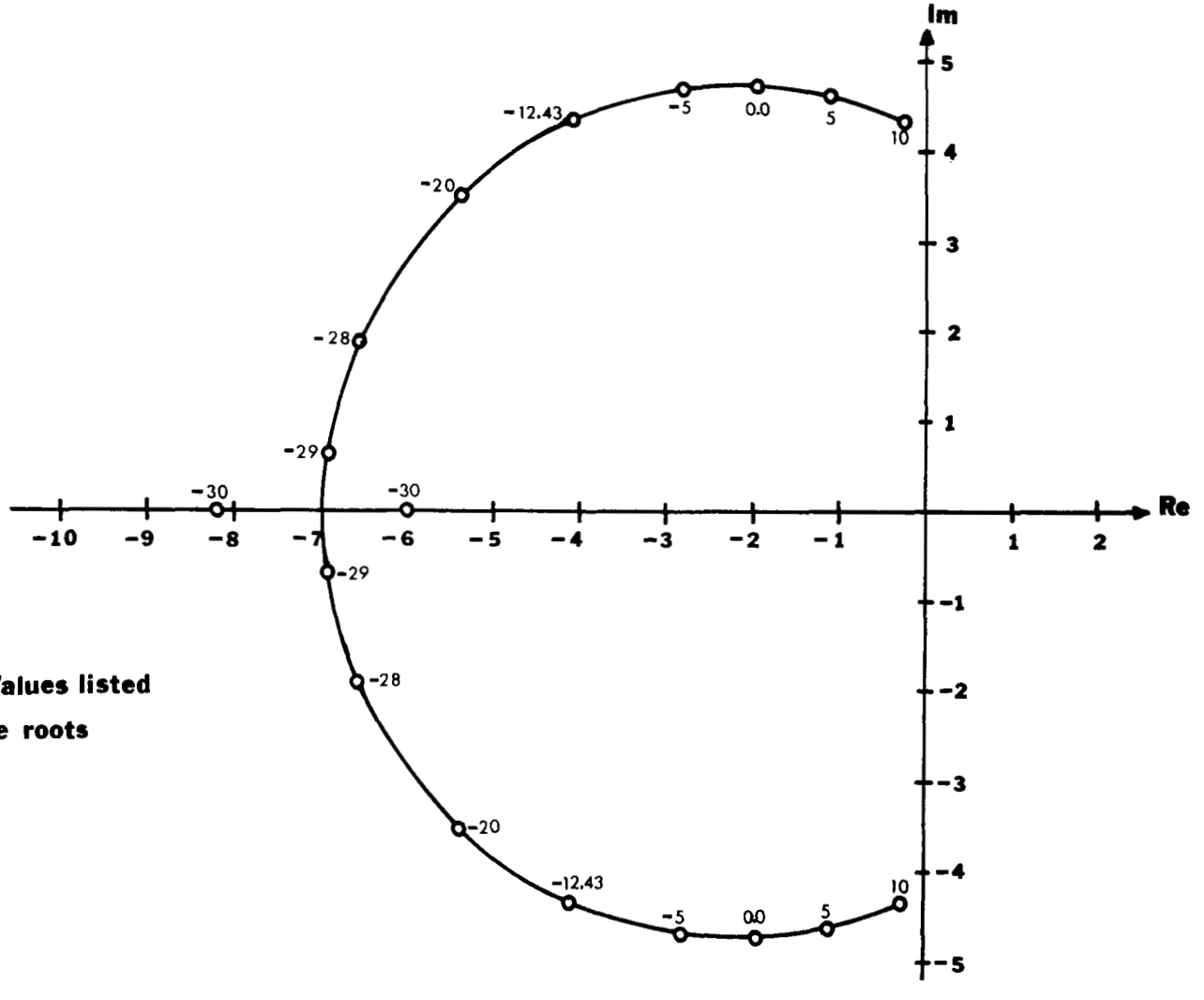

C_{m_q} Values listed beside roots

Figure 95a

Phugoid Mode Roots for the C_{m_q} Variation

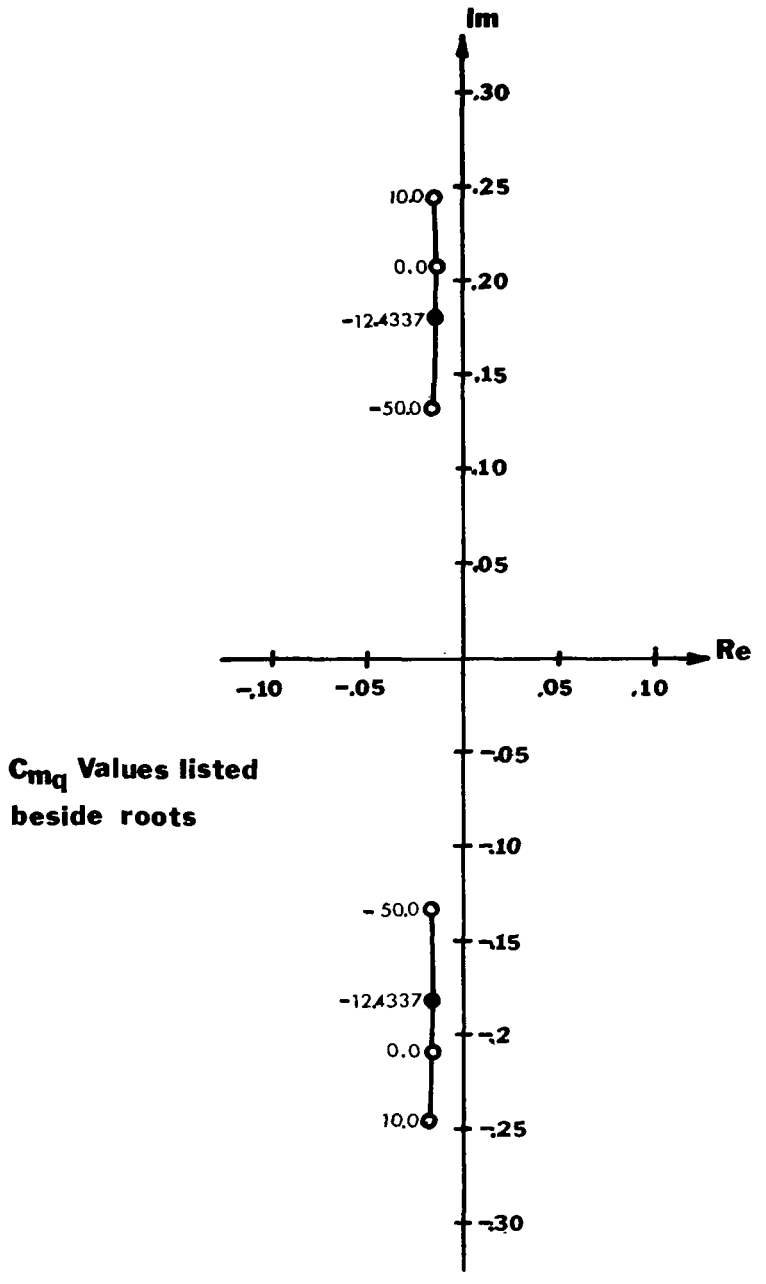

Figure 95b

NUMERATOR ROOTS

STABILITY DERIVATIVE	REAL	IMAGINARY	REAL	REAL
		u		
-50.0	-4.67832	0.0	-21.12196	4.22104
-30.0	-5.26804	0.0	-14.83064	5.33863
-29.0	-5.31297	0.0	-14.51478	5.40867
-28.0	-5.36047	0.0	-14.19800	5.48035
-20.0	-5.88484	0.0	-11.58404	6.11845
-12.4337	-7.68330	0.0	- 7.93156	6.84425
- 5.0	-6.96597	±2.38145		7.69596
0.0	-6.44403	±2.89559		8.35687
5.0	-5.96067	±3.21405		9.09494
10.0	-5.51777	±3.40961		9.91393
		$\Delta\alpha$		
-50.0	-0.01350	±0.20000		-208.22433
-30.0	-0.01413	±0.20333		-201.40389
-29.0	-0.01416	±0.20350		-201.06287
-28.0	-0.01419	±0.20368		-200.72185
-20.0	-0.01446	±0.20506		-197.99364
-12.4337	-0.01472	±0.20640		-195.41333
- 5.0	-0.01498	±0.20774		-192.87823
0.0	-0.01516	±0.20866		-191.17308
5.0	-0.01534	±0.20958		-189.46792
10.0	-0.01552	±0.21053		-187.76275
		θ		
-50.0	-0.04605	0.0	-2.04529	
-30.0	-0.04605	0.0	-2.04529	
-29.0	-0.04605	0.0	-2.04529	
-28.0	-0.04605	0.0	-2.04529	
-20.0	-0.04605	0.0	-2.04529	
-12.4337	-0.04605	0.0	-2.04529	
- 5.0	-0.04605	0.0	-2.04529	
0.0	-0.04605	0.0	-2.04529	
5.0	-0.04605	0.0	-2.04529	
10.0	-0.04605	0.0	-2.04529	

Table 40. Numerator roots for C_{m_q} variations.

NUMERATOR ROOTS

u

STABILITY DERIVATIVE	REAL	IMAGINARY	REAL	REAL
-0.5	-7.58511	±2.06610		7.74177
-0.1	-7.67989	±1.57952		7.35208
0.0	-7.70387	±1.42618		7.25523
0.1	-7.72796	±1.25135		7.15859
0.25	-7.76429	±0.92196		7.01404
0.4268	-7.68330	0.0	- 7.93156	6.84425
0.75	-6.59867	0.0	- 9.17542	6.53544
1.0	-6.22015	0.0	- 9.67839	6.29786
2.0	-5.22593	0.0	-11.17913	5.35625
5.0	-3.13507	0.0	-14.73205	2.47395

$\Delta\alpha$

-0.5	-0.01495	±0.21144		158.94513
-0.1	-0.01484	±0.20920		811.68551
0.0	-0.01482	±0.20868		
0.1	-0.01479	±0.20816		-820.16606
0.25	-0.01476	±0.20734		-330.61069
0.4268	-0.01472	±0.20640		-195.41333
0.75	-0.01465	±0.20472		-113.03072
1.0	-0.01460	±0.20345		- 85.83329
2.0	-0.01442	±0.19859		- 45.03736
5.0	-0.01406	±0.18585		- 20.56030

θ

-0.5	-0.04401	0.0	-2.30446
-0.1	-0.04482	0.0	-2.19391
0.0	-0.04504	0.0	-2.16597
0.1	-0.04526	0.0	-2.13790
0.25	-0.04561	0.0	-2.09556
0.4268	-0.04605	0.0	-2.04529
0.75	-0.04691	0.0	-1.95233
1.0	-0.04765	0.0	-1.87948
2.0	-0.05142	0.0	-1.57923
5.0	-0.09587	0.0	-0.56084

Table 41. Numerator roots for $C_{L_{\delta_E}}$ variations.

NUMERATOR ROOTS

u

STABILITY DERIVATIVE	REAL	IMAGINARY	REAL	REAL
-0.1	-2.09831	± 8.05539	-3.58753	
-0.05	-1.62690	±10.80785	-4.16199	
0.0			-4.92591	136.99857
0.0596	-7.68330	0.0	-7.93156	6.84425
0.1	-6.67433	± 2.63517		4.82778
0.5	-4.76177	± 3.95572		1.29735

$\Delta\alpha$

-0.1	-0.01590	±0.20626		-195.52065
-0.05	-0.01553	±0.20630		-195.48703
0.0	-0.01516	±0.20635		-195.45341
0.0596	-0.01472	±0.20640		-195.41333
0.1	-0.01442	±0.20644		-195.38617
0.5	-0.01145	±0.20676		-195.11722

θ

-0.1	-0.03843	0.0	-2.05190
-0.05	-0.04081	0.0	-2.04983
0.0	-0.04320	0.0	-2.04776
0.0596	-0.04605	0.0	-2.04529
0.1	-0.04798	0.0	-2.04361
0.5	-0.06731	0.0	-2.02679

Table 42. Numerator roots for $C_{D_{\delta_E}}$ variations.

NUMERATOR ROOTS

STABILITY DERIVATIVE	REAL	IMAGINARY	REAL	REAL
		u		
-15.0	-5.25815	0.0	-33.18891	29.67621
-10.0	-5.30278	0.0	-27.27432	23.80632
- 5.0	-5.44662	0.0	-19.44515	16.12106
- 3.0	-5.66806	0.0	-15.01042	11.90781
- 1.283	-7.68330	0.0	- 7.93156	6.84425
- 0.75	-6.66992	±2.51054		4.56927
0.0	-3.96317	±4.21546		- 0.84424
0.5	-2.55070	±6.96412		- 3.66917
1.0	-2.25392	±9.10942		- 4.26274
		Δα		
-15.0	-0.01522	±0.20851		-2239.746
-10.0	-0.01519	±0.20839		-1494.563
- 5.0	-0.01512	±0.20807		- 749.38113
- 3.0	-0.01503	±0.20767		- 451.30835
- 1.283	-0.01472	±0.20640		- 195.41333
- 0.75	-0.01434	±0.20486		- 115.97763
0.0	-0.00003	0.0	-4.23938	0.01042
0.5	-0.01682	±0.21467		70.32293
1.0	-0.01602	±0.21158		144.83956
		θ		
-15.0	-0.04267	0.0	- 2.15785	
-10.0	-0.04282	0.0	- 2.15263	
- 5.0	-0.04327	0.0	- 2.13696	
- 3.0	-0.04388	0.0	- 2.11600	
- 1.283	-0.04605	0.0	- 2.04529	
- 0.75	-0.04899	0.0	- 1.95623	
0.0	0.01042	0.0	-15.26480	
0.5	-0.03486	0.0	- 2.47223	
1.0	-0.03832		- 2.32224	

Table 43. Numerator roots for $C_{m_{\delta_E}}$ variations.

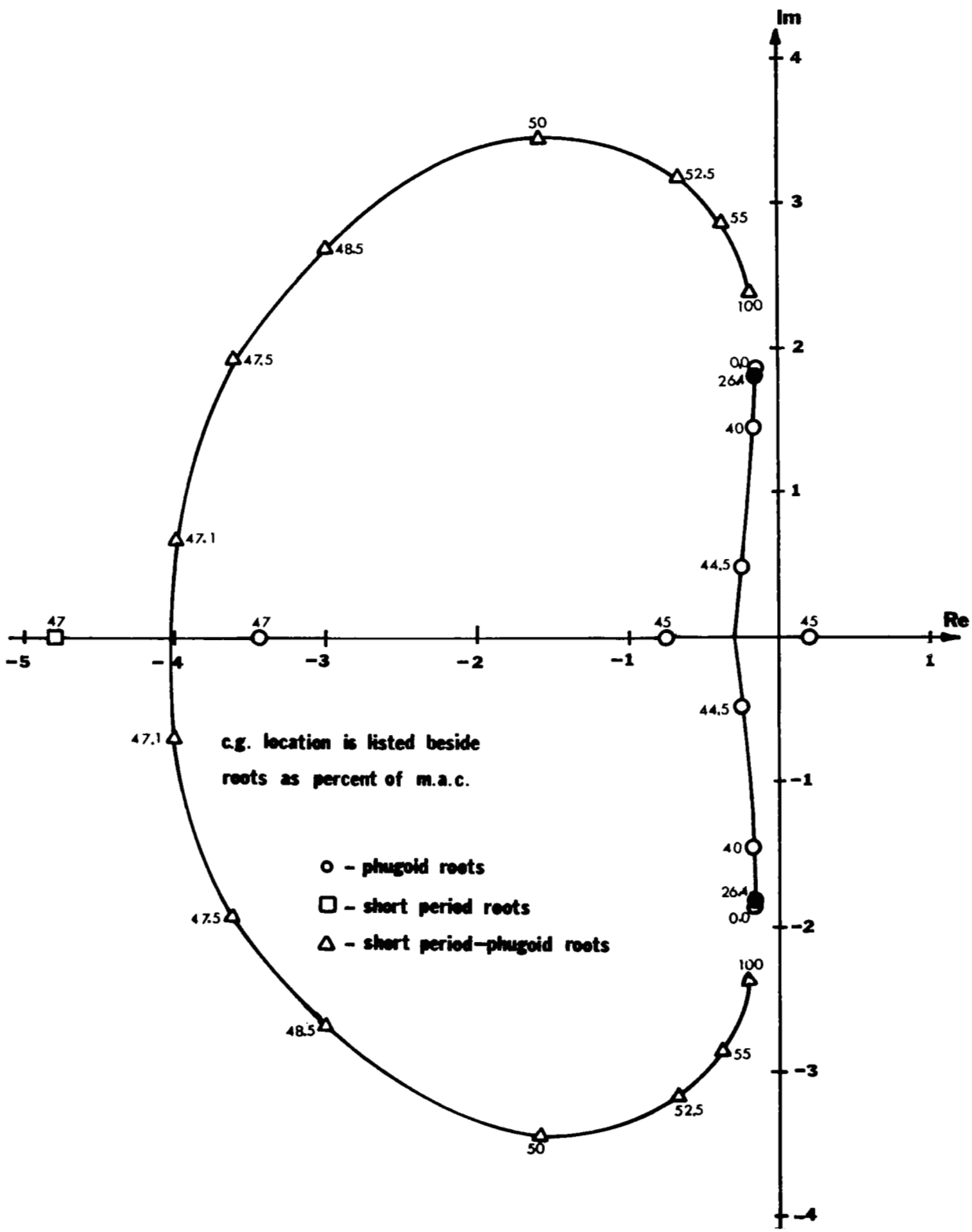
Short Period and Phugoid Roots for c.g. Variation
Im
Re
4
3
2
1
-1
-2
-3
-4
-5
-4
-3
-2
-1
1
50
52.5
55
100
48.5
47.5
47.1
47
47
45
45
0.0
26.4
40
44.5
44.5
40
26.4
0.0
47.1
47.5
48.5
50
52.5
55
100
c.g. location is listed beside
roots as percent of m.a.c.
o - phugoid roots
□ - short period roots
△ - short period-phugoid roots

Figure 96

c.g. LOCATION (% m.a.c.)	SHORT PERIOD ROOTS			SHORT PERIOD / PHUGOID		PHUGOID ROOTS		
	Real	Imaginary	Real	Real	Imaginary	Real	Imaginary	Real
0.0	- 4.6345	±7.5094				-0.0136	±0.1865	
26.4	- 4.0848	±4.3679				-0.0136	±0.1801	
42.5	- 5.3421		-2.1568			-0.0182	±0.1175	
45.0	- 6.1725		-1.1979			-0.0763		0.02000
47.0	- 6.6547		-0.4796			-0.3432		0.13957
47.1	- 6.6764			-0.40098	±0.06724			0.14501
47.5	- 6.7615			-0.36069	±0.19146			0.16725
48.5	- 6.9626			-0.26908	±0.30056			0.22966
50.0	- 7.2381			-0.15946	±0.34295			0.35661
52.5	- 7.6453			-0.06470	±0.31623			0.69487
55.0	- 8.0056			-0.03672	±0.28517			1.11858
100.0	-11.5233			-0.01703	±0.23765			7.36681

Table 44. Short Period and Phugoid Roots for c.g. Variations.

Short Period Mode Roots for the S_t Variation

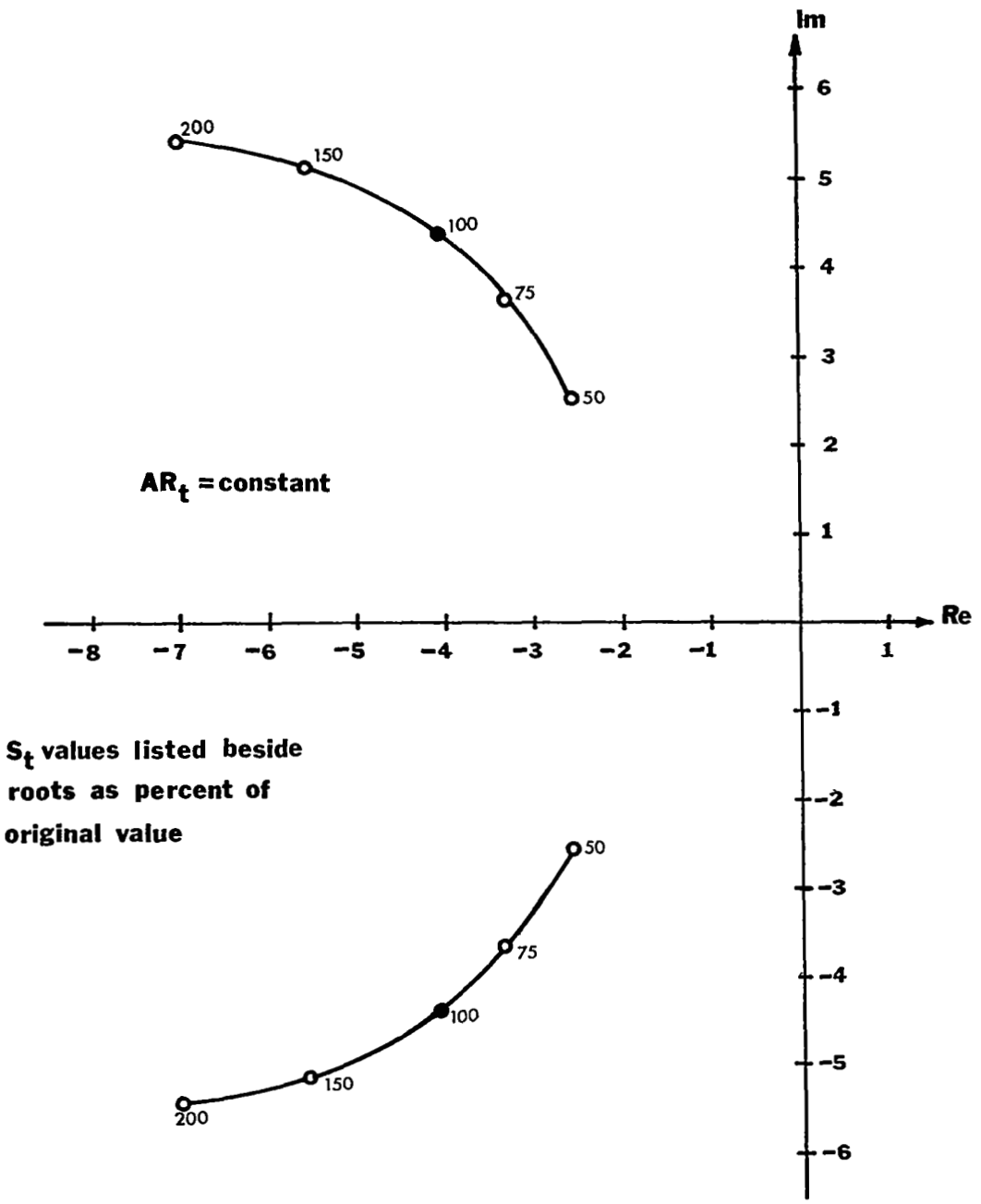

Figure 97a

Phugoid Mode Roots for the S_t Variation

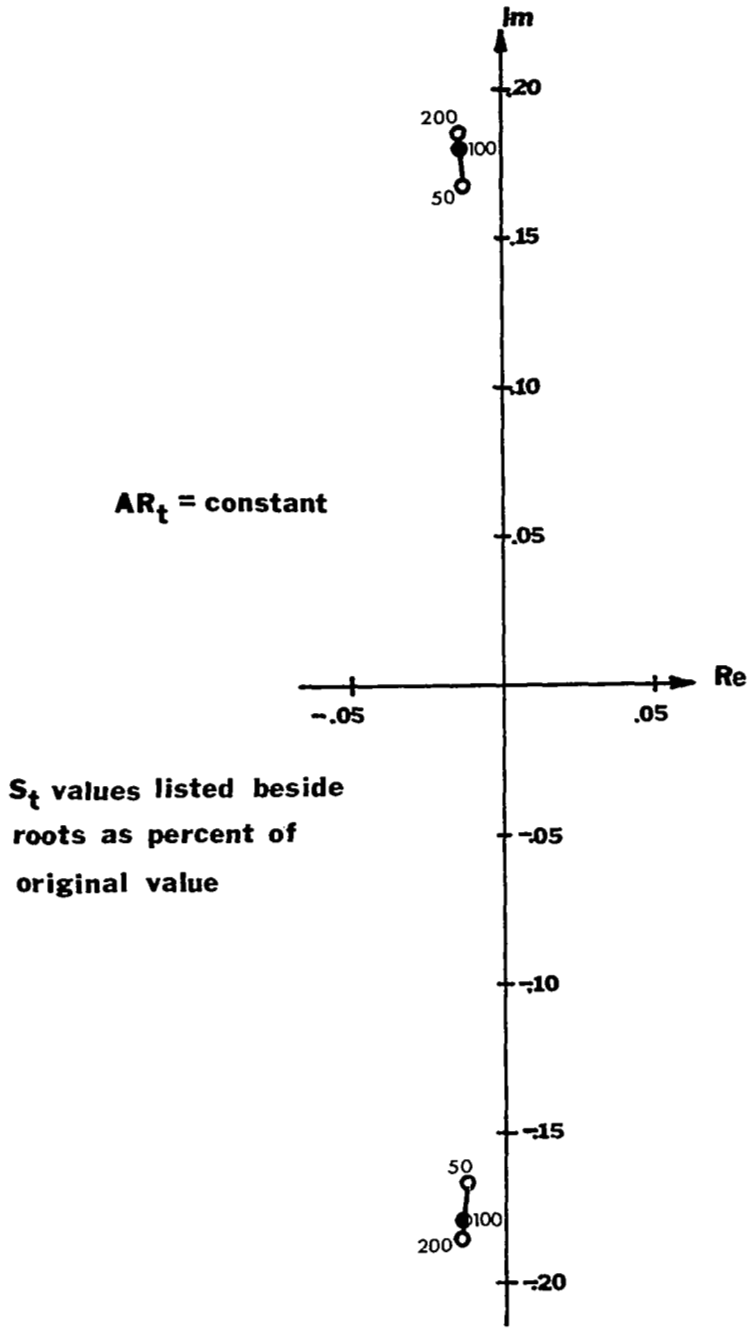

Figure 97b

Short Period Mode Roots for the l_t Variation

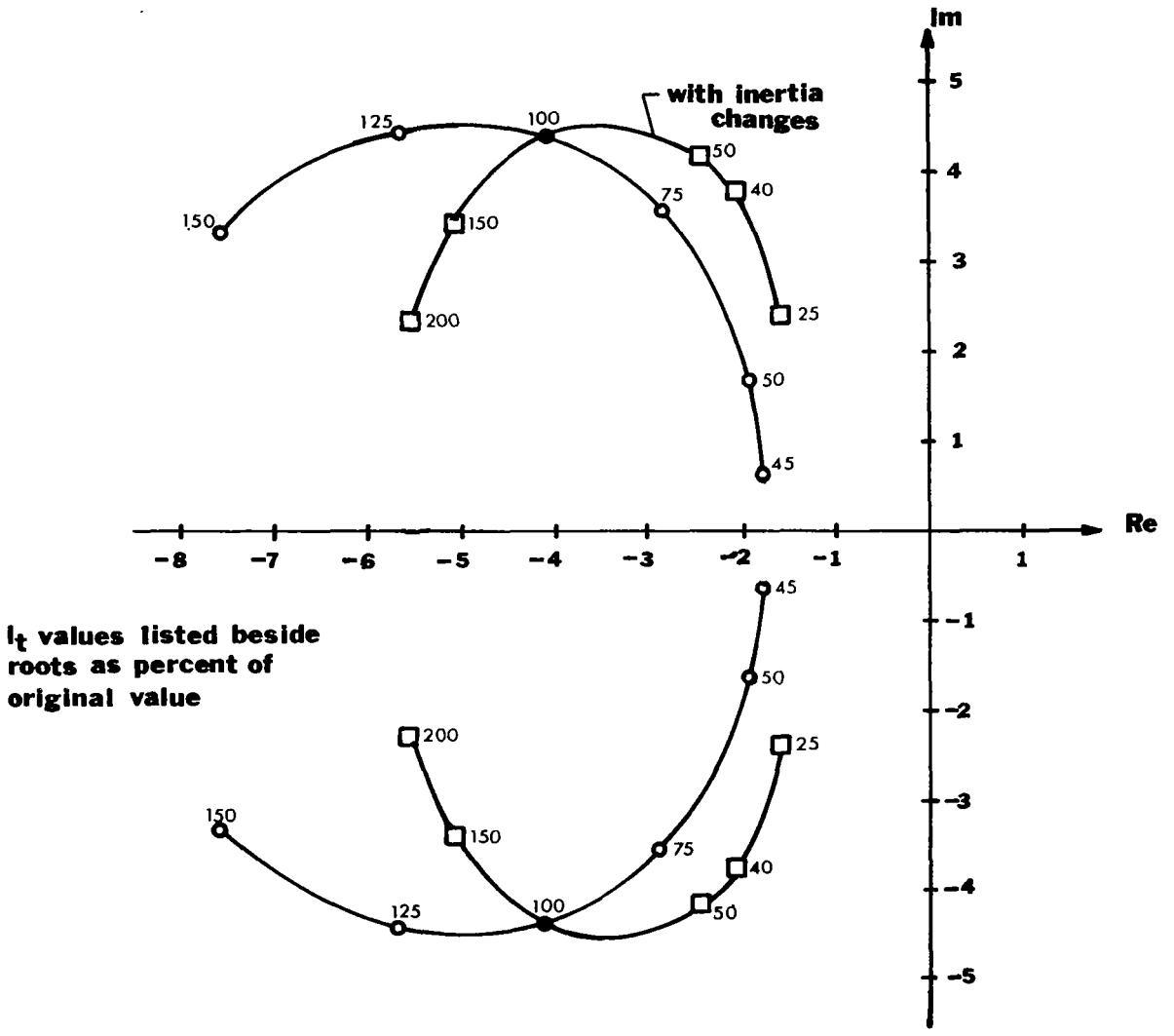

Figure 98a

Phugoid Mode Roots for the I_t Variation

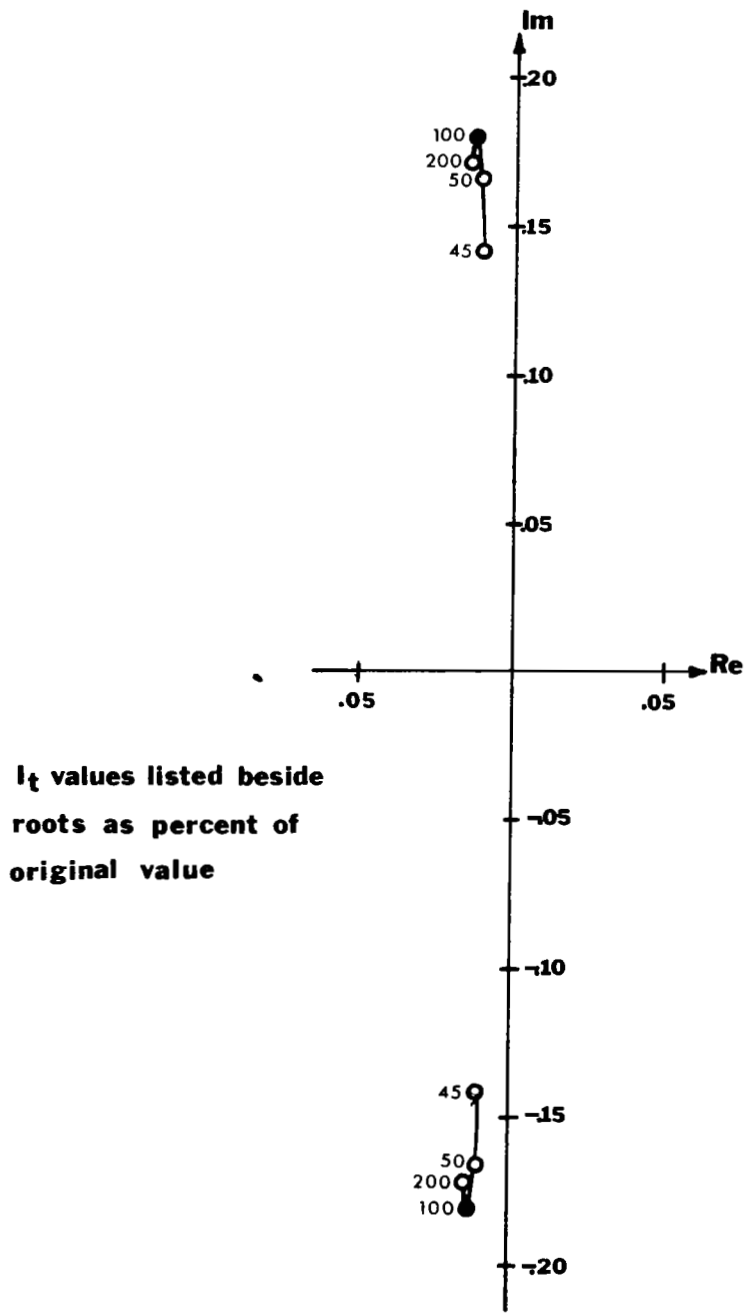

Figure 98b

Short Period Mode Roots for the η_t Variation

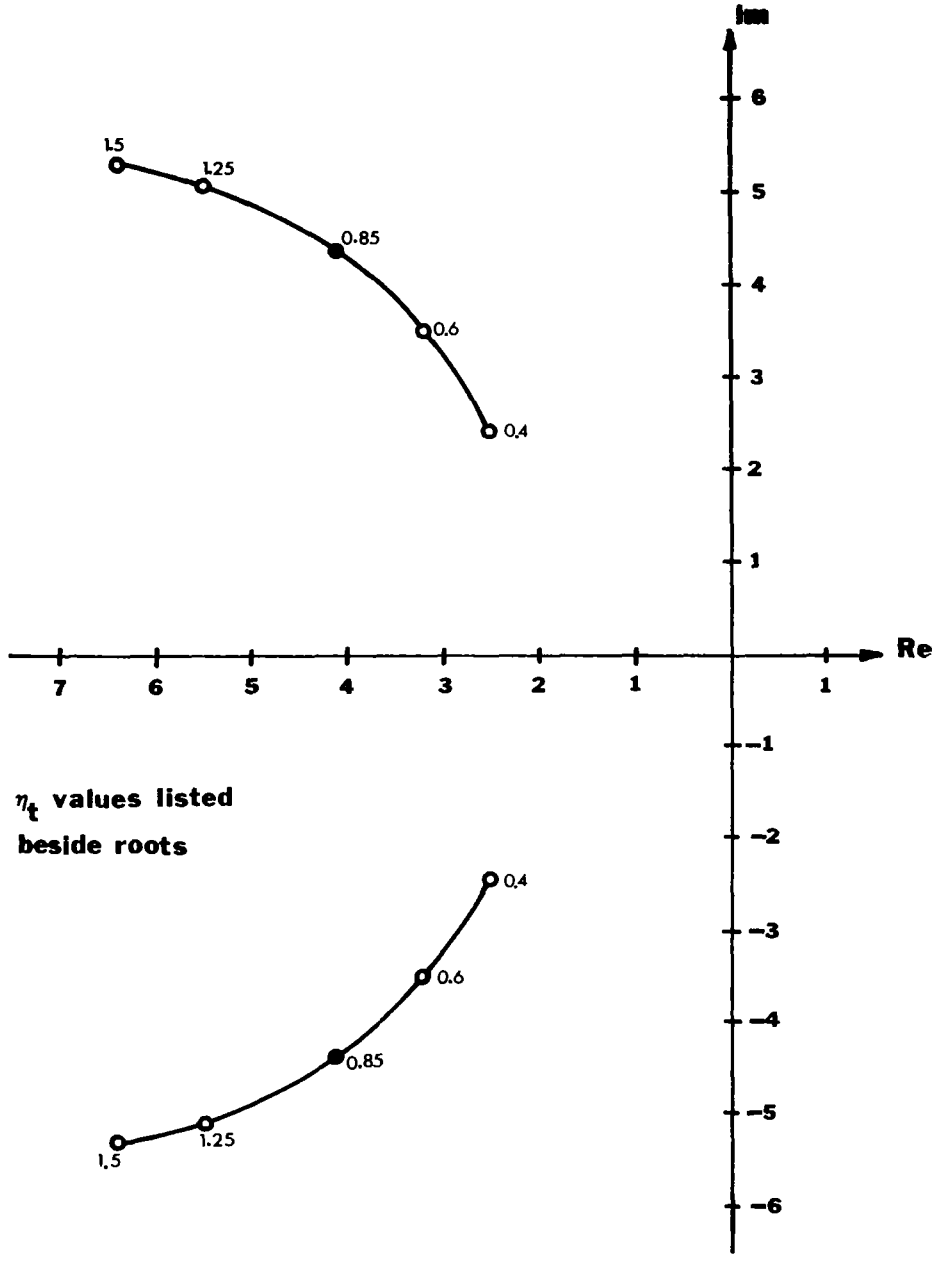

Figure 99a

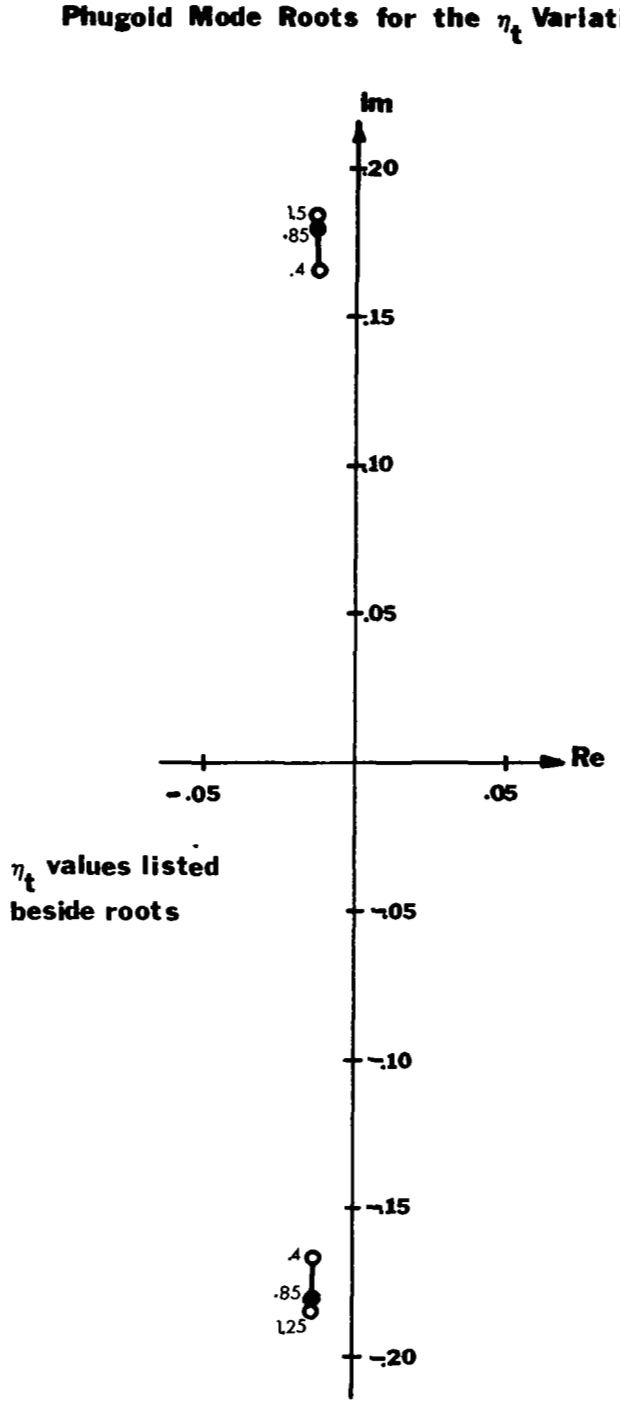
Phugoid Mode Roots for the η_t Variation
Im
.20
.15
.10
.05
Re
-.05
.05
-.05
-.10
-.15
-.20
1.5
.85
.4
.4
.85
1.25
η_t values listed
beside roots

Figure 99b

Dutch Roll Mode Roots for the C_{y_β} Variation

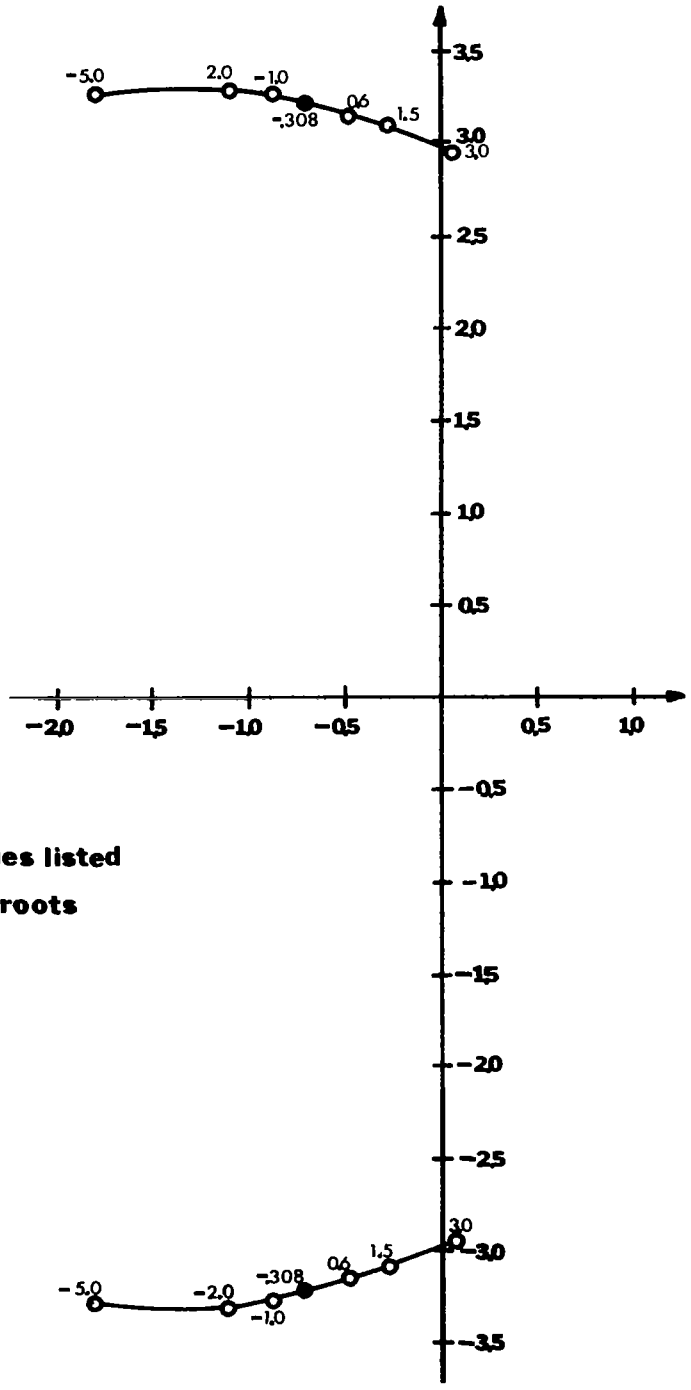

C_{y_β} **Values listed beside roots**

Figure 100a

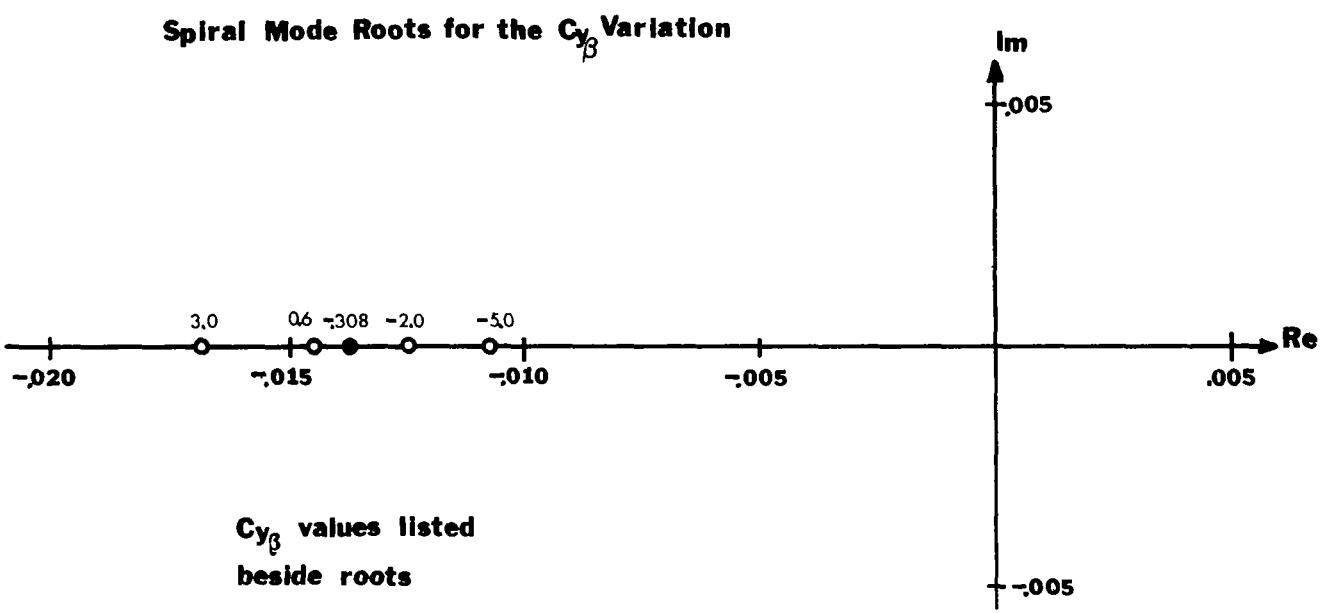

Figure 100b

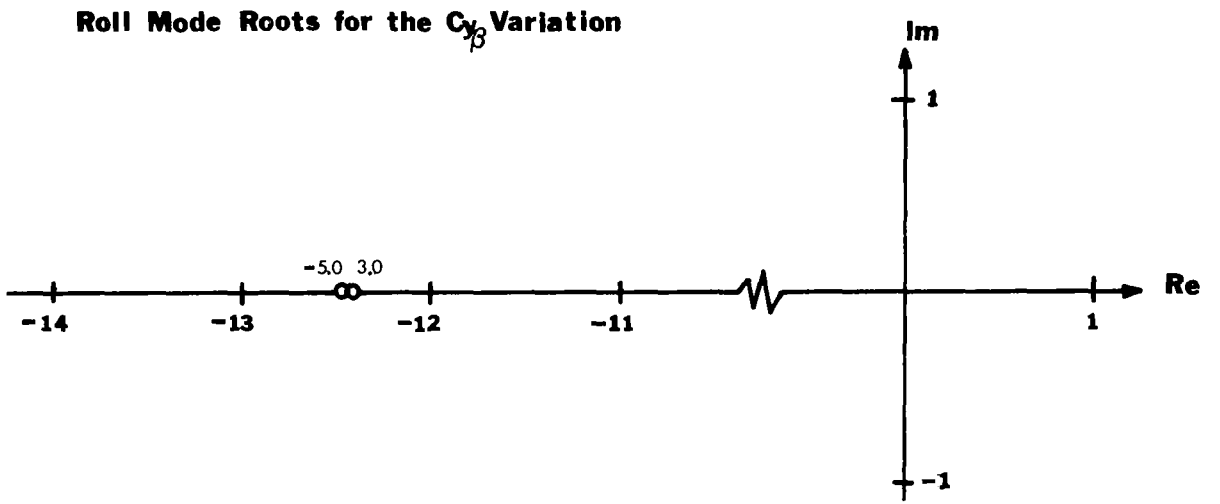

Figure 100c

NUMERATOR ROOTS

STABILITY DERIVATIVE	REAL	IMAGINARY	REAL	REAL
		β		
-5.0	.02272	0.0	-12.58832	-115.40198
-2.0	.02272	0.0	-12.58832	-115.40198
-1.0	.02272	0.0	-12.58832	-115.40198
- .308	.02272	0.0	-12.58832	-115.40198
.6	.02272	0.0	-12.58832	-115.40198
1.5	.02272	0.0	-12.58832	-115.40198
2.5	.02272	0.0	-12.58832	-115.40198
3.0	.02272	0.0	-12.58832	-115.40198
		ϕ		
-5.0	0.0	0.0	-6.81839	9.22719
-2.0	0.0	0.0	-5.86461	9.69719
-1.0	0.0	0.0	-5.55962	9.86678
- .308	0.0	0.0	-5.29036	9.86759
0.6	0.0	0.0	-5.08575	10.15225
1.5	0.0	0.0	-4.82705	10.32069
2.5	0.0	0.0	-4.54640	10.51463
3.0	0.0	0.0	-4.40880	10.61431
		ψ		
-5.0	-2.11867	0.0	- .13344	-12.65862
-2.0	- .41643	± .33074		-12.65543
-1.0	- .17978	± .50051		-12.65501
- .308	- .01387	± .52896		-12.65493
0.6	.19895	± .49324		-12.65086
1.5	.41204	± .33633		-12.64990
2.5	.27717	0.0	1.02041	-12.64890
3.0	.21422	0.0	1.32018	-12.04842

Table 45. Numerator roots for C_{Y_β} variations.

Dutch Roll Mode Roots for the C_{l_β} Variation

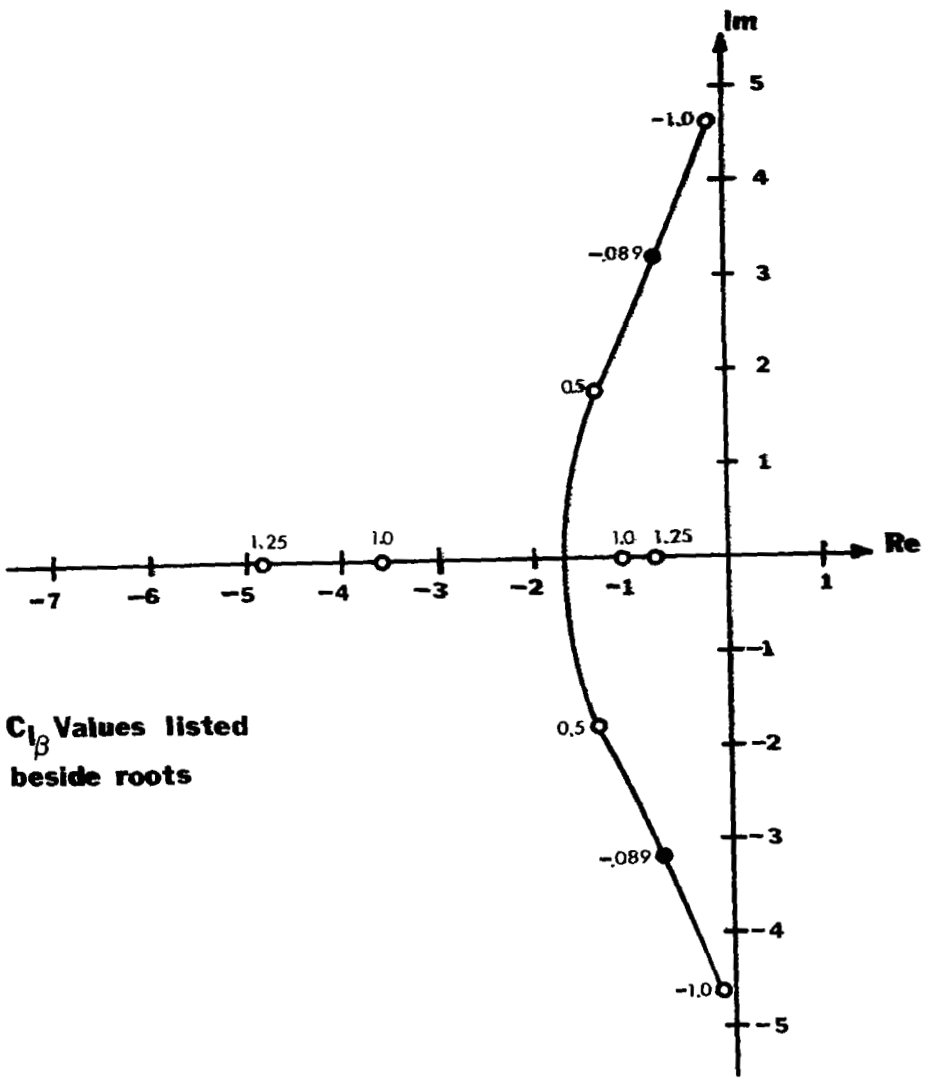

Figure 101a

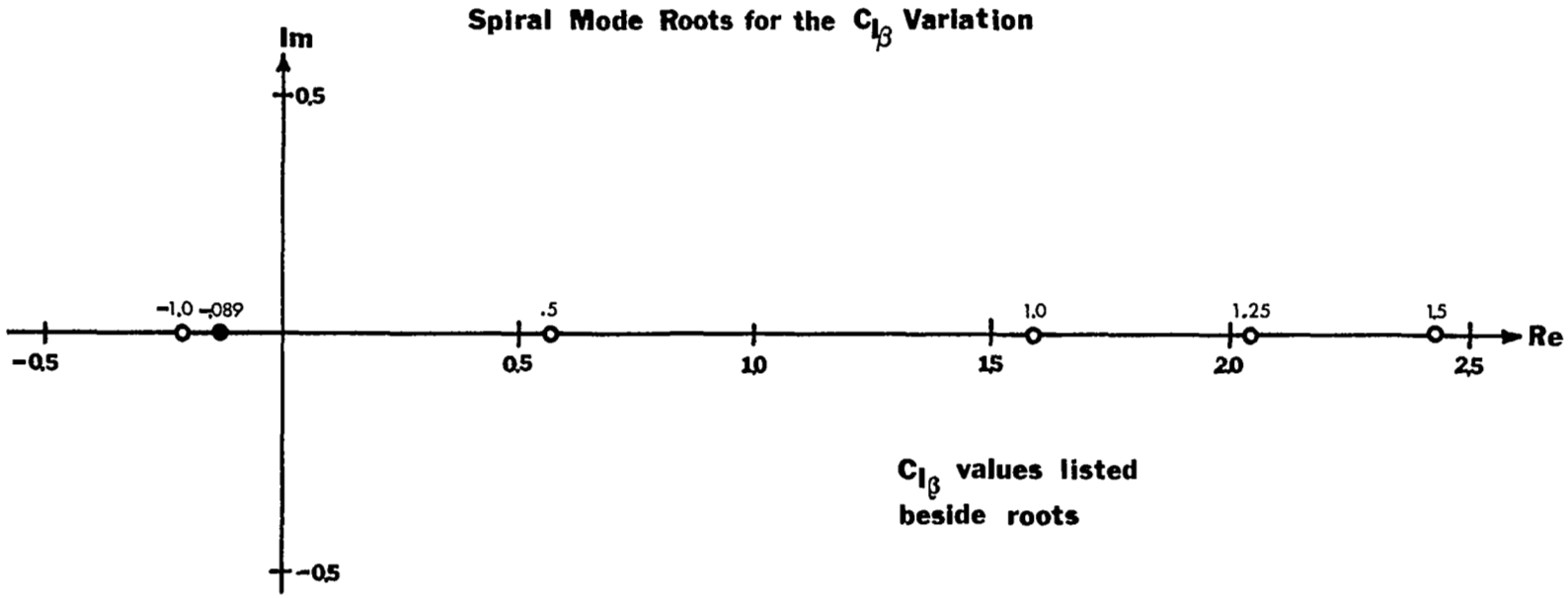

Figure 101b

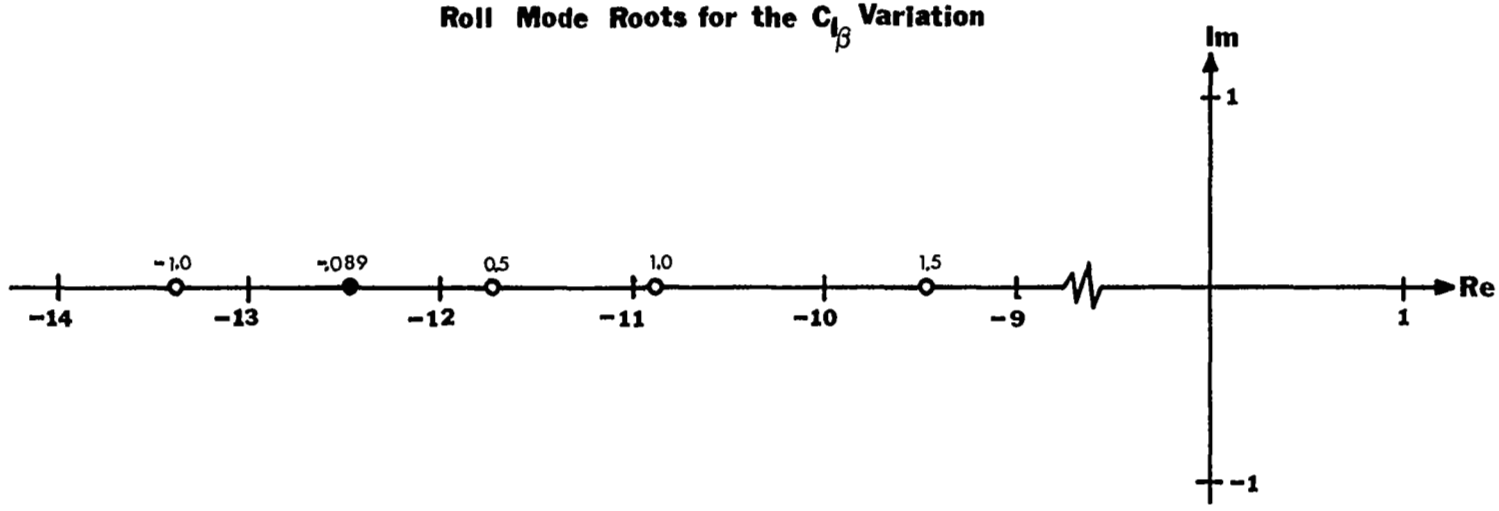

Figure 101c

NUMERATOR ROOTS

STABILITY DERIVATIVE	REAL	IMAGINARY	REAL	REAL
		β		
-1.0	.02272	0.0	-12.588	-115.42
- .089	.02272	0.0	-12.588	-115.42
.5	.02272	0.0	-12.588	-115.42
1.0	.02272	0.0	-12.588	-115.42
1.25	.02272	0.0	-12.588	-115.42
1.5	.02272	0.0	-12.588	-115.42
		ϕ		
-1.0	-21.8216	0.0	31.9475	0.0
- .089	- 5.2904	0.0	9.8676	0.0
.5	.54328	±19.03747		0.0
1.0	- .96334	±26.741		0.0
1.25	- 1.71665	±29.8279		0.0
1.5	- 2.4700	±32.6067		0.0
		ψ		
-1.0	.16499	±1.8909		-13.0132
- .089	- .01387	± .52896		-12.65493
.5	-1.5533	0.0	1.26811	-12.3981
1.0	-2.2648	0.0	1.74875	-12.16725
1.25	-2.57468	0.0	1.9370	-12.04559
1.5	-2.86861	0.0	2.10452	-11.91919

Table 46. Numerator roots for C_{ℓ_β} variations.

Dutch Roll Mode Roots for the C_{n_β} Variation

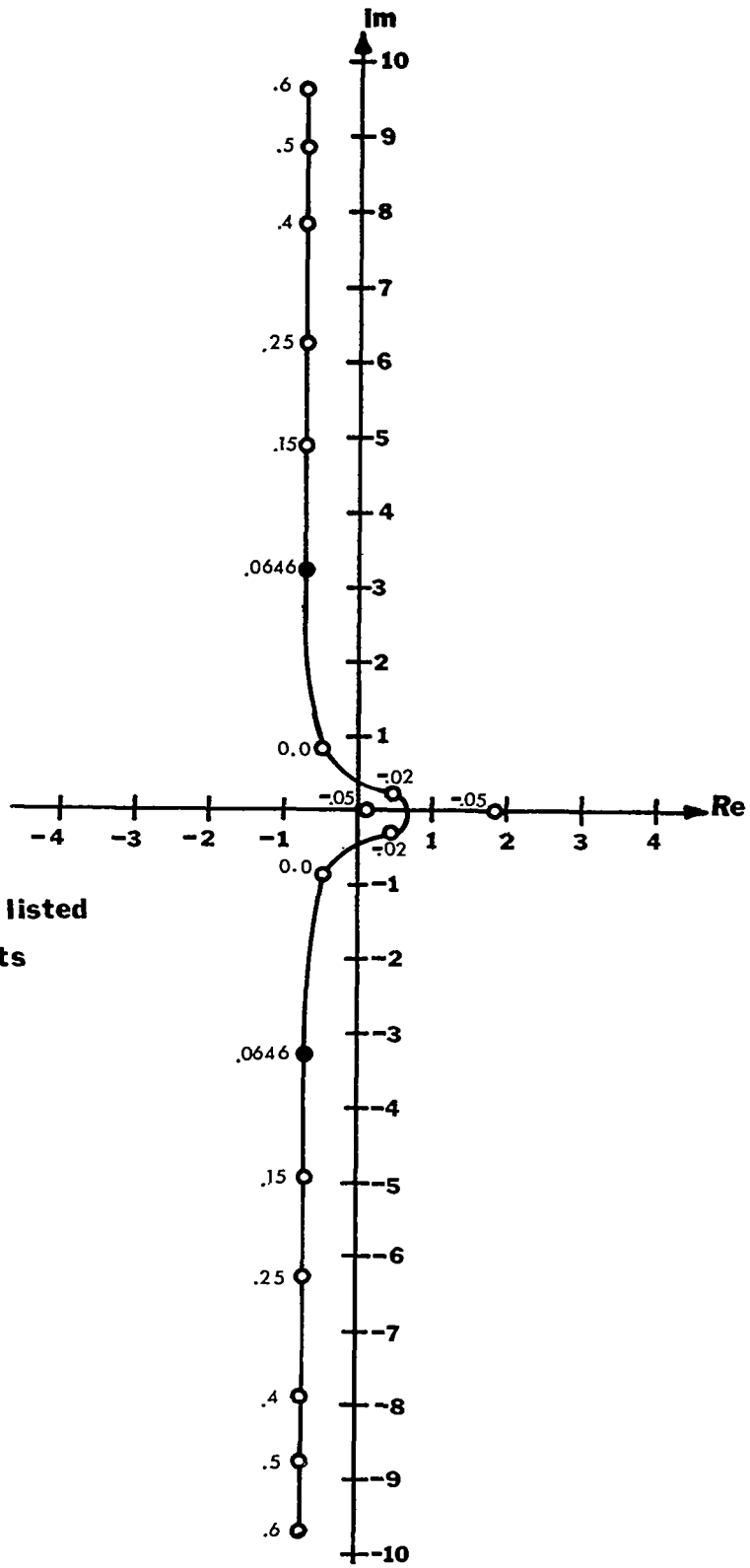

C_{n_β} Values listed beside roots

Figure 102a

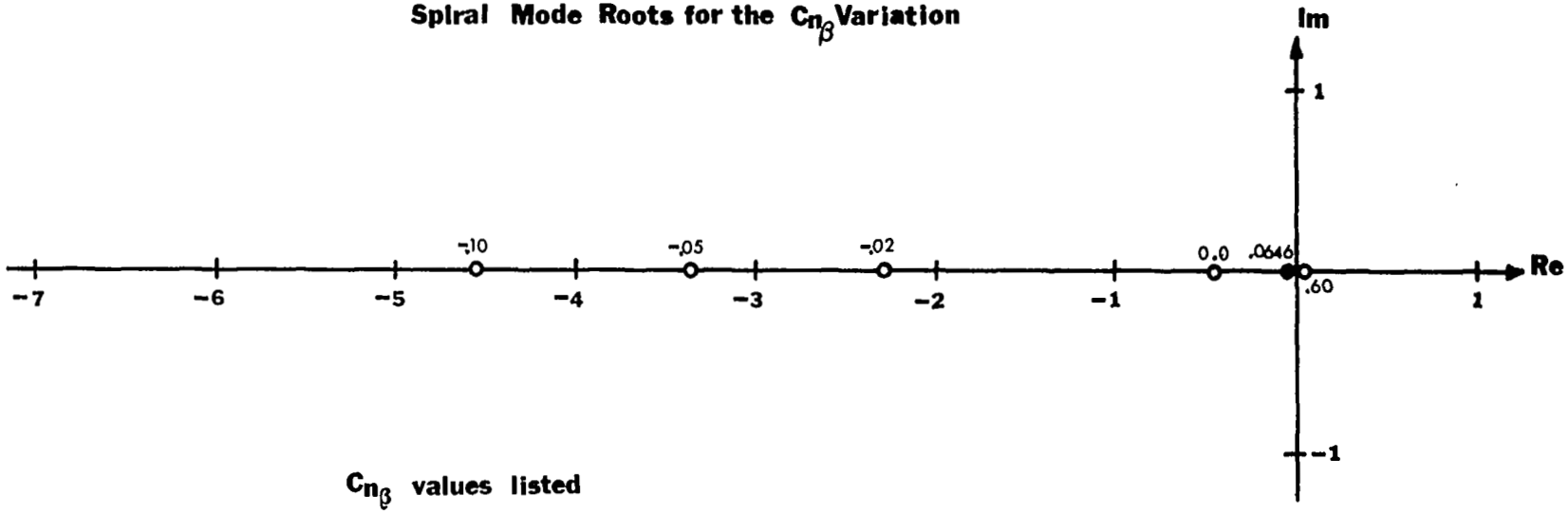

Figure 102b

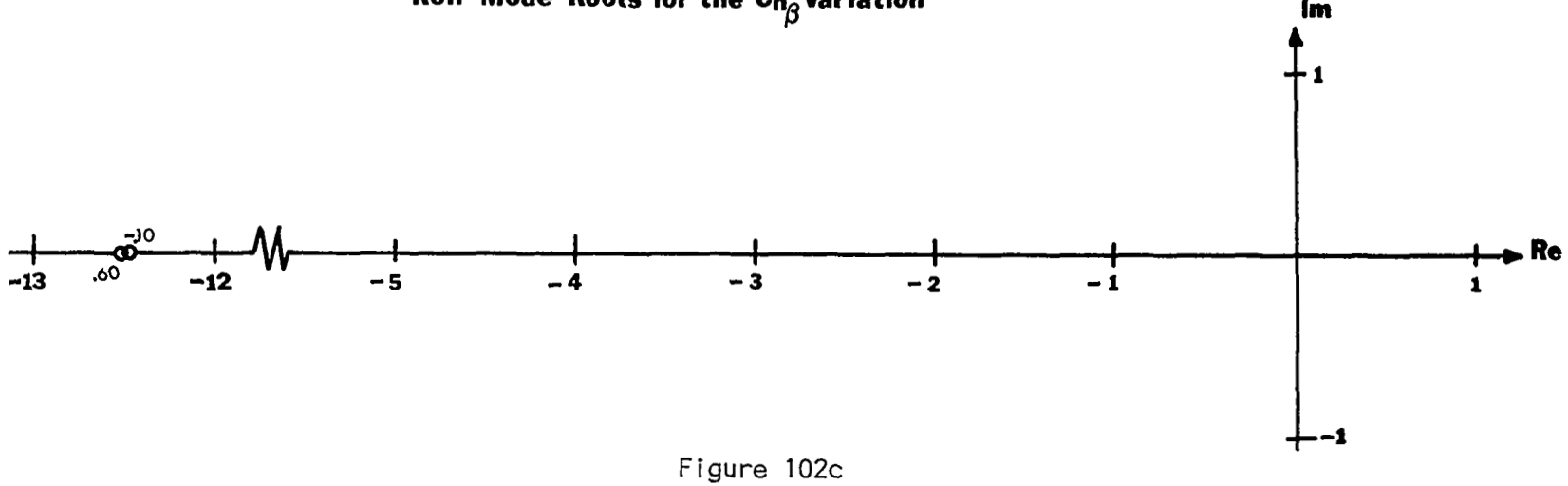

Figure 102c

NUMERATOR ROOTS

STABILITY DERIVATIVE	REAL	IMAGINARY	REAL	REAL
		β		
- .05	.02272	0.0	-12.588	-115.402
- .02	.02272	0.0	-12.588	-115.402
0.0	.02272	0.0	-12.588	-115.402
.06455	.02272	0.0	-12.588	-115.402
.15	.02272	0.0	-12.588	-115.402
.25	.02272	0.0	-12.588	-115.402
.4	.02272	0.0	-12.588	-115.402
.5	.02272	0.0	-12.588	-115.402
.6	.02272	0.0	-12.588	-115.402
		ϕ		
- .05	11.0918	0.0	-6.4556	0.0
- .02	10.81052	0.0	-6.17427	0.0
0.0	10.61768	0.0	-5.98144	0.0
.06455	9.86759	0.0	-5.29036	0.0
.15	8.9962	0.0	-4.3599	0.0
.25	7.6478	0.0	-3.0116	0.0
.4	4.3478	0.0	.28833	0.0
.5	2.31811	±3.47434		0.0
.6	2.31811	±5.31620		0.0
				0.0
		ψ		
- .05	-.08494	± .60700		-12.66270
- .02	-.06641	± .5886		-12.6598
0.0	-.05405	± .5756		-12.65785
0.06455	-.01387	± .52896		-12.6549
0.15	.03877	± .45654		-12.64358
0.25	.10076	± .34167		-12.63429
0.4	.00538	0.0	.38233	-12.62066
0.5	-.12719	0.0	.63929	-12.61177
0.6	-.19755	0.0	.83419	-12.60305

Table 47. Numerator roots for C_{n_β} variations.

Dutch Roll Mode Roots for the Cy_p Variation

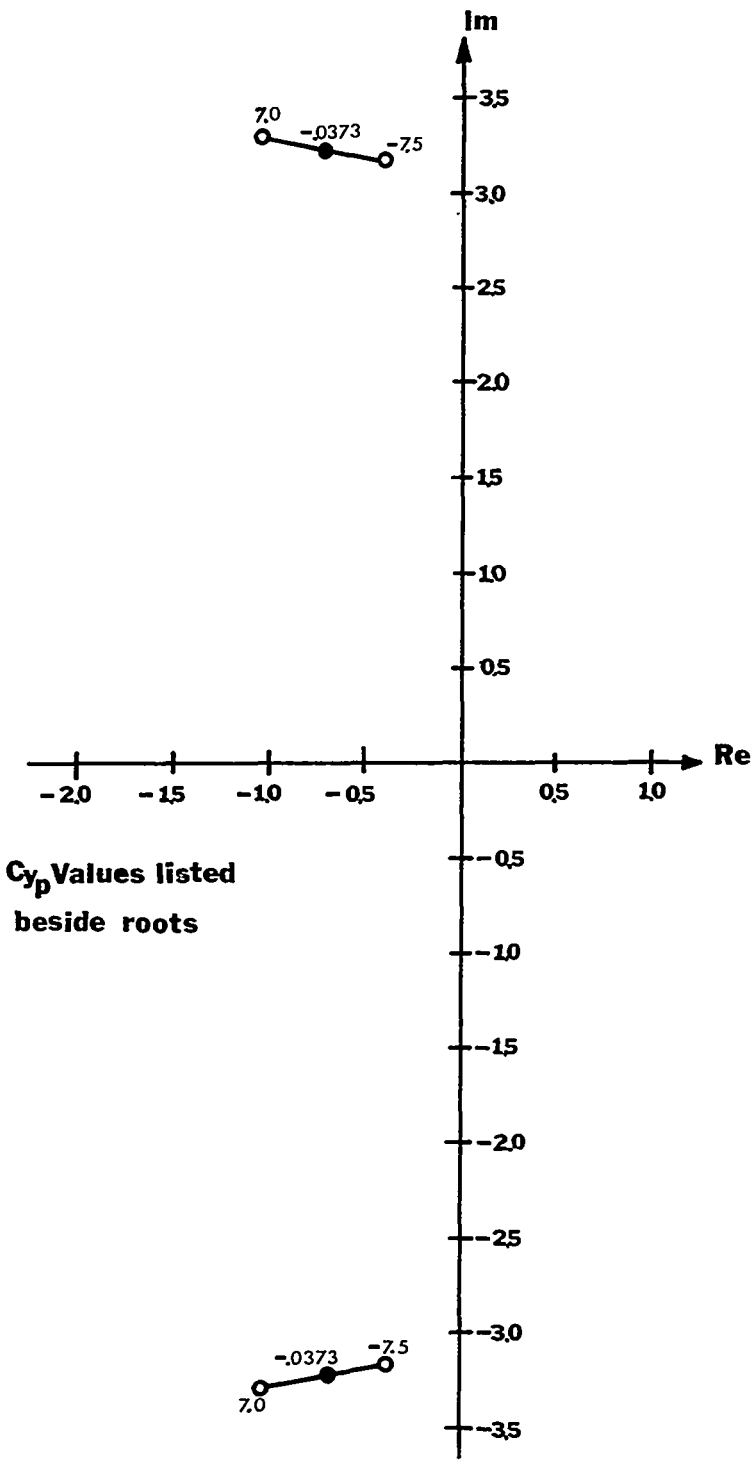

Figure 103a

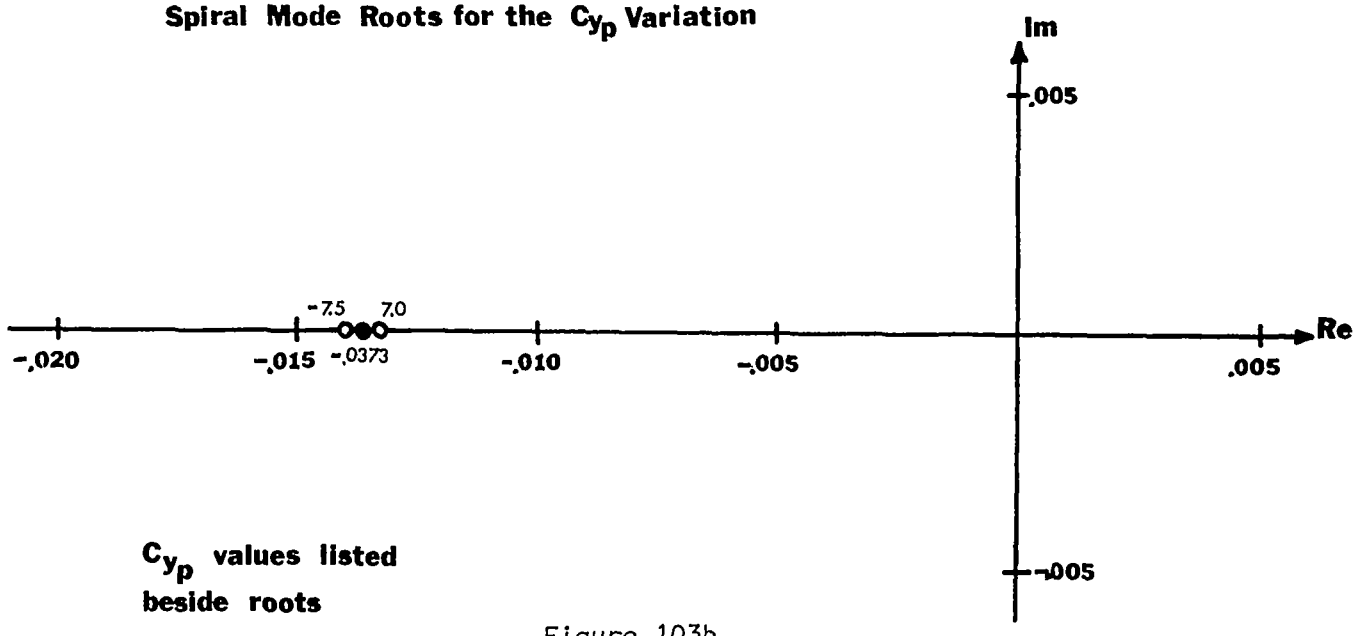

Figure 103b

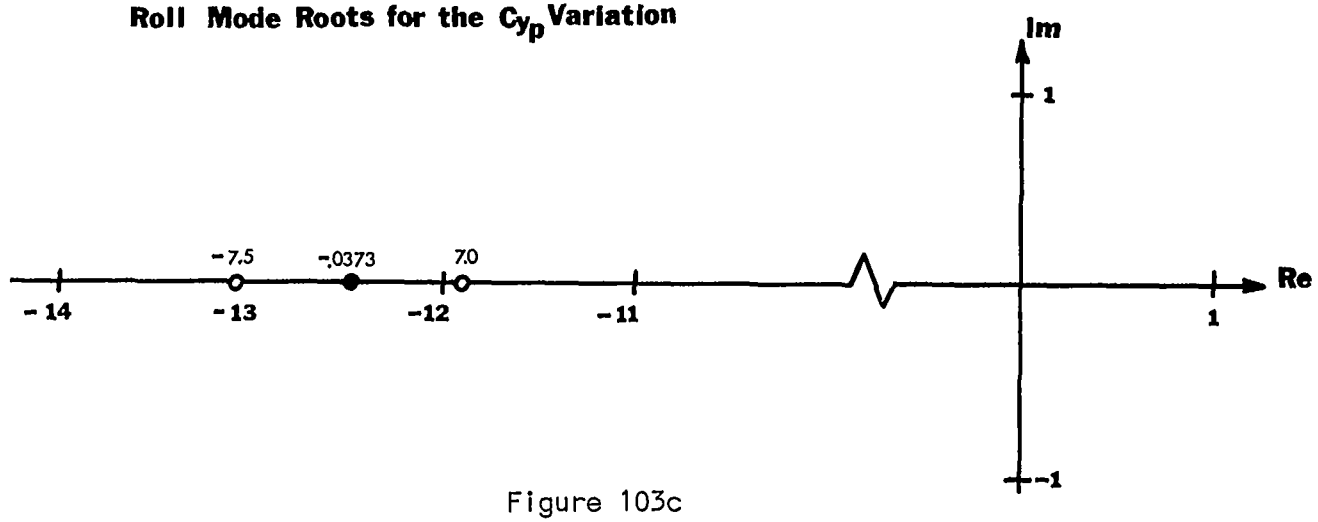

Figure 103c

STABILITY DERIVATIVE	REAL	IMAGINARY	REAL	REAL
		NUMERATOR ROOTS		
		β		
-7.5	0.02177	0.0	-15.624	- 98.470
- .0373	0.02272	0.0	-12.588	-115.402
7.0	0.02373	0.0	-10.552	-133.746
		ϕ		
-7.5	0.0	0.0	-5.2904	9.8676
- .0373	0.0	0.0	-5.2904	9.8676
7.0	0.0	0.0	-5.2904	9.8676
		ψ		
-7.5	0.25191	±0.45598		-13.187
- .0373	-0.01387	±0.52896		-12.655
7.0	-0.29057	±0.45964		-12.102

Table 48. Numerator roots for C_{y_p} variations.

Dutch Roll Mode Roots for the C_{l_p} Variation

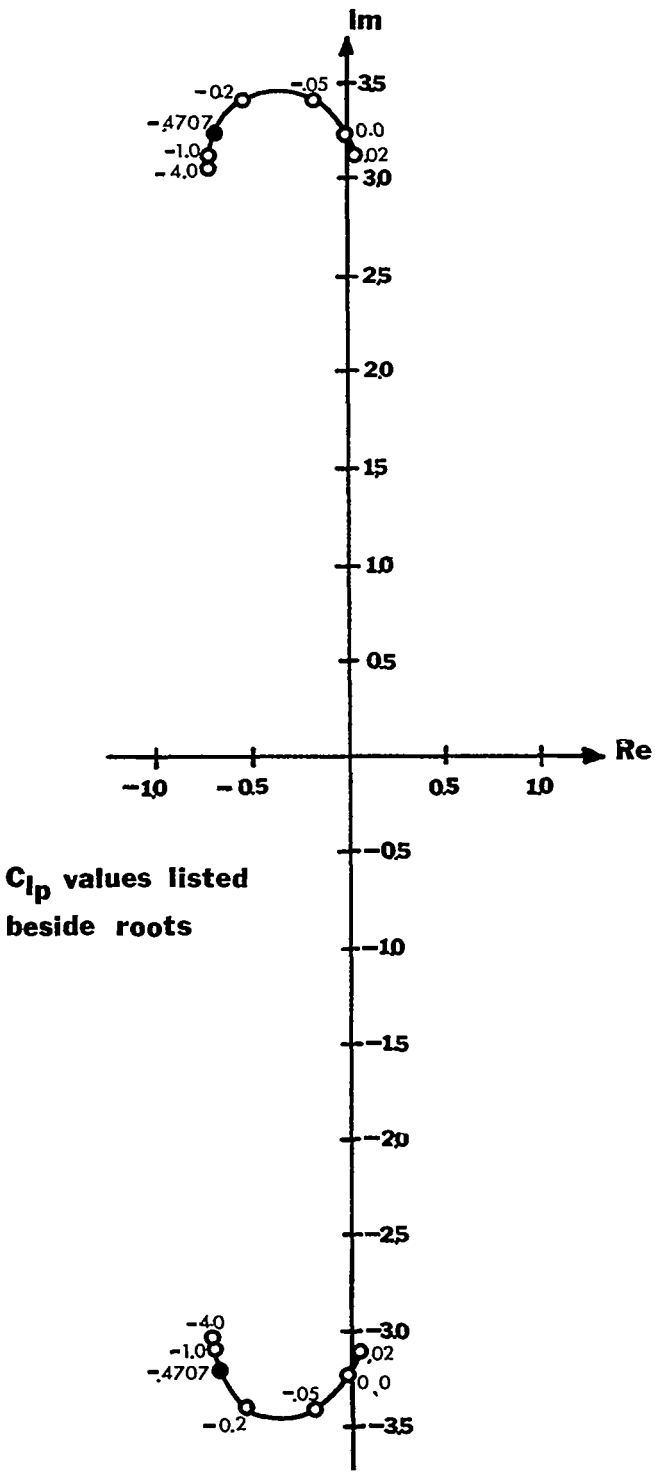

Figure 104a

Spiral Mode Roots for the C_{lp} Variation

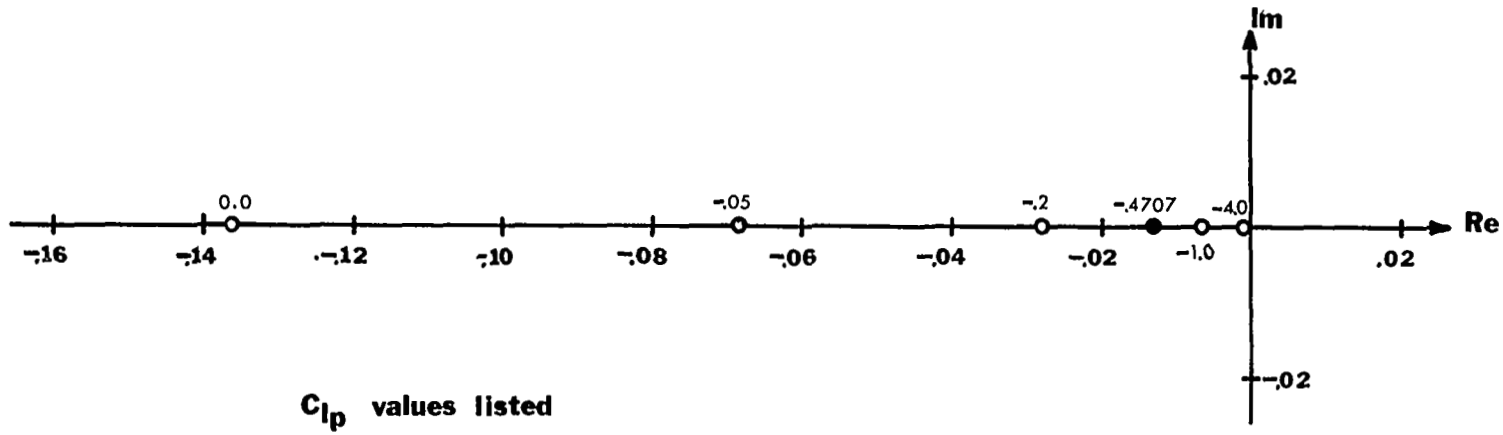

C_{lp} values listed beside roots

Figure 104b

Roll Mode Roots for the C_{lp} Variation

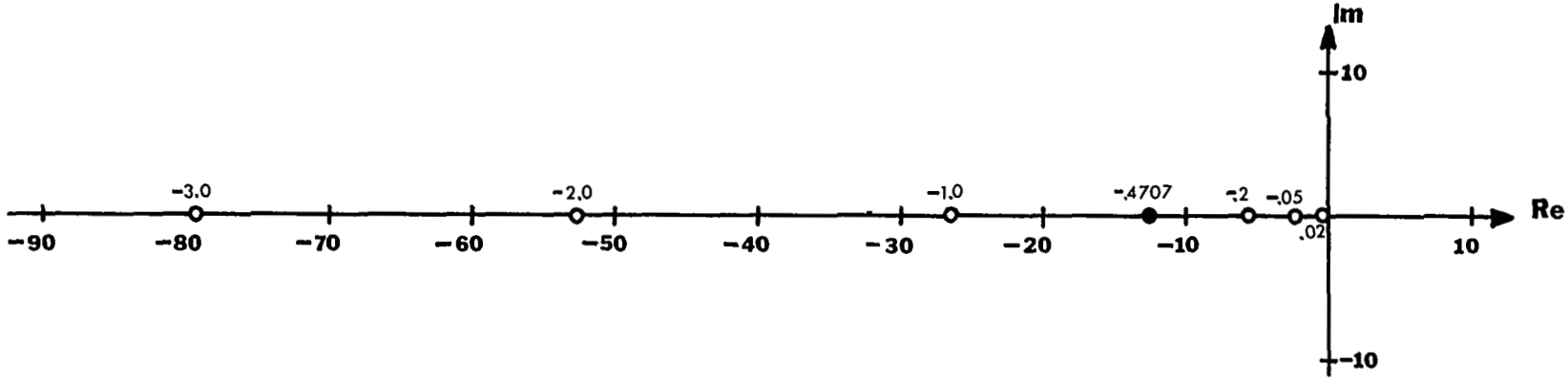

Figure 104c

NUMERATOR ROOTS

STABILITY DERIVATIVE	REAL	IMAGINARY	REAL	REAL
		β		
-4.0	.00270	0.0	-107.822	-115.135
-3.0	.00360	0.0	- 79.796	-116.713
-2.0	.00539	0.0	- 53.132	-116.934
-1.0	.01076	0.0	- 26.599	-117.025
- .4708	.02272	0.0	- 12.588	-117.032
- .2	.05256	0.0	- 5.4426	-117.066
- .05	.17927	0.0	- 1.5962	-117.0724
0.0	.49080	0.0	- .58346	-117.0743
.02	1.15326	0.0	- .35271	-117.0769
		φ		
-4.0	-5.29036	0.0	9.8676	0.0
-3.0	-5.29036	0.0	9.8676	0.0
-2.0	-5.29036	0.0	9.8676	0.0
-1.0	-5.29036	0.0	9.8676	0.0
- .4708	-5.29036	0.0	9.8676	0.0
- .2	-5.29036	0.0	9.8676	0.0
- .05	-5.29036	0.0	9.8676	0.0
0.0	-5.29036	0.0	9.8676	0.0
.02	-5.29036	0.0	9.8676	0.0
		ψ		
-4.0	- .03070	± .18119		-105.960
-3.0	- .03039	± .20996		- 79.514
-2.0	- .02969	± .25798		- 53.068
-1.0	- .02673	± .36562		- 26.628
- .4708	- .01387	± .52896		- 12.6549
- .2	.03660	± .79875		- 5.59728
- .05	.35341	±1.20658		- 2.26388
0.0	.70033	±1.30297		- 1.63539
.02	1.00127	±1.17834		- 1.45731

Table 49. Numerator roots for $C\ell_p$ variations.

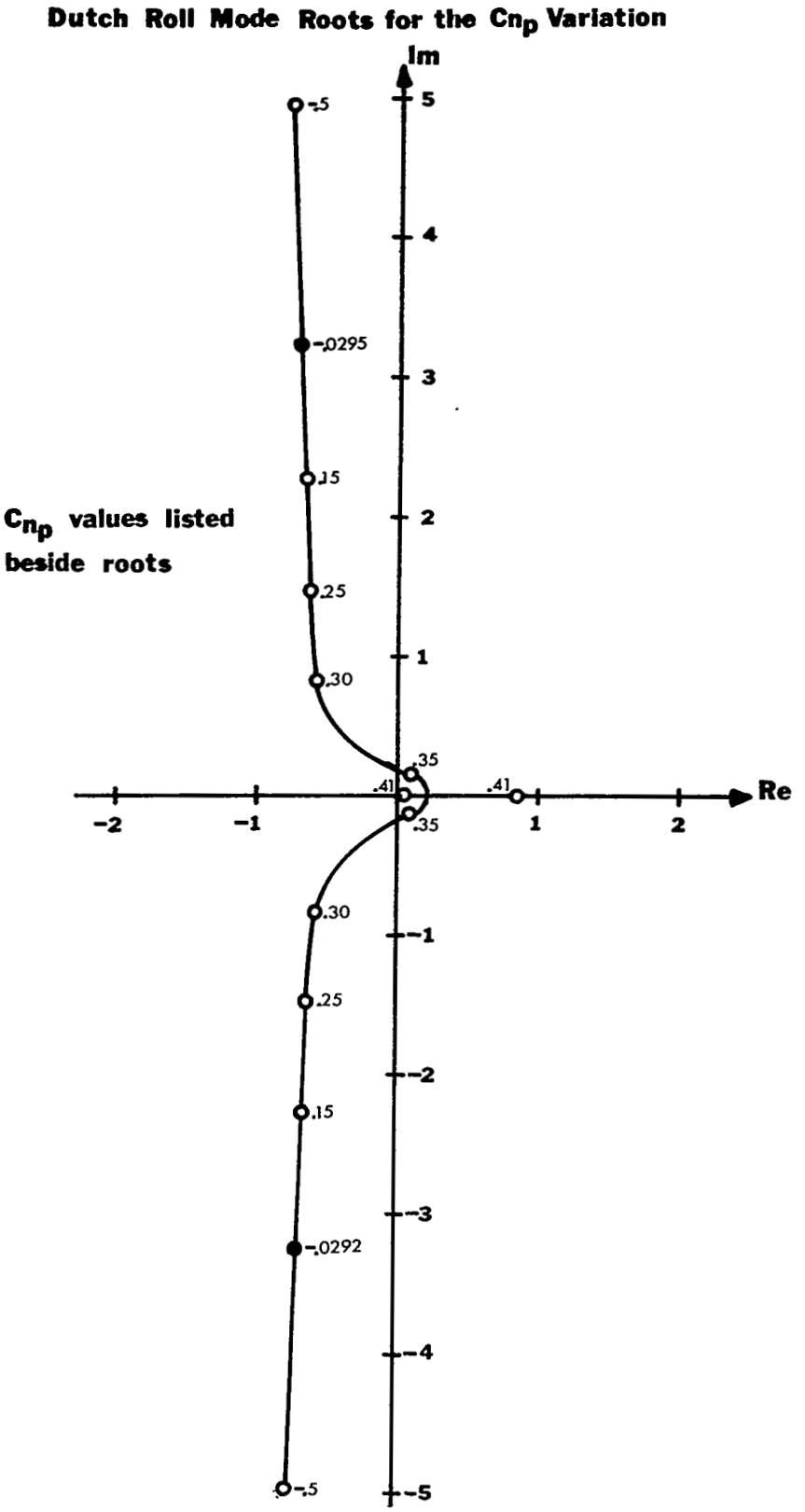
Dutch Roll Mode Roots for the Cn_p Variation
Im
Re
Cn_p values listed beside roots
-.5
-.0295
.15
.25
.30
.35
.41
.41
.35
.30
.25
.15
-.0292
-.5
5
4
3
2
1
-1
-2
-3
-4
-5
-2
-1
1
2

Figure 105a

Spiral Mode Roots for the C_{n_p} Variation

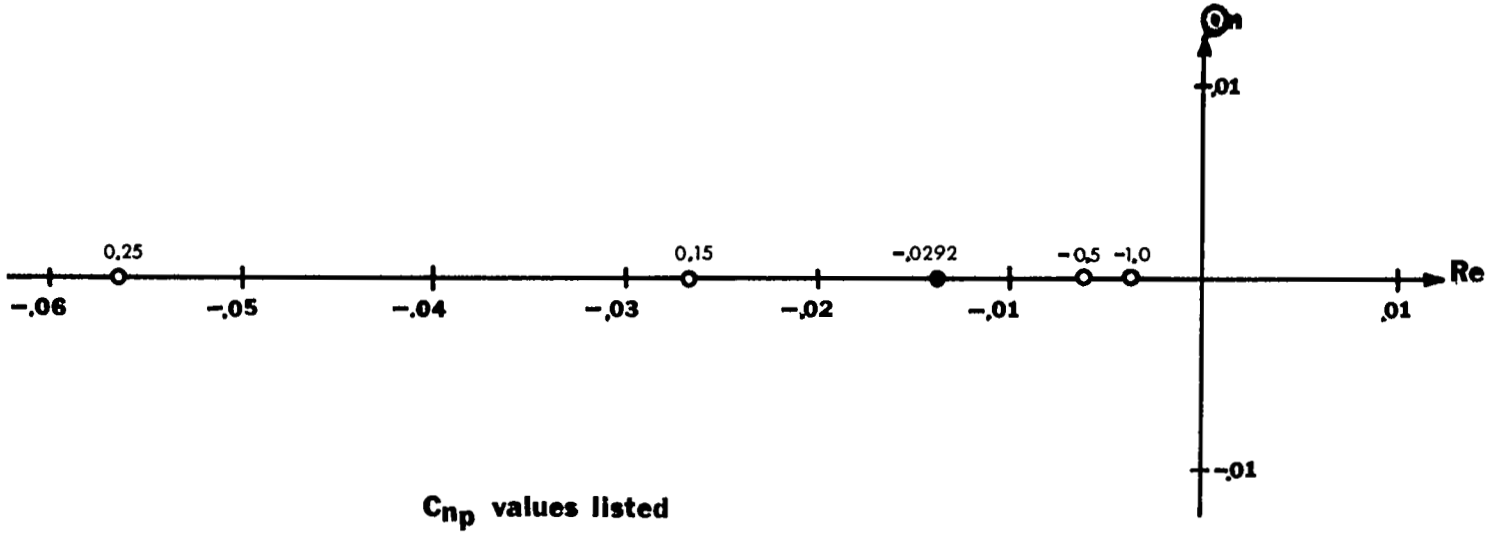

C_{n_p} values listed beside roots

Figure 105b

Roll Mode Roots for the C_{n_p} Variation

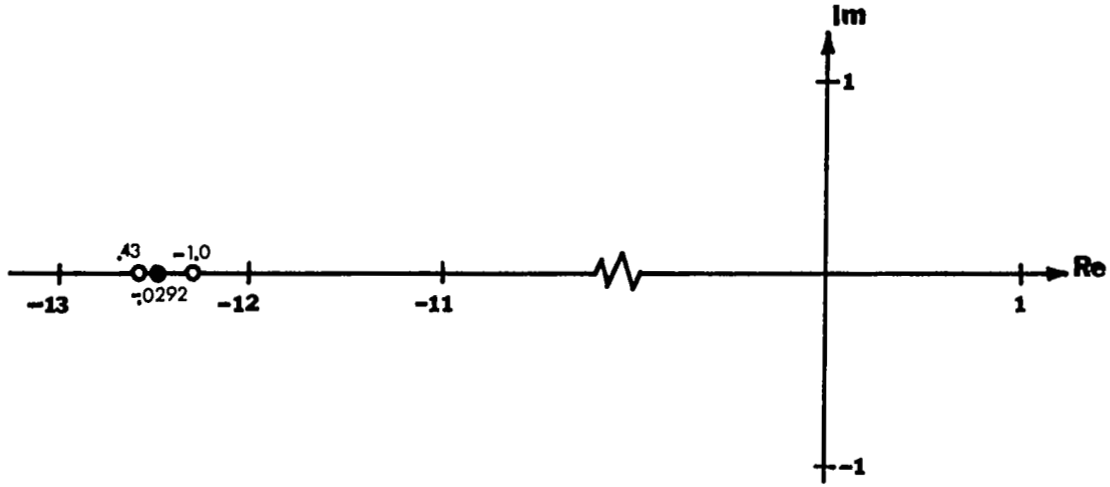

Figure 105c

NUMERATOR ROOTS

STABILITY DERIVATIVE	REAL	IMAGINARY	REAL	REAL
		β		
-1.0	.01584	0.0	-19.1345	-110.497
- .5	.01877	0.0	-15.6501	-113.984
- .02923	.02272	0.0	-12.58832	-115.402
.15	.02472	0.0	-11.46221	-118.178
.25	.02599	0.0	-10.84717	-118.794
.30	.02667	0.0	-10.54233	-119.099
.41	.02831	0.0	- 9.87778	-119.766
		ϕ		
-1.0	9.86759	0.0	-5.29036	0.0
- .5	9.86759	0.0	-5.29036	0.0
- .02923	9.86759	0.0	-5.29036	0.0
.15	9.86759	0.0	-5.29036	0.0
.25	9.86759	0.0	-5.29036	0.0
.30	9.86759	0.0	-5.29036	0.0
.41	9.86759	0.0	-5.29036	0.0
		ψ		
-1.0	.04698	±.43785		-18.45365
- .5	.02029	±.48044		-15.47606
- .02923	-.01387	±.52896		-12.655
.15	-.03371	±.55521		-11.56659
.25	-.04523	±.56965		-10.95871
.30	-.05145	±.57728		-10.65385
.41	-.06638	±.59510		- 9.98065

Table 50. Numerator roots for C_{n_p} variations.

Dutch Roll Mode Roots for the C_{y_r} Variation

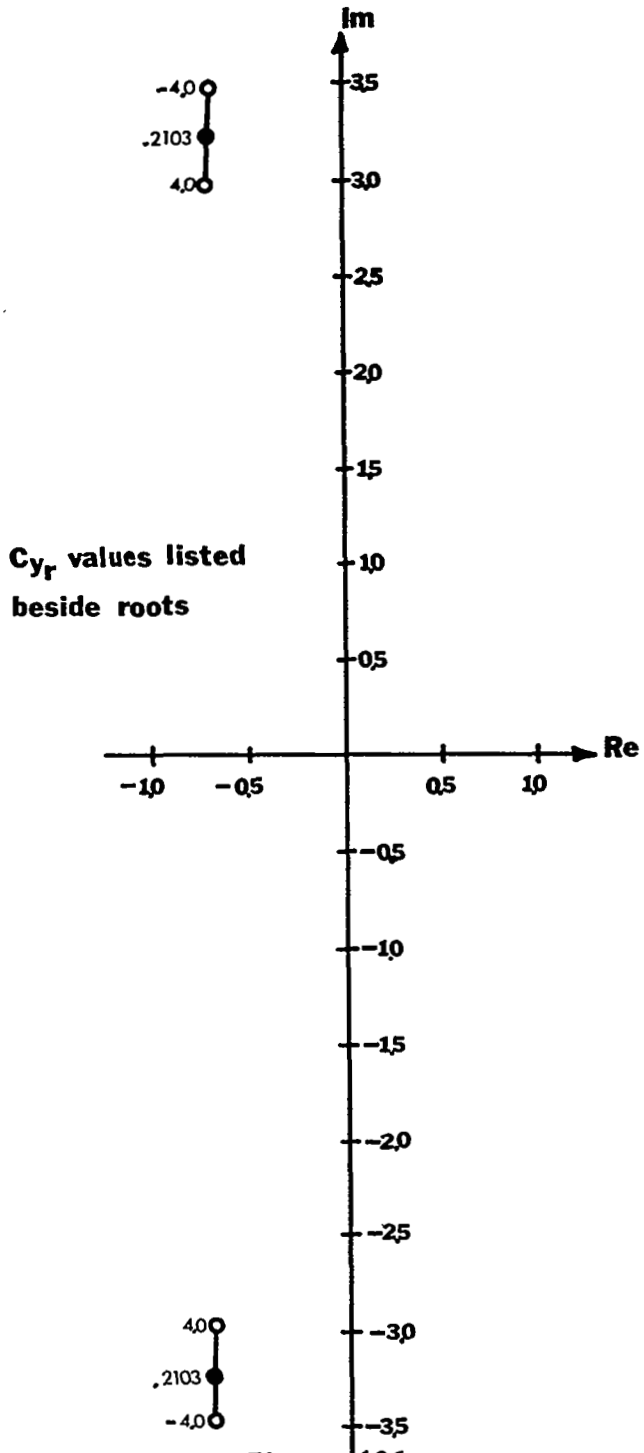

Figure 106a

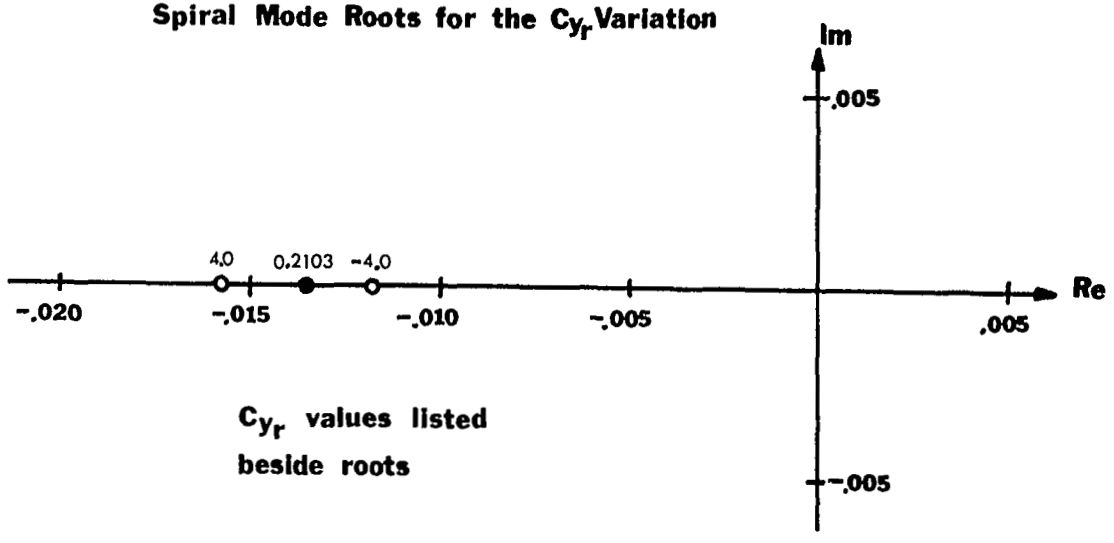

Figure 106b

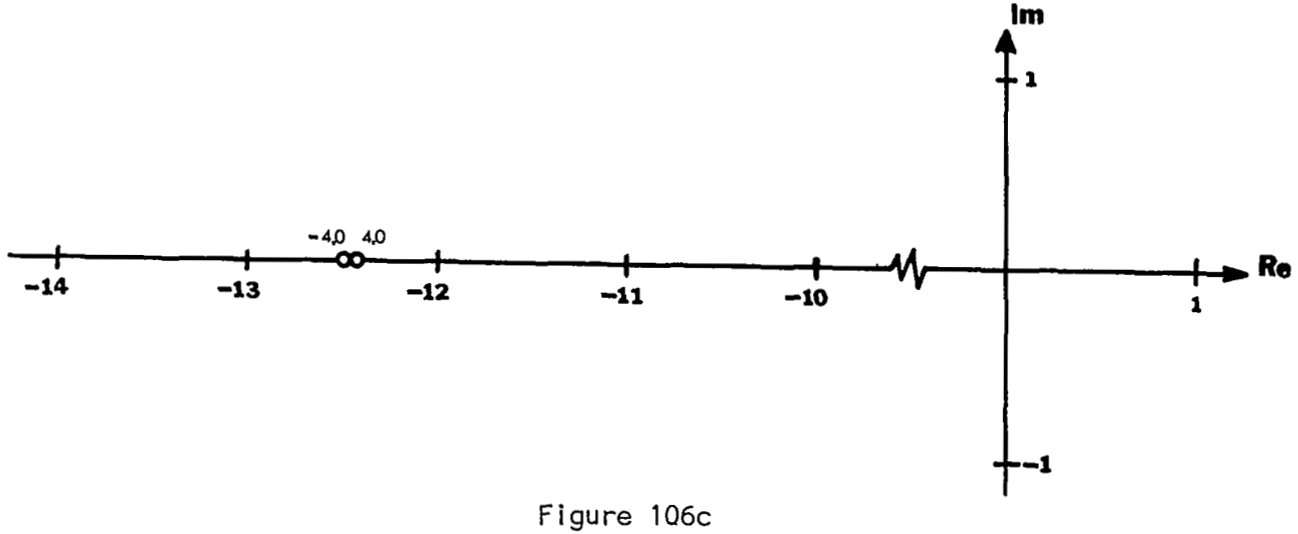

Figure 106c

	NUMERATOR ROOTS			
	β			
STABILITY DERIVATIVE	REAL	IMAGINARY	REAL	REAL
-4.0	.01953	0.0	-12.589	-136.167
.2103	.02272	0.0	-12.588	-115.402
4.0	.02666	0.0	-12.5767	- 99.875
	ϕ			
-4.0	0.0	0.0	-5.8982	10.5344
.2103	0.0	0.0	-5.2904	9.8676
4.0	0.0	0.0	-4.8256	9.4618
	ψ			
-4.0	-.01387	±.52896		-12.655
.2103	-.01387	±.52896		-12.655
4.0	-.01387	±.52896		-12.655

Table 51. Numerator roots for C_{y_r} variations.

Dutch Roll Roots for the C_{l_r} Variation

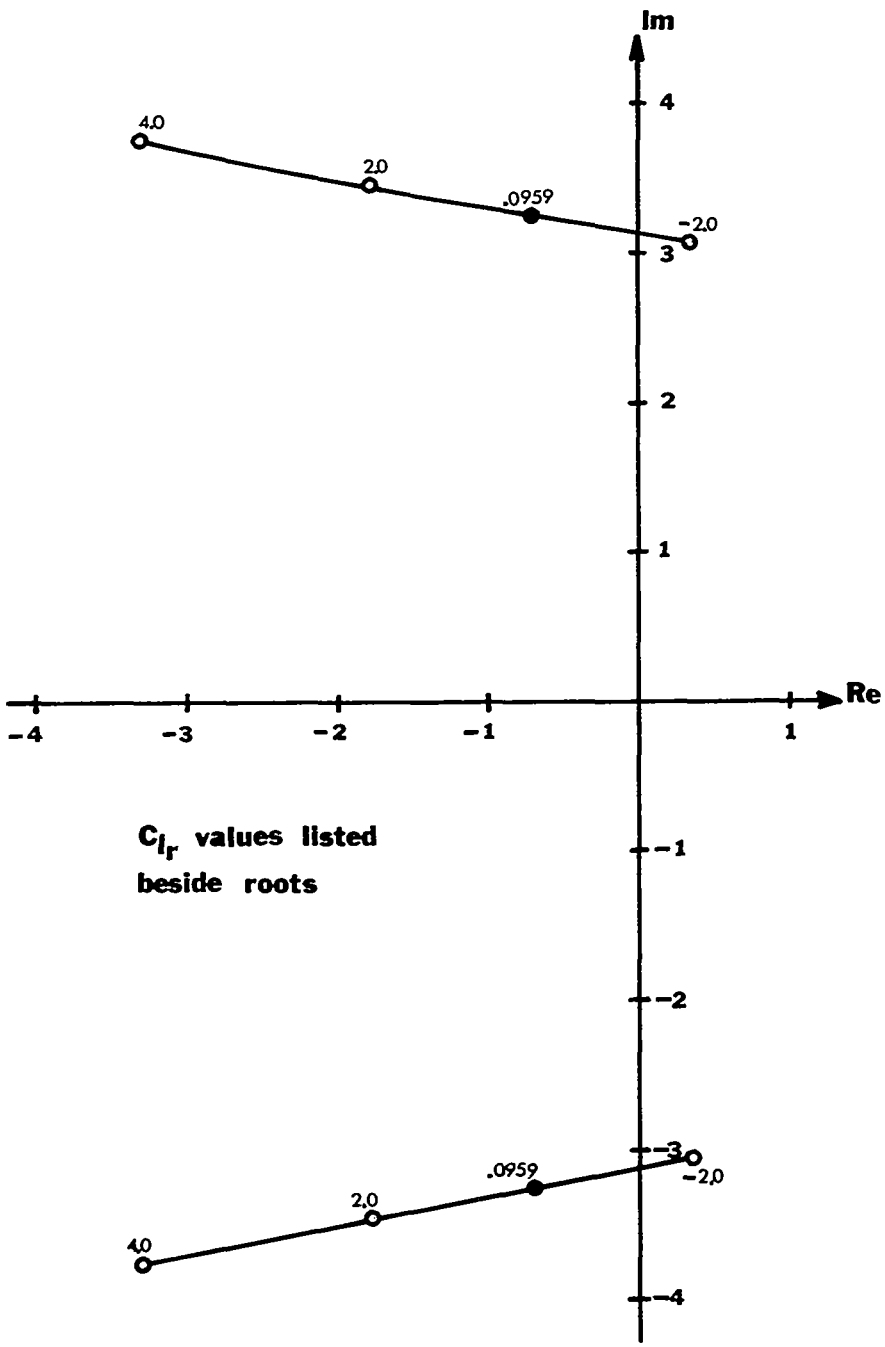

Figure 107a

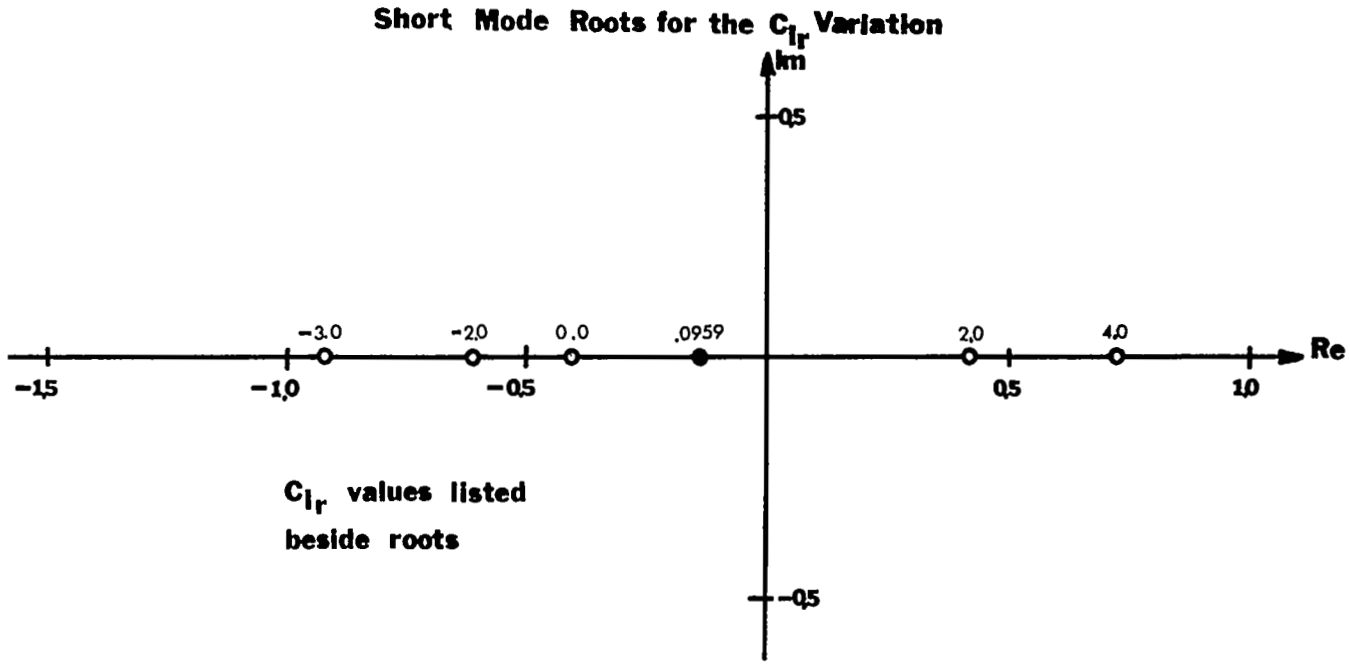

Figure 107b

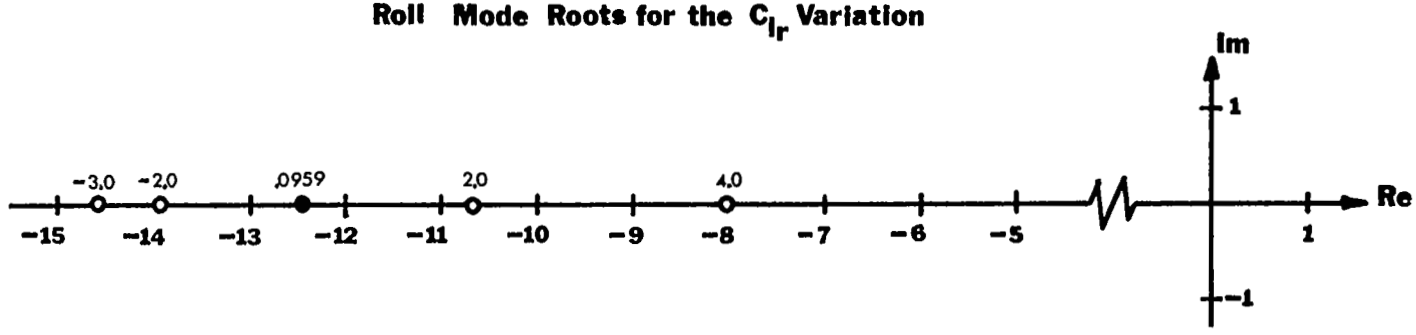

Figure 107c

NUMERATOR ROOTS

STABILITY DERIVATIVE	REAL	IMAGINARY	REAL	REAL
		β		
-5.0	-1.8946	0.0	-10.26117	-116.459
-3.0	-1.03898	0.0	-11.2754	-116.30101
-2.0	- .66903	0.0	-11.72497	-116.0221
0.0	- .00695	0.0	-12.54671	-115.8325
0.0959	0.02272	0.0	-12.588	-115.402
2.0	0.57860	0.0	-13.29262	-114.901
4.0	1.10784	0.0	-13.98292	-114.740
5.0	1.35548	0.0	-14.31136	-114.659
7.0	1.82262	0.0	-14.94063	-114.497
		ϕ		
-5.0	-289.21	0.0	0.12108	0.0
-3.0	-174.06	0.0	.24276	0.0
-2.0	-116.57	0.0	.39352	0.0
0.0	- 7.75308	0.0	6.85029	0.0
0.0959	- 5.29036	0.0	9.8676	0.0
2.0	- .52488	0.0	114.8989	0.0
4.0	- .29323	0.0	229.9438	0.0
5.0	- .24677	0.0	287.5357	0.0
7.0	- .19355	0.0	402.759	0.0
		ψ		
-5.0	-.01387	±.52896		-12.65493
-3.0	-.01387	±.52896		-12.65493
-2.0	-.01387	±.52896		-12.65493
0.0	-.01387	±.52896		-12.65493
.0959	-.01387	±.52896		-12.65493
2.0	-.01387	±.52896		-12.65493
4.0	-.01387	±.52896		-12.65493
5.0	-.01387	±.52896		-12.65493
7.0	-.01387	±.52896		-12.65493

Table 52. Numerator roots for C_{ℓ_r} variations.

Roots for the C_{n_r} Variation

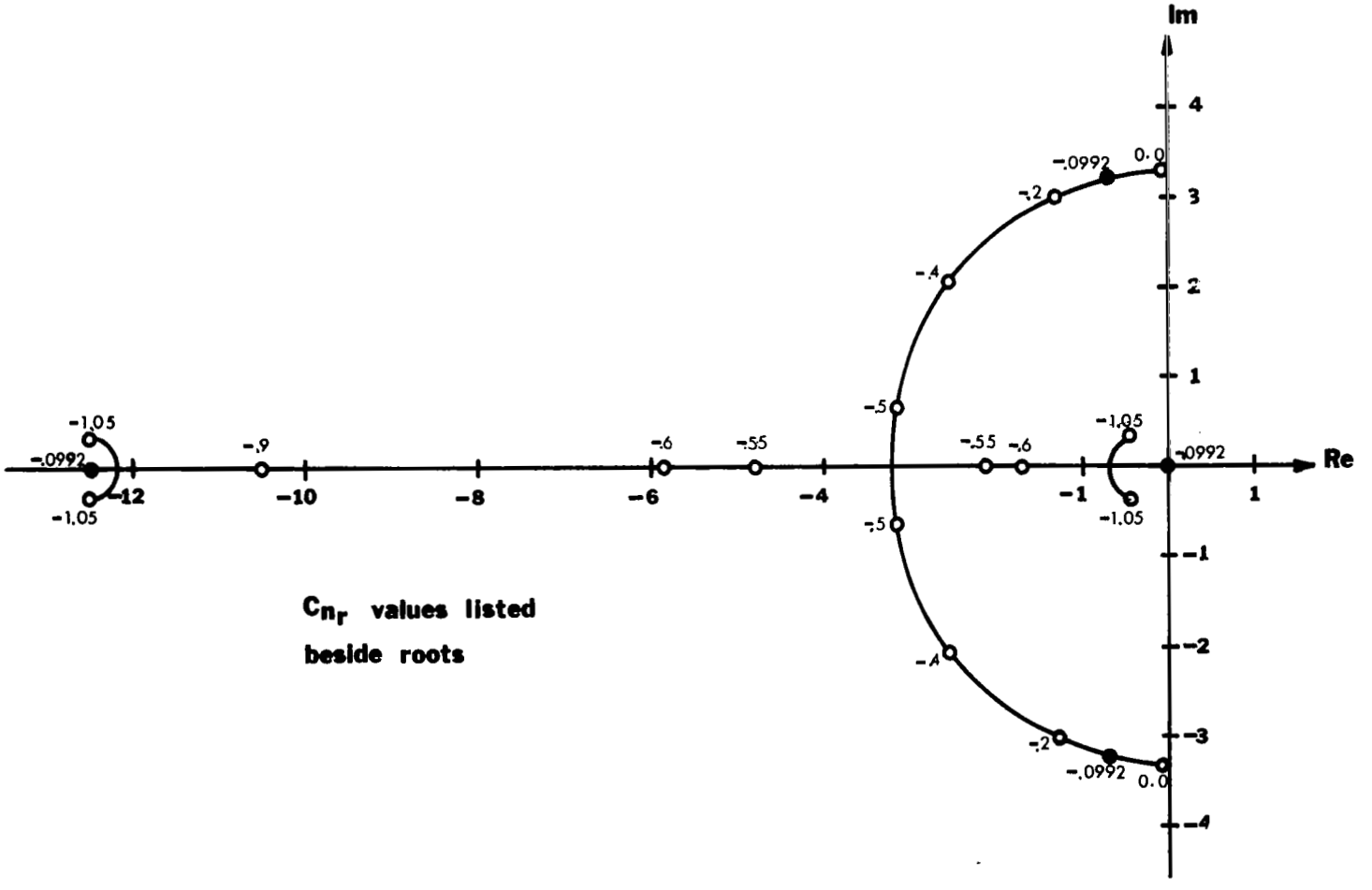

Figure 108

NUMERATOR ROOTS

STABILITY DERIVATIVE	REAL	IMAGINARY	REAL	REAL
		β		
-1.0	-.03548	0.0	-12.4639	-128.568
- .9	-.02947	0.0	-12.4762	-127.287
- .6	-.01077	0.0	-12.51447	-123.444
- .55	-.00755	0.0	-12.52111	-122.803
- .5	-.00430	0.0	-12.5278	-122.163
- .4	.00229	0.0	-12.5415	-120.881
- .2	.01586	0.0	-12.5697	-118.317
- .09924	.02272	0.0	-12.588	-115.402
- .07	.02496	0.0	-12.589	-114.650
- .05	.02638	0.0	-12.592	-114.394
0.0	.02996	0.0	-12.599	-113.752
		ϕ		
-1.0	4.93162	-11.748		0.0
- .9	5.28858	-10.840		0.0
- .6	6.6698	- 8.3875		0.0
- .55	6.94212	- 8.0225		0.0
- .5	7.2278	- 7.6709		0.0
-. 4	7.8399	- 7.0084		0.0
- .2	9.2274	- 5.8466		0.0
- .09924	9.8676	- 5.2904		0.0
- .07	10.2420	- 5.2042		0.0
- .05	10.4055	- 5.1128		0.0
0.0	10.823	- 4.893		0.0
		ψ		
-1.0	-.01387	±.52896		-12.65493
- .9	-.01387	±.52896		-12.65493
- .6	-.01387	±.52896		-12.65493
- .55	-.01387	±.52896		-12.65493
- .5	-.01387	±.52896		-12.65493
- .4	-.01387	±.52896		-12.65493
- .2	-.01387	±.52896		-12.65493
- .09924	-.01387	±.52896		-12.65493
- .07	-.01387	±.52896		-12.65493
- .05	-.01387	±.52896		-12.65493
0.0	-.01387	±.52896		-12.65493

Table 53. Numerator roots for C_{n_r} variations.

NUMERATOR ROOTS

STABILITY DERIVATIVE	REAL	IMAGINARY	REAL	REAL
		β		
-1.0	.02418	0.0	-12.55031	20.22192
- .75	.02377	0.0	-12.55567	27.3650
- .5	.02333	0.0	-12.56214	41.64652
- .25	.02272	0.0	-12.57005	84.47888
0.0	.02297	0.0	-12.58048	
.1874	.02272	0.0	-12.59078	-115.40684
.25	.02264	0.0	-12.59431	- 86.79281
.5	.02232	0.0	-12.61223	- 43.95034
.75	.02202	0.0	-12.63853	- 29.64899
1.00	.02172	0.0	-12.68051	- 22.46934
		φ		
-1.0	0.0	0.0	-6.57089	7.74879
- .75	0.0	0.0	-6.26998	8.16388
- .5	0.0	0.0	-5.98623	8.59611
- .25	0.0	0.0	-5.71911	9.04498
0.0	0.0	0.0	-5.46802	9.50987
.187	0.0	0.0	-5.28991	9.86846
.25	0.0	0.0	-5.23228	9.99012
.5	0.0	0.0	-5.01116	10.48499
.75	0.0	0.0	-4.80392	10.99373
1.00	0.0	0.0	-4.60975	11.51555
		ψ		
-1.0	-.31014	±.4297		-12.61691
- .75	-.24760	±.46833		-12.62560
- .5	-.18515	±.49616		-12.63411
- .25	-.12278	±.51497		-12.64245
0.0	-.06049	±.52576		-12.65062
.1874	-.01386	±.52892		-12.65664
.25	.00171	±.52906		-12.65863
.5	.06384	±.52503		-12.66649
.75	.12589	±.51353		-12.67420
1.00	.18787	±.49407		-12.68176

Table 54. Numerator roots for $C_{y_{\delta_R}}$ variations.

NUMERATOR ROOTS

STABILITY DERIVATIVE	REAL	IMAGINARY	REAL	REAL
		β		
-3.0	- .48468	0.0	-168.74511	25.38497
-2.0	- .57868	0.0	-153.71383	15.71175
-1.0	- 1.17612	0.0	-136.61884	4.47829
0.0001	-12.32283	0.0	-115.75927	.03009
.01475	-12.59078	0.0	-115.40684	.02272
.05	-13.24437	0.0	-114.55102	.00605
.15	-15.16965	0.0	-112.0589	- .03437
.50	-22.91592	0.0	-102.37878	- .12576
1.0	-39.3933	0.0	- 83.20187	- .19315
2.0	-58.6349	±41.37965		- .25419
3.0	-55.98877	±62.39119		- .28250
		ϕ		
-3.0	- .72027	±3.15419		0.0
-2.0	- .72763	±3.17672		0.0
-1.0	- .74972	±3.24328		0.0
0.0001	-10.29436	0.0	892.35499	0.0
.01475	- 5.28991	0.0	9.86846	0.0
.05	- 2.69752	0.0	3.05337	0.0
.15	- .41106	±1.96457		0.0
.50	- .6172	±2.81787		0.0
1.0	- .66137	±2.96712		0.0
2.0	- .68346	±3.03875		0.0
3.0	- .69082	±3.06222		0.0
		ψ		
-3.0	2.51434	0.0	22.92565	- 2.50023
-2.0	3.29649	0.0	10.61332	- 2.78665
-1.0	1.70459	±3.08103		- 4.10259
.0001	- .01042	± .58161		-12.49040
.01475	- .01386	± .52892		-12.65664
.05	- .02153	± .38078		-13.05783
.15	- .48245		.40343	-14.20363
.50	-1.09987		.94997	-18.26858
1.0	-1.42295		1.23465	-24.13854
2.0	-1.68133		1.47382	-35.93603
3.0	-1.79385		1.58414	-47.75055

Table 55. Numerator roots for $C_{\ell_{\delta_R}}$ variations.

NUMERATOR ROOTS

STABILITY DERIVATIVE	REAL	IMAGINARY	REAL	REAL
		β		
-.12	-12.47042	0.0	.02617	-209.71058
-.10	-12.49848	0.0	.02532	-174.92893
-.08	-12.54195	0.0	.02407	-140.13146
-.0658	-12.59078	0.0	.02272	-115.40684
-.04	-12.78700	0.0	.01796	- 70.37482
-.02	-13.49442	0.0	.00657	- 34.90327
-.005	-11.14076	±4.97905	-.04503	
.005	-10.91735	0.0	.21055	5.75643
.01	-11.38982	0.0	.09625	15.03131
.02	-11.76114	0.0	.05942	32.81567
		φ		
-.12	-6.59921	0.0	15.66940	0.0
-.10	-6.20569	0.0	13.61845	0.0
-.08	-5.71878	0.0	11.47411	0.0
-.0658	-5.28991	0.0	9.86846	0.0
-.04	-4.19447	0.0	6.63494	0.0
-.02	-2.62335	0.0	3.40639	0.0
-.005	- .23002	±2.27629		0.0
.005	- .64437	±3.77708		0.0
.01	- .85155	±4.32203		0.0
.02	-1.26591	±5.22012		0.0
		ψ		
-.12	-.0335	± .55252		-12.57804
-.10	-.02871	± .54692		-12.59717
-.08	-.02155	± .53837		-12.62581
-.0658	-.01386	± .52892		-12.65664
-.04	.01380	± .49251		-12.76809
-.02	.08232	± .37954		-13.04833
-.005	-.28175		1.16989	-14.63102
.005	-.78637	± .85217		- 9.87907
.01	-.37960 =	± .79577		-11.26536
.02	-.21060	± .70841		-11.88973

Table 56. Numerator roots for $C_{n_{\delta_R}}$ variations.

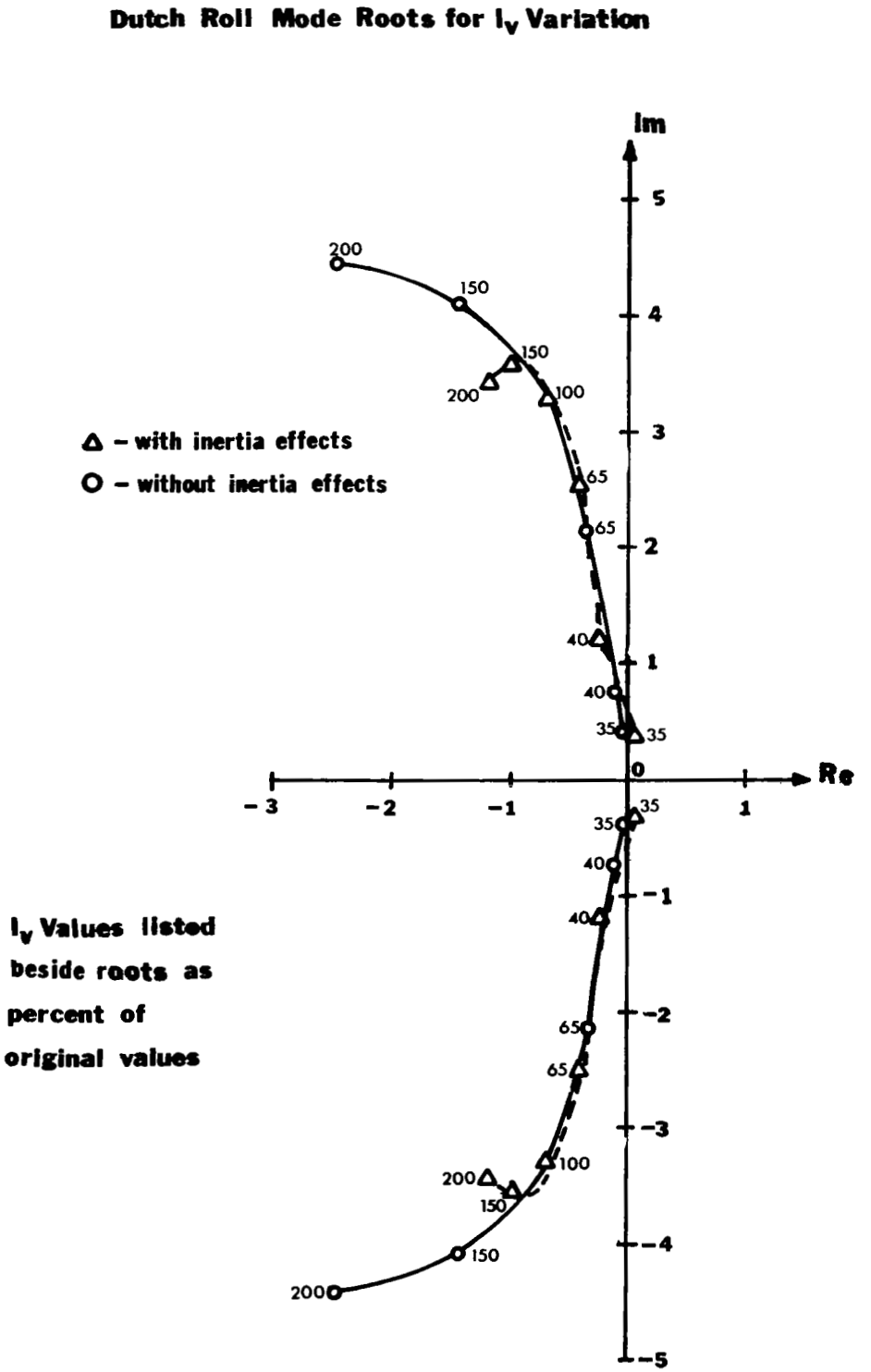
Dutch Roll Mode Roots for I_v Variation
Im
Re
△ – with inertia effects
○ – without inertia effects
I_v Values listed beside roots as percent of original values
200
150
150
200
100
65
65
40
40
35
35
35
40
40
65
65
100
200
150
150
200
5
4
3
2
1
0
-1
-2
-3
-4
-5
-3
-2
-1
1

Figure 109a

Spiral Mode Roots for I_v Variation

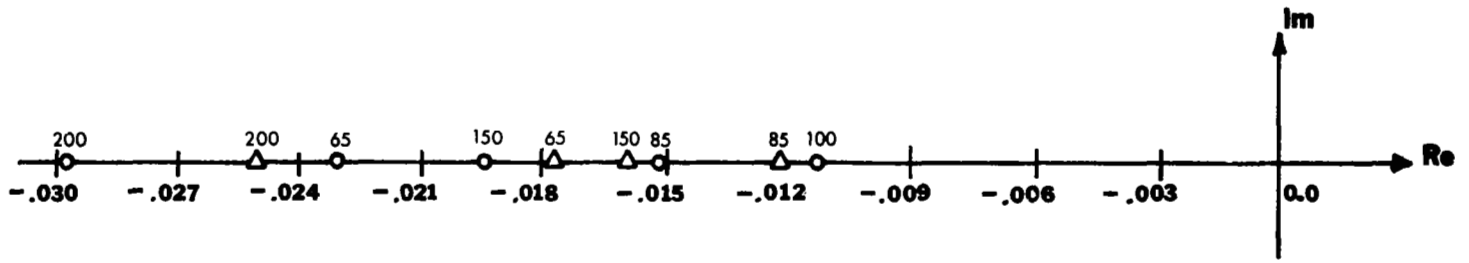

Δ – with inertia effects

O – without inertia effects

I_v values listed beside roots as percent of original value

Figure 109b

Roll Mode Roots for I_v Variation

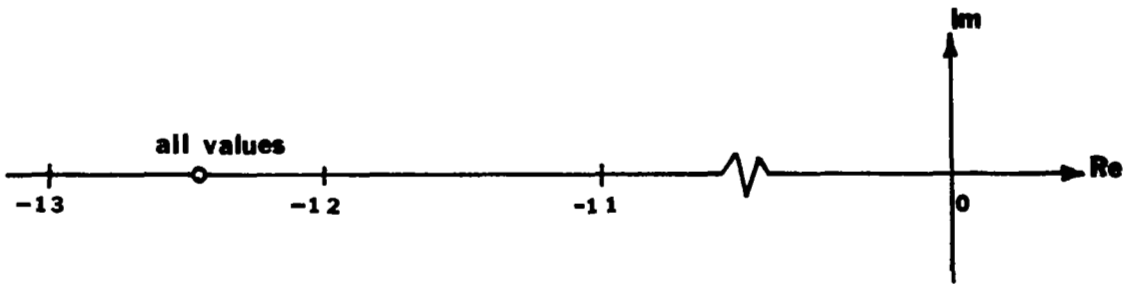

Figure 109c

Dutch Roll Mode Roots for S_v Variation with Constant AR

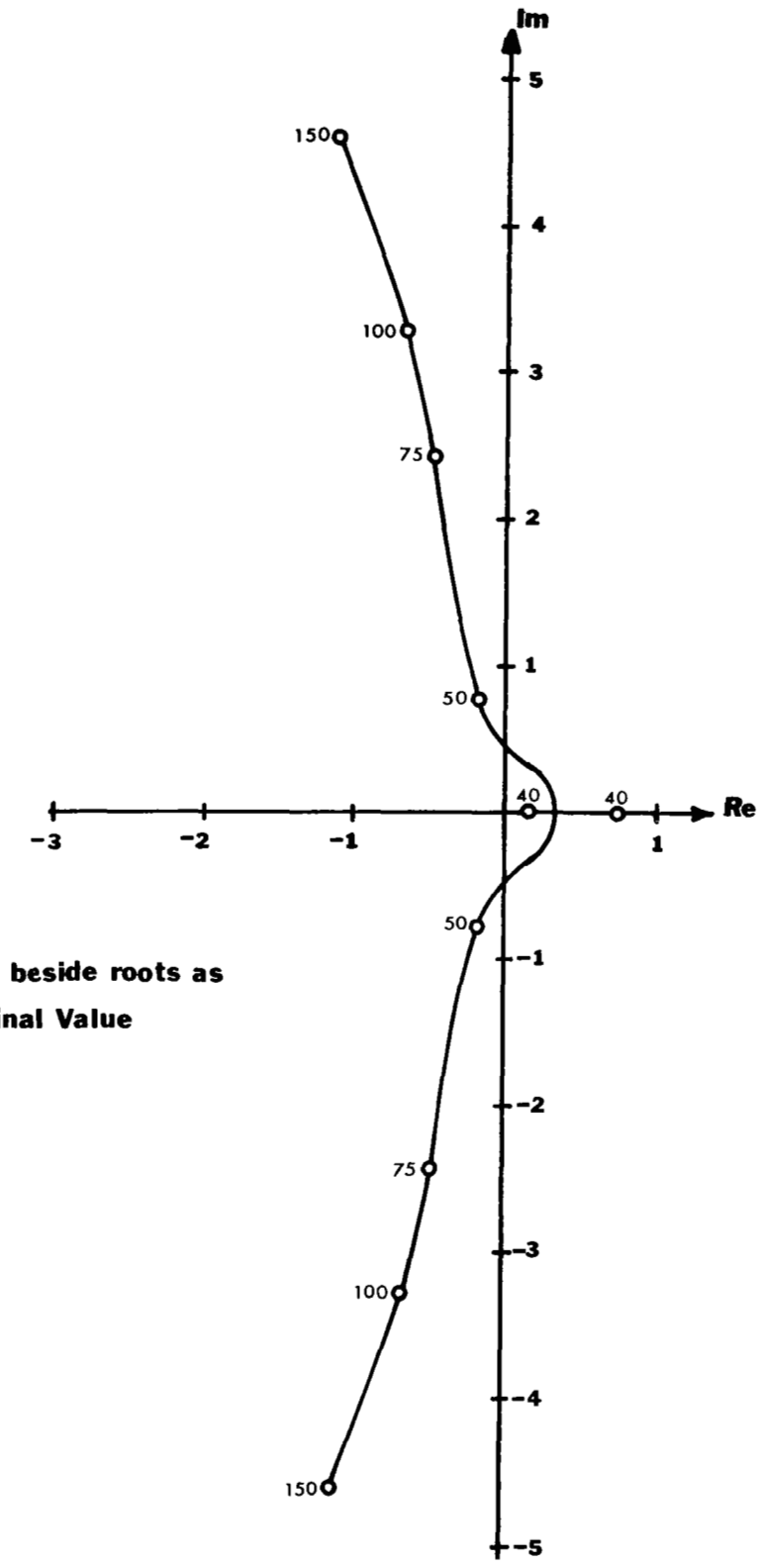

S_v Values listed beside roots as percent of original Value

Figure 110a

Spiral Mode Roots for S_V Variation

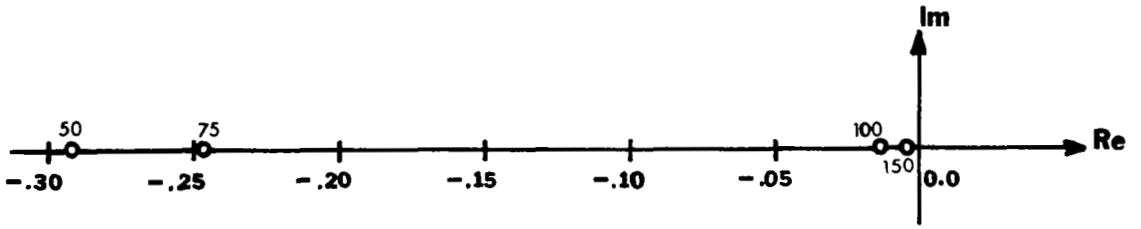

S_V values listed beside roots

as percent of original values

Figure 110b

Roll Mode Roots for S_V Variation

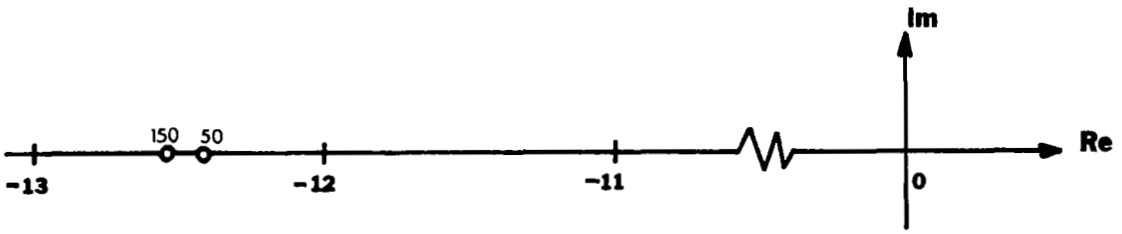

Figure 110c

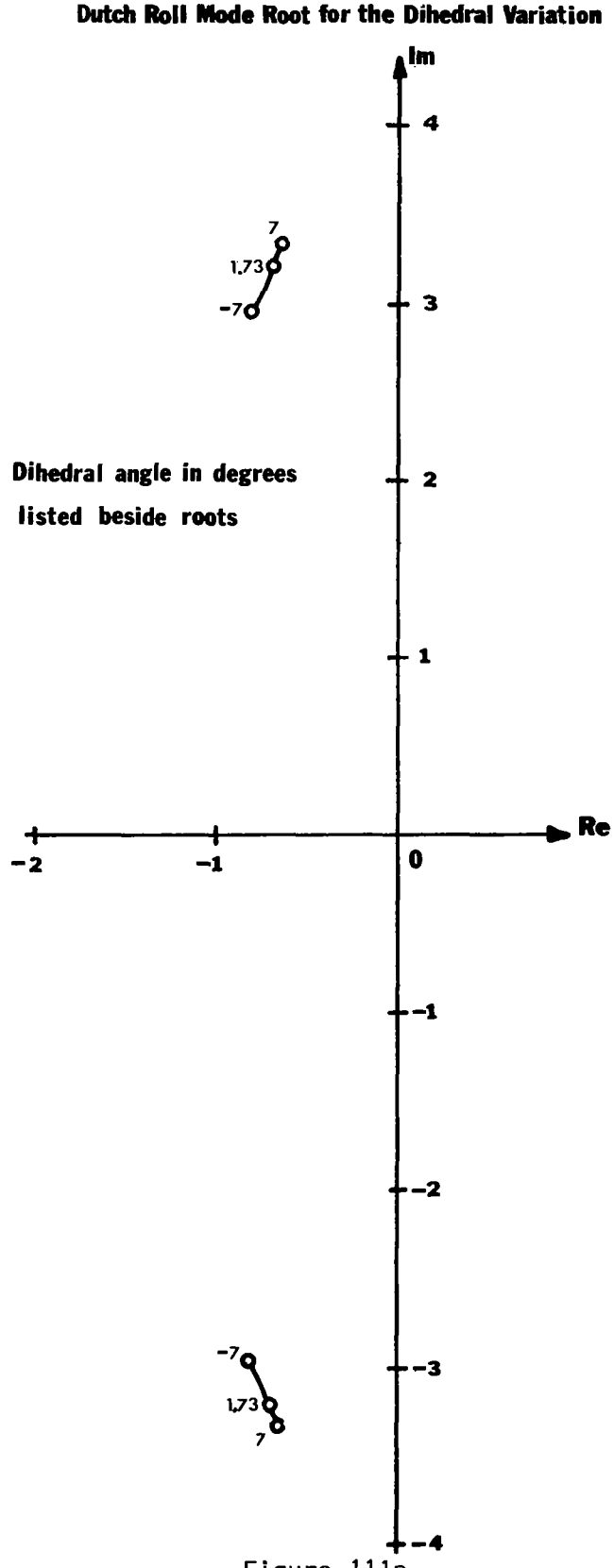
Dutch Roll Mode Root for the Dihedral Variation
Im
4
3
2
1
-1
-2
-3
-4
Re
-2
-1
0
7
1.73
-7
-7
1.73
7
Dihedral angle in degrees
listed beside roots

Figure 111a

Spiral Mode Roots for Dihedral Variation

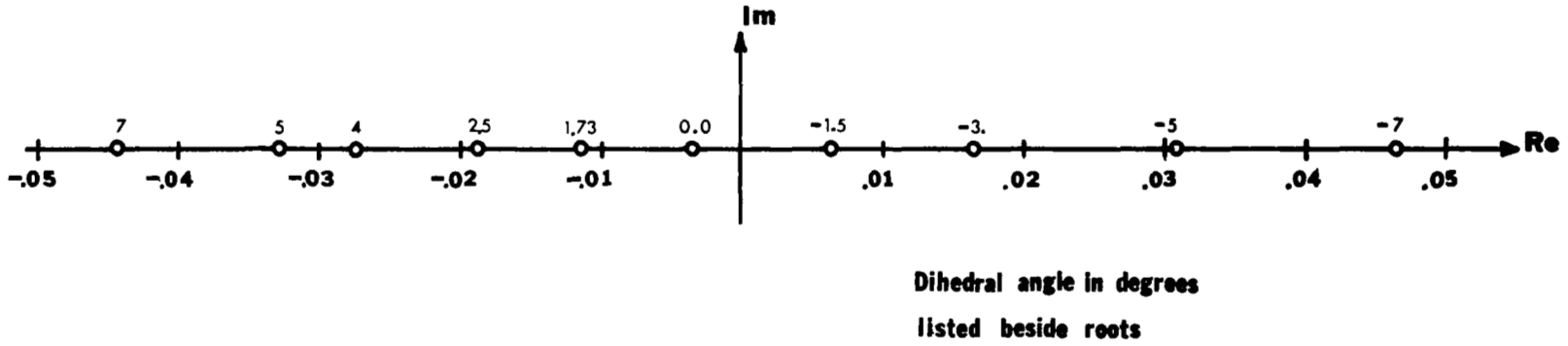

Figure 111b

Roll Mode Roots for Dihedral Variation

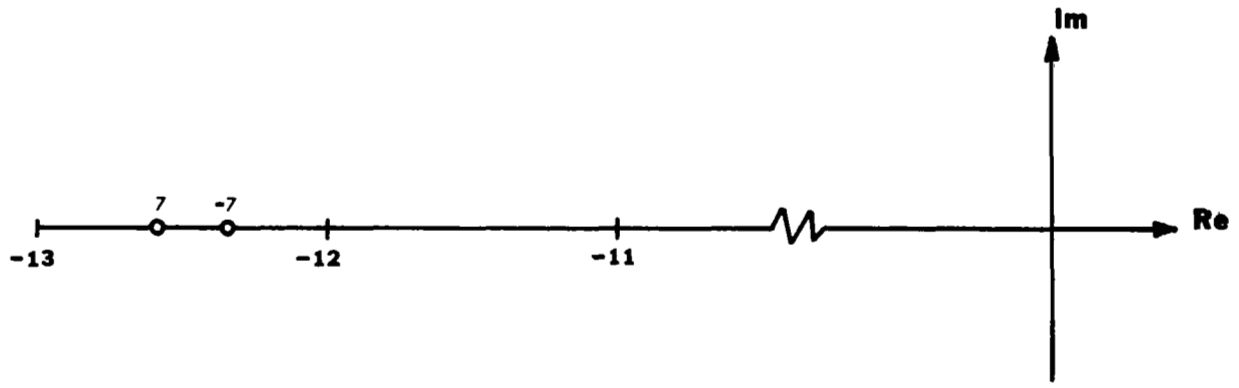

Figure 111c

Dutch Roll Mode Roots for Dihedral and S_v Variation

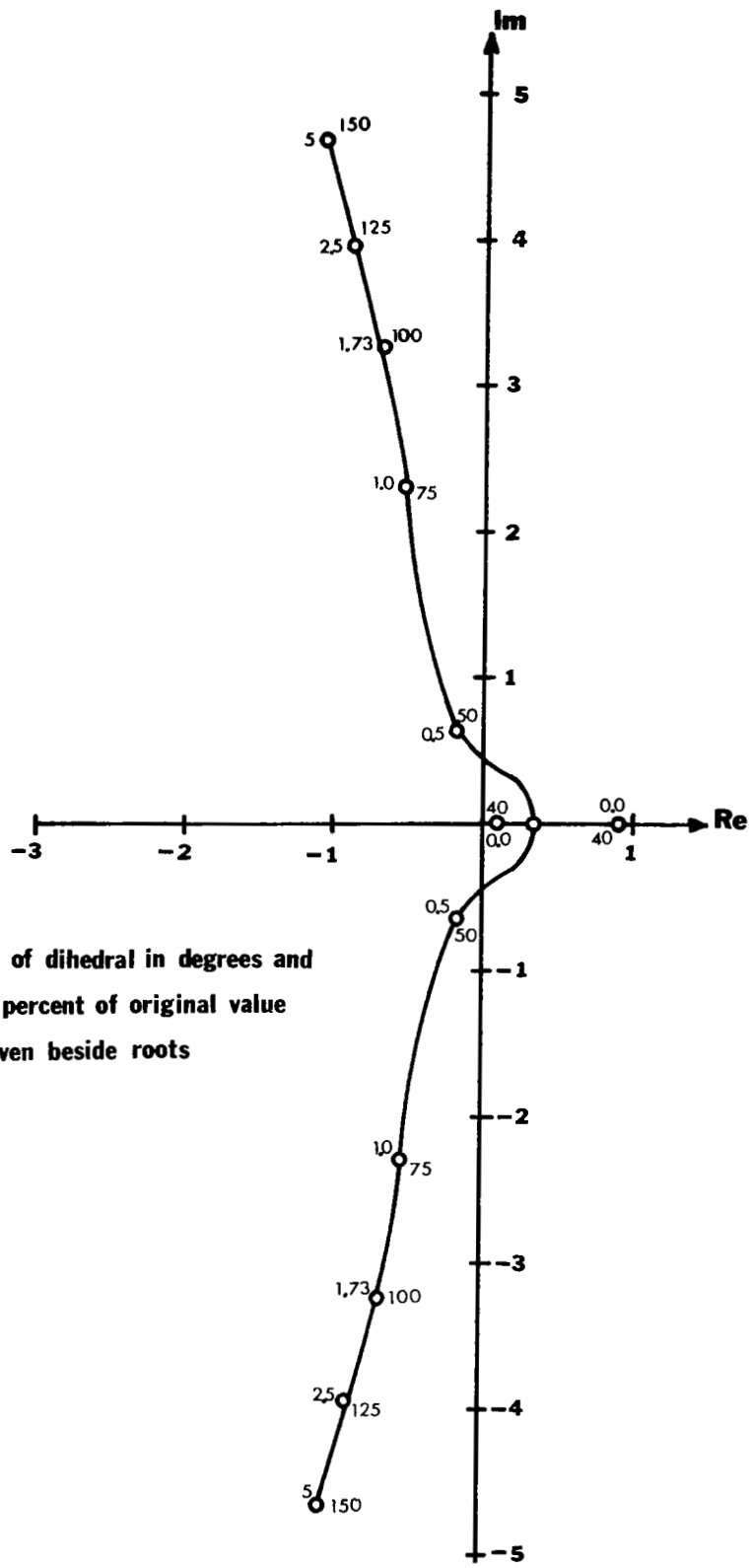

Figure 112a

Spiral Mode Roots for Dihedral and S_V Variation

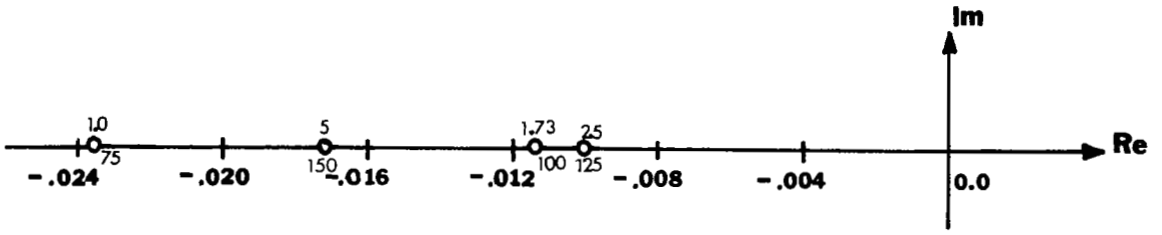

Values of dihedral in degrees and
S_V as percent of original value
are given beside roots

Figure 112b

Roll Mode Roots for Dihedral and S_V Variation

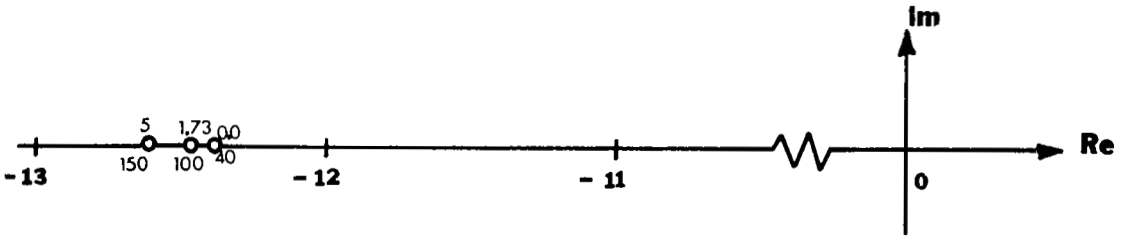

Figure 112c

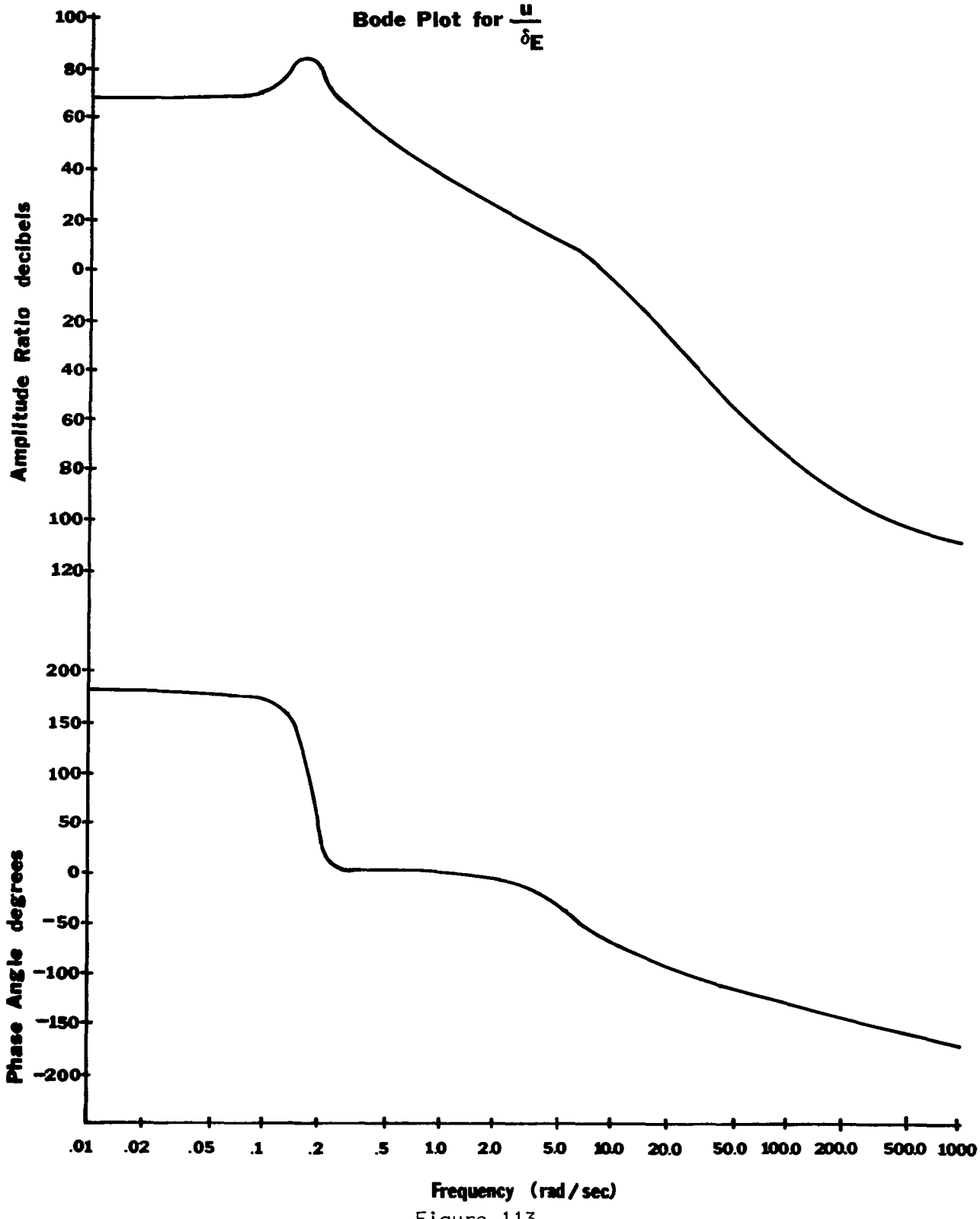
Bode Plot for u/δE
Amplitude Ratio decibels
100
80
60
40
20
0
20
40
60
80
100
120
Phase Angle degrees
200
150
100
50
0
-50
-100
-150
-200
.01
.02
.05
.1
.2
.5
1.0
2.0
5.0
10.0
20.0
50.0
100.0
200.0
500.0
1000
Frequency (rad/sec)

Figure 113

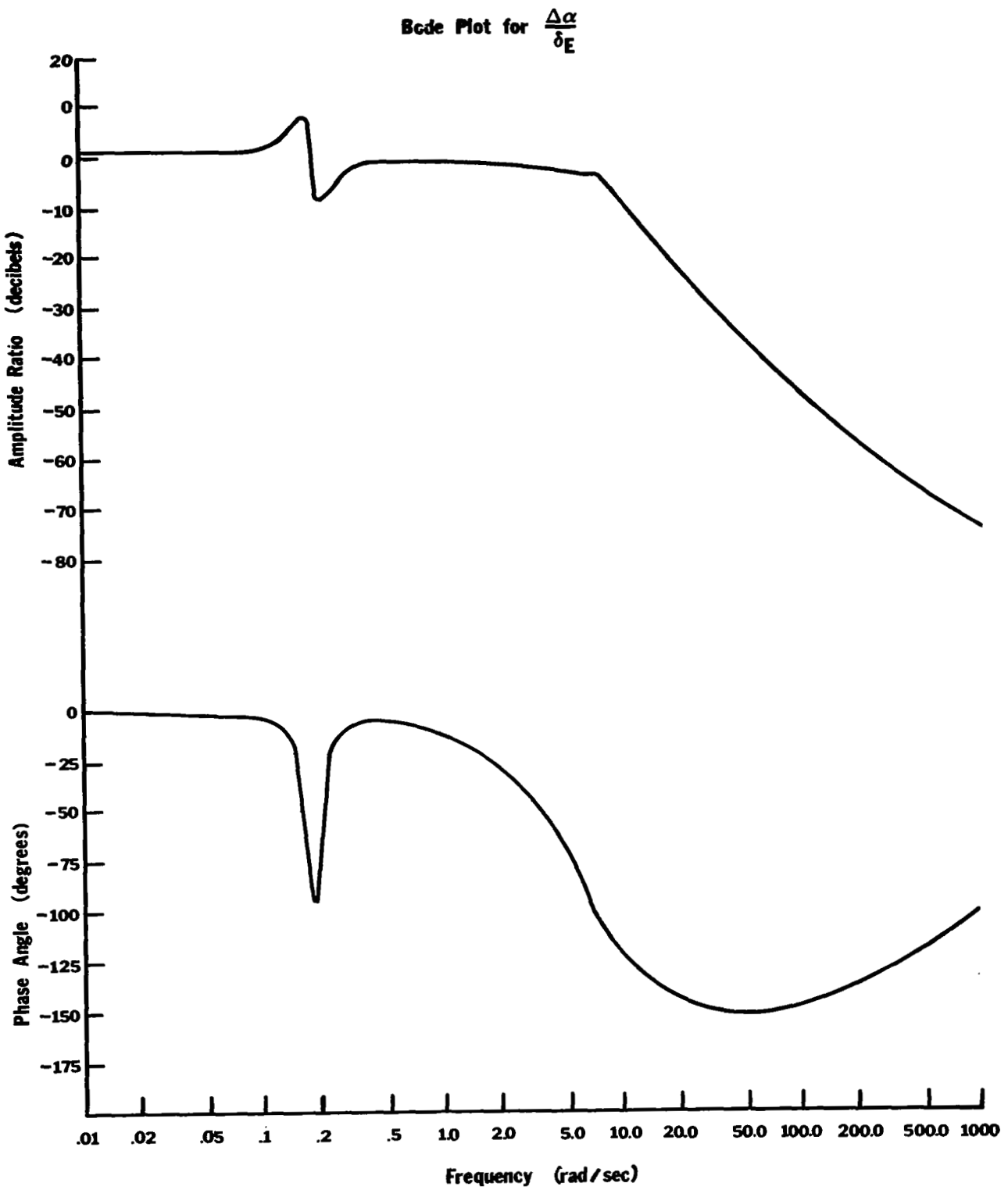
Bode Plot for $\frac{\Delta\alpha}{\delta_E}$
Amplitude Ratio (decibels)
20
0
0
-10
-20
-30
-40
-50
-60
-70
-80
Phase Angle (degrees)
0
-25
-50
-75
-100
-125
-150
-175
.01
.02
.05
.1
.2
.5
1.0
2.0
5.0
10.0
20.0
50.0
100.0
200.0
500.0
1000
Frequency (rad/sec)

Figure 114

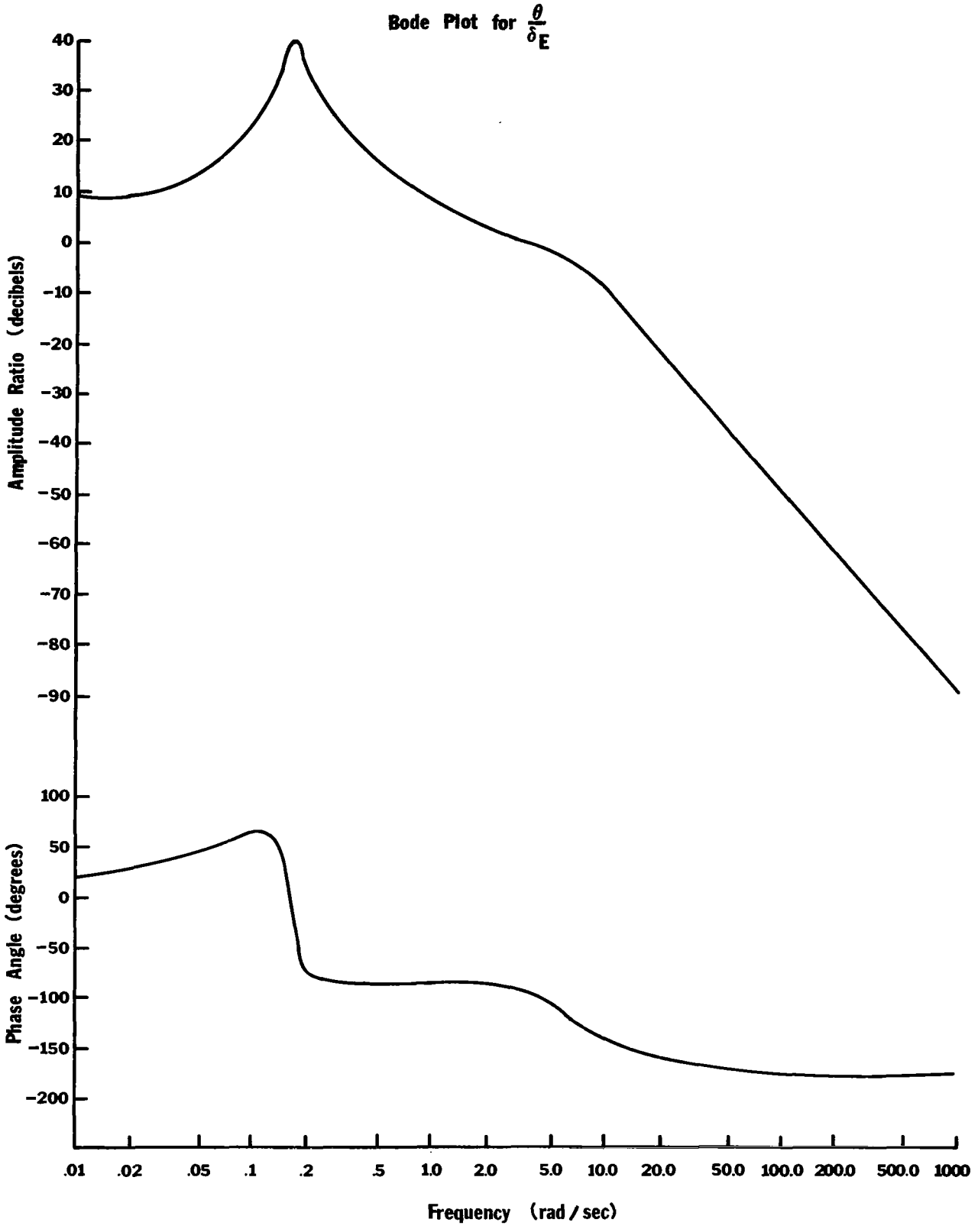
Bode Plot for $\frac{\theta}{\delta_E}$
Amplitude Ratio (decibels)
40
30
20
10
0
-10
-20
-30
-40
-50
-60
-70
-80
-90
Phase Angle (degrees)
100
50
0
-50
-100
-150
-200
.01
.02
.05
.1
.2
.5
1.0
2.0
5.0
10.0
20.0
50.0
100.0
200.0
500.0
1000
Frequency (rad / sec)

Figure 115

Bode Plot for $\frac{\beta}{\delta_R}$

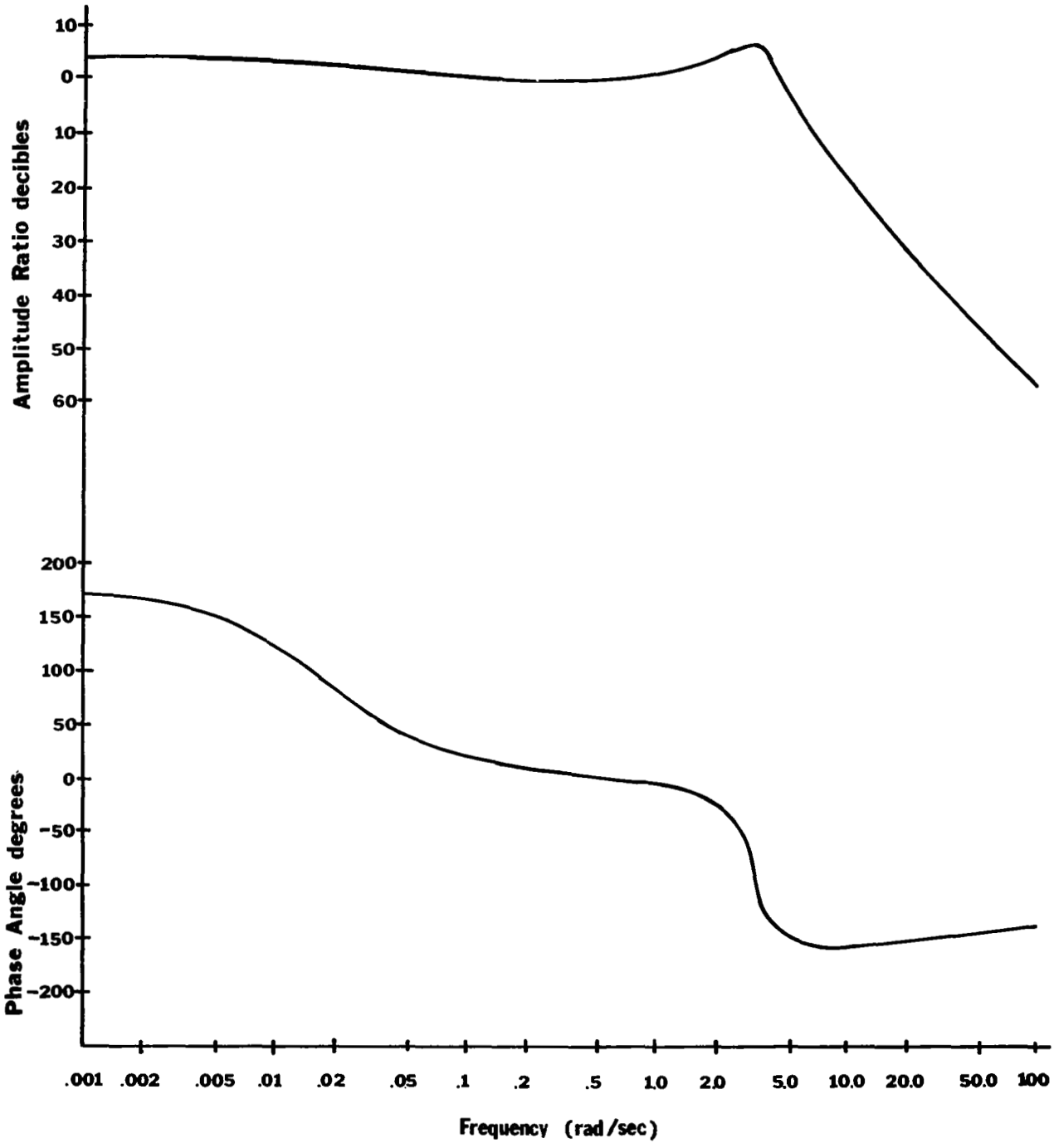

Figure 116

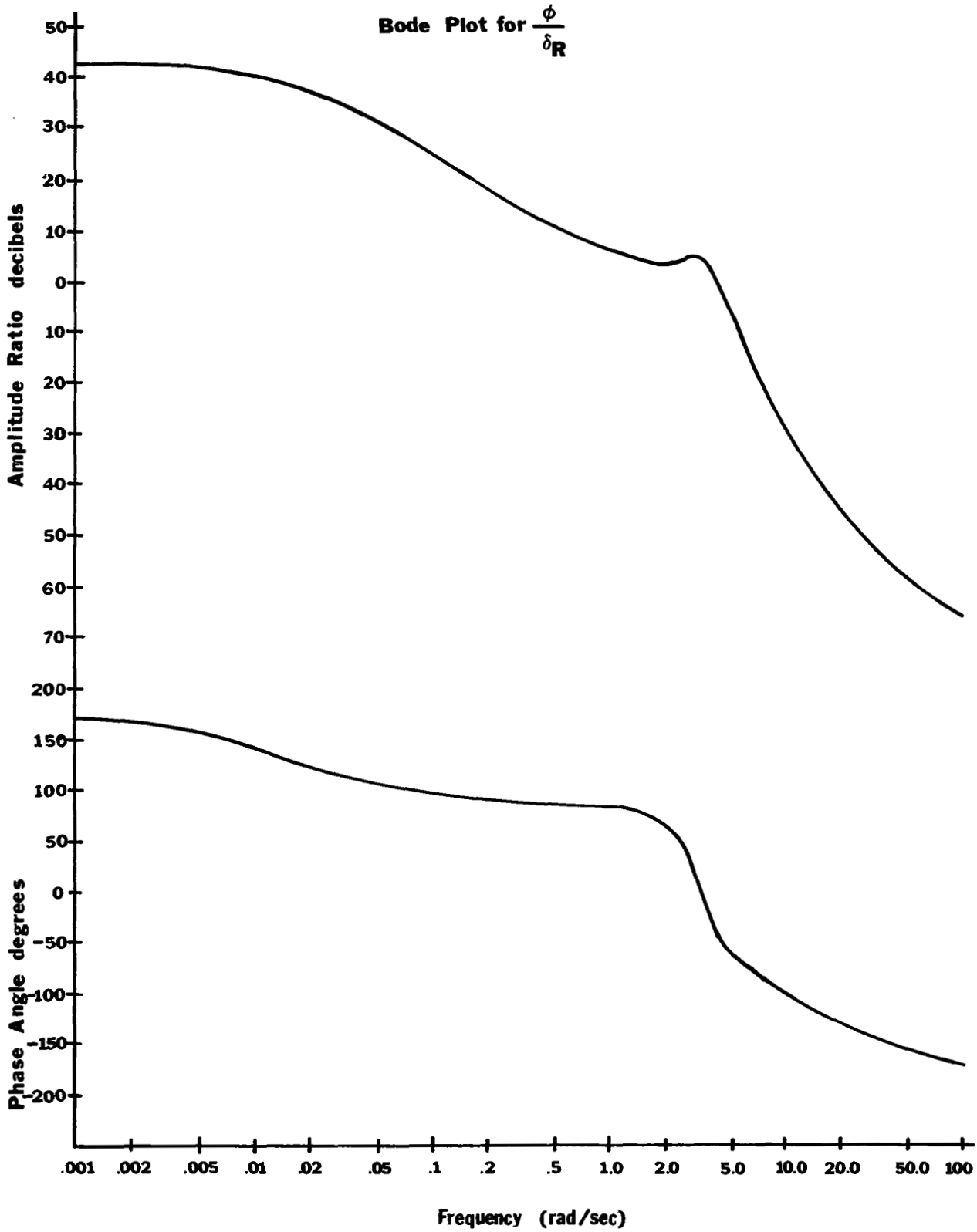
Bode Plot for $\frac{\phi}{\delta_R}$
Amplitude Ratio decibels
50
40
30
20
10
0
10
20
30
40
50
60
70
200
150
100
50
0
-50
-100
-150
-200
Phase Angle degrees
.001
.002
.005
.01
.02
.05
.1
.2
.5
1.0
2.0
5.0
10.0
20.0
50.0
100
Frequency (rad/sec)

Figure 117

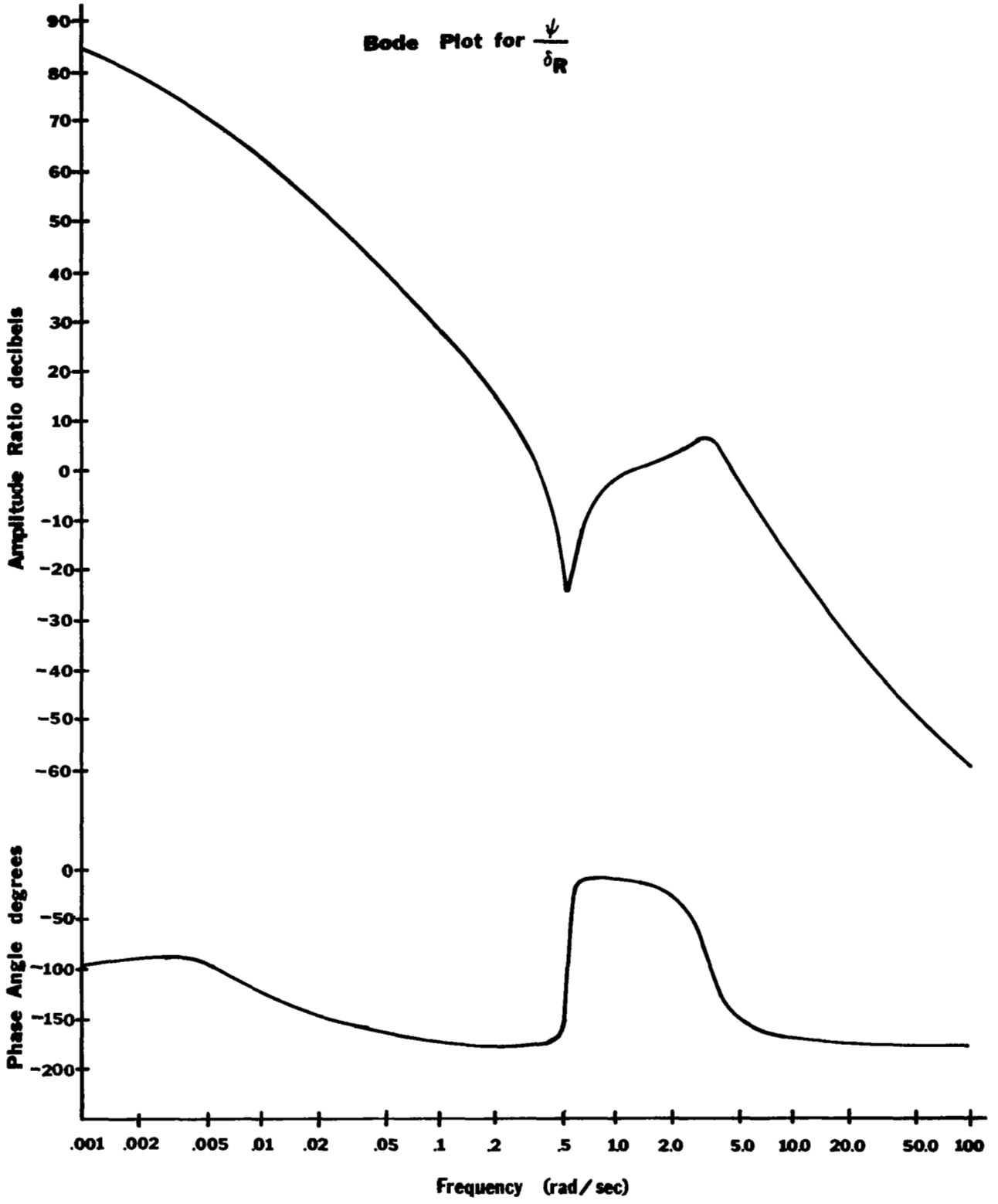
Bode Plot for $\frac{\psi}{\delta_R}$
Amplitude Ratio decibels
90
80
70
60
50
40
30
20
10
0
-10
-20
-30
-40
-50
-60
Phase Angle degrees
0
-50
-100
-150
-200
.001
.002
.005
.01
.02
.05
.1
.2
.5
1.0
2.0
5.0
10.0
20.0
50.0
100
Frequency (rad/sec)

Figure 118

REFERENCES

1. Smetana, Frederick O.: "A Study of NACA and NASA Published Information of Pertinence in the Design of Light Aircraft, Volume I - Structures". NASA CR-1484, February 1970.

2. Williams, James C., III; Summey, Delbert C.; and Perkins, John N.: "A Study of NACA and NASA Published Information of Pertinence in the Design of Light Aircraft, Volume II - Aerodynamics and Aerodynamic Loads". NASA CR-1485, February 1970.

3. Moore, Clifford J.; and Phillips, Dennis M.: "A Study of NACA and NASA Published Information of Pertinence in the Design of Light Aircraft, Volume III - Propulsion Subsystems, Performance, Stability and Control, Propellers, and Flight Safety". NASA CR-1486, February 1970.

4. Chalk, C. R.; Neal, T. P.; Harris, T. M; Pritchard, F. E.; and Woodcock, R. J.: "Background Information and User Guide for MIL-F-8785B(ASG), 'Military Specification - Flying Qualities of Piloted Airplanes'". AFFDL-TR-69-72, August 1969.

5. Ellison, Don E.; and Hoak, Donald E.: Stability Derivative Estimation at Subsonic Speeds. New York Academy of Sciences, Annals, Vol. 154, Nov. 1968.

6. Von Mises, Richard: Theory of Flight. McGraw-Hill Book Company, Inc., 1945.

7. Abbott, Ira H.; and von Doenhoff, Albert E.: Theory of Wing Sections. Dover Publications, Inc., 1959.

8. Abbott, Ira H.; von Doenhoff, Albert E.; and Stivers, Louis S., Jr.: "Summary of Airfoil Data". NACA TR-824, 1945.

9. Jacobs, Eastman N.; and Ward, Kenneth E.: "Interference of Wing and Fuselage from Tests of 209 Combinations in the N. A. C. A. Variable-Density Tunnel". NACA TR-540, 1935.

10. Hoak, D. E.; and Ellison, D. E.: "USAF Stability and Control Datcom". October 1960 (Rev. August 1968).

11. Perkins, Courtland D.; and Hage, Robert E.: Airplane Performance Stability and Control. John Wiley and Sons, Inc., 1949.

12. Wood, K. D.: Aerospace Vehicle Design, Volume I - Aircraft Design. Johnson Publishing Company, 1968.

13. Wood, Karl D.: Technical Aerodynamics. McGraw-Hill Book Comapny, Inc., 1947.

14. Hoerner, Sighard F.: Fluid-Dynamic Drag. Midland Park, N. J., 1958.

15. Mulally, Alan R.: An Investigation of Aerodynamic Design Modifications which Lead to Performance Gains and the Preliminary Design of a New Light Airplane. University of Kansas, 1968.

16. Phillips, William H.: "Appreciation and Prediction of Flying Qualities". NACA TR-927, 1949.

17. Bureau of Aeronautics, Navy Department: "Dynamics of the Airframe". BU AER Rep. AE-61-4II, September 1952.

18. Blakelock, John H.: Automatic Control of Aircraft and Missiles. John Wiley and Sons, Inc., 1965.

19. Dommasch, Daniel O.; Sherby, Sydney S.; and Connolly, Thomas F.: Airplane Aerodynamics. Pitman Publishing Corporation, 1967.

20. Jacobs, Eastman N.: "Characteristics of Two Sharp-nosed Airfoils Having Reduced Spinning Tendencies". NACA TN-416, April 1932.

21. Gilruth, R. R.; and White, M. D.: "Analysis and Prediction of Longitudinal Stability of Airplanes". NACA TR-711, 1941.

22. Multhopp, H.: "Aerodynamics of the Fuselage". NACA TM-1036, December 1942.

23. Greenberg, Harry; and Sternfield, Leonard: "A Theoretical Investigation of Longitudinal Stability of Airplanes with Free Controls Including Effect of Friction in Control System". WR L-430, February 1944.

24. Durand, William Frederick: Aerodyanmic Theory, Vol. V, Dynamics of the Airplane, Airplane Performance. Dover Publications, Inc., 1963.

25. Greenberg, Harry; and Sternfield, Leonard: "A Theoretical Investigation of Longitudinal Stability of Airplanes with Free Controls Including Effect of Friction in Control System". NACA TR-791, 1944.

26. Silverstein, Abe; and Katzoff, S.: "Aerodynamic Characteristics of Horizontal Tail Surfaces". NACA TR-688.

27. Campbell, John P.; and McKinney, Marion O.: "Summary of Methods for Calculating Dynamic Lateral Stability and Response and for Estimating Lateral Stability Derivatives". NACA TR-1098, 1952.

28. Toll, Thomas A.; and Queijo, M. J.: "Approximate Relations and Charts for Low-Speed Stability Derivatives of Swept Wings". NACA TN-1581, 1948.

29. Shortal, Joseph A.; and Draper, John W.: "Free-Flight-Tunnel Investigation of the Effect of the Fuselage Length and the Aspect Ratio and Size of the Vertical Tail on Lateral Stability and Control". WR L-487, April 1943.

30. McKinney, Marion O., Jr.: "Experimental Determination of the Effects of Dihedral, Vertical-Tail Area, and Lift Coefficient on Lateral Stability and Control Characteristics". NACA TN-1094, July 1946.

31. Queijo, M. J.: "Theoretical Span Load Distributions and Rolling Moments for Sideslipping Wings of Arbitrary Plan Form in Incompressible Flow". NACA TR-1269, 1956.

32. Hoerner, Sighard: "Forces and Moments on a Yawed Airfoil". NACA TM-906, August 1939.

33. Goodman, Alex; and Fisher, Lewis R.: "Investigation at Low Speeds of the Effect of Aspect Ratio and Sweep on Rolling Stability Derivatives of Untapered Wings". NACA TR-968, 1950.

34. Booth, Katherine W.: "Effect of Horizontal-tail Chord on the Calculated Subsonic Span Loads and Stability Derivatives of Isolated Unswept Tail Assemblies in Sideslip and Steady Roll". NASA MEMO 4-1-59L, March 1959.

35. Michael, William H., Jr.: "Analysis of the Effects of Wing Interference on the Tail Contributions to the Rolling Derivatives". NACA TR-1086, 1952.

36. Klawans, Bernard B; and White, Jack A.: "A Method Utilizing Data on the Spiral, Roll-Subsidence, and Dutch Roll Modes for Determining Lateral Stability Derivatives for Flight Measurements". NACA TN-4066, August 1957.

37. Bird, John P.: "Some Theoretical Low-Speed Span Loading Characteristics of Swept Wings in Roll and Sideslip". NACA TN-1839, March 1949.

38. Queijo, M. J.; and Jaquet, Byron M.: "Calculated Effects of Geometric Dihedral on the Low-Speed Rolling Derivatives of Swept Wings. NACA TN-1732, October 1948.

39. Goodman, Alex; and Adair, Glenn H.: "Estimation of the Damping in Roll of Wings through the Normal Flight Range of Lift Coefficient". NACA TN-1924, July 1949.

40. Wolhart, Walter D.: "Influence of Wing and Fuselage on the Vertical Tail Contribution to the Low Speed Rolling Derivative of Midwing Airplane Models with 45° Sweptback Surfaces". NACA TN-2587, December 1951.

41. MacLachlan, Robert; and Letko, William: "Correlation of Two Experimental Methods of Determining the Rolling Characteristics of Unswept Wings". NACA TN-1309, May 1947.

42. Michael, William H., Jr.: "Analysis of the Effects of Wing Interference on the Tail Contributions to the Rolling Derivatives. NACA TN-2332, April 1951.

43. Goodman, Alex; and Brewer, Jack D.: "Investigation at Low Speeds of the Effect of Aspect Ratio and Sweep on Static and Yawing Stability Derivatives of Untapered Wings". NACA TN-1669, August 1948.

44. Bird, John D.; Fisher, Lewis R.; and Hubbard, Sadie M.: "Some Effects of Frequency on the Contribution of a Vertical Tail to the Free Aerodynamic Damping of a Model Oscillating in Yaw". NACA TR-1130, 1953.

45. Zimmerman, Charles H.: "An Analysis of Lateral Stability in Power-Off Flight with Charts for Use in Design". NACA TR-589, 1937.

46. Campbell, John P.; and Goodman, Alex: "A Semiempirical Method for Estimating the Rolling Moment Due to Yawing of Airplanes". NACA TN-1984, December 1949.

47. Cotter, William E., Jr.: "Summary and Analysis of Data on Damping in Yaw and Pitch for a Number of Airplane Models". NACA TN-1080, May 1946.

48. Campbell, John P.; and Mathews, Ward O.: "Experimental Determination of the Yawing Moment Due to Yawing Contributed by the Wing, Fuselage, and Vertical Tail of a Midwing Airplane Model". WR L-387, June 1943.

49. Pearson, Henry A.; and Jones, Robert T.: "Theoretical Stability and Control Characteristics of Wings with Various Amounts of Taper and Twist". NACA TR-635, 1938.

50. Etkin, Bernard: Dynamics of Flight, Stability and Control. John Wiley and Sons, Inc., 1959.

51. Goett, Harry J.; Jackson, Roy P.; and Belsley, Steven E.: "Wing-Tunnel Procedure for Determination of Critical Stability and Control Characteristics of Airplanes". NACA TR-781, 1944.

52. Langley Research Staff (compiled by Toll, Thomas A.): "Summary of Lateral-Control Research". NACA TR-868, 1947.

53. Faber, Stanley; and Crane, Harold L.: "A Longitudinal Control Feel System for In-flight Research on Response Feel". NASA TN D-632, January 1961.

54. Federal Aviation Agency: "Federal Aviation Regulations, Part 23, Airworthiness Standards Normal, Utility, and Acrobatic Category Airplanes". 1967.

55. Barber, Marvin R.; Jones, Charles K.; Sisk, Thomas R.; and Haise, Fred W.: "An Evaluation of the Handling Qualities of Seven General-Aviation Aircraft". NASA TN D-3726, November 1966.

56. Lay, L. W.; and Ikerd, L. R.: "Flying Qualities Tests Results". Cessna Rep. No. F-M337-12, January 1968.

57. Grantham, William D.; Moore, Frederick L.; Deal, Perry L.; and Patton, James M., Jr.: "Simulator Study of Coupled Roll-Spiral Mode Effects on Lateral-Directional Handling Qualities". NASA TN D-5466, March 1970.

58. Taylor, Lawrence W., Jr.; and Day, Richard E.: "Flight Controllability Limits and Related Human Transfer Functions as Determined from Simulator and Flight Tests". NASA TN D-746, May 1961.

59. McFadden, Norman M.; Vomaske, Richard F.; and Heinle, Donovan R.: "Flight Investigation Using Variable-Stability Airplanes of Minimum Stability Requirements for High-Speed, High-Altitude Vehicles". NASA TN D-779, April 1961.

60. Kuehnel, Helmut A.: "In-flight Measurement of the Time Required for a Pilot to Respond to an Aircraft Disturbance". NASA TN D-221, March 1960.

61. Russell, Walter R.; Sjoberg, S. A.; and Alford, William L.: "Flight Investigation of Automatic Stabilization of an Airplane Having Static Longitudinal Instability". NASA TN D-173, December 1959.

62. Adams, James J.: "A Simplified Method for Measuring Human Transfer Functions". NASA TN D-1782, April 1963.

63. Fink, Marvin P.; and Freeman, Delma C., Jr.: "Full-Scale Wind-Tunnel Investigation of Static Longitudinal and Lateral Characteristics of a Twin-Engine Airplane. NASA TN D-4983, January 1969.

64. Fink, Marvin P.; Freeman, Delma C., Jr.; and Greer, H. Douglas: "Full-Scale Wind-Tunnel Investigation of the Static Longitudinal and Lateral Characteristics of a Light Single-Engine Airplane". NASA TN D-5700, March 1970.

65. Shivers, James P.; Fink, Marvin P.; and Ware, George M.: "Full-Scale Wind-Tunnel Investigation of the Static Longitudinal and Lateral Characteristics of a Light Single-Engine Low-Wing Airplane". NASA TN D-5857, June 1970.

66. Jarvis, Calvin R.; Loschke, Paul C.; and Enevoldson, Einar K.: "Evaluation of the Effect of a Yaw-Rate Damper on the Flying Qualities of a Light Twin-Engine Airplane". NASA TN D-5890, July 1970.

67. Perkins, Courtland D.: "Development of Airplane Stability and Control Technology". Journal of Aircraft, July-August 1970.

68. Soulé, Hartley A.; and Miller, Marvel P.: "The Experimental Determination of the Moments of Inertia of Airplanes". NACA TR-467, 1933.

69. Gracey, William: "Measured Moments of Inertia of 32 Airplanes". NACA TN-780, October 1940.

70. Kirschbaum, H. W.: "Estimation of Moments of Inertia of Airplanes from Design Data". NACA TN-575, July 1936.

71. McCullough, George B.; and Gault, Donald E.: "Examples of Three Representative Types of Airfoil-Section Stall at Low Speed:. NACA TN-2502, September 1951.

72. Soulé, H. A.; and Anderson, R. F.: "Design Charts Relating to the Stalling of Tapered Wings". NACA TR-703, 1940.

73. Sweberg, Harold H.; and Dingeldein, Richard C.: "Summary of Measurements in Langley Full-Scale Tunnel of Maximum Lift Coefficients and Stalling Characteristics of Airplanes". NACA WR L-145, April 1945.

74. Jacobs, Eastman N.: "Tapered Wings, Tip Stalling, and Preliminary Results from Tests of the Stall-Control Flap". NACA WR L-296, November 1937.

75. Anderson, Seth B.: "Correlation of Pilot Opinion of Stall Warning with Flight Measurements of Various Factors which Produce the Warning". NACA TN-1868, April 1949.

76. Zalovcik, John A.: "Summary of Stall-Warning Devices". NACA TN-2676, May 1952.

77. Stone, Ralph W., Jr.; Garner, William G.; and Gale, Lawrence J.: "Study of Motion of Model of Personal-Owner or Liaison Airplane through the Stall and into the Incipient Spin by Means of a Free-Flight Testing Technique". NACA TN-2923, April 1953.

78. Bowman, James S.: "Airplane Spinning". NASA SP-83, May 1965.

79. Neihouse, Anshal I.; Klinar, Walter J.; and Scher, Stanley H.: "Status of Spin Research for Recent Airplane Designs". NASA TR R-57, 1960.

80. Neihouse, Anshal I.: "A Mass-Distribution Criterion for Predicting the Effect of Control Manipulation on the Recovery from a Spin". NACA WR L-168, August 1942.

81. Neihouse, Anshal I.; Lichtenstein, Jacob H.; and Pepoon, Philip W.: "Tail-Design Requirements for Satisfactory Spin Recovery". NACA TN-1045, April 1946.

82. Neihouse, A. I.: "Tail-Design Requirements for Satisfactory Spin Recovery for Personal-Owner-Type Light Airplanes". NACA TN-1329, June 1947.

83. Klinar, Walter J.; and Wilson, Jack H.: "Spin-Tunnel Investigation of the Effects of Mass and Dimensional Variations on the Spinning Characteristics of a Low-Wing Single-Vertical-Tail Model Typical of Personal-Owner Airplanes". NACA TN-2352, May 1951.

84. Seidman, Oscar; and Neihouse, A. I.: "Free-Spinning Wind-Tunnel Tests of a Low-Wing Monoplane with Systematic Changes in Wings and Tails - IV. Effect of Center-of-Gravity Location". NACA TR-672, 1939.

85. Siedman, Oscar; and Neihouse, A. I.: "Free-Spinning Wind-Tunnel Tests of a Low-Wing Monoplane with Systematic Changes in Wings and Tails - V. Effect of Airplane Relative Density". NACA TR-691, 1940.

86. Zimmerman, C. H.: "Effect of Changes in Tail Arrangement upon the Spinning of a Low-Wing Monoplane Model". NACA TN-570, June 1936.

87. Seidman, Oscar; and Neihouse, A. I.: "Free-Spinning Wind-Tunnel Tests of a Low-Wing Monoplane with Systematic Changes in Wings and Tails, I. Basic Loading Condition". NACA TN-608, August 1937.

88. Gale, Lawrence J.; and Jones, Ira P., Jr.: "Effects of Antispin Fillets and Dorsal Fins on the Spin and Recovery Characteristics of Airplanes as Determined from Free-Spinning-Tunnel Tests". NACA TN-1779, December 1948.

89. Klinar, Walter J.; and Gale, Lawrence J.: "Wind-Tunnel Investigation of the Spinning Characteristics of a Model of a Twin-Tail Low-Wing Personal-Owner-Type Airplane with Linked and Unlinked Rudder and Aileron Controls". NACA TN-1801, January 1949.

90. Headquarters, Air Force Systems Command: "Design Handbook, Series 1-0, General, Personnel Subsystems". AFSC DH 1-3, January 1969.

91. Morgan, C. T.; Cook, J. S.; Chapanis, A.; and Lund, M. W.: Human Engineering Guide to Equipment Design. McGraw-Hill, 1963.

92. Damon, Albert; Stroudt, Howard W.; and McFarland, Ross A.: The Human Body in Equipment Design. Cambridge, Harvard University Press, 1966.

93. Bureau of Aeronautics, Navy Department: "The Human Pilot". BU AER Rep. AE-61-4III, August 1954.

94. Woodson, Wesley E.; and Conover, Donald W.: Human Engineering Guide for Equipment Designers. University of California Press, 1964.

95. McCormick, Ernest J.: Human Factors Engineering. McGraw-Hill Book Company, 1964.

96. Orlansky, J.: "Psychological Aspects of Stick and Rudder Controls in Aircraft", Aeronautical Engineering Review. Vol. 8, January 8, 1949.

97. Tufts College, Institute of Applied Experimental Psychology: "Handbook of Human Engineering Data". Special Devices Center, Technical Report No. SDC 199-1-2, November 1952.

98. McFarland, Ross A.: Human Factors in Air Transportation. McGraw-Hill Book Company, Inc., 1953.

99. Harper, R. P.: "Flight Evaluations of Various Longitudinal Handling Qualities in a Variable Stability Jet Fighter". WADC TR-55-299, July 1955.

100. Sevant, C. J., Jr.: Control System Design. McGraw-Hill Book Company, Inc., 1964.

101. Wolowicz, Chester H.; and Holleman, Euclid C.: "Stability Derivative Determination from Flight Data." AGARD Report 224, October 1958.

102. Recant, Isidore G.; and Swanson, Robert S.: "Determination of the Stability and Control Characteristics of Airplanes from Flight Tests of Powered Models." NACA WR L-710, July 1942.

103. Katzoff, S.: "Longitudinal Stability and Control with Special Reference to Slipstream Effects." NACA TR-690, 1940.

104. Weil, Joseph; and Sleeman, William C., Jr.: "Perdiction of the Effects of Propeller Operation on the Static Longitudinal Stability of Single-Engine Tractor Monoplanes with Flaps Retracted." NACA TR-941, 1949.

105. Hagerman, John R.: "Wind-Tunnel Investigation of the Effect of Power and Flaps on the Static Longitudinal Stability and Control Characteristics of a Single-Engine High-Wing Airplane Model." NACA TN-1339, July 1947.

106. Hagerman, John R.: "Wind-Tunnel Investigation of the Effect of Power and Flaps on the Static Lateral Stability and Control Characteristics of a Single-Engine High-Wing Airplane Model." NACA TN-1379, July 1947.

107. Tamburello, Vito; and Weil, Joseph: "Wind-Tunnel Investigation of the Effect of Power and Flaps on the Static Lateral Characteristics of a Single-Engine Low-Wing Airplane Model." NACA TN-1327, June 1947.

108. Purser, Paul E.; and Spear, Margaret F.: "Wind-Tunnel Investigation of Effects of Unsymmetrical Horizontal-Tail Arrangements on Power-On Static Longitudinal Stability of a Single-Engine Airplane Model." NACA TN-1474, October 1947.

109. Schade, Robert O.: "Free-Flight Investigation of Dynamic Longitudinal Stability as Influenced by the Static Stability Measured in Wind-Tunnel Force Tests under Conditions of Constant Thrust and Constant Power." NACA TN-2075, April 1950.

110. Barber, Marvin R.; Jones, Charles K.; Sisk, Thomas R.; and Haise, Fred W.: "An Evaluation of the Handling Qualities of Seven General Aviation Aircraft." NASA TN D-3726, November 1966.

111. Marr, Roger L.: "A Method for Analyzing Power-on Static Longitudinal Stability." SAE Paper 700238, 1970.

112. Fink, Marvin P.; and Freeman, Delma C., Jr.: "Full-Scale Wind-Tunnel Investigation of Static Longitudinal and Lateral Characteristics of a Light Twin-Engine Airplane." NASA TN D-4983, January 1969.

113. Fink, Marvin P.; Freeman, Delma C., Jr.; and Greer, H. Douglas: "Full-Scale Wind-Tunnel Investigation of the Static Longitudinal and Lateral Characteristics of a Light Single-Engine Airplane." NASA TN D-5700, March 1970.

114. Ribner, Herbert S.: "Notes on the Propeller and Slipstream in Relation to Stability." NACA WR L-25, October 1944.

115. Ribner, Herbert S.: "Formulas for Propellers in Yaw and Charts of the Side-Force Derivative." NACA WR L-217, May 1943.

116. Ellis, David R.: "Flying Qualities Criteria for Small General Aviation Airplanes as Determined by In-Flight Simulation." SAE Paper 710373, March 24-26, 1971.

APPENDIX A

DERIVATION OF THE EQUATIONS OF MOTION

Derivation for the equations of motion, following Dynamics of the Airframe (Ref. 17), is based on Newton's laws, ie., motion with reference to axes fixed in space. The several assumptions which form the basis for this derivation will be presented throughout the following discussion as they are needed to clarify the various steps of the derivation. The first two of these assumptions specify the nature of the body being studied and the atmosphere in which it is set.

Assumption I — The airframe is assumed to be a rigid body; thus, the distance between any specified points in the body are invarient.

Assumption II — The earth is assumed to be fixed in space, and the earth's atmosphere is assumed to be fixed with respect to the earth.

Table A-1, with the aid of Figure A-1, defines the direction of the axes with respect to the airplane, as well as the nomenclature needed to apply Newton's laws.

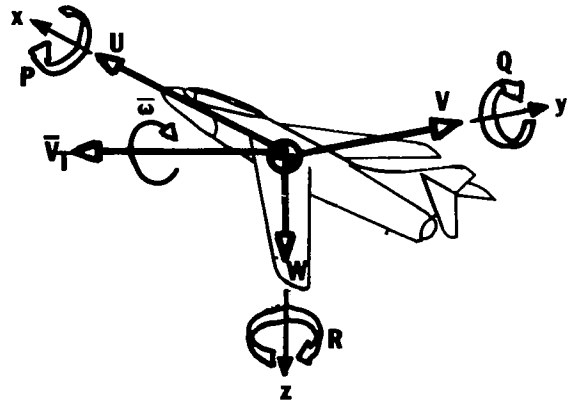

Figure A-1. Direction of the axes with respect to the airplane.

Axis	Linear Velocity Along Axis	Angular Velocity Along Axis	Summation of Moments About Axis	Summation of Forces Along Axis	Displacements About Axis	Moments of Momentum About Axis	Moment of Inertia
x	U	P Rolling Vel.	ΣL	ΣF_x	Φ	h_x	I_{xx}
y	V	Q Pitching Vel.	ΣM	ΣF_y	θ	h_y	I_{yy}
z	W	R Yawing Vel.	ΣN	ΣF_z	Ψ	h_z	I_{zz}

Table A-1. Direction of the axes with respect to the airplane and nomenclature needed to apply Newton's Laws.

Newton's second law of motion states that the rate of change of momentum of a body is proportional to the net force applied to the body and that the rate of change of the moment of momentum is proportional to the net torque applied to the body. The mathematical statements of the law can be written

$$\Sigma F_x = \frac{d}{dt}(mU)$$
$$\Sigma F_y = \frac{d}{dt}(mV)$$
$$\Sigma F_z = \frac{d}{dt}(mW) \qquad \text{(A-1)}$$

and

$$\Sigma L = \frac{dh_x}{dt}$$
$$\Sigma M = \frac{dh_y}{dt}$$
$$\Sigma N = \frac{dh_z}{dt} \qquad \text{(A-2)}$$

Assumption III The mass of the airplane is assumed to remain constant for the duration for any particular dynamic analysis.

Assumption III permits the mass of the airplane to be written outside the differentiation sign in Equations (A-1).

The moments of momentum referred to in Equations (A-2) can be expanded by using an element of mass of the airplane dm which is rotating with the angular velocity $\bar{\omega}(\bar{\omega} = Pi + Qj + Rk)$. This element of mass is at the point (x,y,z) measured relative to the c.g. of the airplane. The motion of the element of mass can be approximated by six linear velocity components (Py, Pz, Qx, Qz, Rx, and Ry), as seen in Figure A-2.

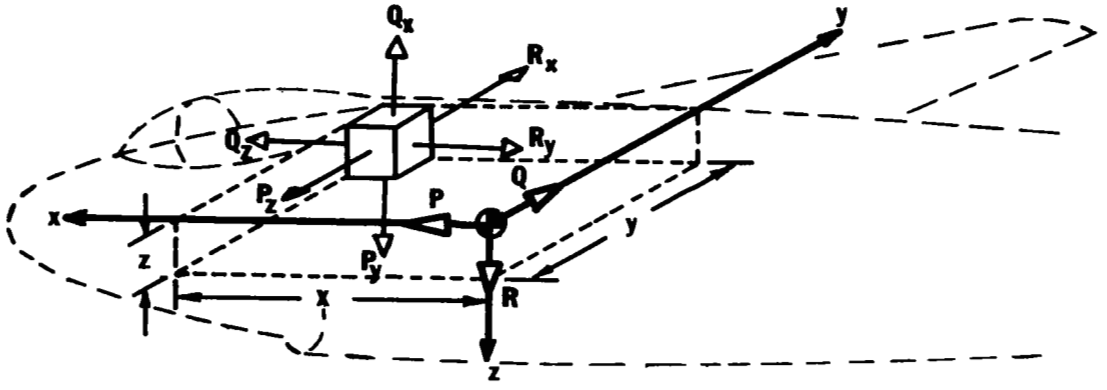

Figure A-2. Linear velocity components of an element of mass caused by an angular velocity $\bar{\omega}$ having components P, Q, and R.

The x, y, and z components of the moment of momentum are calculated by summing the moments of these velocity components about each axis and multiplying by mass dm. For example,

$$dh_x = y(yP)dm + z(zP)dm - z(xR)dm - y(xQ)dm.$$

Thus, if the moments are taken about the x, y, and z axes, the following set of equations is obtained:

$$\begin{aligned} dh_x &= (y^2 + z^2)P\ dm - zx\ R\ dm - yx\ Q\ dm \\ dh_y &= (z^2 + x^2)Q\ dm - xy\ P\ dm - yz\ R\ dm \\ dh_z &= (x^2 + y^2)R\ dm - zx\ P\ dm - zy\ Q\ dm \end{aligned} \qquad \text{(A-3)}$$

For a finite mass, the components of the moment of momentum are the integrals of Equations (A-3). Taking $I_{xx} = \int(y^2 + z^2)dm$, $I_{xz} = \int xzdm$, and $I_{yz} = I_{zy}$ the integral relations become

$$h_x = PI_{xx} - QI_{xy} - RI_{xz}$$

$$h_y = QI_{yy} - RI_{yz} - PI_{xy}$$

$$h_z = RI_{zz} - PI_{xz} - QI_{yz} \qquad \text{(A-4)}$$

The derivative dh/dt may be found by differentiating Equations (A-4) with respect to time. Thus, the equations of motion relative to inertial axes become

$$\Sigma F_x = m \frac{dU}{dt}$$

$$\Sigma F_y = m \frac{dV}{dt}$$

$$\Sigma F_z = m \frac{dW}{dt}$$

$$\Sigma L = \frac{dh_x}{dt} = \dot{P}I_{xx} + P\dot{I}_{xx} - \dot{Q}I_{xy} - Q\dot{I}_{xy} - \dot{R}I_{xz} - R\dot{I}_{xz}$$

$$\Sigma M = \frac{dh_y}{dt} = \dot{Q}I_{yy} + Q\dot{I}_{yy} - \dot{R}I_{yz} - R\dot{I}_{yz} - \dot{P}I_{xy} - P\dot{I}_{xy}$$

$$\Sigma N = \frac{dh_z}{dt} = \dot{R}I_{zz} + R\dot{I}_{zz} - \dot{P}I_{xz} - P\dot{I}_{xz} - \dot{Q}I_{yz} - Q\dot{I}_{yz} \qquad \text{(A-5)}$$

For ease in interpreting flight measurements, one desires to change the fixed axes system to an Eulerian axis system, ie., a right-hand system of orthogonal coordinate axes which has its origin at the center of gravity of the airplane and its orientation fixed with respect to the airplane. Velocities of the airplane measured relative to these axes are absolute velocities, since, at any instant, the Eulerian axes are considered to be fixed in space. Also, moments and products of inertia in the Eulerian axis system are independent of time, since these axes are fixed in the airplane; thus, dI/dt = 0. Since the Eulerian axis system moves with respect to inerital space, the absolute acceleration (measured in the Eulerian system) can be written

$$\bar{A}_{abs} = d\bar{V}_T/dt + \bar{\omega} \times \bar{V}_T$$

If U, V, and W are components of $\bar{V}_T$ and P, Q, and R are the components of $\bar{\omega}$, then

$$a_x = \dot{U} + QW - RV$$

$$a_y = \dot{V} + RU - PW$$

$$a_z = \dot{W} + PV - QU \qquad \text{(A-6)}$$

In a similar manner, the change in the moment of momentum can be written

$$d\bar{h}_{abs}/dt = d\bar{h}/dt + \bar{\omega} \times \bar{h}$$

$$\text{where } \bar{\omega} \times \bar{h} = \begin{vmatrix} i & j & k \\ P & Q & R \\ h_x & h_y & h_z \end{vmatrix}$$

Thus,

$$\left(\frac{dh_x}{dt}\right)_{abs} = \frac{dh_x}{dt} + h_zQ - h_yR$$

$$\left(\frac{dh_y}{dt}\right)_{abs} = \frac{dh_y}{dt} + h_xR - h_zP$$

$$\left(\frac{dh_z}{dt}\right)_{abs} = \frac{dh_z}{dt} + h_yP - h_xQ \qquad \text{(A-7)}$$

Assumption IV The xz plane is assumed to be a plane of symmetry.

Using Assumption IV and the orientation convention of Figure A-1, the equations of motion can be written

$$\Sigma F_x = m(\dot{U} + QW - RV)$$

$$\Sigma F_y = m(\dot{V} + RU - PW)$$

$$\Sigma F_z = m(\dot{W} + PV - QU)$$

$$\Sigma L = \dot{P}I_{xx} - \dot{R}I_{xz} + QR(I_{zz} - I_{yy}) - PQI_{xz}$$

$$\Sigma M = \dot{Q}I_{yy} + PR(I_{xx} - I_{zz}) - R^2I_{xz} + P^2I_{xz}$$

$$\Sigma N = \dot{R}I_{zz} - \dot{P}I_{xz} + PQ(I_{yy} - I_{xx}) + QRI_{xz} \qquad \text{(A-8)}$$

Eulerian angles are those angles through which one axis system must be rotated to superimpose it upon another having an initial angular displacement from the first. Because the angles are not orthogonal, the order of rotation is important, if the indicated operations are to yield correct results. The sequence of these angular changes are yaw, pitch, and roll. To carry out this superposition, one first yaws through a positive angle ψ in accordance with a right-hand system so that

$$\overline{X}_1 = \overline{X}\cos\psi + \overline{Y}\sin\psi$$

$$\overline{Y}_1 = \overline{Y}\cos\psi - \overline{X}\sin\psi$$

$$\overline{Z}_1 = \overline{Z} \qquad \text{(A-9)}$$

(see Figure A-3)

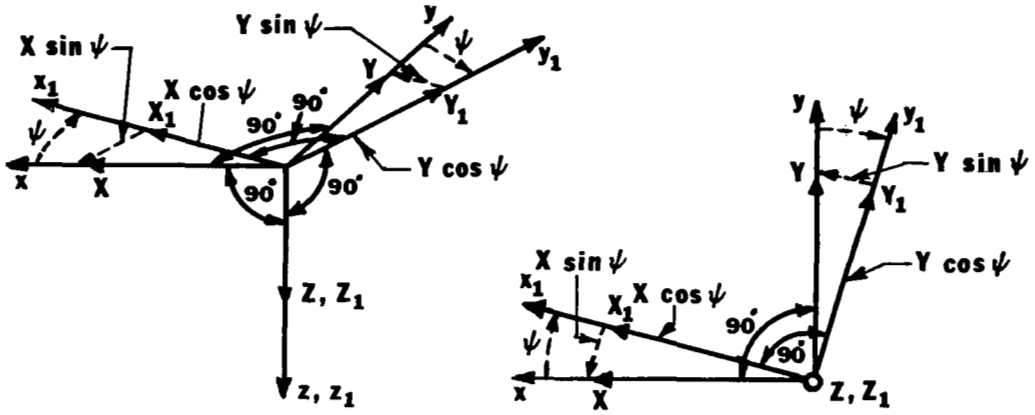

Figure A-3. Yaw through a positive angle ψ in accordance with a right-hand system.

The next rotation (Figure A-4) is a positive pitch through the angle θ, which gives

$$\overline{X}_2 = \overline{X}_1 \cos\theta - \overline{Z}_1 \sin\theta$$

$$\overline{Y}_2 = \overline{Y}_1$$

$$\overline{Z}_2 = \overline{Z}_1 \cos\theta + \overline{X}_1 \sin\theta \qquad \text{(A-10)}$$

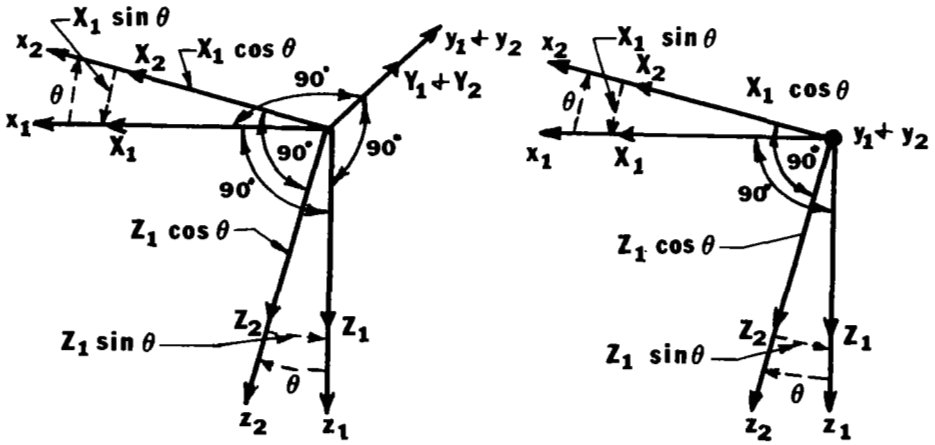

Figure A-4. Positive pitch through the angle θ.

The final rotation (Figure A-5) is through the roll angle ϕ, which gives

$$\begin{aligned}
\overline{X}_3 &= \overline{X}_2 \\
\overline{Y}_3 &= \overline{Y}_2 \cos\phi + \overline{Z}_2 \sin\phi \\
\overline{Z}_3 &= \overline{Z}_2 \cos\phi - \overline{Y}_2 \sin\phi
\end{aligned} \tag{A-11}$$

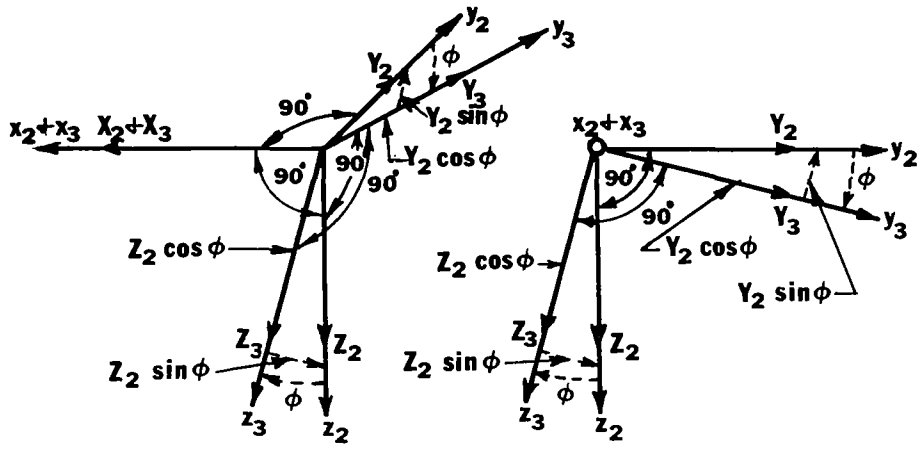

Figure A-5. Rotation through the roll angle ϕ.

Substituting Equations (A-9) and (A-10) into Equations (A-11) yields the transformation needed to convert the initial axis system to the final system:

$$\begin{aligned}
\overline{X}_3 &= \overline{X}\cos\theta\cos\psi + \overline{Y}\cos\theta\sin\psi - \overline{Z}\sin\theta \\
\overline{Y}_3 &= \overline{X}(\cos\psi\sin\theta\sin\phi - \sin\psi\cos\phi) \\
&\quad + \overline{Y}(\cos\psi\cos\phi + \sin\psi\sin\theta\sin\phi) \\
&\quad + \overline{Z}(\cos\theta\sin\phi) \\
\overline{Z}_3 &= \overline{X}(\cos\psi\sin\theta\cos\phi + \sin\psi\sin\phi) \\
&\quad + \overline{Y}(\sin\psi\sin\theta\cos\phi - \cos\psi\sin\phi) \\
&\quad + \overline{Z}(\cos\theta\cos\phi)
\end{aligned} \tag{A-12}$$

The analysis of flight motions is concerned primarily with the vehicle's behavior in response to disturbances from initial conditions. It is convenient, therefore, to chose as the initial conditions flight behavior for which the velocities and accelerations are well known and in which the aircraft spends most of its flight time. Equilibrium (unaccelerated) flight is flight along a straight

path during which the linear velocity vector measured relative to a fixed space is invarient, and the angular velocity is zero. "Steady flight" is flight during which the linear and angular velocities in the Eulerian reference frame remain constant. Hence, equilibrium flight and flight with constant angular velocity are both forms of steady flight.

Always acting on the aircraft even during periods of steady flight is gravity. Since it is unidirectional, it provides an orientation to the motion. The components of gravity acting along the steady flight aircraft axes relative to inertial space can be determined from Figure A-6 by direct resolution of the gravity force along the x_o, y_o, and z_o (steady flight) axes.

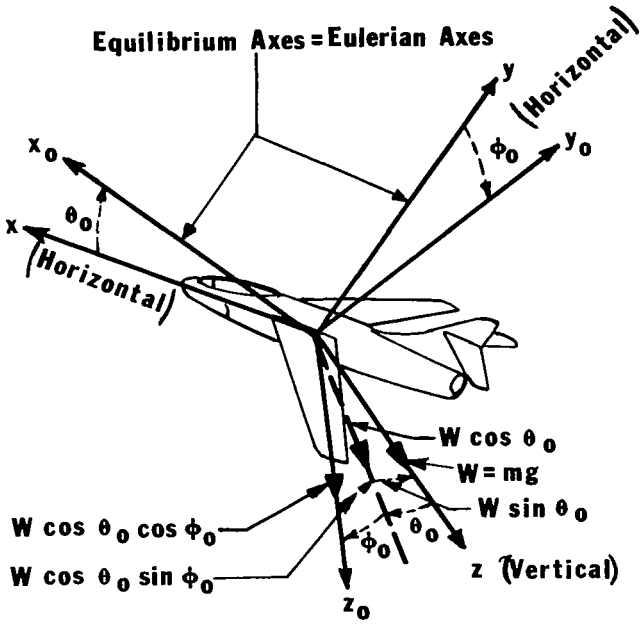

Figure A-6. Gravity acting on an airplane in steady flight with initial angles θ_o and ϕ_o with respect to the gravity vector.

Thus,

$$X_o = -W \sin \theta_o$$

$$Y_o = W \cos \theta_o \sin \phi_o$$

$$Z_o = W \cos \theta_o \cos \phi_o \qquad \text{(A-13)}$$

The components of gravity, acting along the disturbed Eulerian axes, are then

$$X_3 = (-W \sin \theta_o)\cos \theta \cos \psi + (W \cos \theta_o \sin \phi_o)\cos \theta \sin \psi$$

$$- (W \cos \theta_o \cos \phi_o)\sin \theta$$

$$
\begin{aligned}
Y_3 &= (-W \sin \theta_o)(\cos \psi \sin \theta \sin \phi - \sin \psi \cos \phi) \\
&\quad + (W \cos \theta_o \sin \phi_o)(\cos \psi \cos \phi + \sin \psi \sin \theta \sin \phi) \\
&\quad + (W \cos \theta_o \cos \phi_o)(\cos \theta \sin \phi) \\
Z_3 &= (-W \sin \theta_o)(\cos \psi \sin \theta \cos \phi + \sin \psi \sin \phi) \\
&\quad + (W \cos \theta_o \sin \phi_o)(\sin \psi \sin \theta \cos \phi - \cos \psi \sin \phi) \\
&\quad + (W \cos \theta_o \cos \phi_o)(\cos \theta \cos \phi) \qquad \text{(A-14)}
\end{aligned}
$$

The right-hand sides of Equations (A-8) express the aircraft acceleration in terms of the linear and angular velocities. The left-hand sides of Equations (A-8) represent the unbalanced forces (thrust forces, aerodynamic forces, and gravity forces) which produce the airplane motion. The gravity forces have already been expanded and transformed to the Eulerian axes (A-13); ideally, the same procedure could be applied to the thrust and aerodynamic forces. Because of the difficulty in expressing the aerodynamic and thrust forces explicitly in terms of the linear and angular velocities, it is customary to represent these forces by Taylor series expansions, taking a sufficient number of terms to insure adequate accuracy for the maneuver being considered.

Because of this special requirement, it is helpful to separate the aerodynamic and thrust forces from the gravity forces, thus:

$$
\begin{aligned}
\Sigma F_x &= \Sigma F'_x + X_3 \\
\Sigma F_y &= \Sigma F'_y + Y_3 \\
\Sigma F_z &= \Sigma F'_z + Z_3 \qquad \text{(A-15)}
\end{aligned}
$$

where the primed quantities are the summations of the aerodynamic and thrust forces, and X_3, Y_3, and Z_3 are the gravity components derived in Equations (A-14). It should be noted that, if the instant under consideration occurs during the steady flight condition, then $\theta = \phi = \psi = 0$, and the components X_3, Y_3, and Z_3 reduce to Equations (A-13). The force relations from Equations (A-8), with the gravity terms transposed to the right side, are rewritten

$$
\begin{aligned}
\Sigma F'_x &= m(\dot{U} + QW - RV) - X_3 \\
\Sigma F'_y &= m(\dot{V} + RU - PW) - Y_3 \\
\Sigma F'_z &= m(\dot{W} + PV - QU) - Z_3 \qquad \text{(A-16)}
\end{aligned}
$$

By substituting Equations (A-14) in Equations (A-16), Equations (A-8) may be written

$$\Sigma F'_x = m(\dot{U} + QW - RV) + (W \sin \theta_o)\cos \theta \cos \psi$$

$$-(W \cos \theta_o \sin \phi_o)\cos \theta \sin \psi + (W \cos \theta_o \cos \phi_o)\sin \theta$$

$$\Sigma F'_y = m(\dot{V} + RU - PW) + (W \sin \theta_o)(\cos \psi \sin \theta \sin \phi - \sin \psi \cos \phi)$$

$$-(W \cos \theta_o \sin \phi_o)(\cos \psi \cos \phi + \sin \psi \sin \theta \sin \phi)$$

$$-(W \cos \theta_o \cos \phi_o)(\cos \theta \sin \phi)$$

$$\Sigma F'_z = m(\dot{W} + PV - QU) + (W \sin \theta_o)(\cos \psi \sin \theta \cos \phi + \sin \psi \sin \phi)$$

$$-(W \cos \theta_o \sin \phi_o)(\sin \psi \sin \theta \cos \phi - \cos \psi \sin \phi)$$

$$-(W \cos \theta_o \cos \phi_o)(\cos \theta \cos \phi)$$

$$\Sigma L = \dot{P}I_{xx} - \dot{R}I_{xz} + QR(I_{zz} - I_{yy}) - PQI_{xz}$$

$$\Sigma M = \dot{Q}I_{yy} + PR(I_{xx} - I_{zz}) - R^2I_{xz} + P^2I_{xz}$$

$$\Sigma N = \dot{R}I_{zz} - \dot{P}I_{xz} + PQ(I_{yy} - I_{xx}) + QRI_{xz} \qquad \text{(A-17)}$$

These equations are then complete, except for the external forces and moments on the left side, which include aerodynamic and thrust forces as well as moments resulting from control surface deflections.

Definitions of the Eulerian axis system and the Eulerian angles, discussed above, show that the rates of change of the Eulerian angles $\dot{\psi}$, $\dot{\theta}$, and $\dot{\phi}$ are not orthogonal. The fixed axis angular velocities when written in terms of the rates of change of the Eulerian angles become

$$P = \dot{\phi} - \dot{\psi} \sin \theta$$

$$Q = \dot{\theta} \cos \phi + \dot{\psi} \sin \phi \cos \theta$$

$$R = \dot{\psi} \cos \phi \cos \theta - \dot{\theta} \sin \phi \qquad \text{(A-18)}$$

Equations (A-17) match the aerodynamic and thrust forces acting on an airplane to the gravity and resulting inertia forces. These equations are non-linear, since (1) they can contain products of the dependent variables and (2) the dependent variables appear as transcendental functions. The airframe motion can always be considered the result of disturbances to the airframe from some steady flight condition. Accordingly, each of the total instantaneous velocity components of the airframe can be written as the sum of a velocity component during the steady flight condition and a change in velocity caused by the disturbance:

$$U = U_o + u$$

$$V = V_o + v$$

$$W = W_o + w$$

$$P = P_o + p$$

$$Q = Q_o + q$$

$$R = R_o + r \qquad \text{(A-19)}$$

The zero subscripts of Equations (A-19) indicate the steady flight velocities, and the lower case letters represent the disturbance velocities. By substituting Equations (A-19) into Equations (A-17) and noting that derivatives with respect to time of the steady state conditions are zero, Equations (A-17) become

$$\begin{aligned}
\Sigma F'_x &= m[\dot{u} + Q_oW_o + W_oq + Q_ow + wq \\
&\quad - R_oV_o - R_ov - V_or - vr \\
&\quad + (g \sin\theta_o)\cos\theta\cos\psi - (g\cos\theta_o \sin\phi_o)\cos\theta\sin\psi \\
&\quad + (g\cos\theta_o\cos\phi_o)\sin\theta] \\
\Sigma F'_y &= m[\dot{v} + U_oR_o + U_or + R_ou + ru - P_oW_o - P_ow - W_op \\
&\quad - wp + (g\sin\theta_o)(\cos\psi\sin\theta\sin\phi - \sin\psi\cos\phi) \\
&\quad - (g\cos\theta_o\sin\phi_o)(\cos\psi\cos\phi + \sin\psi\sin\theta\sin\phi) \\
&\quad - (g\cos\theta_o\cos\phi_o)(\cos\theta\sin\phi)] \\
\Sigma F'_z &= m[\dot{w} + P_oV_o + P_ov + V_op + pv - Q_oU_o - Q_ou - U_oq - qu \\
&\quad + (g\sin\theta_o)(\cos\psi\sin\theta\cos\phi + \sin\psi\sin\phi) \\
&\quad - (g\cos\theta_o\sin\phi_o)(\sin\psi\sin\theta\cos\phi - \cos\psi\sin\phi) \\
&\quad - g(\cos\theta_o\cos\phi_o)(\cos\theta\cos\phi)] \\
\Sigma L &= \dot{p}I_{xx} - \dot{r}I_{xz} + (Q_oR_o + Q_or + R_oq + qr)(I_{zz} - I_{yy}) \\
&\quad - (P_oQ_o + P_oq + Q_op + pq)I_{xz} \\
\Sigma M &= \dot{q}I_{yy} + (P_oR_o + P_or + R_op + pr)(I_{xx} - I_{zz}) \\
&\quad - (R_o^2 + 2R_or + r^2)I_{xz} + (P_o^2 + 2P_op + p^2)I_{xz} \\
\Sigma N &= \dot{r}I_{zz} - \dot{p}I_{xz} + (P_oQ_o + P_oq + Q_op + pq)(I_{yy} - I_{xx}) \\
&\quad + (Q_oR_o + Q_or + R_oq + qr)I_{xz}
\end{aligned} \qquad \text{(A-20)}$$

Assumption V The disturbances from the steady flight condition are assumed to be small enough so that the products and squares of the changes in velocities are negligible in comparison to the changes themselves. Also, the disturbance angles are assumed to be small enough so that the sines of these angles may be set equal to the angles and the cosines set equal to one. Products of these angles are also approximately zero and can be neglected. Since the disturbances are small, the change in air density encountered by the airplane during any disturbance can be considered zero.

If Assumption V is applied to Equations (A-20), they become

$$\Sigma F'_x = m[\dot{u} + Q_oW_o + W_oq + Q_ow - R_oV_o - R_ov - V_or + g \sin\theta_o - (g \cos\theta_o \sin\phi_o)\psi + (g \cos\theta_o \cos\phi_o)\theta]$$

$$\Sigma F'_y = m[\dot{v} + U_oR_o + U_or + R_ou - P_oW_o - P_ow - W_op - (g \sin\theta_o)\psi - g \cos\theta_o \sin\phi_o - (g \cos\theta_o \cos\phi_o)\phi]$$

$$\Sigma F'_z = m[\dot{w} + P_oV_o + P_ov + V_op - Q_oU_o - Q_ou - U_oq + (g \sin\theta_o)\theta + (g \cos\theta_o \sin\phi_o)\phi - (g \cos\theta_o \cos\phi_o)]$$

$$\Sigma L = \dot{p}I_{xx} - \dot{r}I_{xz} + (Q_oR_o + Q_or + R_oq)(I_{zz} - I_{yy}) - (P_oQ_o + P_oq + Q_op)I_{xz}$$

$$\Sigma M = \dot{q}I_{yy} + (P_oR_o + P_or + R_op)(I_{xx} - I_{zz}) - (R_o^2 + 2R_or)I_{xz} + (P_o^2 + 2P_op)I_{xz}$$

$$\Sigma N = \dot{r}I_{zz} - \dot{p}I_{xz} + (P_oQ_o + P_oq + Q_op)(I_{yy} - I_{xx}) + (Q_oR_o + Q_or + R_oq)I_{xz} \qquad \text{(A-21)}$$

Equations (A-21) limit the applicability of the analysis to so-called small perturbations. In the strictly mathematical sense, Equations (A-21) are applicable only to infinitesimal disturbances; however, experience has shown that quite accurate results can be obtained by applying these equations to disturbances of finite, non-zero magnitude. An additional application of Assumption

V is the reduction of Equations (A-18) to

$$P = \dot{\phi} - \dot{\psi}\theta$$

$$Q = \dot{\theta} + \dot{\psi}\phi$$

$$R = \dot{\psi} - \dot{\theta}\phi \qquad \text{(A-22)}$$

If the products of perturbations are neglected, the above equations are reduced to

$$P = \dot{\phi}$$

$$Q = \dot{\theta}$$

$$R = \dot{\psi} \qquad \text{(A-23)}$$

Equations (A-23) show that, within the limits of small perturbation theory, the instantaneous angular velocities P, Q, and R may be set equal to the rates of change of the Eulerian angles.

Assumption VI During the steady flight condition, the airplane is assumed to be flying with wings level and with all components of velocity zero except U_o and W_o. Thus, $V_o = P_o = Q_o = R_o = \phi_o = \psi_o = 0$.

Assumption VI reduces the equations of motion to

$$\Sigma F'_x = m[\dot{u} + W_o q + g \sin\theta_o + g\theta \cos\theta_o]$$

$$\Sigma F'_y = m[\dot{v} + U_o r - W_o p - g\psi \sin\theta_o - g\phi \cos\theta_o]$$

$$\Sigma F'_z = m[\dot{w} - U_o q + g\theta \sin\theta_o - g \cos\theta_o]$$

$$\Sigma L = \dot{p}I_{xx} - \dot{r}I_{xz}$$

$$\Sigma M = \dot{q}I_{yy}$$

$$\Sigma N = \dot{r}I_{zz} - \dot{p}I_{xz} \qquad \text{(A-24)}$$

The aerodynamic forces and moments are then expressed in coefficient form as

$L = C_L \frac{1}{2}\rho V^2 S$ = Lift

$D = C_D \frac{1}{2}\rho V^2 S$ = Drag

$X = C_X \frac{1}{2}\rho V^2 S$ = Aerodynamic Force Along x Axis

$$Y = C_Y \tfrac{1}{2}\rho V^2 S \quad = \text{Aerodynamic Force Along y Axis}$$

$$Z = C_Z \tfrac{1}{2}\rho V^2 S \quad = \text{Aerodynamic Force Along z Axis}$$

$$L = C_l \tfrac{1}{2}\rho V^2 Sb \quad = \text{Rolling Moment}$$

$$M = C_m \tfrac{1}{2}\rho V^2 Sc \quad = \text{Pitching Moment}$$

$$N = C_n \tfrac{1}{2}\rho V^2 Sb \quad = \text{Yawing Moment} \qquad \text{(A-25)}$$

where

S = Wing Area

c = Mean Aerodynamic Chord = The wing chord which has the average characteristics of all chords in the wing.

b = Wing span

The lift and drag are the forces acting normal and parallel respectively to the flight path.

As noted previously, each of the forces and moments can be expressed as a function of the variables by expanding the forces and moments in a Taylor series. The series has the form

$$F = F_o + (\partial F/\partial \alpha)_o \alpha + (\partial F/\partial \beta)_o \beta + (\partial F/\partial \delta)_o \delta + \ldots \qquad \text{(A-26)}$$

where α, β, and δ are variables, and the subscript zero indicates that the quantities are evaluated at the steady flight condition. In Equation (A-26), terms of the order $(\partial^2 F/\partial \alpha^2)(\alpha^2/2!)$ and all higher order terms are omitted in accordance with Assumption V. Before expanding each of the forces and moments in the above form, a simplification can be made. Because the xz plane is a plane of symmetry, the rate of change of the X and Z forces and the moment M, with respect to the disturbance velocities p, r, and v, is zero. Thus, the forces and moments acting on a disturbed airplane can be expressed

$$X = X_o + \frac{\partial X}{\partial u} u + \frac{\partial X}{\partial \dot{u}} \dot{u} + \frac{\partial X}{\partial q} q + \frac{\partial X}{\partial \dot{q}} \dot{q} + \frac{\partial X}{\partial w} w + \frac{\partial X}{\partial \dot{w}} \dot{w} + \frac{\partial X}{\partial \delta_E} \delta_E$$

$$+ \frac{\partial X}{\partial \dot{\delta}_E} \dot{\delta}_E + \frac{\partial X}{\partial \ddot{\delta}_E} \ddot{\delta}_E + \frac{\partial X}{\partial \delta_F} \delta_F + \frac{\partial X}{\partial \dot{\delta}_F} \dot{\delta}_F$$

$$Y = Y_o + \frac{\partial Y}{\partial r} r + \frac{\partial Y}{\partial \dot{r}} \dot{r} + \frac{\partial Y}{\partial v} v + \frac{\partial Y}{\partial \dot{v}} \dot{v} + \frac{\partial Y}{\partial p} p + \frac{\partial Y}{\partial \dot{p}} \dot{p} + \frac{\partial Y}{\partial \delta_A} \delta_A$$

$$+ \frac{\partial Y}{\partial \dot{\delta}_A} \dot{\delta} + \frac{\partial Y}{\partial \ddot{\delta}_A} \ddot{\delta}_A + \frac{\partial Y}{\partial \delta_R} \delta_R + \frac{\partial Y}{\partial \dot{\delta}_R} \dot{\delta}_R + \frac{\partial Y}{\partial \ddot{\delta}_R} \ddot{\delta}_R$$

$$
\begin{aligned}
Z &= Z_o + \frac{\partial Z}{\partial u} u + \frac{\partial Z}{\partial \dot{u}} \dot{u} + \frac{\partial Z}{\partial q} q + \frac{\partial Z}{\partial \dot{q}} \dot{q} + \frac{\partial Z}{\partial w} w + \frac{\partial Z}{\partial \dot{w}} \dot{w} + \frac{\partial Z}{\partial \delta_E} \delta_E \\
&\quad + \frac{\partial Z}{\partial \dot{\delta}_E} \dot{\delta}_E + \frac{\partial Z}{\partial \ddot{\delta}_E} \ddot{\delta}_E + \frac{\partial Z}{\partial \delta_F} \delta_F + \frac{\partial Z}{\partial \dot{\delta}_F} \dot{\delta}_F \\
L &= L_o + \frac{\partial L}{\partial r} r + \frac{\partial L}{\partial \dot{r}} \dot{r} + \frac{\partial L}{\partial v} v + \frac{\partial L}{\partial \dot{v}} \dot{v} + \frac{\partial L}{\partial p} p + \frac{\partial L}{\partial \dot{p}} \dot{p} + \frac{\partial L}{\partial \delta_A} \delta_A \\
&\quad + \frac{\partial L}{\partial \dot{\delta}_A} \dot{\delta}_A + \frac{\partial L}{\partial \ddot{\delta}_A} \ddot{\delta}_A + \frac{\partial L}{\partial \delta_R} \delta_R + \frac{\partial L}{\partial \dot{\delta}_R} \dot{\delta}_R + \frac{\partial L}{\partial \ddot{\delta}_R} \ddot{\delta}_R \\
M &= M_o + \frac{\partial M}{\partial u} u + \frac{\partial M}{\partial \dot{u}} \dot{u} + \frac{\partial M}{\partial q} q + \frac{\partial M}{\partial \dot{q}} \dot{q} + \frac{\partial M}{\partial w} w + \frac{\partial M}{\partial \dot{w}} \dot{w} + \frac{\partial M}{\partial \delta_E} \delta_E \\
&\quad + \frac{\partial M}{\partial \dot{\delta}_E} \dot{\delta}_E + \frac{\partial M}{\partial \ddot{\delta}_E} \ddot{\delta}_E + \frac{\partial M}{\partial \delta_F} \delta_F + \frac{\partial M}{\partial \dot{\delta}_F} \dot{\delta}_F \\
N &= N_o + \frac{\partial N}{\partial v} v + \frac{\partial N}{\partial \dot{v}} \dot{v} + \frac{\partial N}{\partial r} r + \frac{\partial N}{\partial \dot{r}} \dot{r} + \frac{\partial N}{\partial p} p + \frac{\partial N}{\partial \dot{p}} \dot{p} + \frac{\partial N}{\partial \delta_R} \delta_R \\
&\quad + \frac{\partial N}{\partial \dot{\delta}_R} \dot{\delta}_R + \frac{\partial N}{\partial \ddot{\delta}_R} \ddot{\delta}_R + \frac{\partial N}{\partial \delta_A} \delta_A + \frac{\partial N}{\partial \dot{\delta}_A} \dot{\delta}_A + \frac{\partial N}{\partial \ddot{\delta}_A} \ddot{\delta}_A
\end{aligned}
\qquad \text{(A-27)}
$$

where

δ_E = Angle of deflection of elevator

δ_F = Angle of deflection of flaps

δ_A = Angle of deflection of ailerons

δ_R = Angle of deflection of rudder

The thrust force previously mentioned in Equations (A-15) can be introduced into the equations of motion in much the same way as the gravity force was introduced. The thrust in considered to be a function of the power plant revolutions per minute and the forward speed of the airplane. With the power plant located in the plane of symmetry, the thrust contributes to the X and Z forces and to the moment M. With the aid of Figure A-7, it is evident that, by setting the steady flight thrust equal to T_o, the equations for the steady flight condition become

$$
\begin{aligned}
X_o &= T_o \cos \xi \\
Z_o &= - T_o \sin \xi \\
M_o &= T_o z_j
\end{aligned}
\qquad \text{(A-28)}
$$

where ξ = angle between x axis and thrust line
z_j = perpendicular distance from c.g. to thrust line

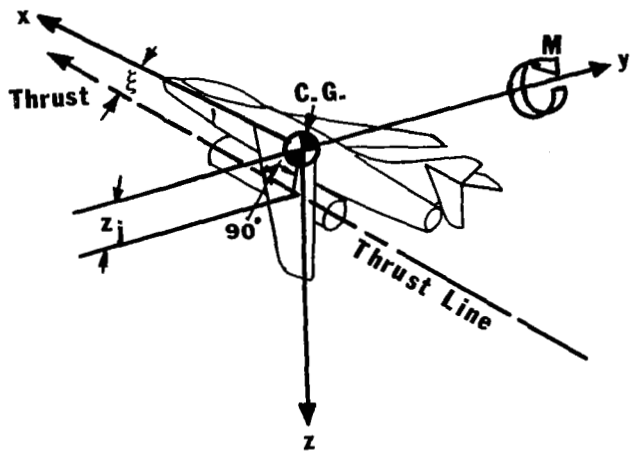

Figure A-7. Thrust force relationship to X and Z forces and moment M.

Since the Eulerian axes remain fixed with reference to the airplane during a disturbance, the thrust components relative to the disturbed axes become

$$X = T_1 \cos \xi$$

$$Z = - T_1 \sin \xi$$

$$M = T_1 z_j \qquad \text{(A-29)}$$

where T_1 (the thrust during the disturbance) $= T_o + \Delta T$

If a Taylor series expansion is assumed, then

$$\Delta T = \frac{\partial T}{\partial u} u + \frac{\partial T}{\partial \delta_{RPM}} \delta_{RPM}$$

Thus,

$$X = T_o \cos \xi + (\cos \xi) \frac{\partial T}{\partial u} u + (\cos \xi) \frac{\partial T}{\partial \delta_{RPM}} \delta_{RPM}$$

$$Z = - T_o \sin \xi - (\sin \xi) \frac{\partial T}{\partial u} u - (\sin \xi) \frac{\partial T}{\partial \delta_{RPM}} \delta_{RPM}$$

$$M = T_o z_j + z_j \frac{\partial T}{\partial u} u + z_j \frac{\partial T}{\partial \delta_{RPM}} \delta_{RPM} \qquad \text{(A-30)}$$

The individual contributions to the equations of motion have now been examined in some detail, giving perhaps some insight into the basis of the complete equations of motion of the airframe. Before continuing, however, it is well to

note that the equations for steady flight can be found by substituting the steady flight values of the aerodynamic, weight and thrust forces and moments into Equations (A-24) and setting the disturbance terms equal to zero:

$$
\begin{aligned}
X_o - W \sin\theta_o + T_o \cos\xi &= 0 \\
Y_o + \quad 0 \quad + \quad 0 \quad &= 0 \\
Z_o + W \cos\theta_o - T_o \sin\xi &= 0 \\
L_o + \quad 0 \quad + \quad 0 \quad &= 0 \\
M_o + \quad 0 \quad + T_o z_j \quad &= 0 \\
N_o + \quad 0 \quad + \quad 0 \quad &= 0
\end{aligned}
\qquad \text{(A-31)}
$$

The equations of motion for the disturbed airplane are then found by substituting the disturbed values of the forces and moments into Equations (A-24):

$$
\begin{aligned}
m\left[\dot{u} + W_o q + \boxed{g \sin\theta_o} + g\theta \cos\theta_o\right] &= \boxed{X_o} + \frac{\partial X}{\partial u} u + \frac{\partial X}{\partial \dot{u}} \dot{u} \\
&+ \frac{\partial X}{\partial q} q + \frac{\partial X}{\partial \dot{q}} \dot{q} + \frac{\partial X}{\partial w} w + \frac{\partial X}{\partial \dot{w}} \dot{w} + \frac{\partial X}{\partial \delta_E} \delta_E + \frac{\partial X}{\partial \dot{\delta}_E} \dot{\delta}_E + \frac{\partial X}{\partial \ddot{\delta}_E} \ddot{\delta}_E + \frac{\partial X}{\partial \delta_F} \delta_F \\
&+ \frac{\partial X}{\partial \dot{\delta}_F} \dot{\delta} + \boxed{T_o \cos\xi} + (\cos\xi) \frac{\partial T}{\partial u} u + (\cos\xi) \frac{\partial T}{\partial \delta_{RPM}} \delta_{RPM} \\
m\left[\dot{v} + U_o r - W_o p - g\psi \sin\theta_o - (g \cos\theta_o)\phi\right] &= \boxed{Y_o} + \frac{\partial Y}{\partial r} r + \frac{\partial Y}{\partial \dot{r}} \dot{r} + \frac{\partial Y}{\partial v} v \\
&+ \frac{\partial Y}{\partial \dot{v}} \dot{v} + \frac{\partial Y}{\partial p} p + \frac{\partial Y}{\partial \dot{p}} \dot{p} + \frac{\partial Y}{\partial \delta_A} \delta_A + \frac{\partial Y}{\partial \dot{\delta}_A} \dot{\delta}_A + \frac{\partial Y}{\partial \ddot{\delta}_A} \ddot{\delta}_A + \frac{\partial Y}{\partial \delta_R} \delta_R + \frac{\partial Y}{\partial \dot{\delta}_R} \dot{\delta}_R + \frac{\partial Y}{\partial \ddot{\delta}_R} \ddot{\delta}_R \\
m\left[\dot{w} - U_o q + g\theta \sin\theta_o - \boxed{g \cos\theta_o}\right] &= \boxed{Z_o} + \frac{\partial Z}{\partial u} u + \frac{\partial Z}{\partial \dot{u}} \dot{u} + \frac{\partial Z}{\partial q} q + \frac{\partial Z}{\partial \dot{q}} \dot{q} \\
&+ \frac{\partial Z}{\partial w} w + \frac{\partial Z}{\partial \dot{w}} \dot{w} + \frac{\partial Z}{\partial \delta_E} \delta_E + \frac{\partial Z}{\partial \dot{\delta}_E} \dot{\delta}_E + \frac{\partial Z}{\partial \ddot{\delta}_E} \ddot{\delta}_E + \frac{\partial Z}{\partial \delta_F} \delta_F + \frac{\partial Z}{\partial \dot{\delta}_F} \dot{\delta}_F \\
&- \boxed{T_o \sin\xi} - (\sin\xi) \frac{\partial T}{\partial u} u - (\sin\xi) \frac{\partial T}{\partial \delta_{RPM}} \delta_{RPM} \\
\dot{p} I_{xx} - \dot{r} I_{xz} &= \boxed{L_o} + \frac{\partial L}{\partial r} r + \frac{\partial L}{\partial \dot{r}} \dot{r} + \frac{\partial L}{\partial v} v + \frac{\partial L}{\partial \dot{v}} \dot{v} + \frac{\partial L}{\partial p} p + \frac{\partial L}{\partial \dot{p}} \dot{p} + \frac{\partial L}{\partial \delta_A} \delta_A \\
&+ \frac{\partial L}{\partial \dot{\delta}_A} \dot{\delta}_A + \frac{\partial L}{\partial \ddot{\delta}_A} \ddot{\delta}_A + \frac{\partial L}{\partial \delta_R} \delta_R + \frac{\partial L}{\partial \dot{\delta}_R} \dot{\delta}_R + \frac{\partial L}{\partial \ddot{\delta}_R} \ddot{\delta}_R
\end{aligned}
$$

$$\dot{q}I_{yy} = \boxed{M_o} + \frac{\partial M}{\partial u}u + \frac{\partial M}{\partial \dot{u}}\dot{u} + \frac{\partial M}{\partial q}q + \frac{\partial M}{\partial \dot{q}}\dot{q} + \frac{\partial M}{\partial w}w + \frac{\partial M}{\partial \dot{w}}\dot{w} + \frac{\partial M}{\partial \delta_E}\delta_E + \frac{\partial M}{\partial \dot{\delta}_E}\dot{\delta}_E$$
$$+ \frac{\partial M}{\partial \ddot{\delta}_E}\ddot{\delta}_E + \frac{\partial M}{\partial \delta_F}\delta_F + \frac{\partial M}{\partial \dot{\delta}_F}\dot{\delta}_F + \boxed{T_o z_j} + z_j\frac{\partial T}{\partial u}u + z_j\frac{\partial T}{\partial \delta_{RPM}}\delta_{RPM}$$
$$\dot{r}I_{zz} - \dot{p}I_{xz} = \boxed{N_o} + \frac{\partial N}{\partial v}v + \frac{\partial N}{\partial \dot{v}}\dot{v} + \frac{\partial N}{\partial r}r + \frac{\partial N}{\partial \dot{r}}\dot{r} + \frac{\partial N}{\partial p}p + \frac{\partial N}{\partial \dot{p}}\dot{p} + \frac{\partial N}{\partial \delta_R}\delta_R$$
$$+ \frac{\partial N}{\partial \dot{\delta}_R}\dot{\delta}_R + \frac{\partial N}{\partial \ddot{\delta}_R}\ddot{\delta}_R + \frac{\partial N}{\partial \delta_A}\delta_A + \frac{\partial N}{\partial \dot{\delta}_A}\dot{\delta}_A + \frac{\partial N}{\partial \ddot{\delta}_A}\ddot{\delta}_A \qquad \text{(A-32)}$$

The quantities in boxes disappear because of the steady flight conditions of Equations (A-31). Dividing the force equations by the mass m and the moment equations by the appropriate moments of inertia yields terms of the form

$$\frac{1}{m}\frac{\partial X}{\partial u}u \text{ and } \frac{1}{I_{xx}}\frac{\partial L}{\partial r}r.$$

Replacing $(1/m)(\partial X/\partial u)$ by X_u and $(1/I_{xx})(\partial L/\partial r)$ by L_r simplifies the notation. These quantities are called either "dimensional stability derivatives" or simply "stability derivatives." By eliminating those terms whose sum, in accordance with Equations (A-32), is zero because of the steady flight conditions, and by using the previous shorthand notation, Equations (A-32) are reduced to the form:

$$\dot{u} + W_o q + g\theta\cos\theta_o = X_u u + X_{\dot{u}}\dot{u} + X_q q + X_{\dot{q}}\dot{q} + X_w w + X_{\dot{w}}\dot{w} + X_{\delta_E}\delta_E$$
$$+ X_{\dot{\delta}_E}\dot{\delta}_E + X_{\ddot{\delta}_E}\ddot{\delta}_E + X_{\delta_F}\delta_F + X_{\dot{\delta}_F}\dot{\delta}_F + \cos\xi\, T_u u + \cos\xi\, T_{\delta_{RPM}}\delta_{RPM}$$
$$\dot{v} + U_o r - W_o p - g\psi\sin\theta_o - g\phi\cos\theta_o = Y_r r + Y_{\dot{r}}\dot{r} + Y_v v + Y_{\dot{v}}\dot{v}$$
$$+ Y_p p + Y_{\dot{p}}\dot{p} + Y_{\delta_A}\delta_A + Y_{\dot{\delta}_A}\dot{\delta}_A + Y_{\ddot{\delta}_A}\ddot{\delta}_A + Y_{\delta_R}\delta_R + Y_{\dot{\delta}_R}\dot{\delta}_R + Y_{\ddot{\delta}_R}\ddot{\delta}_R$$
$$\dot{w} - U_o q + g\theta\sin\theta_o = Z_u u + Z_{\dot{u}}\dot{u} + Z_q q + Z_{\dot{q}}\dot{q} + Z_w w + Z_{\dot{w}}\dot{w} + Z_{\delta_E}\delta_E$$
$$+ Z_{\dot{\delta}_E}\dot{\delta}_E + Z_{\ddot{\delta}_E}\ddot{\delta}_E + Z_{\delta_F}\delta_F + Z_{\dot{\delta}_F}\dot{\delta}_F - (\sin\xi)T_u u - (\sin\xi)T_{\delta_{RPM}}\delta_{RPM}$$
$$\dot{p} - \dot{r}\frac{I_{xz}}{I_{xx}} = L_r r + L_{\dot{r}}\dot{r} + L_v v + L_{\dot{v}}\dot{v} + L_p p + L_{\dot{p}}\dot{p} + L_{\delta_A}\delta_A + L_{\dot{\delta}_A}\dot{\delta}_A$$
$$+ L_{\ddot{\delta}_A}\ddot{\delta}_A + L_{\delta_R}\delta_R + L_{\dot{\delta}_R}\dot{\delta}_R + L_{\ddot{\delta}_R}\ddot{\delta}_R$$
$$\dot{q} = M_u u + M_{\dot{u}}\dot{u} + M_q q + M_{\dot{q}}\dot{q} + M_w w + M_{\dot{w}}\dot{w} + M_{\delta_E}\delta_E + M_{\dot{\delta}_E}\dot{\delta}_E + M_{\ddot{\delta}_E}\ddot{\delta}_E$$
$$+ M_{\delta_F}\delta_F + M_{\dot{\delta}_F}\dot{\delta}_F + \frac{z_j m}{I_{yy}}T_u u + \frac{z_j m}{I_{yy}}T_{\delta_{RPM}}\delta_{RPM}$$
$$\dot{r} - \dot{p}\frac{I_{xz}}{I_{zz}} = N_v v + N_{\dot{v}}\dot{v} + N_r r + N_{\dot{r}}\dot{r} + N_p p + N_{\dot{p}}\dot{p} + N_{\delta_R}\delta_R + N_{\dot{\delta}_R}\dot{\delta}_R$$
$$+ N_{\ddot{\delta}_R}\ddot{\delta}_R + N_{\delta_A}\delta_A + N_{\dot{\delta}_A}\dot{\delta}_A + N_{\ddot{\delta}_A}\ddot{\delta}_A \qquad \text{(A-33)}$$

Assumption VII The flow is assumed to be quasi-steady.

Because of Assumption VII, all derivatives with respect to the rates of change of velocities are ommitted, with the exception of those involving $\dot{w}$, which are retained to account for the effect on the horizontal tail of the downwash from the wing. It should also be pointed out that the change in angle of attack can be approximated by $\Delta\alpha = w/U$.

The only restrictions thus far imposed on the orientation of the Eulerian axes with respect to the airplane are that the y axis be a principal axis and that the origin be located at the center of gravity of the airplane. When the x axis is oriented so that it is a principal axis, the Eulerian axes are referred to as principal axes, but when the x axis in the airplane is parallel to the relative wind during steady flight, the Eulerian axes are referred to as stability axes. When the airframe is disturbed from the steady flight condition, the Eulerian axes rotate with the airframe and do not change direction with respect to the airplane. Consequently, the disturbed x axis may or may not be parallel to the relative wind while the airplane is in the disturbed flight condition. It should be noted that for small angles of attack the moments of inertia about the stability axes are approximately equal to those about the body axes; however, at low speeds (high angles of attack) the moments of inertia about the stability axes can differ significantly from those about the body axes and this fact should be considered in dynamic analyses. The use of the stability axes eliminates the terms containing W_o from Equations (A-33) by eliminating the following quantities: (1) all terms containing W_o, which disappears because of the direction of the stability axes; (2) all aerodynamic partial derivatives with respect to rates of change of velocities, except those with respect to W; and (3) all aerodynamic partial derivatives with respect to rates of change of control surface deflections. Equations (A-33) then reduce to Equations (A-34 and (A-35). To avoid confusion with body axis coordinate systems, where θ_o is the inclination of the x axis with respect to the horizon, the angles between the horizontal and the x stability axis is called γ_o. It will be recognized that because of the way the stability axis system is defined γ_o is indeed the angle of the flight path with respect to the earth.

$$\dot{u} + g\theta \cos \gamma_o = T_u(\cos \xi)u + T_{\delta_{RPM}}\delta_{RPM} \cos \xi + X_u u + X_q q + X_w w + X_{\dot{w}}\dot{w} + X_{\delta_E}\delta_E + X_{\delta_F}\delta_F$$

$$\dot{w} - U_o q + g\theta \sin \gamma_o = - T_u(\sin \xi)u - T_{\delta_{RPM}}\delta_{RPM} \sin \xi + Z_u u + Z_q q + Z_w w + Z_{\dot{w}}\dot{w} + Z_{\delta_E}\delta_E + Z_{\delta_F}\delta_F$$

$$\dot{q} = \frac{z_{jm}}{I_{yy}} T_u u + \frac{z_{jm}}{I_{yy}} T_{\delta_{RPM}}\delta_{RPM} + M_u u + M_q q + M_w w + M_{\dot{w}}\dot{w} + M_{\delta_E}\delta_E + M_{\delta_F}\delta_F \qquad \text{(A-34)}$$

$$\dot{v} + U_o r - g\psi \sin \gamma_o - g\phi \cos \gamma_o = Y_r r + Y_v v$$
$$+ Y_p p + Y_{\delta_A} \delta_A + Y_{\delta_R} \delta_R$$
$$\dot{p} - \frac{I_{xz}}{I_{xx}} \dot{r} = L_r r + L_v v + L_p p + L_{\delta_A} \delta_A + L_{\delta_R} \delta_R$$
$$\dot{r} - \frac{I_{xz}}{I_{zz}} \dot{p} = N_r r + N_v v + N_p p + N_{\delta_A} \delta_A + N_{\delta_R} \delta_R \qquad \text{(A-35)}$$

An examination of these equations shows that Equations (A-34) are functions of the variables u, θ, and w, whereas Equations (A-35) are functions of the variables v, r, and p. As a result of the assumptions made in this analysis, the equations of motion can be treated as two independent sets of three equations with Equations (A-34) describing the longitudinal or x-z plane motions and Equations (A-35) the lateral motions.

APPENDIX B

DEFINITION OF STABILITY DERIVATIVES

In this appendix the dimensional stability derivatives which appeared in the equations of motion are defined. For each dimensional stability derivative an equation is given which, for the most part, relates it to a non-dimensional derivative thus simplifying the evaluation of the dimensional derivatives.

Longitudinal Stability Derivatives:

$$X_u = \frac{\rho US}{m}\left(-\frac{U}{2}\frac{\partial C_D}{\partial u} - C_D\right)$$

$$Z_u = \frac{\rho US}{m}\left(-\frac{U}{2}\frac{\partial C_L}{\partial u} - C_L\right)$$

$$M_u = \frac{\rho USc}{I_{yy}}\left(\frac{U}{2}\frac{\partial C_m}{\partial u} + C_m\right)$$

$$T_u = \frac{\rho US}{m}\left(\frac{U}{2}\frac{\partial C_T}{\partial u} + C_T\right)$$

$$X_w = \frac{\rho US}{2m}\left(C_L - \frac{\partial C_D}{\partial \alpha}\right)$$

$$Z_w = \frac{\rho US}{2m}\left(-\frac{\partial C_L}{\partial \alpha} - C_D\right)$$

$$M_w = \frac{\rho USc}{2I_{yy}}\frac{\partial C_m}{\partial \alpha}$$

$$X_{\dot{w}} = -\frac{\rho Sc}{4m}\frac{\partial C_D}{\partial\left(\frac{\dot{\alpha}c}{2U}\right)} \simeq 0$$

$$Z_{\dot{w}} = -\frac{\rho Sc}{4m}\frac{\partial C_L}{\partial\left(\frac{\dot{\alpha}c}{2U}\right)}$$

$$M_{\dot{w}} = \frac{\rho Sc^2}{4I_{yy}}\frac{\partial C_m}{\partial\left(\frac{\dot{\alpha}c}{2U}\right)}$$

$$X_q = -\frac{\rho USc}{4m}\frac{\partial C_D}{\partial\left(\frac{qc}{2U}\right)} \simeq 0$$

$$Z_q = -\frac{\rho USc}{4m}\frac{\partial C_L}{\partial\left(\frac{qc}{2U}\right)}$$

$$M_q = \frac{\rho U S c^2}{4 I_{yy}} \frac{\partial C_m}{\partial \left(\frac{qc}{2U}\right)}$$

$$T_{\delta_{RPM}} = \frac{30\ \rho U S c}{m} \frac{\partial C_T}{\partial \left(\frac{30\ c}{u}\ \delta_{RPM}\right)}$$

$$X_{\delta_E} = - \frac{\rho U^2 S}{2m} \frac{\partial C_D}{\partial \delta_E}$$

$$Z_{\delta_E} = - \frac{\rho U^2 S}{2m} \frac{\partial C_L}{\partial \delta_E}$$

$$M_{\delta_E} = \frac{\rho U^2 S c}{2 I_{yy}} \frac{\partial C_m}{\partial \delta_E}$$

$$X_{\delta_F} = - \frac{\rho U^2 S}{2m} \frac{\partial C_D}{\partial \delta_F}$$

$$Z_{\delta_F} = - \frac{\rho U^2 S c}{2m} \frac{\partial C_L}{\partial \delta_F}$$

$$M_{\delta_F} = \frac{\rho U^2 S c}{2 I_{yy}} \frac{\partial C_m}{\partial \delta_F}$$

Lateral Stability Derivatives:

$$Y_v = \frac{\rho U S}{2m} \frac{\partial C_y}{\partial \beta}$$

$$L_v = \frac{\rho U S b}{2 I_{xx}} \frac{\partial C_\ell}{\partial \beta}$$

$$L_\beta = U_o L_v$$

$$N_v = \frac{\rho U S b}{2 I_{zz}} \frac{\partial C_n}{\partial \beta}$$

$$N_\beta = U_o N_v$$

$$Y_p = \frac{\rho U S b}{4m} \frac{\partial C_y}{\partial \left(\frac{pb}{2U}\right)}$$

$$L_p = \frac{\rho U S b^2}{4 I_{xx}} \frac{\partial C_\ell}{\partial \left(\frac{pb}{2U}\right)}$$

$$N_p = \frac{\rho U S b^2}{4 I_{zz}} \frac{\partial C_n}{\partial \left(\frac{pb}{2U}\right)}$$

$$Y_r = \frac{\rho U S b}{4m} \frac{\partial C_y}{\partial \left(\frac{rb}{2U}\right)}$$

$$L_r = \frac{\rho U S b^2}{4 I_{xx}} \frac{\partial C_\ell}{\partial \left(\frac{rb}{2U}\right)}$$

$$N_r = \frac{\rho U S b^2}{4 I_{zz}} \frac{\partial C_n}{\partial \left(\frac{rb}{2U}\right)}$$

$$Y_{\delta_R} = \frac{\rho U^2 S}{2m} \frac{\partial C_y}{\partial \delta_R}$$

$$L_{\delta_R} = \frac{\rho U^2 S b}{2 I_{xx}} \frac{\partial C_\ell}{\partial \delta_R}$$

$$N_{\delta_R} = \frac{\rho U^2 S b}{2 I_{zz}} \frac{\partial C_n}{\partial \delta_R}$$

$$Y_{\delta_A} = \frac{\rho U^2 S}{2m} \frac{\partial C_y}{\partial \delta_A}$$

$$L_{\delta_A} = \frac{\rho U^2 S b}{2 I_{xx}} \frac{\partial C_\ell}{\partial \delta_A}$$

$$N_{\delta_A} = \frac{\rho U^2 S b}{2 I_{zz}} \frac{\partial C_n}{\partial \delta_A}$$

It should be noted that derivatives with respect to angles or rates of angular change are defined per radian.

APPENDIX C

DERIVATION OF THE TRANSFER FUNCTIONS

Equations (A-34) and (A-35) from Appendix A may be converted by the use of determinants into the transfer functions considered earlier in this study.

The angle of attack and the angle of sideslip can be written in approximate form based on the velocity components and the perturbation velocity components:

$$\Delta\alpha \simeq \frac{w}{U_o} \quad \text{and} \quad \beta \simeq \frac{v}{U_o}$$

The angle between the equilibrium flight path and the disturbed flight path is defined as Ξ. It should be pointed out that only when Ξ equals zero is the sideslip angle β equal to the negative of the yaw angle.

The longitudinal equations can be written by modifying Equations (A-34), as shown below:

$$\begin{aligned}
&\dot{u} - X_u u - (T_u \cos\xi)u - X_q q + g\theta\cos\gamma_o - X_{\dot{w}}\dot{w} - X_w w \\
&\qquad = X_{\delta_E}\delta_E + T_{\delta_{RPM}}\delta_{RPM} + X_{\delta_F}\delta_F \\
&-Z_u u + (T_u \sin\xi)u - U_o q - Z_q q + g\theta\sin\gamma_o + \dot{w} - Z_{\dot{w}}\dot{w} - Z_w w \\
&\qquad = Z_{\delta_E}\delta_E - (T_{\delta_{RPM}}\sin\xi)\delta_{RPM} + Z_{\delta_F}\delta_F \\
&-M_u u - \frac{z_j m}{I_{yy}} T_u u + \dot{q} - M_q q - M_{\dot{w}}\dot{w} - M_w w \\
&\qquad = M_{\delta_E}\delta_E + \frac{z_j m}{I_{yy}} T_{\delta_{RPM}}\delta_{RPM}
\end{aligned} \tag{C-1}$$

The lateral equations of motion, Equations (A-35), are rearranged by substititing βU for v and dividing by U_o. Thus,

$$\begin{aligned}
&\dot{\beta} - Y_v\beta - \frac{Y_p}{U_o}p - \left(\frac{g}{U_o}\cos\gamma_o\right)\phi + r - \frac{Y_r}{U_o}r - \left(\frac{g}{U_o}\sin\gamma_o\right)\psi \\
&\qquad = \frac{Y_{\delta_A}}{U_o}\delta_A + \frac{Y_{\delta_R}}{U_o}\delta_R \\
&-L_\beta\beta + \dot{p} - L_p p - \frac{I_{xz}}{I_{xx}}\dot{r} - L_r r = L_{\delta_A}\delta_A + L_{\delta_R}\delta_R \\
&-N_\beta\beta - \frac{I_{xz}}{I_{zz}}\dot{p} - N_p p + \dot{r} - N_r r = N_{\delta_A}\delta_A + N_{\delta_R}\delta_R
\end{aligned} \tag{C-2}$$

The right sides of Equations (C-1) and (C-2) are the control forces and represent the means by which either the human pilot or an autopilot can control the motion of the airframe. The thrust and the control surface inputs are the forcing functions which determine the resultant motion of the airframe. Since the airframe equations of motion are linear equations, the principle of superposition may be used to obtain a solution. For instance, the response to simultaneous application of elevator and rudder deflections can be determined by calculating the response to each of these deflections separately and then adding the results to complete the solution.

The transfer functions are obtained by applying the method of Laplace transforms. If Equations (C-1) and (C-2) are transformed into the Laplacian domain,

$$[s - (X_u + A')]u(s) - (sX_{\dot{w}} + X_w)w(s) - (sX_q - g\cos\gamma_o)\theta(s)$$
$$= X_{\delta_E}\delta_E(s) + B'\delta_{RPM}(s) + X_{\delta_F}\delta_F(s)$$

$$-(Z_u - C')u(s) + [s(1 - Z_{\dot{w}}) - Z_w]w(s) - [s(U_o + Z_q) - g\sin\gamma_o]\theta(s)$$
$$= Z_{\delta_E}\delta_E(s) - D'\delta_{RPM}(s) + Z_{\delta_F}\delta_F(s)$$

$$-(M_u + E')u(s) - (sM_{\dot{w}} + M_w)w(s) + (s^2 - M_q s)\theta(s)$$
$$= M_{\delta_E}\delta_E(s) + F'\delta_{RPM}(s) + M_{\delta_F}\delta_F(s)$$

$$(s - Y_v)\beta(s) - (s\frac{Y_p}{U_o} + \frac{g}{U_o}\cos\gamma_o)\phi(s) + [s(1 - \frac{Yr}{U_o}) - \frac{g}{U_o}\sin\gamma_o]\psi(s)$$
$$= [Y_{\delta_A}\delta_A(s) + Y_{\delta_R}\delta_R(s)]\frac{1}{U_o}$$

$$-L_\beta\beta(s) + (s^2 - sL_p)\phi(s) - (A_1 s^2 + sL_r)\psi(s)$$
$$= L_{\delta_A}\delta_A(s) + L_{\delta_R}\delta_R(s)$$

$$-N_\beta\beta(s) - (B_1 s^2 + sN_p)\phi(s) + (s^2 - sN_r)\psi(s)$$
$$= N_{\delta_A}\delta_A(s) + N_{\delta_R}\delta_R(s) \qquad \text{(C-3)}$$

where

$$A' = T_u\cos\xi \qquad F' = \frac{z_j m}{I_{yy}}T_{\delta_{RPM}}$$
$$B' = T_{\delta_{RPM}}\cos\xi$$
$$C' = T_u\sin\xi \qquad A_1 = \frac{I_{xz}}{I_{xx}}$$
$$D' = T_{\delta_{RPM}}\sin\xi$$
$$E' = \frac{z_j m}{I_{yy}}T_u \qquad B_1 = \frac{I_{xz}}{I_{zz}}$$

It should be noted that p, q, and r were replaced by $\dot{\phi}$, $\dot{\theta}$, and $\dot{\psi}$ respectively. This is permitted because of the small perturbation approximation. Using Equations (C-3) and Cramer's rule for solving equations by determinants, the longitudinal transfer function for $U(s)/\delta_E(s)$ with $\delta_F=0$ and $\delta_{RPM}=0$ can be written

$$\frac{u(s)}{\delta_E(s)} = \frac{\begin{vmatrix} X_{\delta_E} & -(sX_{\dot{w}} + X_w) & -(sX_q - g\cos\gamma_o) \\ Z_{\delta_E} & [s(1 - Z_{\dot{w}}) - Z_w] & -[s(U_o + Z_q) - g\sin\gamma_o] \\ M_{\delta_E} & -(sM_{\dot{w}} + M_w) & (s^2 - M_q s) \end{vmatrix}}{\begin{vmatrix} [s - (X_u + A')] & -(sX_{\dot{w}} + X_w) & -(sX_q - g\cos\gamma_o) \\ -(Z_u - C') & [s(1 - Z_{\dot{w}}) - Z_w] & -[s(U_o + Z_q) - g\sin\gamma_o] \\ -(M_u + E') & -(sM_{\dot{w}} + M_w) & (s^2 - M_q s) \end{vmatrix}} = \frac{N_u/\delta_E}{D_1} \qquad \text{(C-4)}$$

The denominator determinant is the determinant of the homogeneous equations denoted by D_1. The expansion of D_1 gives

$$D_1 = As^4 + Bs^3 + Cs^2 + Ds + E, \qquad \text{(C-5)}$$

where $A = 1 - Z_{\dot{w}}$

$$B = -(1 - Z_{\dot{w}})[(X_u + A') + M_q] - Z_w - M_{\dot{w}}(U_o + Z_q) - X_{\dot{w}}(Z_u - C')$$

$$C = (X_u + A')[M_q(1 - Z_{\dot{w}}) + Z_w + M_{\dot{w}}(U_o + Z_q)] - (M_u + E')[X_{\dot{w}}(U_o + Z_q) + X_q(1 - Z_{\dot{w}})] + M_q Z_w + (Z_u - C')[M_q X_{\dot{w}} - X_w) - X_q M_{\dot{w}}] + M_{\dot{w}} g\sin\gamma_o - M_w(U_o + Z_q)$$

$$D = g\sin\gamma_o[(M_u + E)X_{\dot{w}} + M_w - M_{\dot{w}}(X_u + A')] + g\cos\gamma_o[(Z_u - C')M_{\dot{w}} + (M_u + E')(1 - Z_{\dot{w}})] + (M_u + E')[-X_w(U_o + Z_q) + Z_w X_q] + (Z_u - C')[X_w M_q - X_q M_w] + (X_u + A')[M_w(U_o + Z_q) - M_q Z_w]$$

$$E = g\cos\gamma_o[M_w(Z_u - C') - Z_w(M_u + E')] + g\sin\gamma_o[(M_u + E')X_w - (X_u + A')M_w]$$

The numerator determinant is expanded in Equation (C-6):

$$N_u/\delta_E = A_u s^3 + B_u s^2 + C_u s + D_u \qquad \text{(C-6)}$$

where $A_u = X_{\delta_E}(1 - Z_{\dot{w}}) + Z_{\delta_E} X_{\dot{w}}$

$$B_u = -X_{\delta_E}[(1 - Z_{\dot{w}})M_q + Z_w + M_{\dot{w}}(U_o + Z_q)]$$
$$+ Z_{\delta_E}[X_q M_{\dot{w}} - X_{\dot{w}} M_q + X_w]$$
$$+ M_{\delta_E}[X_{\dot{w}}(U_o + Z_q) + (1 - Z_{\dot{w}})X_q]$$

$$C_u = X_{\delta_E}[M_q Z_w + M_{\dot{w}} g \sin\gamma_o - M_w(U_o + Z_q)]$$
$$+ Z_{\delta_E}[X_q M_w - M_{\dot{w}} g \cos\gamma_o - X_w M_q]$$
$$+ M_{\delta_E}[-X_{\dot{w}} g \sin\gamma_o + X_w(U_o + Z_q) - (1 - Z_{\dot{w}})g\cos\gamma_o - Z_w X_q]$$

$$D_u = X_{\delta_E}(M_w g \sin\gamma_o) - Z_{\delta_E}(M_w g \cos\gamma_o)$$
$$+ M_{\delta_E}(Z_w g \cos\gamma_o - X_w g \sin\gamma_o)$$

Similarly, using the approximation discussed at the beginning of this appendix, $\Delta\alpha(s)/\delta_E(s)$ can be written $w(s)/U_o\delta_E(s)$, as seen below:

$$\frac{\Delta\alpha(s)}{\delta_E(s)} = \frac{\begin{vmatrix} [s - (X_u + A')] & X_{\delta_E}/U_o & -(sX_q - g\cos\gamma_o) \\ -(Z_u - C') & Z_{\delta_E}/U_o & -[s(U_o + Z_q) - g\sin\gamma_o] \\ -(M_u + E) & M_{\delta_E}/U_o & (s^2 - M_q s) \end{vmatrix}}{D_1} = \frac{N_\alpha/\delta_E}{D_1}$$

$$N_\alpha/\delta_E = A_\alpha s^3 + B_\alpha s^2 + C_\alpha s + D_\alpha \qquad \text{(C-7)}$$

where $A_w = Z_{\delta_E}/U_o$

$$B_w = (X_{\delta_E}/U_o)(Z_u - C') + (Z_{\delta_E}/U_o)[-M_q - (X_u + A')] + (M_{\delta_E}/U_o)(U_o + Z_q)$$

$$C_w = (X_{\delta_E}/U_o)[(U_o + Z_q)(M_u + E') - M_q(Z_u - C')]$$
$$+ (Z_{\delta_E}/U_o)[M_q(X_u + A') - (M_u + E')X_q]$$
$$+ (M_{\delta_E}/U_o)[X_q(Z_u - C') - g\sin\gamma_o - (U_o + Z_q)(X_u + A')]$$

$$D_w = (-X_{\delta_E}/U_o)(M_u + E')(g\sin\gamma_o) + (Z_{\delta_E}/U_o)(M_u + E')g\cos\gamma_o$$
$$+ (M_{\delta_E}/U_o)[(X_u + A')g\sin\gamma_o - (Z_u - C')g\cos\gamma_o]$$

also,

$$\frac{\theta(s)}{\delta_E(s)} = \frac{\begin{vmatrix} [s - (X_u + A')] & -(sX_{\dot{w}} + X_w) & X_{\delta_E} \\ -(Z_u - C') & [s(1 - Z_{\dot{w}}) - Z_w] & Z_{\delta_E} \\ -(M_u + E') & -(sM_{\dot{w}} + M_w) & M_{\delta_E} \end{vmatrix}}{D_1} = \frac{N\theta/\delta_E}{D_1}$$

$$N_\theta/\delta_E = A_\theta s^2 + B_\theta s + C_\theta \qquad \text{(C-8)}$$

where $A_\theta = Z_{\delta_E}M_{\dot{w}} + M_{\delta_E}(1 - Z_{\dot{w}})$

$$B_\theta = X_{\delta_E}[(Z_u - C')M_{\dot{w}} + (1 - Z_{\dot{w}})(M_u + E')]$$
$$+ Z_{\delta_E}[M_w - M_{\dot{w}}(X_u + A') + (M_u + E')X_{\dot{w}}]$$
$$+ M_{\delta_E}[-Z_w - (1 - Z_{\dot{w}})(X_u + A') - X_{\dot{w}}(Z_u - C')]$$

$$C_\theta = X_{\delta_E}[M_w(Z_u - C') - Z_w(M_u + E')]$$
$$+ M_{\delta_E}[Z_w(X_u + A') - X_w(Z_u - C')]$$
$$+ Z_{\delta_E}[-M_w(X_u + A) + X_w(M_u + E')]$$

It should be noted from the mechanics of the above derivation that, had it been desirable to derive the transfer functions for any one of the other control inputs, it would have been necessary only to replace δ_E by the appropriate derivative whenever δ_E appeared in the transfer function. This knowledge can also be applied to the lateral transfer functions about to be derived. To make the following transfer functions applicable to aileron deflection δ_A instead of rudder deflection δ_R, it is necessary only to replace δ_R by δ_A whenever δ_R appears, and to replace Y_{δ_R}, L_{δ_R}, and N_{δ_R} by Y_{δ_A}, L_{δ_A}, and N_{δ_A} respectively.

Following this approach, the lateral transfer functions for rudder deflections, (δ_A=0), became:

$$\frac{\beta(s)}{\delta_R(s)} = \frac{\begin{vmatrix} \frac{Y_{\delta_R}}{U_o} & -(s\frac{Y_p}{U_o} + \frac{g}{U_o}\cos\gamma_o) & [s(1 - \frac{Y_r}{U_o}) - \frac{g}{U_o}\sin\gamma_o] \\ L_{\delta_R} & (s^2 - sL_p) & -(A_1s^2 + sL_r) \\ N_{\delta_R} & -(B_1s^2 + sN_p) & (s^2 - sN_r) \end{vmatrix}}{\begin{vmatrix} (s - Y_v) & -(s\frac{Y_p}{U_o} + \frac{g}{U_o}\cos\gamma_o) & [s(1 - \frac{Y_r}{U_o}) - \frac{g}{U_o}\sin\gamma_o] \\ -L_\beta & (s^2 - sL_p) & -(A_1s^2 + sL_r) \\ -N_\beta & -(B_1s^2 + sN_p) & (s^2 - sN_r) \end{vmatrix}} = \frac{N_\beta/\delta_R}{D_2}$$

$$D_2 = s(As^4 + Bs^3 + Cs^2 + Ds + E) \qquad \text{(C-9)}$$

where $A = 1 - A_1B_1$

$$B = -Y_v(1 - A_1B_1) - L_p - N_r - A_1N_p - B_1L_r$$

$$C = N_\beta(1 - \frac{Y_r}{U_o}) + L_p(Y_v + N_r) - \frac{Y_p}{U_o}(A_1N_\beta + L_\beta) + N_p(A_1Y_v - L_r) + Y_v(B_1L_r + N_r) + L_\beta B_1(1 - \frac{Y_r}{U_o})$$

$$D = -N_\beta[(1 - \frac{Y_r}{U_o})L_p + L_r\frac{Y_p}{U_o} + A_1\frac{g}{U_o}\cos\gamma_o + \frac{g}{U_o}\sin\gamma_o] + N_p[L_\beta(1 - \frac{Y_r}{U_o}) + Y_vL_r] - L_pN_rY_v + L_\beta[N_r\frac{Y_p}{U_o} - \frac{g}{U_o}\cos\gamma_o - B_1\frac{g}{U_o}\sin\gamma_o]$$

$$E = \frac{g}{U_o}\cos\gamma_o(L_\beta N_r - N_\beta L_r) + \frac{g}{U_o}\sin\gamma_o(N_\beta L_p - L_\beta N_p)$$

$$N_\beta/\delta_R = s(A_\beta s^3 + B_\beta s^2 + C_\beta s + D_\beta) \qquad \text{(C-10)}$$

where $A_\beta = (1 - A_1B_1)\frac{Y_{\delta_R}}{U_o}$

$$B_\beta = \frac{Y_{\delta_R}}{U_o}[-L_p - N_r - A_1N_p - B_1L_r] + L_{\delta_R}[\frac{Y_p}{U_o} - B_1(1 - \frac{Y_r}{U_o})] + N_{\delta_R}[A_1\frac{Y_p}{U_o} - (1 - \frac{Y_r}{U_o})]$$

$$C_\beta = \frac{Y_{\delta_R}}{U_o}[L_p N_r - N_p L_r] + L_{\delta_R}[\frac{g}{U_o}\cos\gamma_o - N_r\frac{Y_p}{U_o} - N_p(1 - \frac{Y_r}{U_o}) + B_1\frac{g}{U_o}\sin\gamma_o] + N_{\delta_R}[\frac{Y_p}{U_o}L_r + A_1\frac{g}{U_o}\cos\gamma_o + L_p(1 - \frac{Y_r}{U_o}) + \frac{g}{U_o}\sin\gamma_o]$$

$$D_\beta = L_{\delta_R}\frac{g}{U_o}[-N_r\cos\gamma_o + N_p\sin\gamma_o] + N_{\delta_R}\frac{g}{U_o}[L_r\cos\gamma_o - L_p\sin\gamma_o]$$

$$\frac{\phi(s)}{\delta_R(s)} = \frac{\begin{vmatrix} (s - Y_v) & \frac{Y_{\delta_R}}{U_o} & [s(1 - \frac{Y_r}{U_o}) - \frac{g}{U_o}\sin\gamma_o] \\ -L_\beta & L_{\delta_R} & -(A_1 s^2 + sL_r) \\ -N_\beta & N_{\delta_R} & (s^2 - sN_r) \end{vmatrix}}{D_2} = \frac{N_\phi/\delta_R}{D_2}$$

$$N_\phi/\delta_R = s(A_\phi s^2 + B_\phi s + C_\phi + D_\phi/s) \qquad \text{(C-11)}$$

where $A_\phi = L_{\delta_R} + N_{\delta_R}A_1$

$$B_\phi = \frac{Y_{\delta_R}}{U_o}(L_\beta + A_1 N_\beta) + L_{\delta_R}(-N_r - Y_v) + N_{\delta_R}(L_r - A_1 Y_v)$$

$$C_\phi = \frac{Y_{\delta R}}{U_o}[+L_r N_\beta - L_\beta N_r] + L_{\delta_R}[Y_v N_r + N_\beta(1 - \frac{Y_r}{U_o})] + N_{\delta_R}[-L_\beta(1 - \frac{Y_r}{U_o}) - Y_v L_r]$$

$$D_\phi = (N_{\delta_R}L_\beta - L_{\delta_R}N_\beta) - \frac{g}{U_o}\sin\gamma_o$$

$$\frac{\psi(s)}{\delta_R(s)} = \frac{\begin{vmatrix} (s - Y_v) & -(s\frac{Y_p}{U_o} + \frac{g}{U_o}\cos\gamma_o) & \frac{Y_{\delta_R}}{U_o} \\ -L_\beta & (s^2 - sL_p) & L_{\delta_R} \\ -N_\beta & -(B_1 s^2 + sN_p) & N_{\delta_R} \end{vmatrix}}{D_2} = \frac{N_\psi/\delta_R}{D_2}$$

$$N_\psi/\delta_R = A_\psi s^3 + B_\psi s^2 + C_\psi s + D_\psi \qquad \text{(C-12)}$$

$$\text{where } A_\psi = N_{\delta_R} + B_1 L_{\delta_R}$$

$$B_\psi = \frac{Y_{\delta_R}}{U_o}(N_\beta + B_1 L_\beta) + L_{\delta_R}(N_p - B_1 Y_v) + N_{\delta_R}(-Y_v - L_p)$$

$$C_\psi = \frac{Y_{\delta_R}}{U_o}(L_\beta N_p - N_\beta L_p) + L_{\delta_R}(\frac{Y_p}{U_o} N_\beta - Y_v N_p)$$
$$+ N_{\delta_R}(L_p Y_v - \frac{Y_p}{U_o} L_\beta)$$

$$D_\psi = (L_{\delta_R} N_\beta - N_{\delta_R} L_\beta)\frac{g}{U_o}\cos \gamma_o$$

The above transfer functions completely describe the airframe within the limits of the assumptions made in Appendix A of this study.

By substituting $j\omega$ for s the transfer functions are transformed into the frequency domain. If one then writes the numerator and denominator each as a magnitude and phase angle and plots the ratio of magnitudes and the difference in phase angles against frequency, the results indicate the magnitude and phase relationship of the aircraft response to a sinusoidal control input of unit magnitude at any given frequency. These "Bode" plots are quite useful in visualizing frequency regions of excessive aircraft response (regions of poor damping), the frequency above which aperiodic motions decrease rapidly in amplitude, frequency regions which should be avoided by structural and control system resonances because of the possibility of coupling, and, if measured in flight, the presence and effect of non-linearities. Control system and autopilot designers find such plots particularly useful when the scales are logarithmic since among other advantages the amplitude of the actual aircraft response is merely subtracted from the desired response to find the effective transfer function which the autopilot or control system must supply.

The denominator of the transfer function is the Laplace transform of the characteristic equation of the system. It can be thought of as representing the general solution in the mathematical sense, for the response of the system. The numerator terms, combined with the time history of the control surface motions, are responsible for the particular solution. To obtain the time history of the response to a particular control surface input it is necessary to obtain the inverse transform of the transfer function. Fairly extensive tables of Laplace transforms are available and the proper form can often be found therein. It may, however, be necessary to perform a partial fraction expansion to reduce the transfer function to a sum of simpler functions whose inverses do appear in a table. For details, the reader is referred to a standard text on control system design such as Savant (Ref.100).

APPENDIX D

SIMPLIFIED RESPONSE CHARACTERISTICS

The equations developed in Appendices A, B, and C, although already linearized, are still difficult to solve by hand. (For those with digital computer facilities, the programs presented in the present report may be used to obtain time solutions to the complete system.) For preliminary design purposes it is desirable to be able to make rapid, approximate calculations of the effect of geometric or loading changes on the dynamics of the aircraft. It is therefore of interest to determine the extent to which the equations and their solutions can be simplified before the characteristic behavior is lost.

In this connection, it is convenient to assume that

$$\gamma_o,\ z_j,\ x_{\dot{w}},\ Z_{\dot{w}},\ X_q,\ X_{\delta_E},\ Z_{\delta_E},\ X_{\delta_F},\ M_{\delta_F},\ Z_q,\ T_u,\ \text{and}\ T_{\delta_{RPM}} = 0$$

It has long been common knowledge that for the longitudinal case the phugoid oscillation is accompanied by little or no change in vertical velocity while the short period oscillation takes place at constant speed if the magnitude of the pitch angle change is kept small. This suggests that the general three-degree-of-freedom system can be approximated by two two-degree-of-freedom systems.

Equations A-34 may be written

$$\begin{aligned} \dot{u} + g\theta &= X_u u + X_w w \\ \dot{w} - U_o q &= Z_u u + Z_w w + Z_{\delta_E}\delta_E \\ \dot{q} &= M_u u + M_q q + M_w w + M_{\dot{w}}\dot{w} + M_{\delta_E}\delta_E \end{aligned} \tag{1}$$

It should be noted that the pertubation velocities, i.e., u, w, and q,are zero when the unperturbed variable is constant during a particular maneuver. Taking advantage of this fact, one finds that the system (1) reduces to three equations in two unknowns, one equation of which is therefore redundant. For the short period approximation, the equation describing linear acceleration along the x-axis is redundant. (The acceleration is zero and the remaining forces reduce to an identity.) Similarly for the phugoid case, the equation describing pitch is redundant.

$$\begin{aligned} \dot{w} - U_o q &= Z_w w + Z_{\delta_E}\delta_E \\ \dot{q} &= M_q q + M_w w + M_{\dot{w}}\dot{w} + M_{\delta_E}\delta_E \end{aligned} \tag{2}$$

for the short period mode

and

$$\begin{aligned} \dot{u} &= X_u u - g\theta \\ -U\dot{\theta} &= Z_u u + Z_{\delta_E}\delta_E \end{aligned} \tag{3}$$

for the phugoid mode.

Equations (2) and (3) have been written to reflect these considerations. Transformed to the frequency domain these become

$$\begin{aligned}(s - Z_w)\, w(s) - sU_o\theta(s) &= Z_{\delta_E}\delta_E(s)\\ (s^2 - sM_q)\,\theta(s) - (M_{\dot{w}}s + M_w)\, w(s) &= M_{\delta_E}\delta_E(s)\end{aligned} \tag{4}$$

short period

and

$$\begin{aligned}(s - X_u)\, u(s) + g\theta(s) &= 0\\ -U_s\theta(s) - Z_u u(s) &= Z_{\delta_E}\delta_E(s)\end{aligned} \tag{5}$$

phugoid.

Substitution of the first equation of (4) into the second yields

$$\frac{\theta}{\delta_E} = \frac{(M_{\dot{w}}+M_{\delta_E})s + (M_w Z_{\delta_E} - M_{\delta_E} Z_w)}{s[s^2 - (Z_w + M_q + U_o M_{\dot{w}})s + (M_q Z_w - M_w U_o)]} \tag{6}$$

The oscillatory roots of the denominator of (6) describe the short period damping and frequency. Since in general the transfer function of an oscillatory mode can be described by

$$\frac{1}{s^2 + 2\zeta\omega_n s + \omega_n^2}$$

it is readily seen that the frequency of the short period mode is given by

$$\omega_{n_{sp}} = (M_q Z_w - M_w U_o)^{1/2} \tag{7}$$

while the damping ratio is

$$\zeta_{sp} = -\frac{U_o M_{\dot{w}} + Z_w + M_q}{2\omega_n} \tag{8}$$

In terms of the stability derivatives, (7) and (8) may be written

$$\omega_{n_{sp}} \simeq \frac{\rho U S c}{2\sqrt{I_{yy}}}\left[-\frac{g}{2W} C_{L_\alpha} C_{m_q} - \frac{2C_{m_\alpha}}{\rho S c}\right]^{1/2} \tag{9}$$

$$\zeta_{sp} \simeq -\frac{\rho S U c^2}{4 I_{yy}\omega_n}\left[C_{m_{\dot{\alpha}}} + \frac{C_{m_q}}{2} - \frac{I_{yy}}{Wc^2} g C_{L_\alpha}\right] \tag{10}$$

For the equivalent values from the phugoid approximation one solves equations (5) for

$$\frac{u}{\delta_E} = \frac{Z\delta_E g/U_o}{s^2 - X_u s - \frac{Z_u g}{U_o}} \tag{11}$$

from which it is apparent that

$$\omega_{n_p} = \sqrt{-\frac{Z_u g}{U_o}} = \sqrt{\frac{\rho S g^2}{W} C_L} \simeq 1.4\ g/U_o \tag{12}$$

$$\zeta_p = -\frac{X_u}{2\omega_n} = C_D \frac{U}{2}\sqrt{\frac{\rho S}{W C_L}} \simeq 0.707\ \frac{D}{W} \tag{13}$$

The approximate lateral-directional characteristics are obtained in a similar fashion. The reader will recall that the solution of the second equation of A-35

$$\dot{p} = L_p p + L_{\delta_A}\ \delta_A \tag{14}$$

for motion restricted to that about the x-axis is given on page 137 as

$$\phi = -\left(\frac{C\ell_{\delta_A}}{C\ell_p}\right)\frac{U}{b}\,\delta_A t + \frac{\left[1 - e^{\left[\frac{C\ell_p\ b^2 q\ S_w}{2U\ I_{xx}}\ t\right]}\right]}{\frac{C\ell_p\ b^2 q S_w}{2U\ I_{xx}}} \tag{15}$$

The first term is the steady state portion of the solution and the time required for the transient solution to attain 63% of its final value is

$$\tau_R = -\frac{4I_{xx}}{C\ell_p\ b^2 \rho S_w U_o}\ \text{seconds} \tag{16}$$

The Dutch roll is assumed for purposes of approximation to consist of a yawing motion about the z-axis. Thus the motion lies entirely in the x-y plane, i.e., the bank angle remains constant and there is no L_r, V, or L_v. With the additional assumptions that $V = U_o\beta$, and $r = \dot{\psi}$, $\psi = -\beta$, $Y_{\delta R}$ and $Y_r = 0$. equations A-35 reduce to

$$\ddot{\beta} - N_r\beta + N_v U_o\beta + N_{\delta_r}\delta_r = 0, \tag{17}$$

which when transformed becomes

$$(s^2 - N_r s + N_v U_o)\beta(s) = -N_{\delta_r}\delta_r(s); \tag{18}$$

thus

$$\omega_{n_d} = (N_v U_o)^{1/2} = \left(\frac{b\rho SU^2}{2I_{zz}} C_{n_\beta}\right)^{1/2} \tag{19}$$

$$\zeta_d = \frac{-N_r}{2(N_v U_o)^{1/2}} = -\left(\frac{\rho Sb^3}{2I_{zz}}\right)^{1/2} \frac{C_{n_r}}{\sqrt{C_{n_\beta}}} \quad . \tag{20}$$

Unfortunately, the spiral mode is not readily approximated with accuracy by a one-or-two-degree-of-freedom system. However, by discarding small quantities from the general fifth order characteristic equation of lateral motion and grouping the remaining terms to match the expansion of

$$s\left(s + \frac{1}{\tau_s}\right)\left(s + \frac{1}{\tau_R}\right)\left(s^2 + 2\zeta\omega_n s + \omega_n{}^2\right) ,$$

Ref. 17 was able to show that

$$\tau_s \simeq \frac{\frac{\rho SUb}{4W} C_{\ell_\beta} C_{\ell_p} C_{n_r} + \frac{U_o}{g} C_{\ell_p} C_{n_\beta} + \frac{4I_{zz}}{\rho SUb^2} C_{\ell_\beta}}{C_{n_\beta} C_{\ell_r} - C_{\ell_\beta} C_{n_r}} \quad . \tag{21}$$

Note that unless the yaw damping and the side force due to sideslip are both very large numerically, the first term in the numerator may be neglected. At cruise, the last term is generally about 10^{-2} times the second term so that one commonly sees

$$\tau_s = \frac{U_o}{g}\left(\frac{C_{\ell_p} C_{n_\beta}}{C_{n_\beta} C_{\ell_r} - C_{\ell_\beta} C_{n_r}}\right) .$$

The stability of the spiral mode may be deduced by examining the sign of the net denominator since the numerator will almost always be negative. C_{n_r} by definition is negative while C_{ℓ_r} is positive. The sign of C_{ℓ_β} depends upon the dihedral angle but the aircraft is usually configured so that C_{ℓ_β} is negative. C_{n_β} depends upon the area distribution in the xz plane but is usually positive. Thus, if $C_{\ell_\beta} C_{n_r}$ is larger than $C_{n_\beta} C_{\ell_r}$, the aircraft will be spirally stable. It should be noted, however, that the geometric changes needed to improve spiral stability will usually result in poorer Dutch roll performance so that some compromise is necessary in the absence of an artificial stability system. Usually one will opt for a very slightly unstable spiral mode in order to obtain satisfactory Dutch roll performance.

APPENDIX E

USE OF THE NON-LINEAR FORM OF THE EQUATIONS OF MOTION

There are occasions in the analysis of flight motions when one would wish to study large departures from equilibrium, circumstances where the aerodynamic forces and moments are highly non-linear, and the rare situations where there is extensive directional-longitudinal cross-coupling. The general equations* of course describe these situations as well as they do those involving small departures from equilibrium. There are, however, no extensively-developed techniques analogous to the transfer-function, root-locus procedures for examining the characteristics of solutions of systems of non-linear, partial differential equations. With the advent of very large digital computers, converting the equations to difference equations for solution or using a variety of forward integration techniques became feasible. In order for such techniques to retain sufficient accuracy when computing slowly decaying oscillations, however, extreme precision must be maintained. Inherently, the computation requires considerable time on a large machine.

Conceptually, a simpler approach is to employ an analog computer. Here, too, a large machine with many function generators is required. Also the availability of skilled analog programmers seems to be limited while the number of "canned" digital programs is multiplying. Thus the user who finds it necessary to analyze non-linear motions is advised to secure a suitable program from others who have employed it.

---

* See equations A-8 and A-27.

APPENDIX F

SOME NOTES ON THE CONSTRUCTION AND INTERPRETATION OF BODE PLOTS AND ROOT LOCUS DIAGRAMS

The use of Bode plots to study airframe response dates from the early 1950's. The Bode plot was by then a familiar tool to the control system engineer and when he was given responsibility for developing advanced autopilots, it was natural for him to employ a representation of the airframe dynamics which would facilitate his task. How it does this is outlined below.

The aircraft alone can be considered as one block in a combined aircraft-automatic control system feedback loop.

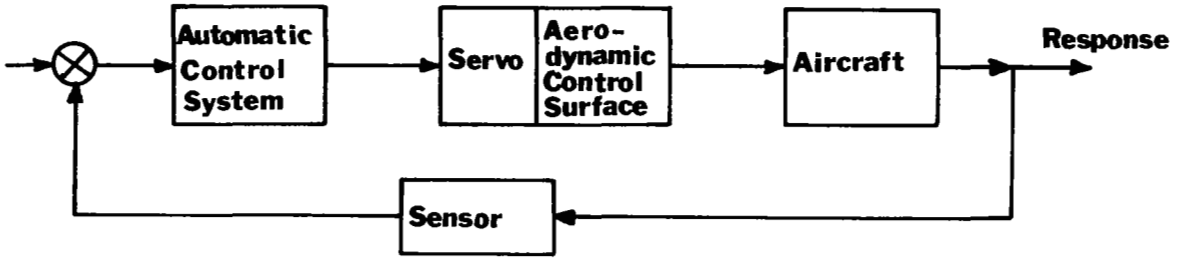

Figure F-1. Sample block diagram.

Each block is described by one or more differential equations, according to Newton's Second Law of Motion or its electrical equivalent. To combine the characteristics of each block so as to form the characteristics of the overall system is quite difficult because a signal is modified in both phase and amplitude in going through each block. By applying the Laplace transform

$$F(s) = \int_0^\infty f(t)e^{-st}\,dt$$

to the describing differential equations one obtains an algebraic representation for each block in the system. It is then convenient to arrange this representation in the form of a transfer function, i.e., as a ratio of block response to block excitation. These transfer functions can then be multiplied together to yield system response to system excitation. It is a relatively straight forward procedure because each transfer function is merely a ratio of polynomials in the Laplace operator s.

A transfer function can be made to display additional physical significance by allowing $j\omega$ to replace s, where ω is a frequency and $j = \sqrt{-1}$. The resulting transfer function is then a ratio of products of vector quantities, such as for example

$$\frac{(3+4j)(5+6j)}{(2+j)\ (7+5j)}\ , \text{ etc.}$$

The rules for reducing this complex quotient to its simplest form are (1) write each factor as an amplitude and a phase angle, (2) multiply the numerator amplitudes together, (3) multiply the denominator amplitudes together, (4) add the numerator phase angles, (5) add the denominator phase angles, (6) form the ratio of numerator to denominator amplitudes (7) form the difference between numerator and denominator phase angles. The total transfer function is then represented by a single amplitude and a single phase angle. The numerical values of amplitude and phase angle are computed at each frequency of interest. (The amplitude and phase angle of the first factor in the example are Amp = $\sqrt{3^2+4^2}$ = 5 and phase $\tan^{-1}$ 4/3.)

By choosing a log-log or db-log frequency representation to plot the amplitude ratio and a linear-log frequency plot for phase angle, one can simply add amplitude ratios and phase angles of components graphically to obtain transfer functions of the entire system. One can also do this for the factors in a transfer function.

Certain shape amplitude ratios-frequency plots can be shown to be associated with certain time responses. For example, the transfer function of a simple series resistor-capacitor circuit

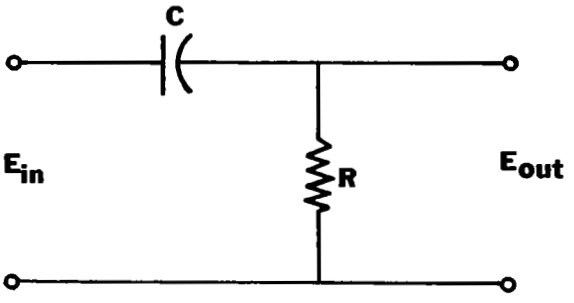

Figure F-2. Sample resistor-capacitor circuit.

can be written

$$\frac{E_o}{E_i} = \frac{j\omega}{\frac{1}{RC} + j\omega} .$$

The differential equation describing the current flow in this situation is of first order; hence, the transfer function shown is said to be that of a first order system. If E_i is a step, E_o will rise instantaneously to the value of E_i and then decay with time, reaching 37% of E_i in RC seconds. Such time response is then characteristic of first order systems.

It will be noted that when $\omega \gg 1/RC$, $|E_o/E_i| \simeq 1$, i.e., independent of frequency and when $\omega \ll 1/RC$, $|E_o/E_i| \simeq RC\omega$. A line such as $RC\omega$ when plotted on a log amplitude, log frequency plot has a slope of +1. Since

$$db = 20 \log(E_o/E_i),$$

this represents a slope of +6db per octave or +20 db per decade. The slope for large values of ω is 0 db per octave and the change begins in the neighborhood of $\omega=1/RC$. The phase angle will change a total 90° in going from $\omega=0$ to $\omega=\infty$.

If E_i is made a sine wave of frequency ω', the plot of $|E_o/E_i|$ indicates that for $\omega'=1/2RC$, $E_o/E_i \simeq 1/2$; for $\omega'=1/10$ RC, $E_o/E_i = 1/10$, and the phase angle is about--90°. For $\omega'>1/RC$, $E_o/E_i = 1$ and the phase angle is zero. Thus the circuit transmits sine wave with frequencies greater than 1/RC essentially unchanged in phase or amplitude but differentiates, i.e., changes phase angle by 90° and amplitude by the factor ω, sine waves with frequencies less than 1/RC.

Interchanging the resistor and capacitor results in the transfer function for a low frequency integrating circuit

$$\frac{E_o}{E_i} = \frac{\frac{1}{RC}}{\frac{1}{RC} + j\omega}$$

Note that the denominator of the transfer function is the same for both circuits. Thus this circuit will also exhibit the characteristic of a first order system in response to a step in E_i: E_o will reach 63% or E_j in RC seconds.

Systems described by a second order differential equation, i.e., a mass-spring-damper system or a inductance-capacitance-resistance system, yield transfer function denominators of the form

$$\omega_n^2 - \omega^2 + j2\zeta\omega_n\omega$$

where ω_n is the natural frequency of the system, that is, the frequency at which the system would oscillate or resonate indefinitely if there were no damping or resistance. ζ is the damping ratio. It describes the envelope of a decaying sinusoid:

$$f(t) = e^{-\zeta\omega_n t} \sin\left(\omega_n\sqrt{1-\zeta^2}\, t\right)$$

On the Bode plot, a second order denominator factor will begin as a horizontal line at low frequencies. The amplitude will slowly increase and peak in the neighborhood of ω_n, the ratio of horizontal asymptote to peak height varying directly with ζ. Beyond ω_n the amplitude falls off rapidly with a final slope of -12 db per octave. The total phase angle change is 180° with the 90° point occurring at $\omega=\omega_n$.

It will be appreciated that any order polynomial can always be factored to appear as a product of first and second order factors. Thus given a transfer function one can always graph it readily by factoring it, graphing the factors, adding, and plotting the sum.

To obtain a reasonably good indication of the characteristic motions of a new airplane one need only evaluate the constants in the transfer functions and plot. The graph of the $|\theta/\delta_e|$ transfer function will probably exhibit two peaks, a high, sharp peak at low frequencies and a modest peak at much larger frequencies. These of course correspond to the phugoid and short period

modes respectively. The frequencies at which they occur and their damping are immediately evident from the plot. The zero frequency value of $\dot{\theta}/\delta_e$ is the steady state pitching velocity which can be produced by a unit elevator deflection at a given forward speed, e.g., location, altitude, weight, and angle of attack. It is thus a measure of elevator effectiveness.

By measuring $\dot{\theta}$ and δ_e as functions of time in flight and performing a harmonic analysis of the time histories it is possible to construct an experimentally-determined $|\dot{\theta}/\delta_e|$ transfer function. This can then be compared with the one calculated from the equations of motion. Note that the later will have two peaks and only two peaks. Flight test records are commonly unreliable at frequencies less than 1 rad/sec. so that the phugoid is seldom evident. Distinct peaks may appear on the flight test Bode plot at frequencies other than the short period frequency. These can be due to

(1) structural resonances excited by the airframe motion
(2) inertial cross coupling (from the dutch roll)
(3) nonlinearities in the motion producing harmonics of the short period mode or intermodulation with other modes
(4) absence of significant harmonic content in the δ_e trace at the particular frequency (a spurious peak, therefore)
(5) poor quality data or data processing.

Careful analysis, however, will usually reveal the source of the extra peaks. One may then compare the measured values of the short period and phugoid frequencies and damping ratios with the predicted values. Knowledge of the frequency and damping ratio also permit one to extract flight values of C_{m_q} and C_D if C_{m_α} is known.

This very brief discussion of the construction and utility of Bode plots is sufficient to point out the fact that they are not very efficient means of studying the effect on the motion of aircraft of varying the amount of control system feedback since a new plot must be made for each value of feedback gain. The same is true for the variation in basic airframe dynamic characteristics resulting from changes in geometry or mass distribution. The root locus diagram was developed to overcome this difficulty. As the name implies it shows on one figure, the trajectory the frequency and damping of characteristic modes follow as system parameters are changed.

Consider the transfer function

$$\frac{O}{I} = \frac{K(s+a)(s^2+bs+c)}{s(s+d)(s+e)(s^2+fs+g)}$$

the denominator of the transfer function represents the characteristic equation of the system, e.g., the equation describing the free motion of the system (the response independent of control input). It is responsible for the general solution of the system of differential equations. The particular solution comes from the numerator.

It will be observed that all values of s which makes the denominator zero are solutions of the characteristic equation and therefore contribute a term of the type $e^{\lambda t}$ to the time response. Since for these roots the transfer function is undefined, denominator roots are called poles. Numerator roots are

appropriately called zeros. It is customary to plot these poles and zeros on a graph whose abscissa is the real part of s and whose ordinate is the imaginary part. Poles are commonly depicted as x's and zeros as O's. A first order root, e.g., (s+d), will always lie on the abscissa (A second order system has two roots. They may be real, in which case they lie on the abscissa) or they may be complex, in which case they are placed equidistant above and below the abscissa.

Any pole which lies in the right half s-plane represents an unstable motion. Zeros in the right half plane are significant in terms of the type of motion only if the system depicted is a feedback system. In this case the zeros represent the location of the poles when the feedback gain is made infinite. For zeros in the right half plane then, the system will then become unstable at some finite value of feedback gain. Knowledge of the location of the basic aircraft zeros is needed by designers in order to combine the control system characteristics with those of the aircraft so as to obtain the desired response without unexpected instabilities. Note also that a zero placed on top of a pole will eliminate the motion caused by that pole from the time history of the particular variable associated with the numerator (θ in θ/δ_e for example) but from no other time history.

A pole located at s=-3, for example, means that there is a contribution to the time history given by e^{-3t}. Thus, the further to the left the pole, the more rapid is the subsidence. Conversely, a pole at s=3 means the motion has an unstable component described by e^{3t}. Typically the spiral mode in aircraft lies slightly to the right. MIL F8785B requires that double amplitude in bank angle shall not be attained in less than 12 seconds. Since $e^{1.693}=2$, τ_s must be more than 1/0.141 or $s \leq 0.141$.

Stable oscillatory modes, it will be recalled, have roots which can be expressed by

$$s_1, s_2 = -\zeta\omega_n \pm j\omega_n\sqrt{1-\zeta^2}$$

Figure F-3 indicates how varying either frequency or damping ratio separately moves the poles. It also shows that the product $\zeta\omega_n$ determines the time for an oscillation to decay to half amplitude. When $\zeta\omega_n=0.591$ the oscillation will decay to half amplitude in one second. Smaller values of the product mean the time to damp to half amplitude is longer.

The ordinate of the figure is $\omega_n\sqrt{1-\zeta^2}$ called the damped natural frequency. This is the frequency of oscillation which one would measure from flight records and is seen to depend on the damping ratio. Note that for a damping ratio of unity, the oscillation has decayed to a subsidence described by $e^{-2\omega n t}$.

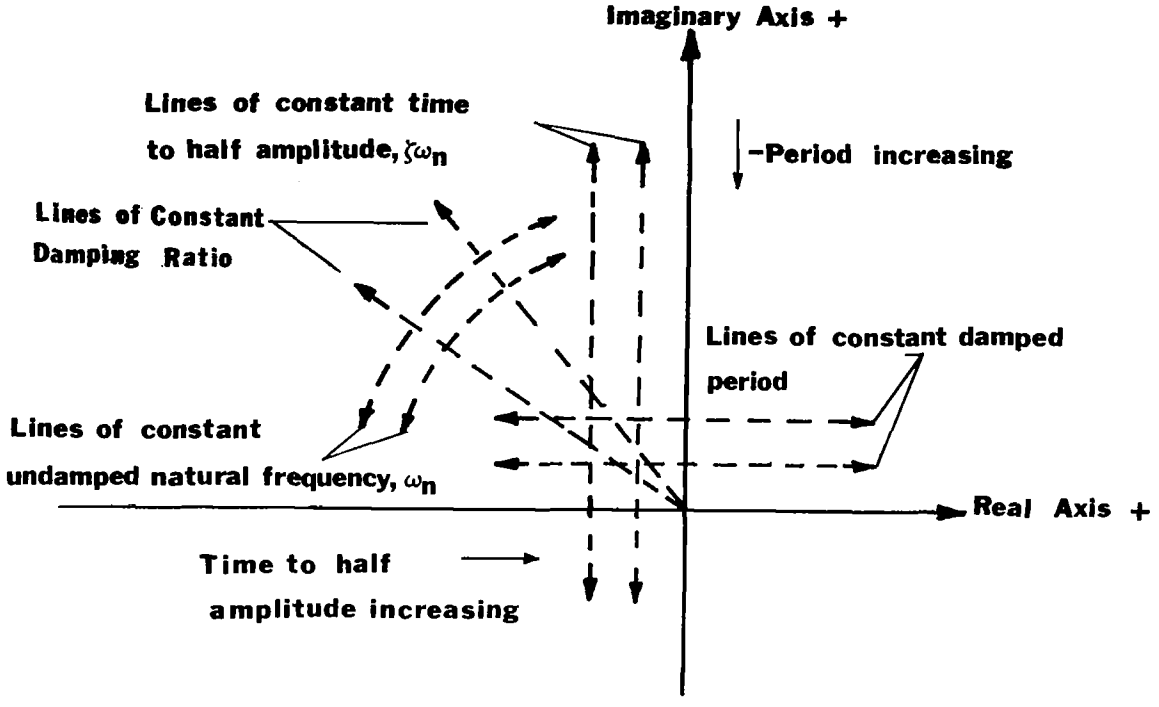

Figure F-3. Variations of frequency and damping ratio.

APPENDIX G

LONGITUDINAL SAMPLE CALCULATIONS

Presented below is a step by step procedure for calculating the longitudinal stability derivatives for the Cessna 182 airplane. A table containing the pertinent geometric dimensions of the airplane is given; geometric and aerodynamic data such as aspect ratio, downwash, and wing lift curve slope are estimated; and formulas for the stability derivatives are delineated, with appropriate numbers for the Cessna 182. These formulas were taken from applicable sections in the text, and the derivatives were calculated only for the cruise condition.

S = 174 ft.^{2}	S_t = 38.71 ft.^{2}	S_E = 16.61 ft.^{2}
b = 35.88 ft.	b_t = 11.54 ft.	
λ = 0.695	λ_t = 0.65	
c.g. located at 26.4% m.a.c.		
fuselage length = 25 ft.	max fuselage width = 4.17 ft.	
length from c.g. to tail quarter-chord = 14.6 ft.		
length from wing quarter-chord to tail quarter-chord = 14.6 ft.		
length from nose to wing quarter-chord = 6.84 ft		
length from c.g. to wing a.c. (chordwise) = 0.1163 ft.		
length from c.g. to wing a.c. (vertical) = 1.67 ft.		
length from c.g. to thrust axis = 0.0 ft.		

Table G-1. Pertinent longitudinal dimensions for the Cessna 182.

1. mean aerodynamic chord $c = \frac{S}{b} = \frac{174}{35.83} = 4.86$ ft.

$$c_t = \frac{38.71}{11.54} = 3.35 \text{ ft.} \qquad c_E = \frac{16.61}{11.54} = 1.44 \text{ ft.}$$

2. aspect ratio $AR = \frac{b}{c} = \frac{35.83}{4.86} = 7.378$ $\qquad AR_t = \frac{11.54}{1.44} = 3.44$

3. incidence angle — the wing incidence angle was assumed to be 1.5°. the tail incidence angle was assumed to be -3.0°.

4. angle of attack — the wing angle of attack is assumed to be 1.5°.

5. wing C_L — the 2-D wing C_L was obtained from Ref. 7 from a plot shown in Figure 1. A Reynolds Number of 5.7×10^6 with an α=1.5° is used to obtain C_ℓ=0.39. The 3-D wing C_L is now found from

$$C_{L_{wing}} = \frac{C_\ell}{1 + 2.0/AR} = \frac{0.39}{1 + 2.0/7.378} = 0.3068$$

6. downwash angle

$$\varepsilon = 20.0\, C_{L_w} \frac{(1/\lambda)^{0.3}}{(AR)^{0.725}} \left(\frac{3.0c}{\ell_t}\right)^{0.25}$$

$$= 20.0 \frac{(1/0.695)^{0.3}}{(7.378)^{0.725}} \left[\frac{(3.0)(4.86)}{14.6}\right]^{0.25} = 1.61°$$

7. horizontal tail α $\alpha_t = \alpha - i_w + i_t - \varepsilon = 1.5-1.5-3.0-1.61 = -4.61°$

8. tail efficiency $\eta_t = q_t/q$ assumed to be 0.85

9. 2-D lift curve slope The 2-D wing lift curve slope is taken from Ref. 7 in the linear region and is found to be 0.103 per degree. Similarly, the tail 2-D lift curve slope is found to be 0.1 per degree (using 0009 section).

10. efficiency factors It is now necessary to approximate the induced-angle span efficiency factor e_1, for both the wing and the tail as well as Oswald's efficiency factor, e, for the wing. For the wing, $e_1 = 1/(1+\tau)$, where τ is approximated (using a taper ratio of 0.695) from Figure 4 as 0.103; thus $e_1 = 1/(1+0.103) = 0.907$. For the tail the same figure is again used (with a taper ratio of 0.65) and τ=0.084, while $e_1 = 1/(1+0.084) = 0.92$. Oswald's efficiency factor is also taken from Figure 4, where $e = 1/(1+\delta)$ and δ is found to be 0.022, while e=0.98.

11. 3-D lift curve slope using steps 9 and 10, the 3-D lift curve slopes can now be calculated.

$$(C_{L_\alpha})_{wing} = \frac{(C_{L_\alpha})_{2\text{-}D}}{1 + \frac{(C_{L_\alpha})_{2\text{-}D} 57.3}{\pi e_1 AR}}$$

$$= \frac{0.103}{1 + \frac{(0.103)\ 57.3}{(3.1416)(.907)(7.378)}} = .085 \text{ per degree or } 4.61 \text{ per radian}$$

$$(C_{L_\alpha})_{tail} = \frac{0.1}{1 + \frac{(0.1)(57.3)}{(3.1416)(.92)(3.44)}} = 0.0635 \text{ per degree or } 3.64 \text{ per radian}$$

12. change in downwash with α

$$\frac{d\varepsilon}{d\alpha} = (20.0)\left(C_{L_{\alpha_w}}\right)_{\text{per degree}} \frac{(1/\lambda)^{0.3}}{AR^{0.725}} \left(\frac{3c}{\ell_t}\right)^{0.25} =$$

$$20.0(0.085)\frac{(1/0.695)}{(7.378)^{0.725}} \left(\frac{3(4.86)}{14.6}\right)^{0.25} = 0.42$$

13. 2-D wing C_{D_α} — The 2-D wing $C_{D\alpha}$ can be approximated from Ref. 7, depending on the angle of attack of the wing. If the angle of attack is relatively small, it may be neglected in many cases. For the cruise condition of the Cessna 182 $(C_{D_\alpha})_{2\text{-}D} \approx 0.0$

14. elevator angle — A procedure for approximating the elevator deflection required for equilibrium flight is given below. The tail lift coefficient, based on the tail area, required for equilibrium flight can be approximated by

$$C_{L_{tail}} = C_{L_{wing}} \frac{x_a}{\ell_t} \frac{S}{S_t} \frac{1}{\eta_t} = (0.307)\left(\frac{0.1163}{14.6}\right)\left(\frac{174}{38.71}\right)\left(\frac{1}{.85}\right)$$

$$= 0.013.$$

The angle of attack required to achieve this lift coefficient is

$$\alpha_{req'd} = \frac{C_{L_t}}{\left(C_{L_{\alpha_t}}\right)_{\substack{per \\ degree}}} = \frac{0.013}{0.0635} = 0.204°.$$

The actual angle of attack of the tail from Ref. 7 is $\alpha_t = -4.61°$. Now the difference between $\alpha_{req'd}$ and α_t is the effective angle of attack produced by deflecting the elevator. From Figure 13,

$$\frac{d\alpha_t}{d\delta_E} = 0.624, \text{ based on } \frac{S_E}{S_t} = 0.43. \quad \text{Thus}$$

$$\delta_E = \frac{\alpha_{req'd} - \alpha_t}{\frac{d\alpha_t}{d\delta_E}} = \frac{0.204 + 4.61}{0.624} = 7.71°.$$

15. parasite drag, C_{D_f} — $(C_{D_f})_{airplane} = \frac{f}{S}$, where S = wing area and $f = \Sigma C_{D_\pi} A_\pi$

C_{D_π} is the drag coefficient of each airplane component part and is multiplied by the area on which it is based and summed for all the components to obtain f.

$f_{wing} = C_{D_w} S_w$, where $C_{D_w} = 0.0065$ (taken from Ref. 7 for $R_N = 5.7 \times 10^6$);

thus,

$f_{wing} = (0.0065)(174 \text{ ft}^2) = 1.131 \text{ ft}^2$

$f_{fuselage} = (C_{D_\pi})_{fuselage} (A_\pi)_{fuselage}$

max. fuselage height ≈ 4.8 ft. height/length = 0.192

max. fuselage width ≈ 4.2 ft. width/length = 0.168

Thus, from fuselage data, $C_{D_\pi} = 0.0063$. Adding 20% for the canopy, $C_{D_\pi} = 0.0756$. Assuming a rectangular area,

$A_\pi = (4.8)(4.2) = 20.2 \text{ ft.}^2$,

$f_{fuselage} = (0.0756)(20.2 \text{ ft.}^2) = 1.525 \text{ ft.}^2$,

$f_{\substack{landing \\ gear}} = (C_{D_\pi} A_\pi)_{\substack{main \\ gear}} + (C_{D_\pi} A_\pi)_{\substack{nose \\ gear}}$.

The value of f for the main gear is found from Table 5 to be 0.74. For the nose gear, where the diameter ≈ 1 foot and the width ≈ 0.5 feet, $C_{D_\pi} = 0.8$ and $A_\pi = (0.5)(1.0) = 0.5 \text{ ft.}^2$. Thus,

$f_{\substack{landing \\ gear}} = 0.74 + (0.8)(0.5) = 1.14 \text{ ft.}^2$

$f_{empennage} = (C_{D_\pi} A_\pi)_{empennage} = (0.007)(38.71) = 0.2715 \text{ ft.}^2$

$f_{total} = 1.131 + 1.525 + 1.14 + 0.271 = 4.067 \text{ ft.}^2$

Adding 10% for mutual interference between component parts and 5% for small protuberances, $f_{airplane} = 4.677 \text{ ft.}^2$. Thus,

$(C_{D_f})_{airplane} = (C_{D_\pi})_{airplane} = 0.0269.$

16. airplane C_L $(C_L)_{airplane} = C_{L_w} + C_{L_t} \frac{S_t}{S_w} \eta_t = 0.307 + 0.0129\left(\frac{38.71}{174}\right)(.85)$

$= 0.309$

17. airplane C_D $(C_D)_{airplane} = (C_{D_\pi})_{airplane} + \frac{C_L^2}{\pi e AR}$

$= .0269 \frac{(0.307)^2}{(3.1416)(.98)(7.378)} = 0.0311$

18. airplane C_m and C_T $C_m = \frac{Tz_T}{\frac{1}{2}\rho U^2 S}$, $C_T = \frac{T}{\frac{1}{2}\rho U^2 S}$, but T = 0.

Thus, $C_m = 0.0$ and $C_T = 0.0$.

19. airplane C_{L_u}, C_{D_u}, C_{m_u}, C_{T_u} $C_{L_u} = C_{D_u} = C_{m_u} = C_{T_u} = 0.0$

20. airplane C_{L_α} $C_{L_\alpha} = (C_{L_\alpha})_{wing} = 4.61$

21. airplane C_{D_α} $(C_{D_\alpha})_{airplane} = \frac{dC_{d_o}}{d\alpha} + \frac{2C_L}{\pi e AR} C_{L_\alpha}$

$= 0.0 + \frac{2(.309)(4.61)}{(3.1416)(.98)(7.378)}$

$= 0.126$

22. airplane C_{m_α} $(C_{m_\alpha})_{airplane} = C_{m_{\alpha_{wing}}} - C_{m_{\alpha_{tail}}} + C_{m_{\alpha_{fus.}}}$

$$(C_{m_\alpha})_{wing} = \left\{\left[1.0 + \frac{2C_L}{\pi e AR}\left(\frac{\alpha - i_w}{57.3}\right) + \frac{C_D}{C_{L_\alpha}}\right]\frac{x_a}{c} + \left[\frac{2C_L}{\pi e AR} - \left(\frac{\alpha - i_w}{57.3}\right) - \frac{C_L}{C_{L_\alpha}}\right]\frac{z_a}{c}\right\} C_{L_\alpha}$$

$$= \left\{\left[1.0 + \frac{2(.309)}{(3.1416)(.98)(7.378)}(0.0) + \frac{0.0311}{4.61}\right]\left[\frac{0.1163}{4.86}\right] + \left[\frac{2(.309)}{(3.1416)(.98)(7.378)} - 0.0 - \frac{0.309}{4.61}\right]\left[\frac{1.67}{4.86}\right]\right\}[4.61]$$

$$(C_{m_\alpha})_{wing} = 0.048$$

$$(C_{m_\alpha})_{tail} = C_{L_{\alpha_t}}\left(1 - \frac{d\varepsilon}{d\alpha}\right)\frac{S_t}{S_w}\frac{\ell_t}{c}\eta_t$$

$$= (3.64)(.58)\left(\frac{38.71}{174}\right)\left(\frac{14.6}{4.86}\right)(.85) = 1.198$$

$$(C_{m_\alpha})_{fus.} = \frac{k_f w_f^2 \ell_b}{S_w c} = \frac{(0.51)(4.17)^2(25.0)}{(174)(4.86)} = 0.265$$

$$(C_{m_\alpha})_{airplane} = 0.048 - 1.2 + 0.265 = -0.885$$

23. airplane $C_{L_{\dot\alpha}}$ $(C_{L_{\dot\alpha}})_{airplane} = 2.0 C_{L_{\alpha_t}}\frac{d\varepsilon}{d\alpha}\frac{\ell_t'}{c}\frac{S_t}{S_w}\eta_t$

$$= (2.0)(3.64)(0.42)\left(\frac{14.6}{4.86}\right)\left(\frac{38.71}{174}\right)(.85) = 1.74$$

24. airplane $C_{D_{\dot\alpha}}$ $C_{D_{\dot\alpha}} = 0.0$

25. airplane $C_{m_{\dot\alpha}}$ $(C_{m_{\dot\alpha}})_{airplane} = -2.0 C_{L_{\alpha_t}}\frac{d\varepsilon}{d\alpha}\frac{\ell_t}{c}\frac{\ell_t'}{c}\frac{S_t}{S_w}\eta_t$

$$= -2.0(3.64)(.42)\left(\frac{14.6}{4.86}\right)\left(\frac{14.6}{4.86}\right)\left(\frac{38.71}{174}\right)(.85)$$

$$= -5.24$$

26. airplane C_{L_q} $(C_{L_q})_{airplane} = 2.0 \frac{x'}{c} C_{L_\alpha} + 2.0 \frac{\ell_t}{c} C_{L_{\alpha_t}} \frac{S_t}{S_w} \eta_t$

$= 2.0 \left(-\frac{0.1163}{4.86}\right)(4.61)$

$+ 2.0\left(\frac{14.6}{4.86}\right)(3.64)\left(\frac{38.61}{174}\right)(.85) = 3.9$

27. airplane C_{D_q} $(C_{D_q})_{airplane} = 0.0$

28. airplane C_{m_q} $(C_{m_q})_{airplane} = -\frac{2x'}{c^2}|x'| C_{L_\alpha} - 2\frac{\ell_t^2}{c^2} C_{L_{\alpha_t}} \frac{S_t}{S_w} \eta_t$

$= -2.0 \frac{(-.1163)}{(4.86)^2}(.1163)(4.61)$

$- 2.0 \left(\frac{14.6}{4.86}\right)^2 (3.64)\left(\frac{38.71}{174}\right)(.85) = -12.43$

29. airplane $C_{L_{\delta_E}}$ $(C_{L_{\delta_E}})_{airplane} = C_{\ell_{\delta_E}} \left(\frac{C_{L_{\alpha_t}}}{C_{\ell_{\alpha_t}}}\right)\left(\frac{(\alpha_\delta)C_L}{(\alpha_\delta)C_\ell}\right)\frac{S_t}{S_w} \eta_t$

$C_{\ell_{\delta_E}}$ can be found from Figure 14 for $c_f/c = \frac{1.43}{3.35} \simeq .43$
or $C_{\ell_{\delta_E}} = 0.06$ per degree or 3.41 per radian.

$\frac{(\alpha_\delta)C_L}{(\alpha_\delta)C_\ell}$ can be found from Figure 16 using a c_f/c ratio of .43. This ratio gives a value of $(\alpha_\delta)C_\ell = -0.77$. Using this value and the tail aspect ratio, 3.44,

$\frac{(\alpha_\delta)C_L}{(\alpha_\delta)C_\ell} = 1.04$ from the lower part of Figure 16. Thus,

$C_{L_{\delta_E}}$ airplane $= (3.41)\frac{(3.64)}{(5.73)}(1.04)\left(\frac{38.71}{174}\right)(.85) = 0.427$

30. airplane $C_{D_{\delta_E}}$ To estimate $C_{D\delta_E}$, the tail surface in Figure 17 which is most like the one in question should be used. The numerical value of $C_{D\delta_E}$ can be taken from plots of C_D versus α for different elevator deflections. From Figure 17 for tail surface 5, $C_{D_{\delta_E}}$ per radian = 0.315. Thus,

$$\left(C_{D_{\delta_E}}\right)_{airplane} = \left(C_{D_{\delta_E}}\right)_{per\ radian} \frac{S_t}{S_w} \eta_t$$

$$= (0.315)\left(\frac{38.71}{174}\right)(.85) = 0.0596 \text{ per radian}$$

31. <u>airplane $C_{m_{\delta_E}}$</u> $\left(C_{m_{\delta_E}}\right)_{airplane} = -\frac{\ell_t}{c} C_{L_{\delta_E}} = -\left(\frac{14.6}{4.86}\right)(0.427) = -1.28$

LATERAL SAMPLE CALCULATIONS

The following is a detailed procedure for calculating the lateral stability derivatives for the Cessna 182 airplane. In Table G-2 the pertinent airplane characteristics are given, from which certain geometric and aerodynamic data such as effective vertical tail aspect ratio, vertical tail lift curve slope, wing and horizontal tail aspect ratio, body side area, and fuselage volume are calculated. Then the formulas for the stability derivatives, from the appropriate sections in the text, are presented with the numbers corresponding to the Cessna 182 for the cruise condition.

S_w = 174 ft.^{2}	b_w = 35.83 ft.	C_L = .307
Γ = 1.73°	z_w = -1.835 ft.	λ = .7
L_b = 25 ft.	x_m = 7.0 ft.	H_1 = 4.8 ft.
H_2 = 1.8 ft.	b_a = 8.9 ft.	c_a = 0.75 ft.
S_R = 6.95 ft.^{2}	H = 4.85 ft.	S_v = 18.57 ft.^{2}
b_v = 5.75 ft.	R1 = 0.73 ft.	z_v = 2.82 ft.
η_v = .85	ℓ_v = 14.8 ft.	W = 4.02 ft.
b_h = 11.6 ft.	S_h = 38.71 ft.^{2}	λ_h = .66
Y_i = 8.34 ft.	C_{D_o} = .0279	U = 219 ft/sec.

ρ = .00205 slugs/ft.^{3}, density at 5,000 feet altitude
HNOSE = 2.7 ft., fuselage height in nose region
WNOSE = 2.8 ft., fuselage width in nose region
HFCY = 3.5 ft., fuselage height at front of canopy
WFCY = 3.6 ft., fuselage width at front of canopy
LFCY = 3.12 ft., length along body centerline from nose to front of canopy
LMH = 6.41 ft., length along body centerline from nose to point of maximum fuselage height
HBCY = 2.9 ft., fuselage height at back of canopy
WBCY = 3.1 ft., fuselage width at back of canopy
LBCY = 12.83 ft., length along body centerline from nose to back of canopy

Table G-2. Pertinent lateral dimensions for the Cessna 182.

1. <u>effective aspect ratio and lift curve slope of vertical tail</u>

$$Ae = 1.55\,\frac{b_v^2}{S_v} = 2.76$$

From Figure 28, $a_v = (C_{L_\alpha})_v$ = .0534/deg.= 3.06/rad.

2. <u>aspect ratio of wing and horizontal tail</u>

$$AR = \frac{b_w^2}{S_w} = 7.378;\ (AR)_h = \left(\frac{b_h}{S_h}\right)^2 = 3.476$$

3. mean aerodynamic chord of wing

$$c_w = \frac{S_w}{b_w} = 4.86 \text{ ft.}$$

4. estimate body side area

The body side area (S_{B_S}) is estimated using four trapezoids by the following formula:

$$S_{B_s} = \frac{(HNOSE + HFCY)(LFCY)}{2.0} + \frac{(H + HFCY)(LMH - LFCY)}{2.0} + \frac{(H + HBCY)(LBCY - LMH)}{2.0} + \frac{(HBCY + 2R_1)(L_b - LBCY)}{2.0}$$

$$= 74.8 \text{ ft.}^2$$

5. estimate fuselage volume

The fuselage volume is estimated using four prismoids by the following formulas:

$$V1 = LFCY[2.0(HNOSE \cdot WNOSE + HFCY \cdot WFCY) + HFCY \cdot WNOSE + HNOSE \cdot WFCY]$$

$$V2 = (LMH-LFCY)[2.0(HFCY \cdot WFCY + H \cdot W) + H \cdot WFCY + HFCY \cdot W]$$

$$V3 = (LBCY-LMH)[2.0(HBCY \cdot WBCY + H \cdot W) + H \cdot WBCY + W \cdot HBCY]$$

$$V4 = (L_b-LBCY)[2.0(HBCY \cdot WBCY + 4.0 \cdot R_1^2) + HBCY \cdot 2.0R_1 + WBCY \cdot 2.0R_1]$$

$$\text{Volume} = (V1+V2+V3+V4)/6.0 = 236.0 \text{ ft.}^3$$

Now each of the stability derivatives will be calculated using the formula from the text which seems best suited for light aircraft.

6. C_{y_β}

$$(C_{y_\beta})_{total} = (C_{y_\beta})_{wing} + (C_{y_\beta})_{fus} + (C_{y_\beta})_{tail}$$

$$(C_{y_\beta})_{wing} = -.0001|\Gamma| = -.000173/\text{deg} = -.00991/\text{rad}$$

$$(C_{y_\beta})_{fus} = -Ki(C_{L_\alpha})_{fus}\left(\frac{\text{Body Reference Area}}{S_w}\right)$$

$(C_{L\alpha})_{fus}$ is assumed equal to 0.1/rad.
Ki from Figure 23 is 1.647.
Body Reference Area = (Fuselage Volume)$^{2/3}$ = 38.19 ft.^{2}.
Therefore,

$$(C_{y_\beta})_{fus} = -1.647(0.1)\left(\frac{38.19}{174}\right) = -.03616/\text{rad.}$$

$$(C_{y_\beta})_{tail} = -K(C_{L_\alpha})_v\left(1 + \frac{\partial\sigma}{\partial\beta}\right)\frac{q_v}{q}\frac{S_v}{S_w}$$

K, from Figure 24, is 1.0

$$\left(1 + \frac{\partial\sigma}{\partial\beta}\right)\frac{q_v}{q} = .724 + 1.53\left(\frac{S_v}{S_w}\right) + .4\frac{z_w}{d} + .009(AR) = 0.802$$

where d is equal to H, the maximum fuselage height.

Thus $(C_{y_\beta})_{tail}$ = -.2619/rad. Therefore,

$$(C_{y_\beta})_{total} = -.00991 - .03616 - .2619 = -.3086/rad.$$

7. C_{ℓ_β}

$$(C_{\ell_\beta})_{total} = (C_{\ell_\beta})_w + (C_{\ell_\beta})_{w,\Gamma=0} + (C_{\ell_\beta})_v + (\Delta C_{\ell_\beta})_1 + (\Delta C_{\ell_\beta})_2$$

$$(C_{\ell_\beta})_w = \left(\frac{C_{\ell_\beta}}{\Gamma}\right)\Gamma, \text{ if the tail shape is ignored.}$$

$\frac{C_{\ell_\beta}}{\Gamma}$ from Figure 26 is -.000238/deg^2, so

$$(C_{\ell_\beta})_w = -.0236/rad.$$

$$(C_{\ell_\beta})_{w,\Gamma=0} = C_L\left[\frac{-K(.71\lambda+.29)}{AR\ \lambda} + .05\right].$$

Assuming that K = 1.25, this gives

$$(C_{\ell_\beta})_{w,\Gamma=0} = -.04313/rad.$$

$$(C_{\ell_\beta})_v = -a_v\frac{S_v}{S_w}\frac{z_v}{b_w}\eta_v = -.02184/rad.$$

From Table 9, values of $(\Delta C_{\ell\beta})_1$ = -.0006 and $(\Delta C_{\ell\beta})_2$ = .00016 are given. Therefore,

$$(C_{\ell_\beta})_{total} = -.0236 - .04313 - .02184 - .0006 + .00016$$
$$= -.089/rad.$$

8. C_{n_β}

$$(C_{n_\beta})_{total} = -K_n\frac{\text{Body Side Area}}{S_w}\frac{\ell_b}{b_w} - (C_{y_\beta})_{tail}\frac{\ell_v}{b_w}$$

From Figure 30, K_n = .002539/deg = 0.1455/rad.
From the C_{y_β} calculation, $(C_{y_\beta})_{tail}$ = -.2619/rad.
Therefore,

$$(C_{n_\beta})_{total} = -.1455\left(\frac{74.8}{174}\right)\frac{25}{35.83} - \left(-.2619\ \frac{14.8}{35.83}\right)$$
$$= .06455/rad.$$

9. C_{ℓ_p}

$$(C_{\ell_p})_{total} = (C_{\ell_p})_w + (C_{\ell_p})_h + (C_{\ell_p})_v$$

Since zero wing sweep:

$$(C_{\ell_p})_w = \left[(C_{\ell_p})_{a_o=2\pi}\right]\left[\frac{AR+4}{(\frac{2\pi}{(a_o)_w})AR+4}\right] - \frac{1}{8}C_D \cdot$$

From Figure 34, $(C_{\ell_p})_{a_o=2\pi} = -.4794/rad.$ Also, from Ref. 7 using a 2412 airfoil $(a_o)_w = 5.9/rad.$ Substituting gives

$$(C_{\ell_p})_w = (-.4794)\left[\frac{7.378+4.0}{(\frac{2\pi}{5.9})7.378+4.0}\right] - \frac{1}{8}(.0279) = -.4643/rad.$$

$$(C_{\ell_p})_h = 0.5\,\frac{S_h}{S_w}\left(\frac{b_h}{b_w}\right)^2\left[(C_{\ell_p})_{a_o=2\pi}\right]\left[\frac{(AR)_h + 4.0}{(\frac{2\pi}{(a_o)_h})(AR)_h+4.0}\right]$$

From Figure 34, using the horizontal tail aspect and taper ratios of 3.476 and 0.66, respectively, gives

$$(C_{\ell_p})_{a_o=2\pi} = -.29/rad.$$

Again from Ref. 7, with a 0009 airfoil, $(a_o)_h = 5.73/rad$, which, when substituted in the above equation, gives $(C_{\ell_p})_h = -.00324/rad.$

$$(C_{\ell_p})_v = 2\left(\frac{z_v}{b_w}\right)^2 (C_{y_\beta})_{tail} = -.00323/rad.$$

Therefore, $(C_{\ell_p})_{total} = -.4708/rad.$

10. C_{y_p}

$$C_{y_p} = \left(\frac{C_{y_p}}{C_L}\right)C_L + \frac{(\Delta C_{y_p})_\Gamma}{(C_{\ell_p})_{\Gamma=0}}\,C_{\ell_p}$$

From Figure 32,

$$\left(\frac{C_{y_p}}{C_L}\right) = -.0795/rad.$$

Figure 33 gives

$$\frac{(\Delta C_{y_p})_\Gamma}{(C_{\ell_p})_{\Gamma=0}} = .02743. \quad \text{Therefore,}$$

$$(C_{y_p}) = (-.0795)(.307) + (.02743)(-.4708) = -.0373/rad.$$

11. C_{n_p}

$$(C_{n_p})_{total} = (C_{n_p})_w + (C_{n_p})_v$$

The wing contribution is given by the following formula:

$$(C_{n_p})_w = C_L \frac{AR+4}{AR+4\cos\Lambda}\left[1+6\left(1+\frac{\cos\Lambda}{AR}\right)\frac{\tan^2\Lambda}{12}\right]\left(\frac{C_{n_p}}{C_L}\right)_{\Lambda=0°}$$

Figure 35, as a function of wing aspect and taper ratio, gives

$\left(\frac{C_{n_p}}{C_L}\right)_{\Lambda=0°} = -.0588/\text{rad.}$ Thus,

$(C_{n_p})_w = (-.0588)(.307) = -.0180/\text{rad.}$

The vertical tail contribution is given by

$$(C_{n_p})_v = \left\{57.3\, a_v \frac{S_v}{S_w}\frac{1}{b_w}(z_v\sin\alpha+\ell_v\cos\alpha)\right\}\left\{\frac{2}{b_w}(z_v\cos\alpha-\ell_v\sin\alpha) - \left[\frac{\partial\sigma_1}{\partial\frac{pb}{2U}}+\frac{\partial\sigma_2}{\partial\frac{pb}{2U}}\right]\right\}$$

From Figure 36, $\frac{\partial\sigma_1}{\partial\frac{pb}{2U}} = 0.24$, where h_t is assumed approximately equal to z_v.

$$\frac{\partial\sigma_2}{\partial\frac{pb}{2U}} = 9.30\left[\frac{z_v-(z_v\cos\alpha-\ell_v\sin\alpha)}{b_w}\right]^2\frac{3}{b_w} = 0.0$$

for zero angle of attack. Therefore,

$(C_{n_p})_v = -.01119/\text{rad.}$ and $(C_{n_p})_{total} = -.0292/\text{rad.}$

12. C_{y_r}

$$(C_{y_r})_{total} = (C_{y_r})_w + (C_{y_r})_{tail}$$

$(C_{y_r})_w = .143C_L - .05 = -.0061/\text{rad.}$

$$(C_{y_r})_{tail} = -2.0\frac{\ell_v}{b_w}(C_{y_\beta})_{tail} = .2164/\text{rad.}$$

Thus, $(C_{y_r})_{total} = .2103/\text{rad.}$

13. C_{ℓ_r}

$$(C_{\ell_r})_{total} = (C_{\ell_r})_{wing} + (C_{\ell_r})_{tail}$$

From Figure 38, $\left(\frac{C_{\ell_r}}{C_L}\right) = 0.2568/\text{rad.}$ Thus,

$(C_{\ell_r})_{wing} = \left(\frac{C_{\ell_r}}{C_L}\right)C_L = 0.0788/rad.$ Also,

$(C_{\ell_r})_{tail} = -2.0 \frac{\ell_v}{b_w} \frac{z_v}{b_w} (C_{y_\beta})_{tail} = 0.0170/rad.$ Thus,

$(C_{\ell_r})_{total} = 0.0958/rad.$

14. C_{n_r}

$(C_{n_r})_{total} = (C_{n_r})_w + (C_{n_r})_{tail}$

$(C_{n_r})_w = -.33\left(\frac{1+3\lambda}{2+2\lambda}\right)C_{D_o} - .02\left(1 - \frac{AR-6}{13} - \frac{1-\lambda}{2.5}\right)C_L^2$

$= -.009852/rad.$

$(C_{n_r})_{tail} = 2\left(\frac{\ell_v}{b_w}\right)^2 (C_{y_\beta})_{tail} = -.08938/rad.$ Thus,

$(C_{n_r})_{total} = -.09924/rad.$

15. $C_{y_{\delta_A}}$

The value of $C_{y\delta_A}$ is assumed zero for conventional light aircraft.

16. $C_{\ell_{\delta_A}}$

$C_{\ell_{\delta_A}} = \left(\frac{C_{\ell_{\delta_A}}}{\tau}\right)\tau$

From Figure 42, $\left(\frac{C_{\ell_{\delta_A}}}{\tau}\right)$ is obtained by first considering the outboard edge of the aileron

$\left(\frac{b_a+y_i}{b_w/2} = .962\right)$ and corresponding to this point getting a value of

$\frac{C_{\ell_{\delta_A}}}{\tau} = 0.786$, then using the inboard edge of the aileron

$\frac{y_i}{b_w/2} = .466$ and, again from Figure 42, getting a corresponding value of

$\frac{C_{\ell_{\delta A}}}{\tau} = 0.231.$ These two values are then subtracted, outboard station minus inboard station, to give a

$\frac{C_{\ell_{\delta A}}}{\tau} = (.786-.231) = 0.555$ over the extent of unit antisymmetrical angle of attack. Now from Figure 41, $\tau = 0.319.$ Therefore,

$$C_{\ell_{\delta_A}} = \left(\frac{C_{\ell_{\delta_A}}}{\tau}\right)\tau = 0.177/\text{rad.}$$

17. $C_{n_{\delta_A}}$

$$C_{n_{\delta_A}} = 2KC_L C_{\ell_{\delta_A}}$$

From Figures 43 and 44, K is determined to be -0.1537. Therefore,

$$C_{n_{\delta_A}} = 2.0(-.1537)(.307)(.177) = -.0167/\text{rad.}$$

18. $C_{y_{\delta_R}}$, $C_{\ell_{\delta_R}}$, $C_{n_{\delta_R}}$

These control derivatives are given by the following formulas:

$$C_{y_{\delta_R}} = a_v \tau \frac{S_v}{S_w}$$

$$C_{\ell_{\delta_R}} = a_v \tau \frac{S_v}{S_w} \frac{z_v}{b_w}$$

$$C_{n_{\delta_R}} = -a_v \tau \frac{S_v}{S_w} \frac{\ell_v}{b_w} n_v$$

From Figure 46 as a function of rudder area to vertical tail area ratio,

$\frac{S_R}{S_v} = 0.374$, it is determined that $\tau = 0.574$. Thus, these three derivatives are evaluated as follows:

$$C_{y_{\delta_R}} = .187/\text{rad.}$$

$$C_{\ell_{\delta_R}} = .0147/\text{rad.}$$

$$C_{n_{\delta_R}} = -.0658/\text{rad.}$$

APPENDIX H

LONGITUDINAL PROGRAM

```
C                                                                       1
C     GIVEN VALUES OF THE STABILITY DERIVATIVES AND AIRCRAFT            2
C     CHARACTERISTICS THIS PROGRAM PERFORMS THE FOLLOWING:              3
C                                                                       4
C                                                                       5
C        1) CALCULATES DIMENSIONAL STABILITY DERIVATIVES                6
C                                                                       7
C        2) FORMS THE TRANSFER FUNCTIONS, TF(S)=N(S)/D(S)               8
C                                                                       9
C        3) SOLVE FOR ROOTS OF D(S) AND N(S)                           10
C                                                                      11
C        4) CALCULATE NATURAL FREQUENCIES, DAMPING RATIOS, TIME TO DAMP 12
C           TO ONE-HALF AMPLITUDE, AND SETTLING TIME                   13
C                                                                      14
C        5) PRODUCES INFORMATION NEEDED FOR BODE PLOT CONSTRUCTION      15
C                                                                      16
C                                                                      17
C     THE DERIVATION OF THE EQUATIONS OF MOTION ON WHICH THIS ANALYSIS IS 18
C     BASED WAS TAKEN FROM 'DYNAMICS OF THE AIRFRAME', BUREAU OF       19
C     AERONAUTICS REPORT, AE-61-4II.                                   20
C                                                                      21
C                                                                      22
C     THE ANALYSIS DESCRIBED ABOVE MUST MEET THE ASSUMPTIONS IMPOSED ON 23
C     THE EQUATIONS OF MOTION WHEN THEY WERE DERIVED.                  24
C      THESE ASSUMPTIONS ARE:                                          25
C                                                                      26
C                                                                      27
C                                                                      28
C        1) THE AIRFRAME IS ASSUMED TO BE A RIGID BODY.                29
C                                                                      30
C        2) THE EARTH IS ASSUMED TO BE FIXED IN SPACE, AND, UNLESS     31
C           SPECIFICALLY STATED OTHERWISE, THE EARTH'S ATMOSPHERE IS   32
C           ASSUMED TO BE FIXED WITH RESPECT TO THE EARTH.             33
C                                                                      34
C        3) THE MASS OF THE AIRPLANE IS ASSUMED TO REMAIN CONSTANT FOR 35
C           THE DURATION OF ANY PARTICULAR DYNAMIC ANALYSIS.           36
C                                                                      37
C        4) THE X-Z PLANE IS ASSUMED TO BE A PLANE OF SYMMETRY.        38
C                                                                      39
C        5) THE DISTURBANCES FROM THE STEADY FLIGHT CONDITION ARE ASSUMED 40
C           TO BE SMALL ENOUGH SO THAT THE PRODUCTS AND SQUARES OF THE 41
C           CHANGES IN VELOCITIES ARE NEGLIGIBLE IN COMPARISON WITH THE 42
C           CHANGES THEMSELVES.  ALSO, THE DISTURBANCE ANGLES ARE ASSUMED 43
C           TO BE SMALL ENOUGH SO THAT THE SINES OF THESE ANGLES MAY BE 44
C           SET EQUAL TO THE ANGLES AND THE COSINES SET EQUAL TO ONE.  45
C           PRODUCTS OF THESE ANGLES ARE ALSO APPROXIMATELY ZERO AND CAN 46
C           BE NEGLECTED.  AND, SINCE THE DISTURBANCES ARE SMALL, THE  47
C           CHANGE IN AIR DENSITY ENCOUNTERED BY THE AIRPLANE DURING ANY 48
C           DISTURBANCE CAN BE CONSIDERED TO BE ZERO.                  49
C                                                                      50
C        6) DURING THE STEADY FLIGHT CONDITION, THE AIRPLANE IS ASSUMED 51
C           TO BE FLYING WITH WINGS LEVEL AND ALL COMPONENTS OF VELOCITY 52
C           ZERO EXCEPT U SUB O.  W SUB O = O BECAUSE THE STABILITY AXES 53
C           WERE CHOSEN AS THE REFERENCE AXES.                         54
C                                                                      55
C                                                                      56
C        7) THE FLOW IS ASSUMED TO BE QUASI-STEADY.                    57
C                                                                      58
C                                                                      59
C     THE FOLLOWING CARDS IMPLY THAT THE PROGRAM IS EXECUTED IN DOUBLE 60
C     PRECISION.                                                       61
C                                                                      62
      IMPLICIT REAL*8(A-H,O-Z)                                         63
      REAL*8 MS,IYY,MU,MW,MDW,MQ,MIN,NUS,NAS,NTHS,KGAIN,KC,KROOT,KKK,KD, 64

     $KN,NWS                                                           65
      COMPLEX*16 P,TST                                                 66
      COMMON   WMSP,ZSP,T12SP,TOSSP,WNP,ZP,T12P,TOSP,WF(21),RRD(10),RRN( 67
     $10),RID(10),RIN(10),AR(21),PHASE(21),ACC,WCYCLE(21),ARDB(21),PHDEG 68
     $(21),KGAIN                                                       69
      COMMON I                                                         70
      DIMENSION NUS(5),NAS(5),NTHS(5),DS(6),ROOTR(10),ROOTI(10),C(5),KC( 71
     $4),QUF(3),QUF2(3),RR1(2),RR2(2),RI1(2),RI2(2),CC(4),RR(3),COFFI(6 72
     $),RI(3),XR(3),XI(3),COF(3),RE(2),RIM(2),ROOT(1),COFF(2),KKK(21),MW 73
     $S(5),P(6)                                                        74
C                                                                      75
C     THE READ STATEMENT IS THE INPUT OF ALL NON-DIMENSIONAL STABILITY 76
C     DERIVATIVES, EXCLUDING CONTROL SURFACE DERIVATIVES.              77
C                                                                      78
C     THE NON-DIMENSIONAL DERIVATIVE CTRPM IS INCLUDED ONLY FOR THE SAKE 79
C     OF COMPLETENESS.  IF THE VALUE OF THIS DERIVATIVE IS KNOWN IT    80
C     SHOULD BE USED, OTHERWISE IT SHOULD BE TREATED SIMILAR TO CTU.   81
C                                                                      82
      READ(1,100)CL,CD,CM,CT,CLA,CDA,CMA,CLQ,CDQ,CMQ,CLDA,CDDA,CMDA,CTRP 83
     $M,CLU,CDU,CMU,CTU                                                84
  100 FORMAT(8F10.6/8F10.6/2F10.6)                                     85
      WRITE(3,200)                                                     86
  200 FORMAT(1X,121('*'),/,1X,'*',119X,'*',/,1X,'*',39X,'LONGITUDINAL ST 87
     $ABILITY DERIVATIVES',46X,'*',/,1X,'*',39X,34('-'),46X,'*',/,1X,'* 88
     $,119X,'*',/,1X,'*',119X,'*')                                     89
      WRITE(3,201)CL,CD,CM,CT,CLA,CDA,CMA,CLQ,CDQ,CMQ,CLDA,CDDA,CMDA,CTR 90
     $PM,CLU,CDU,CMU,CTU                                               91
  201 FORMAT(1X,'*  CL    =',F10.6,4X,'CD    =',F10.6,4X,'CM   =',F10.6,4X 92
     $,'CT   =',F10.6,4X,'CLA  =',F10.6,4X,'CDA  =',F10.6,'  *',/,1X,'* 93
     $CMA  =',F10.6,4X,'CLQ  =',F10.6,4X,'CDQ =',F10.6,4X,'CMQ =',F10.6 94
     $,4X,'CLDA =',F10.6,4X,'CDDA =',F10.6,'  *',/,1X,'*  CMDA =',F10.6, 95
     $4X,'CTRPM =',F10.6,4X,'CLU =',F10.6,4X,'CDU =',F10.6,4X,'CMU  =',F 96
     $10.6,4X,'CTU  =',F10.6,'  *',/,1X,'*',119X,'*',/,1X,'*',119X,'*',/ 97
     $,1X,121('*'),///)                                                98
C                                                                      99
C     INPUT OF PERTINENT AIRCRAFT CHARACTERISTICS                     100
C                                                                     101
      READ(1,101)RHO,U,S,MS,CH,IYY,COSXZ,SINXZ,ZJ,GCOSGM,GSINGM       102
  101 FORMAT(8F10.5/3F10.5)                                           103
C                                                                     104
C     ZJ IS THE PERPENDICULAR DISTANCE FROM THE C.G. TO THRUST LINE,  105
C     POSITIVE FOR C.G. ABOVE THE THRUST LINE                         106
C                                                                     107
C     CH IS THE MEAN AERODYNAMIC CHORD OF THE WING                    108
C                                                                     109
C     U IS THE SPEED OF THE AIRCRAFT IN FEET PER SECOND               110
C                                                                     111
C     COSXZ IS THE COSINE OF ANGLE MADE BETWEEN THE THRUST AXIS AND THE 112
C     WIND AXIS                                                       113
C                                                                     114
C     SINXZ IS THE SINE OF THE ANGLE MADE BETWEEN THE THRUST AXIS AND 115
C     THE WIND AXIS                                                   116
C                                                                     117
C     RHO IS THE DENSITY AT THE ALTITUDE WHICH THE AIRPLANE IS FLYING 118
C                                                                     119
C     S IS THE WING AREA OF THE AIRPLANE                              120
C                                                                     121
C     MS IS THE MASS OF THE AIRPLANE                                  122
C                                                                     123
C     IYY IS THE MOMENT OF INERTIA ABOUT THE Y AXIS                   124
C                                                                     125
C     GCOSGM AND GSINGM ARE THE PRODUCTS OF THE ACCELERATION DUE TO   126
C     GRAVITY (ASSUME = 32.2 FT/SEC**2 FOR THIS ALTITUDE RANGE) AND THE 127
C     COSINE AND SINE RESPECTIVELY OF THE INITIAL FLIGHT PATH ANGLE,  128
C     GAMMA, (USUALLY ZERO FOR LEVEL FLIGHT).                         129
C                                                                     130
      WRITE(3,202)RHO,S,MS,GCOSGM,COSXZ,ZJ,U,CH,IYY,GSINGM,SINXZ      131
  202 FORMAT(1X,130('*'),/,1X,'*',128X,'*',/,1X,'*',46X,'PERTINENT AIRPL 132
     $ANE CHARACTERISTICS',48X,'*',/,1X,'*',46X,34('-'),48X,'*',/,1X,'* 133
     $,128X,'*',/,1X,'*  RHO =',F10.6,3X,'WING AREA =',F10.6,3X,'MASS =' 134
     $,F10.6,3X,'G*COS(GAMMA) =',F10.6,3X,'COS(XZ)  =',F10.6,3X,'ZJ =',F1 135
     $0.6,'  *',/,1X,'*  U    =',F10.6,3X,'CHORD     =',F10.6,3X,'IYY  =' 136
     $,F10.4,3X,'G*SIN(GAMMA) =',F10.6,3X,'SIN(XZ)  =',F10.6,19X,'*',/,1X 137
     $,'*',128X,'*',/,1X,130('*'),///)                                138
      LCOUNT=0                                                         139
C                                                                      140
C     LCOUNT IS A COUNTER WHICH PREVENTS MULTIPLE CALCULATIONS OF THE  141
C     CHARACTERISTIC EQUATION AND NUMERATOR COEFFICIENTS.              142
C                                                                      143
C     LL=1,4 CONSTITUTES SOLUTIONS FOR FOUR DIFFERENT NUMERATORS.      144
C                                                                      145
      DO 35 LL=1,4                                                     146
C                                                                      147
C     THE READ STATEMENT BELOW IS THE INPUT FOR THE VARIABLES EXPLAINED 148
C     BELOW.                                                           149
C                                                                      150
      READ(1,102)CLIN,CDIN,CMIN,K,NUMER,ACC                           151
  102 FORMAT(3F10.6,2I3,E14.7)                                        152
C                                                                     153
C     CLIN, CDIN, AND CMIN ARE THE STABILITY DERIVATIVES DUE TO CONTROL 154
C     SURFACE DEFLECTIONS.  CLIN IS EITHER THE PARTIAL OF CL WITH     155
C     RESPECT TO ELEVATOR DEFLECTION OR FLAP DEFLECTION.  THE VALUE OF K 156
C     DETERMINES WHETHER IT IS CONCERNED WITH FLAPS OR ELEVATOR.      157
C                                                                     158
C     IF K IS GIVEN THE VALUE 1 THEN CLIN, CDIN, AND CMIN ARE PARTIAL 159
C     DERIVATIVES WITH RESPECT TO ELEVATOR DEFLECTION. IF K=2 THEN THE 160
C     PARTIALS ARE TAKEN WITH RESPECT TO FLAP DEFLECTION.             161
C                                                                     162
C     NUMER DEFINES WHICH TRANSFER FUNCTION WE ARE INTERESTED IN, (U, 163
C     ALPHA,THETA,AND W).  NUMER=1 GIVES VARIATIONS IN U, NUMER=2 GIVES 164
C     VARIATIONS IN ALPHA, NUMER=3 GIVES VARIATIONS IN THETA, AND     165
C     NUMER=4 GIVES VARIATIONS IN W.                                  166
C                                                                     167
C     THUS, FOR EXAMPLE, IF K=2 AND NUMER=2 THE TRANSFER FUNCTION WILL 168
C     BE VARIATION IN ALPHA DUE TO DEFLECTION OF THE FLAPS.           169
C                                                                     170
C     WITH THE ABOVE DO LOOP SET FOR LL=1,4 FOUR DATA CARDS MUST BE READ 171
C     WITH THE VALUE OF NUMER CHANGING ON EACH CARD FROM 1 TO 4.  IF IT 172
C     IS DESIRED TO CALCULATE ONLY ONE TRANSFER FUNCTION THEN THE DO  173
C     LOOP RANGE SHOULD BE CHANGED TO DO FROM LL=1,1.                 174
C                                                                     175
C     ACC IS THE ACCURACY USED THROUGHOUT THE PROGRAM TO COMPARE TWO  176
C     NUMBERS TO SEE IF THEY ARE SUFFICIENTLY CLOSE.                  177
C                                                                     178
      LCOUNT=LCOUNT+1                                                 179
      IF(LCOUNT.GE.2)GO TO 4                                          180
      IF(K.NE.1)GO TO 1                                               181
      WRITE(3,203)                                                    182
  203 FORMAT(15X,98('*'),/,15X,'*',96X,'*',/,15X,'*  ',31X,'RESPONSE TO 183
     $ELEVATOR DEFLECTION',30X,'  *')                                 184
      GO TO 2                                                         185
    1 WRITE(3,204)                                                    186
  204 FORMAT(15X,98('*'),/,15X,'*',96X,'*',/,15X,'*  ',33X,'RESPONSE TO 187
     $FLAP DEFLECTION',32X,'  *')                                     188
    2 WRITE(3,205)CLIN,CDIN,CMIN,K,ACC                                189
  205 FORMAT(15X,'*',96X,'*',/,15X,'*',96X,'*',/,15X,'*  ','CLIN =',F10.6 190
     $,4X,'CDIN =',F10.6,4X,'CMIN =',F10.6,4X,'K =',I2,4X,'ACC =',F14.8, 191
     $6X,'*',/,15X,'*',96X,'*',/,15X,98('*'))                         192

C                                                                     193
C     CALCULATION OF DIMENSIONAL STABILITY DERIVATIVES                194
C                                                                     195
C     O AND OC ARE JUST CONSTANTS USED TO CALCULATE THE DIMENSIONAL   196
C     STABILITY DERIVATIVES.                                          197
C                                                                     198
      O=RHO*U*S/MS                                                    199
      OC=RHO*U*S*CH/IYY                                               200
C                                                                     201
C     DIMENSIONAL STABILITY DERIVATIVES                               202
C                                                                     203
      XU=O*(-(CDU+CD))                                                204
      ZU=O*(-(CLU+CL))                                                205
      MU=OC*(CMU+CM)                                                  206
      TU=O*(CTU+CT)                                                   207
      XW=(O/2.0)*(CL-CDA)                                             208
      ZW=(O/2.0)*(-(CLA+CD))                                          209
      MW=(OC/2.0)*CMA                                                 210
      ZDW=-RHO*S*CH*CLDA/(4.0*MS)                                     211
      XDW=-RHO*S*CH*CDDA/(4.0*MS)                                     212
      MDW=RHO*S*CH*CH*CMDA/(4.0*IYY)                                  213
      XQ=-RHO*U*S*CH*CDQ/(4.0*MS)                                     214
      ZQ=-RHO*U*S*CH*CLQ/(4.0*MS)                                     215
      MQ=OC*CH*CMQ/4.0                                                216
      TRPM=30*CH*O*CTRPM                                              217
      XIN=-O*CDIN*U/2.0                                               218
      ZIN=-O*CLIN*U/2.0                                               219
      MIN=OC*CMIN*U/2.0                                               220
C                                                                     221
C     COEFFICIENTS FOR TRANSFER FUNCTION                              222
C                                                                     223
C     A1, A2, A3, A4, A5 ARE CONSTANTS USED TO SIMPLIFY THE CALCULATION 224
C     OF THE DENOMINATOR AND NUMERATOR COEFFICIENTS.                  225
C                                                                     226
      A1=TU*COSXZ+XU                                                  227
      A2=SINXZ*3U-ZU                                                  228
      A3=ZJ*MS*TU/IYY+MU                                              229
      A4=1.0-ZDW                                                      230
      A5=ZQ+U                                                         231
C                                                                     232
C     DENOMINATOR COEFFICIENTS, DS(5)S**4+DS(4)S**3+DS(3)S**2+DS(2)S+ 233
C     DS(1), WHERE S REPRESENTS THE LAPLACIAN OPERATOR.               234
C                                                                     235
      DS(5)=A4                                                        236
      DS(4)=-A4*(MQ+A1)-ZW-MDW*A5+XDW*A2                              237
      DS(3)=A1*(MQ*A4+ZW+MDW*A5)-A3*(XDW*A5+XQ*A4)+MQ*ZW-A2*(MQ*XDW-XW- 238
     $XQ*MDW)+MDW*GSINGM-MW*A5                                        239
      DS(2)=GSINGM*(XDW*A3+MW-MDW*A1)+GCOSGM*(-A2*MDW+A3*A4)+A3*(-XW*A5 240
     $+ZW*XQ)-A2*(-XQ*MW+XM*MQ)+A1*(-MQ*ZW+MW*A5)                     241
      DS(1)=GCOSGM*(MW*(-A2)-ZW*A3)+GSINGM*(XW*A3-MW*A1)              242
C                                                                     243
C     NUMERATOR COEFFICIENTS FOR U VARIATION, NUS(4)S**3+NUS(3)S**2+  244
C     NUS(2)S+NUS(1)                                                  245
C                                                                     246
      NUS(4)=XIN*A4+ZIN*XDW                                           247
      NUS(3)=A4*(XQ*MIN-MQ*XIN)+A5*(XDW*MIN-MDW*XIN)-ZW*XIN+ZIN*(XW-XDW 248
     $*MQ+XQ*MDW)                                                     249
      NUS(2)=A5*(-MW*XIN+MIN*XW)+GSINGM*(MDW*XIN-XDW*MIN)-GCOSGM*(MDW 250
     $*ZIN*A4*MIN)+XIN*MQ*ZW+ZIN*(MW*XQ-MQ*XW)-XQ*ZW*MIN             251
      NUS(1)=GSINGM*(XIN*MW-XW*MIN)+GCOSGM*(ZW*MIN-MW*ZIN)            252
C                                                                     253
C     NUMERATOR COEFFICIENTS FOR ANGLE OF ATTACK VARIATION, NAS(4)S**3+ 254
C     NAS(3)S**2+NAS(2)S+NAS(1)                                       255
C                                                                     256
```

```
      NAS(4)=ZIN/U
      NAS(3)=-ZIN*(A1+MQ)/U+MIN*A5/U+XIN*(1-A2)/U
      NAS(2)=MQ*ZIN+A1/U+XIN*A5*A3/U+MIN*XQ*(-A2)/U-ZIN*XU*A3/U-MIN*A5*A
     $1/U-MIN*GSINGM/U+XIN*MG*(A2)/U
      NAS(1)=-XIN*GSINGM*A3/U+MIN*GCOSGM*A2/U+ZIN*GCOSGM*A3/U+MIN*GSINGM
     $*A1/U
C
C     COEFFICIENTS FOR NUMERATOR FOR PITCH VARIATION, NTHS(3)S**2+
C     NTHS(2)S+NTHS(1)
C
      NTHS(3)=MIN*A4+ZIN*MDW
      NTHS(2)=A1*(-MIN*A4-ZIN*MDW)+A2*(MIN*XDW-XIN*MDW)+A3*(ZIN*XDW+XIN*
     $A4)-MIN*ZW+ZIN*MM
      NTHS(1)=A1*(MIN*ZW-MM*ZIN)+A2*(MIN*XW-XIN*MM)+A3*(ZIN*XW-XIN*ZW)
C
C     COEFFICIENTS FOR NUMERATOR FOR W VARIATION,  NWS(4)S**3 +
C     NWS(3)S**2 + NWS(2)S + NWS(1)
C
      NWS(4)=NAS(4)*U
      NWS(3)=NAS(3)*U
      NWS(2)=NAS(2)*U
      NWS(1)=NAS(1)*U
      WRITE(3,206)DS(5),DS(4),DS(3),DS(2),DS(1),NUS(4),NUS(3),NUS(2),NUS
     $(1),NAS(4),NAS(3),NAS(2),NAS(1),NTHS(3),NTHS(2),NTHS(1),NWS(4),NWS
     $(3),NWS(2),NWS(1)
  206 FORMAT(////2X,123('*'),/,2X,'*',121X,'*',/,2X,'*',32X,'POLYNOMIAL
     $COEFFICIENTS FOR THE DENOMINATOR AND NUMERATOR',32X,'*',/2X,'*',32
     $X,57('-'),32X,'*',/,2X,'*',121X,'*',/,2X,'*',3X,'DS(5)   =',F10.4
     $,5X,'DS(4)   =',F10.4,5X,'DS(3)   =',F10.4,5X,'DS(2)   =',F10.4,5X
     $,'DS(1)   =',F10.4,3X,'*',/,2X,'*',121X,'*',/,2X,'*',27X,'NUS(4)
     $=',F10.4,5X,'NUS(3)   =',F10.4,5X,'NUS(2)   =',F10.4,5X,'NUS(1)   ='
     $,F10.4,3X,'*',/,2X,'*',121X,'*',/,2X,'*',27X,'NAS(4)  =',F10.4,5X,
     $'NAS(3)   =',F10.4,5X,'NAS(2)  =',F10.4,5X,'NAS(1)   =',F10.4,3X,
     $'*',/,2X,'*',121X,'*',/,2X,'*',51X,'NTHS(3) =',F10.4,5X,'NTHS(2) ='
     $,F10.4,5X,'NTHS(1) =',F10.4,3X,'*',/,2X,'*',121X,'*',/,2X,'*',27X,
     $'NWS(4)  =',F10.4,5X,'NWS(3)  =',F10.4,5X,'NWS(2)   =',F10.4,5X,
     $'NWS(1)   =',F10.4,3X,'*',/,2X,'*',121X,'*',/,2X,123('*')/)
C
C     THE DO LOOP BELOW DETERMINES THE ORDER OF THE POLYNOMIAL IN THE
C     DENOMINATOR, MD.
C
      DO 3 I=1,5
      IF(DABS(DS(I)).GT.ACC)MD=I-1
    3 CONTINUE
      IF(MD.NE.0)GO TO 4
C
C     IF MD = 0, THERE IS NO CHARACTERISTIC EQUATION. THEREFORE THE
C     PROGRAM IS TERMINATED.
C
      CALL EXIT
C
C     THE 4 'IF' STATEMENTS BELOW TELL WHICH SET OF NUMERATOR
C     COEFFICIENTS TO EVALUATE DEPENDING ON THE VALUE OF NUMER.
C
    4 IF(NUMER.EQ.1)GO TO 5
      IF(NUMER.EQ.2)GO TO 7
      IF(NUMER.EQ.3)GO TO 9
      IF(NUMER.EQ.4)GO TO 11
    5 WRITE(3,207)
  207 FORMAT('1',    130('*'),/,1X,'*',128X,'*',/,1X,'*',128X,'*',/,1X,'*
     $',52X,'SOLUTION FOR U VARIATION',52X,'*',/,1X,'*',52X,24('-'),52X,
     $'*',/,1X,'*',128X,'*',/,1X,'*',128X,'*',/,2X,'*',55X,'DENOMINATOR
     $ROOTS',56X,'*',/,1X,'*',128X,'*')
C
C     THE DO LOOP BELOW DETERMINES THE ORDER OF THE POLYNOMIAL IN THE
C     NUS NUMERATOR
C
      DO 6 I=1,4
      IF(DABS(NUS(I)).GT.ACC)MN=I-1
    6 CONTINUE
      IF(MN.NE.0)GO TO 13
      WRITE(3,208)MN
  208 FORMAT(1X,'MN=',I3)
      CALL EXIT
    7 WRITE(3,209)
  209 FORMAT('1',    130('*'),/,1X,'*',128X,'*',/,1X,'*',128X,'*',/,1X,'*
     $',45X,'SOLUTION FOR ANGLE OF ATTACK VARIATION',45X,'*',/,1X,'*',45
     $X,38('-'),45X,'*',/,1X,'*',128X,'*',/,1X,'*',128X,'*',/,1X,'*',55X
     $,'DENOMINATOR ROOTS',56X,'*',/,1X,'*',128X,'*')
      DO 8 I=1,4
      IF(DABS(NAS(I)).GT.ACC)MN=I-1
    8 CONTINUE
      IF(MN.NE.0)GO TO 13
      WRITE(3,208)MN
      CALL EXIT
    9 WRITE(3,210)
  210 FORMAT('1',    130('*'),/,1X,'*',128X,'*',/,1X,'*',128X,'*',/,1X,'*
     $',55X,'SOLUTION FOR PITCH VARIATION',          45X,'*',/,1X,'*',55
     $X,28('-'),45X,'*',/,1X,'*',128X,'*',/,1X,'*',128X,'*',/,1X,'*',55X
     $,'DENOMINATOR ROOTS',56X,'*',/,1X,'*',128X,'*')
      DO 10 I=1,3
      IF(DABS(NTHS(I)).GT.ACC)MN=I-1
   10 CONTINUE
      IF(MN.NE.0)GO TO 13
      WRITE(3,208)MN
      CALL EXIT
   11 WRITE(3,211)
  211 FORMAT('1',    130('*'),/,1X,'*',128X,'*',/,1X,'*',128X,'*',/,1X,'*
     $',55X,'SOLUTION FOR   W   VARIATION',          45X,'*',/,1X,'*',55
     $X,28('-'),45X,'*',/,1X,'*',128X,'*',/,1X,'*',128X,'*',/,1X,'*',55X
     $,'DENOMINATOR ROOTS',56X,'*',/,1X,'*',128X,'*')
      DO 12 I=1,4
      IF(DABS(NWS(I)).GT.ACC)MN=I-1
   12 CONTINUE
      IF(MN.NE.0)GO TO 13
      WRITE(3,208)MN
      CALL EXIT
C
C     GETROT IS A SUBROUTINE WHICH, USING OTHER SUBROUTINES, CALCULATES
C     ROOTS, DAMPING RATIOS, AND NATURAL FREQUENCIES, AND THESE ARE
C     TRANSFERRED TO THE MAINLINE BY USE OF A 'COMMON' STATEMENT.
C
   13 CALL GETROT(DS,MD,RRD,RID)
C
C     FOR DAMPING RATIOS GREATER THAN ONE(A NON-OSCILLATORY MODE) THE
C     FOLLOWING FOUR CARDS PREVENT TAKING THE SQUARE ROOT OF A NEGATIVE
C     NUMBER WHEN CALCULATING THE DAMPED NATURAL FREQUENCY.  IF THE
C     DAMPING RATIOS ARE GREATER THAN ONE THEN THE DAMPED NATURAL
C     FREQUENCIES REMAIN 0.0.
C
      WDSP=0.0
      WDP=0.0
      IF(DABS(ZSP).GT.1.0) GO TO 14
      WDSP=WNSP*DSQRT(1.0-ZSP*ZSP)
   14 IF(DABS(ZP).GT.1.0) GO TO 15
      WDP=WNP*DSQRT(1.0-ZP*ZP)
   15 WRITE(3,212)(J,RRD(J),RID(J),J=1,MD)
  212 FORMAT(1X,'*',46X,'ROOT(',I1,') = ',F10.5,'  +J ',F10.5,47X,'*')
      WRITE(3,213)
  213 FORMAT(1X,'*',128X,'*',/,1X,'*',128X,'*',/,1X,'*',34X,'NATURAL FRE
     $Q',5X,'DAMPING RATIO',4X,'TIME FOR 1/2 DAMPING',9X,'SETTLING TIME'
     $,10X,'*',/,1X,'*',31X,'UNDAMPED   DAMPED',80X,'*')
      WRITE(3,214)WNSP,WDSP,ZSP,T12SP,TOSSP
  214 FORMAT(1X,'*',18X,'SHORT PERIOD',F9.5,F10.5,2X,F10.5,11X,F10.5,14X
     $,F10.5,22X,'*',/,1X,'*',128X,'*')
      WRITE(3,215)WNP,WDP,ZP,T12P,TOSP
  215 FORMAT(1X,'*',18X,'PHUGOID',4X,F10.5,F10.5,2X,F10.5,11X,F10.5,14X,
     $F10.5,22X,'*',/,1X,'*',128X,'*',/,1X,'*',35X,58('-'),35X,'*',/,1X,
     $'*',128X,'*')
C
C     CALCULATION OF VALUES OF WF FOR FUTURE USE IN THE BODE ROUTINE.
C     INCLUDED ARE SELECTED VALUES OF WF(.01,.1,1.0,10.0,100.0,1000.0)
C     PLUS 5 VALUES AROUND EACH NATURAL FREQUENCY(2 ABOVE, 2 BELOW, AND
C     THE NATURAL FREQUENCY) TO INCREASE DATA IN THE BODE PLOT CRITICAL
C     AREAS.
C
      WF(1)=.01
      DO 16 IJ=2,6
      IM1=IJ-1
      WF(IJ)=WF(IM1)*10.0
   16 CONTINUE
C
C     KWF IS THE NUMBER OF NATURAL FREQUENCIES TO BE USED IN THE BODE
C     ROUTINE.
C
      KWF=6
C
C     II AND IK ARE COUNTERS USED TO DETERMINE THE MAXIMUM VALUE OF KWF
C     DEPENDING ON THE NUMBER OF NATURAL FREQUENCIES IN BOTH THE
C     NUMERATOR AND THE DENOMINATOR OF A PARTICULAR TRANSFER FUNCTION.
C
      II=0
      IK=0
      IF(I.EQ.0)GO TO 18
      IF(I.EQ.2) GO TO 17
      WF(12)=0.9*WNP
      WF(13)=0.75*WNP
      WF(14)=WNP
      WF(15)=1.1*WNP
      WF(16)=1.25*WNP
      IK=1
      KWF=16
   17 WF(7)=.9*WNSP
      WF(8)=.75*WNSP
      WF(9)=WNSP
      WF(10)=1.1*WNSP
      WF(11)=1.25*WNSP
      II=1
      IF(KWF.EQ.16)GO TO 18
      KWF=11
C
C     GETROT IS USED TO FIND ROOTS OF A PARTICULAR NUMERATOR DEPENDING
C     ON THE VALUE OF NUMER.
C
   18 IF(NUMER.EQ.1)GO TO 19
      IF(NUMER.EQ.2)GO TO 20
      IF(NUMER.EQ.4)GO TO 21
      CALL GETROT(NTHS,MN,RRN,RIN)
      GO TO 22
   19 CALL GETROT(NUS,MN,RRN,RIN)
      GO TO 22
   20 CALL GETROT(NAS,MN,RRN,RIN)
      GO TO 22
   21 CALL GETROT(NWS,MN,RRN,RIN)
   22 WRITE(3,216)
  216 FORMAT(1X,'*',56X,'NUMERATOR ROOTS',57X,'*',/,1X,'*',128X,'*')
      WRITE(3,212)(J,RRN(J),RIN(J),J=1,MN)
      WRITE(3,213)
C
C     IF THE DAMPING RATIO HAS AN ABSOLUTE VALUE GREATER THAN ONE(A NON-
C     OSCILLATORY MODE), THEN A DAMPED NATURAL FREQUENCY IS NOT
C     CALCULATED FOR THE NUMERATOR.  THEREFORE, WDSP AND WDP ARE LEFT AS
C     ZERO.
C
      WDSP=0.0
      WDP=0.0
      IF(DABS(ZSP).GT.1.0) GO TO 23
      WDSP=WNSP*DSQRT(1.0-ZSP*ZSP)
   23 IF(DABS(ZP).GT.1.0) GO TO 24
      WDP=WNP*DSQRT(1.0-ZP*ZP)
C
C     THE TWO WRITE STATEMENTS BELOW PRINT THE PERTINENT INFORMATION FOR
C     OSCILLATORY MODES IN THE NUMERATOR.  IF THE NATURAL FREQUENCIES
C     ARE PRINTED AS ZERO THE MODE IS NON-OSCILLATORY.
C
   24 WRITE(3,217)WNSP,WDSP,ZSP,T12SP,TOSSP
      WRITE(3,217)WNP,WDP,ZP,T12P,TOSP
  217 FORMAT(1X,'*',28X,F9.4,F11.4,3X,F10.4,11X,F10.5,14X,F10.5,22X,'*',
     $/,1X,'*',128X,'*')
      WRITE(3,218)
  218 FORMAT(1X,'*',35X,58('-'),35X,'*',/,1X,'*',128X,'*',/,1X,'*',53X,'
     $MODE OF INFORMATION',54X,'*',/,1X,'*',128X,'*',/,1X,'*',21X,'FRE
     $QUENCY',26X,'AMPLITUDE RATIO',25X,'PHASE ANGLE',21X,'*',/,1X,'*',1
     $5X,'RAD/SEC',8X,'CYCLES/SEC',14X,'PURE',10X,'DECIBELS',15X,'RADIAN
     $S',6X,'DEGREES',15X,'*')
C
C     THE NEXT FEW CARDS ARE A ROUTINE TO FIND MORE VALUES OF WF FOR THE
C     BODE PLOT ROUTINE DEPENDING ON WHETHER OR NOT THE NUMERATOR HAS
C     ANY OSCILLATORY MODES.  THE FREQUENCIES AND THE VALUES OF KWF ARE
C     CHOSEN IN THE SAME MANNER AS THOSE OF THE DENOMINATOR PREVIOUSLY
C     MENTIONED.
C
C     MD1 AND MN1 ARE USED TO PREVENT HAVING ZERO SUBSCRIPTS WHEN
C     CALCULATING THE NUMERATOR AND DENOMINATOR GAINS FOR THE BODE PLOT
C     SUBROUTINE.
C
      MD1=MD+1
      MN1=MN+1
      IF(I.EQ.0)GO TO 27
C
C     II AND IK ARE COUNTERS USED TO DETERMINE THE MAXIMUM VALUE OF KWF.
C
      IF(II.EQ.0.AND.IK.EQ.0)GO TO 26
      IF(II.EQ.1.AND.IK.EQ.0)GO TO 25
      WF(17)=.9*WNSP
      WF(18)=.75*WNSP
      WF(19)=WNSP
      WF(20)=1.1*WNSP
      WF(21)=1.25*WNSP
      KWF=21
      GO TO 27
   25 WF(12)=.9*WNSP
      WF(13)=.75*WNSP
      WF(14)=WNSP
      WF(15)=1.1*WNSP
      WF(16)=1.25*WNSP
```

```
      KWF=16                                                            513
      GO TO 27                                                          514
   26 WF(7)=.9*WNSP                                                     515
      WF(8)=.75*WNSP                                                    516
      WF(9)=WNSP                                                        517
      WF(10)=1.1*WNSP                                                   518
      WF(11)=1.25*WNSP                                                  519
      KWF=11                                                            520
   27 IF(NUMER.NE.1)GO TO 28                                            521
C                                                                       522
C     THE GAIN (KGAIN) FOR THE ROOT LOCUS PLOTS IS CALCULATED FROM THE  523
C     COEFFICIENTS OF THE HIGHEST ORDER TERM IN THE DENOMINATOR AND     524
C     NUMERATOR, TF=KGAIN(S+A)(S+B)/(S+C)(S+D), WHERE A AND B ARE ROOTS 525
C     OF THE NUMERATOR AND C AND D ARE ROOTS OF THE DENOMINATOR.        526
C                                                                       527
      KGAIN=NUS(NN1)/DS(ND1)                                            528
      GO TO 31                                                          529
   28 IF(NUMER.NE.2)GO TO 29                                            530
      KGAIN=NAS(NN1)/DS(ND1)                                            531
      GO TO 31                                                          532
   29 IF(NUMER.NE.3)GO TO 30                                            533
      KGAIN=NTHS(NN1)/DS(ND1)                                           534
      GO TO 31                                                          535
   30 KGAIN=NWS(NN1)/DS(ND1)                                            536
   31 KKWF=KWF                                                          537
C                                                                       538
C     THE NEXT 12 CARDS RANK THE WF'S IN ASCENDING ORDER.               539
C                                                                       540
      WAX=WF(1)                                                         541
      LK=1                                                              542
      DO 33 JD=2,KKWF                                                   543
      IF(WF(JD).GE.WAX)LK=JD                                            544
      IF(WF(JD).GE.WAX)WAX=WF(JD)                                       545
   33 CONTINUE                                                          546
      WSAV=WF(KKWF)                                                     547
      WF(KKWF)=WAX                                                      548
      WF(LK)=WSAV                                                       549
      KKWF=KKWF-1                                                       550
      IF(KKWF.EQ.1)GO TO 34                                             551
      GO TO 32                                                          552
C                                                                       553
C     BODE IS THE SUBROUTINE WHICH CALCULATES AMPLITUDE RATIO AND PHASE 554
C     ANGLE FOR EACH WF.  THE INFORMATION IS TRANSFERRED TO THE MAINLINE 555
C     BY THE USE OF A 'COMMON' STATEMENT.                               556
C                                                                       557
   34 CALL BODE(MD,MN,KWF)                                              558
      WRITE(3,219)(WF(I),WCYCLE(I),AR(I),ARDB(I),PHASE(I),PHDEG(I),I=1, 559
     $KWF)                                                              560
  219 FORMAT(1X,'*',13X,F10.5,6X,F10.5,12X,F10.2,6X,F10.5,12X,F10.5,6X,F 561
     $10.5,13X,'*')                                                     562
      WRITE(3,220)                                                      563
  220 FORMAT(1X,'*',122X,'*',/,1X,130('*'))                             564
   35 CONTINUE                                                          565
      CALL EXIT                                                         566
      END                                                               567
```

```
      SUBROUTINE GETROT(COFFI,M,ROOTR,ROOTI)                            1
C                                                                       2
C     GETROT IS A SUBROUTINE WHICH, USING OTHER SUBROUTINES, CALCULATES 3
C     ROOTS, DAMPING RATIOS, AND NATURAL FREQUENCIES, AND THESE ARE     4
C     TRANSFERRED TO THE MAINLINE BY USE OF A 'COMMON' STATEMENT.       5
C                                                                       6
      IMPLICIT REAL*8(A-H,O-Z)                                          7
      REAL*8 MS,IYY,MU,MW,MDW,MQ,MIN,MUS,MAS,MTHS,KGAIN,KG,KROOT,KKK,KD, 8
     $KN,NWS                                                            9
      COMPLEX*16 P,TST                                                  10
      COMMON   WNSP,ZSP,T12SP,TO5SP,WNP,ZP,T12P,TO5P,WF(21),RRD(10),RRN( 11
     $10),RID(10),RIN(10),AMPR(21),PHASE(21),ACC,WCYCLE(21),AMPRDB(21),P 12
     &HDEG(21),KGAIN                                                    13
      COMMON I                                                          14
      DIMENSION NUS(5),NAS(5),NTHS(5),DS(6),ROOTR(10),ROOTI(10),C(5),KG( 15
     $4),QUFI(3),QUF2(3),RR1(2),RR2(2),RI1(2),RI2(2),CC(4),RR(3),COFF(6 16
     $),RI(3),XR(3),XI(3),COF(3),RE(2),RIN(2),ROOT(1),COFF(2),KKK(21),NW 17
     $S(5),P(6)                                                         18
C                                                                       19
C     THE 3 'IF' STATEMENTS BELOW DECIDE WHICH ROOT-EXTRACTION          20
C     SUBROUTINE TO CALL DEPENDING ON THE VALUE OF M(THE ORDER OF THE   21
C     POLYNOMIAL).                                                      22
C                                                                       23
      IF(M.EQ.4)GO TO 3                                                 24
      IF(M.EQ.3)GO TO 2                                                 25
      IF(M.EQ.2)GO TO 1                                                 26
C                                                                       27
C     THE SUBROUTINES SINGLE, QUAD, CUBE, AND FOURTH SOLVE (THE SOLUTION 28
C     IS ACHIEVED IN CLOSED FORM AND THUS REQUIRES NO ITERATIVE         29
C     PROCEDURE) FOR ROOTS OF FIRST, SECOND, THIRD, AND FOURTH ORDER    30
C     POLYNOMIALS, RESPECTIVELY.                                        31
C                                                                       32
      CALL SINGLE(COFFI,ROOTR,ROOTI)                                    33
      GO TO 4                                                           34
    1 CALL QUAD(COFFI,ROOTR,ROOTI)                                      35
      GO TO 4                                                           36
    2 CALL CUBE(COFFI,ROOTR,ROOTI)                                      37
      GO TO 4                                                           38
    3 CALL FOURTH(COFFI,ROOTR,ROOTI)                                    39
C                                                                       40
C     THE FOLLOWING CARDS TEST THE ROOTS OF THE POLYNOMIAL.  TO CHECK THE 41
C     ACCURACY OF THE ROOT SOLVER SUBROUTINES.  IF THE VALUE OF TST IS  42
C     TOO LARGE A WARNING MESSAGE IS PRINTED.                           43
C                                                                       44
    4 DO 6 I=1,M                                                        45
      P(I)=DCMPLX(ROOTR(I),ROOTI(I))                                    46
      ZERO=0.0                                                          47
      TST=DCMPLX(COFFI(1),ZERO)                                         48
      MJ=M+1                                                            49
      DO 5 J=2,MJ                                                       50
      TST=TST+COFFI(J)*P(J)**(J-1)                                      51
    5 CONTINUE                                                          52
      IF(CDABS(TST).LE.ACC)GO TO 6                                      53
      WRITE(3,100)P(I),TST                                              54
  100 FORMAT(1X,'ROOT = ',2G15.8,'  WHEN SUBSTITUED INTO ITS POLYNOMIA  55
     $L FAILED TO COME WITHIN ACC OF 0.0.',/,1X,'THIS VALUE DIFFERED FR 56
     $OM ZERO BY ',2G15.8,'  THIS IMPLIES EITHER A ROUNDOFF ERROR WHEN  57
     $TESTING THE ROOTS',/,1X,'(ACC TOO SMALL) OR THE VALUE 0.01 USED TO 58
     $ COMPARE WITH TEST IN SUBROUTINE FOURTH IS TOO LARGE.')           59
    6 CONTINUE                                                          60
C                                                                       61
C     I IS A COUNTER WHICH DETERMINES THE NUMBER OF ROOTS WHICH HAVE    62
C     BOTH A REAL AND AN IMAGINARY PART.                                63
C                                                                       64
```

```
C                                                                       65
C     THE NEXT 25 CARDS IS A PROCEDURE WHICH POSITIONS ROOTS WITH BOTH  66
C     REAL AND IMAGINARY PARTS IN THE FIRST L POSITIONS AND THE ROOTS   67
C     WITH ZERO IMAGINARY PARTS IN THE NEXT KK POSITIONS.  FOR EXAMPLE  68
C     IF THERE ARE 4 ROOTS, TWO WITH ONLY REAL PARTS AND TWO COMPLEX,   69
C     THE COMPLEX ROOTS WILL BE IN POSITIONS 1 AND 2 AND THE REAL ROOTS 70
C     WILL BE IN POSITIONS 3 AND 4.  L, K, AND KK ARE COUNTERS USED TO  71
C     FACILITATE THIS PROCEDURE.                                        72
C                                                                       73
C     I IS A COUNTER WHICH DETERMINES THE NUMBER OF ROOTS WHICH HAVE    74
C     BOTH A REAL AND AN IMAGINARY PART.                                75
C                                                                       76
      I=M                                                               77
C                                                                       78
C     N IS A COUNTER WHICH PREVENTS THE ORDER OF THE POLYNOMIAL FROM    79
C     BEING DESTROYED.                                                  80
C                                                                       81
      N=M                                                               82
      L=1                                                               83
      K=M+1                                                             84
      KK=0                                                              85
      DO 8 J=1,M                                                        86
      IF(DABS(RCOTI(J)).GT.ACC)GO TO 7                                  87
      I=I-1                                                             88
      ROOTI(K)=ROOTI(J)                                                 89
      ROOTR(K)=ROOTR(J)                                                 90
      K=K+1                                                             91
      KK=KK+1                                                           92
      GO TO 8                                                           93
    7 RCOTI(L)=ROOTI(J)                                                 94
      RCOTR(L)=ROOTR(J)                                                 95
      L=L+1                                                             96
    8 CONTINUE                                                          97
      IF(KK.EQ.0)GO TO 10                                               98
    9 KI=K-KK                                                           99
      ROOTI(N)=ROOTI(KI)                                                100
      ROOTR(N)=ROOTR(KI)                                                101
      N=N-1                                                             102
      KK=KK-1                                                           103
      IF(KK.EQ.0)GO TO 10                                               104
      GO TO 9                                                           105
C                                                                       106
C     AT THIS POINT THERE ARE I ROOTS THAT HAVE BOTH A REAL AND AN      107
C     IMAGINARY PART AND (M-I) ROOTS WITH JUST A REAL PART.             108
C                                                                       109
C     THIS PART OF THE PROGRAM DETERMINES THE LARGEST REAL PART OF THE  110
C     ROOTS AND RANKS THEM FROM THE BOTTOM IN THE I POSITIONS AVAILABLE. 111
C                                                                       112
   10 RMAX=ROOTR(1)                                                     113
      K=1                                                               114
      IF(I.EQ.0) GO TO 13                                               115
      DO 11 J=1,I                                                       116
      IF(DABS(ROOTR(J)).GT.RMAX)K=J                                     117
      IF(DABS(ROOTR(J)).GT.RMAX)RMAX=ROOTR(J)                           118
   11 CONTINUE                                                          119
      RSAVER=RCOTR(I)                                                   120
      RSAVEI=ROOTI(I)                                                   121
      RCOTR(I)=ROOTR(K)                                                 122
      ROOTI(I)=ROOTI(K)                                                 123
      ROOTR(K)=RSAVER                                                   124
      ROOTI(K)=RSAVEI                                                   125
      M=I-1                                                             126
      DO 12 J=1,M                                                       127
      IF(DABS(RMAX-ROOTR(J)).LE.ACC)L=J                                 128
```

```
   12 CONTINUE                                                          129
      RSAVER=RCOTR(N)                                                   130
      RSAVEI=ROOTI(N)                                                   131
      ROOTR(N)=ROOTR(L)                                                 132
      ROOTI(N)=ROOTI(L)                                                 133
      ROOTR(L)=RSAVER                                                   134
      ROOTI(L)=RSAVEI                                                   135
C                                                                       136
C     THE OUTPUT FOR BOTH NUMERATOR AND DENOMINATOR IS PRINTED IN A FORM 137
C     WHICH REQUIRES TWO OSCILLATORY MODES.  IF ONE OR BOTH OF THE MODES 138
C     ARE NON-OSCILLATORY THEN THE FOLLOWING PROCEDURE IS USED:         139
C          1)  THE DAMPING RATIO IS CHOSEN TO BE THE SMALLER MAGNITUDE OF 140
C              THE REAL ROOTS. SINCE THIS RCOT WILL DOMINATE IN THE TIME 141
C              DOMAIN (A NEGATIVE DAMPING RATIO WOULD INDICATE AN        142
C              UNSTABLE MODE).                                           143
C          2)  THE TIME TO DAMP TO 50% AND 5% OF THE AMPLITUDE ARE       144
C              CALCULATED BASED ON THE ABOVE DAMPING RATIO.  THUS, FOR AN 145
C              UNSTABLE SYSTEM THESE TIMES WILL BE NEGATIVE.             146
C                                                                       147
C     THE REMAINING PORTION OF GETROT CALCULATES THE NATURAL FREQUENCIES 148
C     (WNP & WNSP), DAMPING RATIOS(ZP & ZSP), TIME TO DAMP TO 1/2       149
C     AMPLITUDE(T12P & T12SP), AND SETTLING TIME(TO5P & TO5SP).  THE     150
C     SETTLING TIME IS THE TIME TO DAMP TO 5% OF THE ORIGINAL AMPLITUDE, 151
C     THE SUFFIXES P AND SP REFER TO OSCILLATORY MODES FOR THE NUMERATOR 152
C     OR THE DENOMINATOR DEPENDING ON THE EQUATION BEING SOLVED .       153
C                                                                       154
C     THE SHORT PERIOD AND PHUGOID NATURAL FREQUENCIES ARE DETERMINED BY 155
C     A RANKING OF THE MAGNITUDE OF THE REAL AND IMAGINARY PARTS OF THE 156
C     ROOTS, THE LARGER MAGNITUDE REPRESENTS THE SHORT PERIOD MODE.  IF  157
C     THERE IS ONLY ONE OSCILLATORY MODE THIS MODE IS REFERRED TO AS THE 158
C     SHORT PERIOD MODE AND THE PHUGOID MODE NATURAL FREQUENCY IS        159
C     PRINTED AS ZERO.  WHEN GETROT IS USED FOR A NUMERATOR POLYNOMIAL   160
C     THE SHORT PERIOD INFORMATION IS PRINTED AS A NUMERATOR OSCILLATORY 161
C     MODE(SINCE A CUBIC IS THE LARGEST NUMERATOR POLYNOMIAL POSSIBLE,   162
C     THERE WILL BE ONLY ONE OSCILLATORY MODE AT MOST).                 163
C                                                                       164
   13 IF(M.EQ.1)GO TO 17                                                165
      IF(M.EQ.2.AND.I.EQ.0)GO TO 18                                     166
      IF(M.EQ.2.AND.I.EQ.2)GO TO 21                                     167
      IF(M.EQ.3.AND.I.EQ.0)GO TO 22                                     168
      IF(M.EQ.3.AND.I.EQ.2)GO TO 26                                     169
      IF(M.EQ.4.AND.I.EQ.0)GO TO 27                                     170
      IF(M.EQ.4.AND.I.EQ.2)GO TO 32                                     171
      WN1=DSQRT(ROOTR(3)*ROOTR(3)+ROOTI(3)*ROOTI(3))                    172
      WN2=DSQRT(ROOTR(1)*ROOTR(1)+ROOTI(1)*ROOTI(1))                    173
      IF(WN1.GT.WN2)GO TO 14                                            174
      WNSP=WN2                                                          175
      NX=20                                                             176
      WNP=WN1                                                           177
      GO TO 15                                                          178
   14 WNSP=WN1                                                          179
      NX=10                                                             180
      WNP=WN2                                                           181
   15 IF(NX.NE.20)GO TO 16                                              182
      ZSP=-ROOTR(1)/WNSP                                                183
      TO5SP=(2.9957)/(ZSP*WNSP)                                         184
      T12SP=(.6931471)/(ZSP*WNSP)                                       185
      ZP=-RCOTR(3)/WNP                                                  186
      T12P=(.6931471)/(ZP*WNP)                                          187
      TO5P=(2.9957)/(ZP*WNP)                                            188
      GO TO 35                                                          189
   16 ZSP=-ROOTR(3)/WNSP                                                190
      TO5SP=(2.9957)/(ZSP*WNSP)                                         191
      T12SP=(.6931471)/(ZSP*WNSP)                                       192
```

```
      ZP=-RCOTR(1)/WNP                                                  193
      TO5P=(2.9957)/(ZP*WNP)                                            194
      T12P=(.693147)/(ZP*WNP)                                           195
      GO TO 35                                                          196
   17 WNSP=0.0                                                          197
      WNP=0.0                                                           198
      ZSP=-RCOTR(1)                                                     199
      ZP=0.0                                                            200
      T12SP=.693147/ZSP                                                 201
      TO5SP=2.9957/ZSP                                                  202
      TO5P=0.0                                                          203
      T12P=0.0                                                          204
      GO TO 35                                                          205
   18 IF(DABS(RCOTR(1)).GT.DABS(RCOTR(2)))GO TO 19                      206
      ZSP=-RCOTR(1)                                                     207
      ZP=-RCOTR(2)                                                      208
      GO TO 20                                                          209
   19 ZSP=-RCOTR(2)                                                     210
      ZP=-RCOTR(1)                                                      211
   20 WNSP=0.0                                                          212
      WNP=0.0                                                           213
      T12P=.693147/ZP                                                   214
      TO5P=2.9957/ZP                                                    215
      T12SP=.693147/ZSP                                                 216
      TO5SP=2.9957/ZSP                                                  217
      GO TO 35                                                          218
   21 WNP=0.0                                                           219
      ZP=0.0                                                            220
      T12P=0.0                                                          221
      TO5P=0.0                                                          222
      WNSP=DSQRT(RCOTR(1)*RCOTR(1)+RCOTI(1)*RCOTI(1))                   223
      ZSP=-RCOTR(1)/WNSP                                                224
      T12SP=.693147/(ZSP*WNSP)                                          225
      TO5SP=2.9957/(ZSP*WNSP)                                           226
      GO TO 35                                                          227
   22 RAX=RCOTR(1)                                                      228
      K=1                                                               229
      DO 23 J=1,3                                                       230
      IF(DABS(RCOTR(J)).GT.RAX)K=J                                      231
      IF(DABS(RCOTR(J)).GT.RAX)RAX=RCOTR(J)                             232
   23 CONTINUE                                                          233
      RSAV=RCOTR(3)                                                     234
      RCOTR(3)=RAX                                                      235
      RCOTR(K)=RSAV                                                     236
      IF(DABS(RCOTR(1)).GT.DABS(RCOTR(2)))GO TO 24                      237
      ZSP=-RCOTR(1)                                                     238
      ZP=-RCOTR(2)                                                      239
      GO TO 25                                                          240
   24 ZSP=-RCOTR(2)                                                     241
      ZP=-RCOTR(1)                                                      242
   25 WNSP=0.0                                                          243
      WNP=0.0                                                           244
      T12P=.693147/ZP                                                   245
      TO5P=2.9957/ZP                                                    246
      T12SP=.693147/ZSP                                                 247
      TO5SP=2.9957/ZSP                                                  248
      GO TO 35                                                          249
   26 WNP=0.0                                                           250
      ZP=-RCOTR(3)                                                      251
      T12P=.693147/ZP                                                   252
      TO5P=2.9957/ZP                                                    253
      WNSP=DSQRT(RCOTR(1)*RCOTR(1)+RCOTI(1)*RCOTI(1))                   254
      ZSP=-RCOTR(1)/WNSP                                                255
      T12SP=.693147/(ZSP*WNSP)                                          256

      TO5SP=2.9957/(ZSP*WNSP)                                           257
      GO TO 35                                                          258
   27 RAX=RCOTR(1)                                                      259
      K=1                                                               260
      DO 28 J=1,4                                                       261
      IF(DABS(RCOTR(J)).GT.RAX)K=J                                      262
      IF(DABS(RCOTR(J)).GT.RAX)RAX=RCOTR(J)                             263
   28 CONTINUE                                                          264
      RSAV=RCOTR(4)                                                     265
      RCOTR(4)=RAX                                                      266
      RCOTR(K)=RSAV                                                     267
      RAX=RCOTR(1)                                                      268
      K=1                                                               269
      DO 29 J=1,3                                                       270
      IF(DABS(RCOTR(J)).GT.RAX)K=J                                      271
      IF(DABS(RCOTR(J)).GT.RAX)RAX=RCOTR(J)                             272
   29 CONTINUE                                                          273
      RSAV=RCOTR(3)                                                     274
      RCOTR(3)=RAX                                                      275
      RCOTR(K)=RSAV                                                     276
      IF(DABS(RCOTR(1)).GT.DABS(RCOTR(2)))GO TO 30                      277
      ZSP=-RCOTR(1)                                                     278
      ZP=-RCOTR(2)                                                      279
      GO TO 31                                                          280
   30 ZSP=-RCOTR(2)                                                     281
      ZP=-RCOTR(1)                                                      282
   31 WNSP=0.0                                                          283
      WNP=0.0                                                           284
      T12P=.693147/ZP                                                   285
      TO5P=2.9957/ZP                                                    286
      T12SP=.693147/ZSP                                                 287
      TO5SP=2.9957/ZSP                                                  288
      GO TO 35                                                          289
   32 WNSP=DSQRT(RCOTR(1)*RCOTR(1)+RCOTI(1)*RCOTI(1))                   290
      ZSP=-RCOTR(1)/WNSP                                                291
      WNP=0.0                                                           292
      T12SP=.693147/(ZSP*WNSP)                                          293
      TO5SP=2.9957/(ZSP*WNSP)                                           294
      IF(DABS(RCOTR(3)).GT.DABS(RCOTR(4)))GO TO 33                      295
      ZP=-RCOTR(3)                                                      296
      GO TO 34                                                          297
   33 ZP=-RCOTR(4)                                                      298
   34 T12SP=(2.9957)/(ZSP*WNSP)                                         299
      TO5P=.693147/(ZSP*WNSP)                                           300
   35 RETURN                                                            301
      END                                                               302
```

```
      SUBROUTINE FOURTH(C,ROOTR,ROOTI)                                  1
                                                                        2
C     THIS SUBROUTINE FACTORS A FOURTH ORDER POLYNOMIAL BY A CLOSED FORM  3
C     PROCEDURE WHICH FORMS 2 QUADRATIC FACTORS AND THEN CALLS A        4
C     QUADRATIC FACTORING SUBROUTINE, QUAD, TO OBTAIN THE FOUR ROOTS.   5
C     THE PROCEDURE WAS TAKEN FROM 'INTRODUCTION TO THE THEORY OF       6
C     EQUATIONS' BY M.B. CONKWRIGHT.                                    7
C                                                                       8
                                                                        9
      IMPLICIT REAL*8(A-H,O-Z)                                          10
      REAL*8 MS,IYY,MU,MW,MDW,MQ,MIN,MUS,MAS,MTHS,KGAIN,KC,KROOT,KKK,NMS 11
      DIMENSION C(5),KC(4),QUF1(3),QUF2(3),RR1(2),RR2(2),RI1(2),RI2(2),R 12
     $OOTR(10),ROOTI(10)                                                13
      P=C(4)/C(5)                                                       14
      Q=C(3)/C(5)                                                       15
      R=C(2)/C(5)                                                       16
      S=C(1)/C(5)                                                       17
      KC(4)=1.0                                                         18
      KC(3)=-.5*Q                                                       19
      KC(2)=.25*(P*R-4.0*S)                                             20
      KC(1)=.125*(4.0*C*S-P*P*S-R*R)                                    21
      HKC=(3.0*KC(4)*KC(2)-KC(3)*KC(3))/9.0*KC(4)*KC(4)                 22
      GKC=(2.0*KC(3)*KC(3)*KC(3)-9.0*KC(4)*KC(3)*KC(2)+27.0*KC(4)*KC(4)* 23
     $KC(1))/(27.C*KC(4)*KC(4)*KC(4))                                   24
      RAD=GKC*GKC+4.0*HKC*HKC*HKC                                       25
      IF(RAD.LT.0.0)GO TO 3                                             26
      UKC=((-GKC+DSQRT(GKC*GKC+4.0*HKC*HKC*HKC))/2.0)                   27
      RTUKC=DABS(UKC)**.333333333333333                                 28
      UKC=DSIGN(RTUKC,UKC)                                              29
      VKC=-HKC/UKC                                                      30
      KROOT=UKC+VKC-KC(3)/(3.0*KC(4))                                   31
    1 B=DSQRT(KROOT*KROOT-S)                                            32
      A=DSQRT(2.0*KROOT+P*P*.25-Q)                                      33
      TEST=2.0*A*B+K-KROOT*P                                            34
      IF(TEST.LE..01)GO TO 2                                            35
      A=-A                                                              36
      TEST=2.0*A*B+R-KROOT*P                                            37
      IF(TEST.LE..01)GO TO 2                                            38
      A=-A                                                              39
      B=-B                                                              40
      TEST=2.0*A*B+R-KROOT*P                                            41
      IF(TEST.LE..01)GO TO 2                                            42
      A=-A                                                              43
    2 QUF1(3)=1.0                                                       44
      QUF2(3)=1.0                                                       45
      QUF1(2)=.5*P-A                                                    46
      QUF2(2)=.5*P+A                                                    47
      QUF1(1)=KROOT-B                                                   48
      QUF2(1)=KROOT+B                                                   49
      CALL QUAD(QUF1,RR1,RI1)                                           50
      ROOTR(1)=RR1(1)                                                   51
      ROOTR(2)=RR1(2)                                                   52
      ROOTI(1)=RI1(1)                                                   53
      ROOTI(2)=RI1(2)                                                   54
      CALL QUAD(QUF2,RR2,RI2)                                           55
      ROOTR(3)=RR2(1)                                                   56
      ROOTR(4)=RR2(2)                                                   57
      ROOTI(3)=RI2(1)                                                   58
      ROOTI(4)=RI2(2)                                                   59
      RETURN                                                            60
    3 THETA=DARCOS(-GKC/(2.0*DSQRT(-HKC*HKC*HKC)))                      61
      TH3=THETA/3.0                                                     62
      KROOT = 2.0*DCOS(TH3)*DSQRT(-HKC) - KC(3)/(3.0*KC(4))             63
      GO TO 1                                                           64
      END
```

```
      SUBROUTINE CUBE(CC,XR,XI)                                         1
      IMPLICIT REAL*8(A-H,O-Z)                                          2
      DIMENSION CC(4),RR(3),RI(3),XR(3),XI(3)                           3
C                                                                       4
C     THIS SUBROUTINE FACTORS A THIRD ORDER POLYNOMIAL BY A CLOSED FORM 5
C     PROCEDURE GIVEN IN 'INTRODUCTION TO THE THEORY OF EQUATIONS' BY   6
C     CONKWRIGHT AND MODIFIED BY THE PROCEDURE GIVEN IN 'STANDARD MATH  7
C     TABLES' BY CHEMICAL RUBBER COMPANY.                               8
C                                                                       9
      H=(3.0*CC(4)*CC(2)-CC(3)*CC(3))/(9.0*CC(4)*CC(4))                 10
      G=(2.0*CC(3)*CC(3)*CC(3)-9.0*CC(4)*CC(3)*CC(2)+27.0*CC(4)*CC(4)*CC 11
     $(1))/(27.0*CC(4)*CC(4)*CC(4))                                     12
      RAD=G*G+4.0*H*H*H                                                 13
      IF(RAD.LT.0.0)GO TO 3                                             14
      UROOT3=(-G+DSQRT(G*G+4.0*H*H*H))/2.0                              15
      IF(UROOT3.LT.0.0)GO TO 1                                          16
      UROOT=URGOT3**.333333333333333                                    17
      GO TO 2                                                           18
    1 UROOT=(-UROOT3)**.333333333333333                                 19
      UROOT=-UROOT                                                      20
    2 VROOT=-H/UROOT                                                    21
      RR(1)=UROOT+VROOT                                                 22
      RR(2)=-(UROOT+VROOT)/2.0                                          23
      RR(3)=-(UROOT+VROOT)/2.0                                          24
      RI(1)=0.0                                                         25
      RI(2)=(UROOT-VROOT)*(.866025403784)                               26
      RI(3)=-(UROOT-VROOT)*(.866025403784)                              27
      XR(1)=RR(1)-CC(3)/(3.0*CC(4))                                     28
      XR(2)=RR(2)-CC(3)/(3.0*CC(4))                                     29
      XR(3)=RR(3)-CC(3)/(3.0*CC(4))                                     30
      XI(1)=RI(1)                                                       31
      XI(2)=RI(2)                                                       32
      XI(3)=RI(3)                                                       33
      GO TO 4                                                           34
    3 THETA=DARCOS(-G/(2.0*DSQRT(-H*H*H)))                              35
      TH3=THETA/3.0                                                     36
      XI(1)=0.0                                                         37
      XI(2)=0.0                                                         38
      XI(3)=0.0                                                         39
      XR(1)=2.0*DCOS(TH3)*DSQRT(-H)                                     40
      XR(2)=2.0*DCOS(TH3+2.094395102392)*DSQRT(-H)                      41
      XR(3)=2.0*DCOS(TH3+4.188790204784)*DSQRT(-H)                      42
      SUB=CC(3)/(3.0*CC(4))                                             43
      XR(1)=XR(1)-SUB                                                   44
      XR(2)=XR(2)-SUB                                                   45
      XR(3)=XR(3)-SUB                                                   46
    4 RETURN                                                            47
      END                                                               48
```

```
      SUBROUTINE QUAD(COF,RE,RIM)                                       1
C                                                                       2
C     THIS SUBROUTINE FACTORS A SECOND ORDER POLYNOMIAL BY USING THE    3
C     QUADRATIC FORMULA.                                                4
C                                                                       5
      IMPLICIT REAL*8(A-H,O-Z)                                          6
      DIMENSION COF(3),RE(2),RIM(2)                                     7
      DIS=COF(2)*COF(2)-4.0*COF(3)*COF(1)                               8
      IF(DIS.LT.0.0) GO TO 1                                            9
      RE(1)=(-COF(2)+DSQRT(DIS))/(2.0*COF(3))                           10
      RE(2)=(-COF(2)-DSQRT(DIS))/(2.0*COF(3))                           11
      RIM(1)=0.0                                                        12
      RIM(2)=0.0                                                        13
      GO TO 2                                                           14
    1 RE(1)=-COF(2)/(2.0*COF(3))                                        15
      RE(2)=RE(1)                                                       16
      RIM(1)=(-DSQRT(-DIS))/(2.0*COF(3))                                17
      RIM(2)=(DSQRT(-DIS))/(2.0*COF(3))                                 18
    2 RETURN                                                            19
      END                                                               20
```

```
      SUBROUTINE BODE(L,JJ,KWF)                                         1
C                                                                       2
C     THIS IS A SUBROUTINE WHICH CALCULATES THE INFORMATION NEEDED TO   3
C     CONSTRUCT A BODE PLOT ONCE THE NUMERATOR AND DENOMINATOR          4
C     POLYNOMIALS HAVE BEEN FACTORED.  THE INFORMATION IS TRANSFERRED TO 5
C     THE MAINLINE BY USING A *COMMON* STATEMENT.  THE FREQUENCIES ARE  6
C     GIVEN BOTH IN RADIANS PER SECOND AND CYCLES PER SECOND.  THE      7
C     AMPLITUDE RATIO IS GIVEN BOTH AS A PURE NUMBER AND IN DECIBELS.   8
C     THE PHASE ANGLE IS GIVEN BOTH IN DEGREES AND RADIANS.             9
C                                                                       10
C                                                                       11
      IMPLICIT REAL*8(A-H,O-Z)                                          12
      REAL*8 MS,IVT,MU,MV,MDW,MQ,MIN,MUS,MAS,NTHS,KGAIN,KG,KROOT,KKK,KD, 13
     $KN,MWS,KDSAVE,KNSAVE                                              14
      COMMON   WNSP,ZSP,T12SP,T05SP,WNP,ZP,T12P,T05P,WF(21),RRD(10),RRN( 15
     $10),RID(10),RIN(10),AMPR(21),PHASE(21),ACC,WCYCLE(21),AMPRDB(21),P 16
     $HDEG(21),KGAIN                                                    17
      COMMON I                                                          18
      DIMENSION KKK(21)                                                 19
      DO 9 F=1,KWF                                                      20
      AMPD=1.0                                                          21
      KD=1.0                                                            22
      PHASED=0.0                                                        23
      DO 4 J=1,L                                                        24
      IF(RRD(J).EQ.0.0)GO TO 1                                          25
      GO TO 3                                                           26
    1 AMPD=AMPD*CABS(WF(M)-RID(J))                                      27
      IF(WF(M)-RID(J).LT.0.0)GO TO 2                                    28
      PHASED=PHASED-3.1415926536/2.0                                    29
      GO TO 4                                                           30
    2 PHASED=PHASED+3.1415926536/2.0                                    31
      GO TO 4                                                           32
    3 AMPD=DSQRT(((-WF(M)+RID(J))/RRD(J))**2+1.0)*AMPD                  33
      PHASED=-(DATAN((-RID(J)+WF(M))/(-RRD(J))))+PHASED                 34
      KDSAVE=KD                                                         35
      KD=-RRD(J)*KD                                                     36
      IF(KDSAVE*KD.LT.0.0)PHASED=PHASED-3.1415926536                    37
    4 CONTINUE                                                          38
      PHASER=0.0                                                        39
      KN=KGAIN                                                          40
      AMPN=1.0                                                          41
      DO 8 I=1,JJ                                                       42
      IF(RRN(I).EQ.0.0)GO TO 5                                          43
      GO TO 7                                                           44
    5 AMPN=AMPN*CABS(WF(M)-RIN(I))                                      45
      IF(WF(M)-RIN(I).LT.0.0)GO TO 6                                    46
      PHASEN=PHASEN-3.1415926536/2.0                                    47
      GO TO 8                                                           48
    6 PHASEN=PHASEN+3.1415926536/2.0                                    49
      GO TO 8                                                           50
    7 AMPN=DSQRT(((-WF(M)+RIN(I))/RRN(I))**2+1.0)*AMPN                  51
      PHASEN=DATAN((-RIN(I)+WF(M))/(-RRN(I)))+PHASEN                    52
      KNSAVE=KN                                                         53
      KN=-RRN(I)*KN                                                     54
      IF(KNSAVE*KN.LT.0.0)PHASEN=PHASEN+3.1415926536                    55
    8 CONTINUE                                                          56
      KKK(M)=KN/KD                                                      57
      AMPR(M)=DABS(KKK(M))*AMPN/AMPD                                    58
      AMPRDB(M)=20.0*DLOG10(AMPR(M))                                    59
      PHASE(M)=PHASED+PHASEN                                            60
      PHDEG(M)=PHASE(M)*57.295779513                                    61
      WCYCLE(M)=WF(M)/(2.0*3.1415926536)                                62
    9 CONTINUE                                                          63
      RETURN                                                            64
      END                                                               65
```

```
      SUBROUTINE SINGLE(COFF,ROOT,ROOTI)                                1
C                                                                       2
C     THIS SUBROUTINE FACTORS A FIRST ORDER POLYNOMIAL.                 3
C                                                                       4
      IMPLICIT REAL*8(A-H,O-Z)                                          5
      DIMENSION ROOT(1),COFF(2),ROOTI(1)                                6
      ROOT(1)=-COFF(1)/COFF(2)                                          7
      ROOTI(1)=0.0                                                      8
      RETURN                                                            9
      END                                                               10
```

```
C                                                                       1
C     GIVEN VALUES OF THE STABILITY DERIVATIVES AND AIRCRAFT            2
C     CHARACTERISTICS THIS PROGRAM PERFORMS THE FOLLOWING:              3
C                                                                       4
C                                                                       5
C        1) CALCULATE DIMENSIONAL STABILITY DERIVATIVES                 6
C                                                                       7
C        2) FORMS THE TRANSFER FUNCTIONS, TF(S)=N(S)/D(S)               8
C                                                                       9
C        3) SOLVE FOR ROOTS OF D(S) AND N(S)                           10
C                                                                      11
C        4) CALCULATE NATURAL FREQUENCIES, DAMPING RATIOS, TIME TO DAMP 12
C           TO ONE-HALF AMPLITUDE, AND SETTLING TIME                   13
C                                                                      14
C        5) PRODUCES INFORMATION NEEDED FOR BODE PLOT CONSTRUCTION      15
C                                                                      16
C                                                                      17
C                                                                      18
C     THE DERIVATION OF THE EQUATIONS OF MOTION ON WHICH THIS ANALYSIS IS 19
C     BASED WAS TAKEN FROM 'DYNAMICS OF THE AIRFRAME', BUREAU OF       20
C     AERONAUTICS REPORT, AE-61-4II.                                   21
C                                                                      22
C     THE ANALYSIS DESCRIBED ABOVE MUST MEET THE ASSUMPTIONS IMPOSED ON 23
C     THE EQUATIONS OF MOTION WHEN THEY WERE DERIVED.                  24
C     THESE ASSUMPTIONS ARE:                                           25
C                                                                      26
C        1) THE AIRFRAME IS ASSUMED TO BE A RIGID BODY.                27
C                                                                      28
C        2) THE EARTH IS ASSUMED TO BE FIXED IN SPACE, AND, UNLESS     29
C           SPECIFICALLY STATED OTHERWISE, THE EARTH'S ATMOSPHERE IS   30
C           ASSUMED TO BE FIXED WITH RESPECT TO THE EARTH.             31
C                                                                      32
C        3) THE MASS OF THE AIRPLANE IS ASSUMED TO REMAIN CONSTANT FOR 33
C           THE DURATION OF ANY PARTICULAR DYNAMIC ANALYSIS.           34
C                                                                      35
C        4) THE X-Z PLANE IS ASSUMED TO BE A PLANE OF SYMMETRY.        36
C                                                                      37
C        5) THE DISTURBANCES FROM THE STEADY FLIGHT CONDITION ARE ASSUMED 38
C           TO BE SMALL ENOUGH SO THAT THE PRODUCTS AND SQUARES OF THE 39
C           CHANGES IN VELOCITIES ARE NEGLIGIBLE IN COMPARISON WITH THE 40
C           CHANGES THEMSELVES.  ALSO, THE DISTURBANCE ANGLES ARE ASSUMED 41
C           TO BE SMALL ENOUGH SO THAT THE SINES OF THESE ANGLES MAY BE 42
C           SET EQUAL TO THE ANGLES AND THE COSINES SET EQUAL TO ONE.  43
C           PRODUCTS OF THESE ANGLES ARE ALSO APPROXIMATELY ZERO AND CAN 44
C           BE NEGLECTED.  AND, SINCE THE DISTURBANCES ARE SMALL, THE  45
C           CHANGE IN AIR DENSITY ENCOUNTERED BY THE AIRPLANE DURING ANY 46
C           DISTURBANCE CAN BE CONSIDERED TO BE ZERO.                  47
C                                                                      48
C        6) DURING THE STEADY FLIGHT CONDITION, THE AIRPLANE IS ASSUMED 49
C           TO BE FLYING WITH WINGS LEVEL AND ALL COMPONENTS OF VELOCITY 50
C           ZERO EXCEPT U SUB O.  W SUB O = 0 BECAUSE THE STABILITY AXES 51
C           WERE CHOSEN AS THE REFERENCE AXES.                         52
C                                                                      53
C        7) THE FLOW IS ASSUMED TO BE QUASI-STEADY.                    54
C                                                                      55
C                                                                      56
C                                                                      57
C     THE FOLLOWING CARDS IMPLY THAT THE PROGRAM IS EXECUTED IN DOUBLE 58
C     PRECISION.                                                       59
C                                                                      60
      IMPLICIT REAL*8(A-H,O-Z)                                         61
      COMPLEX*16 P,TST                                                 62
      REAL*8 MS,KGAIN,KC,KROOT,KKK,KD,KN,IXZ,IXX,IZZ,LP,NR,NP,LR,LB,NB,L 63
     $IN,NIN,NPHI,NPSI,NS,LV,NV                                        64
C                                                                      65
      COMMON   WYSP,ZSP,T12SP,TOSSP,WNP,ZP,T12P,TOSP,WF(21),RRD(10),RRN( 66
     $10),RDE(10),RIN(10),AR(21),PHASE(21),ACC,WCYCLE(21),ARDB(21),PHDEG 67
     $(21),KGAIN,NUMER                                                 68
      COMMON I                                                         69
      DIMENSION NS(5),NPHI(5),NPSI(5),DS(6),ROOTR(10),ROOTI(10),CC(5),KCC 70
     $4),CUF1(3),CUF2(3),RK1(2),RR2(2),PI1(2),RI2(2),CC(4),RK(3),COFF(16 71
     $),F1I3),XRI3),AI(3),COFI(3),RE(2),RIM(2),ROOT(11),COFF(2),KKKI(2),PI 72
     $6)                                                               73
C                                                                      74
C     THE READ STATEMENT IS THE INPUT OF ALL NON-DIMENSIONAL STABILITY 75
C     DERIVATIVES, EXCLUDING CONTROL SURFACE DERIVATIVES.              76
C                                                                      77
      READ(1,100)CYB,CLB,CNB,CYP,CLP,CNP,CYR,CLR,CNR                  78
  100 FORMAT(8F10.6/5F10.6)                                            79
      WRITE(3,201)                                                     80
  201 FORMAT(1X,121('*')/,1X,'*',119X,'*'/,1X,'*',44X,'LATERAL STABILI 81
     $TY DERIVATIVES',46X,'*'/,1X,'*',44X,29('-'),46X,'*'/,1X,'*'      82
     $,119X,'*'/,1X,'*',119X,'*')                                      83
      WRITE(3,202)CYB,CLB,CNB,CYP,CLP,CNP,CYR,CLR,CNR                  84
  202 FORMAT(1X,'*   CYB  =',F10.6,4X,'CLB   =',F10.6,4X,'CNB =',F10.6,4X 85
     $,'CYP =',F10.6,4X,'CLP  =',F10.6,4X,'CNP  =',F10.6,'  *'/,1X,'*  86
     $CYR  =',F10.6,4X,'CLR   =',F10.6,4X,'CNR =',F10.6,59X,'  *',    87
     $/,1X,'*',119X,'*'/,1X,'*',119X,'*'/,1X,121('*'),///)            88
C                                                                      89
C     INPUT OF PERTINENT AIRCRAFT CHARACTERISTICS                      90
C                                                                      91
      READ(1,101)RHO,U,S,MS,CH,B,GCOSGM,GSINGM,IXX,IXZ,IZZ             92
  101 FORMAT(6F10.5/5F10.5)                                            93
C                                                                      94
C     GCOSGM AND GSINGM ARE THE PRODUCTS OF THE ACCELERATION DUE TO    95
C     GRAVITY (ASSUME = 32.2 FT/SEC**2 FOR THIS ALTITUDE RANGE) AND THE 96
C     COSINE AND SINE RESPECTIVELY OF THE INITIAL FLIGHT PATH ANGLE,   97
C     GAMMA, (USUALLY ZERO FOR LEVEL FLIGHT).                          98
C                                                                      99
C     IZZ IS THE MOMENT OF INERTIA ABOUT THE Z AXIS                    100
C                                                                      101
C     IXZ IS THE PRODUCT OF INERTIA                                    102
C                                                                      103
C     IXX IS THE MOMENT OF INERTIA ABOUT THE X AXIS                    104
C                                                                      105
C     MS IS THE MASS OF THE AIRPLANE                                   106
C                                                                      107
C     S IS THE WING AREA OF THE AIRPLANE                               108
C                                                                      109
C     RHO IS THE DENSITY AT THE ALTITUDE WHICH THE AIRPLANE IS FLYING  110
C                                                                      111
C     U IS THE SPEED OF THE AIRCRAFT IN FEET PER SECOND                112
C                                                                      113
C     CH IS THE MEAN AERODYNAMIC CHORD OF THE WING                     114
C                                                                      115
C     B IS THE WING SPAN                                               116
C                                                                      117
      WRITE(3,203)RHO,S,MS,GCOSGM,U,CH,B,GSINGM,IXX,IXZ,IZZ            118
  203 FORMAT(1X,121('*')/,1X,'*',119X,'*'/,1X,'*',40X,'PERTINENT AIRPL 119
     $ANE CHARACTERISTICS',45X,'*'/,1X,'*',40X,34('-'),45X,'*'/,1X,'*' 120
     $,119X,'*'/,1X,'*',17X,'RHO =',F10.6,3X,'WING AREA =',F10.6,3X,'MA 121
     $SS =',F10.6,3X,'G*COS(GAMMA) =',F10.6,17X,'*'/,1X,'*',17X,'U   =' 122
     $,F10.4,3X,'CHORD     =',F10.6,3X,'SPAN =',F10.4,3X,'G*SIN(GAMMA) = 123
     $',F10.6,17X,'*'/,1X,'*',17X,'IXX =',F10.4,3X,'IXZ       =',F10.4,4X 124
     $,'IZZ =',F10.4,45X,'*'/,1X,'*',119X,'*'/,1X,121('*'),///)       125
      LCOUNT=0                                                         126
C                                                                      127
C     LCOUNT IS A COUNTER WHICH PREVENTS MULTIPLE CALCULATIONS OF THE  128
C     CHARACTERISTIC EQUATION.                                         129
C                                                                      130
C     LL=1,3 CONSTITUTES SOLUTIONS FOR THREE DIFFERENT NUMERATORS.     131
C                                                                      132
      DO 31 LL=1,3                                                     133
C                                                                      134
C     THE READ STATEMENT BELOW IS THE INPUT FOR THE VARIABLES EXPLAINED 135
C     BELOW.                                                           136
C                                                                      137
      READ(1,102)CYIN,CLIN,CNIN,K,NUMER,ACC                           138
  102 FORMAT(5F10.6,2I3,E14.7)                                         139
C                                                                      140
C     CYIN, CLIN, AND CNIN ARE THE STABILITY DERIVATIVES DUE TO CONTROL 141
C     SURFACE DEFLECTIONS.  CYIN IS EITHER THE PARTIAL OF CY WITH      142
C     RESPECT TO RUDDER DEFLECTION OR AILERON DEFLECTION. THE VALUE OF K 143
C     DETERMINES WHETHER IT IS CONCERNED WITH RUDDER OR AILERON.       144
C                                                                      145
C     IF K IS GIVEN THE VALUE 1 THEN CYIN, CLIN, AND CNIN ARE PARTIAL  146
C     DERIVATIVES WITH RESPECT TO RUDDER DEFLECTION. IF K=2 THEY ARE   147
C     PARTIALS ARE TAKEN WITH RESPECT TO AILERON DEFLECTION.           148
C                                                                      149
C     NUMER DEFINES WHICH TRANSFER FUNCTION WE ARE INTERESTED IN, (BETA, 150
C     PHI, PSI). NUMER=1 GIVES VARIATIONS IN BETA, NUMER=2 GIVES       151
C     VARIATIONS IN PHI, AND NUMER=3 GIVES VARIATIONS IN PSI.          152
C                                                                      153
C     THUS, FOR EXAMPLE, IF K=2 AND NUMER=2 THE TRANSFER FUNCTION WILL 154
C     BE VARIATION IN PHI DUE TO DEFLECTION OF THE AILERONS.           155
C                                                                      156
C     ACC IS THE ACCURACY USED THROUGHOUT THE PROGRAM TO COMPARE TWO    157
C     NUMBERS TO SEE IF THEY ARE SUFFICIENTLY CLOSE.                   158
C                                                                      159
      LCOUNT=LCOUNT+1                                                  160
      IF(LCOUNT.GE.2)GO TO 4                                           161
      IF(K.NE.2)GO TO 1                                                162
      WRITE(3,204)                                                     163
  204 FORMAT(15X,98('*'),/,15X,'*',96X,'*',/,15X,'*  *,32X,'RESPONSE TO 164
     $RUDDER DEFLECTION',31X,'  *')                                    165
      GO TO 2                                                          166
    1 WRITE(3,205)                                                     167
  205 FORMAT(15X,98('*'),/,15X,'*',96X,'*',/,15X,'*  *,31X,'RESPONSE TO 168
     $AILERON DEFLECTION',31X,'  *')                                   169
    2 WRITE(3,206)CYIN,CLIN,CNIN,K,ACC                                 170
  206 FORMAT(15X,'*',90X,'*',/,15X,'*',96X,'*',/15X,'*  *,'CYIN =',F10.6 171
     $,4X,'CLIN =',F10.6,4X,'CNIN =',F10.6,4X,'K =',I2,4X,'ACC =',F14.8, 172
     $6X,'*',/,15X,'*',96X,'*',/,15X,98('*'),///)                      173
C                                                                      174
C     CALCULATION OF DIMENSIONAL STABILITY DERIVATIVES                 175
C                                                                      176
      A=RHO*U*S                                                        177
      F=RHO*U*S*B                                                      178
      H=RHO*U*S*B*B                                                    179
      O=RHO*U*U*S                                                      180
      E=RHO*U*U*S*B                                                    181
C                                                                      182
C     A, F, H, O, E ARE JUST CONSTANTS USED TO CALCULATE THE DIMENSIONAL 183
C     STABILITY DERIVATIVES.                                           184
C                                                                      185
      YV=A*CYB/(2.0*MS)                                                186
      LV=F*CLB/(2.0*IXX)                                               187
      LB=O*LV                                                          188
      NV=F*CNB/(2.0*IZZ)                                               189
      NB=O*NV                                                          190
      YP=F*CYP/(4.0*MS)                                                191
      LP=H*CLP/(4.0*IXX)                                               192
      NP=H*CNP/(4.0*IZZ)                                               193
C                                                                      194
      YR=F*CYR/(4.0*MS)                                                195
      LR=H*CLR/(4.0*IXX)                                               196
      NR=H*CNR/(4.0*IZZ)                                               197
      YIN=O*CYIN/(2.0*MS)                                              198
      LIN=E*CLIN/(2.0*IXX)                                             199
      NIN=E*CNIN/(2.0*IZZ)                                             200
C                                                                      201
C     COEFFICIENTS FOR TRANSFER FUNCTION                               202
C                                                                      203
C     DENOMINATOR COEFFICIENTS, DS(5)S**4+DS(4)S**3+DS(3)S**2+DS(2)S+  204
C     DS(1), WHERE S REPRESENTS THE LAPLACIAN OPERATOR.                205
C                                                                      206
      DS(5)=1.0-(IXZ**2)/(IXX*IZZ)                                     207
      DS(4)=YV*((IXZ**2)/(IXX*IZZ)-1.0)-LP-NR-(IXZ/IXX)*NP-(IXZ/IZZ)*LR 208
      DS(3)=YV*(LP+NR*(IXZ/IXX)*NP+(IXZ/IZZ)*LR)+NR*LP+LO*((IXZ/IZZ)*(1. 209
     $0-YR/U)-YP/U)+NB*((1.0-YR/U)-(IXZ/IXX)*(YP/U)-NP*LR              210
      DS(2)=-NB*(LR*YP/U+(IXZ/IXX)*(GCOSGM/U)+GSINGM/U+LP*(1.0-YR/U))+LB 211
     $*(NP*(1.0-YR/U)-(IXZ/IZZ)*GSINGM/U-GCOSGM/U+NR*YP/U)+YV*(NP*LR-NR* 212
     $LP)                                                              213
      DS(1)=LB*(NR*GCOSGM/U-NP*GSINGM/U)+NB*(LP*GSINGM/U-LR*GCOSGM/U)  214
C                                                                      215
C     NUMERATOR COEFFICIENTS FOR SIDESLIP VARIATION, NS(4)S**3+NS(3)S**2 216
C     +NS(2)S+NS(1)                                                    217
C                                                                      218
      NS(4)=(YIN/U)*(1.0-(IXZ**2)/(IXX*IZZ))                           219
      NS(3)=(YIN/U)*(-NR-LP-(IXZ/IZZ-IXZ*NP/IXX)+LIN*(YP/U-(IXZ/IZZ)*(1.0 220
     $-YP/U))+NIN*((YP/U)*(IXZ/IXX)-(1.0-YR/U))                       221
      NS(2)=(YIN/U)*(LP*NR-LR*NP)+LIN*(GCOSGM/U-YP*NR/U-NP*(1.0-YR/U)+(G 222
     $SINGM/U)*(IXZ/IZZ))+NIN*(GCOSGM*IXZ/(U*IXX)+YP*LR/U+LP*(1.0-YR/U)+ 223
     $GSINGM/U)                                                        224
      NS(1)=(NIN/U)*(LR*GCOSGM-LP*GSINGM)+(LIN/U)*(NP*GSINGM-NR*GCOSGM) 225
C                                                                      226
C     NUMERATOR COEFFICIENTS FOR ROLLING VARIATION, NPHI(4)S**3+       227
C     NPHI(3)S**2+NPHI(2)S+NPHI(1)                                     228
C                                                                      229
      NPHI(4)=LIN+NIN*IXZ/IXX                                          230
      NPHI(3)=LIN*(-YV-NR)+NIN*(LR-IXZ*YV/IZZ)+(YIN/U)*(LB+IXZ*NB/IXX) 231
      NPHI(2)=YV*(LIN*NR-NIN*LR)-(YIN/U)*(LB*NR-LR*NB)+(1.0-YR/U)*(LIN*N 232
     $B-NIN*LB)                                                        233
      NPHI(1)=(GSINGM/U)*(NIN*LB-LIN*NB)                               234
C                                                                      235
C     COEFFICIENTS FOR NUMERATOR FOR YAWING VARIATION, NPSI(4)S**3      236
C     +NPSI(3)S**2+NPSI(2)S+NPSI(1)                                    237
C                                                                      238
      NPSI(4)=NIN*IXZ*LIN/IZZ                                          239
      NPSI(3)=NIN*(-YV-LP)+LIN*(-IXZ*YV/IZZ+NP)+(YIN/U)*(NB+IXZ*LB/IZZ) 240
      NPSI(2)=NIN*(YV*LP-YP*LB/U)+LIN*(YP*NB/U-NP*YV)+(YIN/U)*(NP*LB-LP* 241
     $NB)                                                              242
      NPSI(1)=(GCOSGM/U)*(LIN*NB-NIN*LB)                               243
      WRITE(3,207)DS(5),DS(4),DS(3),DS(2),DS(1),NS(4),NS(3),NS(2),NS(1), 244
     $NPHI(4),NPHI(3),NPHI(2),NPHI(1),NPSI(4),NPSI(3),NPSI(2),NPSI(1)  245
  207 FORMAT(////2X,123('*')/,2X,'*',121X,'*'/,2X,'*',32X,'POLYNOMIAL 246
     $OF COEFFICIENTS FOR THE DENOMINATOR AND NUMERATOR',32X,'*'/,2X,'*',32 247
     $X,'S**5',1X,'=',32X,'*'/,2X,'*',121X,'*'/,2X,'*',3X,'DS(5)  =',F10.4 248
     $,5X,'DS(4)   =',F10.4,5X,'DS(3)   =',F10.4,5X,'DS(2)   =',F10.4,5X 249
     $,'DS(1)   =',F10.4,2X,'*'/,2X,'*',121X,'*'/,2X,'*',27X,'NS(4)  250
     $=',F10.4,5X,'NS(3)   =',F10.4,5X,'NS(2)   =',F10.4,5X,'NS(1)   =' 251
     $,F10.4,3X,'*'/,2X,'*',121X,'*'/,2X,'*',27X,'NPHI(4) =',F10.4,5X, 252
     $'NPHI(3) =',F10.4,5X,'NPHI(2) =',F10.4,5X,'NPHI(1) =',F10.4,3X, 253
     $'*'/,2X,'*',121X,'*'/,2X,'*',27X,'NPSI(4) =',F10.4,3X,'NPSI(3) =' 254
     $,F10.4,5X,'NPSI(2) =',F10.4,5X,'NPSI(1) =',F10.4,3X,'*'/,2X,'*', 255
     $121X,'*'/,2X,123('*'))                                          256
C                                                                      257
C     THE DO LOOP BELOW DETERMINES THE ORDER OF THE POLYNOMIAL IN THE  258
```

```
C     DENOMINATOR, MD.
C
      DO 3 I=1,5
      IF(ABS(DS(I)).GT.ACC)MD=I-1
    3 CONTINUE
      IF(MD.NE.0)GO TO 4
      CALL EXIT
C
C     IF MD = 0, THERE IS NO CHARACTERISTIC EQUATION, THEREFORE THE
C     PROGRAM IS TERMINATED.
C
C     THE 3 'IF' STATEMENTS BELOW TELL US WHICH SET OF NUMERATOR
C     COEFFICIENTS TO EVALUATE DEPENDING ON THE VALUE OF NUMER.
C
    4 IF(NUMER.EQ.1)GO TO 5
      IF(NUMER.EQ.2)GO TO 7
      IF(NUMER.EQ.3)GO TO 9
    5 WRITE(3,208)
  208 FORMAT('1',   130('*'),/,1X,'*',128X,'*',/,1X,'*',128X,'*',/,1X,'*
     $',49X,'SOLUTION FOR SIDESLIP VARIATION',48X,'*',/,1X,'*',52X,24('-
     $'),52X,'*',/,1X,'*',128X,'*',/,1X,'*',128X,'*',/,1X,'*',55X,'DENOM
     $INATOR ROOTS',56X,'*',/,1X,'*',128X,'*')
C
C     THE DO LOOP BELOW DETERMINES THE ORDER OF THE POLYNOMIAL IN THE
C     NUMERATOR, MN.
C
      DO 6 I=1,4
      IF(ABS(NS(I)).GT.ACC)MN=I-1
    6 CONTINUE
      IF(MN.NE.0)GO TO 11
      CALL EXIT
    7 WRITE(3,209)
  209 FORMAT('1',   130('*'),/,1X,'*',128X,'*',/,1X,'*',128X,'*',/,1X,'*
     $',48X,'SOLUTION FOR ROLLING VARIATION',50X,'*',/,1X,'*',45
     $X,36('-'),45X,'*',/,1X,'*',128X,'*',/,1X,'*',128X,'*',/,1X,'*',55X
     $,'DENOMINATOR ROOTS',56X,'*',/,1X,'*',128X,'*')
      DO 8 I=1,4
      IF(ABS(NPHI(I)).GT.ACC)MN=I-1
    8 CONTINUE
      IF(MN.NE.0)GO TO 11
      WRITE(3,210)MN
  210 FORMAT(1X,'MN=',I3)
      CALL EXIT
    9 WRITE(3,211)
  211 FORMAT('1',   130('*'),/,1X,'*',128X,'*',/,1X,'*',128X,'*',/,1X,'*
     $',45X,'SOLUTION FOR YAWING VARIATION',       54X,'*',/,1X,'*',45
     $X,29('-'),54X,'*',/,1X,'*',128X,'*',/,1X,'*',128X,'*',/,1X,'*',55X
     $,'DENOMINATOR ROOTS',56X,'*',/,1X,'*',128X,'*')
      DO 10 I=1,4
      IF(ABS(NPSI(I)).GT.ACC)MN=I-1
   10 CONTINUE
      IF(MN.NE.0)GO TO 11
      WRITE(3,210)MN
      CALL EXIT
C
C     GETROT IS A SUBROUTINE WHICH, USING OTHER SUBROUTINES, CALCULATES
C     ROOTS, DAMPING RATIOS, AND NATURAL FREQUENCIES, AND THESE ARE
C     TRANSFERRED TO THE MAINLINE BY USE OF A 'COMMON' STATEMENT.
C
   11 CALL GETROT(DS,MD,RRD,RID)
C
C     THE FOLLOWING FOUR CARDS ADD A ZERO DENOMINATOR ROOT IF THE
C     TRANSFER FUNCTION IS NOT FOR SIDESLIP.
C


      IF(NUMER.EQ.1)GO TO 12
      MD=MD+1
      RRD(MD)=0.0
      RID(MD)=0.0
   12 WRITE(3,212)(J,RRD(J),RID(J),J=1,MD)
  212 FORMAT(1X,'*',46X,'ROOT(',I1,') = ',F10.5,'  +J ',F10.5,47X,'*')
      WRITE(3,213)
  213 FORMAT(1X,'*',128X,'*',/,1X,'*',128X,'*',/,1X,'*',34X,'NATURAL FRE
     $Q',5X,'DAMPING RATIO',4X,'TIME FOR 1/2 DAMPING',9X,'SETTLING TIME'
     $,18X,'*',/,1X,'*',31X,'UNDAMPED   DAMPED',80X,'*')
C
C     FOR DAMPING RATIOS GREATER THAN ONE(A NON-OSCILLATORY MODE) THE
C     FOLLOWING FOUR CARDS PREVENT TAKING THE SQUARE ROOT OF A NEGATIVE
C     NUMBER WHEN CALCULATING THE DAMPED NATURAL FREQUENCY.  IF THE
C     DAMPING RATIOS ARE GREATER THAN ONE THEN THE DAMPED NATURAL
C     FREQUENCIES REMAIN 0.0.
C
      WDSP=0.0
      WDP=0.0
      IF(DABS(ZSP).GT.1.0) GO TO 13
      WDSP=WNSP*DSQRT(1.0-ZSP*ZSP)
   13 WRITE(3,214)WNSP,WDSP,ZSP,T12SP,T05SP
  214 FORMAT(1X,'*',16X,'NOUTCH ROLL  ',   F9.4, F9.4,F10.5,11X,F10.5,
     $ 14X,F10.5,25X,'*',/,1X,'*',128X,'*')
C
C     CALCULATION OF VALUES OF WF FOR FUTURE USE IN THE BODE ROUTINE.
C     INCLUDED ARE SELECTED VALUES OF WF(.01,.1,1.0,10.0,100.0,1000.0)
C     PLUS 5 VALUES AROUND EACH NATURAL FREQUENCY(2 ABOVE, 2 BELOW, AND
C     THE NATURAL FREQUENCY) TO INCREASE DATA IN THE BODE PLOT CRITICAL
C     AREAS.
C
      WF(1)=.01
      DO 14 I=2,6
      IM1=I-1
      WF(I)=WF(IM1)*10.0
   14 CONTINUE
C
C     KWF IS THE NUMBER OF NATURAL FREQUENCIES TO BE USED IN THE BODE
C     ROUTINE.
C
      KWF=6
C
C     II AND IK ARE COUNTERS USED TO DETERMINE THE MAXIMUM VALUE OF KWF
C     DEPENDING ON THE NUMBER OF NATURAL FREQUENCIES IN BOTH THE
C     NUMERATOR AND THE DENOMINATOR OF A PARTICULAR TRANSFER FUNCTION.
C
      II=0
      IK=0
      IF(I.EQ.0)GO TO 16
      IF(I.EQ.2)GO TO 15
      WF(12)=0.9*WNP
      WF(13)=0.75*WNP
      WF(14)=WNP
      WF(15)=1.1*WNP
      WF(16)=1.25*WNP
      IK=1
      KWF=16
   15 WF(7)=.9*WNSP
      WF(8)=.75*WNSP
      WF(9)=WNSP
      WF(10)=1.1*WNSP
      WF(11)=1.25*WNSP
      II=1
      IF(KWF.EQ.16)GO TO 16
      KWF=11
C
C     GETROT IS USED TO FIND ROOTS OF A PARTICULAR NUMERATOR DEPENDING
C     ON THE VALUE OF NUMER.
C
   16 IF(NUMER.EQ.1)GO TO 17
      IF(NUMER.EQ.2)GO TO 18
      CALL GETROT(NPSI,MN,RRN,RIN)
      GO TO 19
   17 CALL GETROT(NS,MN,RRN,RIN)
      GO TO 19
   18 CALL GETROT(NPHI,MN,RRN,RIN)
   19 WRITE(3,215)
  215 FORMAT(1X,'*',56X,'NUMERATOR ROOTS',57X,'*',/,1X,'*',128X,'*')
      WRITE(3,212)(J,RRN(J),RIN(J),J=1,MN)
      IF(NUMER.NE.3)GO TO 21
      WRITE(3,213)
C
C     IF THE DAMPING RATIO HAS AN ABSOLUTE VALUE GREATER THAN ONE(A NON-
C     OSCILLATORY MODE), THEN A DAMPED NATURAL FREQUENCY IS NOT
C     CALCULATED FOR THE NUMERATOR.  THEREFORE, WDSP AND WDP ARE LEFT AS
C     ZERO.
C
      WDSP=0.0
      WDP=0.0
      IF(DABS(ZSP).GT.1.0) GO TO 20
      WDSP=WNSP*DSQRT(1.0-ZSP*ZSP)
C
C     THE TWO WRITE STATEMENTS BELOW PRINT THE PERTINENT INFORMATION FOR
C     OSCILLATORY MODES IN THE NUMERATOR.  IF THE NATURAL FREQUENCIES
C     ARE PRINTED AS ZERO THE MODE IS NON-OSCILLATORY.
C
   20 WRITE(3,216)WNSP,WDSP,ZSP,T12SP,T05SP
  216 FORMAT(1X,'*',28X,F9.4,F11.4,3X,F10.4,11X,F10.5,14X,F10.5,22X,'*',
     $/,1X,'*',128X,'*')
   21 WRITE(3,217)
  217 FORMAT(1X,'*',35X,58('-'),35X,'*',/,1X,'*',128X,'*',/,1X,'*',53X,'
     $BODE PLOT INFORMATION',54X,'*',/,1X,'*',128X,'*',/,1X,'*',21X,'FRE
     $QUENCY',26X,'AMPLITUDE RATIO',25X,'PHASE ANGLE',21X,'*',/,1X,'*',1
     $5X,'RAD/SEC',8X,'CYCLES/SEC',14X,'PURE',10X,'DECIBELS',19X,'RADIAN
     $S',8X,'DEGREES',15X,'*')
C
C     THE NEXT FEW CARDS ARE A ROUTINE TO FIND MORE VALUES OF WF FOR THE
C     BODE PLOT ROUTINE DEPENDING ON WHETHER OR NOT THE NUMERATOR HAS
C     ANY OSCILLATORY MODES.  THE FREQUENCIES AND THE VALUES OF KWF ARE
C     CHOSEN IN THE SAME MANNER AS THOSE OF THE DENOMINATOR PREVIOUSLY
C     MENTIONED.
C
C     MD1 AND MN1 ARE USED TO PREVENT HAVING ZERO SUBSCRIPTS WHEN
C     CALCULATING THE NUMERATOR AND DENOMINATOR GAINS FOR THE BODE PLOT
C     SUBROUTINE.
C
      MD1=MD+1
      IF(NUMER.NE.1)MD1=MD
      MN1=MN+1
      IF(I.EQ.0)GO TO 24
C
C     II AND IK ARE COUNTERS USED TO DETERMINE THE MAXIMUM VALUE OF KWF.
C
      IF(II.EQ.0.AND.IK.EQ.0)GO TO 23
      IF(II.EQ.1.AND.IK.EQ.0)GO TO 22
      WF(17)=.9*WNSP
      WF(18)=.75*WNSP
      WF(19)=WNSP


      WF(20)=1.1*WNSP
      WF(21)=1.25*WNSP
      KWF=21
      GO TO 24
   22 WF(12)=.9*WNSP
      WF(13)=.75*WNSP
      WF(14)=WNSP
      WF(15)=1.1*WNSP
      WF(16)=1.25*WNSP
      KWF=16
      GO TO 24
   23 WF(7)=.9*WNSP
      WF(8)=.75*WNSP
      WF(9)=WNSP
      WF(10)=1.1*WNSP
      WF(11)=1.25*WNSP
      KWF=11
   24 IF(NUMER.NE.1)GO TO 25
      KGAIN=ASIN(N1)/DS(MD1)
C
C     THE GAIN (KGAIN) FOR THE ROOT LOCUS PLOTS IS CALCULATED FROM THE
C     COEFFICIENTS OF THE HIGHEST ORDER TERM IN THE DENOMINATOR AND
C     NUMERATOR. TF=KGAIN(S+A)(S+B)/(S+C)(S+D), WHERE A AND B ARE ROOTS
C     OF THE NUMERATOR AND C AND D ARE ROOTS OF THE DENOMINATOR.
C
      GO TO 27
   25 IF(NUMER.NE.2)GO TO 26
      KGAIN=NPHI(MN1)/DS(MD1)
      GO TO 27
   26 KGAIN=NPSI(MN1)/DS(MD1)
   27 KKWF=KWF
C
C     THE NEXT 12 CARDS RANK THE WF'S IN ASCENDING ORDER.
C
   28 WAX=WF(1)
      LK=1
      DO 29 JD=2,KKWF
      IF(WF(JD).GE.WAX)LK=JD
      IF(WF(JD).GE.WAX)WAX=WF(JD)
   29 CONTINUE
      WSAV=WF(KKWF)
      WF(KKWF)=WAX
      WF(LK)=WSAV
      KKWF=KKWF-1
      IF(KKWF.EQ.1)GO TO 30
      GO TO 28
C
C     BODE IS THE SUBROUTINE WHICH CALCULATES AMPLITUDE RATIO AND PHASE
C     ANGLE FOR EACH WF.  THE INFORMATION IS TRANSFERRED TO THE MAINLINE
C     BY THE USE OF A 'COMMON' STATEMENT.
C
   30 CALL BODE(MD,MN,KWF)
      WRITE(3,218)(WF(I),WCYCLE(I),AR(I),ARDB(I),PHASE(I),PHDEG(I),I=1,K
     $WF)
  218 FORMAT(1X,'*',13X,F10.5,6X,F10.5,12X,F10.2,6X,F10.5,12X,F10.5,6X,F
     $10.5,13X,'*')
      WRITE(3,219)
  219 FORMAT(1X,'*',128X,'*',/,1X,130('*'))
      IF(NUMER.NE.1)NO=ND-1
   31 CONTINUE
      CALL EXIT
      END
```

```
      SUBROUTINE GETROT(COFFI,N,ROOTR,ROOTI)
C
C     GETROT IS A SUBROUTINE WHICH, USING OTHER SUBROUTINES, CALCULATES
C     ROOTS, DAMPING RATIOS, AND NATURAL FREQUENCIES, AND THESE ARE
C     TRANSFEARED TO THE MAINLINE BY USE OF A 'COMMON' STATEMENT.
C
      IMPLICIT REAL*8(A-H,O-Z)
      COMPLEX*16 P,TST
      REAL*8 MS,IYY,MU,MW,MDW,MQ,MIN,MUS,MAS,MTHS,KGAIN,KG,KROOT,KKK,KD,
     $KN
      COMMON   WNSP,ZSP,T12SP,TOSSP,WNP,ZP,T12P,TOSP,WF(21),RRD(10),RRN(
     $10),RID(10),RIN(10),AR(21),PHASE(21),ACC,WCYCLE(21),ARDB(21),PHDEG
     $(21),KGAIN,NUMER
      COMMON I
      DIMENSION NUS(5),NAS(5),NTHS(5),DS(6),ROOTR(10),ROOTI(10),C(5),KC(
     $4),QUF1(3),QUF2(3),RR1(2),RR2(2),RI1(2),RI2(2),CC(4),RR(3),COFFI(6
     $),RI(5),XR(3),XI(3),COF(3),RE(2),RIM(2),ROOT(11),COFF(2),KKK(21),P(
     $6)
C
C     THE 3 'IF' STATEMENTS BELOW DECIDE WHICH ROOT-EXTRACTION
C     SUBROUTINE TO CALL DEPENDING ON THE VALUE OF MITHE ORDER OF THE
C     POLYNOMIAL).
C
      IF(N.EQ.4)GO TO 3
      IF(N.EQ.3)GO TO 2
      IF(N.EQ.2)GO TO 1
C
C     THE SUBROUTINES SINGLE, QUAD, CUBE, AND FOURTH SOLVE (THE SOLUTION
C     IS ACHIEVED IN CLOSED FORM AND THUS REQUIRES NO ITERATIVE
C     PROCEDURE) FOR ROOTS OF FIRST, SECOND, THIRD, AND FOURTH ORDER
C     POLYNOMIALS, RESPECTIVELY.
C
      CALL SINGLE(COFFI,ROOTR,ROOTI)
      GO TO 4
    1 CALL QUAD(COFFI,ROOTR,ROOTI)
      GO TO 4
    2 CALL CUBE(COFFI,ROOTR,ROOTI)
      GO TO 4
    3 CALL FOURTH(COFFI,ROOTR,ROOTI)
C
C     THE FOLLOWING CARDS TEST THE ROOTS OF THE POLYNOMIAL  TO CHECK THE
C     ACCURACY OF THE ROOT SOLVER SUBROUTINES.  IF THE VALUE OF TST IS
C     TOO LARGE A WARNING MESSAGE IS PRINTED.
C
    4 DO 6 I=1,N
      P(I)=DCMPLX(ROOTR(I),ROOTI(I))
      ZERO=0.0
      TST=DCMPLX(COFF)(1),ZERO)
      MJ=M+1
      DO 5 J=2,MJ
      TST=TST+CCFF(J)*P(I)**(J-1)
    5 CONTINUE
      IF(CDABS(TST).LE.ACC)GO TO 6
      WRITE(3,100)P(I),TST
  100 FORMAT(1X,'ROOT = ',2G15.8,'  WHEN SUBSTITUTED INTO ITS POLYNOMI
     $AL FAILED TO COME WITHIN ACC OF 0.0+0.',/,1X,'THIS VALUE DIFFERED FR
     $OM ZERO BY ',2G15.8,'  THIS IMPLIES EITHER A ROUNDOFF ERROR WHEN
     $TESTING THE ROOTS',/,1X,'ACC TOO SMALL) OR THE VALUE 0.01 USED TO
     $ COMPARE WITH TEST IN SUBROUTINE FOURTH IS TOO LARGE.')
    6 CONTINUE
C
C     I IS A COUNTER WHICH DETERMINES THE NUMBER OF ROOTS WHICH HAVE
C     BOTH A REAL AND AN IMAGINARY PART.
C
C
C     THE NEXT 25 CARDS IS A PROCEDURE WHICH POSITIONS ROOTS WITH BOTH
C     REAL AND IMAGINARY PARTS IN THE FIRST L POSITIONS AND THE ROOTS
C     WITH ZERO IMAGINARY PARTS IN THE NEXT KK POSITIONS.  FOR EXAMPLE
C     IF THERE ARE 4 ROOTS, TWO WITH ONLY REAL PARTS AND TWO COMPLEX,
C     THE COMPLEX ROOTS WILL BE IN POSITIONS 1 AND 2 AND THE REAL ROOTS
C     WILL BE IN POSITIONS 3 AND 4.  L, K, AND KK ARE COUNTERS USED TO
C     FACILITATE THIS PROCEDURE.
C
C     I IS A COUNTER WHICH DETERMINES THE NUMBER OF ROOTS WHICH HAVE
C     BOTH A REAL AND AN IMAGINARY PART.
C
      I=M
C
C     M IS A COUNTER WHICH PREVENTS THE ORDER OF THE POLYNOMIAL FROM
C     BEING DESTROYED.
C
      M=M
      L=1
      K=M+1
      KK=0
      DO 8 J=1,N
      IF(DABS(RCOTI(J)).GT.ACC)GO TO 7
      I=I-1
      ROOTI(K)=RCOTI(J)
      RCOTR(K)=RCOTR(J)
      K=K+1
      KK=KK+1
      GO TO 8
    7 RCOTI(L)=ROOTI(J)
      ROOTR(L)=ROOTR(J)
      L=L+1
    8 CONTINUE
      IF(KK.EQ.0)GO TO 10
    9 KI=K-KK
      ROOTI(M)=ROOTI(KI)
      RCOTR(M)=RCOTR(KI)
      M=M-1
      KK=KK-1
      IF(KK.EQ.0)GO TO 10
      GO TO 9
C
C     AT THIS POINT THERE ARE I ROOTS THAT HAVE BOTH A REAL AND AN
C     IMAGINARY PART AND (M-I) ROOTS WITH JUST A REAL PART.
C
C     THIS PART OF THE PROGRAM DETERMINES THE LARGEST REAL PART OF THE
C     ROOTS AND RANKS THEM FROM THE BOTTOM IN THE I POSITIONS AVAILABLE.
C
   10 RMAX=RCOTR(1)
      K=1
      IF(I.EQ.0) GO TO 13
      DO 11 J=1,I
      IF(DABS(RCOTR(J)).GT.RMAX)K=J
      IF(DABS(RCOTR(J)).GT.RMAX)RMAX=ROOTR(J)
   11 CONTINUE
      RSAVER=RCOTR(I)
      RSAVEI=ROOTI(I)
      ROOTR(I)=ROOTR(K)
      RCOTI(I)=ROOTI(K)
      ROOTR(K)=RSAVER
      RCOTI(K)=RSAVEI
      N=I-1
      DO 12 J=1,N
      IF(DABS(RMAX-ROOTR(J)).LE.ACC)L=J
   12 CONTINUE
      RSAVER=ROOTR(N)
      RSAVEI=RCOTI(N)
      ROOTR(N)=ROOTR(L)
      ROOTI(N)=ROCTI(L)
      ROOTR(L)=RSAVER
      ROOTI(L)=RSAVEI
C
C     THE OUTPUT FOR BOTH NUMERATOR AND DENOMINATOR IS PRINTED IN A FORM
C     WHICH REQUIRES TWO OSCILLATORY MODES.  IF ONE OR BOTH OF THE MODES
C     ARE NON-OSCILLATORY THEN THE FOLLOWING PROCEDURE IS USED:
C         1)  THE DAMPING RATIO IS CHOSEN TO BE THE SMALLER MAGNITUDE OF
C             THE REAL ROOTS, SINCE THIS ROOT WILL DOMINATE IN THE TIME
C             DOMAIN (A NEGATIVE DAMPING RATIO WOULD INDICATE AN
C             UNSTABLE MODE).
C         2)  THE TIME TO DAMP TO 50% AND 5% OF THE AMPLITUDE ARE
C             CALCULATED BASED ON THE ABOVE DAMPING RATIO.  THUS, FOR AN
C             UNSTABLE SYSTEM THESE TIMES WILL BE NEGATIVE.
C
C     THE REMAINING PORTION OF GETROT CALCULATES THE NATURAL FREQUENCIES
C     (WNP & WNSP), DAMPING RATIOS(ZP & ZSP), TIME TO DAMP TO 1/2
C     AMPLITUDE(T12P & T12SP), AND SETTLING TIME(TOSP & TOSSP).  THE
C     SETTLING TIME IS THE TIME TO DAMP TO 5% OF THE ORIGINAL AMPLITUDE.
C     THE SUFFIXES P AND SP REFER TO OSCILLATORY MODES FOR THE NUMERATOR
C     OR THE DENOMINATOR DEPENDING ON THE EQUATION BEING SOLVED .
C
C     THE SHORT PERIOD AND PHUGOID NATURAL FREQUENCIES ARE DETERMINED BY
C     A RANKING OF THE MAGNITUDE OF THE REAL AND IMAGINARY PARTS OF THE
C     ROOTS, THE LARGER MAGNITUDE REPRESENTS THE SHORT PERIOD MODE.  IF
C     THERE IS ONLY ONE OSCILLATORY MODE THIS MODE IS REFERRED TO AS THE
C     SHORT PERIOD MODE AND THE PHUGOID MODE NATURAL FREQUENCY IS
C     PRINTED AS ZERO.  WHEN GETROT IS USED FOR A NUMERATOR POLYNOMIAL
C     THE SHORT PERIOD INFORMATION IS PRINTED AS A NUMERATOR OSCILLATORY
C     MODE(SINCE A CUBIC IS THE LARGEST NUMERATOR POLYNOMIAL POSSIBLE,
C     THERE WILL BE ONLY ONE OSCILLATORY MODE AT MOST).
C
   13 IF(M.EQ.1)GO TO 17
      IF(M.EQ.2.AND.I.EQ.0)GO TO 18
      IF(M.EQ.2.AND.I.EQ.2)GO TO 21
      IF(M.EQ.3.AND.I.EQ.0)GO TO 22
      IF(M.EQ.3.AND.I.EQ.2)GO TO 26
      IF(M.EQ.4.AND.I.EQ.0)GO TO 27
      IF(M.EQ.4.AND.I.EQ.2)GO TO 32
      WN1=DSQRT(RCOTR(3)*ROOTR(3)+ROOTI(3)*ROOTI(3))
      WN2=DSQRT(RCOTR(1)*ROOTR(1)+ROOTI(1)*ROOTI(1))
      IF(WN1.GT.WN2)GO TO 14
      WNSP=WN2
      NX=20
      WNP=WN1
      GO TO 15
   14 WNSP=WN1
      NX=10
      WNP=WN2
   15 IF(NX.NE.20)GO TO 16
      ZSP=-ROOTR(1)/WNSP
      TOSSP=(2.9957)/(ZSP*WNSP)
      T12SP=(.693147)/(ZSP*WNSP)
      ZP=-RCOTR(3)/WNP
      T12P=(.693147)/(ZP*WNP)
      TOSP=(2.9957)/(ZP*WNP)
      GO TO 35
   16 ZSP=-ROOTR(3)/WNSP
      TOSSP=(2.9957)/(ZSP*WNSP)
      T12SP=(.693147)/(ZSP*WNSP)

      ZP=-RCOTR(1)/WNP
      TOSP=(2.9957)/(ZP*WNP)
      T12P=(.693147)/(ZP*WNP)
      GO TO 35
   17 WNSP=0.0
      WNP=0.0
      ZSP=-ROOTR(1)
      ZP=0.0
      T12SP=.693147/ZSP
      TOSSP=2.9957/ZSP
      TOSP=0.0
      T12P=0.0
      GO TO 35
   18 IF(DABS(RCOTR(1)).GT.DABS(ROOTR(2)))GO TO 19
      ZSP=-ROOTR(1)
      ZP=-RCOTR(2)
      GO TO 20
   19 ZSP=-ROOTR(2)
      ZP=-RCOTR(1)
   20 WNSP=0.0
      WNP=0.0
      T12P=.693147/ZP
      TOSP=2.9957/ZP
      T12SP=.693147/ZSP
      TOSSP=2.9957/ZSP
      GO TO 35
   21 WNP=0.0
      ZP=0.0
      T12P=0.0
      TOSP=0.0
      WNSP=DSQRT(RCOTR(1)*RCOTR(1)+ROOTI(1)*ROOTI(1))
      ZSP=-ROOTR(1)/WNSP
      T12SP=.693147/(ZSP*WNSP)
      TOSSP=2.9957/(ZSP*WNSP)
      GO TO 35
   22 RMAX=RCOTR(1)
      K=1
      DO 23 J=1,3
      IF(DABS(RCOTR(J)).GT.RMAX)K=J
      IF(DABS(ROOTR(J)).GT.RMAX)RMAX=ROOTR(J)
   23 CONTINUE
      RSAV=ROOTR(3)
      ROOTR(3)=RMAX
      RCOTR(K)=RSAV
      IF(DABS(RCOTR(1)).GT.DABS(ROOTR(2)))GO TO 24
      ZSP=-RCOTR(1)
      ZP=-RCOTR(2)
      GO TO 25
   24 ZSP=-ROOTR(2)
      ZP=-ROOTR(1)
   25 WNSP=0.0
      WNP=0.0
      T12P=.693147/ZP
      TOSP=2.9957/ZP
      T12SP=.693147/ZSP
      TOSSP=2.9957/ZSP
      GO TO 35
   26 WNP=0.0
      ZP=-ROOTR(3)
      T12P=.693147/ZP
      TOSP=2.9957/ZP
      WNSP=DSQRT(ROOTR(1)*RCOTR(1)+ROOTI(1)*ROOTI(1))
      ZSP=-ROOTR(1)/WNSP
      T12SP=.693147/(ZSP*WNSP)
```

```
      TOSSP=2.9957/(ZSP*WNSP)                                           257
      GO TO 35                                                          258
   27 RAX=ROOTR(1)                                                      259
      K=1                                                               260
      DO 28 J=1,4                                                       261
      IF(DABS(ROOTR(J)).GT.RAX)K=J                                      262
      IF(DABS(ROOTR(J)).GT.RAX)RAX=ROOTR(J)                             263
   28 CONTINUE                                                          264
      RSAV=ROOTR(4)                                                     265
      ROOTR(4)=RAX                                                      266
      ROOTR(K)=RSAV                                                     267
      RAX=ROOTR(1)                                                      268
      K=1                                                               269
      DO 29 J=1,3                                                       270
      IF(DABS(ROOTR(J)).GT.RAX)K=J                                      271
      IF(DABS(ROOTR(J)).GT.RAX)RAX=ROOTR(J)                             272
   29 CONTINUE                                                          273
      RSAV=ROOTR(3)                                                     274
      ROOTR(3)=RAX                                                      275
      ROOTR(K)=RSAV                                                     276
      IF(DABS(ROOTR(1)).GT.DABS(ROOTR(2)))GO TO 30                      277
      ZSP=-ROOTR(1)                                                     278
      ZP=-ROOTR(2)                                                      279
      GO TO 31                                                          280
   30 ZSP=-ROOTR(2)                                                     281
      ZP=-ROOTR(1)                                                      282
   31 WNSP=0.0                                                          283
      WNP=0.0                                                           284
      T12P=.693147/ZP                                                   285
      TO5P=2.9957/ZP                                                    286
      T12SP=.693147/ZSP                                                 287
      TO5SP=2.9957/ZSP                                                  288
      GO TO 35                                                          289
   32 WNSP=DSQRT(ROOTR(1)*ROOTR(1)+ROOTI(1)*ROOTI(1))                   290
      ZSP=-ROOTR(1)/WNSP                                                291
      WNP=0.0                                                           292
      T12SP=.693147/(ZSP*WNSP)                                          293
      TO5SP=2.9957/(ZSP*WNSP)                                           294
      IF(DABS(ROOTR(3)).GT.DABS(ROOTR(4)))GO TO 33                      295
      ZP=-ROOTR(3)                                                      296
      GO TO 34                                                          297
   33 ZP=-ROOTR(4)                                                      298
   34 T12SP=(2.9957)/(ZSP*WNSP)                                         299
      TO5SP=.693147/(ZSP*WNSP)                                          300
   35 RETURN                                                            301
      END                                                               302
```

```
      SUBROUTINE CUBE(CC,XR,XI)                                         1
      IMPLICIT REAL*8(A-H,O-Z)                                          2
      DIMENSION CC(4),RR(3),RI(3),XR(3),XI(3)                           3
C                                                                       4
C     THIS SUBROUTINE FACTORS A THIRD ORDER POLYNOMIAL BY A CLOSED FORM 5
C     PROCEDURE GIVEN IN 'INTRODUCTION TO THE THEORY OF EQUATIONS' BY   6
C     CONKWRIGHT AND MODIFIED BY THE PROCEDURE GIVEN IN 'STANDARD MATH  7
C     TABLES' BY CHEMICAL RUBBER COMPANY.                               8
C                                                                       9
C                                                                       10
      H=(3.0*CC(4)*CC(2)-CC(3)*CC(3))/(9.0*CC(4)*CC(4))                 11
      G=(2.0*CC(3)*CC(3)*CC(3)-9.0*CC(4)*CC(3)*CC(2)+27.0*CC(4)*CC(4)*CC 12
     $(1))/(27.0*CC(4)*CC(4)*CC(4))                                     13
      RAD=G*G+4.0*H*H*H                                                 14
      IF(RAD.LT.0.0)GO TO 3                                             15
      UROOT3=(-G+DSQRT(G*G+4.0*H*H*H))/2.0                              16
      IF(UROOT3.LT.0.0)GO TO 1                                          17
      UROOT=UROOT3**.333333333333333                                    18
      GO TO 2                                                           19
    1 UROOT=(-UROOT3)**.333333333333333                                 20
      UROOT=-UROOT                                                      21
    2 VROOT=-H/UROOT                                                    22
      RR(1)=UROOT+VROOT                                                 23
      RR(2)=-(UROOT+VROOT)/2.0                                          24
      RR(3)=-(UROOT+VROOT)/2.0                                          25
      RI(1)=0.0                                                         26
      RI(2)=(UROOT-VROOT)*(.866025403784)                               27
      RI(3)=-(UROOT-VROOT)*(.866025403784)                              28
      XR(1)=RR(1)-CC(3)/(3.0*CC(4))                                     29
      XR(2)=RR(2)-CC(3)/(3.0*CC(4))                                     30
      XR(3)=RR(3)-CC(3)/(3.0*CC(4))                                     31
      XI(1)=RI(1)                                                       32
      XI(2)=RI(2)                                                       33
      XI(3)=RI(3)                                                       34
      GO TO 4                                                           35
    3 THETA=DARCOS(-G/(2.0*DSQRT(-H*H*H)))                              36
      TH3=THETA/3.0                                                     37
      XI(1)=0.0                                                         38
      XI(2)=0.0                                                         39
      XI(3)=0.0                                                         40
      XR(1)=2.0*DCOS(TH3)*DSQRT(-H)                                     41
      XR(2)=2.0*DCOS(TH3+2.094395102392)*DSQRT(-H)                      42
      XR(3)=2.0*DCOS(TH3+4.188790204784)*DSQRT(-H)                      43
      SUB=CC(3)/(3.0*CC(4))                                             44
      XR(1)=XR(1)-SUB                                                   45
      XR(2)=XR(2)-SUB                                                   46
      XR(3)=XR(3)-SUB                                                   47
    4 RETURN                                                            48
      END
```

```
      SUBROUTINE FOURTH(C,ROOTR,ROOTI)                                  1
C                                                                       2
C     THIS SUBROUTINE FACTORS A FOURTH ORDER POLYNOMIAL BY A CLOSED FORM 3
C     PROCEDURE WHICH FORMS 2 QUADRATIC FACTORS AND THEN CALLS A        4
C     QUADRATIC FACTORING SUBROUTINE, QUAD, TO OBTAIN THE FOUR ROOTS.   5
C     THE PROCEDURE WAS TAKEN FROM 'INTRODUCTION TO THE THEORY OF       6
C     EQUATIONS' BY N.B. CONKWRIGHT.                                    7
C                                                                       8
      IMPLICIT REAL*8(A-H,O-Z)                                          9
      REAL*8 MS,IYY,MU,MW,MDW,MQ,MIN,MUS,MAS,MTHS,KGAIN,KC,KROOT,KKK    10
      DIMENSION C(5),KC(4),QUF1(3),QUF2(3),RR1(2),RR2(2),RI1(2),RI2(2),R 11
     $OOTR(10),ROOTI(10)                                                12
      P=C(4)/C(5)                                                       13
      Q=C(3)/C(5)                                                       14
      R=C(2)/C(5)                                                       15
      S=C(1)/C(5)                                                       16
      KC(4)=1.0                                                         17
      KC(3)=-.5*Q                                                       18
      KC(2)=.25*(P*R-4.0*S)                                             19
      KC(1)=.125*(4.0*Q*S-P*P*S-R*R)                                    20
      HKC=(3.0*KC(4)*KC(2)-KC(3)*KC(3))/9.0*KC(4)*KC(4)                 21
      GKC=(2.0*KC(3)*KC(3)*KC(3)-9.0*KC(4)*KC(3)*KC(2)+27.0*KC(4)*KC(4)* 22
     $KC(1))/(27.0*KC(4)*KC(4)*KC(4))                                   23
      RAD=GKC*GKC+4.0*HKC*HKC*HKC                                       24
      IF(RAD.LT.0.0)GO TO 3                                             25
      UKC=((-GKC+DSQRT(GKC*GKC+4.0*HKC*HKC*HKC))/2.0)                   26
      RTUKC=DABS(UKC)**.333333333333333                                 27
      UKC=DSIGN(RTUKC,UKC)                                              28
      VKC=-HKC/UKC                                                      29
      KROOT=UKC+VKC-KC(3)/(3.0*KC(4))                                   30
    1 B=DSQRT(KROOT*KROOT-S)                                            31
      A=DSQRT(2.0*KROOT+P*P*.25-Q)                                      32
      TEST=2.0*A*B+R-KROOT*P                                            33
      IF(TEST.LE..01)GO TO 2                                            34
      A=-A                                                              35
      TEST=2.0*A*B+R-KROOT*P                                            36
      IF(TEST.LE..01)GO TO 2                                            37
      A=-A                                                              38
      B=-B                                                              39
      TEST=2.0*A*B+R-KROOT*P                                            40
      IF(TEST.LE..01)GO TO 2                                            41
      A=-A                                                              42
    2 QUF1(3)=1.0                                                       43
      QUF2(3)=1.0                                                       44
      QUF1(2)=-.5*P-A                                                   45
      QUF2(2)=-.5*P+A                                                   46
      QUF1(1)=KROOT-B                                                   47
      QUF2(1)=KROOT+B                                                   48
      CALL QUAD(QUF1,RR1,RI1)                                           49
      ROOTR(1)=RR1(1)                                                   50
      ROOTR(2)=RR1(2)                                                   51
      ROOTI(1)=RI1(1)                                                   52
      ROOTI(2)=RI1(2)                                                   53
      CALL QUAD(QUF2,RR2,RI2)                                           54
      ROOTR(3)=RR2(1)                                                   55
      ROOTR(4)=RR2(2)                                                   56
      ROOTI(3)=RI2(1)                                                   57
      ROOTI(4)=RI2(2)                                                   58
      RETURN                                                            59
    3 THETA=DARCOS(-GKC/(2.0*DSQRT(-HKC*HKC*HKC)))                      60
      TH3=THETA/3.0                                                     61
      KROOT = 2.0*DCOS(TH3)*DSQRT(-HKC) - KC(3)/(3.0*KC(4))             62
      GO TO 1                                                           63
      END                                                               64
```

```
      SUBROUTINE QUAD(COF,RE,RIM)                                       1
C                                                                       2
C     THIS SUBROUTINE FACTORS A SECOND ORDER POLYNOMIAL BY USING THE    3
C     QUADRATIC FORMULA.                                                4
C                                                                       5
      IMPLICIT REAL*8(A-H,O-Z)                                          6
      DIMENSION COF(3),RE(2),RIM(2)                                     7
      DIS=COF(2)*COF(2)-4.0*COF(3)*COF(1)                               8
      IF(DIS.LT.0.0) GO TO 1                                            9
      RE(1)=(-COF(2)+DSQRT(DIS))/(2.0*COF(3))                           10
      RE(2)=(-COF(2)-DSQRT(DIS))/(2.0*COF(3))                           11
      RIM(1)=0.0                                                        12
      RIM(2)=0.0                                                        13
      GO TO 2                                                           14
    1 RE(1)=-COF(2)/(2.0*COF(3))                                        15
      RE(2)=RE(1)                                                       16
      RIM(1)=(-DSQRT(-DIS))/(2.0*COF(3))                                17
      RIM(2)=(DSQRT(-DIS))/(2.0*COF(3))                                 18
    2 RETURN                                                            19
      END                                                               20
```

```
      SUBROUTINE SINGLE(COFF,ROOT,ROOTI)                                1
C                                                                       2
C     THIS SUBROUTINE FACTORS A FIRST ORDER POLYNOMIAL.                 3
C                                                                       4
      IMPLICIT REAL*8(A-H,O-Z)                                          5
      DIMENSION ROOT(1),COFF(2),ROOTI(1)                                6
      ROOT(1)=-COFF(1)/COFF(2)                                          7
      ROOTI(1)=0.0                                                      8
      RETURN                                                            9
      END                                                               10
```

```
      SUBROUTINE BODE(L,JJ,KWF)                                         1
C                                                                       2
C     THIS IS A SUBROUTINE WHICH CALCULATES THE INFORMATION NEEDED TO   3
C     CONSTRUCT A BODE PLOT ONCE THE NUMERATOR AND DENOMINATOR          4
C     POLYNOMIALS HAVE BEEN FACTORED.  THE INFORMATION IS TRANSFERRED TO 5
C     THE MAINLINE BY USING A 'COMMON' STATEMENT.  THE FREQUENCIES ARE  6
C     GIVEN BOTH IN RADIANS PER SECOND AND CYCLES PER SECOND.  THE      7
C     AMPLITUDE RATIO IS GIVEN BOTH AS A PURE NUMBER AND IN DECIBELS.   8
C     THE PHASE ANGLE IS GIVEN BOTH IN DEGREES AND RADIANS.             9
C                                                                       10
      IMPLICIT REAL*8(A-H,O-Z)                                          11
      REAL*8 MS,IYY,MU,MW,MDW,MQ,MIN,NUS,NAS,NTHS,KGAIN,KC,KROOT,KKK,KD, 12
     $KN,NWS,KDSAVE,KNSAVE                                              13
      COMMON   WNSP,ZSP,T12SP,TQ5SP,WNP,ZP,T12P,TQ5P,WF(21),RRD(10),RRN( 14
     $10),RID(10),RIN(10),AMPR(21),PHASE(21),ACC,NCYCLE(21),AMPRDB(21),P 15
     $HDEG(21),KGAIN                                                    16
      COMMON I                                                          17
      DIMENSION KKK(21)                                                 18
      DO 9 M=1,KWF                                                      19
      AMPD=1.0                                                          20
      KD=1.0                                                            21
      PHASED=0.0                                                        22
      DO 4 J=1,L                                                        23
      IF(RRD(J).EQ.0.0)GO TO 1                                          24
      GO TO 3                                                           25
    1 AMPD=AMPD*DABS(WF(M)-RID(J))                                      26
      IF(WF(M)-RID(J).LT.0.0)GO TO 2                                    27
      PHASED=PHASED-3.1415926536/2.0                                    28
      GO TO 4                                                           29
    2 PHASED=PHASED+3.1415926536/2.0                                    30
      GO TO 4                                                           31
    3 AMPD=DSQRT(((-WF(M)+RID(J))/RRD(J))**2+1.0)*AMPD                  32
      PHASED=-(DATAN((-RID(J)+WF(M))/(-RRD(J))))+PHASED                 33
      KDSAVE=KD                                                         34
      KD=-RRD(J)*KD                                                     35
      IF(KDSAVE*KD.LT.0.0)PHASED=PHASED-3.1415926536                    36
    4 CONTINUE                                                          37
      PHASEN=0.0                                                        38
      KN=KGAIN                                                          39
      AMPN=1.0                                                          40
      DO 8 I=1,JJ                                                       41
      IF(RRN(I).EQ.0.0)GO TO 5                                          42
      GO TO 7                                                           43
    5 AMPN=AMPN*DABS(WF(M)-RIN(I))                                      44
      IF(WF(M)-RIN(I).LT.0.0)GO TO 6                                    45
      PHASEN=PHASEN+3.1415926536/2.0                                    46
      GO TO 8                                                           47
    6 PHASEN=PHASEN-3.1415926536/2.0                                    48
      GO TO 8                                                           49
    7 AMPN=DSQRT(((-WF(M)+RIN(I))/RRN(I))**2+1.0)*AMPN                  50
      PHASEN=DATAN((-RIN(I)+WF(M))/(-RRN(I)))+PHASEN                    51
      KNSAVE=KN                                                         52
      KN=-RRN(I)*KN                                                     53
      IF(KNSAVE*KN.LT.0.0)PHASEN=PHASEN+3.1415926536                    54
    8 CONTINUE                                                          55
      KKK(M)=KN/KD                                                      56
      AMPR(M)=DABS(KKK(M))*AMPN/AMPD                                    57
      AMPRDB(M)=20.0*DLOG10(AMPR(M))                                    58
      PHASE(M)=PHASED+PHASEN                                            59
      PHDEG(M)=PHASE(M)*57.295779513                                    60
      NCYCLE(M)=WF(M)/(2.0*3.1415926536)                                61
    9 CONTINUE                                                          62
      RETURN                                                            63
      END                                                               64
```

LONGITUDINAL OUTPUT

LONGITUDINAL STABILITY DERIVATIVES

CL	= 0.309300	CD	= 0.031100	CM	= 0.0	CY	= 0.0	CLA	= 4.408000	CDA	= 0.129400
CMA	= -0.885300	CLQ	= 3.918800	CDQ	= 0.0	CNQ	= -12.433700	CLDA	= 1.741900	CDDA	= 0.0
CMDA	= -5.237000	CTRPH	= 0.0	CLU	= 0.0	CDU	= 0.0	CMU	= 0.0	CTU	= 0.0

PERTINENT AIRPLANE CHARACTERISTICS

RHO = 0.002048	WING AREA = 174.000000	MASS = 82.300000	G*COS(GAMMA) = 32.200000	COSI(Z) = 0.998100	ZJ = 0.0
U = 219.000000	CHORD = 4.850000	IYY = 1346.0000	G*SIN(GAMMA) = 0.0	SINI(Z) = 0.061050	

RESPONSE TO ELEVATOR DEFLECTION

CLIN = 0.426800 CDIN = 0.039600 CMIN = -1.283000 K = 1 ACC = 0.00010000

POLYNOMIAL COEFFICIENTS FOR THE DENOMINATOR AND NUMERATOR

DS(5) = 1.0091	DS(4) = 9.2563	DS(3) = 36.2921	DS(2) = 1.2477	DS(1) = 1.1755
	NUS(4) = -6.2451	NUS(3) = -54.7696	NUS(2) = 294.7416	NUS(1) = 2620.3525
	NAS(4) = -0.2024	NAS(3) = -39.5490	NAS(2) = -1.1313	NAS(1) = -1.7036
		NTHS(3) = -39.5057	NTHS(2) = -82.5573	NTHS(1) = -3.6350
	NHS(4) = -44.3161	NHS(3) = -8861.2244	NHS(2) = -247.7452	NHS(1) = -373.0955

SOLUTION FOR U VARIATION

DENOMINATOR ROOTS

RDOT(1) =	-0.01359	+J	-0.18010
RDOT(2) =	-0.01359	+J	0.18010
RDOT(3) =	-4.07716	+J	4.36873
RDOT(4) =	-4.07716	+J	-4.36873

	NATURAL FREQ UNDAMPED	NATURAL FREQ DAMPED	DAMPING RATIO	TIME FOR 1/2 DAMPING	SETTLING TIME
SHORT PERIOD	5.97570	4.36873	0.68229	0.17001	0.73475
PHUGOID	0.18062	0.18010	0.07523	51.01581	220.48435

NUMERATOR ROOTS

RDOT(1) =	-7.11923	+J	0.0
RDOT(2) =	-8.55107	+J	0.0
RDOT(3) =	0.89625	+J	0.0

	NATURAL FREQ UNDAMPED	NATURAL FREQ DAMPED	DAMPING RATIO	TIME FOR 1/2 DAMPING	SETTLING TIME
	0.0	0.0	7.1192	0.09742	0.42103
	0.0	0.0	8.9511	0.08106	0.35033

BODE PLOT INFORMATION

FREQUENCY RAD/SEC	FREQUENCY CYCLES/SEC	AMPLITUDE RATIO PURE	AMPLITUDE RATIO DECIBELS	PHASE ANGLE RADIANS	PHASE ANGLE DEGREES
0.01000	0.00159	2235.83	66.98679	3.13208	179.45488
0.10000	0.01592	3192.39	70.08428	3.01045	172.48527
0.12344	0.02226	4934.16	73.86279	2.87347	164.63790
0.16255	0.02587	9561.27	79.61032	2.50357	143.44397
0.18062	0.02875	14629.84	83.42273	1.54985	88.79972
0.19868	0.03162	8344.44	78.42002	0.69439	39.78573
0.22577	0.03593	3763.85	71.51265	0.29646	16.98389
1.00000	0.15915	77.31	37.76492	-0.09042	-5.18238
4.48178	0.71330	5.18	14.29374	-0.69219	-39.65928
5.37813	0.85596	3.60	11.40300	-0.86592	-49.61357
9.97570	1.58804	3.15	9.94254	-0.97134	-55.64721
9.57327	1.04617	2.64	8.41907	-1.04589	-61.07103
7.44963	1.18483	2.04	6.27932	-1.14330	-67.79798
10.00000	1.59155	1.17	1.35938	-1.38707	-79.47313
99.99998	15.91549	0.04	-24.84201	-1.57435	-90.21640
999.99979	159.15491	0.01	-44.16396	-1.57138	-90.03370

LATERAL OUTPUT

LATERAL STABILITY DERIVATIVES

CYB	= -0.306000	CLB	= -0.089000	CNB	= 0.064600	CYP	= -0.037300	CLP	= -0.470800	CNP	= -0.029200
CYR	= 0.210000	CLR	= 0.095900	CNR	= -0.099200						

PERTINENT AIRPLANE CHARACTERISTICS

RHO = 0.002630	WING AREA = 174.000000	MASS = 82.300000	G*COS(GAMMA) = 32.200000
U = 219.0000	CHORD = 4.850000	SPAN = 35.9100	G*SIN(GAMMA) = 0.0
IXX = 948.0000	IXZ = 0.0	IZZ = 1967.0000	

RESPONSE TO RUDDER DEFLECTION

CYIN = 0.187400 CLIN = 0.014700 CNIN = -0.065800 K = 1 ACC = 0.00010000

POLYNOMIAL COEFFICIENTS FOR THE DENOMINATOR AND NUMERATOR

DS(5) = 1.0000	DS(4) = 13.8617	DS(3) = 28.6339	DS(2) = 143.5812	DS(1) = 1.5997
	NS(4) = 0.0889	NS(3) = 11.3819	NS(2) = 128.9475	NS(1) = -2.9397
	NPHI(4) = 4.7524	NPHI(3) = -21.8582	NPHI(2) = -249.0351	NPHI(1) = 0.0
	NPSI(4) = -10.2925	NPSI(3) = -130.0279	NPSI(2) = -6.4616	NPSI(1) = -34.3408

SOLUTION FOR SIDESLIP VARIATION

DENOMINATOR ROOTS

RDOT(1) =	-0.68793	+J	-3.29399
RDOT(2) =	-0.68793	+J	3.29399
RDOT(3) =	-12.47536	+J	0.0
RDOT(4) =	-0.01130	+J	0.0

	NATURAL FREQ UNDAMPED	NATURAL FREQ DAMPED	DAMPING RATIO	TIME FOR 1/2 DAMPING	SETTLING TIME
DUTCH ROLL	3.3650	3.294C	0.20432	4.35718	1.00817

NUMERATOR ROOTS

RDOT(1) =	-12.38789	+J	0.0
RDOT(2) =	-115.41020	+J	0.0
RDOT(3) =	0.02275	+J	0.0

BODE PLOT INFORMATION

FREQUENCY RAD/SEC	FREQUENCY CYCLES/SEC	AMPLITUDE RATIO PURE	AMPLITUDE RATIO DECIBELS	PHASE ANGLE RADIANS	PHASE ANGLE DEGREES
0.01000	0.00159	1.51	3.56115	3.09174	177.14148
0.10000	0.01592	0.93	-0.60331	0.32684	18.72189
1.00000	0.15915	0.99	-0.08442	-0.09043	-5.18107
2.52373	0.40166	1.71	4.67107	-0.57746	-33.08607
3.02848	0.48200	2.21	6.88316	-1.09831	-62.94961
3.36498	0.53535	2.24	6.99712	-1.53378	-87.87905
3.70147	0.58911	1.84	5.31162	-1.96902	-112.81680
4.20822	0.66996	1.20	1.60921	-2.34291	-134.26176
10.00000	1.59155	0.12	-18.75262	-2.90230	-166.28926
99.99998	15.91549	0.00	-37.33084	-2.41461	-138.34718
999.99979	159.15491	0.00	-80.96069	-1.68440	-96.50910

TIME RESPONSE PROGRAM

The time response program is a program which will give a tabulated output of a transfer function due to an impulse or a step input by taking the inverse Laplace transform of the transfer function. When using this program there are two important restrictions:

1) If an impulse is used the order of the numerator polynomial must be lower than the order of the denominator polynomial.

2) If a step is used the order of the numerator polynomial must be less than or equal to the order of the denominator polynomial.

Use of the program requires the input of the variables listed below:

MN - order of the numerator polynomial

MD - order of the denominator polynomial

ITYPE - variable which indicates the type of response desired
(ITYPE = 0 is the signal for an impulse response
ITYPE = 1 is the signal for a step response)

GAIND - coefficient of the highest order term in the denominator polynomial

FORCE - the magnitude of the input (If FORCE is 3.0 then the response will correspond to a 3^{o} control surface input)

NS(I) - coefficients of the numerator polynomial beginning with the lowest ordered term

ROOTR(I), ROOTI(I) } the real and imaginary parts of the roots to the denominator polynomial

The output variables are defined in the program, and a sample output has been included at the end of the program. It should be noted that all the pertinent input information needed for this program has been included as output information in both the Longitudinal and Lateral programs preceding this program.

```
      IMPLICIT REAL*4 (M)
      DIMENSION NS(10),DS(10),ROOTR(10),ROOTI(10),OUTPUT(1000),T(1000)
    1 READ(1,100)MN,MD,ITYPE,GAINO,FORCE
  100 FORMAT(3I1,2F15.7)
      IF(MN.EQ.0)CALL EXIT
      MN1=MN+1
      READ(1,101)(NS(I),I=1,MN1)
      READ(1,101)(ROOTR(I),ROOTI(I),I=1,MD)
  101 FORMAT(5F15.7)
      IF(ITYPE.EQ.1)GO TO 2
      WRITE(3,201)FORCE
  201 FORMAT('1',////10X,'TIME RESPONSE FOR AN IMPULSE INPUT =',F7.2,'
     $DEGREES')
      GO TO 3
    2 WRITE(3,202)FORCE
  202 FORMAT('1',////10X,'TIME RESPONSE FOR A STEP INPUT =',F7.2,'  DEGR
     $EES')
    3 WRITE(3,203)
  203 FORMAT(////10X,'THE COEFFICIENTS OF THE NUMERATOR'/)
      WRITE(3,204)(I,NS(I),I=1,MN1)
  204 FORMAT(10X,'NS(',I1,')=',F15.7)
      WRITE(3,205)
  205 FORMAT(////10X,'THE ROOTS OF THE DENOMINATOR',/)
      WRITE(3,206)(I,ROOTR(I),ROOTI(I),I=1,MD)
  206 FORMAT(10X,'ROOT(',I1,')=',F15.7,'   +  J ',F15.7)
      GAINDG=GAINO/FORCE
      IF(ITYPE.EQ.1)GO TO 4
      CALL TYME(OUTPUT,T,IO,NS,MN1,ROOTR,RCOTI,MD,GAINDG,ICODE)
      GO TO 5
    4 MD=MD+1
      ROOTR(MD)=0.00
      ROOTI(MD)=0.0
      CALL TYME(OUTPUT,T,IO,NS,MN1,ROOTR,ROOTI,MD,GAINDG,ICODE)
    5 WRITE(3,207)ICODE
  207 FORMAT(1H1,///,10X,'ICODE = ',I2)
      IF(ICODE.EQ.1)WRITE(3,208)
  208 FORMAT(//10X,'THE COMPLEX PART OF THE OUTPUT VECTOR BECAME SIGNIFI
     $CANT')
      IF(ICODE.EQ.2)WRITE(3,209)
  209 FORMAT(//10X,'MULTIPLE ROOTS ENCOUNTERED')
      IF(ICODE.EQ.3)WRITE(3,210)
  210 FORMAT(//10X,'BAD ENTRY - CHECK POLYNOMINAL ORDERS OF TRANSFER FUN
     $CTION')
      IF(ICODE.NE.0)GO TO 1
      WRITE(3,211)
  211 FORMAT(////16X,'TIME',19X,'OUTPUT')
      WRITE(3,212)(T(I),OUTPUT(I),I=1,IO)
  212 FORMAT(/14X,F7.2,14X,F15.7)
      GO TO 1
      END
```

```
      SUBROUTINE CPVAL(RES,ARG,X,IDIMX)
      COMPLEX*8 RES,ARG
      DIMENSION X(20)
      RES=(0.,0.)
      J=IDIMX
    1 IF(J)3,3,2
    2 RES=RES*ARG+X(J)
      J=J-1
      GO TO 1
    3 RETURN
      END
```

```
C
C
C*****************************************************************
C
C     PURPOSE:
C
C
C        THE PURPOSE OF THIS SUBROUTINE IS TO DETERMINE THE TIME
C        RESPONSE OF AN INPUT TO A TRANSFER FUNCTION BY TAKING THE
C        INVERSE LAPLACE TRANSFORM.
C
C
C     METHOD:
C
C        THE METHOD OF RESIDUES IS USED TO GENERATE THE TIME RESPONSES.
C
C
C     VARIABLES:
C
C        OUTPUT - VECTOR OF CALCULATED RESPONCE AMPLITUDE VALUES
C        T - VECTOR OF SEQUENTIAL TIME VALUES DIRECTLY RELATED TO OUTPUT
C        IO - NUMBER OF OUTPUT VALUES (CALCULATED)
C        NG - VECTOR OF NUMERATOR COEFFICIENTS
C        ING - DIMENSION OF THE NUMERATOR COEFFICIENTS
C        ROOTR - VECTOT OF REAL PARTS OF THE ROOTS
C        ROOTI - VECTOR OF IMAGINARY PARTS OF THE ROOTS
C        IDGM1 - NUMBER OF ROOTS (ORDER OF THE DENOMINATOR)
C        GAINDG - GAIN OF THE DENOMINATOR
C        ICODE - RETURN CODE VARIABLE
C                ICODE=0 IMPLIES NORMAL EXECUTION
C                ICODE=1 IMPLIES THAT THE COMPLEX PART OF THE OUTPUT
C                        VECTOR BECAME SIGNIFICANT.
C                ICODE=2 IMPLIES THAT MULTIPLE ROOTS WERE ENCOUNTERED
C                        IN THE DENOMINATOR.
C                ICODE=3 IMPLIES THAT THE ORDER OF THE DENOMINATOR WAS
C                        NOT GREATER THAN THE ORDER OF THE NUMERATOR.
C
C
C     SUBROUTINES CALLED:
C
C        CPVAL - COMPLEX EVALUATION OF A POLYNOMIAL
C
C
C     REMARKS:
C
C        THIS SUBROUTINE IS DESIGNED TO GENERATE THE TIME RESPONSE OF A
C        GENERAL OUTPUT FUNCTION XO(S) = X1(S)G(S).  IN THIS
C        EVALUATION TWO IMPORTANT ASSUMPTIONS ARE MADE.
C                1)  THE ORDER OF THE DENOMINATOR OF THE OUTPUT FUNCTION
C                    OF THE OUTPUT FUNCTION.
C                    MUST BE LARGER THAN THE ORDER OF THE NUMERATOR
C                2)  MULTIPLE ROOTS OF THE DENOMINATOR MAY NOT EXIST.
C
C
C     REFERENCE:
C
C        INTRODUCTION TO AUTOMATIC CONTROL SYSTEMS - ROBERT N. CLARK
C        (PP 70 - 77).
C
C*****************************************************************
C
C
C
```

```
      SUBROUTINE TYME(OUTPUT,T,IO,NG,ING,ROOTR,ROOTI,IDGM1,GAINDG,ICODE)
      IMPLICIT COMPLEX*8 (C,K),REAL*4 (N)
      COMPLEX*8 P,S,CUT,CUT1
      DIMENSION P(10),NG(10),K(10),OUT(1000),OUTPUT(1000),T(1000),
     $          ROOTR(10),ROOTI(10)
C
C        CHECK FOR BAD ENTRY
C
      IF(IDGM1.LT.ING) GO TO 9
C
C        CHECK FOR MULTIPLE ROOTS
C
      DO 1 I=1,IDGM1
      RRP1=ROOTR(I)+.001
      RRM1=ROOTR(I)-.001
      RIP1=ROOTI(I)+.001
      RIM1=ROOTI(I)-.001
      DO 1 J=1,IDGM1
      IF(I.EQ.J) GO TO 1
      RRJ=ROOTR(J)
      RIJ=ROOTI(J)
      IF(RRM1.LT.RRJ.AND.RRP1.GT.RRJ.AND.RIM1.LT.RIJ.AND.RIP1.GT.RIJ)
     $GO TO 8
    1 CONTINUE
      ICODE=0
C
C        DETERMINE TMAX
C
      SMALL=1.E6
      TDEL=.1
      MAX=TDEL*1000
      TROOT=6./MAX
      DO 2 I=1,IDGM1
      ABSR=ABS(ROOTR(I))
      IF(ABSR.LT.TROOT)   GO TO 2
      IF(ABSR.LT.SMALL) SMALL=ABSR
    2 CONTINUE
      TMAX=6./SMALL
      IF(TMAX.GT.99.) TMAX=99.
      DO 3 I=1,IDGM1
    3 P(I)=CMPLX(ROOTR(I),ROOTI(I))
C
C        DETERMINE THE K'S
C
      DO 5 J=1,IDGM1
      S=P(J)
      CALL CPVAL(KKUM,S,NG,ING)
      KJ=1.
      DO 4 L=1,IDGP1
      IF(L.EQ.J) GO TO 4
      KJ=KJ/(S-P(L))
    4 CONTINUE
      K(J)=KJ*KKUM/GAINDG
    5 CONTINUE
C
C        DETERMINE THE TIME RESPONSE
C
      IO=0
      T1=-TDEL
    6 IO=IO+1
      CUT1=(0.,0.)
      T1=T1+TDEL
      DO 7 J=1,IDGM1
      IF(ROOTR(J)*T1.LT.-15.) GO TO 7

      CUT1=CUT1+K(J)*CEXP(T1*P(J))
    7 CONTINUE
      OUTPUT(IO)=REAL(CUT1)
      UNREAL=AIMAG(CUT1)
      IF(ABS(UNREAL).GT..001) ICODE=1
      T(IO)=T1
      IF(T1.LT.TMAX) GO TO 6
      RETURN
    8 ICODE=2
      RETURN
    9 ICODE=3
      RETURN
      END
```

SAMPLE OUTPUT

TIME RESPONSE FOR AN IMPULSE INPUT = 1.00 DEGREES

THE COEFFICIENTS OF THE NUMERATOR

NS(1)= 48.0000000
NS(2)= 72.0000000
NS(3)= 24.0000000

THE ROOTS OF THE DENOMINATOR

ROOT(1)= -1.0000000 + J 1.7320490
ROOT(2)= -3.0000000 + J 0.0
ROOT(3)= -4.0000000 + J 0.0
ROOT(4)= -1.0000000 + J -1.7320490

ICODE = 0

TIME	OUTPUT
0.0	-0.0000038
0.10	1.7742138
0.20	2.6069489
0.30	2.8446970
0.40	2.7188845
0.50	2.3841696

APPENDIX I

BIBLIOGRAPHY

1. Knight, Montgomery; and Wenzinger, Carl J.: "Rolling Moments Due to Rolling and Yaw for Four Wing Models in Rotation." NACA TR-379, 1931.

2. Freeman, Hugh B.: "The Effect of Small Angles of Yaw and Pitch on the Characteristics of Airplane Propellers." NACA TR-389, 1931.

3. Knight, Montgomery; and Noyes, Richard W.: "Span-Load Distribution as a Factor in Stability in Roll." NACA TR-393, 1931.

4. Weick, Fred E.; and Wenzinger, Carl J.: "Wind-Tunnel Research Comparing Lateral Control Devices, Particularly at High Angles of Attack. I--Ordinary Ailerons on Rectangular Wings." NACA TR-419, 1932.

5. Weick, Fred E.; and Wenzinger, Carl J.: "Wind-Tunnel Research Comparing Lateral Control Devices, Particularly at High Angles of Attack. III--Ordinary Ailerons Rigged Up 10° When Neutral." NACA TR-423, 1932.

6. Weick, Fred E.; and Harris, Thomas A.: "Wind-Tunnel Research Comparing Lateral Control Devices, Particularly at High Angles of Attack. IV--Floating Tip Ailerons on Rectangular Wings." NACA TR-424, 1932.

7. Dryden, Hugh L.; and Monish, B.H.: "The Effect of Area and Aspect Ratio on the Yawing Moments of Rudders at Large Angles of Pitch on Three Fuselages." NACA TR-437, 1932.

8. Weick, Fred E.; and Shortal, Joseph A.: "Wind-Tunnel Research Comparing Lateral Control Devices, Particularly at High Angles of Attack. V--Spoilers and Ailerons on Rectangular Wings." NACA TR-439, 1932.

9. Soulé, Hartley A.; and Wheatley, John B.: "A Comparison Between the Theoretical and Measured Longitudinal Stability Characteristics of an Airplane." NACA TR-442, 1933.

10. Weick, Fred E.; and Soulé, Hartley A.; and Gough, Melvin N.: "A Flight Investigation of the Lateral Control Characteristics of Short Wide Ailerons And Various Spoilers with Different Amounts of Wing Dihedral." NACA TR-494. 1934.

11. Weick, Fred E.; and Wenzinger, Carl J.: "Wind-Tunnel Research Comparing Lateral Control Devices, Particularly at High Angles of Attack. XII--Upper-Surface Ailerons on Wings with Split Flaps."NACA TR-499, 1934.

12. Weick, Fred E.; and Noyes, Richard W.:. "Wind-Tunnel Research Comparing Lateral Control Devices, Particularly at High Angles of Attack. XIII--Auxiliary Airfoils Used as External Ailerons." NACA TR-510, 1935.

13. Soulé, H.A.; and McAvoy, W.H.: "Flight Investigation of Lateral Control Devices for Use With Full-Span Flaps." NACA TR-517, 1935.

14. Shortal, Joseph A.: "Effect of Tip Shape and Dihedral on Lateral-Stability Characteristics." NACA TR-548, 1936.

15. Jones, Robert T.: "A Simplified Application of the Method of Operators to the Calculation of Disturbed Motions of an Airplane." NACA TR-560, 1936.

16. Weick, Fred E.; and Jones, Robert T.: "The Effect of Lateral Controls in Producing Motion of an Airplane as Computed from Wind-Tunnel Data." NACA TR-570, 1936.

17. Soulé, Hartley A.: "Flight Measurements of the Dynamic Longitudinal Stability of Several Airplanes and a Correlation of the Measurements with Pilots' Observations of Handling Characteristics." NACA TR-578, 1937.

18. Jones, Robert T.: "A Study of the Two-Control Operation of an Airplane." NACA TR-579, 1937.

19. Weick, Fred E.; and Jones, Robert T.: "Résumé and Analysis of N.A.C.A. Lateral Control Research." NACA TR-605, 1937.

20. Jones, Robert T.: "The Influence of Lateral Stability on Disturbed Motions of an Airplane with Special Reference to the Motions Produced by Gusts." NACA TR-638, 1938.

21. Sherman, Albert: "Interference of Tail Surfaces and Wing and Fuselage From Tests of 17 Combinations in the N.A.C.A. Variable-Density Tunnel. NACA TR-678, 1939.

22. Katzoff, S.: "Longitude Stability and Control with Special Reference to Slipstream Effects." NACA TR-690, 1940.

23. Imlay, Frederick H.: "A Theoretical Study of Lateral Stability with an Automatic Pilot." NACA TR-693,1940.

24. Soulé, H.A.: "Preliminary Investigation of the Flying Qualities of Airplanes." NACA TR-700, 1940.

25. House, Rufus O.; and Arthur R. Wallace: "Wind-Tunnel Investigation of Effect of Interference on Lateral-Stability Characteristics of Four NACA 23012 Wings, an Elliptical and a Circular Fuselage, and Vertical Fins." NACA TR-705, 1941.

26. Jones, Robert T.; and Cohen, Doris: "An Analysis of the Stability of an Airplane with Free Controls." NACA TR709, 1941.

27. Gilruth, R.R.; and Turner, W.N.: "Lateral Control Required for Satisfactory Flying Qualities Based on Flight Tests of Numerous Airplane." NACA TR-715, 1941.

28. Greenberg, Harry; and Sternfield, Leonard: "A Theoretical Investigation of the Lateral Oscillations of an Airplane with Free Rudder with Special Reference to the Effect of Friction." NACA TR-762, 1943.

29. Cohen, Doris: "A Theoretical Investigation of the Rolling Oscillations of an Airplane with Ailerons Free." NACA TR-787,1944.

30. Jones, Robert T.; and Greenburg, Harry: "Effect of Hinge-Moment Parameters on Elevator Stick Forces in Rapid Maneuvers." NACA TR-798, 1944.

31. Ribner, Herbert S.: "Formulas for Propellers in Yaw and Charts of the Side-Force Derivative." NACA TR-819, 1945.

32. Kayten, Gerald G.: "Analysis of Wind Tunnel Stability and Control Tests in Terms of Flying Qualities of Full-Scale Airplanes." NACA TR-825, 1945.

33. Sawyer, Richard H.: "Flight Measurements of the Lateral Control Characteristics of Narrow-Chord Ailerons on the Trailing Edge of a Full-Span Slotted Flap." NACA TR-883, 1947.

34. Weil, Joseph; and Sleeman, William C.,Jr.: "Prediction of the Effects of Propeller Operation on the Static Longitudinal Stability of Single-Engine Tractor Monoplanes with Flaps Retracted." NACA TR-941, 1949.

35. Sternfield, Leonard; and Gates, Ordway B., Jr.: "A Simplified Method for the Determination and Analysis of the Neutral-Lateral-Oscillatory-Stability Boundary." NACA TR-943, 1949.

36. Johnson, Harold I.: "Flight Investigation of the Effect of Various Vertical-tail Modifications on the Directional Stability and Control Characteristics of a Propeller-Driven Fighter Airplane." NACA TR-973, 1950.

37. Curfam, Howard J.; and Gardiner, Robert A.: "Method for Determining the Frequency-Response Characteristics of an Element or System from the System Transient Output Response to a Known Input Function." NACA TR-984, 1950.

38. McKinney, Marion O., Jr.: "Analysis of Means of Improving the Uncontrolled Lateral Motions of Personal Airplanes." NACA TR-1035, 1951.

39. Donegan, James J.; and Pearson, Henry A.: "Matrix Methods of Determining the Longitudinal-Stability Coefficients and Frequency Response of an Aircraft from Transient Flight Data." NACA TR-1070, 1952.

40. Stone, Ralph W., Jr.: "Estimation of the Maximum Angle of Sideslip for Determination of Vertical-Tail Loads in Rolling Maneuvers." NACA TR-1136, 1953.

41. Schade, Robert O.; and Hassell, James L., Jr.: "The Effects on Dynamic Lateral Stability and Control of Large Artificial Variations in the Rotary Stability Derivatives." NACA TR-1151, 1953.

42. Martina, Albert P.: "Method for Calculating the Rolling and Yawing Moments Due to Rolling for Unswept Wings With or Without Flaps or Ailerons by Use of Nonlinear Section Lift Data." NACA TR-1167, 1954.

43. Donegan, James J.: "Matrix Methods for Determining the Longitudinal-Stability Derivatives of an Airplane from Transient Flight Data." NACA TR-1169, 1954.

44. Campbell, John P.; and McKinney, Marion O., Jr.: "A Study of the Problem of Designing Airplanes With Satisfactory Inherent Damping of the Dutch Roll Oscillation." NACA TR-1199, 1954.

45. Donegan, James J.; Robinson, Samuel W., Jr.; and Gates, Ordway B., Jr.: "Determination of Lateral-Stability Derivatives and Transfer-Function Coefficients from Frequency-Response Data for Lateral Motions." NACA TR-1225, 1955.

46. Riley, Donald R.: "Effect of Horizontal-Tail Span and Vertical Location on the Aerodynamic Characteristics of an Unswept Tail Assembly in Sideslip." NACA TR-1171, 1954.

47. Eggleston, John M.; and Mathews, Charles W.: "Application of Several Methods for Determining Transfer Functions and Frequency Response of Aircraft from Flight Data." NACA TR-1204, 1954.

48. Weick, Fred E.; and Wenzinger, Carl J.: "Effect of Length of Handley Page Tip Slots on the Lateral-Stability Factor Damping in Roll." NACA TN-423, July, 1932.

49. Bamber, M.J.; and Zimmerman, C.H.: "Effect of Stabilizer Location Upon Pitching and Yawing Moments in Spins as Shown by Tests with the Spinning Balance." NACA TN-474, November, 1933.

50. Soulé, Hartley A.; and Wetmore, J.W.: "The Effect of Slots and Flaps on Lateral Control of a Low-Wing Monoplane as Determined in Flight." NACA TN-478, November, 1933.

51. Bamber, Millard J.: "Aerodynamic Rolling and Yawing Moments Produced by Floating Wing-Tip Ailerons, As Measured by the Spinning Balance." NACA TN-493, March, 1934.

52. Shortal, J.A.: "Effect of Retractable-Spoiler Location on Rolling and Yawing-Moment Coefficients." NACA TN-499, July, 1934.

53. Wenzinger, Carl J.; and Bamber, Millard J.: "Wind-Tunnel Tests of Three Lateral Control Devices in Combination with a Full-Span Slotted Flap on an N.A.C.A. 23012 Airfoil." NACA TN-659, August, 1938.

54. Bamber, M.J.; and House, R.O.: "Wind-Tunnel Investigation of Effect of Yaw on Lateral-Stability Characteristics. I--Four NACA 23012 Wings of Various Plan Forms with and without Dihedral." NACA TN-703, April, 1939.

55. Jones, Robert T.; and Fehlner, Leo F.: "Transient Effects of the Wing Wake on the Horizontal Tail." NACA TN-771, August, 1940.

56. Pass, H.R.: "Analysis of Wind-Tunnel Data on Directional Stability and Control." NACA TN-775, September, 1940.

57. Bamber, Millard J.: "Effect of Some Present-Day Airplane Design Trends on Requirements for Lateral Stability." NACA TN-814, June, 1941.

58. Recant, Isidore G.; and Wallace, Arthur R.: "Wind-Tunnel Investigation of Effect of Yaw of Lateral-Stability Characteristics. III--Symmetrically Tapered Wing at Various Positions on Circular Fuselage with and without a Vertical Tail." NACA TN-825, September, 1941.

59. Donlan, C.J.; and Recant, I.G.: "Methods of Analyzing Wind-Tunnel Data for Dynamic Flight Conditions." NACA TN-828, October, 1941.

60. Jones, Robert T.: "Notes on the Stability and Control of Tailless Airplanes." NACA TN-837, December, 1941.

61. Ankenbruck, Herman O.: "Effects of Tip Dihedral on Lateral Stability and Control Characteristics on Determined by Tests of a Dynamic Model in the Langley Free-Flight Tunnel." NACA TN-1059, July, 1946.

62. Phillips, William H.: "An Investigation of Additional Requirements for Satisfactory Elevator Control Characteristics." NACA TN-1060, June, 1946.

63. Bishop, Robert C.; and Lomax, Harvard: "A Simplified Method for Determining from Flight Data the Rate of Change of Yawing-Moment Coefficient with Sideslip." NACA TN-1076, June, 1946.

64. Shortal, Joseph A.; and Maggin, Bernard: "Effect of Sweepback and Aspect Ratio on Longitudinal Stability Characteristics of Wings at Low Speeds." NACA TN-1093, July, 1946.

65. Drake, Hubert M.: "Experimental Determination of the Effects of Directional Stability and Rotary Damping in Yaw on Lateral Stability and Control Characteristics." NACA TN-1104, July, 1946.

66. Spahr, J. Richard: "Lateral-Control Characteristics of Various Spoiler Arrangements as Measured in Flight." NACA TN-1123, January, 1947.

67. Purser, Paul E.; and Spear, Margaret F.: "Tests to Determine Effects of Slipstream Rotation on the Lateral Stability Characteristics of a Single-Engine Low-Wing Airplane Model." NACA TN-1146, September, 1946.

68. Harper, Charles W.; and Jones, Arthur L.: "A Comparison of the Lateral Motion Calculated for Tailless and Conventional Airplanes." NACA TN-1154, February, 1947.

69. Malvestuto, Frank S., Jr.: "Formulas for Additional-Mass Corrections to the Moments of Inertia of Airplanes." NACA TN-1187, February, 1947.

70. Sawyer, Richard H.: "Flight Measurements of the Lateral Control Characteristics of Narrow-Chord Ailerons on the Trailing Edge of a Full-Span Slotted Flap." NACA TN-1188, February, 1947.

71. Hunter, P.A.; and Vensel, J.R.: "A Flight Investigation to Increase the Safety of a Light Airplane." NACA TN-1203, March, 1947.

72. Hanson, Carl M.; and Anderson, Seth B.: "Flight tests of a Double-Hinged Horizontal Tail Surface with Reference to Longitudinal-Stability and Control Characteristics." NACA TN-1224, May, 1947.

73. Wallace, Arthur R.; Rossi, Peter F.; Wells, Evalyn G.: "Wind-Tunnel Investigation of the Effects of Power and Flaps on the Static Longitudinal Stability Characteristics of a Single-Engine Low-Wing Airplane Model." NACA TN-1239, April, 1947.

74. Rathert, George A., Jr.: "Flight Investigation of the Effects on Airplane Static Longitudinal Stability of a Bungee and Engine-Tilt Modifications." NACA TN-1260, May, 1947.

75. Bates, William R.: "Collection and Analysis of Wind-Tunnel Data on the Characteristics of Isolated Tail Surfaces with and without End Plates." NACA TN-1291, May, 1947.

76. Murray, Harry E.; and Wells, Evalyn G.: "Wind-Tunnel Investigation of the Effect of Wing-Tip Fuel Tanks on Characteristics of Unswept Wings in Steady Roll." NACA TN-1317, June, 1947.

77. Tamburello, Vito; and Weil, Joseph: "Wind-Tunnel Investigation of the Effect of Power and Flaps on the Static Lateral Characteristics of a Single-Engine Low-Wing Airplane Model." NACA TN-1327, June, 1947.

78. Hagerman, John R.: "Wind-Tunnel Investigation of the Effect of Power and Flaps on the Static Longitudinal Stability and Control Characteristics of a Single-Engine High-Wing Airplane Model." NACA TN-1339, July, 1947.

79. Maggin, Bernard: "Experimental Verification of the Rudder-Free Stability Theory for an Airplane Model Equipped with a Rudder Having Positive Floating Tendencies and Various Amounts of Friction." NACA TN-1359, July, 1947.

80. Hagerman, John R.: "Wind-Tunnel Investigation of the Effect of Power and Flaps on the Static Lateral Stability and Control Characteristics of a Single-Engine High-Wing Airplane Model." NACA TN-1379, July, 1947.

81. Fischel, Jack; and Ivey, Margaret F.: "Collection of Test Data for Lateral Control with Full-Span Flaps." NACA TN-1404, April, 1948.

82. Tosti, Louis P.: "Low-Speed Static Stability and Damping-in-Roll Characteristics of some Swept and Unswept Low-Aspect-Ratio Wings." NACA TN-1468, October, 1947.

83. Polhamus, Edward C.; and Moss, Robert J.: "Wind-Tunnel Investigation of the Stability and Control Characteristics of a Complete Model Equipped with a Vee Tail." NACA TN-1478, November, 1947.

84. Lomax, Harvard: "Sideslip Angles and Vertical-Tail Loads Developed by Periodic Control Deflections." NACA TN-1504, January, 1948.

85. Hunter, Paul A.: "Flight Measurement of the Flying Qualities of Five Light Airplanes." NACA TN-1573, May, 1948.

86. Weil, Joseph; and Sleeman, William C., Jr.: "Prediction of the Effects of Propeller Operation on the Static Longitudinal Stability of Single-Engine Tractor Monoplanes with Flaps Retracted." NACA TN-1722, October, 1948.

87. Schneitez, Leslie E.; and Naeseth, Rodger L.: "Wind-Tunnel Investigation at Low Speed of the Lateral Control Characteristics of Ailerons Having Three Spans and Three Trailing-Edge Angles on a Semispan Wing Model." NACA TN-1738, November, 1948.

88. Johnson, Harold S.: "Wind-Tunnel Investigation of Effects of Tail Length on the Longitudinal and Lateral Stability Characteristics of a Single-Propeller Airplane Model." NACA TN-1766, December, 1948.

89. Kauffman, Smith, Liddell, and Copper: "Flight Tests of an Apparatus for Varying Dihedral Effect in Flight." NACA TN-1788, December, 1948.

90. Goodman, Alex; and Fisher, Lewis R.: "Investigation at Low Speeds of the Effect of Aspect Ratio and Sweep on Rolling Stability Derivatives of Untapered Wings." NACA TN-1835, March, 1949.

91. Curfman, Howard J., Jr.; and Gardiner, Robert A.: "Method for Determining the Frequency-Response Characteristics of an Element or System From the System Output Response to a Known Input Function." NACA TN-1964, October, 1949.

92. Mazelsky, Bernard; and Diederich, Franklin W.: "Two Matrix Methods for Calculating Forcing Functions from Known Responses." NACA TN-1965, October, 1949.

93. McKinney, Marion O., Jr.: "Analysis of Means of Improving the Uncontrolled Lateral Motions of Personal Airplanes." NACA TN-1997, December, 1949.

94. Mokrzycki, G.A.: "Application of the Laplace Transformation to the Solution of the Lateral and Longitudinal Stability Equations." NACA TN-2002, January, 1950.

95. Bird, John D.; and Jaquet, Byron M.: "A Study of the Use of Experimental Stability Derivatives in the Calculation of the Lateral Disturbed Motions of a Swept-Wing Airplane and Comparison with Flight Results." NACA TN-2013, January, 1950.

96. Mazelsky, Bernard; and Diederich, Franklin W.: "A Method of Determining the Effect of Airplane Stability on the Gust Load Factor." NACA TN-2035, February, 1950.

97. Schade, Robert O.: "Free-Flight-Tunnel Investigation of Dynamic Longitudinal Stability as Influenced by the Static Stability Measured in Wind-Tunnel Force Tests Under Conditions of Constant Thrust and Constant Power." NACA TN-2075, April, 1950.

98. Murray, Harry E.; and Grant, Frederick C.: "Method of Calculating the Lateral Motions of Aircraft Based on the Laplace Transform." NACA TN-2129, July, 1950.

99. Johnson, Harold S.; and Hagerman, John R.: "Wind-Tunnel Investigation at Low-Speed of the Lateral Control Characteristics of an Unswept Untapered Semispan Wing of Aspect Ratio 3.13 Equipped with Various 25-percent-chord Plain Ailerons." NACA TN-2199, October, 1950.

100. Shinbrot, Marvin: "A Least Squares Curve Fitting Method with Applications to the Calculations of Stability Coefficients From Transient-Response Data." NACA TN-2341, April, 1951.

101. Campbell, Hunter, Hewes, and Whitten: "Flight Investigation of the Effect of Control Centering Springs on the Apparent Spiral Stability of A Personal-Owner Airplane." NACA TN-2413, July, 1951.

102. Marino, Alfred A.; and Mastrocola, N.: "Wind-Tunnel Investigation of the Contribution of a Vertical Tail To the Directional Stability of a Fighter Type Airplane." NACA TN-2488, January, 1952.

103. Goodman, Alex: "Effects of Wind Position and Horizontal-Tail Position on the Static Stability Characteristics of Models Unswept and 45° Swept Back to Mutual Reference." NACA TN-2504, October, 1951.

104. Shrinbot, Marvin: "A Description and a Comparison of Certain Nonlinear Curve-Fitting Techniques with Applications to the Analysis of Transient-Response Data." NACA TN-2622, February, 1952.

105. Donegan, James J.: "Matrix Methods for Determining the Longitudinal-Stability Derivatives of an Airplane from Transient Flight Data." NACA TN-2902, March, 1953.

106. Briggs, Benjamin R.; and Jones, Arthur L.: "Techniques for Calculating Parameters of Nonlinear Dynamic Systems from Response Data." NACA TN-2977, July, 1953.

107. Eggleston, John M.; and Mathews, Charles W.: "Application of Several Methods for Determining Transfer Functions and Frequency Response of Aircraft from Flight Data." NACA TN-2997, September, 1953.

108. Donegan, J.J.; and Robinson, S.W., Jr.; and Gates, Ordway B., Jr.: "Determination of Lateral Stability Derivatives and Transfer-Function Coefficients from Frequency Response Data for Lateral-Motions." NACA TN-3083, May, 1954.

109. Fisher, Lewis R.: "Some Effects of Aspect Ratio and Tail Length on the Contribution of a Vertical Tail to Unsteady Lateral Damping and Directional Stability of a Model Oscillating Continuously in Yaw." NACA TN-3121, January, 1954.

110. Canning, Thomas N.: "A Simple Mechanical Analogue for Studying the Dynamic Stability of Aircraft Habing Nonlinear Moment Characteristics." NACA TN-3125, February, 1954.

111. Gates, Ordway B., Jr.; and Woodling, C.H.: "A Method for Estimating Variations in the Roots of the Lateral-Stability Quartic due to Changes in Mass and Aerodynamic Parameters of an Airplane." NACA TN-3134, January, 1954.

112. Fisher, Lewis R.; and Fletcher, Herman S.: "Effect of Lag Sidewash on the Vertical-Tail Contribution to Oscillatory Damping in Yaw of Airplane Models." NACA TN-3356, January, 1955.

113. Bates, William R.: "Static Stability of Fuselages Having a Relatively Flat Cross Section." NACA TN-3429, March, 1955.

114. Letko, William; and Williams, James L.: "Experimental Investigation at Low Speed of Effects of Fuselage Cross Section on Static Longitudinal and Lateral Stability Characteristics of Models Having 0° and 45° Sweptback Surfaces." NACA TN-3551, December, 1955.

115. Fisher, Lewis R.; and Lichtenstein, Jacob H.; and Williams, Katherine D.: "A Preliminary Investigation of the Effects of Frequency and Amplitude on the Rolling Derivatives of an Unswept-Wing Model Oscillating in Roll." NACA TN-3554, January, 1956.

116. Wolhart, Walter D.; and Thomas, David F., Jr.: "Static Longitudinal and Lateral Stability Characteristics at Low Speed of Unswept-Midwing Models Having Wings with an Aspect Ratio of 2, 4, or 6." NACA TN-3649, May, 1956.

117. Weick, Fred E.; and Abramson, H. Norman: "Investigation of Lateral Control Near the Stall. Analysis For Required Longitudinal Trim Characteristics and Discussion of Design Variables." NACA TN-3677, June, 1956.

118. Klawans, Bernard B.: "A Simple Method for Calculating the Characteristics of the Dutch Roll Motion of an Airplane." NACA TN-3754, October, 1956.

119. Gault, Donald E.: "A Correlation of Low-Speed, Airfoil Section Stalling Characteristics with Reynolds Number and Airfoil Geometry." NACA TN-3963, March, 1957.

120. Pratt, Kermit G.; and Bennett, Floyd V.: "Charts for Estimating the Effects of Short-Period Stability Characteristics on Airplane Vertical-Acceleration and Pitch-Angle Response in Continuous Atmospheric Turbulence." NACA TN-3992, June, 1957.

121. Eggleston, John M.; and Phillips, William H.: "A Method for the Calculation of the Lateral Response of Airplanes to Random Turbulence." NACA TN-4196, February, 1958.

122. Gates, Ordway B., Jr.; and Woodling, C.H.: "A Theoretical Analysis of the Effect of Engine Angular Momentum on Longitudinal and Directional Stability in Steady Rolling Maneuvers." NACA TN-4249, April, 1958.

123. Crane, Robert M.: "Computation of Hinge-Moment Characteristics of Horizontal Tails from Section Data." NACA WR A-11, April, 1945.

124. Holtzclaw, R.N.; and Crane, R.M.: "Wind-Tunnel Investigation of Ailerons on a Low-Drag Airfoil. III--The Effect of Tabs." NACA WR A-18, November, 1944.

125. Laitone, Edmund V.; and Summers, James L.: "An Additional Investigation of the High-Speed Lateral-Control Characteristics of Spoilers." NACA WR A-21, July, 1945.

126. Spahr, J. Richard; and Christophersen, Don R.: "Measurements in Flight of the Stability, Lateral-Control, and Stalling Characteristics of an Airplane Equipped with Full-Span Zap Flaps and Spoiler-Type Ailerons." NACA WR A-28, December, 1943.

127. Spahr, J. Richard; and Christophersen, Don R.: "Measurements in Flight of the Lateral-Control Characteristics of an Airplane Equipped with Full-Span Zap Flaps and Simple Circular-Arc-Type Ailerons." NACA WR A-32, September 1944.

128. Crane, Robert M.; and Holtzclaw, Ralph W.: "Wind-Tunnel Investigation of Ailerons on a Low-Drag Airfoil. I--The Effect of Aileron Profile." NACA WR A-55, January, 1944.

129. Clousing, Lawrence A.; and McAvoy, William H.: "Flight Measurements of the Lateral Control Characteristics of an Airplane Equipped with a Combination Aileron-Spoiler Control System." NACA WR A-68, September, 1942.

130. Turner, William N.; and Adams, Betty: "Flight Measurements of the Effect of Various Amounts of Aileron Droop on the Low-Speed Lateral-Control Characteristics of an Observation Airplane." NACA WR A-79, August, 1943.

131. Hollingsworth, Thomas A.: "Investigation of Effect of Sideslip on Lateral-Stability Characteristics. II--Rectangular Midwing on Circular Fuselage with Variations in Vertical-Tail Area and Fuselage Length with and without Horizontal Tail Surface." NACA WR L-8, April, 1945.

132. Fehlner, Leo F.; and MacLachlan, Robert: "Investigation of Effect of Sideslip on Lateral Stability Characteristics. I--Circular Fuselage with Variations in Vertical-Tail Area and Tail Length with and without Horizontal Tail Surface." NACA WR L-12, May, 1944.

133. Hollingsworth, Thomas A.: "Investigation of Effect of Sideslip on Lateral Stability Characteristics. III--Rectangular Low-Wing on Circular Fuselage with Variations in Vertical-Tail Area and Fuselage Length with and without Horizontal Tail Surface." NACA WR L-17, April, 1945.

134. Ribner, Herbert S.: "Notes on the Propeller and Slipstream in Relation to Stability." NACA WR L-25, October, 1944.

135. Sjoberg, S.A.: "Flight Tests of Two Airplanes Having Moderately High Effective Dihedral and Different Directional Stability and Control Characteristics." NACA WR L-40, October, 1945.

136. Swanson, Robert S.; and Priddy, E. LaVerne: "Lifting-Surface-Theory Values of the Damping in Roll and of the Parameter used in Estimating Aileron Stick Forces." NACA WR L-53, August, 1945.

137. McKinney, Marion O., Jr.: "Experimental Determination of the Effect of Negative Dihedral on Lateral Stability and Control Characteristics at High Lift Coefficients." NACA WR L-54, January, 1946.

138. Campbell, John P.; and Paulson, John W.: "The Effects of Static Margin and Rotational Damping in Pitch on the Longitudinal Stability Characteristics of an Airplane as Determined by Tests of a Model in the NACA Free-Flight Tunnel." NACA WR L-55, January, 1944.

139. Drake, Hubert M.: "The Effect of Lateral Area on the Lateral Stability and Control Characteristics of an Airplane as Determined by Tests of a Model in the Langley Free Flight Tunnel." NACA WR L-103, February, 1946.

140. Purser, Paul E.; and McKinney, Elizabeth G.: "Comparison of Pitching Moments Produced by Plain Flaps and by Spoilers and Some Aerodynamic Characteristics of an NACA 23012 Airfoil with Various Types of Aileron." NACA WR L-124, April, 1945.

141. Vogeley, A.N.: "Climb and High Speed Tests of a Curtiss No. 714-lC2-12 Four-Blade Propeller on the Republic P-47C Airplane." NACA WR L-177, December, 1944.

142. McKinney, Marion O., Jr.; and Maggin, Bernard: "Experimental Verification of the Rudder-Free Stability Theory for an Airplane Model Equipped with Rudders Having Negative Floating Tendency and Negligible Friction." NACA WR L-184, November, 1944.

143. Ribner, Herbert S.: "Formulas for Propellers in Yaw and Charts of the Side-Force Cerivative." NACA WR L-217, May, 1943.

144. Bailey, F.J., Jr.; and O'Sullivan, William J.: "A Theoretical Analysis of the Effect of Aileron Inertia and Hinge Moment on the Maximum Rolling Acceleration of Airplanes in Abrupt Aileron Rolls." NACA WR L-302, February, 1942.

145. Donlan, Charles J.: "Some Theoretical Considerations of Longitudinal Stability in Power-on Flight with Special Reference to Wind-Tunnel Testing." NACA WR L-309, November, 1922.

146. Harris, Thomas A.; and Purser, Paul E.: "Wind-Tunnel Investigation of Plain Ailerons for a Wing with a Full-Span Flap Consisting of an Inboard Fowler and an Outboard Retractable Split Flap." NACA WR L-317, March, 1941.

147. Imlay, Frederick H.; and Bird, J.D.: "Wind-Tunnel Tests of Hinge-Moment Characteristics of Spring Tab Ailerons." NACA WR L-318, January, 1944.

148. Letko, W.; and Kemp, W.B.: "Wind-Tunnel Tests of Ailerons at Various Speeds. III--Ailerons of a 0.2 Airfoil Chord and True Contour with .35-Aileron-Chord Frise Balance on the NACA 23012 Airfoil." NACA WR L-325, September, 1943.

149. Fehlner, Leo F.: "A Study of the Effects of Vertical Tail Area and Dihedral on the Lateral Maneuverability of an Airplane." NACA WR L-347, October, 1941.

150. Cohen, Doris: "A Theoretical Investigation of the Rolling Oscillations of an Airplane with Ailerons Free." NACA WR L-361, January, 1944.

151. MacDougall, George F.: "Tests of Inverted Spins in the NACA Free-Spinning Tunnels." NACA WR L-370, December, 1943.

152. Sears, R.I.; and Hoggard, H.P., JR.: "Characteristics of Plain and Balanced Elevators on a Typical Pursuit Fuselage at Attitudes Simulating Normal-Flight and Spin Conditions." NACA WR L-379, March, 1942.

153. Goranson, R. Fabian: "Calculated Effects of Full-Span Slotted and Fowler Flaps on Longitudinal Stability and Control Characteristics for a Typical Fighter Type Airplane with Various Tail Modifications." NACA WR L-392, July, 1942.

154. Harmon, Sidney M.: "Determination of the Damping Moment in Yawing for Tapered Wings with Partial-Span Flaps." NACA WR L-395, August, 1943.

155. Seidman, Oscar; and Klinar, J.W.: "Elevator Stick Forces in Spins as Computed from Wind-Tunnel Measurements." NACA WR L-422, October, 1942.

156. Wallace, Arthur R.; and Turner, Thomas R.: "Wind-Tunnel Investigation of Effect of Yaw on Lateral-Stability Characteristics. V--Symmetrically Tapered Wing with a Circular Fuselage Having a Horizontal and a Vertical Tail." NACA WR L-459, June, 1943.

157. Campbell, John P.; and Seacord, Charles L., Jr.: "Effect of Wing Loading and Altitude on Lateral Stability and Control Characteristics of an Airplane as Determined by Tests of a Model in the Free-Flight Tunnel." NACA WR L-522, April, 1943.

158. Nissen, J.M.; and Phillips, W.H.: "Measurements of the Flying Qualities of a Hawker Hurricane Airplane." NACA WR L-565, April, 1942.

159. Phillips, W.H.; and Crane, H.L.: "Flight Tests of Various Tail Modifications on the Brewster XSBA-1 Airplane. II--Measurements of Flying Qualities with Tail Configuration Number Two." NACA WR L-598, December, 2, 1943.

160. Johnson, Harold I.; "Résumé of NACA Stability and Control Tests of the Bell P-63 Series Airplane." NACA WR L-601, October, 1944.

161. Johnson, H.I.; and Liddell, C.J.; and Hoover, H.H.: "Veasurements of the Flying Qualities of a Bell P-390-1 Airplane." NACA WR L-602, September, 1943.

162. Stability and Control Section of Flight Research Division at Langley Laboratory: "Charts Showing Stability and Control Characteristics of Airplanes in Flight." NACA WR L-706, December, 1944.

163. Lowry, John G.; and Toll, Thomas A.: "Power-On Longitudinal-Stability and Control Tests of the 1/8-Scale Model of the Brewster FZA Airplane Equipped with Full-Span Slotted Flaps and A New Horizontal Tail." NACA WR L-709, March, 1942.

164. Recant, Isidore G.; and Swanson, Robert S.: "Determination of the Stability and Control Characteristics of Airplanes from Tests of Powered Models." NACA WR L-710, July, 1942.

165. Johnson, Harold I.: "Flight Investigation to Improve the Dynamic Longitudinal Stability and Control-Feel Characteristics of the P-63A-1 Airplane with Closely Balanced Experimental Elevators." NACA WR L-730, July, 1946.

166. Goett, Harry J.; and Pass, H.R.: "Effect of Propeller Operation on the Pitching Moments of Single-Engine Monoplanes." NACA WR L-761, May, 1941.

167. Goett, Harry J.; and Jackson, Roy P.; and Belsley, Steven E.: "Wind-Tunnel Procedure for Determination of Critical Stability and Control Characteristics of Airplanes." NACA WR W-5, April, 1944.

168. Conway, H.M.: "Notes on Maximum Airplane Angular Velocities." NACA WR W-101, May, 1943.

169. Mathias, Gotthold: "The Calculation of Lateral Stability with Free Controls." NACA TM-741, April, 1934.

170. Hübner, Walter: "Additional Test Data on Static Longitudinal Stability." NACA TM-752, August, 1934.

171. Schmidt, Rudolf: "The Effect of the Masses of the Controls on the Longitudinal Stability with Free Elevator." NACA TM-900, July, 1939.

172. Martinov, A.; and Kolosov, E.: "Some Data on the Static Longitudinal Stability and Control of Airplanes (Design and Control Surfaces)." NACA TM-941, May, 1940.

173. Raikh, A.: "Calculation of the Lateral-Dynamic Stability of Aircraft." NACA TM-1264, February, 1952.

174. Kramer, M.; and Zober, Th.; and Esche, C.G.: "Lateral Control by Spoilers at the DVL." NACA TM-1307, August, 1951.

175. Hoene, H.: "Influence of Static Longitudinal Stability on the Behavior of Airplanes in Gusts." NACA TM-1323, November, 1951.